



University Free State



34300000106595

Universiteit Vrystaat

HIERDIE EKSEMPLAAR MAG ONDER
GEEN OMSTANDIGHEDE UIT DIE
BIBLIOTEEK VERWYDER WORD NIE

**STRATIGRAPHY, PETROCHEMISTRY AND
GENESIS OF THE MAKWASSIE FORMATION,
VENTERSDORP SUPERGROUP**

PETRUS GERHARDUS MEINTJES

This dissertation is submitted in fulfillment of the requirements for the degree
of Philosophiae Doctor in the Faculty of Science, Department of Geology,
University of the Orange Free State, Bloemfontein

OCTOBER 1998

SUPERVISOR:
Prof. W.A. van der WESTHUIZEN

CO-SUPERVISOR:
Dr H. de BRUIYN

The observer, when he seems to himself to be observing a stone, is really, if physics is to be believed, observing the effects of the stone upon himself.

Bertrand Russell

ABSTRACT

This study resulted in the subdivision of the former Makwassie Formation of S.A.C.S. (1980) into the lower Goedgenoeg Formation, characterised by feldspar porphyries, and the overlying quartz-feldspar porphyries of the Makwassie Formation proper (Meeting of the Ventersdorp Task Group, Feb. 1994). Non-porphyrific mafic lavas are interbedded with the porphyries of both the formations, while minor sedimentary rocks occur at the base and top of the Goedgenoeg Formation. The Garfield Member (Winter, 1976) is a unit of feldspar porphyries and mafic lavas which proved to occur locally within the Makwassie Formation and which is restricted to a limited area within the Bothaville area only.

The Goedgenoeg and Makwassie igneous rocks are of extrusive origin and both the feldspar and quartz-feldspar porphyries were emplaced subaerially as pyroclastic ash-flows, in most cases as extremely welded and recrystallised high-temperature ash-flows. Normal welded ash-flows and rheomorphic ash-flows also do occur. The non-porphyrific lavas and some of the less porphyritic feldspar porphyries represent normal liquid lava flows. These volcanic rocks must have originated from calderas, but none could be identified as yet.

The volcanic rocks are subalkaline, metaluminous to peraluminous and generally high in potassium. The tholeiitic Goedgenoeg rocks range from high-andesitic to dacitic in composition and four geochemical facies are recognised in the Bothaville area. The Makwassie porphyries are calc-alkaline in composition and classify as dacites to rhyodacites, with two geochemical facies being identified in the Bothaville area.

The Goedgenoeg and Makwassie Formations occur widespread throughout the Ventersdorp Supergroup depository and are preserved in deep graben structures, which developed during a rifting phase over a broad area of the western Kaapvaal Craton. Extremely thick successions of over 3 000 m accumulated in some areas, possibly representing intra-caldera successions, while the general outflow sheets reach an accumulated thickness of up to a 1 000 m. The overall volume of extruded magma must be in excess of 100 000 km³. The geochemical facies or magma types which were identified in the Bothaville area are also

represented in other Platberg grabens throughout the depository, though not all the facies are necessarily developed at any specific locality.

Neither the Goedgenoeg nor the Makwassie volcanics have a direct genetic link to any of the Klipriviersberg Group magmas. These volcanics originated from an enriched source and evolved through processes such as fractional crystallisation with periodic replenishment, assimilation and magma mixing, with the rhyodacitic Makwassie rocks being from a separate source.

TABLE OF CONTENTS

ABSTRACT.....	i
TABLE OF CONTENTS	iii
LIST OF FIGURES.....	vii
LIST OF TABLES.....	ix
 1. INTRODUCTION.....	 1
1.1 Review of the Ventersdorp Supergroup.....	1
1.1.1 General Background.....	1
1.1.2 History.....	1
1.1.3 Distribution.....	2
1.1.4 Stratigraphy.....	3
1.1.5 Geochronology.....	5
1.1.6 Geochemistry.....	5
1.1.7 Tectonic Setting.....	7
1.2 Aim of the Study.....	7
1.3 The Study Area.....	8
1.4 Study Methods.....	8
1.5 Definition of Nomenclature.....	10
 2. REVIEW OF THE GOEDGENOEG AND MAKWASSIE FORMATIONS.....	 14
2.1 Introduction.....	14
2.2 Previous Descriptions.....	14
2.3 Stratigraphy.....	17
2.4 Distribution.....	19
2.5 Age.....	21
2.6 Geochemistry and petrogenesis.....	21
 3. THE STRATIGRAPHY OF THE GOEDGENOEG AND MAKWASSIE FORMATIONS IN THE BOTHAVILLE AREA.....	 23
3.1 Introduction.....	23
3.2 Stratigraphy.....	23
3.2.1 The Goedgenoeg Formation.....	23
3.2.2 The Makwassie Formation.....	26
3.3 Lithology and Petrography.....	26
3.3.1 Comments on Alteration.....	26
3.3.2 Quartz-feldspar Porphyry.....	27
3.3.2.1 Macroscopic description.....	27
3.3.2.2 Petrographic description.....	30
3.3.3 Feldspar porphyry.....	36
3.3.3.1 Macroscopic description.....	36
3.3.3.2 Petrographic description.....	37
3.3.4 Non-porphyritic Lava.....	37

3.3.4.1 Macroscopic description.....	37
3.3.4.2 Petrographic description.....	37
3.3.5 Tuffaceous Rocks.....	37
3.3.5.1 Macroscopic description.....	37
3.3.5.2 Petrographic description.....	38
3.3.6 Epiclastic Sedimentary Rocks.....	38
3.4 Flow Morphology.....	38
3.4.1 Description.....	38
3.4.2 Interpretation.....	44
3.5 Discussion.....	47
 4. DISTRIBUTION OF THE GOEDGENOEG AND MAKWASSIE FORMATIONS IN THE BOTHAVILLE AREA.....	 52
4.1 Introduction.....	52
4.2 Thickness.....	52
4.2.1 The Goedgenoeg and Makwassie Formations combined.....	52
4.2.2 The Goedgenoeg Formation.....	53
4.2.3 The Makwassie Formation.....	54
4.2.4 The Garfield Member.....	54
4.3 Subtopography.....	58
4.3.1 Base of the Goedgenoeg Formation.....	58
4.3.2 Contact of the Goedgenoeg and Makwassie Formations.....	58
4.3.3 The Makwassie Formation top.....	59
4.4 Correlation diagrams.....	61
4.5 Discussion and structure.....	63
 5. GEOCHEMICAL COMPOSITION OF THE GOEDGENOEG AND MAKWASSIE FORMATIONS IN THE BOTHAVILLE AREA.....	 79
5.1 Introduction.....	79
5.2 Downhole geochemical plots.....	79
5.3 Alteration.....	80
5.4 Analytical Results.....	82
5.5 Geochemical classification.....	87
5.6 The Goedgenoeg Formation.....	92
5.7 The Makwassie Formation.....	96
5.8 The Garfield Member and interbedded mafic lava in the Makwassie Formation..	99
5.9 Discussion.....	101
 6. THE STRATIGRAPHY, PETROGRAPHY AND GEOCHEMISTRY OF THE GOEDGE- NOEG AND MAKWASSIE FORMATIONS OUTSIDE THE BOTHAVILLE AREA.....	 103
6.1 Introduction.....	103
6.2 The Makwassie Hills outcrop.....	104
6.2.1 Quartz-feldspar porphyry.....	105
6.2.2 Feldspar porphyry.....	106

6.2.3 Borehole LLE1.....	108
6.2.3.1 The Goedgenoeg Formation.....	109
6.2.3.2 The Makwassie Formation.....	109
6.2.3.3 The Garfield Member and interbedded mafic unit.....	109
6.2.3.4 Discussion.....	109
6.3 Suboutcrop in the Kimberley Mines.....	111
6.3.1 Stratigraphy.....	112
6.3.2 Detail of the examined ash-flow units.....	113
6.3.3 Geochemical composition.....	117
6.3.4 Discussion.....	117
6.3.5 Note on the Ritchie Formation.....	119
6.4 Outcrop on Vaal Koppies 8, between Welkom and Bultfontein.....	120
6.5 Outcrops on Sweet Home 280 and Wildebeestfontein 471, between Bultfontein and Dealesville.....	120
6.6 Outcrops on Honiglaagte 124, Honigkop 1002 and Goudkop 1496, north of Boshoff.....	120
6.7 The Vryburg area.....	121
6.7.1 Outcrop on Vaarwel 683 and Schatkist 716.....	121
6.7.2 Kareefontein Formation, northwest of Vryburg.....	121
6.7.3 Geochemical composition.....	123
6.8 The T'Kuip Quartz Porphyry Formation, Sodium Group.....	125
6.9 The Ritchie Formation.....	126
6.10 The Hereford Formation.....	126
6.11 Outcrop to the southwest of Warrenton.....	127
6.12 The Phokwane Formation of the Hartswater Group near Taung.....	127
6.13 The Paardefontein Formation of the Amalia Group.....	127
6.14 Outcrops at Klerkskraal Townlands, the Buffelsfontein Graben and at Platberg	128
6.15 Outcrops at the Vredefort Dome.....	128
6.16 Outcrops at the Johannesburg Dome.....	128
6.17 Outcrops in southeastern Botswana and north of Mafikeng, North Cape.....	128
6.18 The Witfonteinrand Formation of the Buffelsfontein Group, Thabazimbi.....	129
6.19 Summary.....	129
 7. PETROGENESIS OF THE GOEDGENOEG AND MAKWASSIE FORMATIONS	131
7.1 Introduction.....	131
7.2 Emplacement.....	131
7.2.1 Intrusive vs. extrusive origin.....	131
7.2.2 Eruption style.....	135
7.2.3 Eruption source.....	135

7.2.4 Eruption and magma volumes.....	137
7.2.5 Lack of interbedded sedimentary rocks.....	137
7.3 Tectonic setting.....	138
7.3.1 The Witwatersrand Supergroup.....	138
7.3.2 The Ventersdorp Supergroup.....	139
7.3.3 Geochemical classification.....	145
7.4 Petrogenesis.....	147
7.4.1 Introduction.....	147
7.4.2 Note on the chemical analysis of porphyritic rocks.....	147
7.4.3 Previous genetic models.....	148
7.4.4 Genetic modelling.....	149
 8. SUMMARY.....	 155
8.1 Lithostratigraphy.....	155
8.2 Geochemical composition.....	157
8.3 Distribution.....	158
8.4 Genesis	161
8.5 Stratigraphic recognition.....	162
8.6 Potential for economic mineral deposits.....	163
8.7 Recommendations.....	164
 ACKNOWLEDGEMENTS.....	 166
 REFERENCES.....	 167
 APPENDIX A.....	 184
APPENDIX B.....	227
APPENDIX C.....	239
APPENDIX D.....	244
APPENDIX E.....	322
APPENDIX F.....	324

LIST OF FIGURES

Figure 1.1: The lithostratigraphy and tectonic evolution of the Ventersdorp Supergroup	4
Figure 1.1: The distribution of the Ventersdorp Supergroup	9
Figure 2.1: The lithostratigraphy of the Makwassie and Rietgat Fm. stratotypes	18
Figure 2.2: The distribution of the Makwassie Fm.	20
Figure 3.1: Map of the Bothaville area	24
Figure 3.2: The general stratigraphy of the Goedgenoeg and Makwassie Fms.	25
Figure 3.3: Highly epidotized quartz-feldspar porphyry	27
Figure 3.4: Irregular alteration of the Makwassie Fm. quartz-feldspar porphyry	28
Figure 3.5: Colour-banded texture of the Makwassie Fm. quartz-feldspar porphyry	28
Figure 3.6: Typical Makwassie Fm. quartz-feldspar porphyry in borehole core	29
Figure 3.7: Quartz-feldspar porphyry with chloritic laminae	30
Figure 3.8: Rounded, embayed and fractured quartz phenocrysts	31
Figure 3.9: An altered plagioclase phenocryst	32
Figure 3.10: Complex skeletal feldspar phenocryst	33
Figure 3.11: An aggregate of euhedral apatite, spinel, sphene and zircon crystals...	34
Figure 3.12: A quench-textured apatite crystal	34
Figure 3.13: Felsitic texture of the quartz-feldspar porphyry matrix	35
Figure 3.14: Goedgenoeg Fm. feldspar porphyry	36
Figure 3.15a: Unwelded glass-shard textures in a tuffaceous sedimentary bed	39
Figure 3.15b: View of fig. 3.23a under crossed nicols	39
Figure 3.16a: Partially-welded glass textures in a tuffaceous bed	40
Figure 3.16b: View of fig. 3.24a under crossed nicols	40
Figure 3.17: Generalized flow unit of the quartz-feldspar porphyry	41
Figure 3.18: Non-porphyritic inclusion, hosted in quartz-feldspar porphyry	43
Figure 3.19: Parallel, elongated amygdales in the top zone of a subunit	43
Figure 3.20: Idealized sections of the three main types of pyroclastic flow deposits	45
Figure 3.21: Gas vesicles that coalesced, flattened against, and flowed around...	46
Figure 3.22: Growth habit variation of plagioclase	48
Figure 3.23: Protuberances on a growing crystal projecting into more undercooled liquid	49
Figure 3.24: Perlitic-crack textures in devitrified glass...	50
Figure 3.25: The influence of temperature on nucleation rate, crystal growth rate...	51
Figure 4.1: Collar positions of the boreholes in the Bothaville area...	55
Figure 4.2: Isopach map of the combined total thickness of the Goedg. and Makw. Fms.	56
Figure 4.3: Isopach map of the Goedgenoeg Fm.	56
Figure 4.4: Isopach map of the Makwassie Fm.	57
Figure 4.5: Confirmed occurrence and thickness of the Garfield Member	57
Figure 4.6: Subtopography of the basal contact of the Goedgenoeg Fm.	59

Figure 4.7: Subtopography of the top of the Goedgenoeg Fm.	60
Figure 4.8: Subtopography of the top of the Makwassie Fm.	60
Figure 4.9: Correlation diagrams of the Ventersdorp Supergroup Fms. between boreholes	64
Figure 4.10: Structural control during deposition of the Goedgenoeg and Makwassie Fms.	78
Figure 5.1: Harker diagrams of 319 samples from the Goedgenoeg and Makwassie Fms...	83
Figure 5.2: Selected histograms of the element distribution in the Goedg. and Makw. Fms.	86
Figure 5.3: Alumina saturation of the Goedg. and Makw. Fms. in the Bothaville area	88
Figure 5.4: Subalkaline classification of the Goedgenoeg and Makwassie Fm. samples	88
Figure 5.5a: Classification of the Goedg. and Makw. Fm. samples as calc-alkaline	89
Figure 5.5b: Classification of the Goedg. and Makw. Fm. samples as calc-alkaline	89
Figure 5.6: Classification of the Goedg. and Makw. Fms. samples on a Jensen diagram	90
Figure 5.7: The Goedg. and Makw. Fms. samples classify as oversaturated...	90
Figure 5.8: The volcanic rocks of the Goedg. and Makw. Fms. are mostly high in potassium	91
Figure 5.9a: Classification of the volcanics as high andesites, dacites and rhyodacites	91
Figure 5.9b: Classification of the Goedgenoeg and Makwassie Fm. volcanics	91
Figure 5.10: Selected Harker diagrams of the Goedgenoeg Fm. in the Bothaville area	93
Figure 5.11: Selected Harker diagrams of the geochemical facies of the Makw. Fm.	98
Figure 5.12: Selected Harker diagrams of the Garfield Member and interbedded mafic lavas	100
Figure 5.13: Scattergram of P/Cr vs Zr/Cr ...	102
Figure 6.1: Outcrops of the Makw. and Goedg. Fms. in the Ventersdorp S.group depository	103
Figure 6.2: Red-coloured quartz-feldspar porphyry of the Makwassie Fm. near Witpoort	105
Figure 6.3: Clastic beds with contorted bedding, Makw. Fm. on Bezuidenhoutskraal 64	106
Figure 6.4: Makwassie Fm. quartz-feldspar porphyry breccia near Wolmaransstad	107
Figure 6.5: Litho- and chemostratigraphy of borehole LLE1	108
Figure 6.6: P_2O_5/Cr vs Zr/Cr plot of borehole LLE1's samples	110
Figure 6.7: Stratigraphic section of the Kimberley Mines	112
Figure 6.8: Litho- and chemostratigraphy of the Goedg. and Makw. Fms. in Wesselton Mine	113
Figure 6.9: Upper Makwassie ash-flow unit (760 - 820 m) in Wesselton Mine	114
Figure 6.10: Contorted lamination and tight flow-folds in the porphyry	115
Figure 6.11: Contorted lamination in the basal part of the 760 - 820 m flow-unit	115
Figure 6.12: The dark-coloured 820 m flow-unit with abundant inclusions	116
Figure 6.13: Part of the 820 m flow-unit	117
Figure 6.14: P_2O_5/Cr vs Zr/Cr plot of porphyry samples from Wesselton Mine	118
Figure 6.15: Silicification front, visible as a purplish-coloured band	122
Figure 6.16: Detail of the silicification front in Fig. 6.15	123
Figure 6.17: P_2O_5/Cr - Zr/Cr plot of porphyry samples from the Vryburg area	124
Figure 6.18: P_2O_5/Cr - Zr/Cr plot of T'Kuip Fm. samples	126
Figure 7.1: A simplified and idealized east-west cross section	143
Figure 7.2: Individual rift zones in the Platberg multiple rift system	144
Figure 7.3: Within plate (WPG) classification of the Goedgenoeg and Makwassie Fms.	146

Figure 7.4: (RRG+CEUG) classification of the Goedgenoeg and Makwassie Formations	146
Figure 7.5: Classification of the geochemical facies of the Goedg. and Makw. Fms.	147
Figure 7.7: Spidergram of Primitive Chondrite normalised data...	153
Figure 7.8: Fractionation of Alberton as source magma in terms of 10% intervals	154
Figure 7.9: Possible fractionation trends for the Gm facies	154
Figure 7.10: Fractionation of Gm as source magma in terms of 10% intervals	153

LIST OF TABLES

TABLE 1.1: Rb-Sr, Pb-Pb and U-Pb ages for the Ventersdorp Supergroup	6
TABLE 2.1: Average of 3 geochemical analyses of the Makwassie quartz porphyry	15
TABLE 5.1: Sample groups for 447 samples of the Goedg. and Makw. Fms.	79
TABLE 5.2: The geochemical compositions of the Goedg. and Makw. Fms.	82
TABLE 5.3: The geochemical composition of the individual geochemical facies...	94
TABLE 5.4: The projected intersections of the geochemical facies of the Goedg. Fm...	95
TABLE 5.5: The depths at which the geochemical facies of the Makw. Fm. were intersected...	97
TABLE 5.6: The geochemical composition of the geochemical facies of the Makw. Fm.	97
TABLE 5.7: The geochemical compositions of the Garfield Member and interbedded mafic...	99
TABLE 6.1: Average geochemical compositions of Goedg. and Makw. Fm. in borehole LLE1	111
TABLE 6.2: Average geochemical compositions of the flow-units in Wesseltown Mine	118
TABLE 6.3: Average geochemical compositions of samples from the Vryburg area	124
TABLE 6.4: Comparison between the interpreted mode of deposition	130
TABLE 7.1: Possible high-temperature rhyolitic ash-flow tuff localities	133
TABLE 7.2: Criteria for distinction between ash-flows, rhyolite lavas and high-T ash-flows	134
TABLE 7.3: Examples of ash-flow tuff deposits with high phenocryst content	134
TABLE 7.4: Volume calculations for the Goedg. and Makwassie Fm. volcanics	137
TABLE 7.5: Data depicting the mixing of 18.23% Gm and 81.77% Gz to produce Gi	152
TABEL 7.6: Data depicting the mixing of Gi and Mr to produce Gs and Md	152
TABLE 8.1: Macroscopic lithological characteristics of the 3 main rock types of the Makw...	157
TABLE 8.2: The average compositions of the geochemical facies of the Goedg. and Makw...	159

1. INTRODUCTION

1.1 REVIEW OF THE VENTERSDORP SUPERGROUP

1.1.1 General Background

The Ventersdorp Supergroup represents a late Archaean volcano-sedimentary supracrustal sequence on the Kaapvaal Craton. Subsequent to the stabilization of the Kaapvaal Craton between 3.2 and 3 Ga (Anhaeusser, 1973; Hunter and Pretorius, 1981), four epicratonic basins developed on the craton between 3 and 2.1 Ga, namely the Pongola, Witwatersrand, Ventersdorp and Transvaal Basins (Hunter and Pretorius, 1981). Of these, the Ventersdorp Supergroup exemplifies the largest and most widespread volcanic sequence. The combined thickness of maximum intersections of the Ventersdorp Supergroup is 8 000 m and it extends over a roughly elliptical area with dimensions of 750 km by 350 km (Winter, 1976).

Knowledge of this largely volcanic succession is important as an aid in exploration for extensions of Witwatersrand Supergroup gold deposits outside the known Witwatersrand Basin. The Ventersdorp Supergroup largely suboutcrops in the Witwatersrand Basin and numerous exploration boreholes therefore have penetrated the Ventersdorp succession. Access to this borehole data is restricted due to its confidential nature and, as a result, research on the Ventersdorp Supergroup has been limited and many aspects still have to be clarified.

During the seventies and eighties, much attention was given to the lithostratigraphy and geochemistry of the Klipriviersberg Group (Wyatt, 1976; M.P. Bowen, 1984; T.B. Bowen, 1984; Schweitzer and Kröner, 1985; Crow and Condie, 1988; R.E. Myers *et al.*, 1990; Winter, 1995). The lithostratigraphy, petrography and geochemistry of the Platberg Group, however, received little attention and the lithostratigraphy of the Makwassie Formation is still based on mesoscopic descriptions of borehole core (Winter, 1976).

1.1.2 History

The first mention of rocks that are today regarded as part of the Ventersdorp Supergroup, is found in a report by Wyley (1859) on a journey into the interior from 1857 to 1858. Since then, numerous publications on rocks that are now classified as belonging to the Ventersdorp Supergroup have been printed. A comprehensive bibliography of early literature on the Ventersdorp System, other

pre-Bushveld extrusives and associated sedimentary rocks was compiled by Simpson (1964). Haughton (1969) compiled a literature review of the geology of South Africa, including the Ventersdorp Supergroup. An exhaustive historical assessment of the investigation of the Witwatersrand triad lavas can be found in an unpublished thesis by T.B. Bowen (1984). (The Witwatersrand triad lavas comprise extrusives of the Dominion Group, Witwatersrand Supergroup and Ventersdorp Supergroup). A paper by Van der Westhuizen *et al.* (1991) presents an overview of the Ventersdorp Supergroup and also contains a thorough bibliography of literature on the Supergroup.

1.1.3 Distribution

The Ventersdorp rocks extend for about 750 km from Soudia in the Northern Cape Province (Grobler and Emslie, 1975-76) to Derdepoort in the North West Province (Tyler, 1979a). This roughly elliptical area is in excess of 200 000 km² (Fig. 1.2), encompassing most of the distribution of the Dominion, West Rand and Central Rand Groups (Tankard *et al.*, 1982). The Ventersdorp sequence is best exposed in the southern and western regions of the North West Province and the northern region of the Northern Cape Province. Determination of the true extent of the Ventersdorp Supergroup is hampered by poor exposure; it is extensively covered by especially the Transvaal and Karoo Supergroups. Denudation prior to the deposition of the above mentioned overlying formations may also have had an influence on the present distribution of the Ventersdorp Supergroup, especially since the Karoo Supergroup is only of Phanerozoic age while the Ventersdorp Supergroup is of Late Archaean age.

The Klipriviersberg Group is confined to the northern and northwestern regions of the Ventersdorp Supergroup depository and has an average thickness of between 1 500 m and 2 000 m (R.E. Myers *et al.*, 1990). The Platberg Group is mostly absent from the northeastern region of the Ventersdorp depository and outcrops inconsistently over the rest of the area, where large thickness variations occur. The succession between Welkom and Klerksdorp is described by Winter (1976) and in the Klerksdorp area by Myers (1990). Recent drilling in the vicinity of Witpoort near Leeudoringstad revealed a Platberg thickness in excess of 3 600 m (Borehole LLE1, this study), with no evidence of duplication.

The southern and western regions of the Ventersdorp depository are composed of Platberg and Pniel Group rocks. These are the Soudia, Zoetlief, Amalia, and Hartswater Groups, also the Ritchie, Hereford, Bosch Kop, and Zeekoebaart Formations (SACS, 1980).

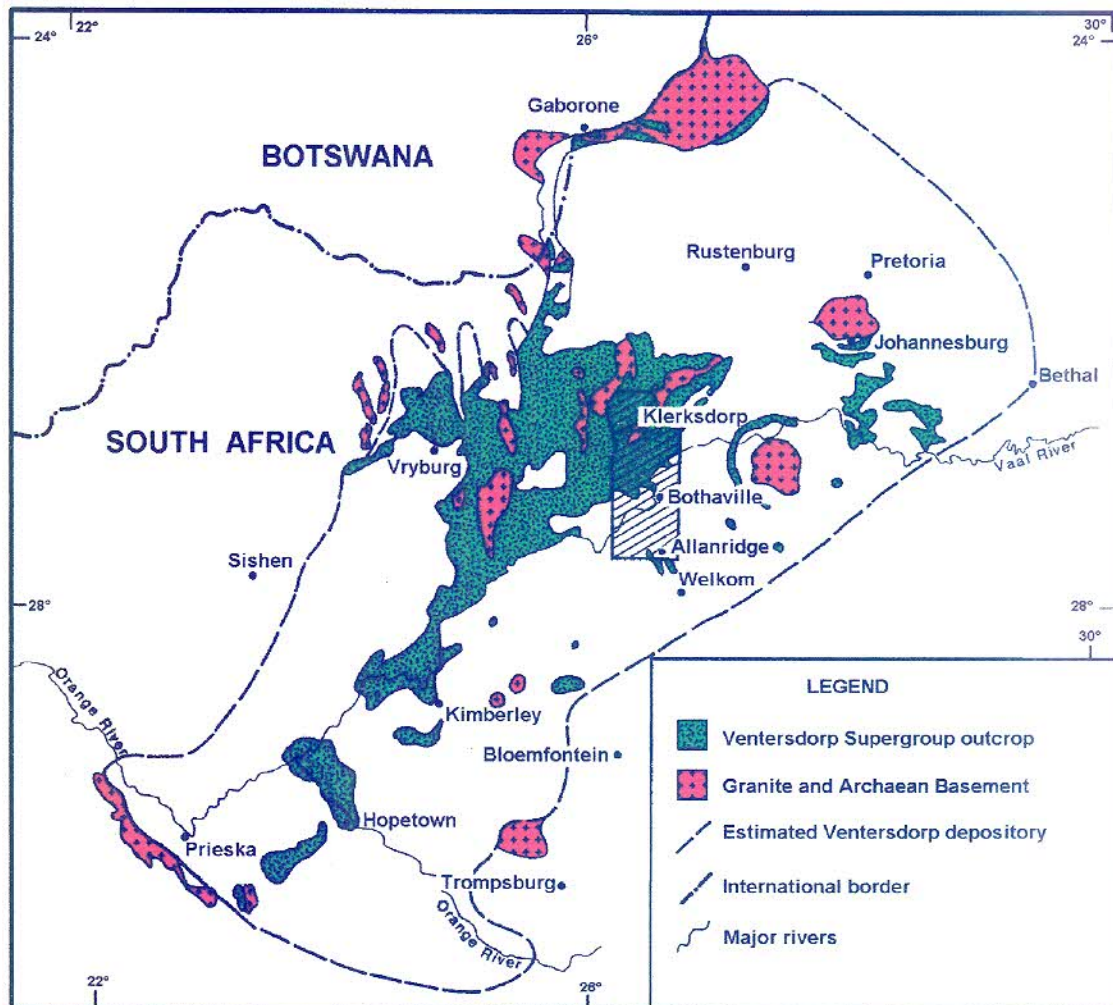


FIGURE 1.1: The distribution of the Ventersdorp Supergroup. The main study area, designated the Bothaville area, is indicated by hatching.

(NOTE: Although the “Pniel Group”, as termed by Winter (1976) and being composed of the Bothaville and Allanridge Formations, is not acknowledged by SACS (1980), the term has become widely accepted and will be used in this thesis to describe the upper volcanic-sedimentary succession of the Ventersdorp Supergroup).

The arenaceous sedimentary rocks of the Bothaville Formation are more mature than the other Ventersdorp sediments. It tends to have a regional distribution, whereas the Platberg sedimentary rocks have a localized setting. Allanridge Formation lavas cover the underlying rocks over large areas in the Northern Cape, North West and Free State Provinces, and the lavas are in turn extensively covered by Phanerozoic rocks of the Karoo Supergroup.

1.1.4 Stratigraphy

The Ventersdorp Supergroup is positioned between the underlying Witwatersrand Supergroup and the overlying Transvaal Supergroup. An angular unconformity separates the Ventersdorp and Witwatersrand rocks in the western region of the Witwatersrand Basin (Tankard *et al.*, 1982), but these successions are apparently conformable in the Central Rand, East Rand, Heidelberg and Welkom areas (Nel and Jansen, 1957; Coetzee, 1960; Tankard *et al.*, 1982). Where the lower volcanics are absent, younger Ventersdorp formations onlap pre-Ventersdorp rocks (Winter, 1976).

The stratigraphic subdivision of the Ventersdorp succession remained uncertain until sufficient data became available through exploration boreholes. The low relief, poor exposure, low dip, repeated rock types and alteration of the rocks hampered the stratigraphic efforts of earlier workers like Nel (1935), Beetz (1936), Jacobsen (1940; 1943), Matthysen (1953), Pienaar (1956) and Coetzee (1960). Through information obtained from 200 exploration boreholes between the Klerksdorp and Free State goldfields, Winter (1965) modified previous stratigraphic subdivisions by Matthysen (1953) and Pienaar (1956), thereby presenting a new stratigraphic subdivision for the Ventersdorp Supergroup in 1976 (Winter, 1976), which is still in use at present.

The Ventersdorp Supergroup is subdivided into a lower, middle and upper succession, viz the basal Klipriviersberg Group (mafic volcanics), Platberg Group (rudites, mafic, intermediate and felsic volcanics) and the upper Pniel Group (arenites and mafic volcanics). Pronounced unconformities separate the 3 subdivisions. The lithostratigraphy of the Ventersdorp Supergroup is summarized on Figure 1.2.

The Pniel Group is composed of the Bothaville and Allanridge Formations with no common lithology between the two Formations (Winter, 1976). Even though there is structural concordance between the two formations, the age concordance between the Pniel Group and Platberg Group is still uncertain. The unconformity at the base of Pniel is proposed as the Archaean-Proterozoic boundary in the Kaapvaal Province by Cheney *et al.* (1990).

It must be stressed that Winter's lithostratigraphic subdivision of the Ventersdorp Supergroup is based on lithological criteria; petrographic and geochemical characteristics were not incorporated. The type area of the Ventersdorp Supergroup (Winter, 1976) centers around Bothaville, between the Klerksdorp and Free State Goldfields. Significant outcrops of the Ventersdorp

GROUP	FORMATION	VOLCANIC ROCKS				SEDIMENTARY ROCKS		TECTONICS		
		FELSIC	INTERME - DIATE	MAFIC	PYRO - CLASTIC	RUDITES	ARENITES	TOPO - GRAPHY	GRA - BENS	MAJOR UNCON - FORMITY
PNIEL	ALLANRIDGE									
	BOTHAVILLE									
PLATBERG	RIETGAT									
	MAKWASSIE									
	GOEDGENOEG									
	KAMEELDOORNS									
KLIPRIVERS - BERG	EDENVILLE									
	LORAINE									
	JEANNETTE									
	ORKNEY									
	ALBERTON									
	WESTONARIA									

FIGURE 1.2: The lithostratigraphy and tectonic evolution of the Ventersdorp Supergroup (after Winter, 1976; modified after Grobler *et al.*, 1989).

Supergroup are absent in this area, but complete stratigraphic intersections were obtained from boreholes drilled in the area. As exploration efforts were extended to areas outside the Central Rand Basin, a more complete picture of the stratigraphic variation and deviation from the type area became apparent. Modifications of the standard stratigraphic subdivision (SACS, 1980) are therefore envisaged.

The geochemical stratigraphy of Ventersdorp volcanics has become increasingly useful as an aid in exploration. Geochemical profiles for the Klipriviersberg volcanics have been published by R.E. Myers *et al.* (1990). Linton *et al.* (1990) have demonstrated that formational recognition in the Klipriviersberg Group based solely on lithological characteristics is inadequate, but can be enhanced by the use of geochemistry.

1.1.5 Geochronology

The Witwatersrand Supergroup is difficult to date by any direct means (Armstrong *et al.*, 1986), but by dating the Ventersdorp Supergroup a minimum age can be obtained for the former. Numerous age determinations have been made on Ventersdorp Supergroup rocks, as summarized in Table 1.1. The most recent age determination, based on single zircon analyses, indicated an age of 2714 ± 8 Ma for the Klipriviersberg lavas and 2708 ± 5 Ma for the Makwassie quartz-feldspar porphyry (Armstrong *et al.*, 1992).

TABLE 1.1: Rb-Sr, Pb-Pb and U-Pb ages for the Ventersdorp Supergroup.

ROCK UNIT	AGE	REFERENCE
Acid lava, Zoetlief Formation	2310 ± 50	Burger and Coertze, 1973/4
Makwassie quartz porphyry	2142 ± 213	Armstrong <i>et al.</i> , 1986
Plantation Porphyry, Botswana	2154 ± 210	Harding <i>et al.</i> , 1974
Derdepoort Acid Volcanics	2150	Crampton, 1973
T'Kuip Quartz Porphyry Formation	1920 ± 100	Cornell, 1978
Makwassie quartz porphyry	$2286 + 40 / - 41$	Van Niekerk and Burger, 1964
Makwassie quartz porphyry	$2351 + 411 / - 576$	Armstrong <i>et al.</i> , 1986
Klipriviersberg	2370 ± 70	Armstrong <i>et al.</i> , 1986
Makwassie quartz porphyry	2238 ± 110	Burger and Coertze, 1973/4
Makwassie quartz porphyry	2245 ± 90	Burger and Coertze, 1973/4
Ritchie Formation quartz porphyry	2602 ± 8	Van Niekerk and Burger, 1978
Makwassie quartz porphyry	2699 ± 50	Retief, In: Walraven <i>et al.</i> , 1990
Makwassie quartz porphyry	2708 ± 5	Armstrong <i>et al.</i> , 1992
Klipriviersberg	2714 ± 8	Armstrong <i>et al.</i> , 1992

1.1.6 Geochemistry

The Ventersdorp volcanics are extensively altered and mobile element concentrations are adversely affected (SiO_2 , K_2O , Na_2O and CaO). It is widely accepted that the Ventersdorp Supergroup was altered by greenschist facies metamorphism (Cornell, 1978; Tyler, 1979a; Schweitzer and Kröner, 1985; Crow and Condie, 1988; Grobler *et al.*, 1989).

The Ventersdorp Supergroup volcanics have been described as a weakly bimodal, tholeiitic, basic-acid volcanic suite of subalkaline, tholeiitic character (T.B. Bowen *et al.*, 1986). Schweitzer and Kröner (1985) portrayed the volcanics as bimodal alkali-rich, tholeiitic basaltic andesites, andesites and rhyolites with a slight alkaline affinity. Crow and Condie (1988) stated that the Edenville and Loraine Formations (Klipriviersberg Group) fall in the calc-alkaline field while samples from more evolved units (mostly Platberg and Pniel samples) plot in the tholeiitic field. They concluded that the Ventersdorp volcanics are tholeiitic with a mild calc-alkaline affinity, especially in the more mafic samples.

Komatiitic affinities have been recognized at the base of the Klipriviersberg Group (Meredale Member; Wyatt, 1976; McIver *et al.*, 1982) and at the base of the Allanridge Formation (Grobler *et al.*, 1986; Van der Westhuizen *et al.*, in prep.).

Geochemical stratigraphy has become increasingly useful as an aid in exploration. Studies by M.P. Bowen (1984) and T.B. Bowen (1984) on the Witwatersrand triad volcanics indicated a clear geochemical stratigraphy in the Ventersdorp Supergroup volcanics. A discrimination diagram (involving Ti, P and Zr) was devised to distinguish between the Witwatersrand triad volcanics.

Klipriviersberg geochemical stratigraphy was first reported by Wyatt (1976) and later by Palmer *et al.* (1986). R.E. Myers *et al.* (1990) presented geochemical stratigraphic profiles for the Klipriviersberg lavas in different localities in the Klipriviersberg depository.

1.1.7 Tectonic Setting

The diverse nature of the opinions advanced by different authors illustrate the complexity of the tectonism associated with the Ventersdorp Supergroup. There is consequently still controversy as to the tectonic setting for the Ventersdorp Supergroup. Burke *et al.* (1985) see the Ventersdorp Supergroup as a rift system which is related to collision between the Kaapvaal and Zimbabwe

cratons. Winter (1986; 1987) describes the Ventersdorp as a cratonic foreland in a back-arc plate tectonic setting, while Clendenin *et al.* (1988a) relates it to roll-back of a subducted slab following collision, with resulting intraplate deformation. Clendenin *et al.* (1988b) further view the Ventersdorp as part of a fully evolved rift system, with the Klipriviersberg volcanics part of a pre-graben stage whilst the Platberg - Pniel represents the graben stage.

Roering *et al.* (1990) perceive a single pre- to syn-Klipriviersberg contractional deformational event, during which folding and thrusting prevailed which influenced upper Witwatersrand sedimentation along the western margin of the Witwatersrand Basin. Middle-Ventersdorp (Platberg) times experienced extensional tectonics, while pre-late Ventersdorp (Pniel) times experienced thrust faulting.

Hartnady and Stowe (1991) relate extensional deformation during the Platberg era to retro-arc tectonics behind an active Andean-type continental margin along the northwestern leading edge of the combined Kaapvaal - Zimbabwe continental plate.

1.2 AIM OF THE STUDY

The aim of the study was to define stratigraphic and geochemical variation of the Makwassie Formation in the Bothaville area and compare it with Makwassie Formation occurrences in the rest of the Ventersdorp depository. During exploration programmes some boreholes intersected unusually thick successions of Makwassie Formation, while other boreholes encountered facies unfamiliar to the Makwassie Formation. The question arose as to whether these boreholes may have penetrated volcanic feeder dikes or very thick sills, in which case the timeous cessation of the boreholes will save costs. The Makwassie Formation porphyries may represent high-temperature ash-flow deposits (Winter, 1976; Van der Westhuizen *et al.*, 1988; Twist *et al.*, 1989), or in some cases, shallow subvolcanic intrusives (Jacobsen, 1943).

A stratigraphic description and study of the lithological and geochemical variation of the Makwassie Formation would therefore be beneficial to exploration, especially if a technique could be devised to differentiate between various facies of the Makwassie Formation.

1.3 THE STUDY AREA

The Makwassie Formation was studied in detail in the Bothaville area, designated as the area between Allanridge and Klerksdorp (Fig. 1.1), which largely coincides with the area on which Winter (1976) based his subdivision of the Ventersdorp Supergroup. It was subsequently compared with other occurrences as well.

The Makwassie Formation only suboutcrops in the Bothaville area and the use of borehole data is therefore imperative. Outcrops in the vicinity of Klerksdorp were not investigated during this study, as it was already being investigated by another researcher (Myers, 1990). The outcrop at Makwassie Hills near Wolmaransstad was, however, included in this study.

A limited number of Makwassie Formation outcrops and boreholes intersections outside the Bothaville area were also investigated. The specific localities of these occurrences are discussed in Chapter 6. The Makwassie Formation as exposed in the Wesselton Mine at Kimberley was also studied.

1.4 STUDY METHODS

Since a stratigraphic model for the Makwassie Formation does not exist, analysis of the lithogeochemistry would only be realistic after a proper basis for the stratigraphy had been established. Genetic modelling is a final stage in the investigation.

Research on the Bothaville area was conducted on borehole core supplied by Anglo American Corporation, which included some of the boreholes that were used by Winter (1965; 1976) in his study of the lithostratigraphy of the Ventersdorp Supergroup. Additional borehole information (borehole ST2) was made available by African Selection Trust. A total of $\pm 25\ 000$ m of Makwassie core, which represents Makwassie intersections of 23 boreholes in the Bothaville area and 3 boreholes outside this area, were logged on a scale of 1:200. The boreholes were sampled for petrographic and geochemical analyses. The draft logs were reduced to a scale of 1:2500 to enable representation (Appendix A).

Sampling for geochemical and petrographic studies was done on a controlled basis, with the aim of representing the complete Makwassie succession of each borehole. Zones with abnormal alteration or atypical rock types were avoided, except when the nature of the alteration or lithology was to be investigated. Sampling was done on the most homogeneous parts of recognized subunits.

Subunits in boreholes OT1, SYF1, WS3, WS4 and YYS1 were sampled in more detail to establish within-flow compositional variations. Nine hundred thin sections were petrographically investigated. Thin sections of samples selected for geochemical analyses were used to explain anomalous geochemical results.

Geochemical analyses of major and trace elements were conducted on 586 samples, of which 447 originated from the Makwassie Formation in boreholes in the Bothaville area and the remainder from localities outside this area. Data of an additional set of 63 samples, from previous research for Anglo American Prospecting Services, were also included in this study.

An initial non-genetic approach to the Makwassie Formation was attempted. Application of genetic terminology was a final step after lithological characteristics had been evaluated. Such a study would be of more value to future researchers on the same rocks since the non-genetic descriptions and terminology can easily be reinterpreted. Cas and Wright (1988; p349-350) stressed the need for a cautious approach to studies of ancient volcanic successions, as follows:

"It should always be clear that genetic terminology cannot always be immediately applied, especially to ancient volcanoclastic rocks, because of the problems caused by poor exposure, lack of exposure of contact relationships, weathering, alteration, metamorphism and deformation."

Cas and Wright (1988; p355) further stated that:

"The approach (to metamorphosed volcanoclastic rocks) therefore initially has to be more objective and less genetic, with the overall context, extent and characteristics of the lithological unit(s) having to be established."

Other factors which complicate the genetic interpretation and classification of lithified volcanoclastics include: devitrification, recrystallization, new mineral growth during diagenesis and low grade metamorphism, and deformation, all of which lead to modification of original textures and mineralogy to varying degrees. ...It is then a brave person who walks up to an outcrop and applies a genetic classification or terminology."

1.5 DEFINITION OF NOMENCLATURE

The **main study area** between Klerksdorp and Allanridge, and westwards to Witpoort is designated the **Bothaville area**.

Quartz porphyries of igneous origin always contain feldspar phenocrysts, but the term **quartz-feldspar porphyry** is preferred in this dissertation.

The terms **basic**, **mafic**, **felsic** and **acidic** will be used in the same context used by Cas and Wright (1988):

- Basic** - igneous rocks with low SiO₂ contents (<52% SiO₂)
- Mafic** - igneous rocks with high modal ferromagnesian mineral contents
- Acidic** - igneous rocks with high SiO₂ contents, also called silicic (>63% SiO₂)
- Felsic** - igneous rocks with high modal contents of light coloured minerals, such as quartz and feldspar

Although the feldspar porphyry succession which forms the lower part of the Makwassie Formation is unofficially known as the Goedgenoeg Formation, this is as yet an unofficial subdivision and will not be regarded as a separate formation. The Platberg Group subdivision as defined by SACS (1980) is accepted.

Volcanological terms and concepts (from Cas and Wright (1988), unless otherwise indicated):

Lava flows: The effusive eruption of magma as coherent lava. The exsolved volatile content of the magma chamber immediately before eruption, and of the magma during eruption, must be sufficiently low to prevent the build-up of gas pressure which could cause explosive fragmentation. Basic magmas, such as basalt, mostly erupt as lava flows.

Pahoehoe and aa lava flows: These Hawaiian names denote the end members of lava flows. Pahoehoe lavas are characterized by smooth, billowy and ropy surfaces, while aa lavas have exceedingly rough spinose and fragmented surfaces. **Block lavas** are less spinose, consisting of lava blocks with more regular fragments than aa lavas. Pahoehoe and aa lavas, with all transitional forms, may form in the same lava flow. The transition of pahoehoe to aa lava is regarded to be the result of viscosity increase caused by cooling, gas loss and greater crystallinity with time. A single lava flow may have pahoehoe at the base and aa at the top, e.g. lavas of the Roque Nublo Group, Gran Canaria.

Pyroclastic deposits: Pyroclastic deposits form directly from the fragmentation of magma and rock by explosive volcanic activity. These deposits are grouped into three generic types according to their mode of transport and deposition:

Pyroclastic fall deposits: Such a deposit forms through gravitational fall-back of lithics from an eruptive column after the material has been explosively ejected from a vent. The size of the lithic fall-back can range from ash (ash-fall) to blocks (ballistic clasts). Pyroclastic fall deposits form mantle bedding.

Pyroclastic flow deposits: These deposits are emplaced by surface flows of pyroclastic debris which travel as a high particle concentration gas-solid dispersion. These flows are hot and are controlled by gravity and topography, except for some high-velocity flows which may also show mantle bedding. Pyroclastic flow deposits may be termed **ash-flow deposits** if more than 50 volume percent of the deposit is of ash-size ($1/_{16}$ mm) or less (Fisher and Schmincke, 1984). The term **ignimbrite** is used in many different contexts in the literature, but will be used here in a lithological sense, referring to successive pyroclastic flow deposits which form a coherent succession, possibly through cooling of these flows as a single unit after rapid emplacement.

Pyroclastic surge deposits: These deposits originate through a pyroclastic flow of expanded, turbulent, low particle concentration gas-solid dispersion along the surface. Such deposits show unidirectional sedimentary bedforms such as low-angle cross stratification, climbing dune forms, and chute and swell structures. Pyroclastic surges differ from pyroclastic flows by being low particle flows, while the latter are high particle flows. The deposits of the two types of flows differ markedly.

Tuff: The lithified equivalent of an ash deposit, deposited through any pyroclastic process in which the grain size was less than 2 mm. With increasing proportions of lapilli (pyroclastic clasts between 4 and 64 mm) and blocks (clasts larger than 64 mm), the terms lapilli-tuff and block-tuff can be introduced. Similarly, terms such as ash-flow tuff, ash-fall tuff and pyroclastic-flow tuff can be used.

Spherulitic texture: Spherulites are spherulitic bodies in a rock, which are composed of an aggregate of fibrous crystals of one or more minerals radiating from a nucleus, with glass or other crystals in between (MacKenzie *et al.*, 1982).

Axiolitic texture: This texture is similar to spherulites, but differs in that radiating fibres extend from either end of a linear nucleus, rather than from a point (MacKenzie *et al.*, 1982).

Variolitic texture: This is a fan-like arrangement of diverging, often branching, fibres which form conical bundles of acicular crystals (MacKenzie *et al.*, 1982). This texture differs from spherulites in that no discrete spherical bodies are identifiable.

Amygdales: This term is commonly used for gas vesicles in ancient volcanic successions which have become filled with minerals. (Originally the term referred to the almond shape (L. *amygdala*; Gr. *amygdalé*) of the vesicles).

Facies: The term facies is used for distinctive intervals or associations of rock types that are distinguishable from other such associations and will therefore not denote lateral gradation of one rock type into another, as it is often used in sedimentology. Cas and Wright (1988) stated that this enables identifying, describing and interpreting distinctive intervals and/or associations of rock(s) which recur many times in a stratigraphic succession.

2. REVIEW OF THE GOEDGENOEG AND MAKWASSIE FORMATIONS

2.1 INTRODUCTION

The Makwassie Formation consists of quartz-feldspar porphyries, also *"quartz-free porphyritic and non-porphyritic volcanic rocks and minor bodies of sediments"* (Winter, 1976; p.42). The name Makwassie Formation was proposed by Winter (1965), after a town in the North West Province where a major outcrop of this formation occurs.

The formational status of the Goedgenoeg Formation was only recently approved (Meeting of the Ventersdorp Task Group, S.A.C.S., 1990). It is defined as the feldspar porphyry succession underlying the quartz-feldspar porphyries of the Makwassie Formation proper. Previously it formed part of the Makwassie Formation. As a result of this recent division, few references to the Goedgenoeg Formation are found in the literature and previous studies of the Makwassie volcanics included that of the Goedgenoeg Formation.

2.2 PREVIOUS DESCRIPTIONS

Numerous descriptions of quartz-porphyry occurrences appear in early publications on the Ventersdorp "System" and most of these quartz porphyries are currently correlated with the Makwassie Formation. Quartz porphyries of the Ventersdorp System at the Makwassie Hills and in the Kimberley mines were described by Hatch and Corstorphine (1905). They mentioned that these occurrences were also noted by Dahms (1891) and Hatch (1898; 1903).

Du Toit (1906) described the geology in the Vryburg and Mafikeng areas and named an assemblage of volcanics and sedimentary rocks the "Zoetlief Beds" (now correlated with the Platberg Group), which form part of the Ventersdorp System. The middlemost unit of this assemblage is composed of quartz porphyries. Du Toit (1907) also described quartz porphyries at the confluence of the Riet and Modder Rivers south of Kimberley (the Ritchie locality; Potgieter and Lock, 1978), and in the diamond mines at Kimberley which he correlated with the Zoetlief Beds at Vryburg. Du Toit (1907) mentioned that the Kimberley quartz porphyries *"... show the same corrosion of the quartz-phenocrysts, the pseudomorphs after enstatite, the alteration of the feldspar, and the extensive silicification of the whole rock ..."* as the Vryburg quartz porphyries. Du Toit (1907) further mentioned that some specimens from ± 420 m below surface in

the De Beers Mine and from ± 660 m below surface in the Kimberley Mine are "orthoclase-porphyrines", which possibly correlate with the Goedgenoeg Formation (this study).

Rogers and Du Toit (1909) described rocks of the northern Cape Colony and mentioned the Zoetlief, "Kuip" and the Pniel series. The present correlatives of these series are the Kameeldoorns, Makwassie, Rietgat, Bothaville and Allanridge Formations.

Williams' (1932) account of the geology in the Kimberley diamond mines is largely similar to that of Du Toit (1907). Williams, however, cited 3 chemical analyses of the quartz porphyry, which were probably the earliest analyses of the Makwassie quartz porphyries. The averages of Williams' quartz porphyry analyses are listed in Table 2.1. (Note that an analysis published by Horwood in 1911 was of the Klipriviersberg "amygdaloidal diabase").

TABLE 2.1: Average of 3 chemical analyses of the Makwassie quartz porphyry in the Kimberley diamond mines (Williams, 1932).

SiO ₂	65.21	MnO	0.13	CO ₂	3.21
Al ₂ O ₃	5.67	NiO	nil	P ₂ O ₅	0.29
Cr ₂ O ₃	-	CaO	6.66	H ₂ O ⁻	0.09
Fe ₂ O ₃	3.56	MgO	0.36	H ₂ O ⁺	2.18
FeO	5.41	K ₂ O	3.31		
TiO ₂	1.37	Na ₂ O	1.61		

Holmes (1907) described the geology of south-western Transvaal, including the quartz-feldspar porphyry outcrop at "Makuassiberg" close to the town of Makwassie. He mentioned that quartz porphyries in the centre of the "structure" appeared akin to granites. To the edges of the "structure", the quartz porphyry had characteristics corresponding to fine-grained felsite with smaller phenocrysts than in the central part. The weathered parts of the outcrop had a reddish colour. Holmes (1907) also mentioned a quartz porphyry outcrop at Kareelaagte to the west of Schweizer-Reneke, 32 km north of Mafikeng and also at Crocodile Pools *"in the extreme north-western part of Transvaal"*. Van Eeden (1946) later reported on the correlation of the quartz porphyries in the Schweizer-Reneke area and correlated part of the Zoetlief in this area with the Dominion Reef series at Ottosdal.

In his description of the geology of the Klerksdorp-Ventersdorp area, Nel (1935) described the quartz porphyry outcrops and their petrography in great detail. The geology of the Klerksdorp District was investigated by Beetz (1936), whose

account was based on outcrop and exploration boreholes. The large variation in thickness of the Ventersdorp succession led him to speculate on the role of faulting and tectonics in the area. He further postulated that the quartz porphyries are lava sheets rather than intrusive dykes.

Truter and Strauss (1942) reported on the pre-Transvaal rocks at "*Taungs*" in the North Cape and accounted for Pniel and Zoetlief rocks in the area, while Jacobsen (1943) gave a detailed account of the Platberg succession in the Buffelsdoorn area, Klerksdorp Townlands and inner area of Klerksdorp town.

The Ventersdorp System in the Taungs area was subdivided into the Zoetlief and Pniel Series by Matthysen (1953), while only the Pniel Series occur in the Christiana area. Matthysen further described the Ventersdorp System in the Free State and he subdivided the System into three Series, viz the Upper Ventersdorp or Pniel Series, the Middle Ventersdorp or Zoetlief Series and the Lower Ventersdorp or Klipriviersberg Amygdaloid Series.

Pienaar (1956) presented a detailed stratigraphic and preliminary structural study of the Ventersdorp rocks in the Free State Goldfield. He proposed a subdivision of the Ventersdorp System into the Lower Lava, Upper Sediments and Upper Lava. In a description of the geology of the Free State Goldfield, Coetzee (1960) gave only a brief description of the Upper Volcanic Stage of the Ventersdorp System, which is today correlated with the Makwassie, Rietgat, Bothaville and Allanridge Formations.

Quartz porphyries were also noted by Von Backström (1962) in the vicinity of Ottosdal, whilst Nel and Verster (1962) described it in boreholes between Bothaville and Vredefort. Subsequently the stratigraphy of the Ventersdorp System was finalised by Winter (1965; 1976) and since then the stratigraphic position and correlation of the Makwassie quartz porphyries are better understood.

Whiteside (1970) gave an account of the volcanic rocks of the Ventersdorp Supergroup and he also presented the stratigraphy of a number of boreholes from the Bothaville-Klerksdorp area. These boreholes intersected intermediate lavas underlying the quartz porphyries, which are now recognized as the Goedgenoeg Formation (this study).

During the period 1970-1980 a number of theses on the geology of the Northern Cape, North West and western Free State Provinces were produced at the University of the Free State. Quartz porphyry outcrops in these areas were described by Emslie (1972), Joubert (1973), Potgieter (1973), Potgieter (1974), Lemmer (1977), Liebenberg (1977), Kleynhans (1979) and Behounek (1980). This research resulted in a number of publications, *i.e.* Visser *et al.* (1975-76), Grobler and Emslie (1975-76), Potgieter and Visser (1976) and Potgieter and Lock (1978), wherein the quartz porphyry outcrops were described.

In the Lobatse and Ramotswa areas of south-eastern Botswana, quartz porphyries of the Plantation Porphyry were correlated with the Ventersdorp Supergroup (Crockett, 1971). Nearby quartz porphyries of the Tshwene-Tshwene, Seokangwana and Derdepoort belts in North West Province were also correlated with the Makwassie Formation (Tyler, 1979a), but those of the Buffalo Springs Group near Thabazimbi were assigned to the Wolkberg Group by Tyler (1979b).

M.P. Bowen (1984) and T.B. Bowen (1984) greatly contributed to the knowledge of the geochemistry and genesis of the Makwassie volcanics. They presented analyses of Makwassie samples from boreholes in the Bothaville area and devised geochemical discrimination diagrams to distinguish between the Witwatersrand triad lavas (M.P. Bowen, 1984; T.B. Bowen, 1984; M.P. Bowen *et al.*, 1986).

The eruptive style of the Platberg volcanics in the Hartbeesfontein Basin was discussed by Karpeta (1990). Quartz-feldspar porphyries are absent in this area, but feldspar porphyries of the Goedgenoeg Formation are present. The most recent research on the Platberg Group volcanics, with detail on the Goedgenoeg and Makwassie Formations, was completed by Myers (1990). This research was presented by Booth (1987), Myers *et al.* (1988) and J.M. Myers *et al.* (1990).

2.3 STRATIGRAPHY

The Makwassie Formation is represented by the type section of borehole DF1, south-west of Orkney (SACS, 1980). The lithostratigraphy of the Makwassie and Rietgat Formation stratotypes are depicted in Fig. 2.1. Winter (1976) stated that the Makwassie quartz-feldspar porphyries occur together with quartz-free porphyritic and non-porphyritic volcanic rocks and minor bodies of sediment (now part of the Goedgenoeg Formation). Winter (1976) commented that such a subdivision of the Makwassie Formation may be possible.

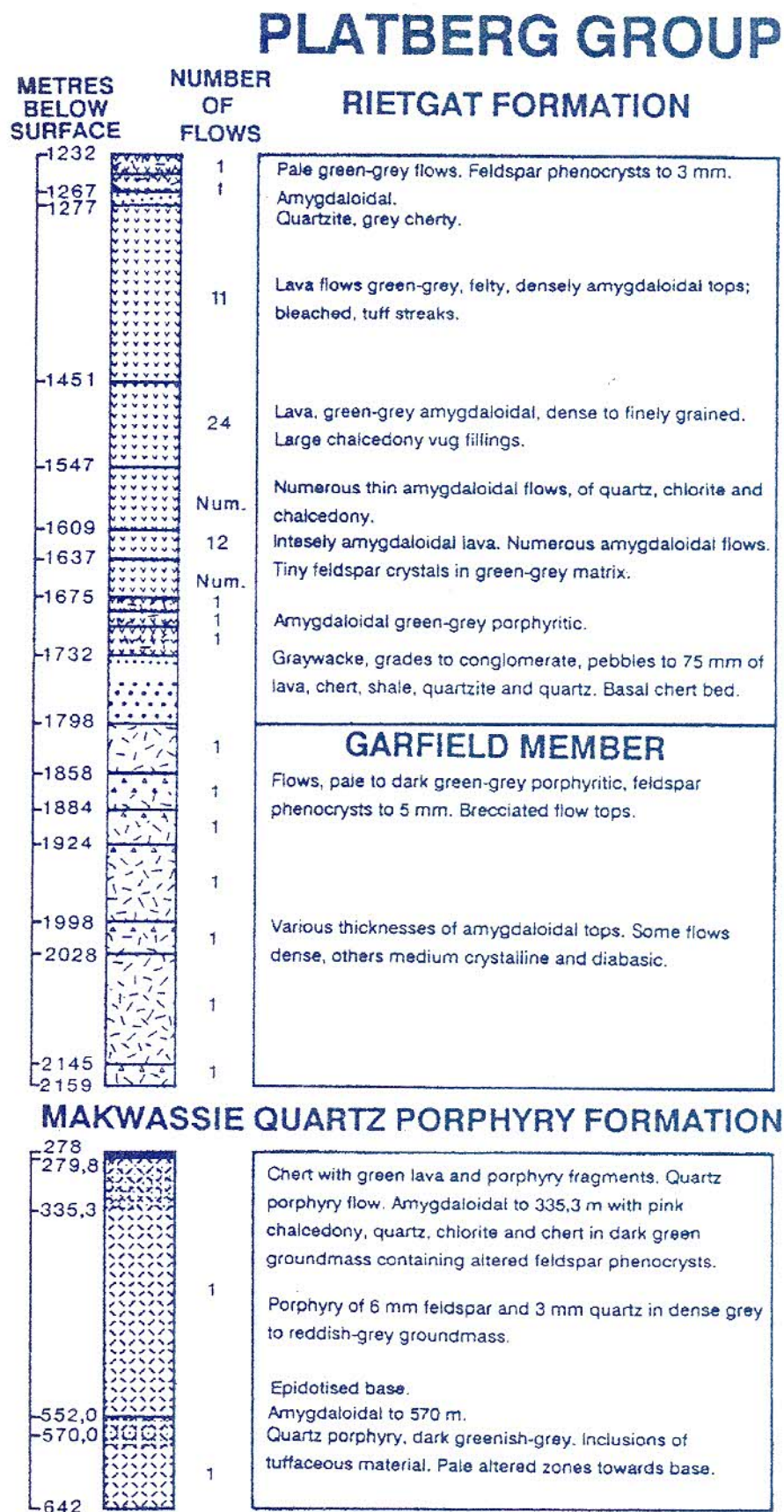


FIGURE 2.1: The lithostratigraphy of the Makwassie and Rietgat Formation stratotypes, according to Winter (1976).

The Garfield Member (type section borehole LL1, east of Bothaville; SACS, 1980) was identified as green-grey, porphyritic lavas which are distinguished from the Makwassie quartz-feldspar porphyries by their more mafic character. Winter (1976) states that the Garfield Member generally occurs within the lower portion of the Rietgat Formation, but it may "locally become a member of the Makwassie Formation", as in borehole KRF1. Elsewhere, it can contain minor intercalations of sediments and non-porphyritic lavas.

The Goedgenoeg Formation overlies the sedimentary Kameeldoorns Formation, or where it is absent, the Klipriviersberg Group or older units. The Goedgenoeg Formation is overlain by the Makwassie Formation. The Rietgat Formation covers the Makwassie porphyries over large areas, but where the Rietgat lavas are absent, the Bothaville Formation truncates the porphyries. (There is a major unconformity between the Platberg Group and Pniel Group; Winter, 1976).

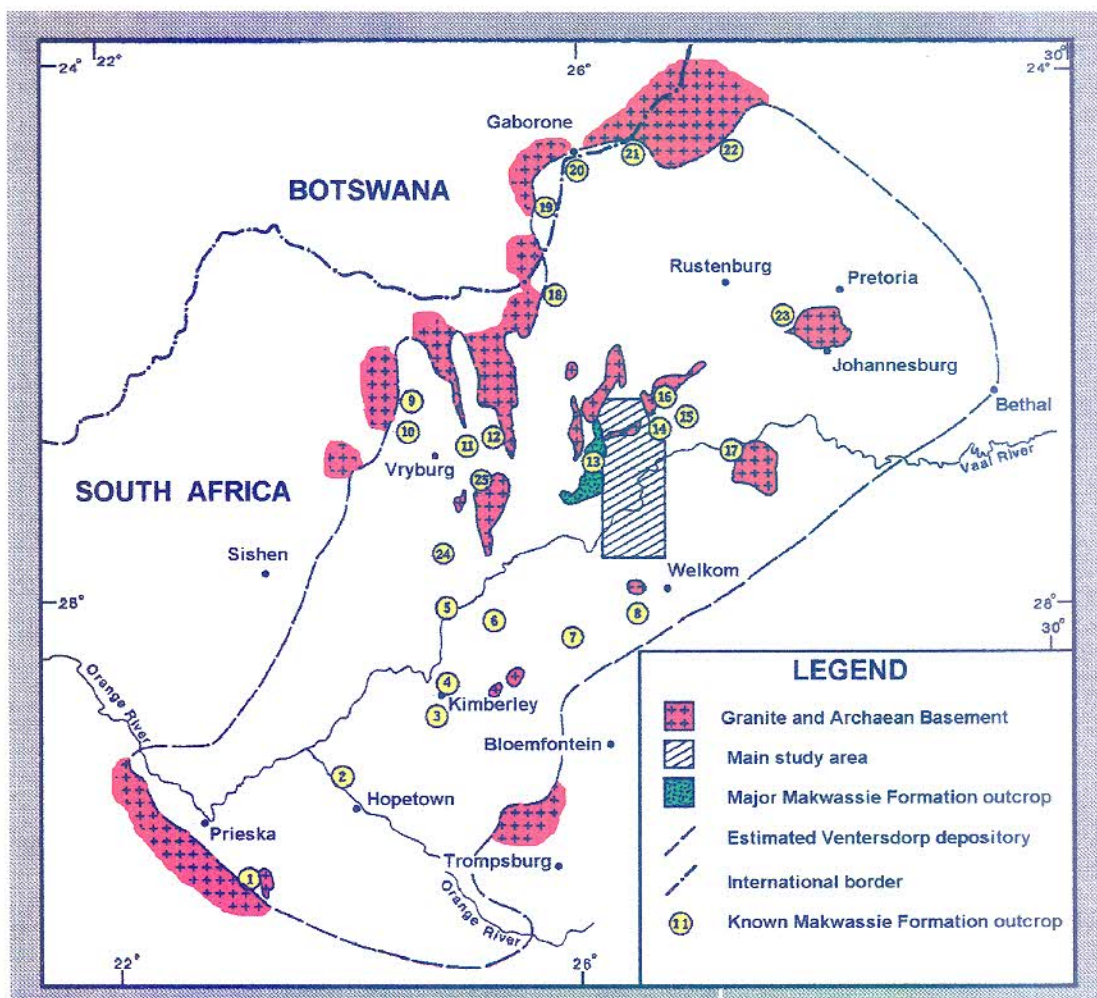
A succession of *"shales, tuffs, quartzites, conglomerates, andesitic lavas, pyroclastics and feldspar and quartz-feldspar porphyries"* that underlies the Klipriviersberg Group west and south-west of Klerksdorp, was described by Whiteside (1970) in collaboration with P.M. Strydom. They proposed the name Vaal Bend unit for this succession. The stratigraphic position of this unit was not clear (Winter, 1976; SACS, 1980). Further borehole information, however, indicate that the Vaal Bend unit is a basal member of the Goedgenoeg Formation and that the overlying 'Klipriviersberg Group' lavas are in fact intermediate and mafic lavas of the Goedgenoeg Formation (personal communication; P.M. Strydom, 1988).

2.4 DISTRIBUTION

The Goedgenoeg and Makwassie Formations occur inconsistently over almost the entire Ventersdorp depository and are largely restricted to suboutcrop only (Fig. 2.2). Outcrops are limited and the stratigraphy is poorly exposed, so that the true extent and full stratigraphy are only revealed by exploration boreholes. Outcrops of the Goedgenoeg Formation are even more limited and largely undocumented compared to the Makwassie Formation. Detailed accounts of particular Makwassie Formation occurrences as depicted in Fig. 2.2 are presented in Chapter 6.

FIGURE 2.2: The distribution of the Makwassie Formation (detailed accounts of occurrences are presented in Chapter 6). The numbers represent the following localities:

- 1 - T'Kuip Quartz Porphyry Formation, Sodium Group
- 2 - Hereford Formation
- 3 - Ritchie Quartz Porphyry Formation
- 4 - Suboutcrop in the Kimberley Mines
- 5 - Outcrop, southwest of Warrenton
- 6 - Outcrop north of Boshoff
- 7 - Outcrop between Bultfontein and Dealesville
- 8 - Outcrop between Welkom and Bultfontein
- 9 - Kareefontein Formation, Zoetlief Group
- 10 - Kareefontein Formation, Zoetlief Group
- 11 - Outcrop east of Vryburg
- 12 - Kareefontein Formation, Zoetlief Group
- 13 - Outcrop at Makwassie Hills
- 14 - Outcrop at Klerksdorp Townlands
- 15 - Outcrop and suboutcrop in the Buffelsfontein Graben
- 16 - Outcrop at Platberg
- 17 - Possible outcrop at the Vredefort Dome
- 18 - Outcrop north of Mafikeng
- 19 - Outcrop in south-eastern Botswana
- 20 - Outcrop in the Seokangwana Belt
- 21 - Outcrop in the Derdepoort Belt
- 22 - Witfontein Formation, Buffelsfontein Group (possibly Makwassie Formation correlative)
- 23 - Outcrop and suboutcrop at the Johannesburg Dome
- 24 - Phokwane Formation, Hartswater Group near Taung
- 25 - Paardefontein Quartz Porphyry Formation, Amalia Group



2.5 AGE

The most recent age determination is by Armstrong *et al.* (1992), who reported an age of 2708 ± 8 Ma on single zircons with U-Pb methods on an ion microprobe. Zircon xenocrysts in the Makwassie Formation are reported by Armstrong *et al.* (1992), which indicate that assimilation took place during genesis of Makwassie magma. The age of the Goedgenoeg Formation is still unknown, but is not expected to be significantly older than the Makwassie Formation.

2.6 GEOCHEMISTRY AND PETROGENESIS

Even though the first chemical analyses of the Makwassie porphyry was published by Williams (1932), it was only during the last decade that the petrology of the Makwassie Formation received attention. Liebenberg (1977) and Kleynhans (1979) presented analyses of the Makwassie Formation in the Northern Cape Province. Kleynhans (1979) concluded that the Makwassie porphyries are rhyodacitic in composition and that a possible differentiation series exists between the Makwassie and Rietgat volcanics.

Recent petrological investigations of the Goedgenoeg and Makwassie volcanics were mostly concerned with the geochemical stratigraphy of the Witwatersrand triad. De Bruijn *et al.* (1984) demonstrated the use of lithogeochemistry and multivariate statistics as aids in the stratigraphic characterization of the Ventersdorp Supergroup. Research by M.P. Bowen (1984) and T.B. Bowen (1984) further proved that a distinctive geochemical stratigraphy exists in the Ventersdorp Supergroup (T.B. Bowen *et al.*, 1986; M.P. Bowen *et al.*, 1986).

The geochemical composition of the Makwassie Formation in the Bothaville area (T.B. Bowen *et al.*, 1986) differs from that in the T'Kuip and North West Province areas (De Bruijn *et al.*, 1984). This discrepancy emphasized the need to investigate the lithostratigraphy of the Makwassie Formation in the Ventersdorp depository.

Schweitzer and Kröner (1985) stated that the Ventersdorp volcanics have only one primary source and that the Makwassie volcanics evolved through fractional crystallization from this source. According to Crow and Condie (1988) the Makwassie porphyries are the product of fractional crystallization of a mantle source, separate from the Klipriviersberg mantle source. Crow and Condie (1988) further state that the Makwassie magma was derived through partial melting induced by the rising plume of the Klipriviersberg magma source.

A study of the Platberg volcanics in the Klerksdorp area by Myers *et al.* (1988) and Myers (1990) indicated that the lower intermediate volcanics of the Makwassie Formation (the Goedgenoeg volcanics; see page 23), the quartz-feldspar porphyries of the Makwassie Formation and the Rietgat volcanics are related by differentiation to the same parental basic magma. Myers (1990) found that the Makwassie quartz-feldspar porphyries were derived from the intermediate Goedgenoeg volcanics magma, through ponding and rapid differentiation in the crust to an acidic composition. Increased eruption rates resulted in an upwards basic trend in the Makwassie succession in the Klerksdorp area, eventually ending in direct eruption without ponding and differentiation in the crust (Rietgat facies).

3. THE STRATIGRAPHY AND LITHOLOGY OF THE GOEDGE- NOEG AND MAKWASSIE FORMATIONS IN THE BOTHAVILLE AREA

3.1 INTRODUCTION

The Goedgenoeg and Makwassie Formations suboutcrop in the Bothaville area and the observations from this study are limited to borehole cores. The positions of the relevant boreholes are indicated in Fig. 3.1, which includes the type section of the Makwassie Formation (borehole DF1; S.A.C.S., 1980). In the Bothaville area the Goedgenoeg Formation overlies the sedimentary Kameeldoorns Formation or, where the Kameeldoorns Formation is not developed, the Klipriviersberg Group. The Makwassie Formation overlies the Goedgenoeg Formation. Outside the Klipriviersberg Group depository these formation onlap onto progressively older formations (e.g. the Witwatersrand Supergroup), until it directly overlies Basement Igneous Complex. Where developed, mafic lavas of the Rietgat Formation overlies the Makwassie Formation, otherwise it is overlain by the Pniel Group or younger formations.

3.2 STRATIGRAPHY

As described in Chapter 2, the Makwassie Formation as it was defined by S.A.C.S. (1980), is now divided into a lower feldspar porphyry unit (the Goedgenoeg Formation) and an upper quartz-feldspar porphyry unit (the Makwassie Formation proper (Meeting of the Ventersdorp Supergroup Task Group of SACS, February 1994; see Fig. 3.2).

3.2.1 The Goedgenoeg Formation

The Goedgenoeg Formation is composed of feldspar porphyries and less prominent non-porphyritic mafic lavas. The mafic lavas are interbedded with the feldspar porphyries and become more prominent towards the top of the succession. Subordinate tuffaceous rocks are infrequently interbedded with the porphyries and mafic lavas, while epiclastic sedimentary rocks are rare. The Goedgenoeg Formation is generally thicker than the Makwassie Formation and, in the Bothaville area, reaches a maximum thickness of 1777 m in borehole KRF1 (Appendix A).

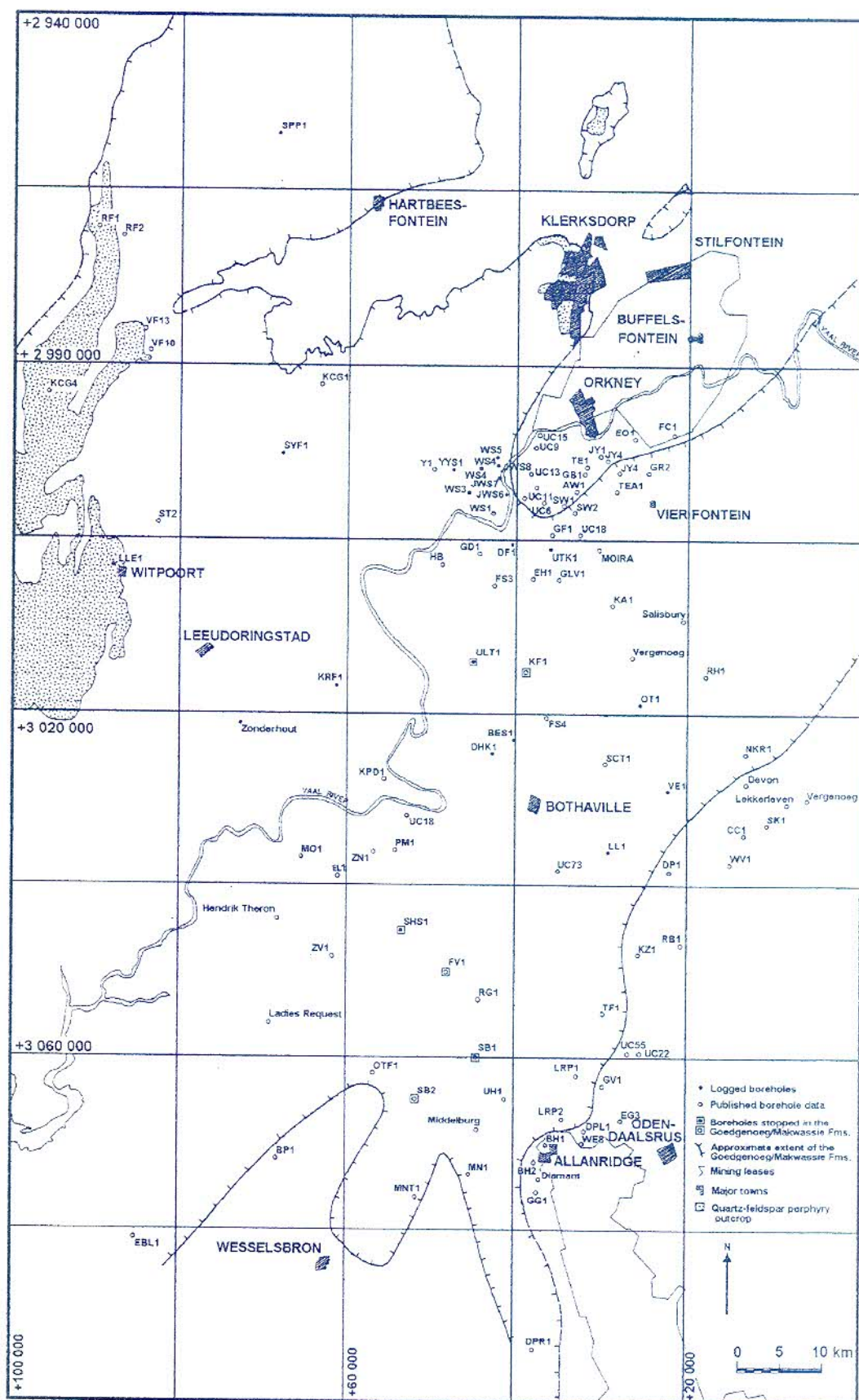


FIGURE 3.1: Map of the Bothaville area which indicates the distribution of quartz-feldspar porphyry outcrop, the position of boreholes and the subsurface distribution of the Makwassie Formation, including the Goedgenoeg Formation.

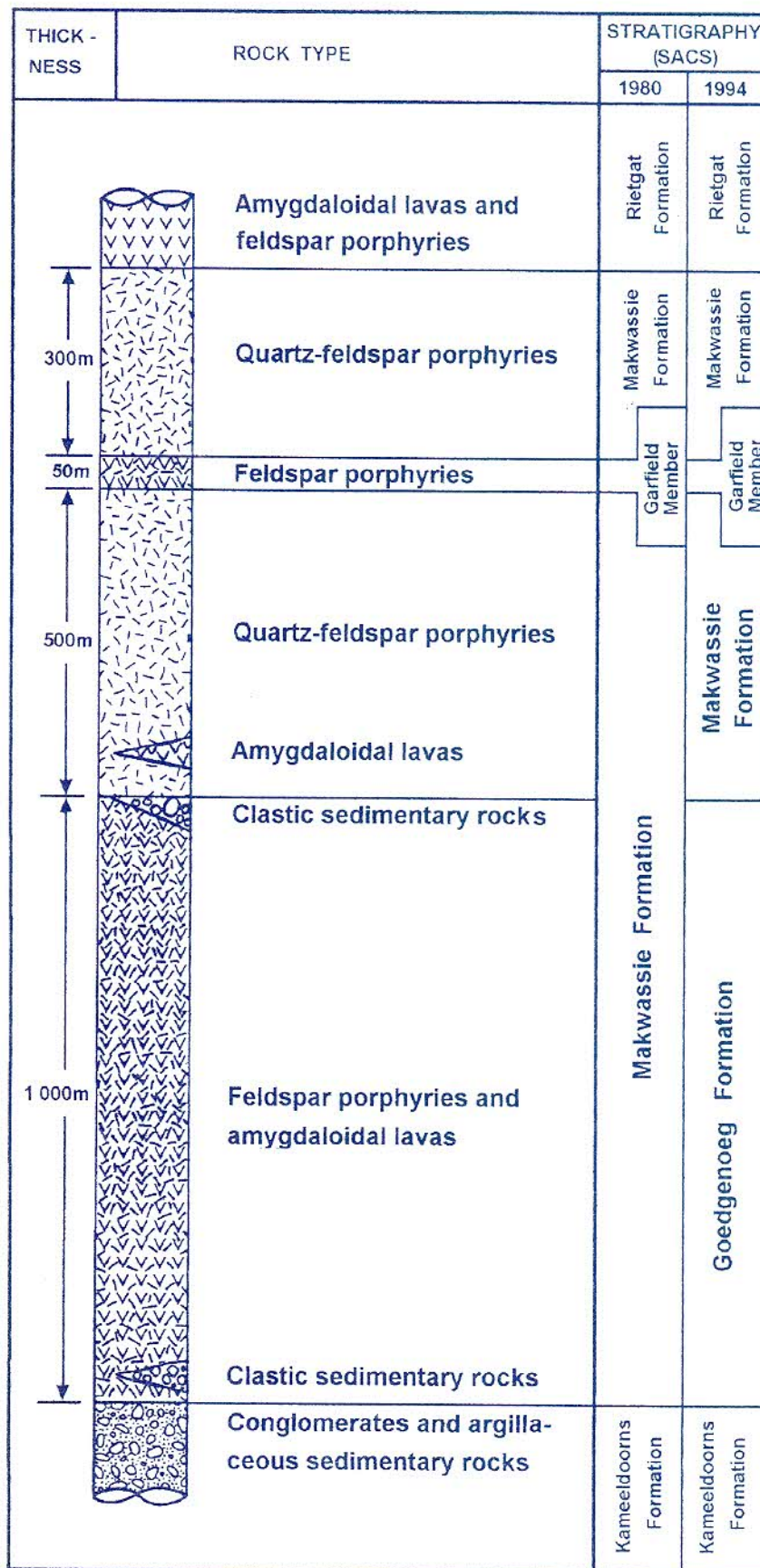


FIGURE 3.2: The general lithostratigraphy of the Goedgenoeg and Makwassie Formations in the Bothaville area.

Minor sedimentary rock units are associated with the lower and upper contacts of the Goedgenoeg Formation (Fig. 3.2). In the most prominent Platberg grabens (*i.e.* where the Goedgenoeg Formation attains its greatest thickness), clastic sedimentary rocks are interbedded with feldspar porphyries in the basal part of the Goedgenoeg Formation. This particular succession was described as the 'Vaal Bend formation' by Whiteside (1970). Some of these clastic beds have unusual textures and seem to be intermingled sediment and juvenile lava, which may indicate that the Kameeldoorns Formation sedimentation was still active at the onset of Goedgenoeg volcanism.

3.2.2 The Makwassie Formation

The Makwassie Formation consists predominantly of quartz-feldspar porphyries, but thin tuffaceous rock units are frequently interbedded with the porphyries. Minor mafic lava flows interbedded with quartz-feldspar porphyries occur locally in the lower part of the Makwassie Formation whilst epiclastic sedimentary rocks are rare. A prominent feldspar porphyry and mafic lava unit occur, however, in the upper part of the Makwassie Formation and this unit is known as the Garfield Member (Winter, 1976). A maximum thickness of 421 m for the Garfield Member was observed in borehole KRF1 (Appendix A). The Garfield Member is unique to the Bothaville area and its distribution can be accurately delineated (Chapter 4). In the eastern part of the Bothaville area the Garfield Member is directly overlain by the Rietgat Formation, whereas it is overlain by Makwassie Formation quartz-feldspar porphyries further to the west.

3.3 LITHOLOGY AND PETROGRAPHY

3.3.1 Comments On Alteration

Alteration of the Makwassie Formation rocks as a result of metamorphism affected the original mineral composition as well as emplacement textures. The Ventersdorp Supergroup was subjected to lower greenschist facies metamorphism (Cornell, 1978; Tyler, 1979a; Schweitzer and Kröner, 1985; Crow and Condie, 1988; Grobler *et al.*, 1989). A metamorphic paragenesis of quartz-chlorite-albite-clinzoisite-actinolite prevails in the Makwassie quartz-feldspar porphyries. Extensive silicification, chloritization and epidotization (Fig. 3.3) destroyed primary flow textures.

Devitrification of the originally glassy Makwassie quartz-feldspar porphyry was accompanied by extensive hydrothermal alteration, as is often the case with ignimbrites (Cas and Wright, 1988). Hydrothermal alteration can take many

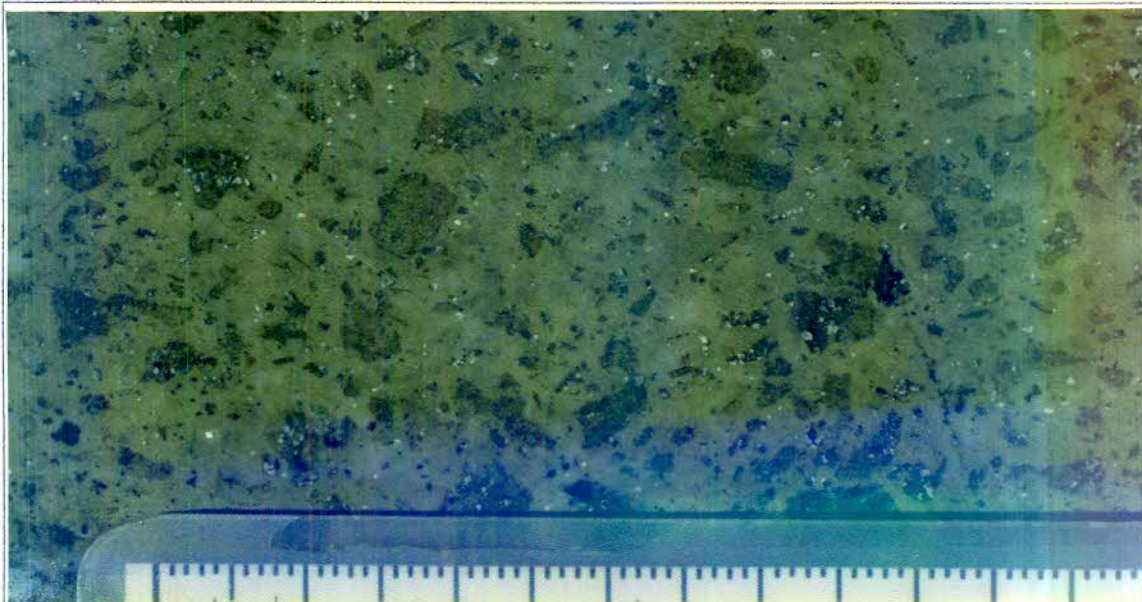


FIGURE 3.3: Highly epidotized quartz-feldspar porphyry in the lower part of the middle layer of a flow unit. Note the altered feldspars and almost totally obscured quartz phenocrysts. The white specs are leucoxene. Sample FVM750; borehole LLE1. (Top to the right and scale in mm).

forms and the resultant minerals can include amorphous silica, quartz, K-feldspar, albite, calcite, montmorillonite, illite, kaolinite, chlorite, zeolite and a host of other low-grade metamorphic minerals. Patchy alteration, transgressing over original textures and mineralogy, may produce an apparent clastic texture. The superimposed textures appear as clasts in a differently coloured and mineralogically different matrix (R. Allen, 1990, personal communication; Cas and Wright, 1988). Hydrothermal alteration is especially visible in the quartz-feldspar porphyry of borehole ZH1 (Zonderhout). Gradational to sharp contacts exist between zones of chlorite-quartz-sericite alteration (Figs. 3.4 and 3.5). Gibson *et al.* (1983) attribute mottled silicification of the Amulet Rhyolite Formation in Quebec to water-rock interaction, related to the circulation of sea water. Although the Makwassie Formation volcanics are not envisaged to have been inundated by seawater, interaction of groundwater with the porphyries could have attributed to the mottled silicification.

3.3.2 Quartz-feldspar Porphyry

3.3.2.1 Macroscopic Description

The quartz-feldspar porphyries are lighter-coloured than the feldspar porphyries and other mafic volcanic facies of the Ventersdorp Supergroup. They are predominantly light green in colour, although variations from grey-green, light yellow, grey-blue to purple-blue also occur. Red-coloured quartz-feldspar porphyry, associated with oxidation zones, is also present.

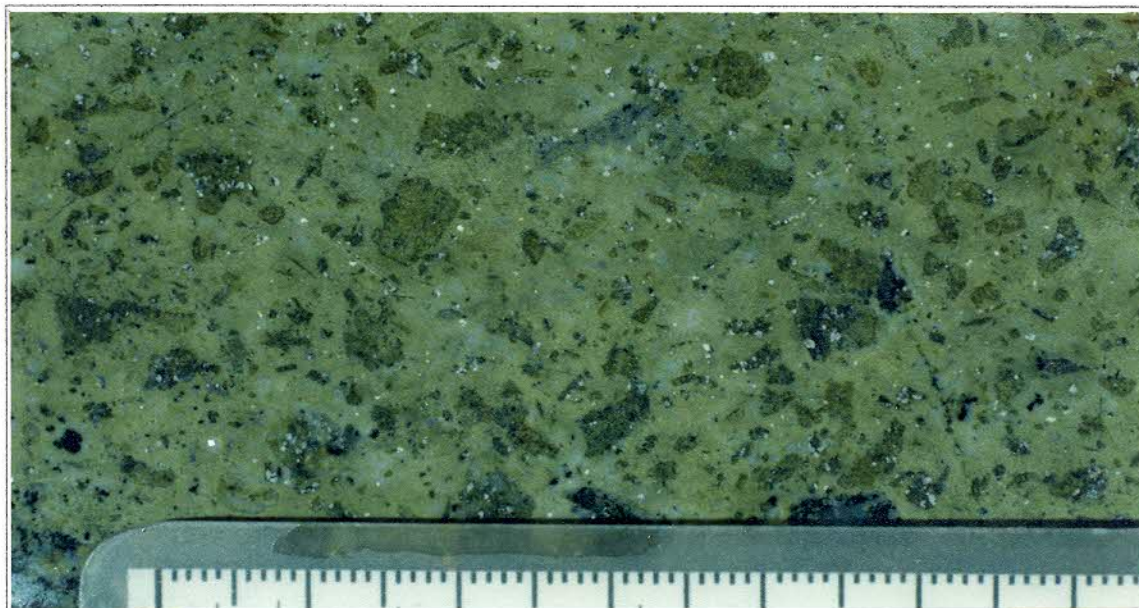


FIGURE 3.3: Highly epidotized quartz-feldspar porphyry in the lower part of the middle layer of a flow unit. Note the altered feldspars and almost totally obscured quartz phenocrysts. The white specs are leucoxene. Sample FVM750; borehole LLE1. (Top to the right and scale in mm).

forms and the resultant minerals can include amorphous silica, quartz, K-feldspar, albite, calcite, montmorillonite, illite, kaolinite, chlorite, zeolite and a host of other low-grade metamorphic minerals. Patchy alteration, transgressing over original textures and mineralogy, may produce an apparent clastic texture. The superimposed textures appear as clasts in a differently coloured and mineralogically different matrix (R. Allen, 1990, personal communication; Cas and Wright, 1988). Hydrothermal alteration is especially visible in the quartz-feldspar porphyry of borehole ZH1 (Zonderhout). Gradational to sharp contacts exist between zones of chlorite-quartz-sericite alteration (Figs. 3.4 and 3.5). Gibson *et al.* (1983) attribute mottled silicification of the Amulet Rhyolite Formation in Quebec to water-rock interaction, related to the circulation of sea water. Although the Makwassie Formation volcanics are not envisaged to have been inundated by seawater, interaction of groundwater with the porphyries could have attributed to the mottled silicification.

3.3.2 Quartz-feldspar Porphyry

3.3.2.1 Macroscopic Description

The quartz-feldspar porphyries are lighter-coloured than the feldspar porphyries and other mafic volcanic facies of the Ventersdorp Supergroup. They are predominantly light green in colour, although variations from grey-green, light yellow, grey-blue to purple-blue also occur. Red-coloured quartz-feldspar porphyry, associated with oxidation zones, is also present.

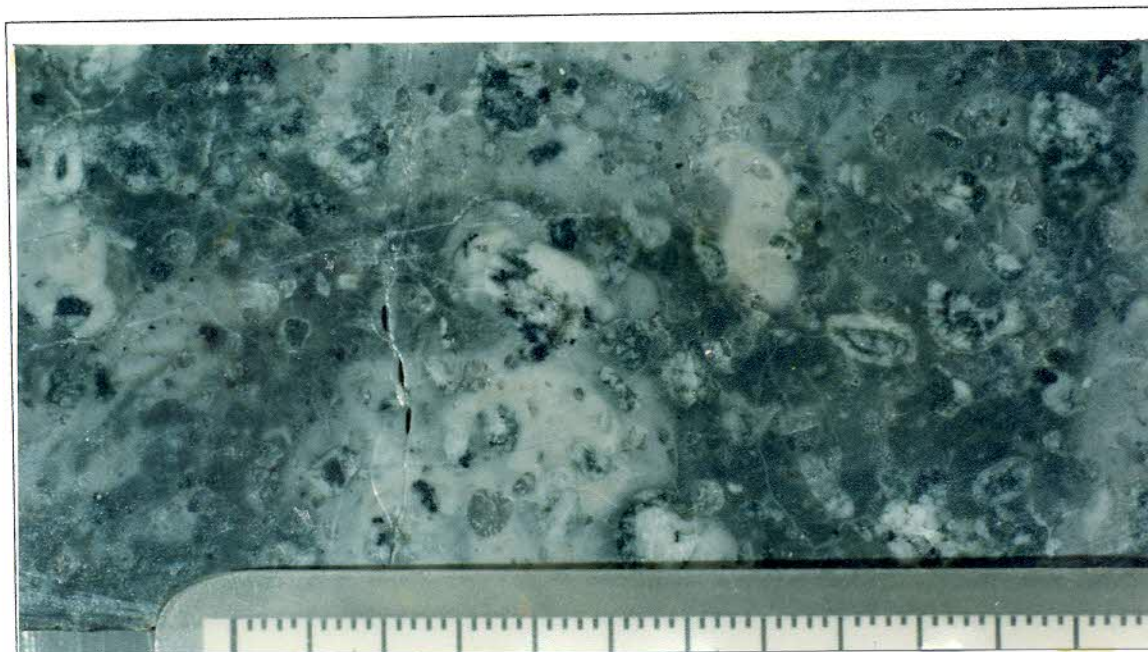


FIGURE 3.4: Irregular alteration of the Makwassie Formation quartz-feldspar porphyry, resulting in an apparent clastic texture (R. Allen, personal communication, 1991). Sample FVM788; borehole ZH1. (Top to the right and scale in mm).

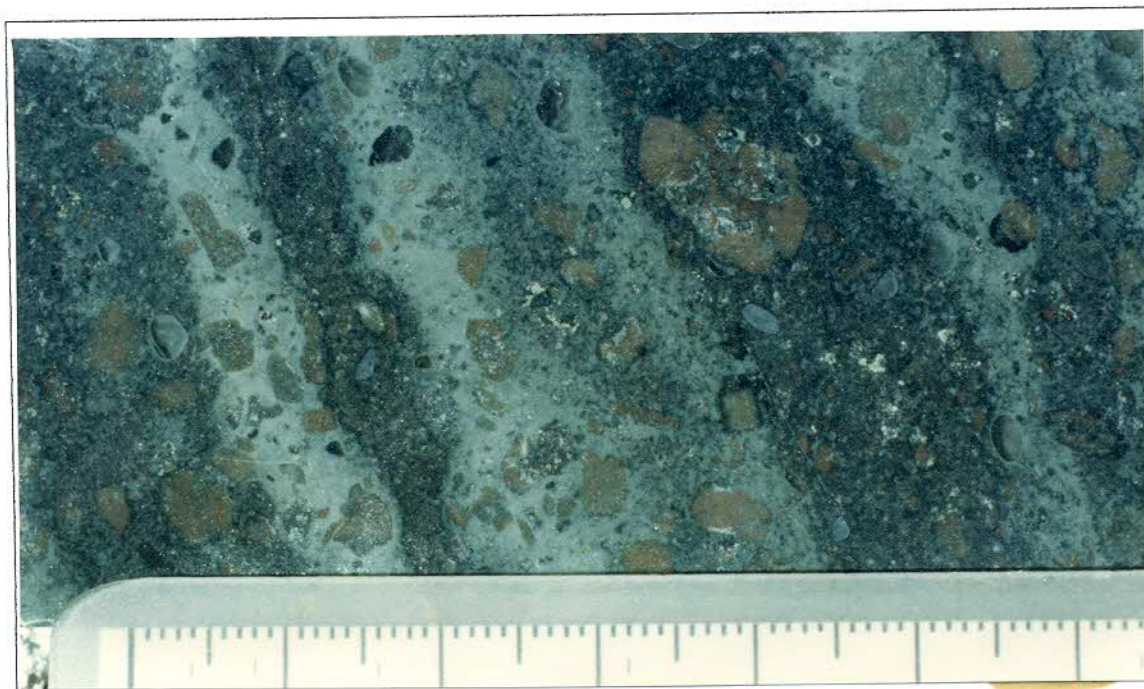


FIGURE 3.5: Colour-banded texture of the Makwassie Formation quartz-feldspar porphyry, attributed to inconsistent alteration. Sample FVM820; borehole DF1. (Top to the right and scale in mm).

Both quartz and feldspar phenocrysts are recognizable in hand specimen (Fig. 3.6). The quartz phenocrysts are round to oval in shape with a diameter from microscopic up to 8 mm and with a mean of 2 mm. Fragmented quartz phenocrysts are also present.

In contrast, the shape of the feldspar phenocrysts are rectangular with rounded edges. They are generally fractured and although small phenocryst fragments are frequently observed, the phenocrysts' size range from microscopic up to 12 mm, with an average of 5 mm. Composite grains of up to 30 mm were also noted. The phenocryst colour varies from white to green and reddish potassic feldspar were frequently observed. The red colour originates as a result of iron exsolution which leads to clouding of the crystals (Poldervaart and Gilkey, 1954). Zonation of some of the feldspar phenocrysts are macroscopically visible and is manifest by a green-coloured chloritic core, surrounded by white feldspar (Fig. 3.7). This phenomenon is often present in altered plagioclase feldspars (Cox *et al.*, 1979). The phenocrysts constitute about 35 volume per cent of the rock and can be divided into 30% feldspar, 10% quartz and 5% composite glomerular phenocrysts.

The porphyry matrix is aphanitic, very dense and has a cherty appearance. The red-coloured quartz-feldspar porphyries are often weakly magnetic.

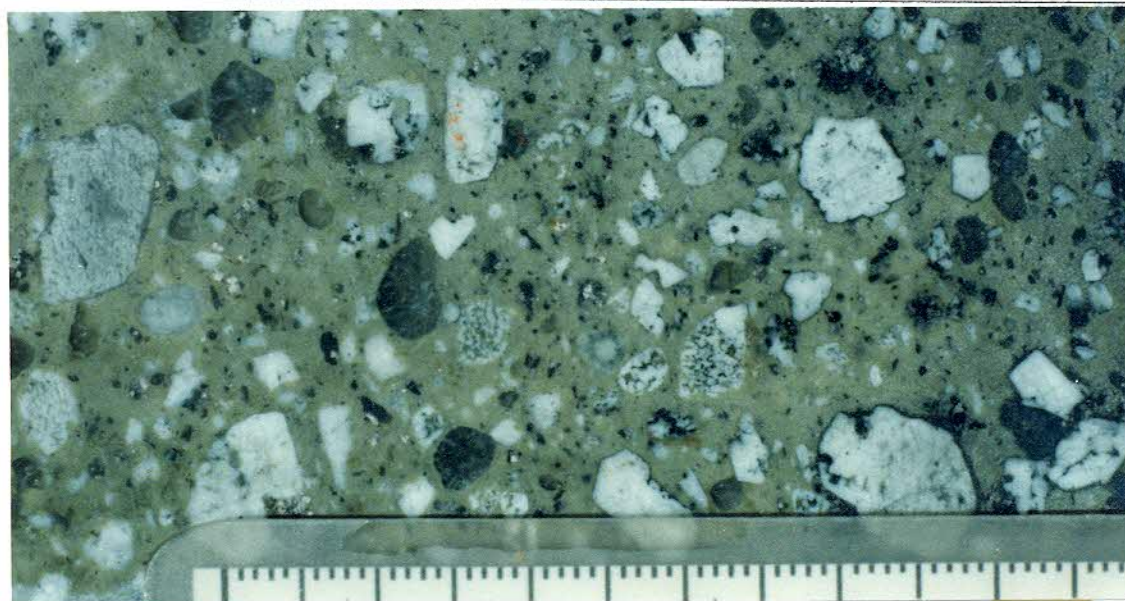


FIGURE 3.6: Typical Makwassie Formation quartz-feldspar porphyry in borehole core. Feldspar phenocrysts are visible as fragmented white crystals, often with skeletal forms. Subrounded quartz phenocrysts appear as grey-coloured crystals. The khaki-green colour of the matrix is attributed to epidotization. Sample FVM728; borehole WS4. (Top to the right and scale in mm).

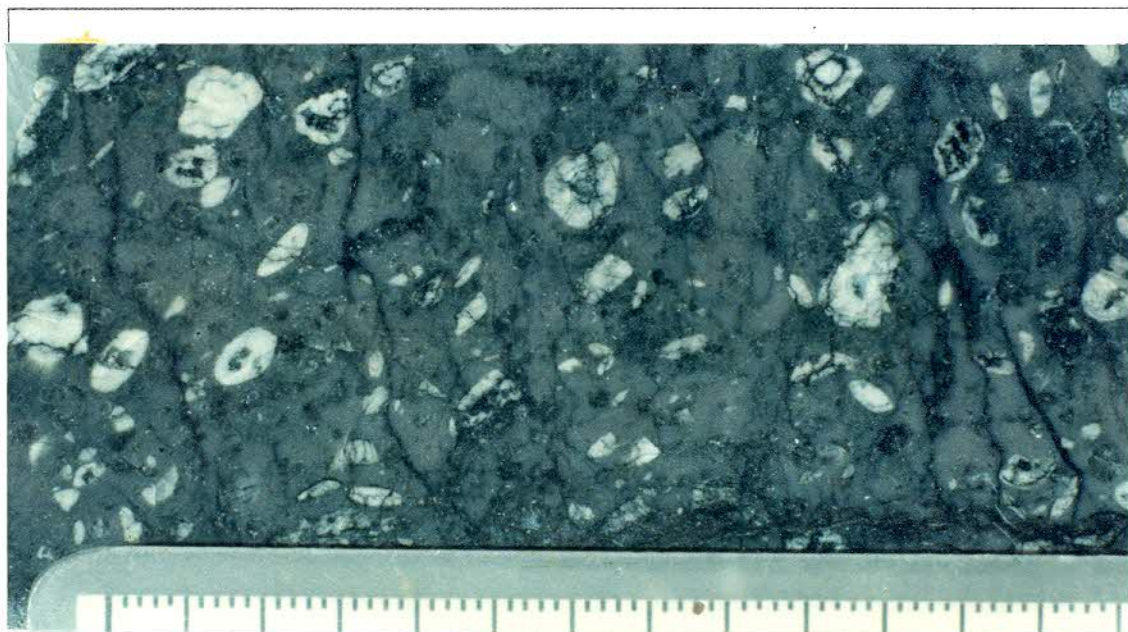


FIGURE 3.7: Quartz-feldspar porphyry with chloritic laminae. Feldspar phenocrysts show zonation, often with chlorite alteration of the core. Quartz phenocrysts are unclear in this sample. Sample FVM149; borehole LLE1. (Top to the right and scale in mm).

3.3.2.2 Petrographic Description

The prevalent porphyritic texture is conspicuous. Feldspar phenocrysts predominate over quartz, with accessory microphenocrysts of apatite, zircon, sphene, spinel and titaniferous magnetite. The total phenocryst content rarely exceeds 35%. Myers (1990), however, reports total phenocryst proportions from 10% to 65% for Makwassie rocks in the Buffelsdoorn graben, Makwassie Townlands and Platberg, near Klerksdorp.

Quartz Phenocrysts

Rounded to oval, embayed and fractured quartz phenocrysts occur in varying concentrations and size in the quartz-feldspar porphyry (Fig. 3.8). The phenocrysts are monocrystalline, but undulatory extinction is often visible. Embayments cut into the crystals and are filled by amorphous minerals of the surrounding matrix. Some phenocrysts are fractured, with segregation of the fragments, especially in the top layer of flow units.

Dark-coloured rims of amorphous minerals surround the quartz phenocrysts. Very fine-crystalline, spindly actinolite is often associated with these rims, penetrating the perimeter of the quartz phenocrysts. The extent of quartz replacement is variable; in some flow units the quartz phenocrysts are almost completely replaced and clouded by an abundance of submicroscopic minerals. Inclusions of apatite and other accessory minerals were observed and bubble trails of very small fluid inclusions are common.

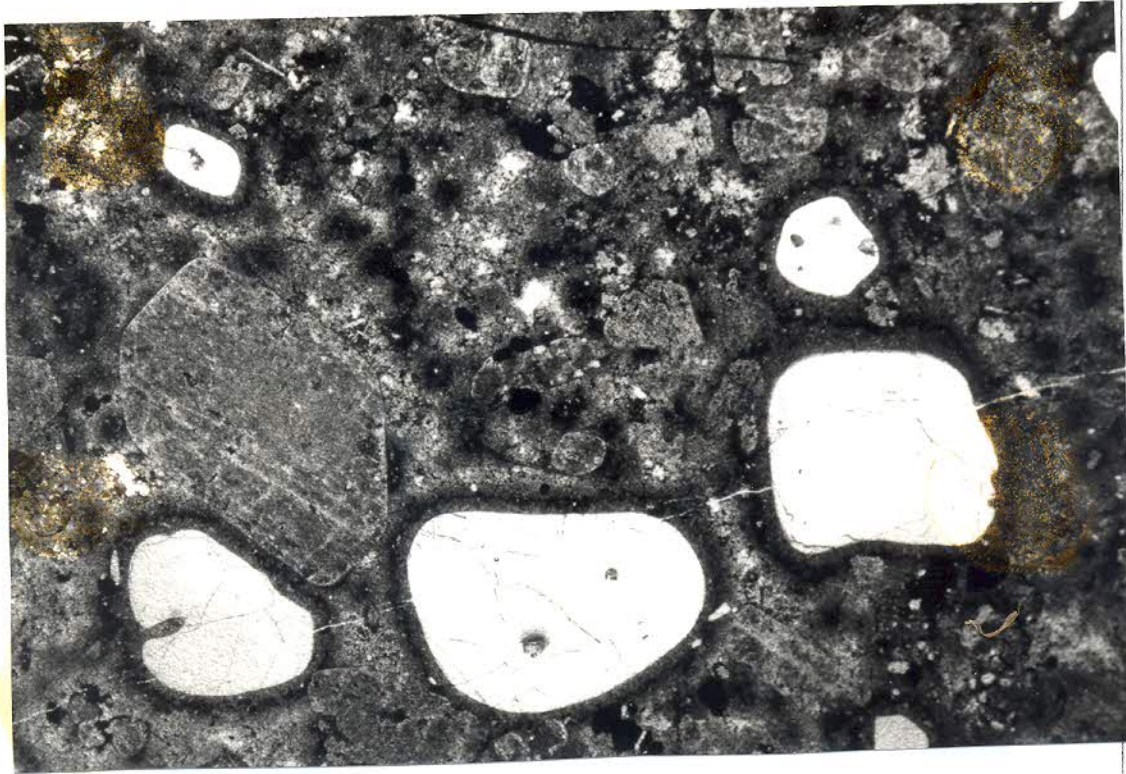


FIGURE 3.8: Rounded, embayed and fractured quartz phenocrysts (white crystals) with dark reaction rims, typical of the Makwassie quartz-feldspar porphyry. Note the altered feldspar phenocrysts and the spherulites (dark blots) in the matrix. Sample FVM096; borehole YYS1. (Plane polarized light. Width of field is 14 mm).

Feldspar Phenocrysts

Feldspar phenocrysts occur as fragmented, subhedral crystals with subrounded edges, while larger crystals may be well rounded (Fig. 3.9). None of the phenocrysts appear intact. The phenocrysts are furthermore intensely affected by saussuritic alteration and in some cases can hardly be distinguished from the groundmass. Although rhythmic zonation is rare, phenocrysts with a core and secondary overgrowth are common.

Plagioclase phenocrysts predominate over alkali-feldspar phenocrysts. Jacobsen (1943) reports albite, oligoclase, orthoclase and microperthite, while M.P. Bowen (1984) and J.M. Myers *et al.* (1990) report plagioclase of oligoclase composition. Electron microprobe analyses performed during this study indicated albitization of the feldspars (Appendix E;). Albitic ($\text{Ab}_{97-99}\text{An}_{1-3}\text{Or}_1$) compositions predominate, with minor oligoclase/andesine ($\text{An}_{29}\text{Ab}_{59}\text{Or}_{12}$). The alkali-feldspars are represented by orthoclase ($\text{Or}_{98}\text{Ab}_1\text{An}_1$) and anorthoclase ($\text{Or}_{24}\text{Ab}_{76}$).



FIGURE 3.9: An altered plagioclase phenocryst mantled by later-stage growth. The primary central part is altered to chlorite, indicating compositional differences between the growth stages. Note the embayed quartz phenocrysts and aphanitic matrix. Sample FVM220; borehole ZH1. (Crossed nicols. Width of field is 11 mm).

Plagioclase phenocrysts exhibit Carlsbad and polysynthetic Albite twinning. Apart from the single-crystal phenocrysts, glomerular phenocrysts also occur. Some plagioclase and especially alkali-feldspar phenocrysts display complex skeletal crystals (Fig. 3.10), which were described as honeycomb-textured feldspars by M.P. Bowen (1984).

Other Phenocrysts

Relict phenocrysts, totally altered to or replaced by chlorite and actinolite, are also present in the quartz-feldspar porphyry, but appear more frequently in the feldspar porphyry. These relict phenocrysts were also reported by previous researchers (Jacobsen, 1943; M.P. Bowen 1984), which Jacobsen (1943) considered to be relicts of hornblende. These subhedral relict phenocrysts are stubby in shape and comprise a mass of secondary chloritic material, often with aligned, fibrous actinolite and opaque oxides. The relict phenocrysts are often associated with aggregates of accessory and secondary minerals. The original composition of these phenocrysts could not be determined. The molecular

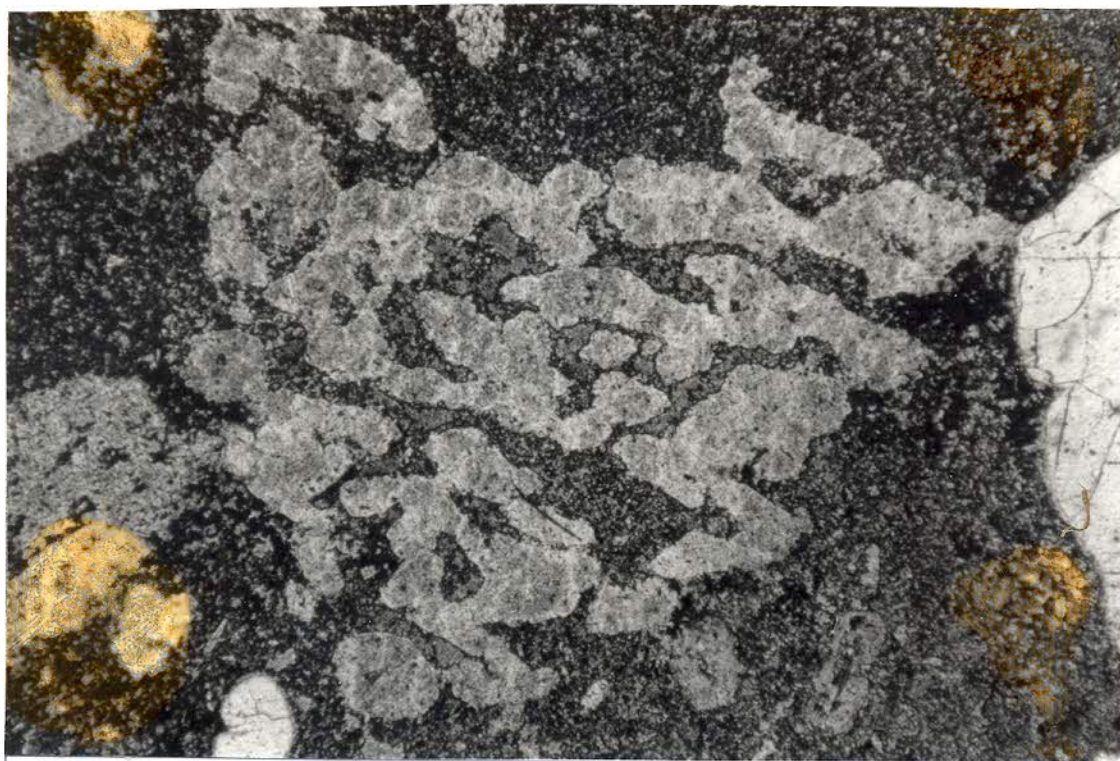


FIGURE 3.10: Complex skeletal feldspar phenocryst with groundmass filling the openings. Sample FVM288; borehole DF1. (Crossed nicols. Width of field is 6 mm).

proportions of Al_2O_3 , CaO and $\text{Na}_2\text{O} + \text{K}_2\text{O}$ determine which mafic minerals will be present in granites and rhyolites (Barker, 1983). The Makwassie felsics are metaluminous (Chapter 5) and it can be expected that amphibole (hornblende?) and/or biotite will be present as a phenocryst phase instead of pyroxene.

Accessory Minerals

Small euhedral crystals of apatite, zircon, sphene and spinel are common in the Makwassie quartz-feldspar porphyry, often occurring as aggregated masses together with titaniferous magnetite (Fig. 3.11) and feldspar. The above accessory minerals are widespread in granites and rhyolites (Barker, 1983). Zircon is relatively rare in the quartz-feldspar porphyry. Discreet apatite laths in the matrix often display quench textures (Fig. 3.12).

Titanomagnetite occurs prevalently as a sandwich or trellis intergrowth of ilmenite and magnetite (Fig. 3.11). The original titanomagnetite ($\text{Fe}_3\text{O}_4\text{-Fe}_2\text{TiO}_4$ - magnetite/ulvöspinel) has been oxidized to ilmenite, magnetite and maghemite ($\text{Fe}_3\text{O}_4 + \text{FeTiO}_3 \pm \text{Fe}_2\text{O}_3$), with the ilmenite exsolved within the magnetite as trellis or sandwich patterns (Elsdon, 1975), similar to that described by Buddington and Lindsley (1964). Ilmenite is altered to leucosene and appears as

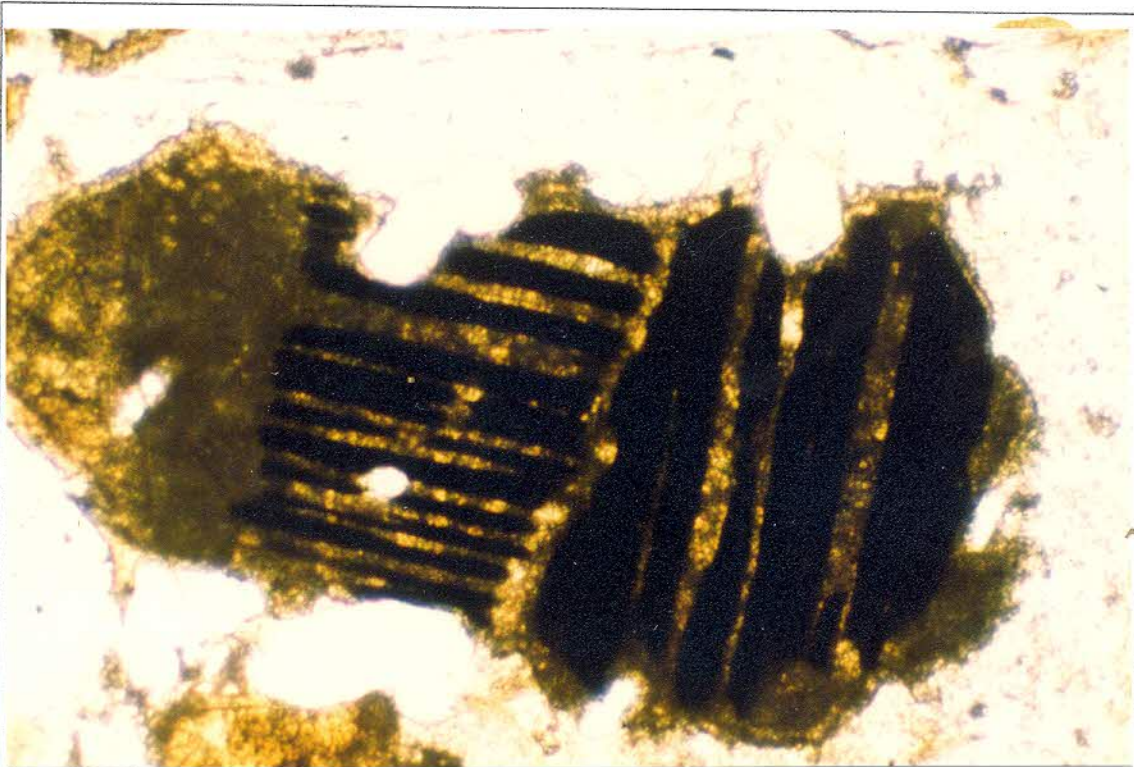


FIGURE 3.11: An aggregate of euhedral apatite, spinel, sphene and zircon crystals (not visible), which surrounds an altered titanomagnetite crystal. The dark lamellae are maghemite and the greenish patches are leucoxene. Sample FVM018; borehole WS3. (Plane polarized light. Width of field is 1 mm).



FIGURE 3.12: A quench-textured apatite crystal (hollow centre of the crystal) in the quartz-feldspar porphyry. Sample FVM285; borehole DF1. (Crossed nicols. Width of field is 1 mm).

white specks in hand specimen, while the magnetite is partially altered to an opaque brownish mass of maghemite. Excess Fe_2O_3 in the magnetite will be present as maghemite (Buddington and Lindsley, 1964).

Matrix

The matrix of the quartz porphyry consists of a fine-crystalline mass of quartz, albite, K-feldspar, chlorite, epidote, calcite, sericite and opaque minerals. Phenocryst fragments or single accessory minerals are interspersed in the matrix. Matrix mineral proportions are variable, especially in the case of quartz, epidote, and chlorite, e.g. some layers are silicified, epidotized, or chloritized. In flow units of the quartz-feldspar porphyry the matrix in the flow-unit base tends to be highly epidotized, while the flow-unit top is mostly silicified. Makwassie quartz-feldspar porphyries with a red-coloured matrix have very finely-dispersed opaque oxides (maghemite?) in the matrix.

The matrix invariably displays a felsitic texture (Fig. 3.13), particularly in the basal and middle parts of flow units (petrographic analysis, Appendix F). A microprobe scan across a very fine-grained example revealed lamellar intergrowths of quartz and K-feldspar, with subordinate albite. The albite is possibly of secondary origin. With a beam diameter of 1 μm , the microprobe was utilized to determine the widths of the intergrown minerals. Quartz lamellae measured less than 30 μm , K-feldspar less than 20 μm , and albite less than 4 μm .

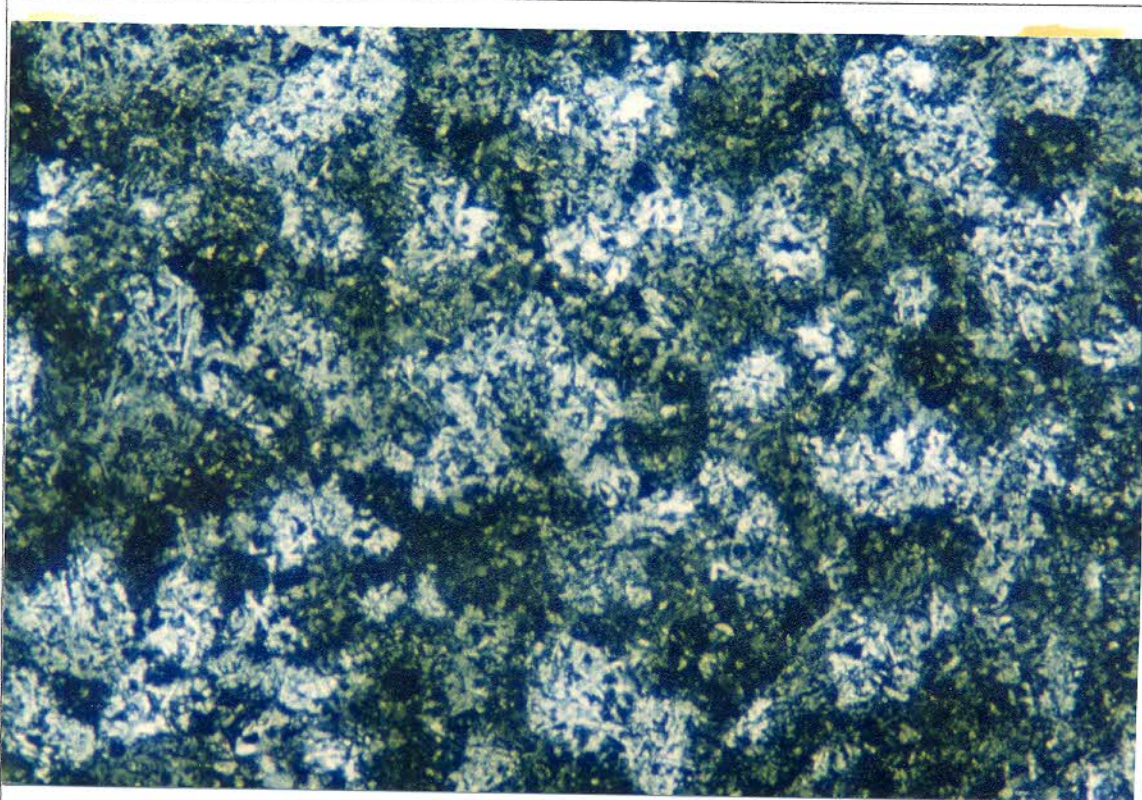


FIGURE 3.13: Felsitic texture of the quartz-feldspar porphyry matrix, composed of a very fine intergrowth of quartz and feldspar. Sample FVM018; borehole WS3. (Crossed nicols. Width of field is 4 mm).

3.3.3 Feldspar Porphyry

3.3.3.1 Macroscopic Description

The most distinctive lithological difference between the feldspar porphyry and quartz-feldspar porphyry is the absence of quartz phenocrysts in the former (Fig. 3.14). The feldspar porphyry is dark green in colour due to a high chlorite content. Phenocryst concentrations vary; some flow units contain only scattered feldspar phenocrysts while others may be very phenocryst-rich. Some feldspar porphyry flow units host rare quartz phenocrysts, which are only recognized in thin section.

Euhedral, intact feldspar phenocrysts occur in phenocryst-poor flows, while phenocrysts are commonly rounded and fragmented in phenocryst-rich flows and also smaller ($\mu 3$ mm) than the feldspar phenocrysts in the quartz-feldspar porphyry. The colour of the feldspar phenocrysts varies from white to shades of green.

Relict phenocrysts, similar to those recognized in the quartz-feldspar porphyries, were frequently observed. Due to alteration, their original composition could not be determined. The matrix of the feldspar porphyry is aphanitic and very dense with a dark-green colour which is attributed to a high chlorite content. The feldspar porphyry can easily be distinguished from the quartz-feldspar porphyry due to its mafic appearance and the absence of quartz phenocrysts.

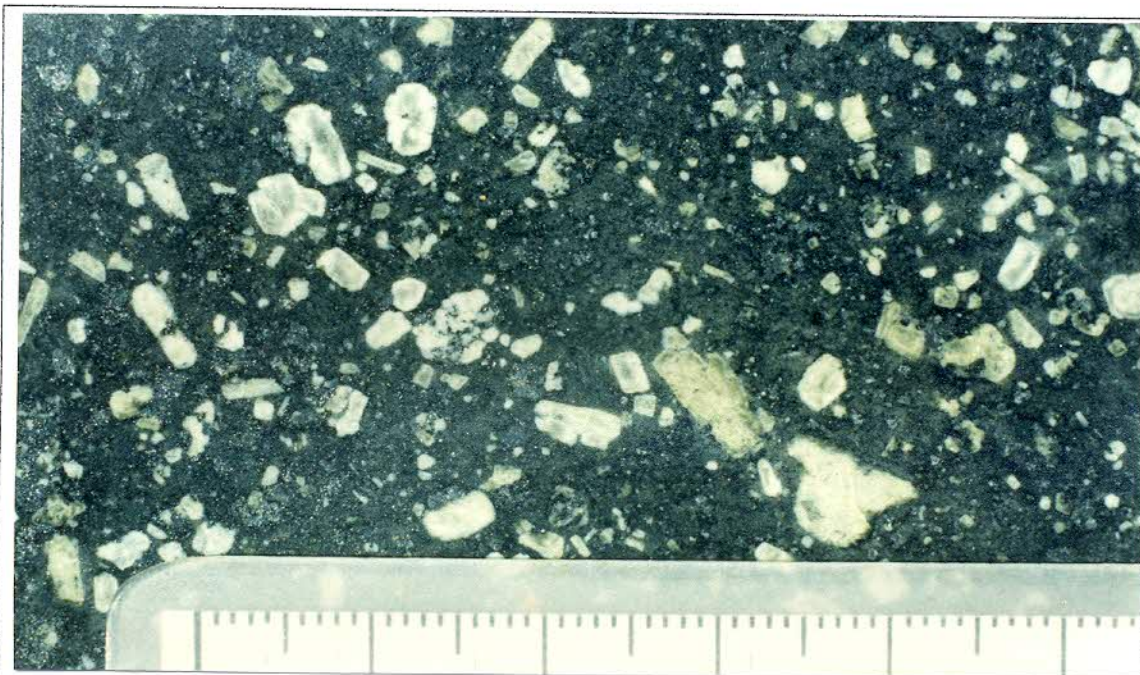


FIGURE 3.14: Goedgenoeg Formation feldspar porphyry with fractured, subrounded feldspar phenocrysts which are smaller than those of the Makwassie quartz-feldspar porphyry. Sample FVM129; borehole LLE1. (Top to the right and scale in mm).

3.3.3.2 Petrographic Description

The petrography of the feldspar porphyries is generally similar to that of the quartz-feldspar porphyry, except for the absence of quartz phenocrysts. Completely chloritized relict phenocrysts are prevalent in the feldspar porphyry while the matrix is also more chlorite-rich than for the quartz-feldspar porphyries.

The feldspar phenocrysts are often euhedral, in contrast to those of the quartz-feldspar porphyry. Skeletal feldspar phenocrysts are rare. Phenocryst-rich flow units, however, have broken feldspars and matrix with felsitic textures similar to the quartz-feldspar porphyry. Less phenocryst-rich flow units display a fine-crystalline matrix.

An electron microprobe analyses (Appendix E) indicated alkali-feldspar phenocrysts of albite ($\text{Ab}_{93-99}\text{An}_{1-6}\text{Or}_{1-2}$) and sanidine ($\text{Or}_{74}\text{Ab}_{25}\text{An}_1$ and $\text{Ab}_{70-76}\text{Or}_{23-28}\text{An}_{1-2}$) composition. Apart from albite, a plagioclase composition of labradorite ($\text{An}_{59}\text{Ab}_{40}\text{An}_1$) was also obtained.

3.3.4 Non-porphyritic Lava

3.3.4.1 Macroscopic Description

Non-porphyritic lava is subordinate to feldspar porphyry in the Goedgenoeg Formation and is only rarely interbedded with the quartz-feldspar porphyries of the Makwassie Formation. The mafic lava has a physical appearance similar to lava from the Rietgat Formation, *i.e.* it is dark-green in colour, fine to medium-crystalline and amygdaloidal at the base and top of flows. Lava breccias occur rarely.

3.3.4.2 Petrographic Description

These rocks display a fine-crystalline texture of altered feldspar laths with interstitial spaces filled by amorphous chlorite, epidote, quartz, calcite and sericite. Feldspar microphenocrysts also occur.

3.3.5 Tuffaceous Rocks

3.3.5.1 Macroscopic Description

The tuffaceous rocks, which occur as thin interbedded layers in the Makwassie quartz-feldspar porphyries, are fine-grained and laminated. Interbedded tuffaceous rocks in the Makwassie Formation often have embedded fragments and clasts of scoriaceous quartz-feldspar porphyry, in which case these clasts indent the laminae. The tuffaceous beds are poorly graded, but an upwards-fining sequence can be defined in some cases. Cross-bedding is absent.

3.3.5.2 Petrographic Description

The fine-grained, tuffaceous beds that separate individual flow units in the quartz-feldspar porphyry are composed of quartz and altered mineral fragments, embedded in an amorphous matrix. Mica flakes and unidentified lithic fragments were also observed. Layering is defined under the microscope by variable crystal-fragment concentrations and although the fine-grained beds are upwards-fining, individual laminae can be either upward-fining or upward-coarsening. Relict unwelded glass-shard textures (Figs. 3.15 and 3.16) were often recognized in the less crystal-rich laminae. Vesicular porphyritic clasts with irregular shapes and a large size range (4-150 mm) are often embedded in these tuff beds and laminae drape over them. Cherty layers also occur, often with bedded accretionary lapilli composed of cherty outer laminae and grained cores.

3.3.6 Epiclastic Sedimentary Rocks

Clastic sedimentary rocks associated with the basal part of the Goedgenoeg Formation consist of chaotic lava breccia in an immature sedimentary matrix. Intermingled lava, clastic and shaley sedimentary material are also present in this stratigraphic position. Similar material is reported by Winter (1976). Poorly sorted, matrix-supported conglomerate with clasts consisting of mafic lava separates the Goedgenoeg and Makwassie Formations in some areas (e.g. boreholes JWS6, JWS7 and JWS8; Appendix A). Silicified, calcareous mudrock was also observed in borehole LLE1 (Appendix A).

3.4 FLOW MORPHOLOGY

3.4.1 Description

Flow units can be distinguished in the feldspar porphyries of the Goedgenoeg Formation, but are difficult to delineate in some intersections. In the feldspar porphyries the flow units are recognized by contrast in phenocryst concentrations, amygdaloidal flow tops and the presence of scoriaceous breccias. In the associated mafic lavas flow units are readily distinguished by amygdaloidal top sections, scoriaceous breccias and sharp flow contacts as well as a decrease in crystallinity towards the contacts.

Superficially the quartz-feldspar porphyries of the Makwassie Formation appears to be massive. On close scrutiny, however, flow units can often be recognized, which consist of a basal, middle and top layer (Fig. 3.17). Individual flow units have sharp contacts and are often separated by a thin layer of tuff. The basal, middle and top layers of the flow units in the quartz-feldspar porphyry are distinguished as described in the following paragraphs.

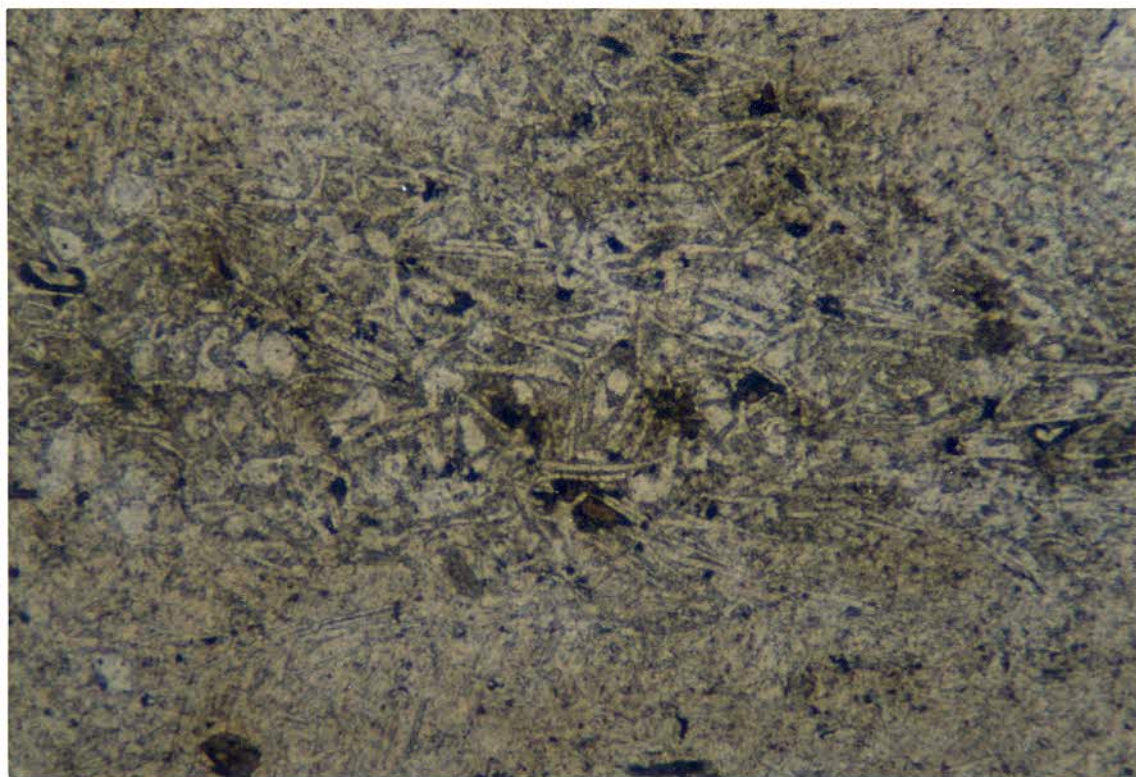


FIGURE 3.15a: Unwelded glass-shard textures in a tuffaceous sedimentary bed. Sample FVM772; borehole LLE1. (Plane polarized light. Width of field is 4 mm).

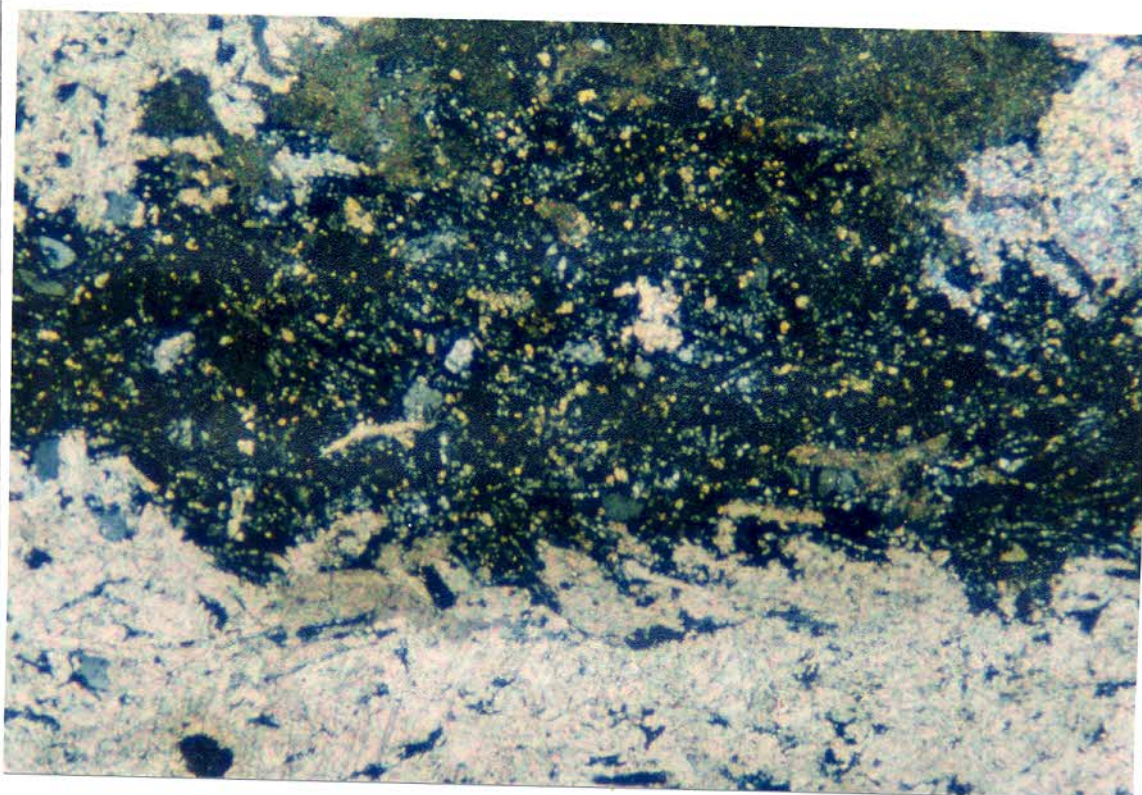


FIGURE 3.15b: View of fig. 3.15a under crossed nicols. Calcification destroyed the glass-shard textures in the lower and upper part of the picture. The glass shards in the middle part are replaced by silica. (Width of field is 4 mm).

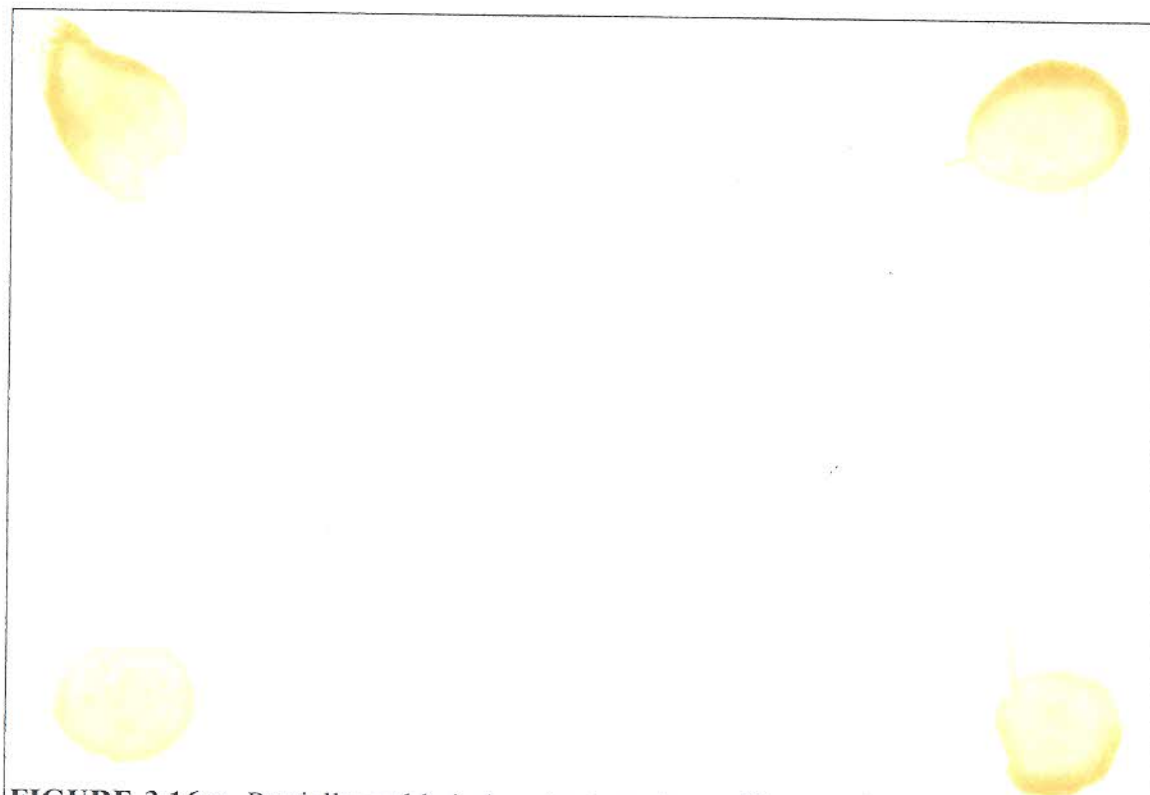


FIGURE 3.16a: Partially-welded glass textures in a tuffaceous bed. Note the draping of shards over lithic and crystal fragments. Sample FVM842; borehole OT1. (Plain polarized light. Width of field is 4 mm).

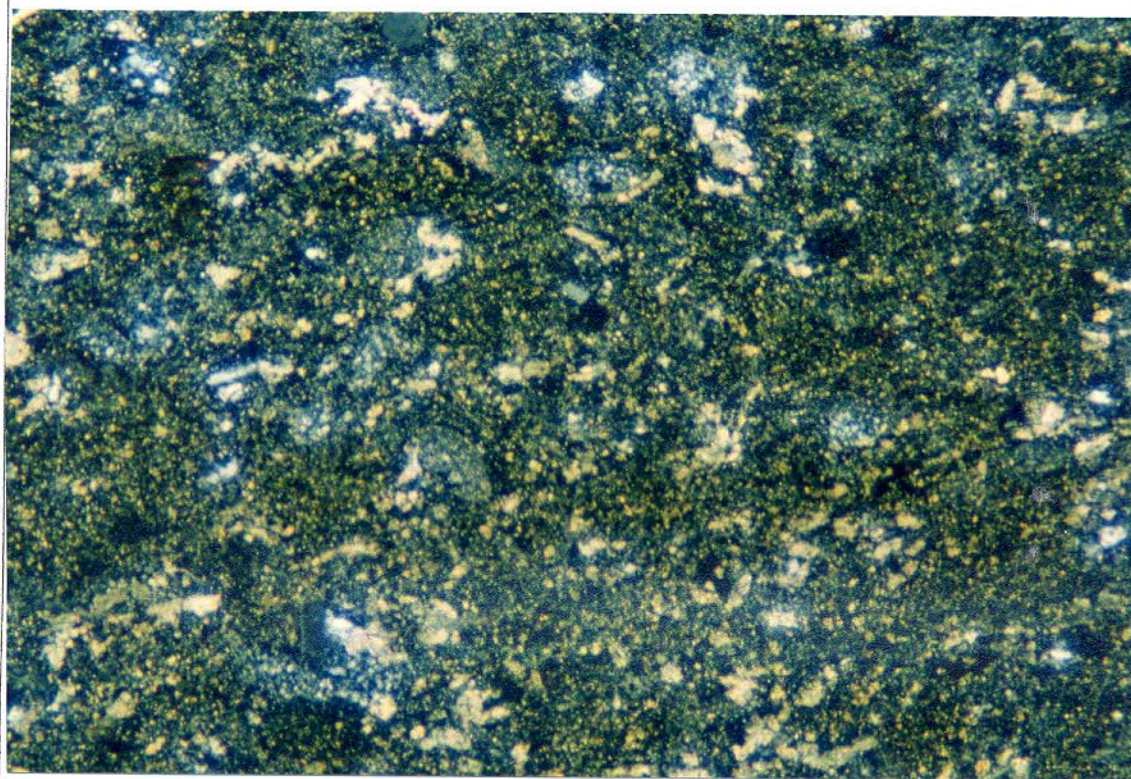


FIGURE 3.16b: View of fig. 3.16a under crossed nicols. The partially-welded texture was partially destroyed by silicification and chloritization. (Width of field is 4 mm).

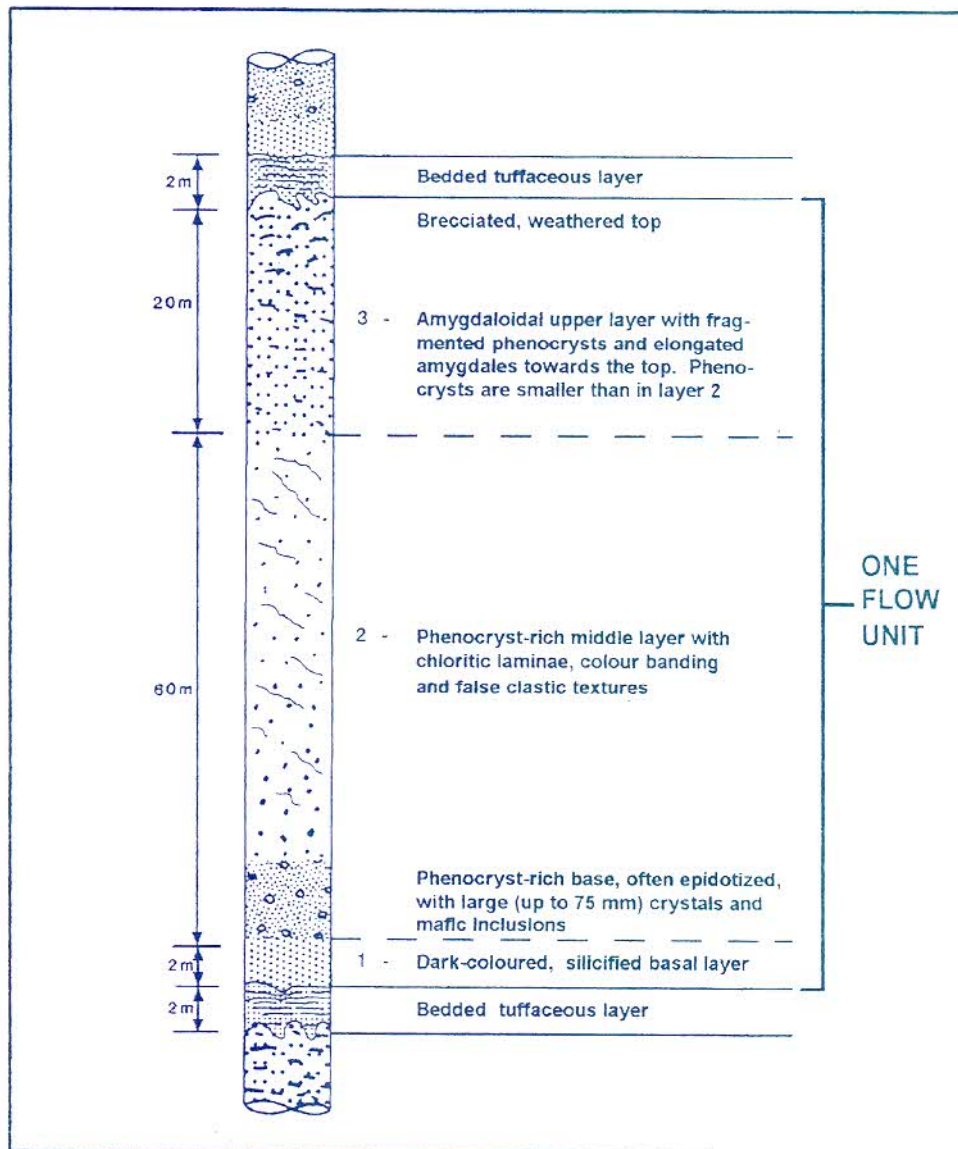


FIGURE 3.17: Generalized flow unit of the quartz-feldspar porphyry.

Basal Layer (Layer 1, Fig. 3.17)

This layer is distinctly darker than the rest of the flow unit and contains poorly visible phenocrysts, which are smaller than those in the overlying middle layer. The matrix appears glassy. The basal layer is seldom thicker than 2 m and the lower contact is sharp. The upper contact is gradational, but nevertheless forms a rapid transition into the overlying middle layer. The basal layer is not always developed, in which case the middle layer forms the base of the flow unit.

Middle Layer (Layer 2, Fig. 3.17)

The lower part of the middle layer is particularly phenocryst-rich, often with phenocrysts larger than 5 mm. Inclusions of quartz-feldspar porphyry and non-porphyritic lava are often present. These inclusions are mostly smaller than 80 mm. The lower part of the middle layer is frequently epidotized (Figs. 3.3 and 3.6). Jacobsen (1943) also reports epidotization near the base of flow-units in the Makwassie porphyries at Klerksdorp.

The rest of the middle layer is also phenocryst-rich, although less so than in the lower part. Infrequent laminae, depicted by very thin (mm scale) parallel chloritic streaks, occur in some flow units (Fig. 3.7). The laminae are spaced far apart and sometimes cut through fractured phenocrysts. Broader (cm scale) colour-banding occurs frequently (Fig. 3.5). Irregular, patchy colour variations are present and form an apparent clastic or brecciated texture in places (Fig. 3.9).

In some flow units numerous non-porphyritic lava inclusions (Fig. 3.18) are present in the middle layer. Their size range from microscopic to ± 100 mm and most are subspherical in shape. Some have a sharply defined outline, while others blend with the matrix of the host quartz-feldspar porphyry and only rarely do they contain amygdaloidal textures. The inclusions are fine-crystalline and sometimes also contain discrete, small feldspar or quartz phenocrysts.

Quartz-feldspar porphyry inclusions, although rarely observed, have the same lithology as the host porphyry, but the phenocryst size and colour may differ somewhat between inclusion and matrix. The inclusions are further delineated by a surrounding chloritic zone. Rounded inclusions of quartzite (<20 mm) were observed infrequently. Towards the top of the middle layer small, rounded amygdales mark the gradation into the top layer.

Top Layer (Layer 3, Fig. 3.17)

This layer is a continuation of the middle layer and contains progressively more amygdales towards the top. The amygdales are very small (<6 mm) and did not develop the typical amygdaloidal texture of more mafic lavas. The amygdales consist of quartz, calcite, chlorite and epidote, but large (up to 100 mm) quartz or calcite-filled vesicles also occur. Towards the upper part of the top layer, the amygdales become elongated and subhorizontally aligned (Fig. 3.19).

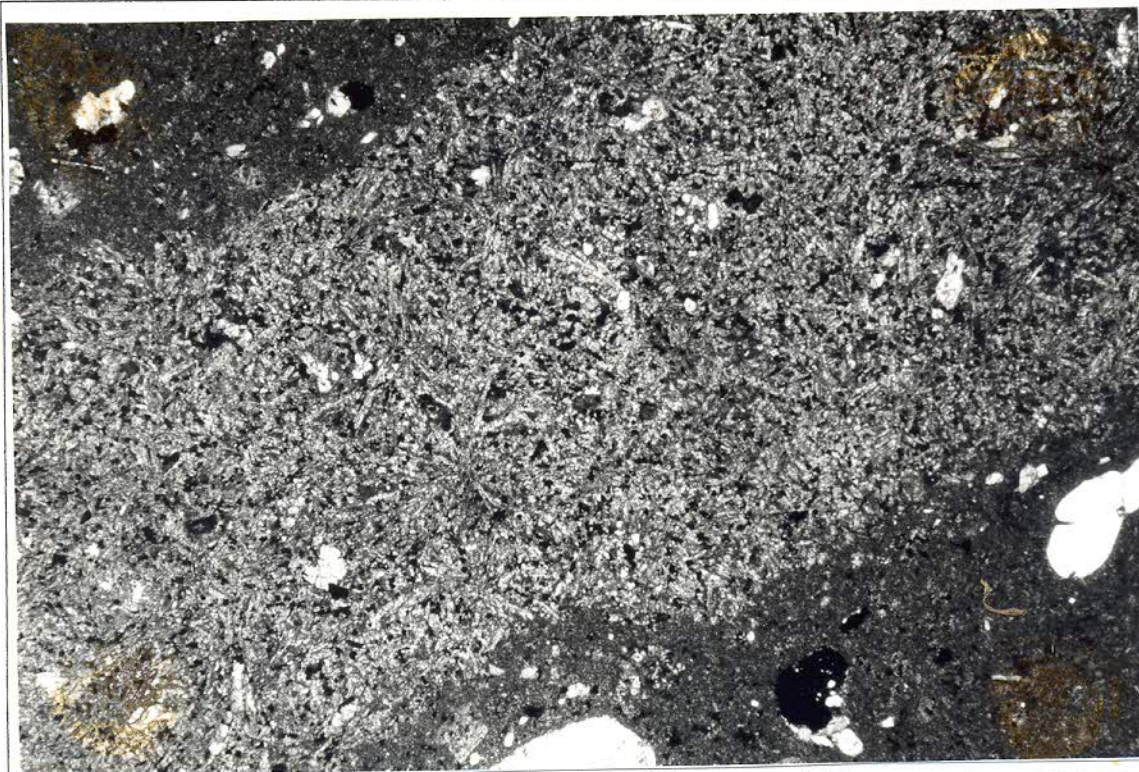


FIGURE 3.18: Non-porphyrific inclusion, hosted in quartz-feldspar porphyry. Note the well-defined, irregular outline and spherulitic feldspar. Sample FVM451; borehole UTK1. (Plane polarized light. Width of field is 12 mm).

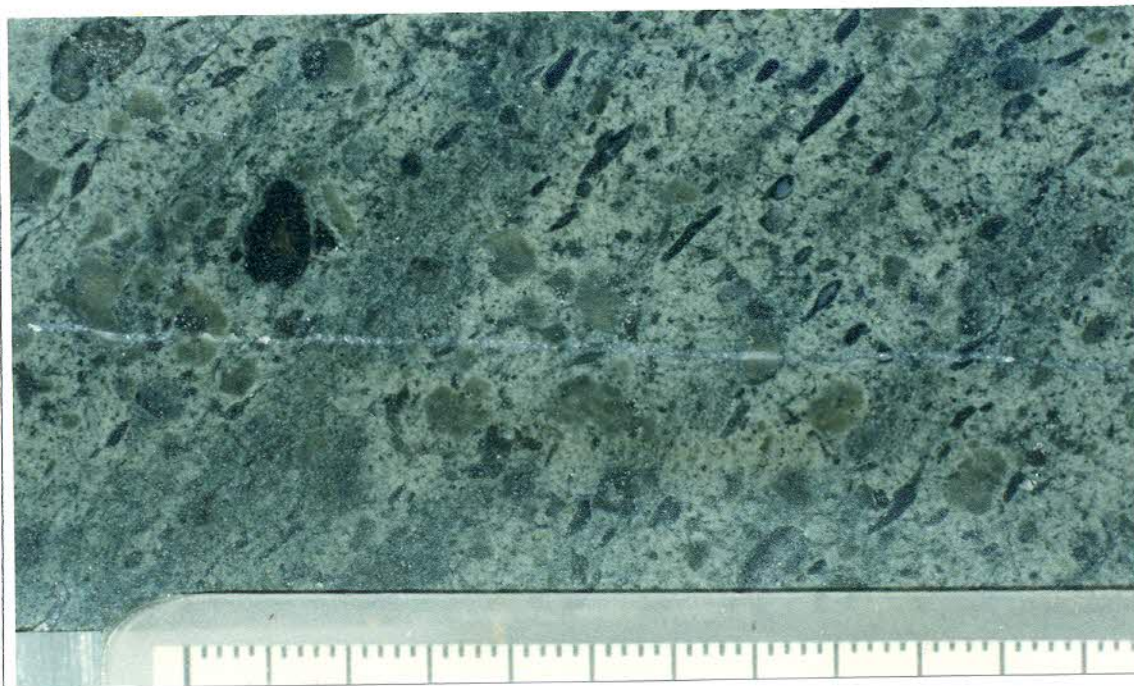


FIGURE 3.19: Parallel, elongated amygdales, filled by secondary chlorite and quartz, in the top layer of a flow unit. Sample FVM891; borehole SHS1. (Top to the right and scale in mm).

The phenocrysts in the top layer are mostly fractured and therefore smaller than those in the middle layer. In some flow units, the upper part of the top layer appears weathered and has a gravelly texture. These textures are clearly visible in flow units at the top of the Makwassie Formation, e.g. at the contact of the Makwassie and Rietgat Formations, indicating a hiatus. The upper contact of the top layer is very uneven and breccia may predominate in some cases, appearing as monolithological, chaotic assemblages. Fine-grained tuffaceous material often fills interstitial openings.

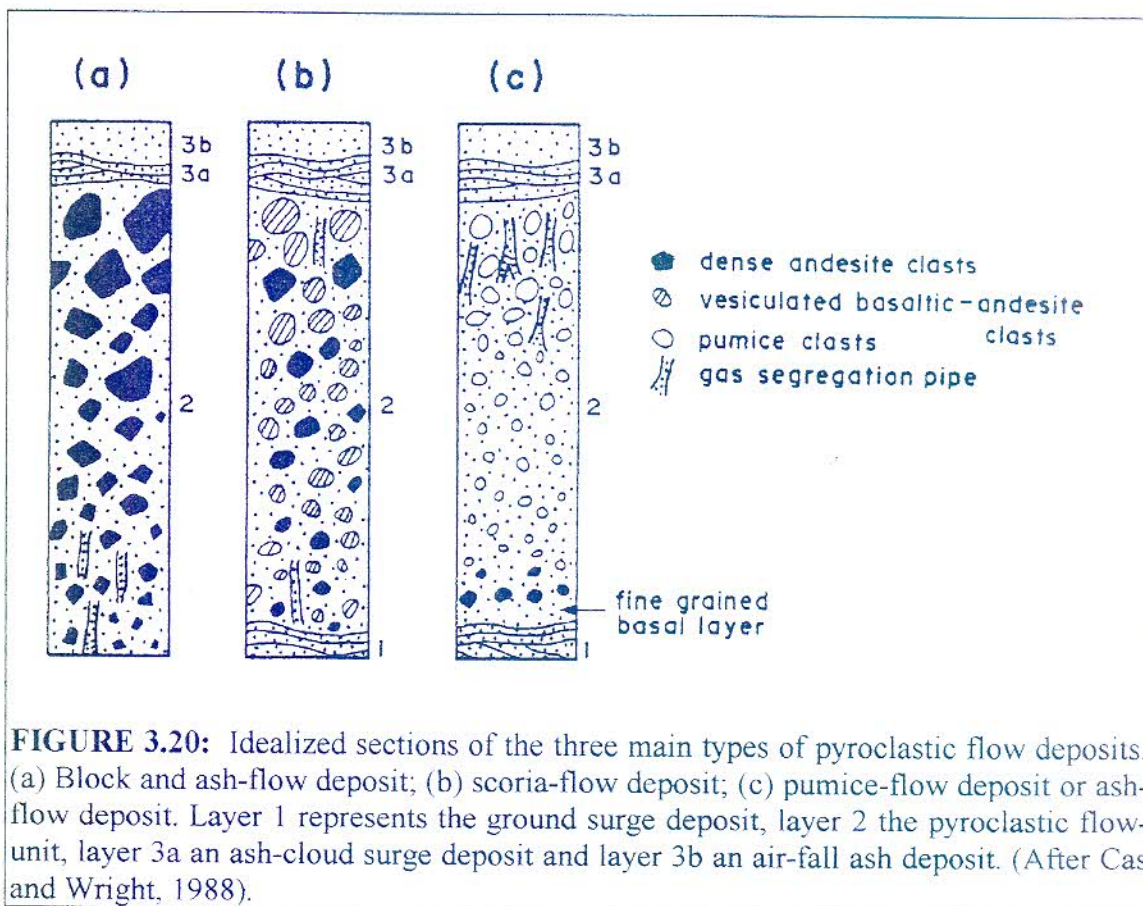
In most cases, the flow units are separated by a thin layer (up to 2 m) of fine-grained, tuffaceous rock (Fig. 3.17). The tuff beds are layered, with the laminae draping over protrusions of the uneven top of the underlying quartz-feldspar porphyry flow unit. Larger, very irregularly shaped, vesicular quartz-feldspar porphyry clasts are often embedded in the fine-grained material with the clasts indenting the layering. The tuffaceous material may penetrate metres down into breccia of the top layer of an underlying flow unit, filling interstitial spaces of the breccia. Where the fine-grained tuffaceous beds are absent, the quartz-feldspar porphyry flow units overlie each other directly with unit thickness varying from 30 m to 250 m (average of 80 m). In very thick flow units, the basal layer is about 2 m thick, whereas the top layer may be as thick as 30 m.

3.4.2 Interpretation

The flow units in the quartz-feldspar porphyries are interpreted as ash-flow units. Their lithology corresponds well with flow units produced by ignimbrite eruptions, as described by Sparks *et al.* (1973) and will be discussed using idealized sections of three main pyroclastic flow deposit types (Fig. 3.20).

The fine-grained basal layer (layer 1, Fig. 3.17) is typical of pyroclastic flows and correlates with the fine-grained basal layer of pumice-flow deposits (column (c) in Fig. 3.20 Sparks *et al.*, 1973; Cas and Wright, 1988). A fine-grained layer at the base of pyroclastic flows is attributed to the flow bottom being a zone of high shear. The shearing induces dispersing pressures on grains which act away from the flow bottom, so that larger grains (e.g. clasts and crystals) will drift away from this zone of maximum shear (Sparks, 1976).

Some of the flow units in the Makwassie porphyries have a cherty and featureless basal layer, interpreted originally to have been vitrophyric through rapid cooling of the flow base during deposition. Basal vitrophyres are typical of



pyroclastic flows and rhyolite lava flows (Ekren *et al.*, 1984). These vitrophyric basal layers are not extensively developed in the Makwassie porphyries, probably due to retention of heat after rapid deposition of successive flows, in which case the flows would cool as a single ignimbrite.

Flow units without distinctive basal layers were also observed in the Makwassie Formation. Pyroclastic flows are high particle concentration, poorly expanded, partially fluidized flows (Sparks, 1976). Wilson (1980) classified pyroclastic flows according to fluidization behaviour into non-expanded, expanded, and segregating types. Pyroclastic flow units without distinctive basal layers can be related to those with only a marginally expanded matrix during the original movement of the flow. Such flows will have high shear-strain rates and shear-induced grading may affect the whole flow, inhibiting the formation of a fine-grained basal layer (Cas and Wright, 1988).

The middle layer (layer 2, Fig. 3.17) forms the main body of the flow units and corresponds with **layer 2b** (Fig. 3.20) of Sparks *et al.* (1973). Quartz-feldspar porphyry clasts that occur in the lower part of this layer represent material of

higher density than the expanded matrix of the moving pyroclastic flow. This higher density material would settle at the flow base through gravitation (Cas and Wright, 1988), thus accounting for the concentration of larger size phenocrysts in the lower part of the middle layer. Preferential concentration of phenocrysts was also observed in ash-flows of the Sleeping Lion Formation in the Davis Mountains, USA, by Franklin *et al.* (1987) and by Henry *et al.* (1989). The chloritic laminae in some of the Makwassie Formation units (Fig. 3.7) could represent shear partings (now demarcated by chlorite) that developed due to high viscosity during the final settling of the flow unit (Fisher and Schminke, 1984).

The top layer (layer 3, Fig. 3.17) contains abundant gas vesicles which are often elongated and flattened (Fig. 3.19). Their elongated shape is attributed to shear strain during the final settling of the flow. The elongated amygdales further indicate that the porphyry matrix was in a liquid state during degassing, illustrated by the flattening of amygdales against overlying feldspar phenocrysts (Fig. 3.21).

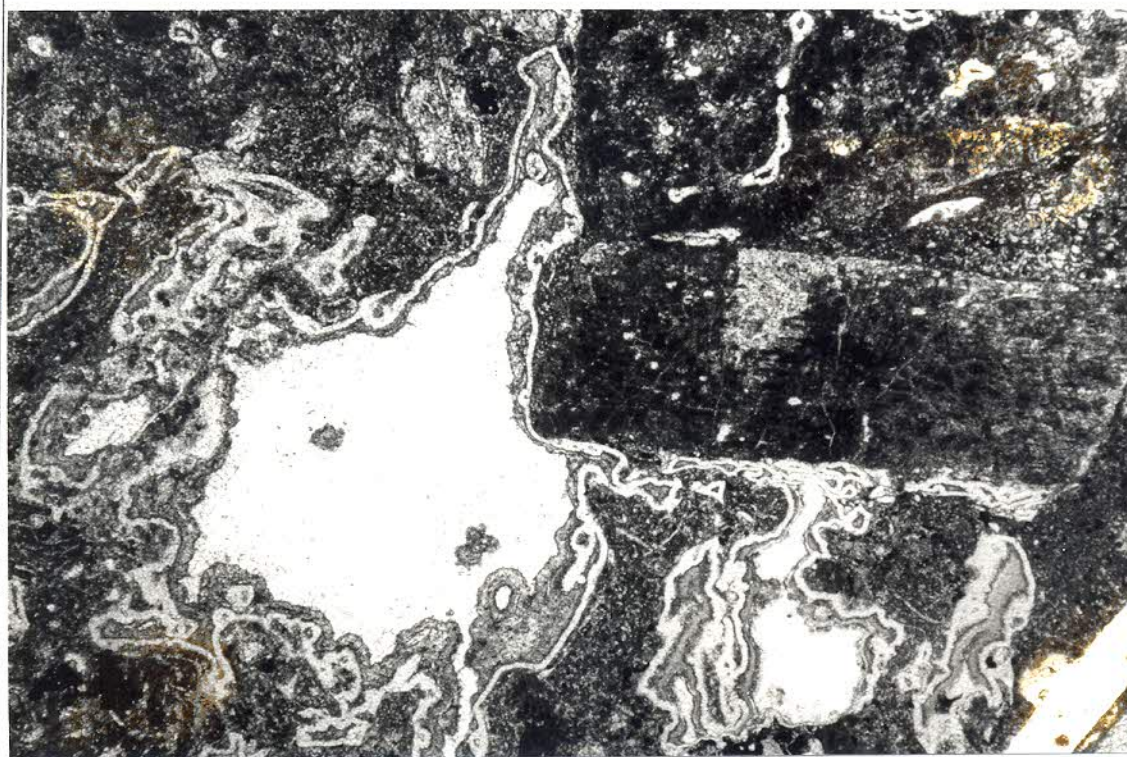


FIGURE 3.21: Gas vesicles that coalesced, flattened against, and flowed around a feldspar phenocryst when the porphyry was still in a liquid stage. The vesicles were progressively filled by very fine-crystalline quartz (narrow, white outer rim), followed by chlorite (irregular, grey rim), and crystalline quartz (white centre). Sample FVM293; borehole DF1. (Plane polarized light. Width of field is 12 mm).

The higher proportion of broken phenocrysts in the top layer of the flow unit reflects the smaller mass and slower settling rate of these fragments. Amygdaloidal-rich clasts were rarely encountered, but numerous small lithic fragments of quartz-feldspar porphyry were observed as breccia in the top layers of flow units.

The tuffaceous beds that separate the individual ash-flow units are interpreted as co-ignimbrite air-fall tuffs. Such ash-falls are an essential component of pyroclastic-flow deposits (Cas and Wright, 1988).

3.5 DISCUSSION

The contact between the Goedgenoeg and overlying Makwassie Formation marks the transition between a lower intermediate and an upper felsic volcanic succession. Interbedded mafic lava occurs throughout the succession, but is far more prevalent in the Goedgenoeg Formation than in the Makwassie Formation.

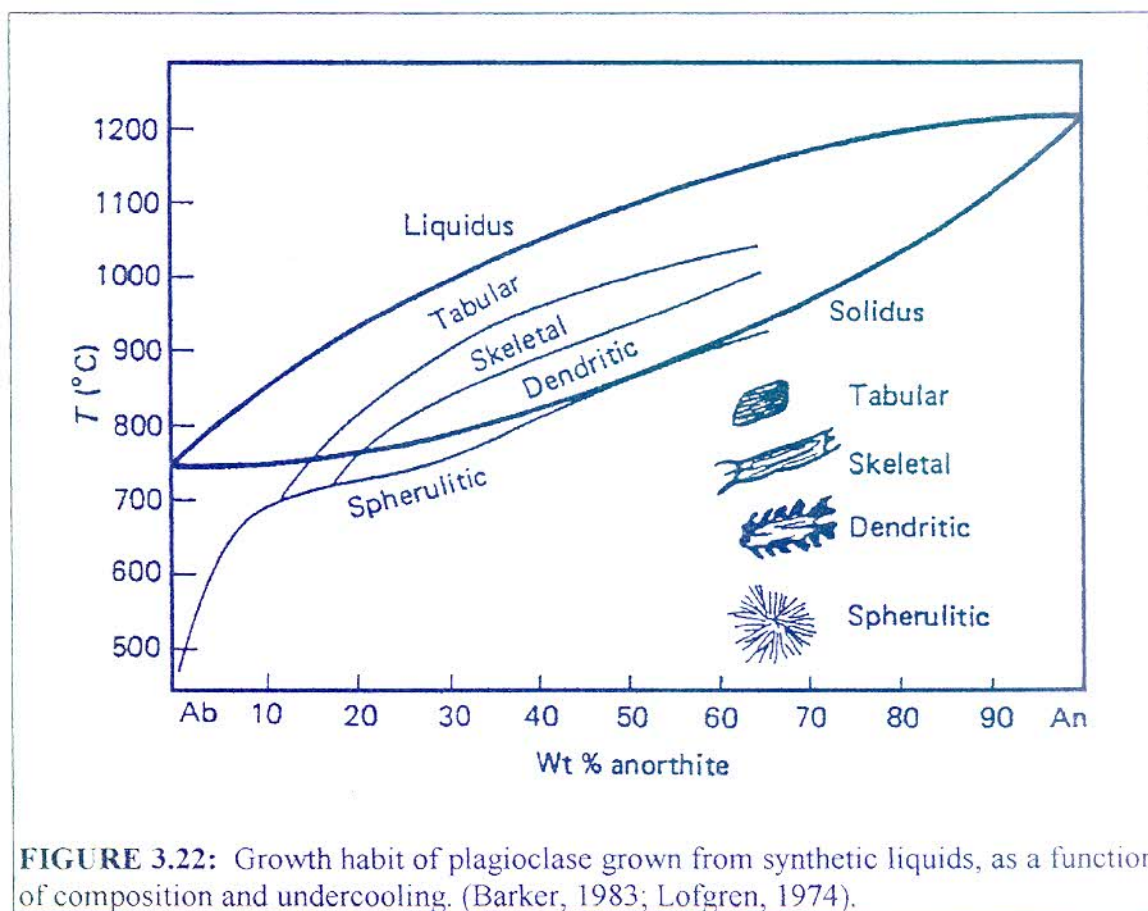
Lithological and petrographical textures indicate that both the Goedgenoeg and Makwassie Formation rocks are of extrusive origin. Original lava flow units can still be recognized in the mafic lavas and some of the feldspar porphyries, while ash-flow units are discernable in the quartz porphyries and some of the feldspar porphyries.

The phenocryst-rich feldspar-porphyry flow units are considered to be ash-flows, similar to the quartz-feldspar porphyries, as substantiated by the presence of fragmented phenocrysts. Less porphyritic flow units are regarded as lava flows which are recognized by amygdaloidal tops and bases, fine-crystalline matrix and intact phenocrysts. Primary textures were destroyed by secondary chloritization. Alteration had a more pronounced effect on the feldspar porphyries than on the quartz-feldspar porphyries; feldspar phenocrysts are altered to the extent that they are microscopically barely recognizable. Similar alteration on dacites was illustrated by Cas and Wright (1988; Fig. 14.3, p. 417). The intense alteration of the feldspar porphyries, compared to the quartz-feldspar porphyries, may be related to their more mafic composition.

The volcanic origin of the quartz-feldspar porphyries is apparent in thin sections. The round shape and embayments of the quartz phenocrysts are attributed to resorption, while fragmentation and the separation of these fragments indicate high strain during emplacement of the porphyry. The undulating extinction of some of the quartz phenocrysts is, however, attributed to tectonic deformation.

Dark amorphous rims around the quartz phenocrysts indicate reaction due to disequilibrium between the quartz and matrix.

Lower-grade greenschist metamorphism affected the original composition of the plagioclase and alkali-feldspar phenocrysts and resulted in the albitization of feldspars. Feldspar crystal embayments are attributed to resorption by the liquid matrix in igneous melts (Cox *et al.*, 1979), while skeletal forms are the result of moderate undercooling (Donaldson, 1976; MacKenzie *et al.*, 1982). For plagioclase, skeletal crystals form at undercooling rates of more or less 100° to 200° C (Fig. 3.22). Moderate to strong undercooling will occur particularly in extrusive or very near-surface intrusive rocks. The skeletal growth is induced by irregularities on the crystal surface which protrude into more undercooled liquid than the rest of the crystal surface, leading to rapid growth of these protuberances (Kirkpatrick, 1975; Barker, 1983; Fig. 3.23). If the crystal does not have the same composition as the melt, a compositional effect (constitutional supercooling) additional to the above thermal effect, can further accelerate the growth rate of protuberances (Kirkpatrick, 1974, 1975).



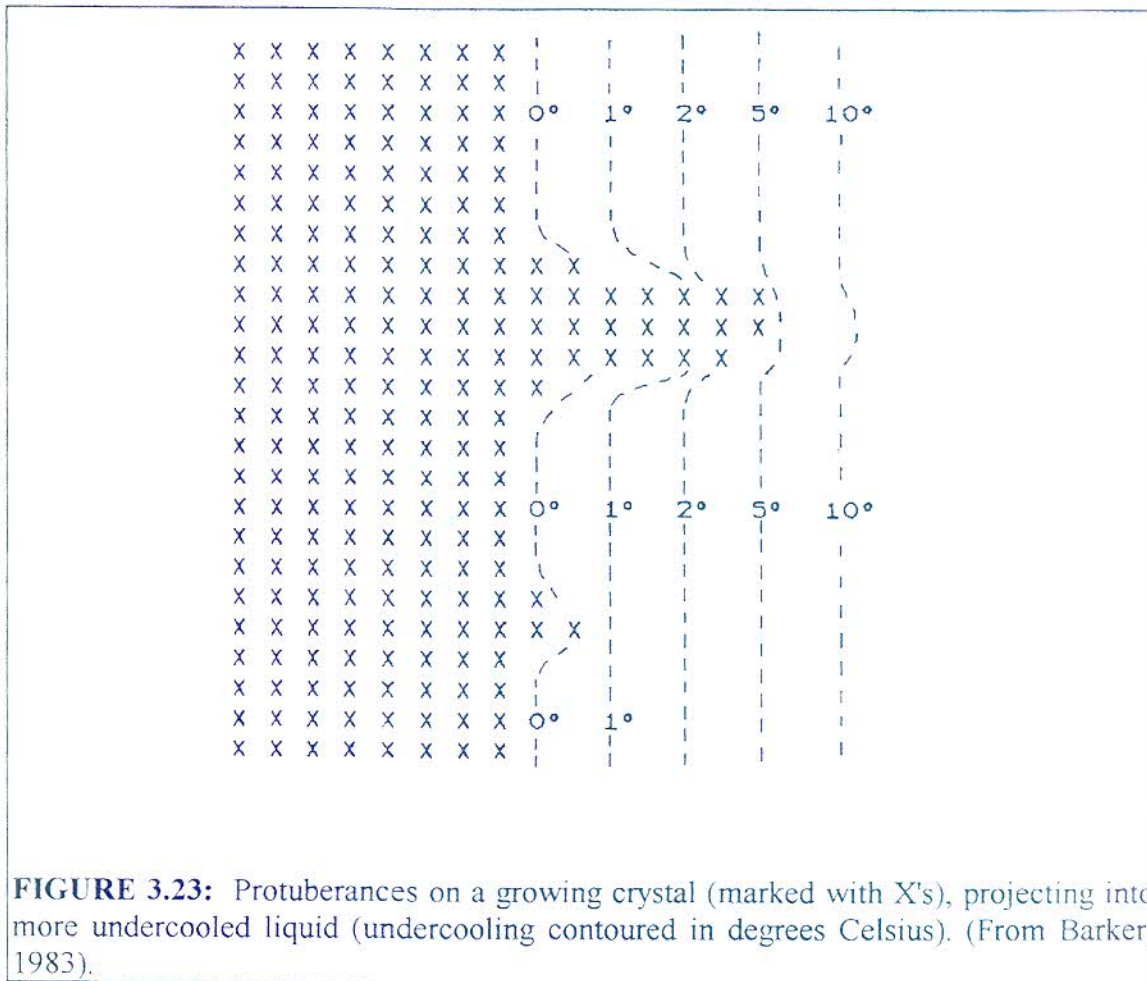


FIGURE 3.23: Protuberances on a growing crystal (marked with X's), projecting into more undercooled liquid (undercooling contoured in degrees Celsius). (From Barker, 1983).

The complex feldspar phenocryst assemblage (skeletal, subrounded and broken crystals, and glomerular phenocrysts) reflects the complex evolution of the Makwassie quartz-feldspar porphyry. The quench textures of apatite further signify rapid cooling of the porphyries. Apatite is capable of forming quench prisms with length to breadth ratios of 100:1, but still retaining an axial cavity for the length of the crystal (Cox *et al.*, 1979).

The felsitic textures in the porphyry matrix imply rapid and simultaneous crystallization of quartz and feldspar from undercooled liquid, vapour, or devitrifying glass in a near-surface environment (Smith, 1974; Barker, 1983). Granophyric devitrification is common in old, devitrified glassy rocks (Cas and Wright, 1988). Evidence for the secondary development of granophyric textures in the Makwassie porphyries as a result of devitrification, is found in the coexistence of granophyric textures and relict perlitic-crack textures (Fig. 3.24 petrographic analysis, Appendix F), and in the presence of relict spherulites. The quartz-feldspar porphyry matrix often displays poorly-visible chloritic spherulites (Fig. 3.8), which are remnants of the spherulitic devitrification stage before the granophyric devitrification stage was reached. The perlitic crack textures

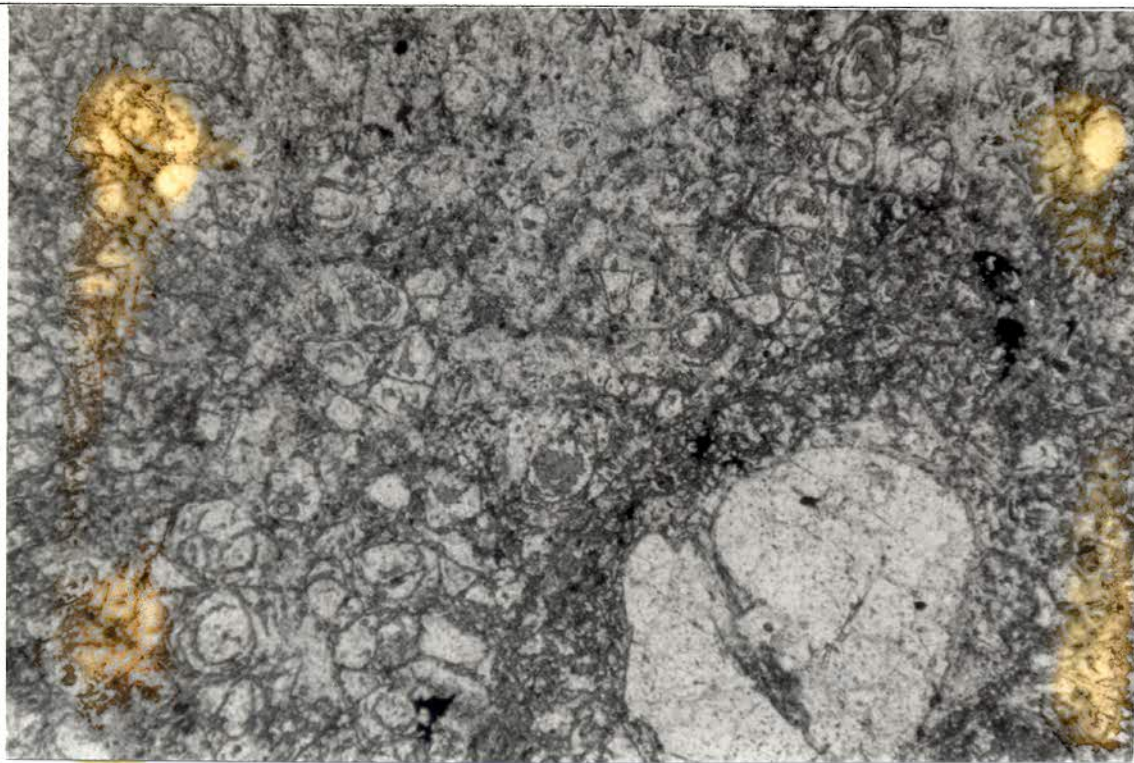


FIGURE 3.24: Perlitic-crack textures in devitrified glass which form the matrix of the quartz-feldspar porphyry in the top layer of a flow unit. The textures are accentuated by chlorite-filling of the original fractures. Sample FVM224; borehole ZH1. (Plane polarized light. Width of field is 6 mm).

developed as a result of volume change by hydration during devitrification of metastable glass (Barker, 1983). The textures were preserved by the original glass being devitrified to hydrous chlorite.

The contrasting presence of large crystals (phenocrysts) in an amorphous groundmass can be explained by the nucleation and growth rate of crystals during cooling of a magma below the liquidus temperature. The nucleation and crystal growth rate reach maxima at specific degrees of undercooling for a specific liquid, but the individual maxima of nucleation and growth rate are not necessarily at the same temperature (Fenn, 1977; Fig. 3.25). If cooling is slow enough, a high crystal growth rate and a low nucleation rate will prevail, leading to the formation of only a few, large-sized crystals (Barker, 1983). A greater cooling rate will produce more but smaller crystals. Progressive cooling rates will reach a point where the maximum growth rate is exceeded before the maximum nucleation rate is achieved, leading to the formation of only small crystals (e.g. the fine-crystalline texture of mafic lavas). If the temperature decreases very rapidly, both nucleation and growth rates will drop to zero and the disordered, although polymeric structure of the liquid will persist metastably in glass.

Devitrification (recrystallization) of the glass can then proceed. Therefore, the phenocrysts form part of the intratelluric (magma chamber) assemblage, while the groundmass represents the quenching stage of the volcanics.

It is important to notice that the presence of small phenocrysts, such as apatite and zircon, are just as significant as the presence of large phenocrysts such as feldspar. Minor phases such as apatite and zircon form small crystals even with slow cooling, but hold important clues as to the geochemical evolution of the magma. Large quantities of elements such as P and Zr are contained by these minerals, which will be reflected in fractionation trends.

The tuffaceous layers that separate the quartz-feldspar porphyry flow-units represent co-ignimbrite air-fall deposits. Lapilli and accretionary lapilli are present in some of these layers, while other layers may have been water-reworked.

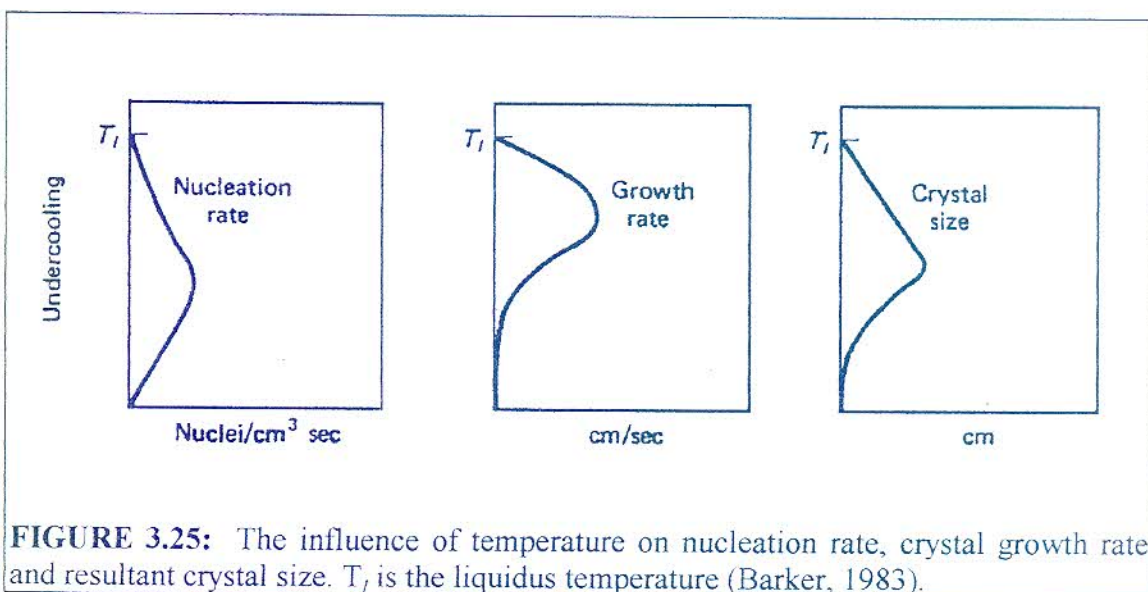


FIGURE 3.25: The influence of temperature on nucleation rate, crystal growth rate and resultant crystal size. T_l is the liquidus temperature (Barker, 1983).

148 731 82

4. DISTRIBUTION AND STRUCTURE OF THE GOEDGENOEG AND MAKWASSIE FORMATIONS IN THE BOTHAVILLE AREA

4.1 INTRODUCTION

The core of 23 boreholes drilled in the Bothaville area were available for this study (Appendix A). Published borehole information was reinterpreted (Appendix B) to enable construction of correlation diagrams and isopach maps. The collar positions of these boreholes and the distribution limits of the Goedgenoeg/Makwassie Formation are illustrated in Fig. 4.1. The depicted distribution limits coincide with those proposed by Winter (1965), except in the southern region where better definition was achieved through data published by Marshall (1986) on the Wesselsbron Dome.

The LO-27 grid system was used to compile the maps. The isopach and subtopographical maps in this chapter illustrate the area between 2 970 000 m and 3 070 000 m south of the equator on the X-axis, and between 10 000 m and 90 000 m west of 27° longitude on the Y-axis.

4.2 THICKNESS

The top contact of the Makwassie Formation is well constrained and so is the basal contact of the Goedgenoeg Formation. The contact between the Goedgenoeg and Makwassie Formations, however, is only known from the borehole cores that were examined during this study and was interpreted for the published borehole data. The constructed isopach trends for the combined Goedgenoeg and Makwassie Formation thickness are therefore more accurate than the isopachs for each Formation individually.

4.2.1 The Goedgenoeg and Makwassie Formations Combined

The combined thickness of the Makwassie and Goedgenoeg Formations increases steadily from the margins of the depository to a maximum in excess of 3 000 m in the vicinity of borehole KRF1 (Fig. 4.2). It thins over the Ontario Arch and southwards towards the Waterpan and Concord Arches, until it discontinues further southeastwards. There is, however, a thickening of about 200 m between the Ontario and Concord Arches, which forms an extension of the South Bothaville Basin. North of the Ontario Arch the Makwassie/Goedgenoeg Formation thickens substantially into the Vierfontein Basin, which appears to be connected to the Harrisburg Basin. It continues northeastwards from the Vierfontein Basin under the cover of Transvaal Supergroup. The northern

distribution limit in this area is defined by the Orkney Arch, forming the Orkney and Klerksdorp Goldfields, where only a thin sequence of Klipriviersberg Group lava overlies the Witwatersrand Supergroup.

The thickening of the Goedgenoeg/Makwassie Formation in the Western Border Trough can be followed northwards into the South Bothaville and Harrisburg Basins. Dramatic thinning in the region of the Zandfontein Arch is indicated by borehole EL1, which intersected rocks of the Lower Witwatersrand Supergroup underlying Bothaville Formation (Winter, 1965). The original stratigraphy of this area is disrupted by a major structural feature of post Platberg or possibly of post Ventersdorp age. This anomalous configuration is also evident in borehole ZN1, which intersected possible West Rand Group rocks underlying the Makwassie Formation. This situation has been reflected in the isopach and subtopography maps (Figs. 4.2-4.4; Figs. 4.6-4.8), but not in the small scale sections (Fig. 4.9d; 4.9i).

Westwards from the Harrisburg Basin the Goedgenoeg/Makwassie Formation gradually thins towards the Makwassie Hills area, where it outcrops (outside the area depicted by Fig. 4.2). Borehole LLE1 was collared in this outcrop and although it was drilled to a depth of 3659 m, failed to penetrate the base of the Goedgenoeg Formation (Chapter 6). A major fault with more or less north-south strike is therefore inferred, which forms the western margin of the Bothaville depository. The southwestern limit of the Goedgenoeg/Makwassie Formation is constrained by the Wesselsbron Dome, while outcrop of Basement Igneous Complex defines the northwestern limit.

4.2.2 The Goedgenoeg Formation

The Goedgenoeg Formation is largely confined to the Western Border Trough, South Bothaville and Harrisburg Basins (Fig. 4.3). It gradually thins towards the Ontario, Concord and Waterpan Arches, while dramatic thinning occurs at the Zandfontein Arch. The Goedgenoeg Formation does not occur in the western parts of the Bothaville area, *i.e.* in the vicinity of borehole Zonderhout. The Goedgenoeg Formation is also absent from the northern parts of the Vierfontein Basin.

Winter (1965) described the 'Langgeleven-type' facies of the Makwassie Formation (equivalent to the Goedgenoeg Formation?), which occurs 'towards the base' of the Makwassie Formation, as occurring only in the northwestern part of the Bothaville area (*i.e.* in the Harrisburg Basin).

Interbedded sedimentary rocks and lava in the basal part of the Goedgenoeg Formation have been intersected in boreholes KRF1 and HB, indicating that this facies is possibly restricted to the Harrisburg Basin. The occurrence of this facies in the South Bothaville Basin could not be established since the boreholes in this area have failed to penetrate the base of the Goedgenoeg Formation.

Note that the absence of the Goedgenoeg Formation from the Zandfontein Arch is due to a major structural feature of post Platberg or possible post Ventersdorp age.

4.2.3 The Makwassie Formation

This Formation thickens gradually westward from the Waterpan and Concord Arches until it reaches more than 1000 m in the western part of the Harrisburg Basin (Fig. 4.4). The Makwassie Formation thickness increases in the eastern part of the Vierfontein Basin. Dramatic thinning on the Zandfontein Arch is conspicuous, but it is apparently a post-depositional structural feature.

Note that the thinning and absence of the Makwassie Formation from the Zandfontein Arch is due to a major structural feature of post Platberg or possible post Ventersdorp age. Originally the Platberg volcanic succession in this area was probably of substantial thickness.

4.2.4 The Garfield Member

Lack of data hampers construction of a detailed isopach map of the Garfield Member. In addition to the thickness indicated in Fig. 4.5, Winter (1965) also reports the occurrence of the Garfield Member in boreholes GR2, TEA1, JY4 and GF1 in the Vierfontein Basin. It therefore appears that the Garfield Member is largely confined only to the Harrisburg and Vierfontein Basins. The interpreted occurrence of this Member in the unlogged boreholes (Appendix B) is probably overoptimistic, which is also reflected in the sections depicted in Figure 4.9.

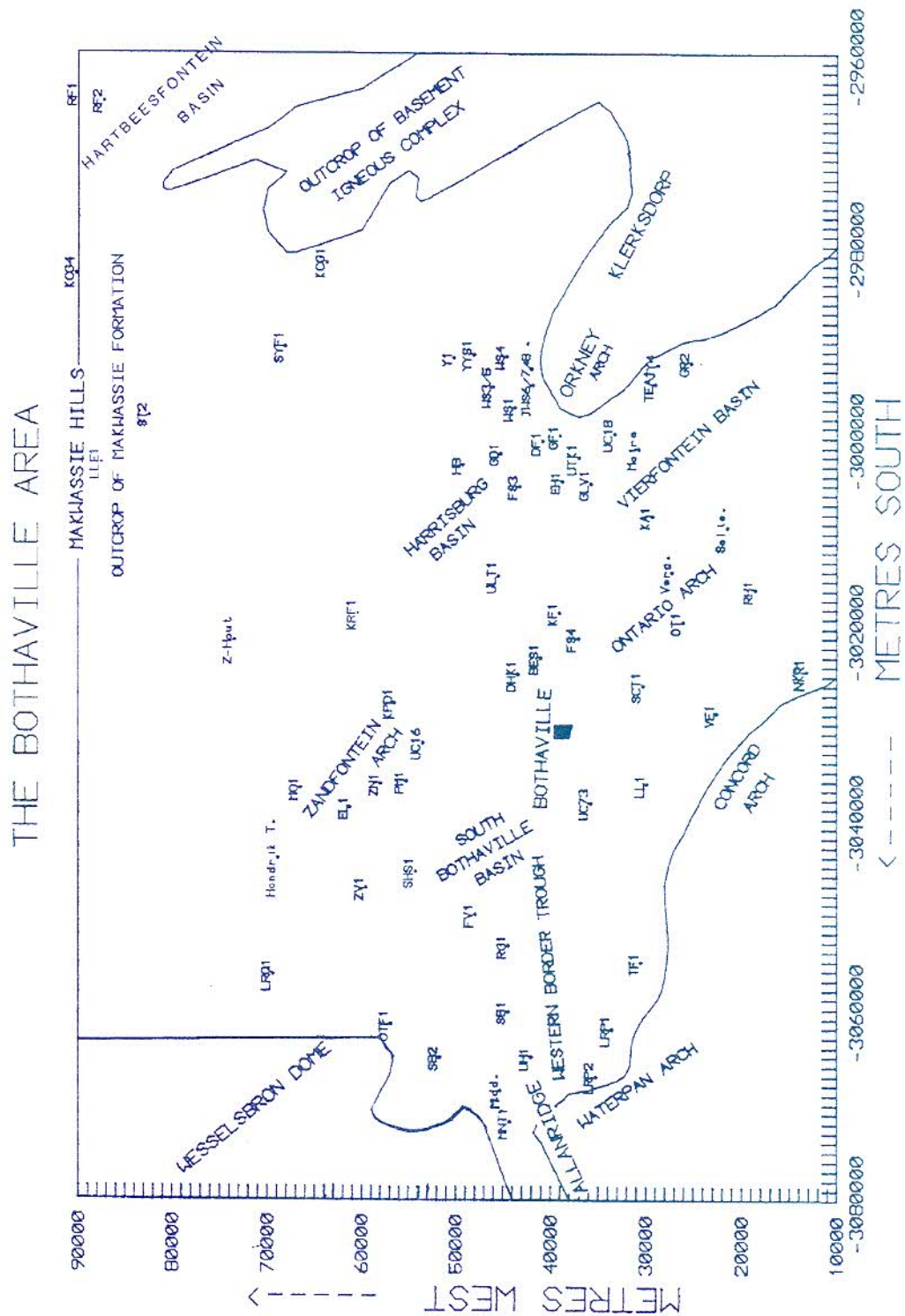


FIGURE 4.1: Collar positions of the boreholes in the Bothaville area which were used to construct the isopach maps. The distribution limits of the Goedgenoeg/Makwassie Formation are indicated by hatched areas. Note that the following isopach maps cover the area between 15 000 m and 85 000 m west of the 27° parallel, and between 2970 000 m and 3070 000 m south of the equator.

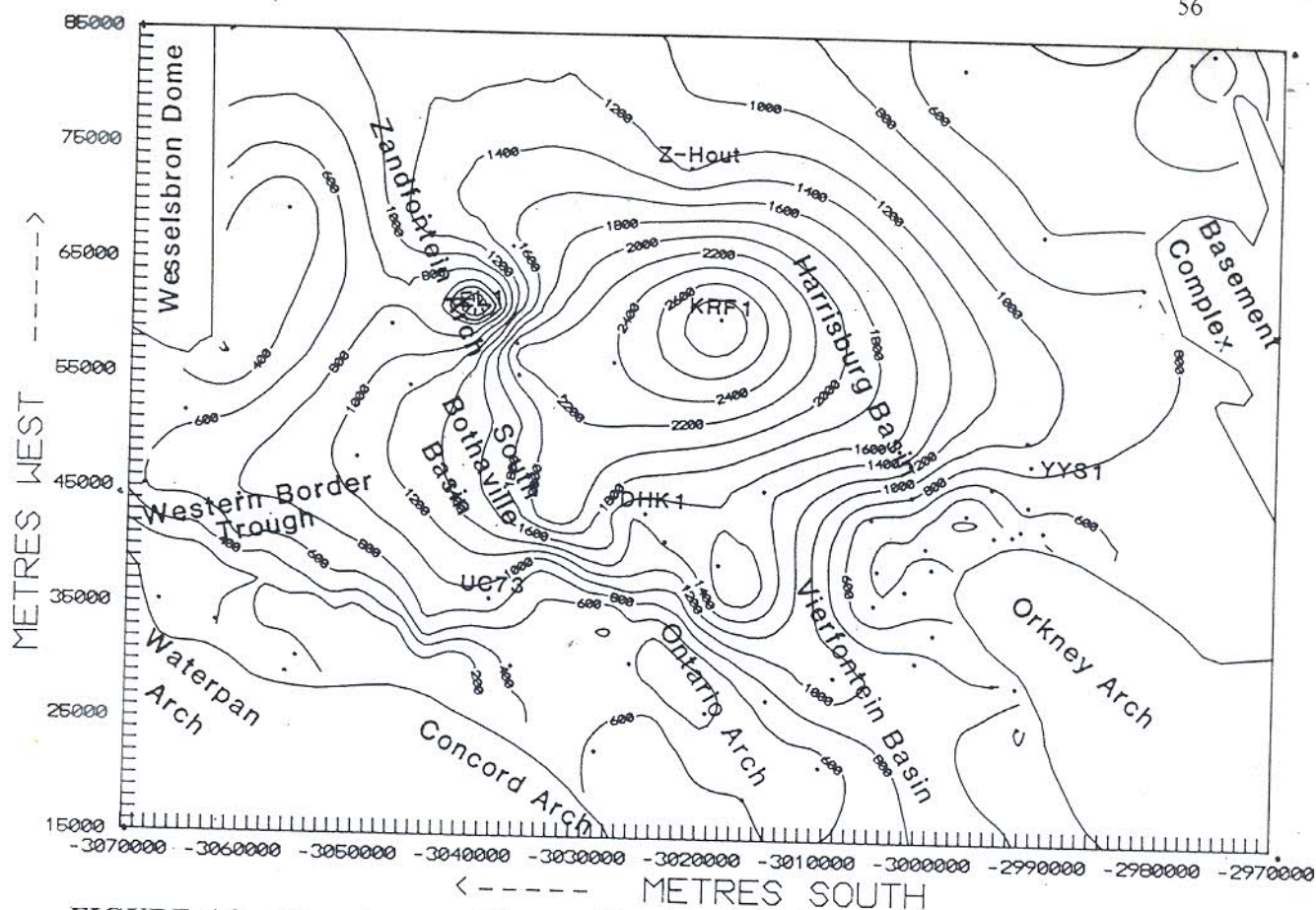


FIGURE 4.2: Isopach map of the combined total thickness of the Goedgenoeg and Makwassie Formations. Isopachs are in 200 m increments.

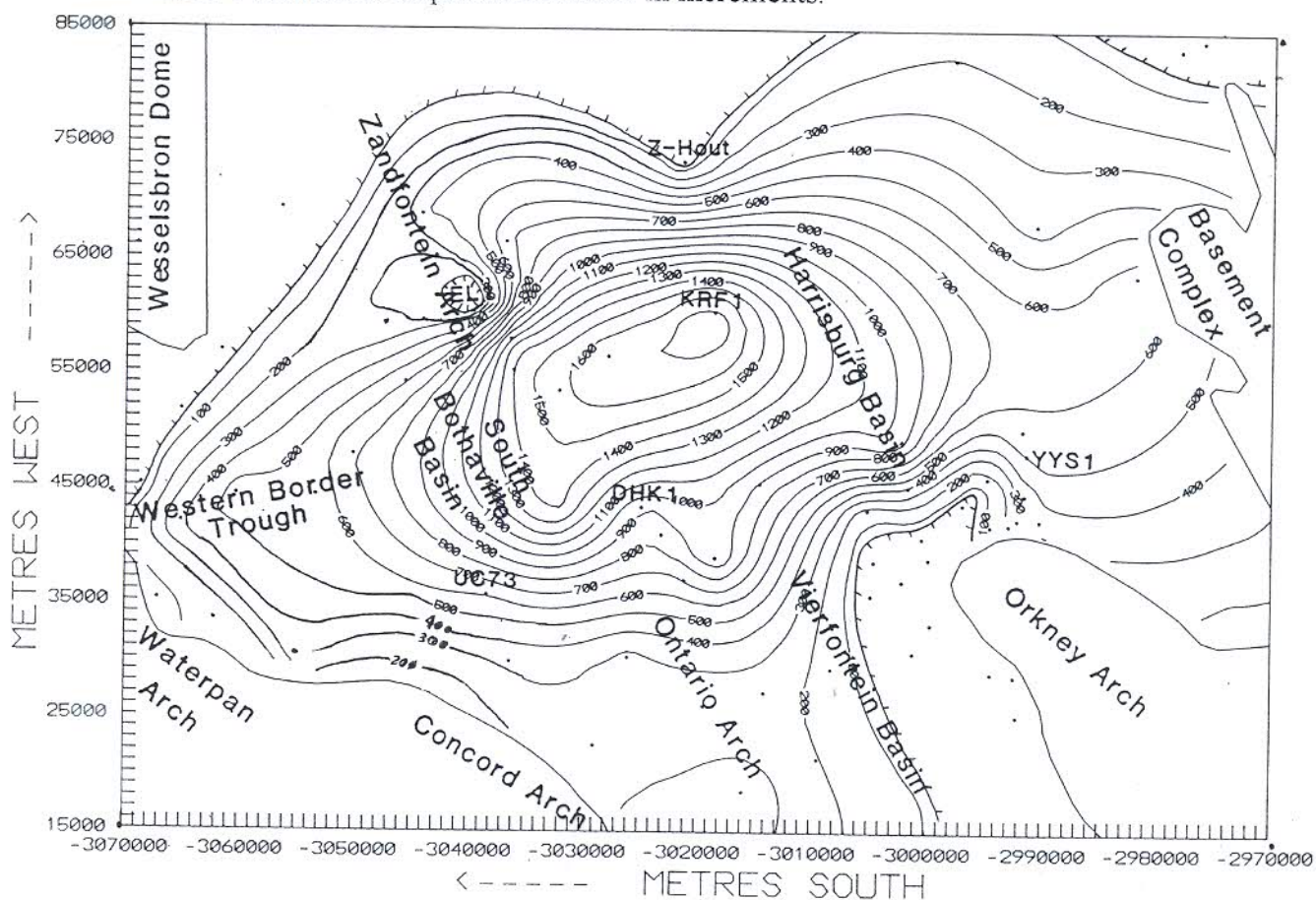


FIGURE 4.3: Isopach map of the Goedgenoeg Formation. The hatched line is the zero isopach. Isopachs are in 100 m increments.

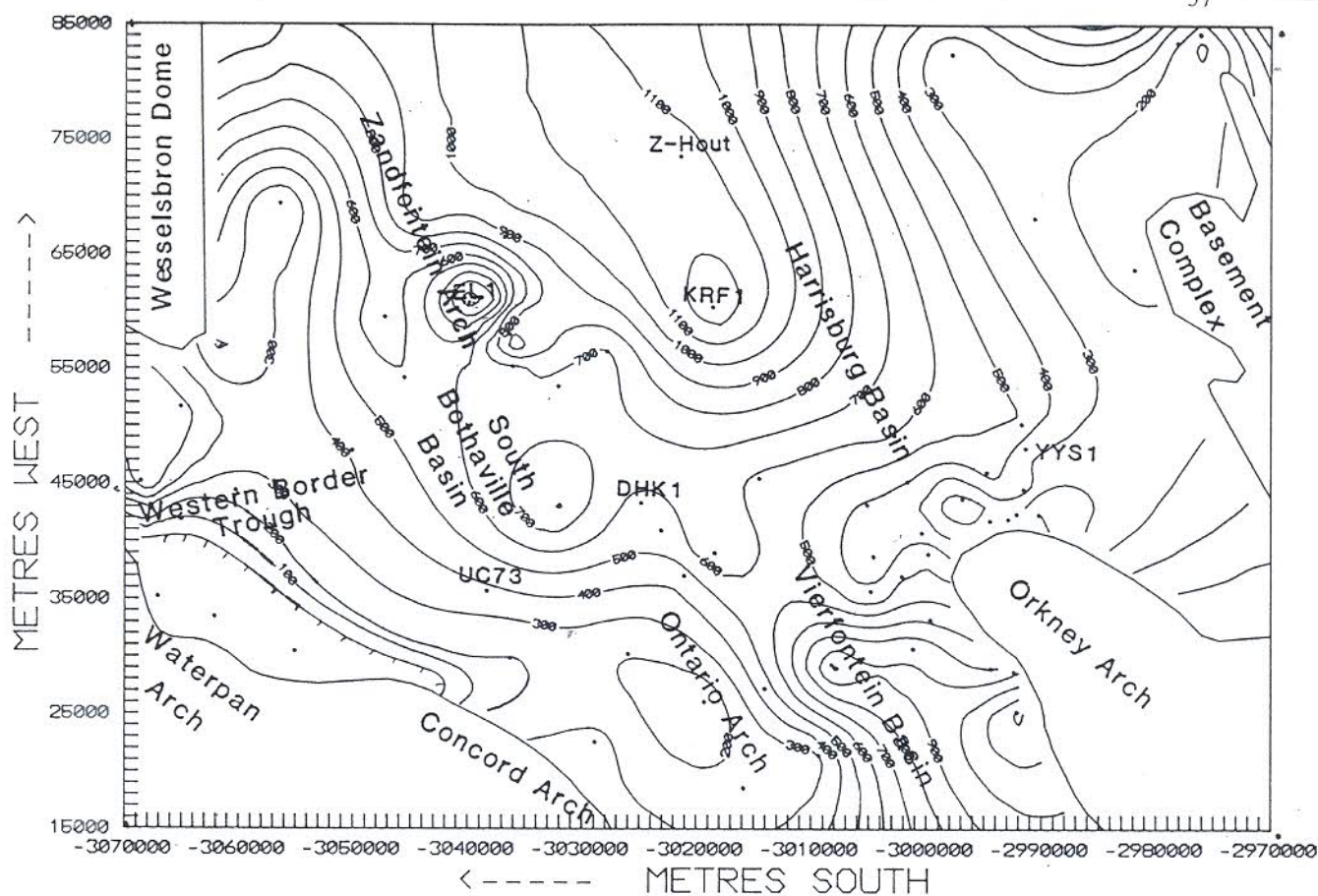


FIGURE 4.4: Isopach map of the Makwassie Formation. Isopachs are in 100 m increments.

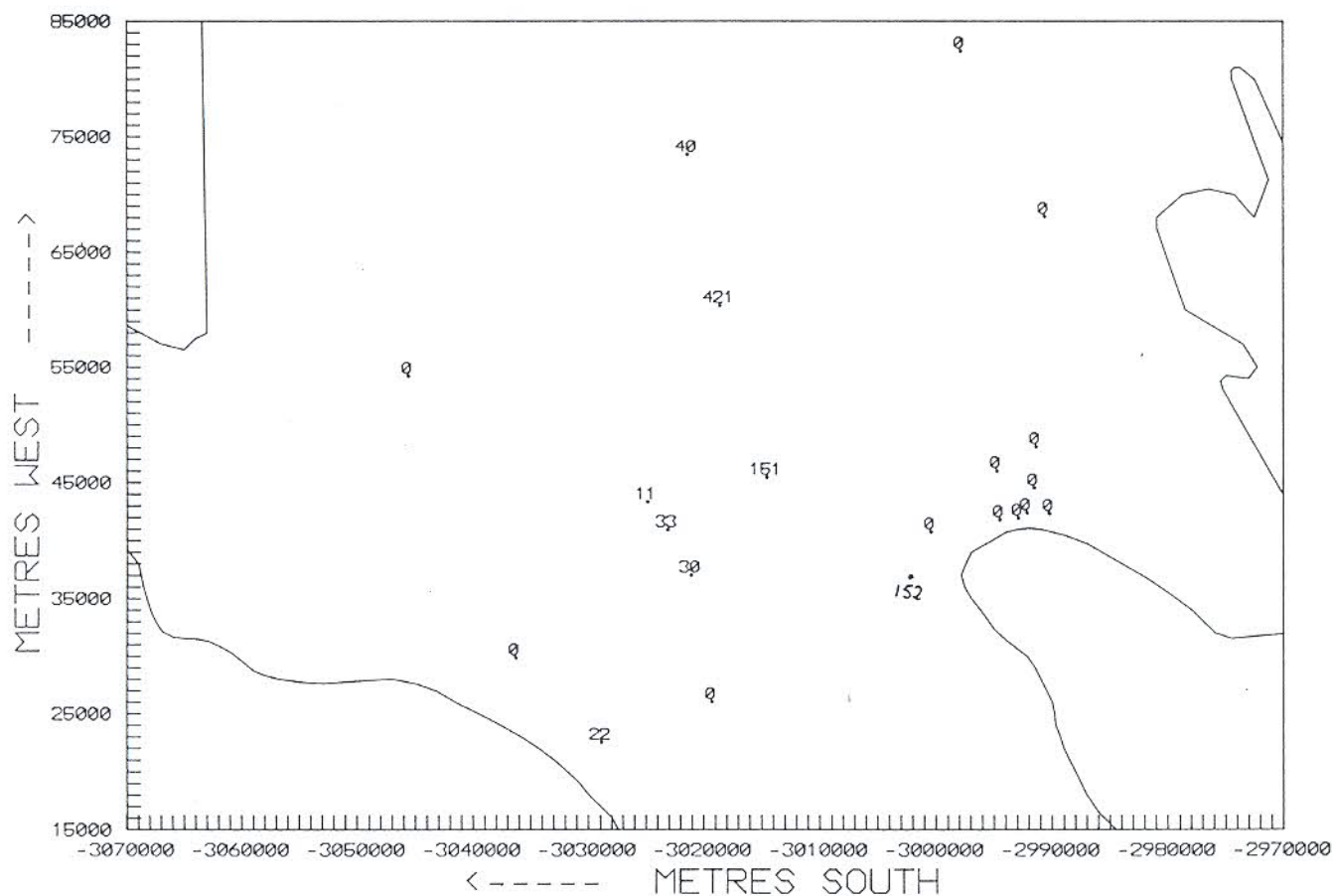


FIGURE 4.5: Confirmed occurrence and thickness (in metres) of the Garfield Member.

4.3 SUBTOPOGRAPHY

The subtopographical maps illustrate the contact between two lithostratigraphic units, e.g. between the Goedgenoeg and Makwassie Formations, thereby depicting the suboutcrop "surface" of the top of the lowermost unit. Where a unit is not developed, the chronological equivalent of the subtopography under discussion is depicted. The subtopographical maps highlight similarities or discrepancies between the thickness and elevation of specific units. This enables recognition of pre- and post-depositional faulting.

The subtopographical maps, however, cannot be regarded as palaeotopographical maps since the palaeotopography has been changed by post-depositional faulting. It must also be kept in mind that the isopach and subtopographical maps depict the *current* distribution of the Makwassie Formation; the original distribution was also affected by post-depositional erosion.

4.3.1 Base of the Goedgenoeg Formation

The subtopography of the Makwassie Formation base defines the depressions of the South Bothaville and Harrisburg Basins (Fig. 4.6). This low area continues along the Western Border Trough and also branches off from the Harrisburg Basin into the Vierfontein Basin. Subtopographical highs are defined by the Concord, Waterpan, Ontario and Zandfontein Arches. Further high-lying areas are associated with the Wesselsbron Dome in the south and with the Orkney Arch in the northeast. The basal subtopography of the Makwassie Formation slowly rises towards the outcrop of Basement Igneous Complex in the northwest.

When the subtopography of the Goedgenoeg Formation basal contact (Fig. 4.6) is compared with the isopachs of the combined Goedgenoeg and Makwassie Formations (Fig. 4.2), it appears that the thickness and floor subtopography largely conform, except in the South Bothaville Basin. The thickness of the Goedgenoeg Formation (Fig. 4.3) and thickness of the Makwassie Formation (Fig. 4.4) also do not conform with the South Bothaville Basin depression.

4.3.2 Contact of the Goedgenoeg and Makwassie Formations

The subtopographical expression of the contact between the Goedgenoeg and Makwassie Formations differs somewhat from that of the Goedgenoeg Formation base (Fig. 4.7 compared to Fig. 4.6). Depressions are still defined by the South Bothaville Basin and Western Border Trough, the western part of the Harrisburg Basin and the eastern part of the Vierfontein Basin. The Ontario and Zandfontein Arches have now become more prominent. The situation along the Orkney Arch,

Wesselsbron Dome and outcrop of Basement Igneous Complex is still unchanged.

The thickness of the Makwassie Formation (Fig. 4.4) compares well with the present subtopography of the Makwassie Formation base (Fig. 4.7), except in the South Bothaville Basin area.

4.3.3 The Makwassie Formation Top

The present subtopography of the Makwassie Formation top shows a consistent slope from west to east, except for a depression formed by the South Bothaville Basin and Western Border Trough (Fig. 4.8). The eastern part of the Vierfontein Basin forms the lowest-lying area. Most of the topographical features discernible in the previous subtopographical maps are now obliterated, e.g. the Harrisburg Basin and Zandfontein Arch.

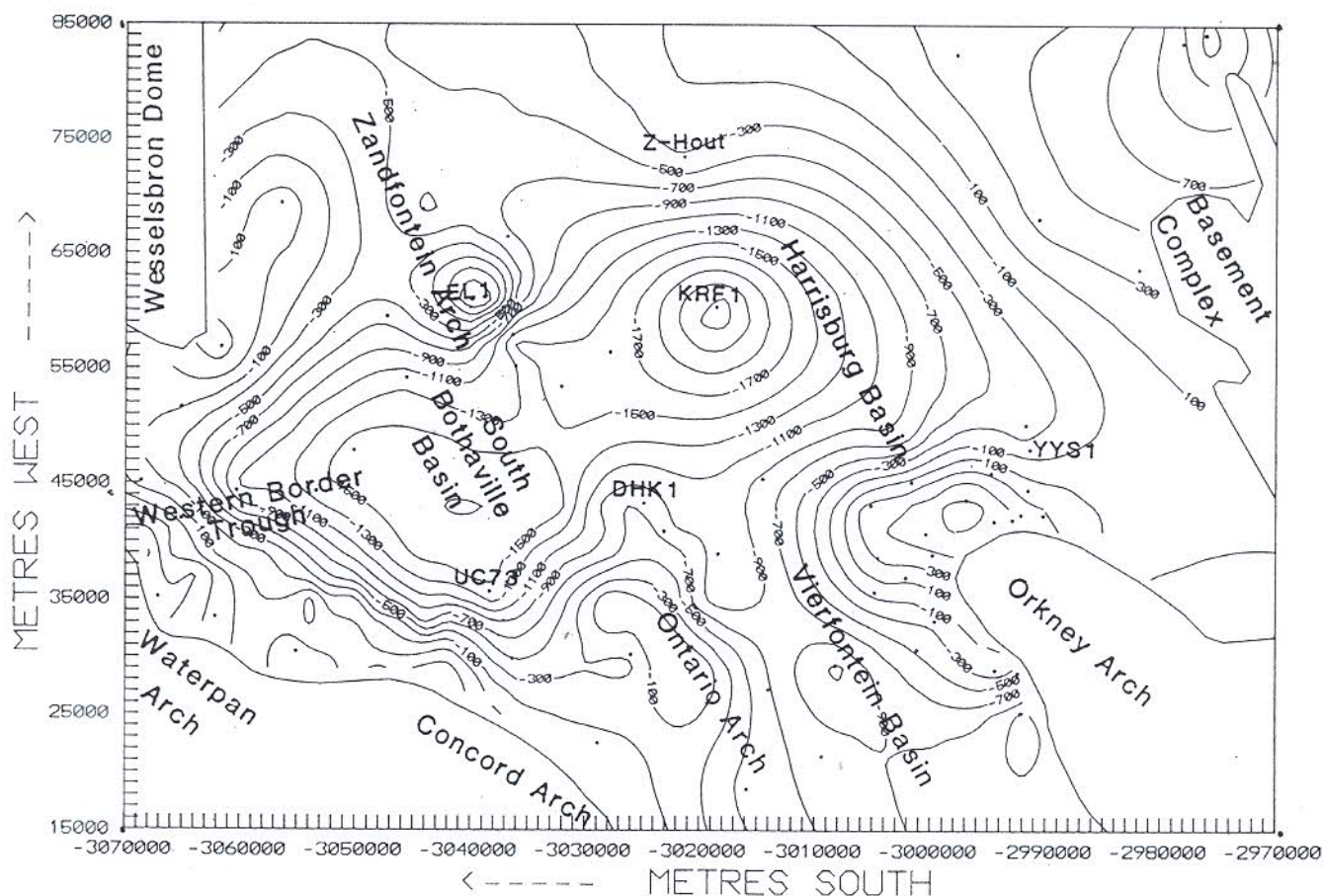


FIGURE 4.6: Subtopography of the basal contact of the Goedgenoeg Formation. (In 200 m increments above or below (minus) sea level).

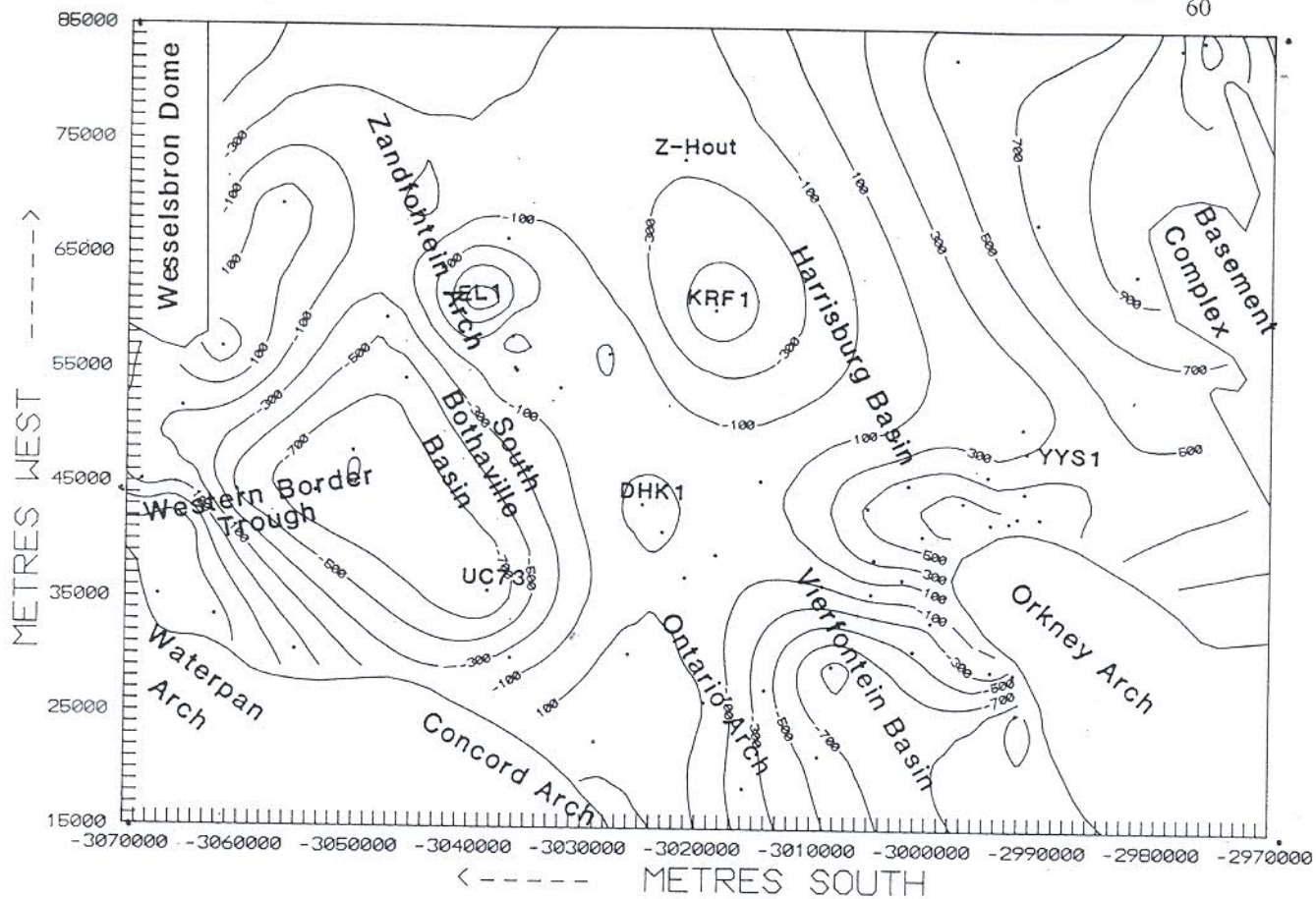


FIGURE 4.7: Subtopography of the top of the Goedgenoeg Formation, i.e. the contact between the Goedgenoeg and Makwassie Formations. (In 200 m increments above or below (minus) sea level).

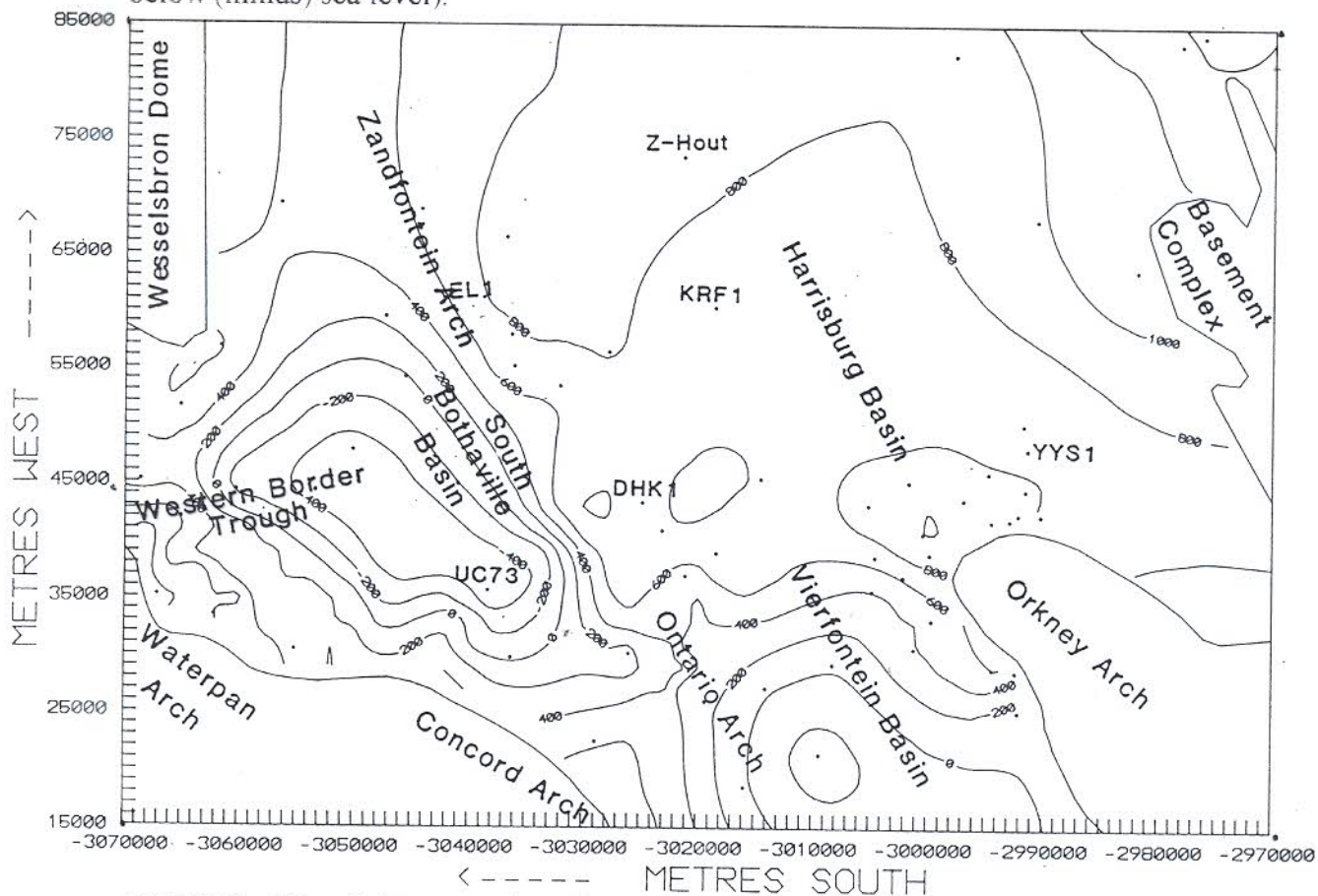


FIGURE 4.8: Subtopography of the top of the Makwassie Formation. (In 200 m increments above or below (minus) sea level).

4.4 CORRELATION DIAGRAMS

Various sections are illustrated in Fig. 4.9, depicting stratigraphic correlation between boreholes in the Bothaville area. Correlation was not restricted to just the Goedgenoeg and Makwassie Formations; all available stratigraphic data were utilized. Only major faults with a throw of over a thousand metres are depicted on these diagrams. Smaller faults which affected the Platberg Group and their throw are indicated at the top of each diagram. The presence of these smaller faults are deduced from correlation discrepancies between boreholes.

The eastern distribution limit of the Goedgenoeg and Makwassie Formations is controlled by a major fault zone, which may be an extension of the De Bron Fault (Fig. 4.9a-c; the fault zone is depicted as a single fault line on the large scale diagram of Fig. 4.9c). The Goedgenoeg and Makwassie Formations thin towards this fault zone and are absent on the Waterpan and Concord Arches to the east of the fault. The western limit is also influenced by a major fault zone, but to the west of this fault the thickness of the Goedgenoeg and Makwassie Formations increases dramatically (Fig. 4.9c), as intersected in borehole LLE1 (Appendix A). The situation further to the south of borehole LLE1 is not known due to lack of data, but it can be expected that the Wesselsbron Dome will have an influence in this extreme southwestern Bothaville area.

Borehole KRF1 (section A; Fig. 4.9c) was drilled into the South Bothaville/Harrisburg Basin between boreholes DHK1 (east) and Zonderhout (west). Between boreholes BES1 (west) and VE1 (east) post-Makwassie subsidence is evident, as a result of information from borehole SCT1. This graben structure was filled by Rietgat Formation lavas. The Goedgenoeg and Makwassie Formations thin towards the eastern fault-controlled limit, where it was partially eroded during Bothaville Formation times.

The Wesselsbron Dome is depicted in sections B and C (Figs. 4.9d and e). Between the Wesselsbron Dome and the eastern distribution limit, a post-Makwassie graben structure is again evident in Fig. 4.9d, forming the Western Border Trough which is filled by Rietgat Formation lavas and Bothaville Formation sediments. The Goedgenoeg and Makwassie Formations initially thicken to the west of the Wesselsbron Dome, but the Goedgenoeg Formation disappears westwards towards borehole Zonderhout so that only the Makwassie Formation is developed in this area.

Further south from section B a narrow valley cuts into the Wesselsbron Dome (section C; Fig. 4.e) and is filled by sediments of the Witwatersrand Supergroup and Kameeldoorns Formation. Although this valley could represent a Witwatersrand erosional feature, the thickness of the Goedgenoeg and Makwassie Formation volcanics also increases into this valley, possibly indicating subsidence. The Kameeldoorns and Makwassie Formations are still present on the central part of the Wesselsbron Dome, but are expected to thin out and disappear further south (higher up on the northwards-sloping dome).

The Orkney Arch is represented in section D (Fig. 4.9f). The Goedgenoeg and Makwassie Formations thin from the west towards this Arch, but in the Vierfontein Basin towards the east, boreholes JY4 and GR2 failed to penetrate the base of the Makwassie Formation while the Goedgenoeg Formation is apparently absent from this area. To the west of the Orkney Arch the Goedgenoeg and Makwassie Formations gradually thin towards the western margin fault zone. West of this fault zone, there is a dramatic increase in thickness. To the south of section D, the Makwassie Formation drapes over a Klipriviersberg Group high (section E; Fig. 4.9g), which forms an extension of the Orkney Arch. This indicates that uplift of this Arch continued after Makwassie Formation times.

Section F (Fig. 4.9h) illustrates that the Makwassie Formation is poorly developed in places and the Garfield Member, which occurs as an interbedded unit in the Makwassie Formation, directly overlies the Goedgenoeg Formation. The Rietgat Formation, Garfield Member and Goedgenoeg Formation now follow directly onto one another. Since these formations have similar lithological characteristics, this stratigraphic sequence may be difficult to recognize.

A section from north to south through the western part of the Bothaville area (section G; Fig. 4.9i) illustrates that the thickness of the Goedgenoeg Formation increases from the Orkney Arch to the Harrisburg and South Bothaville Basins, but discontinues against the Wesselsbron Dome. The thickness increase of the Makwassie Formation is less dramatic. The presence of the Garfield Member was confirmed in boreholes ULT1 and DHK1, but it continues possibly as far south as borehole Hendrik Theron.

Section H (Fig. 4.9j), from north to south through the central part of the Bothaville area, highlights the Vierfontein Basin (boreholes KF1 and FS4), the Ontario Arch (borehole BES1) and the South Bothaville Basin and Western Border Trough (boreholes UC73, RG1 and SB1). In this section the northern limit of the

Goedgenoeg and Makwassie Formations are formed by the Orkney Arch and the southern limit by a fault zone. Note that the South Bothaville Basin and Western Border Trough are largely filled by post-Makwassie formations and therefore underwent subsidence after deposition of the Makwassie Formation.

The relationship between the Orkney Arch, Vierfontein Basin, Ontario Arch and Concord Arch is further illustrated by section I (Fig. 4.9k), which depicts the eastern part of the study area. Note that post Makwassie subsidence of the the Vierfontein is indicated by the thick Rietgat succession in the Basin.

The northwestern margin of the Bothaville area is bordered by Basement Igneous Complex. The Makwassie Formation discontinues against this horst, but the Goedgenoeg Formation does occur in the Hartbeesfontein Basin to the north (sections J and K; Fig. 4.9l and m).

4.5 DISCUSSION AND STRUCTURE

The distribution and thickness of the Makwassie Formation are fault controlled and the volcanics accumulated in graben structures (Clendenin *et al.*, 1988c). The Bothaville area is demarcated by an eastern fault zone, possibly an extension of the De Bron Fault, and apparently by a western fault zone, situated just east of borehole LLE1. Another prominent feature is an extension of the Border Fault of the Free State Goldfields (Fig. 4.9d and 4.9j). The southern and northern borders of the Bothaville area are delimited by horst structures, forming the northern part of the Free State Goldfield in the south and the southern part of the Klerksdorp Goldfield in the north (Fig. 4.10). To the west of both these horst structures, high-lying areas of Basement Igneous Complex occur.

The Goedgenoeg Formation is largely limited to the South Bothaville and Harrisburg Basins, indicating areas of earliest subsidence during deposition of the Platberg Group. Furthermore, the "Vaal Bend formation" of Whiteside (1970), consisting of intermingled lava and sediment related to the onset of volcanism towards the close of Kameeldoorns Formation deposition, occurs at the base of the Goedgenoeg Formation in this area. Deposition of the Goedgenoeg Formation was controlled by north to south trending structures (Figs. 4.10 and 4.3). Prominent faulting and major graben structures apparently only formed after deposition of the Goedgenoeg Formation, as is evident from uplift of the formation along, for example, the Border Fault.

During deposition of the Makwassie Formation the South Bothaville and Harrisburg Basins were still prominent and subsided further, but northeast to southwest trending structures also became prominent. Grabens with this trend started to form the Vierfontein Basin, while associated uplift formed the Ontario and Zandfontein Arches. The Orkney, Concord and Waterpan Arches appear to have been older features which have been reactivated during this period (e.g. the Goedgenoeg Formation truncates against the southern part of the Orkney Arch, but the Makwassie Formation drapes over it and is now uplifted; Fig. 4.9g). The Wesselsbron Dome indicates similar movements (Fig. 4.9e).

Subsidence in the Vierfontein Basin and Western Border Trough continued after deposition of the Makwassie Formation, as is evident by the fill of Rietgat Formation. The thickness of the Allanridge Formation also increases in the Vierfontein Basin.

The absence of Makwassie Formation in borehole EL1 is enigmatic, but could be related to thrusting, as suggested by Winter (1965). If so, this could be a tectonic extension of the Ontario Arch, or it might be related to uplift of the Wesselsbron Dome.

FIGURE 4.9: Correlation diagrams of the Ventersdorp Supergroup Formations between boreholes in the study area. Figures (a) and (b) depict the location of the various sections and (c) to (m) the correlation diagrams. Borehole collar elevations are referenced to sea level and the diagrams therefore show the true elevation. Solid lines indicate known formational positions in the boreholes and dotted lines indicate estimated positions. The approximate position of smaller faults which affected the Platberg Group are indicated at the top of the diagrams. All the correlation diagrams have a horizontal scale 10 times that of the vertical, but all the diagrams are not to the same scale.



FIGURE 4.9a: Distribution map of boreholes in the study area. Sections A-A' to F-F' are depicted.

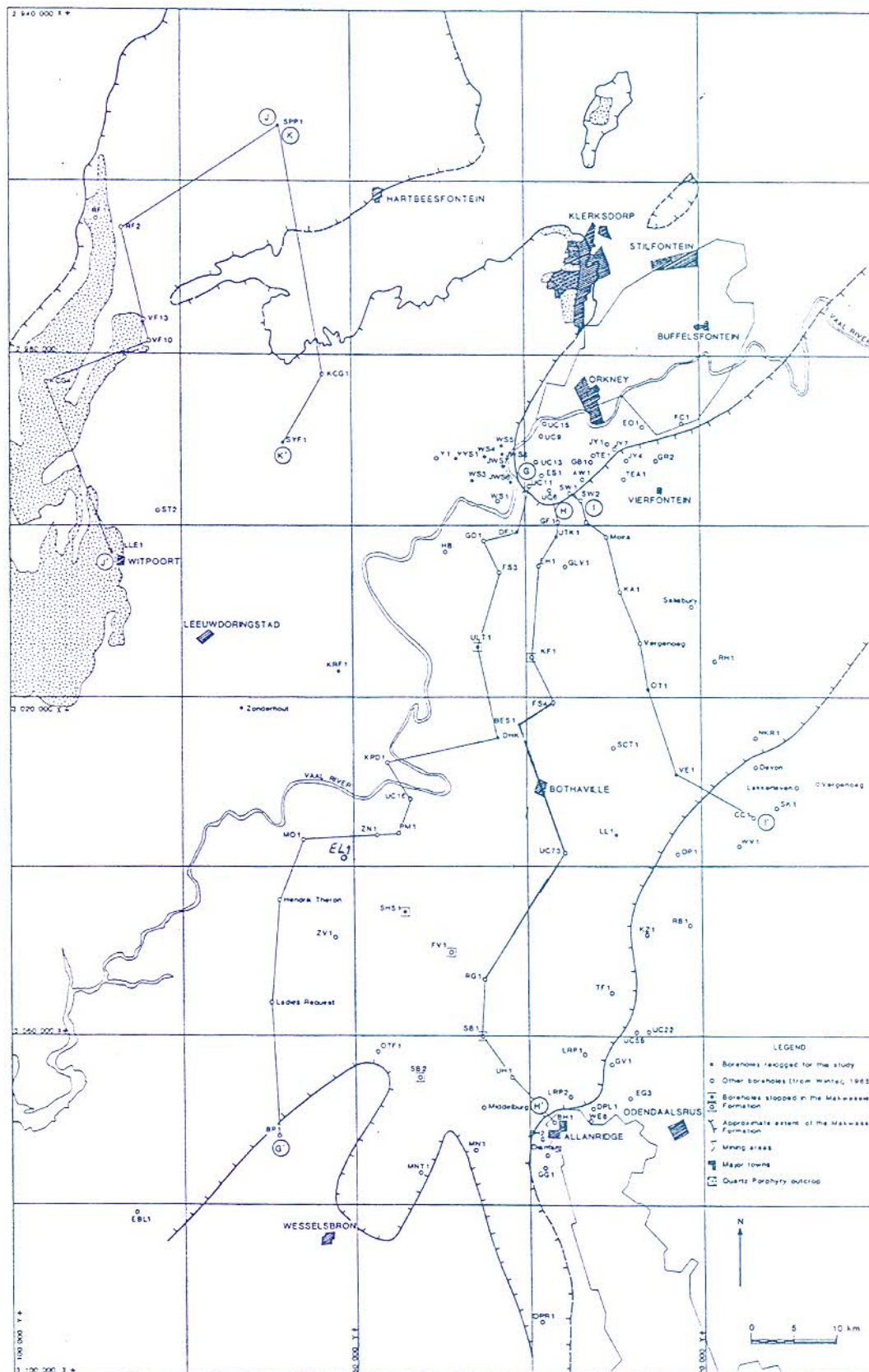
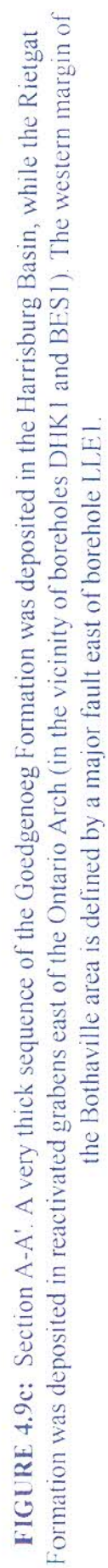


FIGURE 4.9b: Distribution map of boreholes in the study area. Sections G-G' to K-K' are depicted.



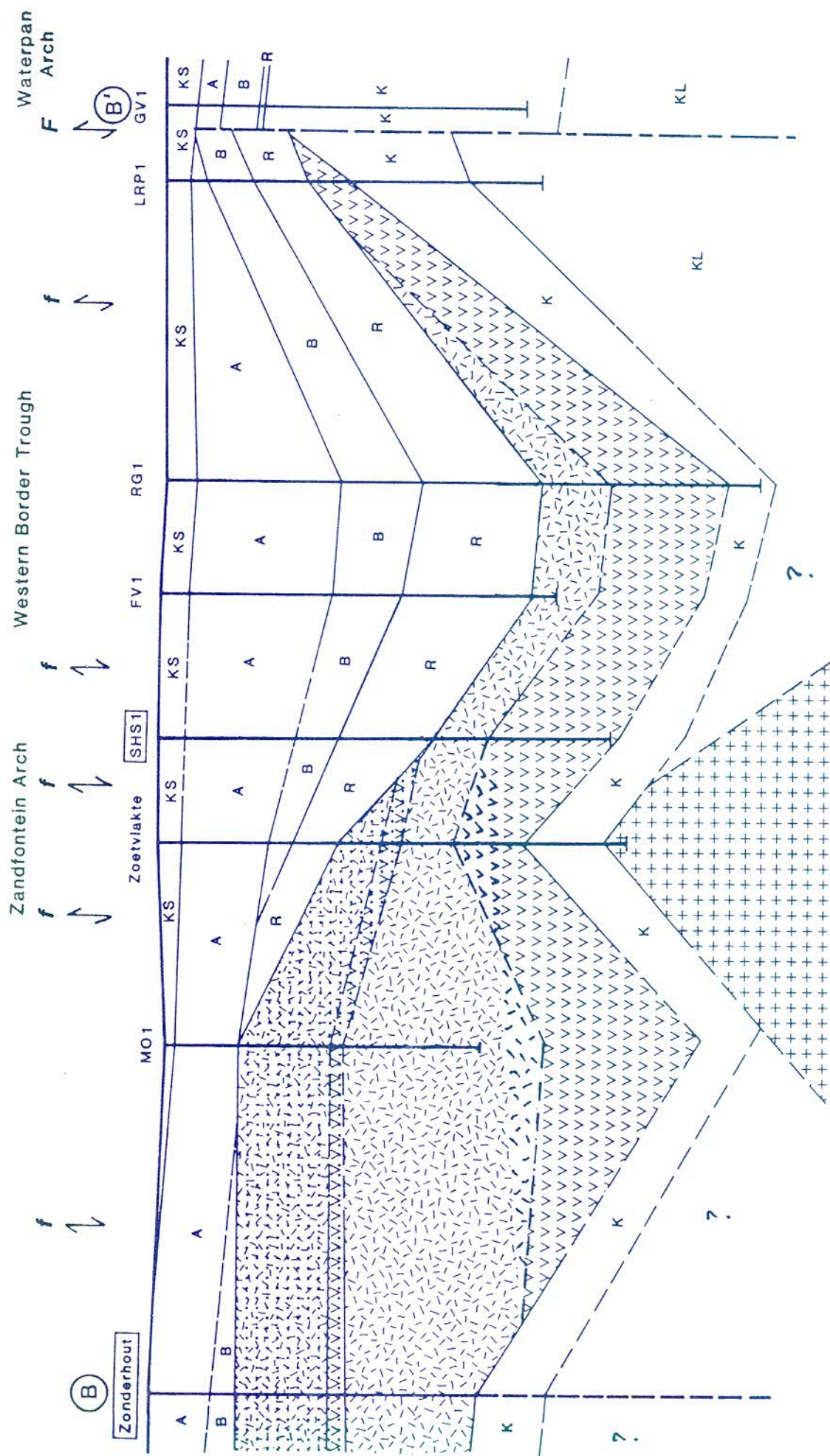


FIGURE 4.9d: Section B-B'. Granite of the Wesselsbron Dome occurs in this section. Post-Makwassie graben subsidence took place in the Western Border Trough east of the Wesselsbron dome, in which the Rietgat and Bothaville Formations were deposited. Between boreholes RG1 and LRP1 uplift on an extension of the Border Fault occurred after deposition of the Goedgenoeg Formation.

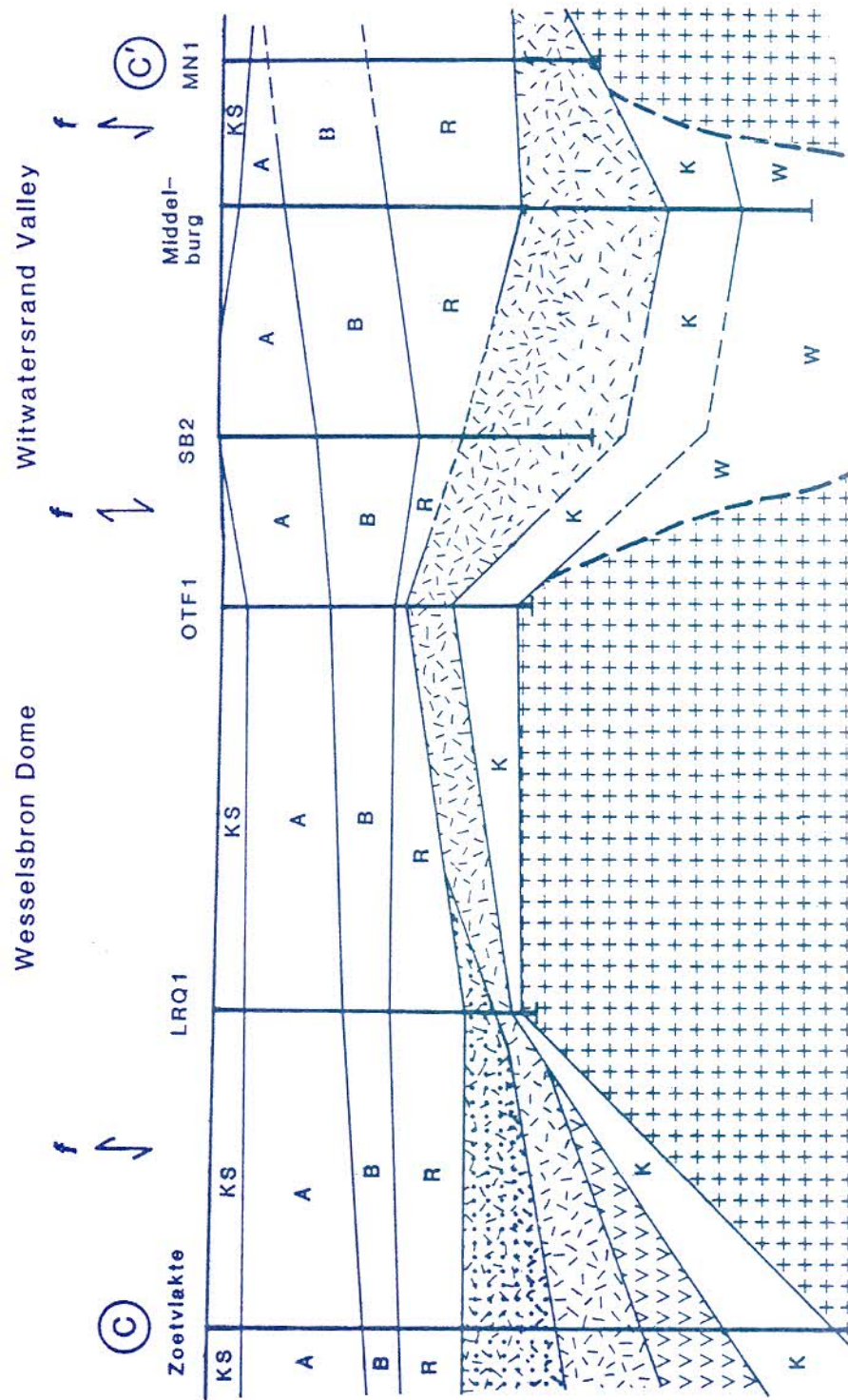


FIGURE 4.9c: Section C-C'. The Basement Igneous Complex is part of the Wesselsbron Dome. A Witwatersrand valley eroded into the dome and the Makwassie Formation is present in this valley.

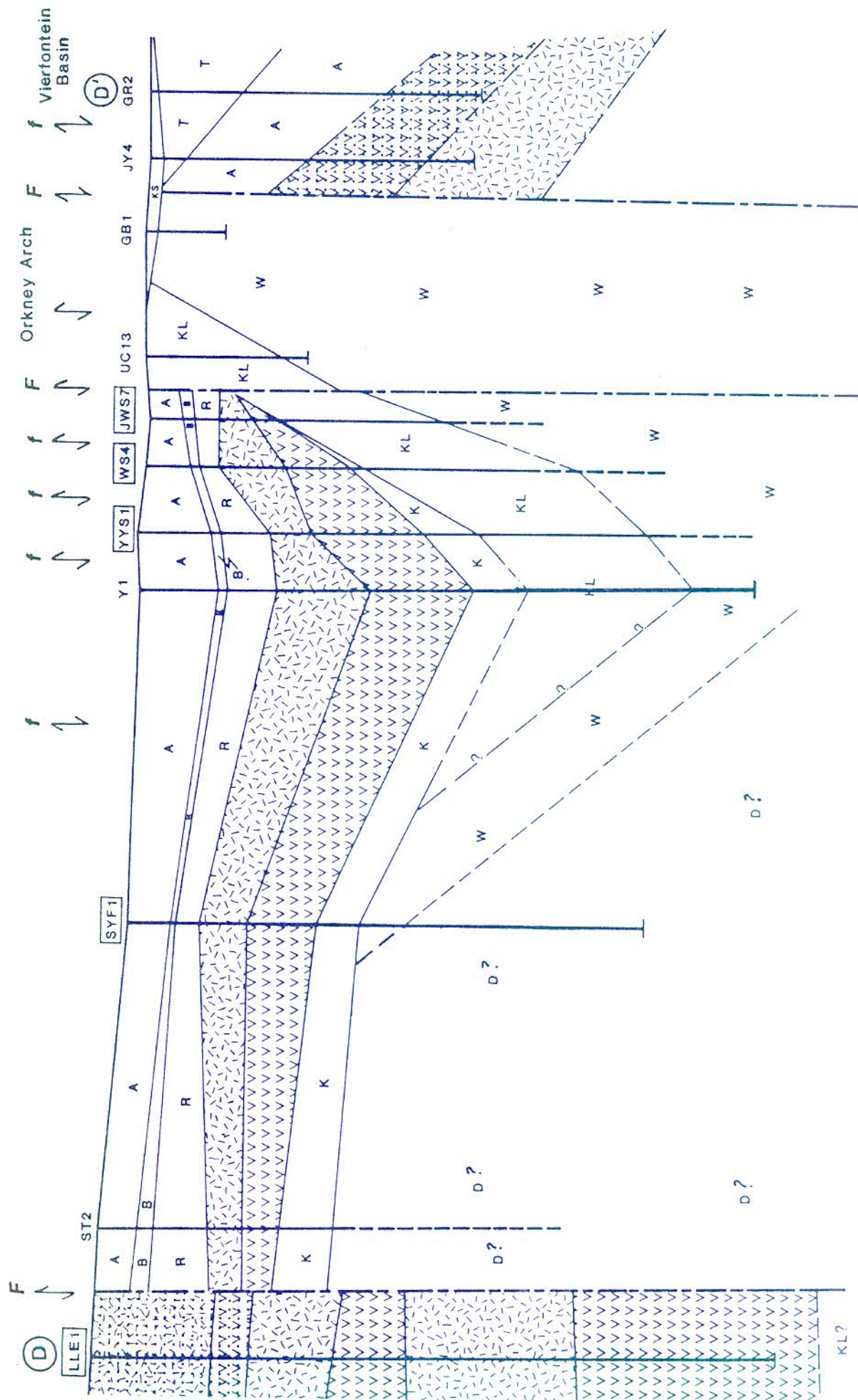


FIGURE 4.9f: Section D-D'. The Orkney Arch is illustrated in this section, on top of which the Platberg Group is absent. The Vierfontein Basin developed to the east of the Orkney Arch.



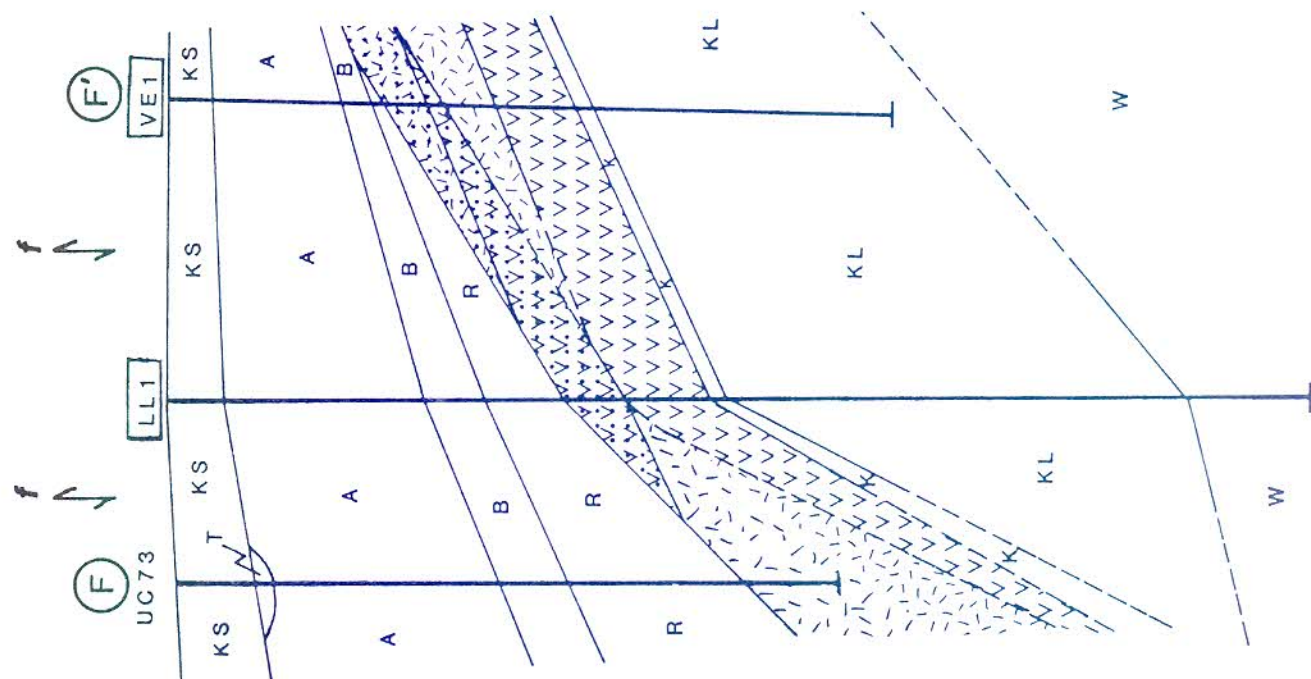


FIGURE 4.9h: Section F-F'. The Garfield Member directly overlies the Goedgenoe Formation in borehole LL1.

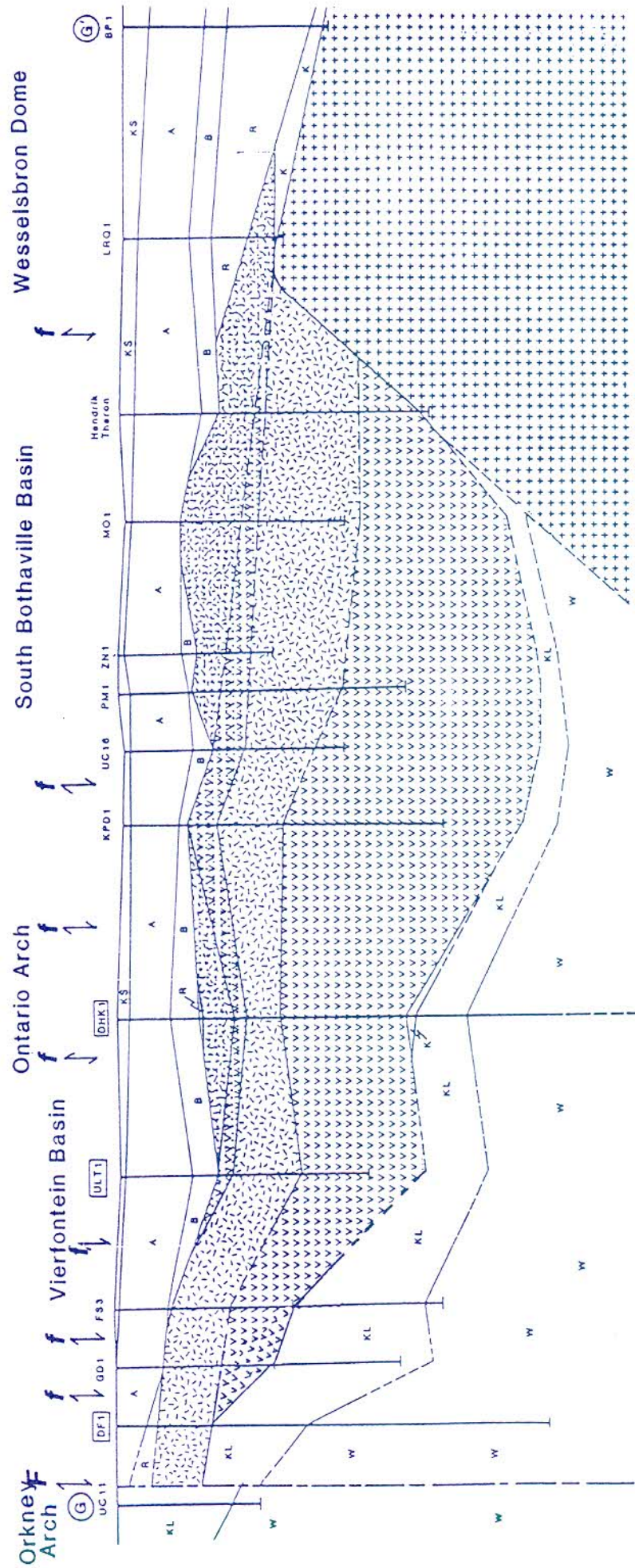


FIGURE 4.9i: Section G-G'. The Wesselsbron Dome in the south obstructed development of the Makwassie Formation. Note the major development of the Rietgat Formation on top of the Basement Igneous Complex dome.

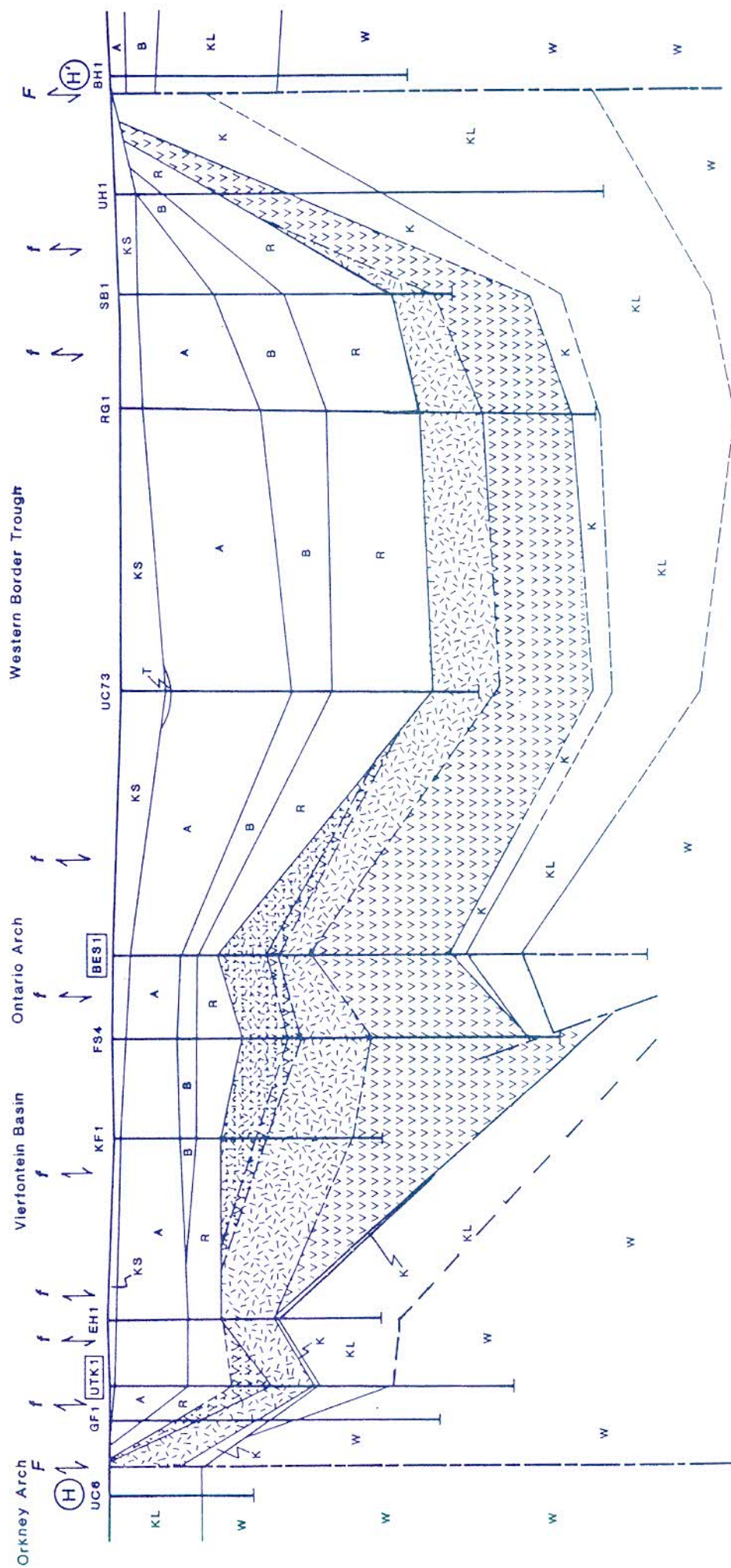


FIGURE 4.9j: Section H-H'. The Western Border Trough subsided further after deposition of the Makwassie Formation. Duplication of the Goedgenoeg Formation occurs in borehole FS4 on the edge of the Ontario Arch.

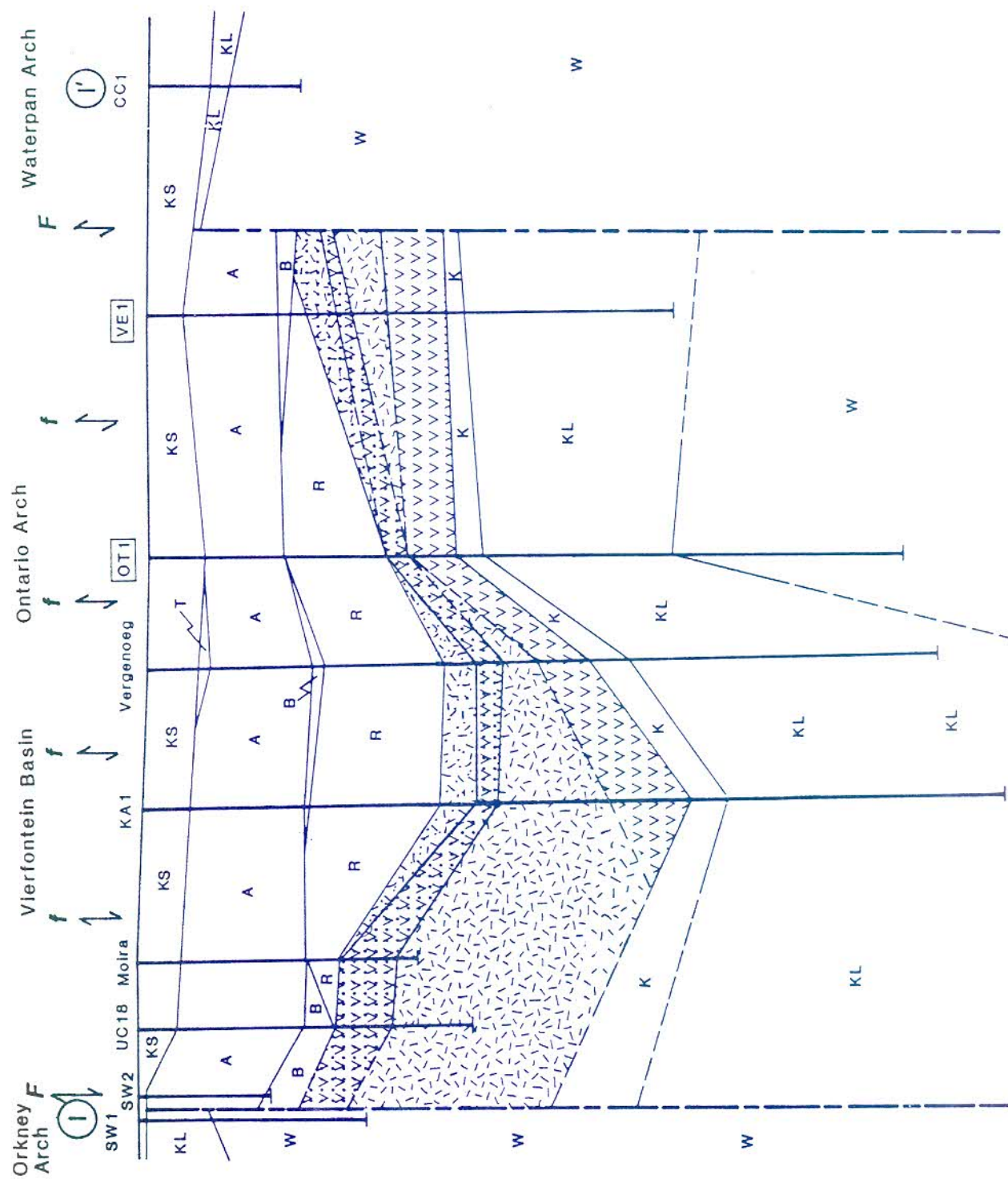
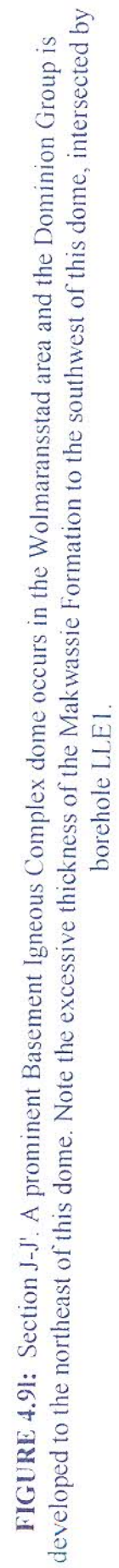


FIGURE 4.9k: Section I-I'. The Garfield Member directly overlies the Goedgevoeg Formation in borehole OT1.



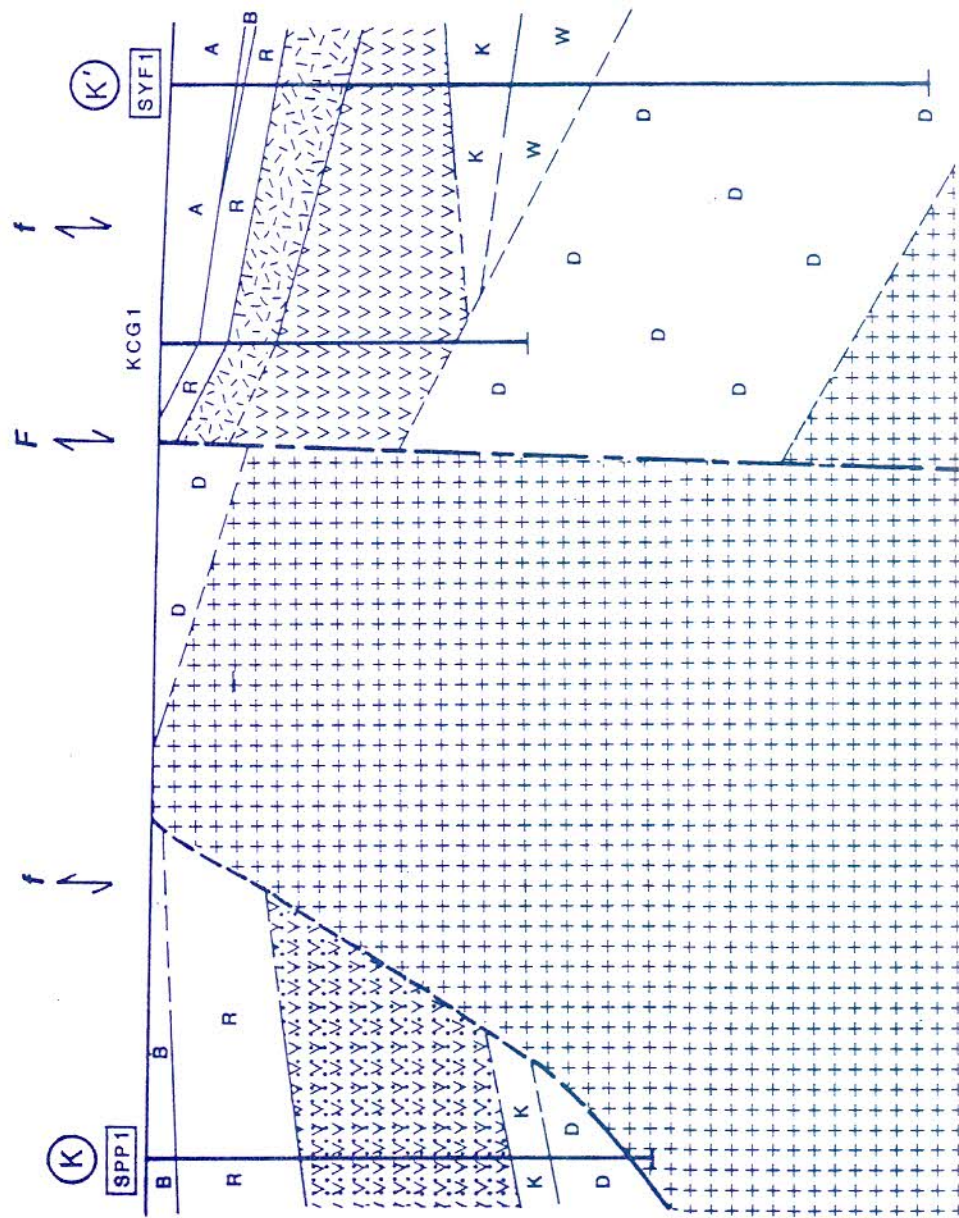


FIGURE 4.9m: Section K-K'. The Makwassie Formation in the Bothaville area is truncated by a major fault south of the Basement Igneous Complex dome, but does occur in the Hartbeesfontein Basin to the north of the dome.

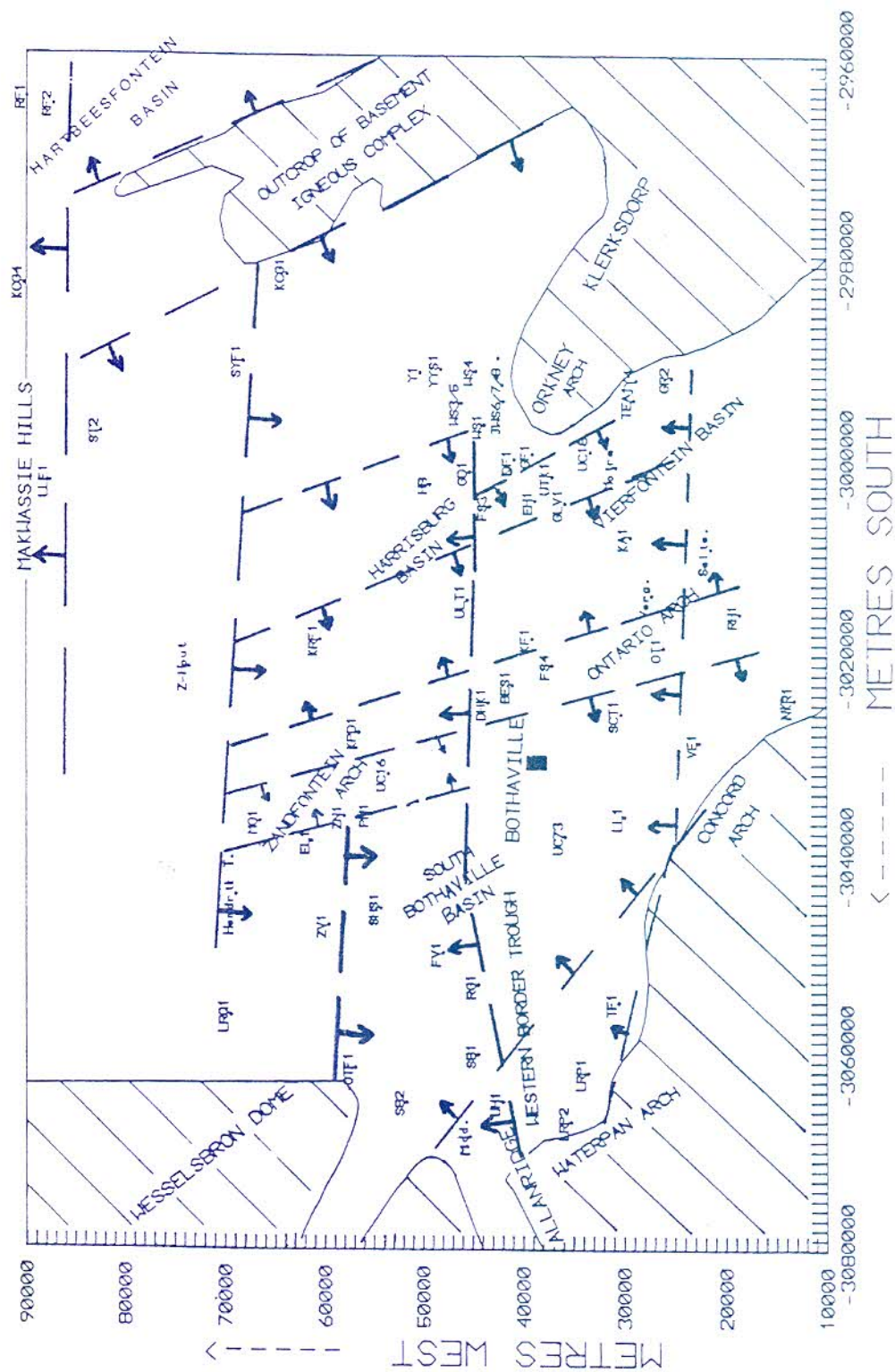


FIGURE 4.10: Structural control during deposition of the Goedgeoeg and Makwassie Formations. Early north-south striking structures were later replaced by SW-NE striking structures.

5. GEOCHEMICAL COMPOSITION OF THE GOEDGENOEG AND MAKWASSIE FORMATIONS IN THE BOTHAVILLE AREA

5.1 INTRODUCTION

Major and trace element analyses of 447 whole rock samples of the Goedgenoeg and Makwassie Formations in the Bothaville area are listed in Appendix C, where the sampling procedures and analytical techniques are also discussed. In this discussion the major elements are presented in weight percent (normalized to a 100% volatile free) and the trace elements in parts per million.

The samples are divided into groups as listed in Table 5.1. Samples from anomalously altered zones (Ga and Ma) and from the inclusion-rich zone of the Makwassie Formation (Mx) are excluded from this discussion. This inclusion-rich zone forms the lower part of the Makwassie quartz-feldspar porphyry in some boreholes and contains abundant mafic inclusions, *i.e.* in boreholes WS3, WS4, YYS1 and SYF1 (Chapter 3). Although samples with macroscopic inclusions were avoided during geochemical analyses, petrographic investigation of the analysed samples revealed that some contain abundant microscopic mafic inclusions. The whole rock geochemical compositions of these inclusion-rich samples vary greatly and they were therefore rejected.

TABLE 5.1: Sample groups for 447 samples of the Goedgenoeg and Makwassie Formations in the Bothaville area. (As listed in Appendix C).

SAMPLE GROUP	CODE	N
Goedgenoeg Formation	Gm, Gi, Gs, Gz	126
Makwassie Formation	Md, Mr	193
Garfield Member	GF	43
Interbedded mafic lava in the Makwassie Formation	Mm	10
Anomalously altered (Goedgenoeg Formation)	Ga	8
Anomalously altered (Makwassie Formation)	Ma	16
Inclusion-rich zone (Makwassie Formation)	Mx	51

5.2 DOWNHOLE GEOCHEMICAL PLOTS (Appendix D)

Downhole geochemical plots of the sampled boreholes demonstrate the geochemical variation with stratigraphy (Appendix D). The Goedgenoeg Formation and Garfield Member (feldspar porphyries and non-porphyritic lavas)

are more basic than the Makwassie Formation (quartz-feldspar porphyries). While the SiO_2 concentrations in the Goedgenoeg Formation and Garfield Member are comparable, it is higher in the Makwassie Formation but for an overlap between 66% and 68%. A well defined break can be observed in the SiO_2 , TiO_2 , Fe_2O_3 , MnO , CaO , P_2O_5 , Zr, Y, Nb, V and Co trends between the Goedgenoeg and Makwassie Formations, and between the Garfield Member and the Makwassie Formation. These elements also define a break between the lower and upper part of the Makwassie Formation in boreholes LLE1, ZH1 and DHK1; in these boreholes the upper part of the Makwassie Formation is more acidic than the lower part. The geochemical compositions of the Goedgenoeg Formation and Garfield Member are, however, comparable.

The trends of Na_2O , K_2O , Zn, Ba, Rb, CaO and Sr are fairly erratic (Appendix D), especially near lithological contacts. Erratic geochemical concentrations also become prominent near lava flow contacts, noticeable in boreholes WS3 and WS4 (Appendix D) which were more intensively sampled than the other boreholes. This variation is also reflected in downhole plots of LOI (Loss On Ignition). It is concluded that preferential alteration took place along formational and flow contacts and these zones should be avoided when determining the bulk composition of the rocks. These anomalously altered samples were discarded as discussed above (Table 5.1).

Mafic non-porphyritic flow-units, which are interbedded with the feldspar porphyries of the Goedgenoeg Formation, are manifested in the downhole geochemical plots by their basic composition (e.g. DHK1). The inclusion-rich zone in the lower part of the Makwassie Formation is reflected by erratic element concentrations, e.g. boreholes WS3, WS4, SYF1 and YYS1.

The overall geochemical parameters of the succession can be determined at a glance from the downhole geochemical plots. They also aid detection of major alteration zones, such as flow contacts and fault zones, as well as alteration associated with lithological contacts. Aberrant samples in the data base can be timeously detected, while inclusion-rich zones (representing mixed magmas?) can also be distinguished.

5.3 ALTERATION

The Goedgenoeg and Makwassie Formations were subjected to pervasive alteration and various stages can be identified. The first stage is characterized by devitrification and hydrothermal alteration (Chapter 3), which starts

immediately after deposition of volcanic rocks (Cas and Wright, 1988). The second stage represents burial metamorphism during which the mineral assemblage was altered to that of lower greenschist facies, while late stage alteration is represented by saussuritization of feldspars.

Elements considered to be mobile during low-grade alteration are particularly the major elements Ca, Na, K and the trace elements Ba, Rb and Sr (Wilson, 1989). Less mobile major and trace elements are Ti, P, Cr, V, Co, Ni, Nb, Zr and Y (Cann, 1970). Many ancient volcanic suites display metamorphic assemblages associated with burial metamorphism, which has reached the greenschist facies (Kuniyoshi and Liou, 1976). Numerous authors have demonstrated that ancient (Viereck *et al.*, 1982; Kranidiotis and MacLean, 1987) as well as more recently erupted volcanic rocks (Hart, 1969; Hart *et al.*, 1974) commonly display redistribution of chemical elements. Volcanic rocks are in extreme chemical disequilibrium with the atmospheric environment at the earth's surface (Cas and Wright, 1988) and due to the glassy nature and physical inhomogeneous make-up of these rocks, they undergo chemical alteration easily and relatively rapidly. Regional greenschist-facies metamorphism of the Ventersdorp Supergroup volcanics, attributed to burial metamorphism, has been demonstrated by Cornell (1978), Tyler (1979a), Schweitzer and Kröner (1985) and Crow and Condie (1988). Grobler *et al.* (1989) demonstrated through the technique of Beswick and Soucie (1978) that depletion of Na and Ca and enrichment in K and Si took place in the T'Kuip mafic and felsic volcanics, while Meintjes (1988) demonstrated the same for the Klipriviersberg Group lavas in the Welkom area. Geochemical classification of the Makwassie volcanics involving these mobile elements must therefore be treated with circumspection. Schweitzer and Kröner (1985) and T.B. Bowen *et al.* (1986) have reported that the elements Ti, P, Zr, Nb, Y, V, Al and Mg were the least mobilized in the case of the Ventersdorp Supergroup.

Most geochemical classification diagrams for volcanic and igneous rocks utilize elements such as silica and the alkalis (*i.e.* Irvine and Barager, 1971; Cox *et al.*, 1979; De La Roche *et al.*, 1980; Wilkinson, 1986), so that these classification schemes are ill-suited for the Ventersdorp Supergroup. Classification diagrams such as Jensen's (1976), which use Fe, Ti, Mg and Al, are considered to be more suitable for low-grade metamorphic assemblages.

As mentioned in the first paragraph, 25 of the 447 Goedgenoeg and Makwassie Formation samples were considered to be anomalously altered (Ga, Gma and

Ma in Appendix C). Most of these samples were taken close to highly altered zones such as lithological contacts and faults. Some also have very high LOI values during analysis, which render them suspect. These 31 samples are excluded from geochemical diagrams in this chapter.

5.4 ANALYTICAL RESULTS

The volcanic rocks of the Goedgenoeg and Makwassie Formations have a wide range in geochemical composition (Table 5.2; Fig. 5.1), which display a weakly bimodal distribution (Fig. 5.2). SiO_2 concentrations in the Goedgenoeg Formation vary between 56% to 69% and between 65% and 80% for the Makwassie Formation. With silica increase there is a decrease in TiO_2 , Fe_2O_3 , MnO , MgO , CaO , P_2O_5 , Sr, Zn, Ni, V, Cr and Co, while K_2O and Rb increase. Al_2O_3 decreases slightly with an increase in silica. In the case of the Goedgenoeg Formation there is an increase in Zr, Y and Nb with a corresponding increase in silica, but a decrease for the Makwassie Formation. Na_2O possibly has the same trend, but it is less clearly discernable due to redistribution during alteration. The Al_2O_3 , MgO , CaO , Na_2O , K_2O , Sr, Rb, Cu, Zn and Ba concentrations show erratic variations, possibly also due to redistribution.

TABLE 5.2: The geochemical compositions of the Goedgenoeg and Makwassie Formations in the Bothaville area. The Goedgenoeg Formation consists of feldspar porphyries and non-porphyritic lavas, while the Makwassie Formation consists of quartz-feldspar porphyries.

ELEMENT	GOEDGENOEG Fm. (G) (126 samples)				MAKWASSIE Fm. (M) (193 samples)			
	Min.	Max.	Avg.	S	Min.	Max.	Avg.	S
SiO_2	55.98	68.84	63.30	3.39	65.15	79.63	70.78	3.30
TiO_2	1.05	1.54	1.30	0.09	0.24	1.25	0.84	0.29
Al_2O_3	12.41	16.11	13.68	0.62	9.95	16.11	12.98	0.77
Fe_2O_3	5.49	10.95	8.08	1.27	1.39	9.11	4.75	1.86
MnO	0.01	0.23	0.12	0.03	0.00	0.18	0.07	0.03
MgO	0.78	6.95	2.48	1.55	0.00	4.29	1.18	0.89
CaO	2.30	8.01	4.64	1.32	0.26	7.27	2.46	1.46
Na_2O	1.18	5.23	2.97	0.72	0.04	6.77	2.59	1.29
K_2O	0.31	4.96	2.91	1.04	0.09	8.61	4.05	1.73
P_2O_5	0.40	0.67	0.52	0.05	0.02	0.52	0.31	0.16
Zr	208	695	492	137	221	563	415	70
Y	36	85	57	9	32	84	53	10
Sr	77	809	376	148	26	2919	358	497
Rb	6	163	79	33	0	278	119	53
Cu	2	62	15	12	0	56	7	7
Zn	55	248	126	32	24	227	88	34
Ni	12	218	49	46	5	22	14	4
Ba	79	4975	1277	543	73	3961	1313	573
Nb	11	24	19	3	14	25	20	3
V	99	231	151	34	7	123	74	33
Cr	14	607	114	139	7	47	24	7
Co	4	43	21	9	2	21	10	4

FIGURE 5.1: (Continued)

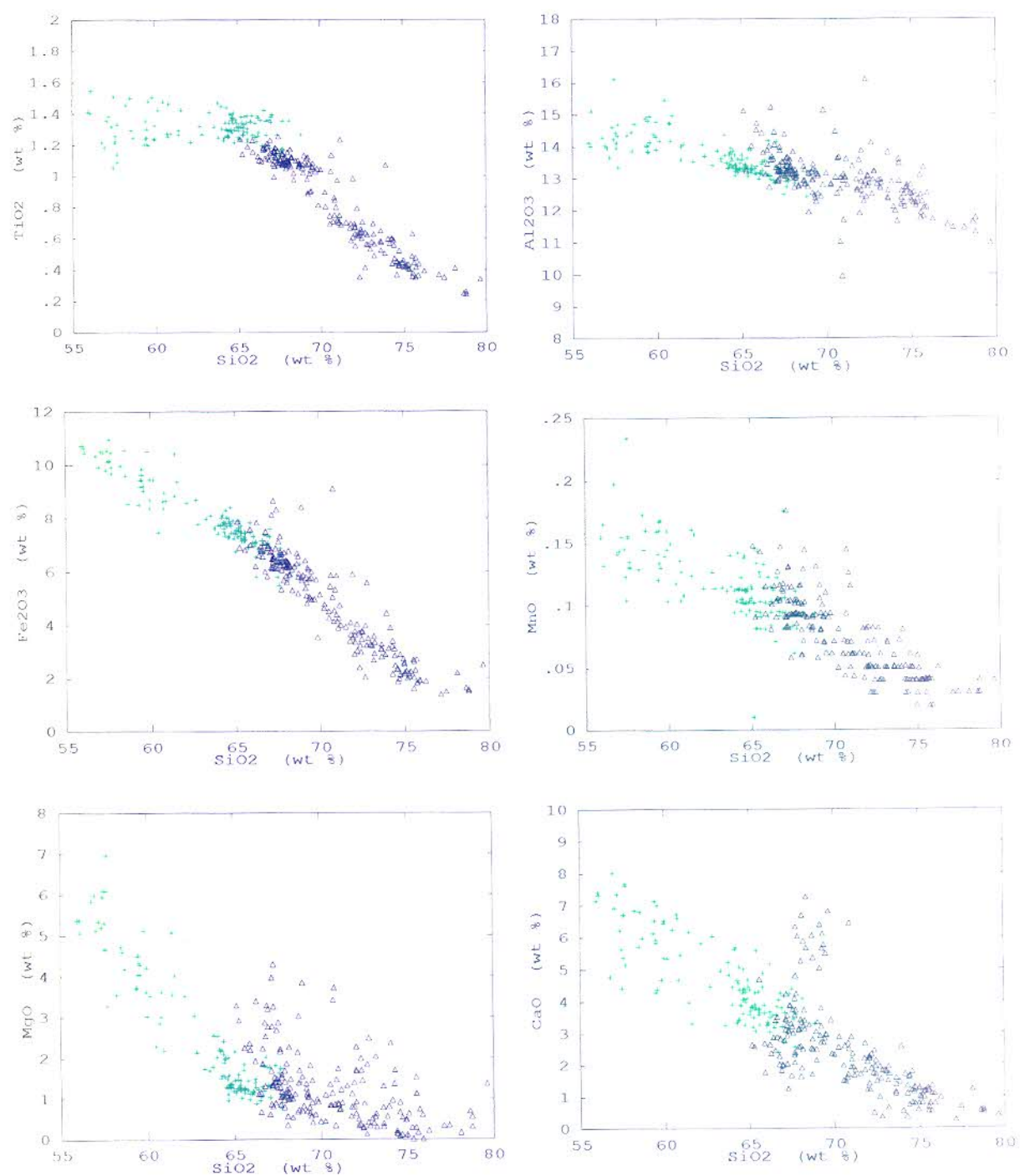


FIGURE 5.1: Harker diagrams of 319 samples from the Goedgenoeg (green) and Makwassie (black) Formations in the Bothaville area, depicting element concentrations against SiO₂.

FIGURE 5.1: (Continued)

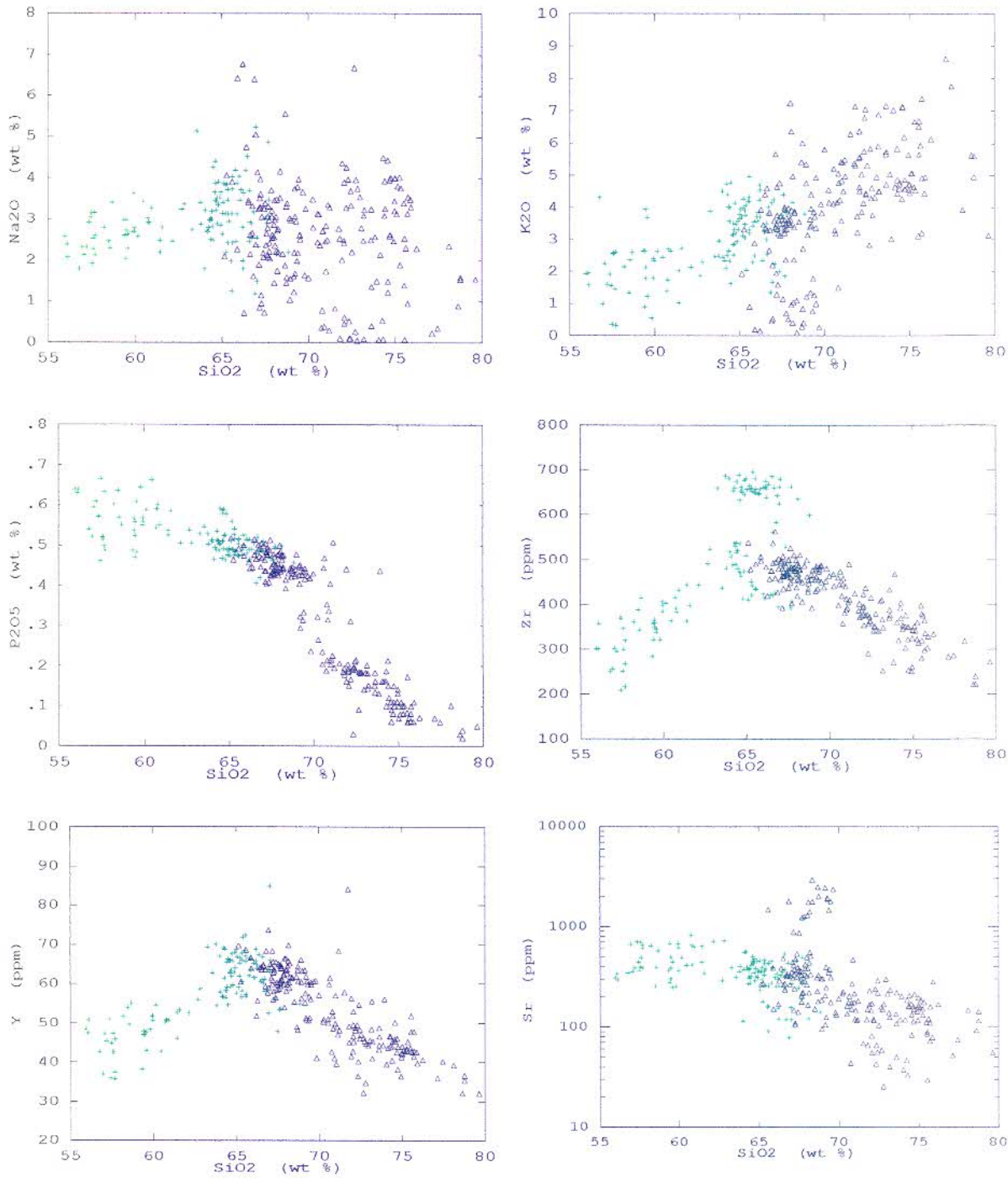
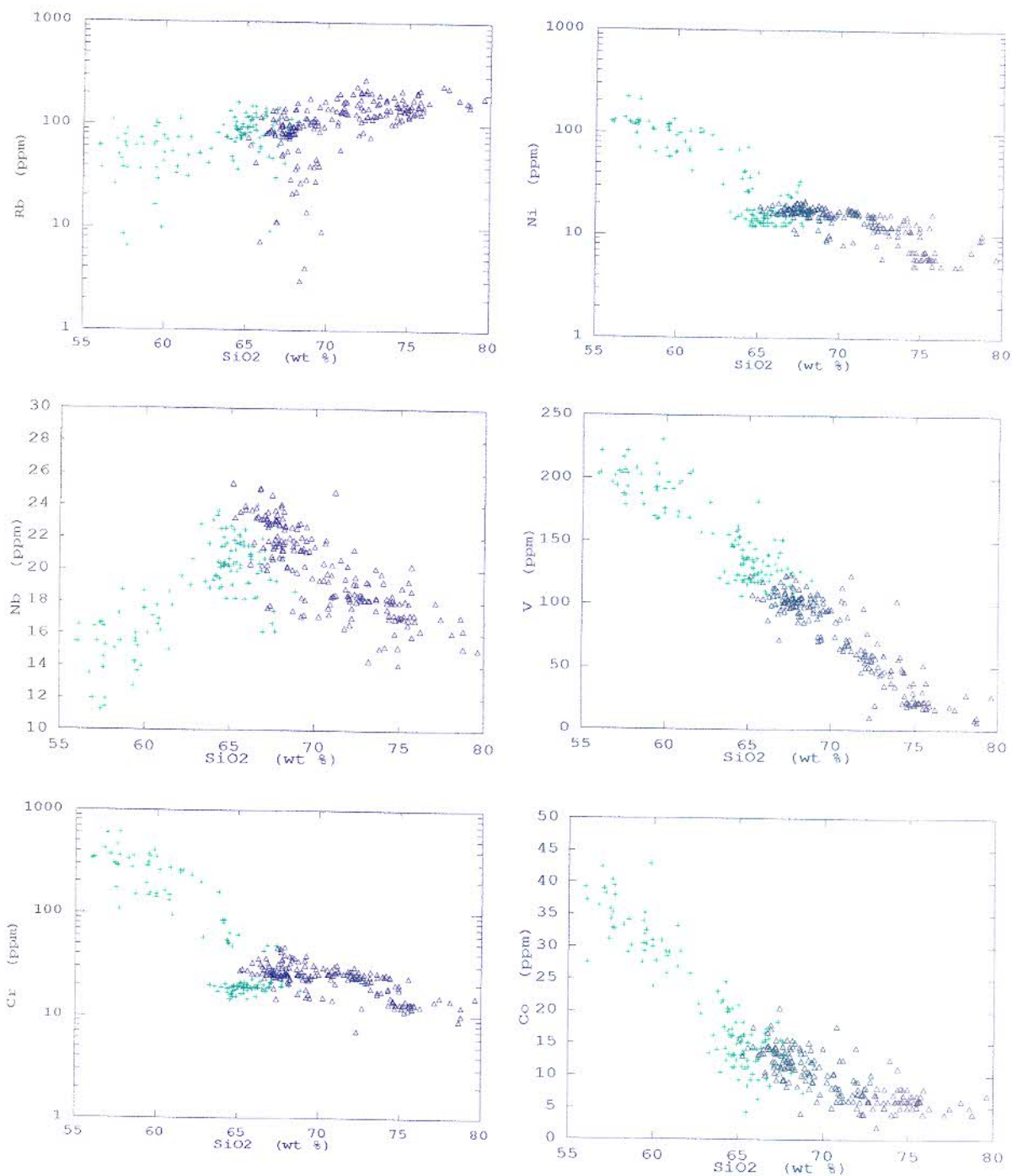


FIGURE 5.1: (Continued)



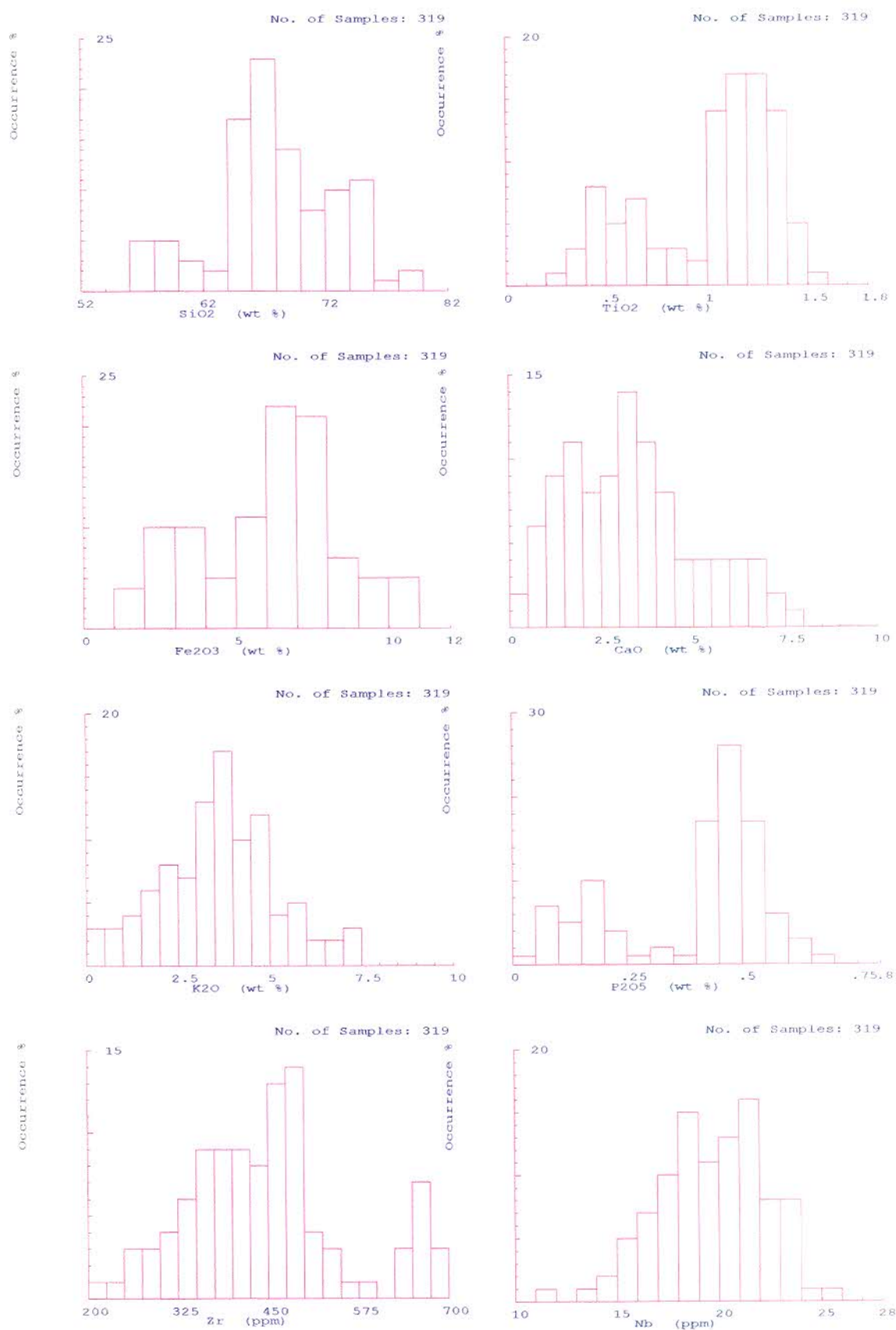


FIGURE 5.2: Selected histograms of the element distribution in the Goedgenoeg and Makwassie Formations, demonstrating the weakly bimodal composition.

5.5 GEOCHEMICAL CLASSIFICATION

The Goedgenoeg and Makwassie volcanics are predominantly metaluminous (Fig. 5.3), whereas some of the Makwassie Formation samples are peraluminous. Metaluminous rhyolites are by far the most common type when compared to peraluminous and peralkaline rhyolites (Barker, 1983). In continental settings, however, a peraluminous composition can be expected (Clarke, 1992).

The subalkaline (tholeiitic) character of the Ventersdorp Supergroup volcanics has been well established (Wyatt, 1976; Grobler *et al.*, 1982; Schweitzer and Kröner, 1985; T.B. Bowen, 1986; Fig. 5.4). The Al_2O_3 contents of the Goedgenoeg and Makwassie Formation samples of this study are <16% (Table 5.2), indicating a tholeiitic composition according to the classification scheme of Irvine and Barager (1971). The Ventersdorp Supergroup volcanics, however, also have a slight calc-alkaline affinity (Schweitzer and Kröner, 1985; M.P. Bowen *et al.*, 1986; Crow and Condie, 1988). On the ternary AFM-diagram of Irvine and Barager (1971), the Goedgenoeg and Makwassie Formation samples plot in the calc-alkaline field (Fig. 5.5a) and display a calc-alkaline trend. This is also evident on the diagram of Miyashiro (1974; Fig. 5.5b). Since these diagrams make use of mobile elements, Schweitzer and Kröner (1985) have attributed a similar calc-alkaline trend they found for the Ventersdorp volcanics to secondary alteration. On the ternary diagram of Jensen (1976), however, the Goedgenoeg and Makwassie samples plot in the tholeiitic and in the calc-alkaline fields when immobile elements are used (Fig. 5.6). Similar results for the Ventersdorp Supergroup were reported by Crow and Condie (1988), Grobler *et al.* (1989) and Nelson *et al.* (1992). The Jensen diagram (Fig. 5.6) classifies the Goedgenoeg Formation samples as tholeiitic dacites and some of the samples as calc-alkaline andesites and high-Fe tholeiitic basalts. The Makwassie Formation samples are mainly classified as calc-alkaline dacites and rhyolites, while some samples classify as tholeiitic dacites and rhyolites.

The total alkali-silica diagram (Fig. 5.7) of Le Bas *et al.* (1986) classify the Goedgenoeg and Makwassie rocks as oversaturated andesites, dacites and rhyolites, while the potassium-silica diagram (Fig. 5.8; Le Maitre, 1989) indicates medium to high potassium for the Goedgenoeg Formation (calc-alkaline and high-K calc-alkaline; Rickwood, 1989) and mostly high potassium for the Makwassie Formation. Potassium mobility could possibly account for the high variation. Note that Rickwood (1989) pointed out that slightly different boundary lines were implicated by the classification parameters of various previous authors for both the TAS and potassium-silica diagrams.

On a Nb/Y vs Zr/TiO₂ diagram of Winchester and Floyd (1977) the Goedgenoeg and Makwassie Formation samples plot as rhyodacite, dacite and andesite (Fig. 5.9a), while

some samples plot as rhyolites and trachy-andesites on a diagram of Zr/TiO_2 vs SiO_2 (Fig. 5.9b). Therefore, mobility of SiO_2 is indicated, as was also reported by Schweitzer and Kröner (1985) for the Ventersdorp Supergroup volcanics.

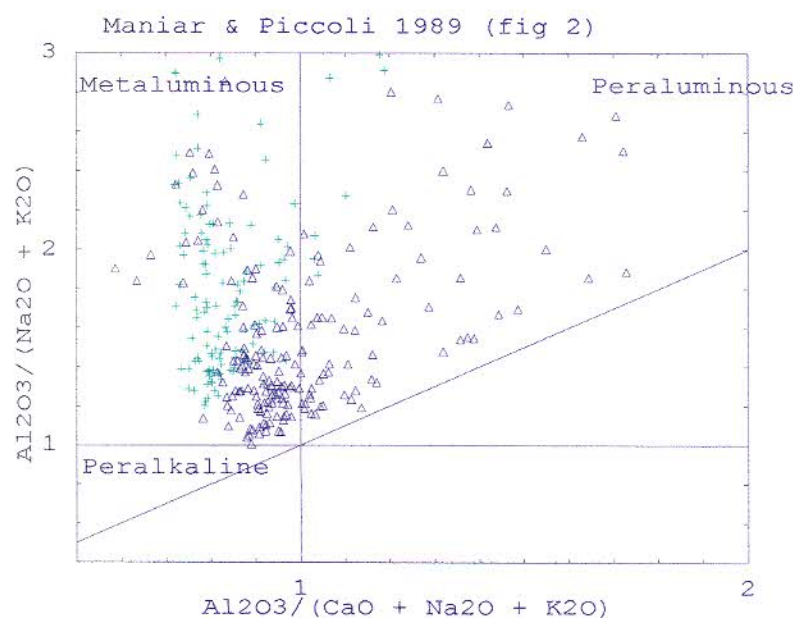


FIGURE 5.3: Alumina saturation of the Goedgenoeg (green) and Makwassie (black) Formations in the Bothaville area (after Shand, 1951 and Maniar and Piccoli, 1989).

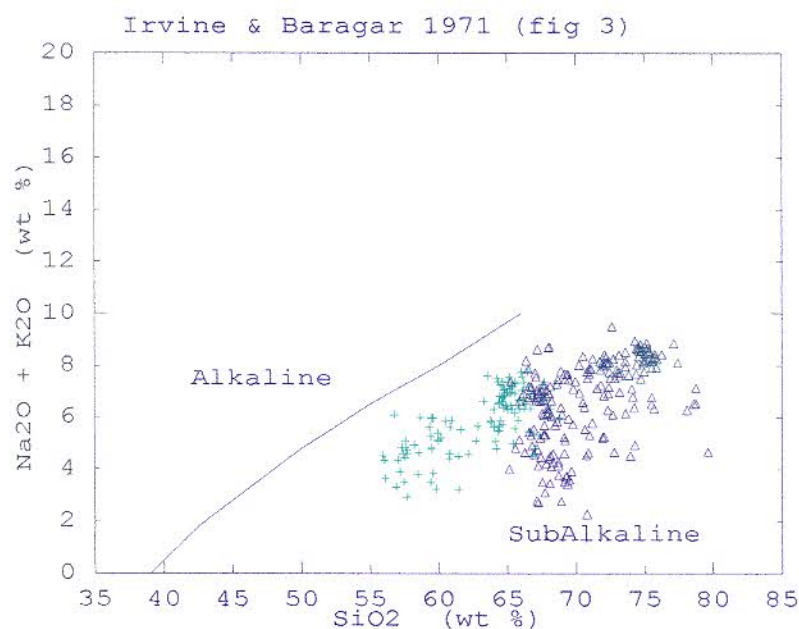


FIGURE 5.4: Subalkaline classification of the Goedgenoeg (green) and Makwassie (black) Formation samples (after Irvine and Baragar, 1971).

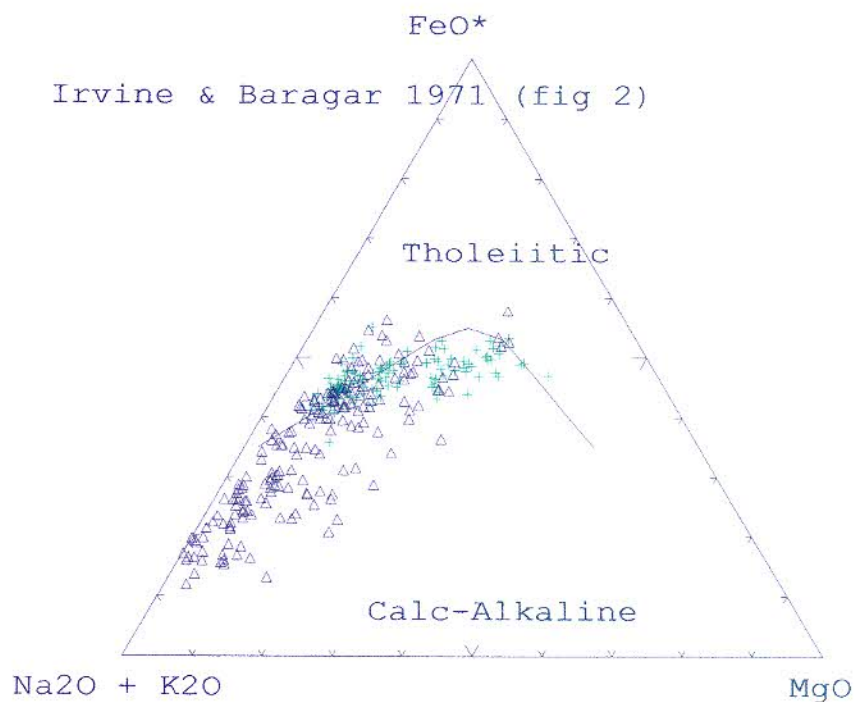


FIGURE 5.5a: Classification of the Goedgenoeg (green) and Makwassie (black) Formation samples as predominantly calc-alkaline (after Irvine and Baragar, 1971).

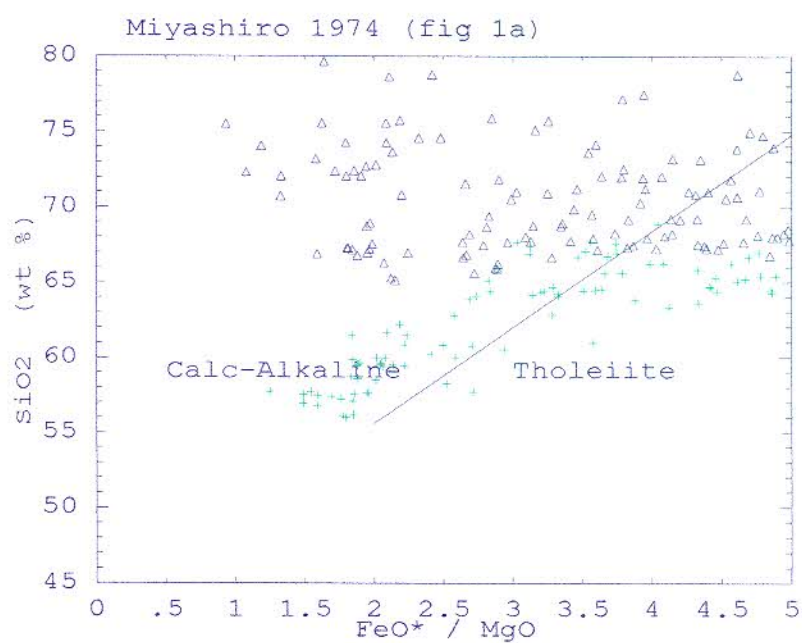


FIGURE 5.5b: Classification of the Goedgenoeg (green) and Makwassie (black) Formation samples as predominantly calc-alkaline (after Miyashiro, 1974).

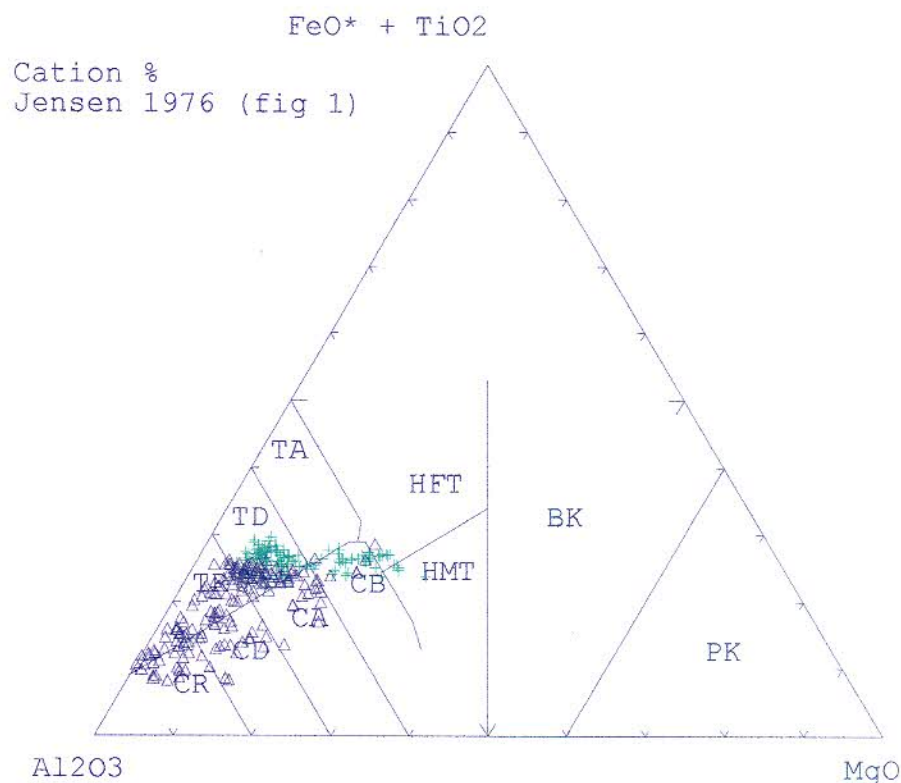


FIGURE 5.6: Classification of the Goedgenoeg (green) and Makwassie (black) Formations samples on a Jensen diagram. The fields are tholeiitic rhyolite (TR), dacite (TD) and andesite (TA), high-iron tholeiitic basalt (HFT), high-Mg tholeiitic basalt (HMT), and calc-alkaline rhyolite (CR), dacite (CD), andesite (CA) and basalt (CB). Other fields are basaltic komatiite (BK) and peridotitic komatiite (PK). (After Jensen, 1976).

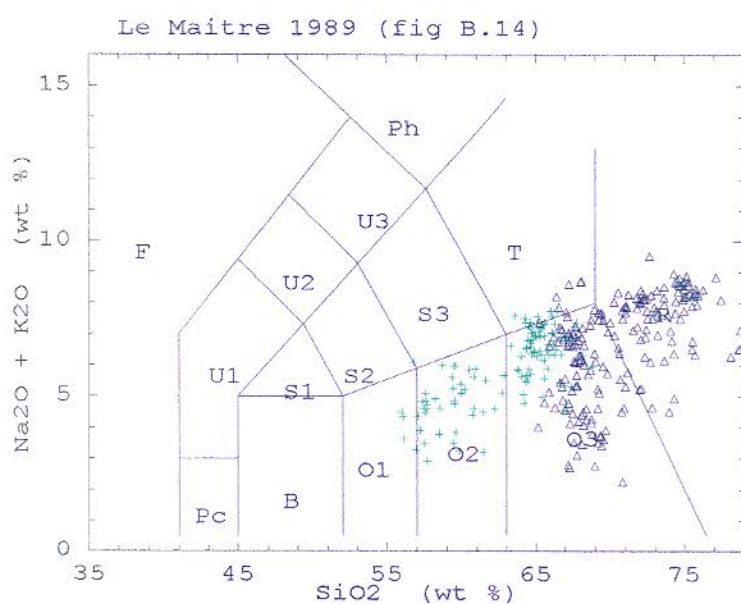


FIGURE 5.7: The Goedgenoeg (green) and Makwassie (black) Formations samples classify as oversaturated basaltic andesite (O1), andesite (O2), dacite (O3) and rhyolite (R) on the total alkali-silica diagram of Le Maitre (1989).

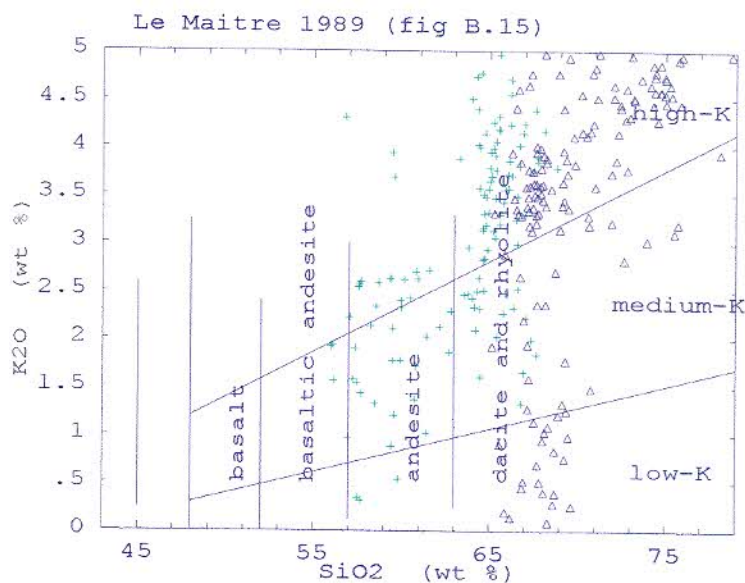


FIGURE 5.8: The volcanic rocks of the Goedgenoeg (green) and Makwassie (black) Formations are mostly high in potassium (after Le Maitre, 1989). (Note that K mobility during alteration influenced the concentrations and that some samples plot off the scale at the top).

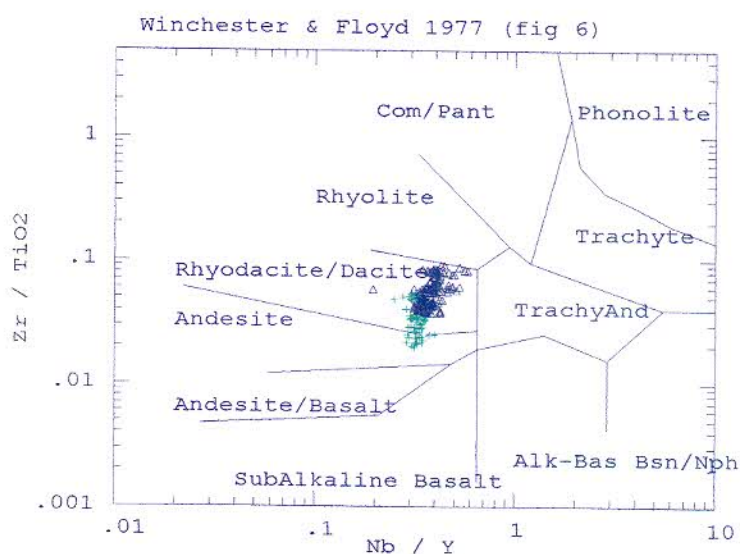


FIGURE 5.9a: Classification of the Goedgenoeg (green) and Makwassie (black) Formation volcanics as high andesites, dacites and rhyodacites (after Floyd and Winchester, 1975).

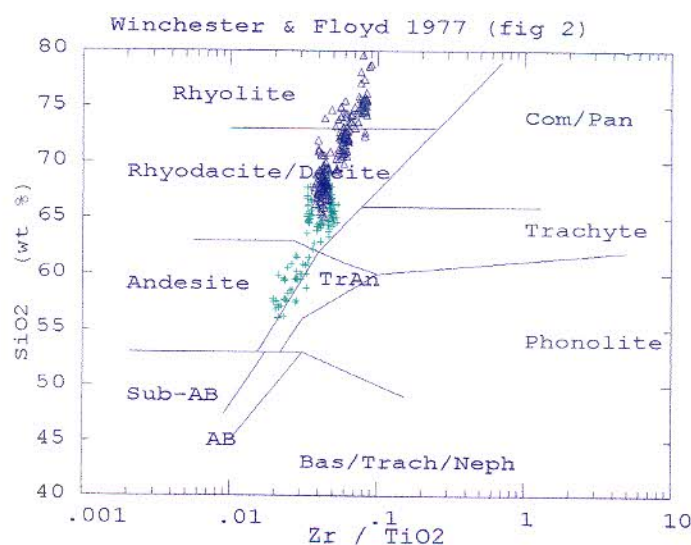


FIGURE 5.9b: Classification of the Goedgenoeg (green) and Makwassie (black) Formation volcanics (after Floyd and Winchester, 1975). Secondary mobility of SiO₂ during alteration has influenced the SiO₂ concentrations.

5.6 THE GOEDGENOEG FORMATION

The average geochemical composition of the Goedgenoeg Formation of this study (Table 5.2) corresponds with compositions cited by Crow and Condie (1988), except for lower SiO_2 concentrations reported by them (54.30 weight % after recalculation to a 100% volatile free). The average composition reported by M.P. Bowen (1986) is more basic and so are compositions published by Nelson *et. al* (1992). The geochemical composition of the Goedgenoeg Formation, however, varies considerably and M.P. Bowen (1984) also found "incoherent" compositional variation in the Goedgenoeg and Rietgat Formations. An average composition is therefore misleading. Furthermore, published geochemical data on the Goedgenoeg Formation are limited and only represent restricted borehole intersections, mostly only from the Klerksdorp area (*i.e.* M.P. Bowen, 1984; T.B. Bowen, 1984; Schweitzer and Kröner, 1985; Crow and Condie, 1988; Myers, 1990). It can thus be expected that the published data do not reflect the total geochemical variation of the Goedgenoeg Formation and discrepancies with the present study, which database covers a wider area, may occur.

This study delineates four geochemical facies in the Goedgenoeg Formation, which can be correlated with the lithostratigraphy. The SiO_2 concentration in the **basic** facies (**Gm**) varies between 56% and 64% and in the **intermediate** facies (**Gi**) it is well-constrained between 63% and 68% (Table 5.3). The Gm facies has lower incompatible and higher compatible element concentrations than the Gi facies (Fig. 5.10). The **high-Zr** facies (**Gz**) and the **low-Zr** facies (**Gs**) differ only slightly from the Gi facies; relative to the Gi facies the Gz facies is enriched in Zr and the Gs facies depleted in Zr (Table 5.3).

The Gm facies comprises mafic, non-porphyritic to slightly porphyritic lava flows interbedded with feldspar porphyries of the Gi facies. The Gm facies occurs interbedded throughout the Goedgenoeg Formation, but becomes predominant towards the top of the succession. Geochemically the facies classifies as high andesites and low dacites, but the major and trace element concentrations are erratic. With SiO_2 increase, however, there is a strong increase in the incompatible elements Zr, Y and Nb, and a strong decrease in compatible elements Ni, Cr and Co (Zr, Y and Cr shown in Fig. 5.10).

The Gi, Gz and Gs facies consist of feldspar porphyries with a dacitic geochemical composition (Table 5.3). The Gz facies occurs interbedded with the Gm facies in the lower part of the Goedgenoeg Formation, while the Gi facies occurs at a higher level. The Gs facies was only detected in borehole DHK1 and

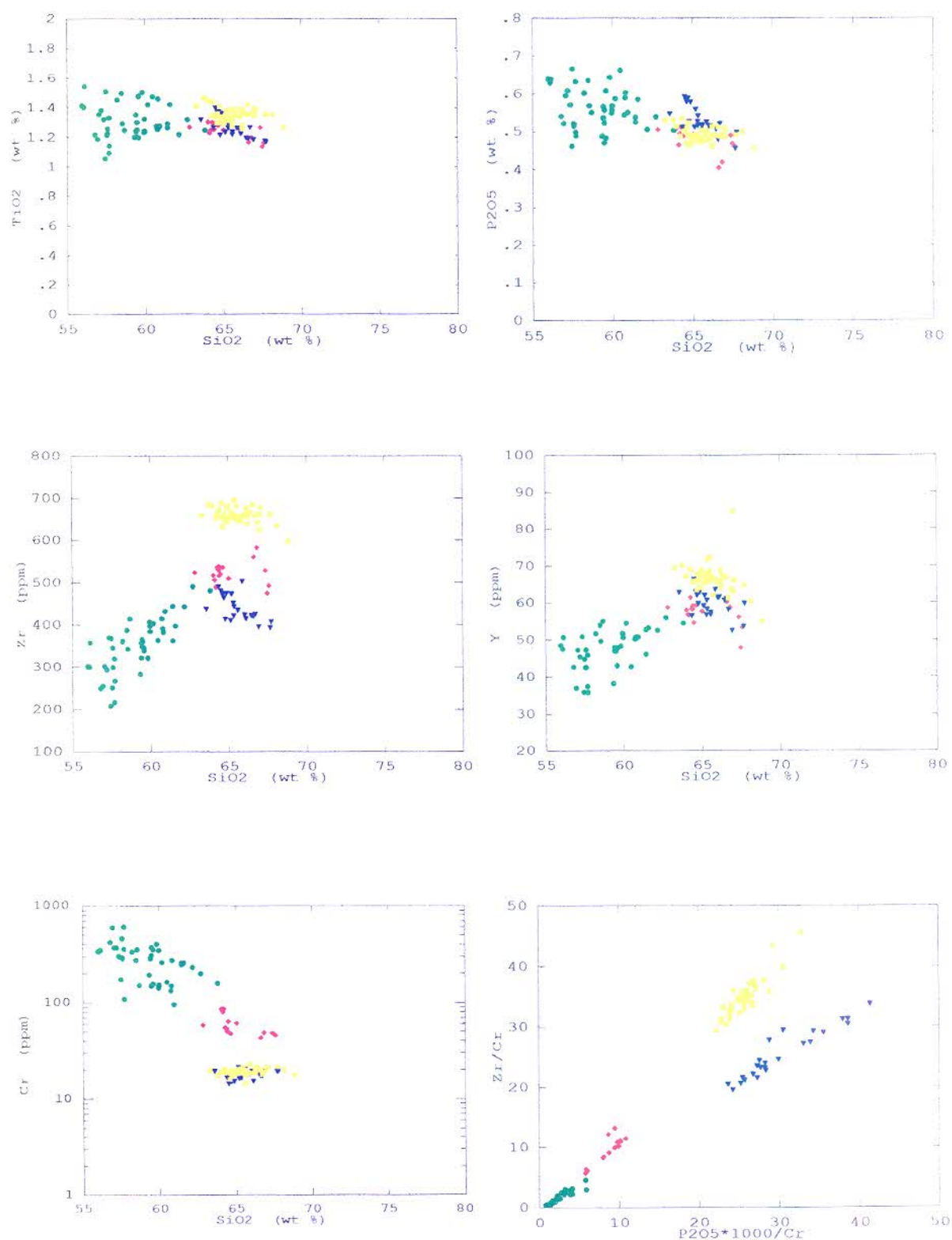


FIGURE 5.10: Selected Harker diagrams of the Goedgenoeg Formation (126 samples) in the Bothaville area, illustrating the concentrations of compatible and incompatible elements. Compare these diagrams with those of Fig. 5.2. The geochemical facies are: Gm (green), Gi (red), Gs (blue) and Gz (yellow).

TABLE 5.3: The geochemical composition of the individual geochemical facies of the Goedgenoeg Formation in the Bothaville area.

ELEMENT	BASIC FACIES (Gm) (44 samples)				INTERMED. FACIES (Gi) (16 samples)			
	Min.	Max.	Avg.	S	Min.	Max.	Avg.	S
SiO ₂	55.98	63.82	59.12	1.84	62.84	67.61	65.18	1.44
TiO ₂	1.05	1.54	1.31	0.12	1.13	1.30	1.24	0.05
Al ₂ O ₃	13.34	16.11	14.29	0.53	12.48	13.94	13.47	0.36
Fe ₂ O ₃	7.46	10.95	9.54	0.86	5.49	8.02	7.21	0.75
MnO	0.10	0.23	0.14	0.02	0.06	0.12	0.10	0.02
MgO	2.18	6.95	4.35	1.10	1.39	2.54	2.00	0.25
CaO	3.30	8.01	5.98	1.11	3.43	6.02	4.60	0.69
Na ₂ O	1.77	3.62	2.65	0.42	2.63	4.25	3.10	0.37
K ₂ O	0.31	4.31	2.06	0.84	1.33	4.38	2.62	0.79
P ₂ O ₅	0.46	0.67	0.56	0.05	0.40	0.51	0.48	0.03
Zr	208	490	350	64	474	583	522	26
Y	36	56	48	5	48	61	57	3
Sr	245	809	466	152	241	719	422	118
Rb	6	113	56	26	30	102	66	22
Cu	6	62	26	12	5	47	17	10
Zn	100	237	137	29	66	126	101	17
Ni	42	218	105	35	20	42	31	6
Ba	79	4975	1069	763	585	1669	1153	265
Nb	11	20	16	2	17	21	19	1
V	155	231	192	17	114	159	143	12
Cr	95	607	279	115	43	85	57	14
Co	21	43	32	5	15	25	19	3
ELEMENT	HIGH-Zr FACIES (Gz) (42 samples)				LOW-Zr FACIES (Gs) (24 samples)			
	Min.	Max.	Avg.	S	Min.	Max.	Avg.	S
SiO ₂	63.30	68.84	65.65	1.15	63.58	67.74	65.58	1.03
TiO ₂	1.25	1.47	1.35	0.05	1.16	1.40	1.27	0.07
Al ₂ O ₃	12.41	14.35	13.38	0.36	12.72	13.86	13.22	0.26
Fe ₂ O ₃	5.68	8.41	7.29	0.57	6.39	8.09	7.38	0.43
MnO	0.08	0.18	0.11	0.02	0.01	0.12	0.09	0.02
MgO	0.88	2.01	1.36	0.26	0.78	2.41	1.32	0.32
CaO	2.30	5.57	3.85	0.67	2.38	4.39	3.57	0.49
Na ₂ O	1.18	4.19	2.80	0.75	2.49	5.23	3.77	0.70
K ₂ O	2.02	4.96	3.71	0.72	1.65	4.77	3.29	0.67
P ₂ O ₅	0.46	0.53	0.49	0.02	0.45	0.59	0.53	0.04
Zr	598	695	659	18	392	502	440	31
Y	55	85	66	4	52	66	60	3
Sr	77	503	263	107	232	488	380	65
Rb	49	151	99	27	9	163	96	28
Cu	2	31	7	5	5	9	8	1
Zn	55	248	130	41	105	137	117	8
Ni	13	24	16	2	12	72	15	12
Ba	736	2269	1444	284	875	2673	1448	358
Nb	19	24	22	1	16	21	19	1
V	106	181	129	14	99	162	122	13
Cr	14	22	19	1	14	21	18	2
Co	4	17	12	3	13	20	16	2

LLE1, where it occurs in the middle and upper part of the Goedgenoeg succession. The geochemical compositions of the Gi, Gz and Gs facies are largely similar, except for the incompatible elements Zr, Y and Nb and the compatible elements Ni, Cr and Co. The Gz facies is strongly enriched in Zr (100 ppm above the concentrations in the Gs and Gi facies). Schweitzer and Kröner (1985) reported Goedgenoeg samples with similar high Zr concentrations, but considered these samples to be altered. M.P. Bowen (1984) also observed a large variation in Zr-concentration in the Goedgenoeg and Rietgat lavas, which he stated to be unrelated to alteration and metamorphism.

The distribution of the four facies of the Goedgenoeg Formation is reflected by the sampled boreholes (Table 5.4). The Gz facies, which is restricted to the basal part of the Goedgenoeg Formation, occurs only in the central part of the Bothaville area where the Formation reaches maximum thickness. The Gi and Gm facies are present wherever the Goedgenoeg Formation is developed in this area.

TABLE 5.4: The projected intersections of the geochemical facies of the Goedgenoeg Formation in the sampled boreholes in the Bothaville area. Depths are in metres below surface. The boreholes marked by an asterisk either did not penetrate the base of the Goedgenoeg Formation, or samples from only a limited section of the stratigraphy were available.

GOEDGENOEG FORMATION					
Borehole	Depth (m)	Basic (Gm)	Interm. (Gi)	High-Zr (Gz)	Low-Zr (Gs)
DHK1	1128 - 1295	X			
	1295 - 1310		X		
	1310 - 1350	X			
	1350 - 1410		X		
	1433 - 1933				X
	1433 - 1912			X	
	1912 - 1996	X			
FS4*	2629(F) - 2645	X			
	2645 - 2688		X		
JWS7*	545 - 555	X			
KRF1*	2765 - 2831			X	
	3091 - 3106		X		
LLE1*	2604 - 3648				X
	3648 - 3659	X			
OT1	1251 - 1392			X	
SHS1*	1603 - 1878	X			
	1878 - 2181			X	
ULT1*	1504 - 1683		X		
VE1	1076 - 1366	X			
WS3*	923 - 960	X			
WS4*	744 - 750	X			
YYS1*	988 - 1030	X			

5.7 THE MAKWASSIE FORMATION

Geochemically the quartz-feldspar porphyries of the Makwassie Formation consist of dacites, rhyodacites and rhyolites. Two geochemical facies can be recognized: the dacitic facies (**Md**) comprises the lower part of the Makwassie Formation and the rhyolitic facies (**Mr**) the upper part. The Mr facies is present only in boreholes LLE1, ZH1, DHK1 and VE1, while the Md facies occurs more widespread (Table 5.5).

The SiO_2 concentration in the Md facies varies between 65% and 74% and in the Mr facies between 70% and 80% (Table 5.6; Fig. 5.11). Secondary addition or loss of silica could possibly account for the overlap in silica composition. The two facies are better discriminated by immobile elements, such as titanium (TiO_2 between 0.80% and 1.25% for the Md facies and between about 0.25 and 0.80 % for the Mr facies; Fig. 5.8) and phosphorous (P_2O_5 between about 0.3% and 0.5% for the Md facies and between 0.02% and 0.3% for the Mr facies; Fig. 5.8). The concentrations of the trace elements Zr, Y, Nb, Ni, Cr and Co, however, overlaps (Table 5.6; Fig. 5.8). Fe_2O_3 , CaO and Sr are higher in the Md facies than in the Mr facies. In general compatible elements have higher concentrations in the Md facies, while incompatible elements are higher in the more acidic Mr facies with the exception of Zr, Y and Nb.

An average composition for the Makwassie Formation published by T.B. Bowen *et al.* (1986) compares well with the Md facies of this study, while that of Crow and Condie (1988) falls between the Md and Mr facies. The geochemical data of J.M. Myers (1990) reflect both these facies, while the compositions cited by Nelson *et al.* (1992) correlate with only the Md facies.

The Mr facies hosts the Garfield Member, which consists of a minor succession of feldspar porphyry and non-porphyritic lava. The Garfield Member is correlated over a large part of the Bothaville area and can be used as a marker horizon. The geochemical composition of the Mr facies underlying the Garfield Member, and the Mr facies overlying the Garfield Member are remarkably similar.

Subdivision of the Mr facies is, however, possible through the incompatible/compatible element ratio, e.g. TiO_2 , P_2O_5 or Zr vs V, Cr or Ni (Fig. 5.11). In boreholes LLE1 and ZH1 the upper part of the Mr facies has a low incompatible/compatible element ratio and the lower part of the facies a high ratio. In borehole DHK1 and VE1 the sequence is inverted in the sense that the upper part of the Mr facies has a high ratio and the lower part a low ratio (Table 5.6). In boreholes ZH1 and VE1 the high/low incompatible/compatible element ratio break coincides with the stratigraphic position of the Garfield Member and in borehole LLE1 the break is associated with a major interbedded mafic sequence in the Mr facies, which apparently does not correlate with the Garfield Member. It therefore appears that the incompatible/compatible element ratio can be used as a local stratigraphic marker in the Mr facies.

TABLE 5.5: The depths at which the geochemical facies of the Makwassie Formation were intersected by boreholes in the Bothaville area. The rhyolitic facies can be subdivided into low and high ratios of incompatible/compatible elements. Note that in borehole VE1 the upper part of the Mr facies has a low ratio, in contrast to the other boreholes. Depths are in metres. (The first 700 m of borehole LLE1 was percussion drilled and samples were not available; between 1299 m and 1687 m mafic lava was intersected).

Borehole	Intersected Depths Of Geochemical Facies			
	Dacitic	Rhyolitic		Garfield M.
		Low Ratio	High Ratio	
DF1	279 - 641			
DHK1	1091 - 1128	700 - 1091	573 - 700	855 - 866
JWS6	279 - 504			
JWS7	365 - 530			
JWS8	390 - 589			
LLE1	2404 - 2604	848 - 1753	1753 - 2387	636 - 848
SHS1	1346 - 1603			
SYF1	387 - 639			
UTK1	980 - 1214			
VE1	absent	896 - 1076	728 - 874	874 - 896
WS3	451 - 923			
WS4	375 - 743			
YYS1	708 - 971			
ZH1	1467 - 1583	427 - 836	896 - 1467	836 - 896

TABLE 5.6: The geochemical composition of the individual geochemical facies of the Makwassie Formation in the Bothaville area.

ELEMENT	DACITIC FACIES (Md) (104 samples)				RHYOLITIC (Mr) (89 samples)			
	Min.	Max.	Avg.	S	Min.	Max.	Avg.	S
SiO ₂	65.15	73.94	68.20	1.44	69.84	79.63	73.80	2.08
TiO ₂	0.80	1.25	1.09	0.08	0.24	0.81	0.54	0.14
Al ₂ O ₃	9.95	15.23	13.21	0.70	10.99	16.11	12.71	0.76
Fe ₂ O ₃	4.45	9.11	6.27	0.85	1.39	5.59	2.97	0.89
MnO	0.00	0.18	0.10	0.02	0.02	0.09	0.05	0.02
MgO	0.35	4.29	1.54	0.89	0.00	3.43	0.75	0.66
CaO	1.28	7.27	3.37	1.36	0.26	2.88	1.39	0.61
Na ₂ O	0.29	6.77	2.71	1.18	0.04	6.68	2.44	1.40
K ₂ O	0.09	7.25	3.07	1.56	2.83	8.61	5.20	1.11
P ₂ O ₅	0.29	0.52	0.44	0.04	0.02	0.31	0.14	0.06
Zr	357	563	466	33	221	480	356	54
Y	41	74	61	5	32	84	45	6
Sr	96	2919	551	613	26	299	133	60
Rb	0	182	85	40	77	278	158	38
Cu	0	56	10	8	0	17	3	3
Zn	49	227	111	25	24	173	62	23
Ni	8	22	17	3	5	18	11	4
Ba	73	3961	1287	734	621	2445	1343	284
Nb	17	25	22	2	14	21	18	1
V	68	123	101	12	7	97	43	20
Cr	14	47	27	6	7	32	20	6
Co	4	21	12	3	2	11	6	2

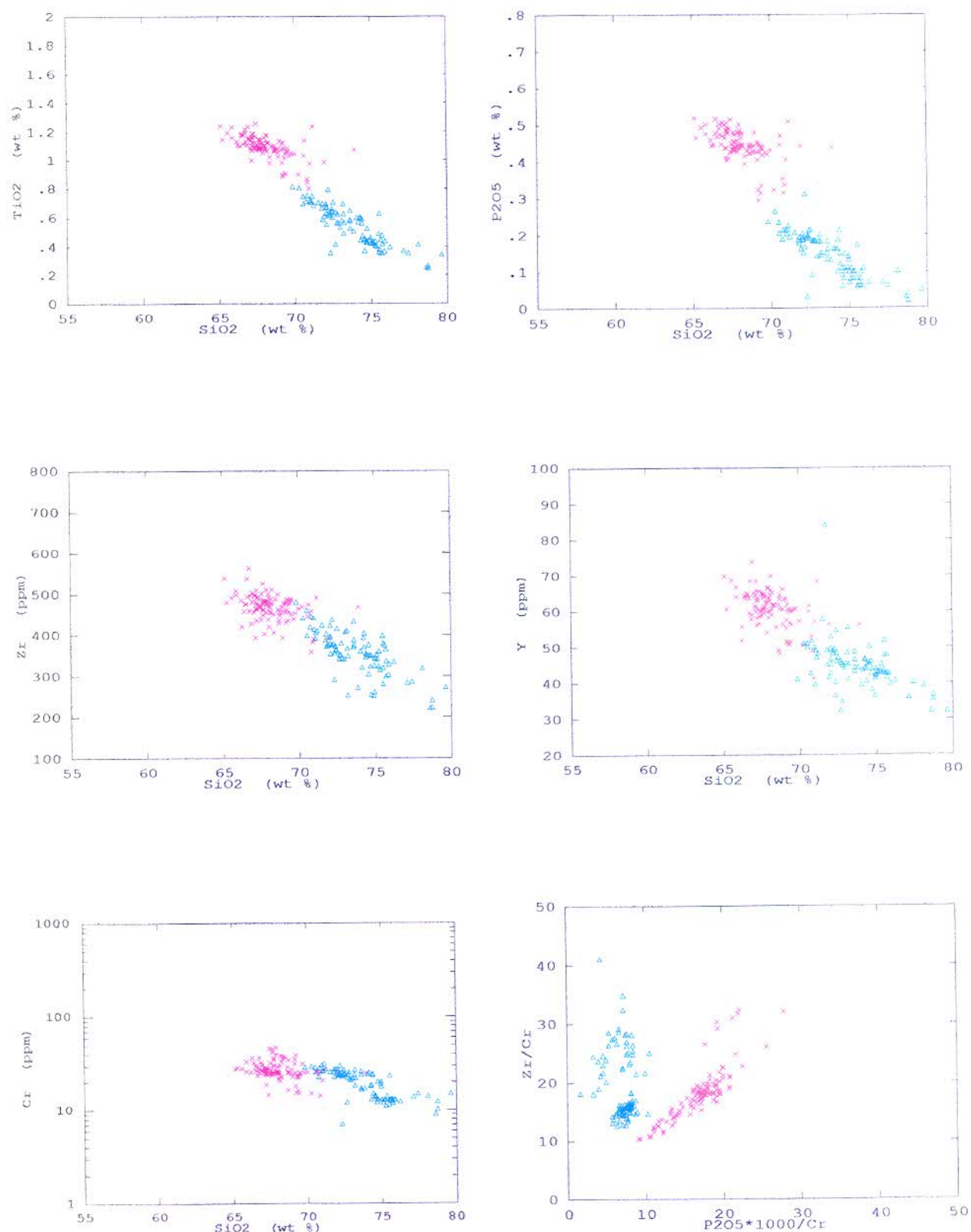


FIGURE 5.11: Selected Harker diagrams of the geochemical facies of the Makwassie Formation in the Bothaville area. The geochemical facies are Md (magenta) and Mr (blue).

5.8 THE GARFIELD MEMBER AND INTERBEDDED MAFIC LAVA IN THE MAKWASSIE FORMATION

Although the Garfield Member was described as long ago as 1965 (Winter, 1965), geochemical analyses of it have not yet been published. Apart from the Garfield Member, other minor mafic lava flows also occur interbedded with the Makwassie quartz-feldspar porphyries. The geochemical compositions of the Garfield Member and of these mafic lava flows reflect the composition of the basic facies (Gm) of the Goedgenoeg Formation (Table 5.7; Fig. 5.12). The Garfield Member and interbedded mafic lava are somewhat enriched in TiO_2 and P_2O_5 compared to the Gm facies, while some samples approach the composition of the Gi facies (Fig. 5.12).

TABLE 5.7: The geochemical compositions of the Garfield Member and interbedded mafic lava flows hosted by the Makwassie Formation in the Bothaville area.

ELEMENT	Garfield Member (43 samples)				Interbedded Mafic Lava (10 samples)			
	Min.	Max.	Avg.	S	Min.	Max.	Avg.	S
SiO_2	55.12	65.86	59.75	2.82	49.09	65.89	56.78	3.84
TiO_2	1.10	1.73	1.34	0.16	0.98	1.78	1.40	0.25
Al_2O_3	12.53	15.52	14.29	0.73	9.91	15.60	13.45	1.63
Fe_2O_3	5.93	12.98	9.44	1.55	6.97	15.13	11.22	2.13
MnO	0.01	0.20	0.14	0.03	0.01	0.33	0.14	0.07
MgO	2.36	6.95	4.45	1.24	2.20	13.28	6.29	2.87
CaO	1.85	8.21	5.24	1.51	3.83	9.71	6.32	1.38
Na_2O	1.41	3.82	2.53	0.65	1.08	3.38	2.41	0.73
K_2O	0.79	3.70	2.25	0.87	0.14	3.24	1.31	0.78
P_2O_5	0.46	0.82	0.57	0.09	0.43	0.94	0.68	0.17
Zr	260	542	365	76	164	559	298	107
Y	34	59	47	7	27	84	50	14
Sr	86	1083	379	247	96	787	418	201
Rb	23	175	63	36	19	230	49	54
Cu	2	54	21	14	24	92	37	17
Zn	104	333	151	53	113	225	137	28
Ni	37	182	106	39	89	431	188	98
Ba	179	1821	912	426	56	1488	705	423
Nb	12	22	16	3	7	17	14	3
V	137	260	197	26	163	251	212	26
Cr	97	510	273	118	209	1442	490	376
Co	13	45	31	8	29	60	45	9

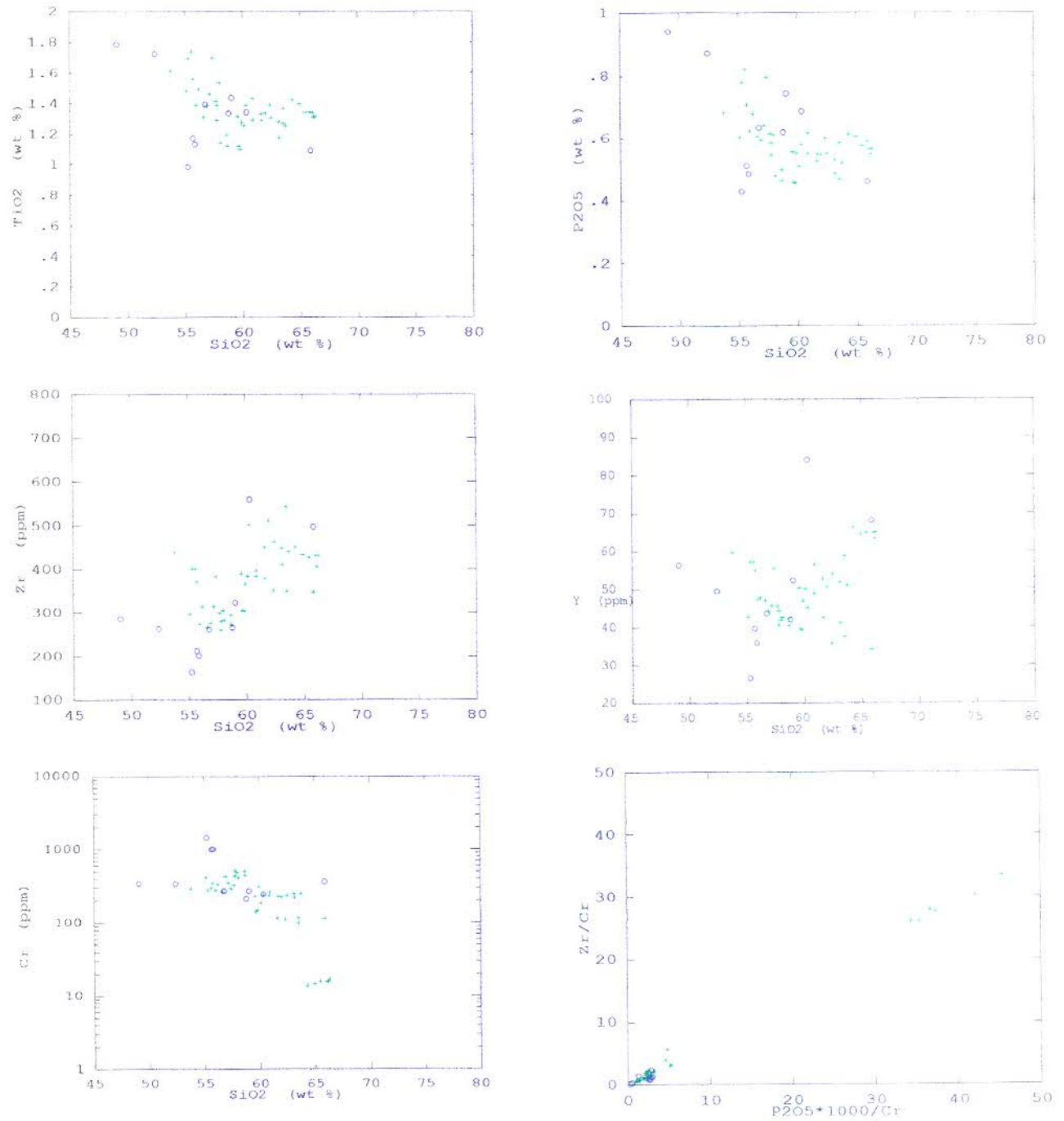


FIGURE 5.12: Selected Harker diagrams of the Garfield Member (green) and interbedded mafic lava flows hosted by the Makwassie Formation (blue). The composition of most of these rocks corresponds to that of the Gm facies of the Goedgenoeg Formation, while some of the Garfield Member rocks compare with the Gs facies (compare with Fig. 5.7).

5.9 DISCUSSION

Pervasive alteration of the Ventersdorp Supergroup has affected the mobile elements, such as the alkalis, so that geochemical classification of these rocks through use of these elements are suspect. Even so, a subalkaline (tholeiitic) to calc-alkaline composition can be recognised. Classification schemes utilizing immobile elements, however, indicate an andesitic to predominant dacitic composition for the Goedgenoeg Formation, while the Makwassie Formation is dacitic to rhyolitic. The Goedgenoeg and Makwassie Formations comprise weakly bimodal volcanics with metaluminous, subalkaline composition. The predominantly tholeiitic Goedgenoeg Formation is contrasted by the predominantly calc-alkaline Makwassie Formation. These rock types match the continental setting of the Goedgenoeg and Makwassie volcanics.

The lithostratigraphy is complimented by chemostratigraphy, which manifests into four geochemical facies (Gm, Gz, Gi and Gs) in the case of the Goedgenoeg Formation. The non-porphyritic to slightly porphyritic Gm facies and the porphyritic Gi facies are prevalent wherever the Goedgenoeg Formation occurs in the Bothaville area, while the other two facies are typically porphyritic and have limited distribution. The Gm facies is interbedded with the other three Goedgenoeg facies and also with the overlying acidic Makwassie Formation, indicating co-eruption of this Gm magma with magmas of more evolved composition. The Makwassie Formation comprises two geochemical facies; the dacitic Md facies at the base and the rhyodacitic Mr facies overlying it. Although both facies occur extensively in the Bothaville area, the Mr facies was possibly eliminated in places by erosion.

The above geochemical facies are reflected in the geochemical data of previous workers, *i.e.* Schweitzer and Kröner (1985), M.P. Bowen *et al.* (1986), T.B. Bowen *et al.* (1986), Crow and Condie (1988) and Grobler *et al.* (1989). None of these data bases, however, comprises all of the above six geochemical facies.

Recognition of the six geochemical facies are facilitated by a simple scattergram of P_2O_5/Cr vs Zr/Cr (Fig. 5.13). The Gi facies field of the Goedgenoeg Formation overlaps somewhat with the Md facies field of the Makwassie Formation. The Gi facies, however, comprises feldspar porphyries while the Md facies consists of quartz-feldspar porphyries. The same argument also holds for the overlap of Md and Gz facies. Subdivision of the Mr facies into a high incompatible/compatible element ratio (Mr+) and low incompatible/compatible element ratio (Mr-) is also possible through this scattergram. It is of interest to note that the felsic porphyries

of the Dominion Group plot outside the depicted field in Fig. 5.13, as their Zr/Cr ratio is higher than 50 (not shown), so that this diagram can also be used to discriminate chemically between Dominion and Makwassie porphyries. This is not adequately performed on the P/Ti vs Zr/P scattergram of T.B. Bowen (1984), as the rhyolitic Makwassie rocks plot in the Dominion porphyry field of this diagram. (T.B. Bowen's database only incorporated Makwassie Formation rocks of the Md facies; Mr facies rocks were lacking).

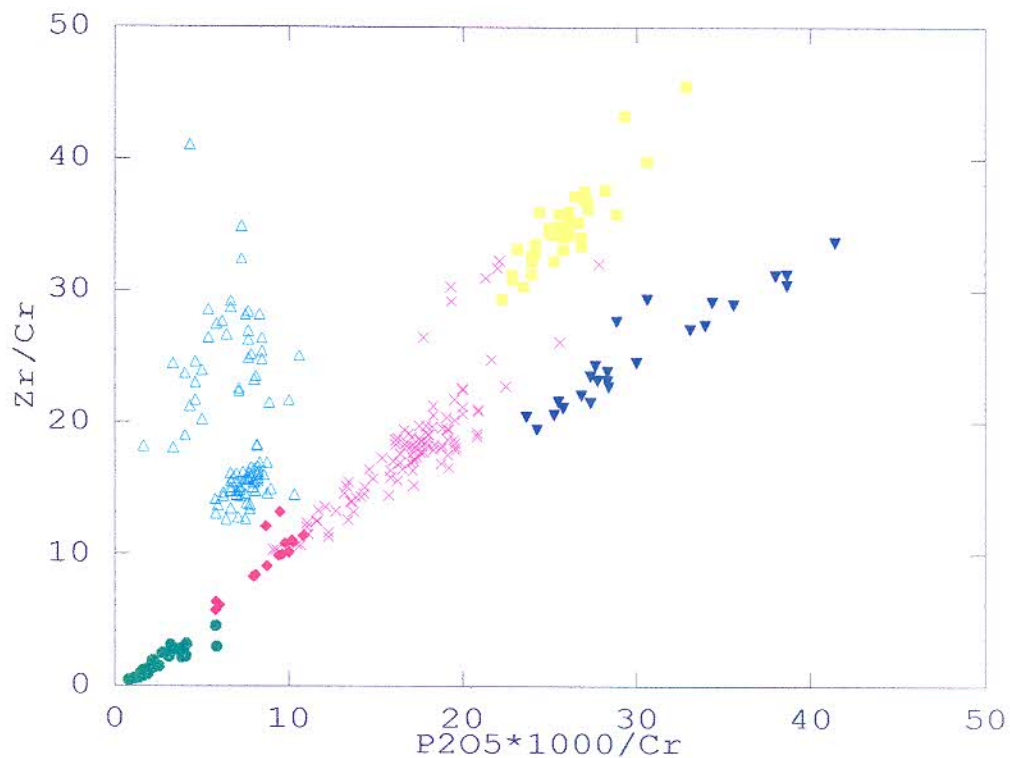


FIGURE 5.13: Scattergram of P/Cr vs Zr/Cr to facilitate discrimination of the Goedgenoeg and Makwassie Formation geochemical facies. Minor overlap occurs between the Gi and Md facies, and between the Md and Gz facies. The Gi and Gz facies consist, however, of feldspar porphyries and the Md facies of quartz-feldspar porphyries. The geochemical facies are Gm (green), Gi (red), Gs (blue), Gz (yellow), Md (magenta) and Mr (turquoise blue).

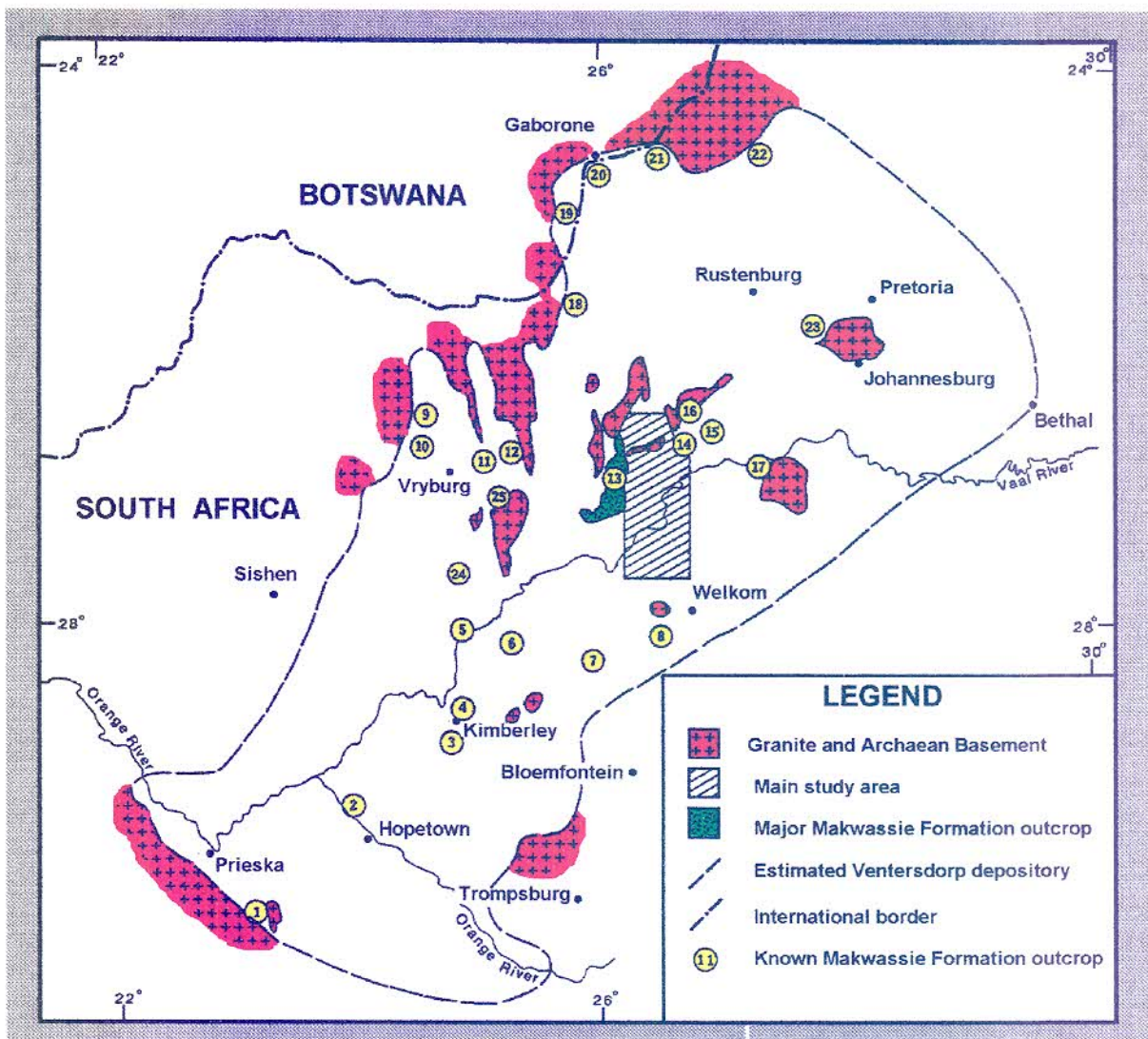
6. THE STRATIGRAPHY, PETROGRAPHY AND GEOCHEMISTRY OF THE GOEDGENOEG AND MAKWASSIE FORMATIONS OUTSIDE THE BOTHAVILLE AREA

6.1 INTRODUCTION

The Makwassie and Goedgenoeg Formations outcrop sporadically throughout the Ventersdorp Supergroup depository (Fig. 6.1). Some of the outcrops were investigated during this study whilst others are described from reports by previous researchers. The Goedgenoeg/Makwassie Formation at Wesselton Mine in Kimberley and outcrops at Makwassie Hills and Vryburg were sampled and analysed geochemically.

FIGURE 6.1: Outcrops of the Makwassie and Goedgenoeg Formations and correlatives in the Ventersdorp Supergroup depository. The occurrences marked by an asterisk are possible correlatives. The numbers represent the following localities

- 1 - T'Kuip Quartz Porphyry Formation, Sodium Group.
- 2 - Hereford Formation.
- 3 - Ritchie Quartz Porphyry Formation.
- 4 - Suboutcrop in the Kimberley Mines.
- 5 - Outcrop southwest of Warrenton.
- 6 - Outcrop on Honiglaagte 1234, Honigkop 1002 and Goudkop 1496, north of Boshoff.
- 7 - Outcrop on Sweet Home 280 and Wildebeestfontein 471, between Bultfontein and Dealesville.
- 8 - Outcrop on Vaalkoppies 8, between Welkom and Bultfontein.
- 9 - Kareefontein Formation, Zoetlief Group.
- 10 - Kareefontein Formation, Zoetlief Group.
- 11 - Outcrop on Vaarwel 683 and Schatkist 716, east of Vryburg.
- 12 - Kareefontein Formation, Zoetlief Group.
- 13 - Makwassie Hills.
- 14 - Klerksdorp Townlands.
- 15 - The Buffelsdoorn Graben.
- 16 - Platberg.
- 17 - Possible outcrop at the Vredefort Dome.
- 18* - Outcrop north of Mafikeng.
- 19* - Outcrop in south-eastern Botswana.
- 20* - The Seokangwana Belt.
- 21* - The Derdepoot Belt.
- 22* - Witfontein Formation, Buffelsfontein Group.
- 23 - Outcrop at the Johannesburg Dome.
- 24 - Phokwane Formation, Hartswater Group near Taung.
- 25 - Paardefontein Quartz Porphyry Formation, Amalia Group.



SECTION A - OUTCROPS EXAMINED DURING THIS STUDY

6.2 THE MAKWASSIE HILLS OUTCROP (Locality 13, Fig. 6.1)

The Makwassie Formation outcrops over a large area to the east, south and north of Wolmaransstad in the North West Province, while outcrop of the Goedgenoeg Formation is limited and still poorly mapped. The description of this occurrence by Dahms (1891) was possibly the first of Makwassie Formation rocks. The outcrop forms north-south striking, low-lying hills which protrude above the surrounding plains, with good exposures along the Wolmaransstad - Leeudoringstad road. Large boulders of relatively fresh porphyry lie next to the road between Witpoort and Wolmaransstad, where a trench was excavated for a water pipeline.

6.2.1 Quartz-Feldspar Porphyry

The Makwassie Hills consist predominantly of light-coloured, massive quartz-feldspar porphyries. The outcrops in the vicinity of Witpoort are conspicuously brownish-red in colour (Fig. 6.2). Holmes (1907) attributed this red colouration to weathering, while Cas and Wright (1988) relate red colouration of volcanic rocks to the remobilization of exsolved iron to form hematite, resulting from recrystallization during devitrification. It may also be due to oxidization of disseminated magnetite to form hematite (Cas and Wright, 1988). These reddish quartz-feldspar porphyry outcrops near Witpoort are very phenocryst-rich ($\pm 45\%$ by volume). The feldspar phenocrysts are up to 15 mm in length and vary from white to greenish (plagioclase) and reddish (K-feldspar) in hand specimen. Quartz phenocrysts are also abundant and reach sizes up to 8 mm.

The quartz-feldspar porphyries weather positively to form ridges, while the negative topographic areas consist of subordinate lithic, layered porphyritic rock units and finer-grained, bedded, tuffaceous rocks. Contorted bedding is apparent in some of the bedded rocks (Fig. 6.3). Good exposures of the above rock types appear on Bezuidenhoutskraal 64, to the south of the Wolmaransstad - Witpoort road and Von Backström (1962) also reported bedding structures on Doornfontein 313, further to the north.

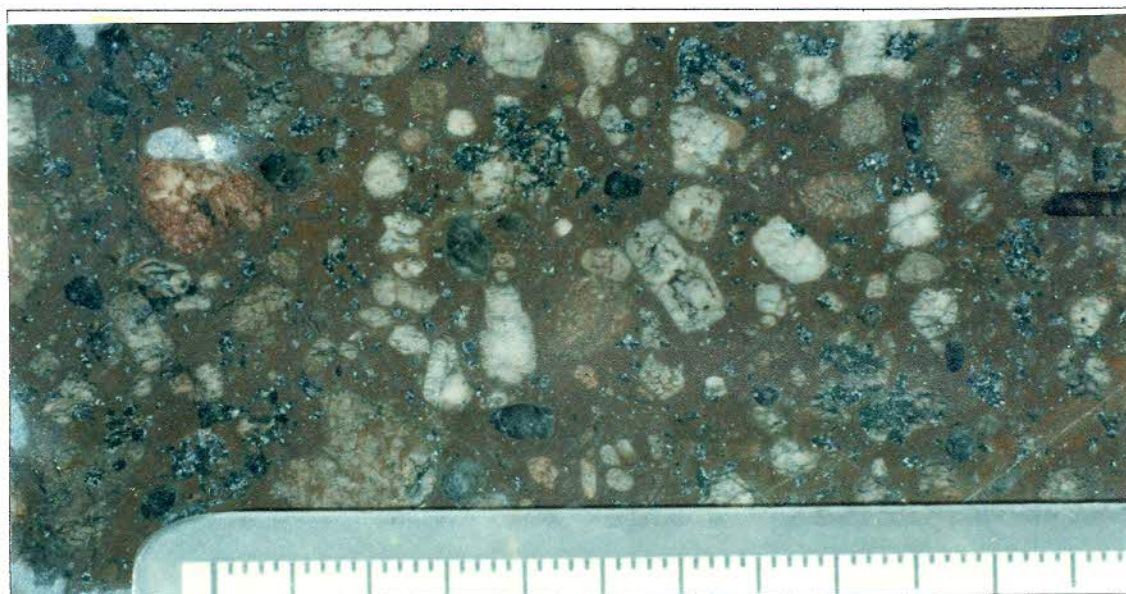


FIGURE 6.2: Red-coloured quartz-feldspar porphyry of the Makwassie Formation near Witpoort. Phenocrysts of K-feldspar appear red and plagioclase are white. (Scale in mm).



FIGURE 6.3: Clastic beds with contorted bedding, Makwassie Formation on Bezuidenhoutskraal 64. (Succession top to the right. Scale in cm).

The massive porphyries often grade into units with breccia textures (Fig. 6.4), well exposed next to the road between Wolmaransstad and Klerksdorp, close to the Palmietfontein turn-off. Although both the breccia fragments and host matrix are similarly porphyritic, thin sections indicate that the matrix is largely silicified, contains fragmented phenocrysts, microscopic devitrified lithics and perlitic-crack textures. These breccias are interpreted as autobreccias, which develop at flow tops of either rhyolite lava flows or rheomorphic ash-flow deposits.

Flow units in the porphyries consist of a dominant middle part of massive quartz-feldspar porphyry which grades upwards into bedded, lithic beds, often with contorted bedding, or into autobreccias. Individual flow units are separated by layered, tuffaceous units. The flow units are interpreted as high-temperature ash-flow units similar to those recognized in the Bothaville area and compares lithologically to the high-temperature ash-flow units of the Jozini rhyolites, described by Bristow (1989b).

6.2.2 Feldspar Porphyry

An outcrop of feldspar porphyry occurs in a low-lying area along the Makwassie Spruit to the northeast of Wolmaransstad. This outcrop is indicated as Rietgat Formation on the Geological Map of South Africa (Geological Survey of South



FIGURE 6.4: Makwassie Formation quartz-feldspar porphyry breccia near Wolmaransstad. (Scale in cm).

Africa, 1984) and on the 1:250 000 geological map of the West Rand (Geological Survey of South Africa, 1986). In hand specimen the feldspar porphyry is dark green-coloured and contains scattered feldspar phenocrysts. In thin section, rare fragments of quartz phenocrysts were identified, while the feldspar phenocrysts display fractured features. The porphyry matrix is cryptocrystalline, but in places display microscopic granophyric textures which are unattached to phenocrysts. The granophyric textures are ascribed to rapid crystal growth from devitrification of glass (Barker, 1970; Lofgren, 1971a), or from rapid crystallization from a melt (Barker, 1970; Lofgren 1971b; Lofgren 1980).

Another feldspar-porphyry is exposed on Palmietfontein 312, next to the Makwassie Spruit. The top is highly amygdaloidal and contains abundant tuffaceous, lithic and devitrified chloritic fragments. Although the complete unit is not exposed, it appears to be a partially-welded pyroclastic-flow unit with well-preserved flow-textures.

As described above, the lithological and petrographic features of these feldspar porphyry outcrops are unlike that of the Rietgat lavas. Since it is overlain by

quartz-feldspar porphyry similar to the Makwassie Formation of the Bothaville area, the feldspar porphyry may be a correlative of the Goedgenoeg Formation, alternatively of the Garfield Member.

6.2.3 Borehole LLE1

Although this borehole was included in the discussion of the Bothaville area (Chapters 3 to 5), some comments are appropriate in this chapter as this borehole was drilled in the quartz-feldspar porphyry outcrop at Makwassie Hills, on the farm Leeuwfontein 29, close to Witpoort. The borehole was drilled through a succession of quartz-feldspar and feldspar porphyries, but failed to penetrate the base of the Goedgenoeg Formation (Fig. 6.5).




Formation	Depth	Log	Lithological Description	Chemical Facies
GARFIELD MEMBER	636 m		Quartz-feldspar porphyry	Percussion Drilled
	700 m		Mafic, amygdaloidal lava	Gm facies
MAKWASSIE FORMATION	848 m		Quartz-feldspar porphyry	Mr facies (low)
	1299 m		Mafic, amygdaloidal lava	Gm facies
	1687 m		Quartz-feldspar porphyry	Mr facies (high)
	2404 m			Md facies
	2604 m			
GOEDGENOEG FORMATION	3648 m		Feldspar porphyry	Gs facies
	3659 m		Mafic, amygdaloidal lava End of hole	Gm facies

FIGURE 6.5: Litho- and chemostratigraphy of borehole LLE1. (Depth in metres below collar. Not to scale).

6.2.3.1 The Goedgenoeg Formation (2604 m to 3659 m)

Although the Goedgenoeg Formation in the central part of the Bothaville area consists of interbedded basic and intermediate volcanics, the succession is less complicated in borehole LLE1. The succession below 2604 m is correlated with the Goedgenoeg Formation (Figs. 6.5; 6.6) and consists of feldspar porphyry and subordinate quartz-feldspar porphyry with an intermediate geochemical composition (Table 6.1). Almost the complete succession below 2604 m correlates with the Gs facies of the Goedgenoeg Formation, while the succession below 3648 m correlates with the Gm facies (Fig. 6.6). The Gi and Gz facies are not represented in this borehole. Since the Gz facies occurs at the base of the Goedgenoeg Formation and borehole LLE1 failed to penetrate the base of the Formation, there is a possibility that the Gz facies may be present deeper down.

6.2.3.2 The Makwassie Formation (surface to 2604 m)

Lithostratigraphically the succession from surface to 2604 m is correlated with the Makwassie Formation (Figs. 6.5; 6.6). Geochemically the lowermost part of the succession (between 2404 m and 2604 m) correlates with the Md facies and the succession from surface to 2404 m with the Mr facies (Fig. 6.6). From just below the mafic unit to the top of the Md facies (1753 m to 2404 m) the Mr facies has a high incompatible/compatible element ratio, while the flow-unit just below the mafic unit (1687 m to 1753 m) and the succession between the Garfield Member and the mafic unit (848 m to 1299 m) have a low ratio. Since the borehole was percussion drilled to approximately 700 m and samples were not available, an outcrop sample was geochemically analysed. The rhyolitic composition of this sample (Table 6.1) correlates with the Mr facies (Fig. 6.6) and has a low incompatible/compatible element ratio, similar to the succession between the Garfield Member and the mafic unit.

6.2.3.3 The Garfield Member (± 600 m to 848 m) and Interbedded Mafic Unit (1299 m to 1687 m)

The Garfield Member (636 m to 848 m) and the interbedded mafic unit (1299 m to 1687 m) have a similar composition as the Gm facies of the Goedgenoeg Formation (Fig. 6.6). These two mafic successions, however, differ significantly in TiO_2 , P_2O_5 , Zr, Ni and Cr contents (Table 6.1) which rules out the possibility of duplication of the succession in the borehole.

6.2.3.4 Discussion

The anomalous combined Goedgenoeg/Makwassie thickness of 3 600 m intersected by this borehole is problematic, as the maximum thickness of this

succession in the Bothaville area is just over 2 000 m. The borehole is situated to the west of a projected fault which separates the Bothaville area from the Makwassie Hills outcrop. Evidence for stratigraphic duplication by faulting or thrusting was not found. Characteristics of intrusive facies (*i.e.* intrusive contacts, cross-cutting units and chill contacts) or caldera facies (*i.e.* steep-dipping units, intra-caldera volcanic facies and excessive hydrothermal alteration) are also absent. It is significant that the Goedgenoeg Formation in borehole LLE1 consists predominantly of the Gs facies, which was only represented in borehole DHK1 in the Bothaville area. The Makwassie Formation in borehole LLE1 hosts a major mafic unit which apparently does not correlate with the Garfield Member.

It is concluded that the Makwassie Hills area represents a separate Platberg rift, separated from the adjacent Bothaville rift by a major north-south striking fault. The style of volcanism, major characteristics and geochemical composition of the erupted material are similar, but the volcanic sequences differ somewhat.

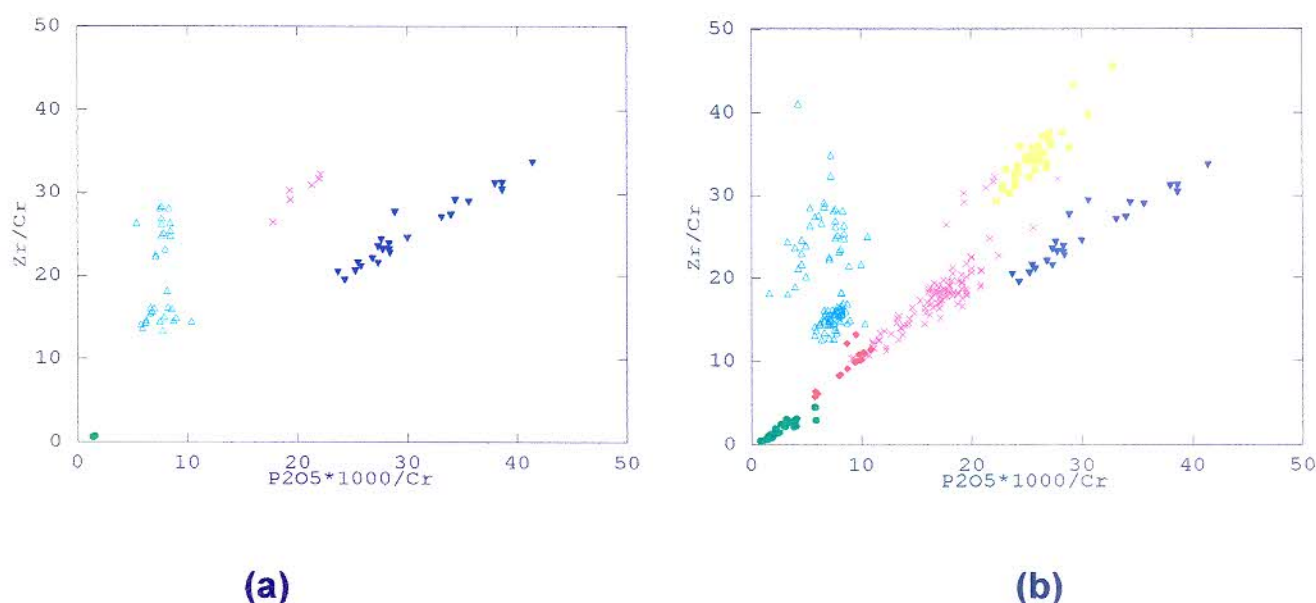


FIGURE 6.6: (a) P_2O_5/Cr vs Zr/Cr plot of borehole LLE1's samples. The symbols represent the following intersections with the correlation in brackets: green - 3648 m to 3659 m (Gm); blue - 2604 m to 3648 m (Gs); magenta - 2404 m to 2604 m (Md); turquoise - 848 m to 1299 m (Mr-low) and 1687 m to 2404 m (Mr-high); green - 636 m to 848 m (Gm) and 1299 m to 1687 m (Gm). (b) A similar diagram for the Goedgenoeg and Makwassie Formations in the Bothaville area. The geochemical facies are indicated by the coloured symbols: green - Gm; red - Gi; blue - Gs; yellow - Gz; magenta - Md; turquoise - Mr.

TABLE 6.1: Average geochemical compositions of Goedgenoeg and Makwassie Formations in borehole LLE1. The interbedded unit of mafic lavas in the Makwassie Formation is listed as *Mafic*. The borehole did not penetrate the base of the Goedgenoeg Formation.

UNIT	GOEDGENOEG		MAKWASSIE				GAR-FIELD	OUT-CROP
FACIES	Gm	Gs	Md	Mr-High	Mafic	Mr-Low	Gm	Mr-Low
N	2	24	6	17	5	13	4	1
Depth From	3659	2604	2404	1687	1299	848	636	
Depth To	3648	3659	2604	2404	1687	1299	848	
SiO ₂	57.57	65.58	69.72	75.00	56.45	72.90	56.01	70.73
TiO ₂	1.07	1.27	0.89	0.43	1.20	0.60	1.67	0.71
Al ₂ O ₃	14.27	13.22	13.08	12.54	12.41	12.75	13.80	12.89
Fe ₂ O ₃	10.50	7.38	4.86	2.16	11.09	3.42	11.12	3.97
MnO	0.13	0.09	0.07	0.04	0.11	0.05	0.16	0.05
MgO	6.01	1.32	0.63	0.05	8.65	0.49	5.44	0.73
CaO	5.38	3.57	2.76	1.21	6.31	1.64	6.97	1.96
Na ₂ O ₃	3.10	3.77	3.46	4.03	1.94	3.52	2.07	4.33
K ₂ O	1.49	3.29	4.22	4.44	1.32	4.45	1.99	4.43
P ₂ O ₅	0.48	0.53	0.32	0.10	0.54	0.18	0.78	0.20
Zr	212	440	470	339	220	367	388	417
Y	37	60	51	43	38	45	56	47
Sr	413	380	308	174	546	196	705	144
Rb	38	96	114	130	31	125	43	113
Cu	52	8	5	2	31	6	35	-
Zn	124	117	83	51	124	59	132	-
Ni	124	13	9	7	262	12	126	-
Ba	1115	1405	1411	1311	755	1421	1102	1499
Nb	11	19	18	18	11	18	19	21
V	195	122	72	22	200	52	205	59
Cr	325	18	16	16	784	25	299	24
Co	38	16	9	7	47	8	41	5

6.3 SUBOUTCROP IN THE KIMBERLEY MINES (Locality 4, Fig. 6.1)

In the Kimberley Mines the Ventersdorp Supergroup overlies the Basement Igneous Complex and is in turn overlain by rocks from the Karoo Supergroup. During this study the Goedgenoeg and Makwassie Formations could only be accessed in Wesselton Mine, as the other Kimberley Mines have already progressed below the base of the Ventersdorp Supergroup. Du Toit (1907) described the Ventersdorp System in the Kimberley Mines, but at that time the full Ventersdorp succession had only been penetrated in the De Beers Mine. Joubert (1973) gave further descriptions of the Ventersdorp rocks in a number of the Kimberley Mines.

6.3.1 Stratigraphy

The stratigraphy of the Ventersdorp Supergroup in the Kimberley area is illustrated by a section from the Kimberley Mine to Wesselton Mine (Fig. 6.7). The Ventersdorp succession consists of the complete Platberg and Pniel sequences. A topographic high of Archaean Basement Igneous Complex is present in the vicinity of the Bultfontein and Du Toitspan Mines with the Makwassie Formation abutting against this horst. A thick succession of Rietgat Formation lavas and sedimentary rocks of the Bothaville Formation is preserved on this horst. The horst is of pre-Goedgenoeg age and was being eroded during deposition of the Kameeldoorns Formation.

In Wesselton Mine, the Goedgenoeg and Makwassie Formations were intersected between 550 m and ± 995 m below surface. The levels below 904 m were still being developed at the time of this investigation. The succession consists of five distinctive units, interpreted as ash-flow units, which occur from 550 m to ± 650 m, ± 650 m to 760 m, 760 m to 820 m, 820 m to ± 920 m, and ± 920 m to 995 m respectively (Fig. 6.8). The thicknesses of the individual ash-flow units are 100 m, 110 m, 60 m, 100 m and 75 m respectively.

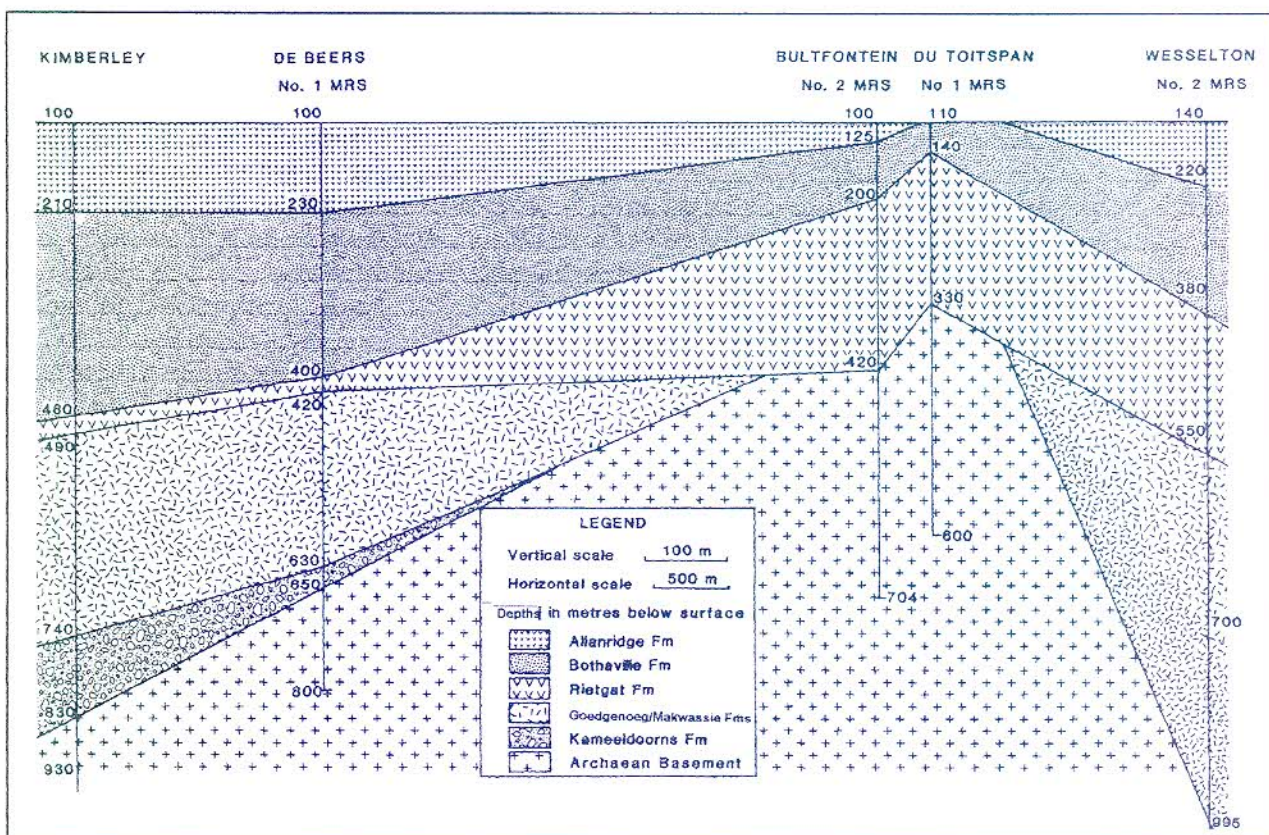


FIGURE 6.7: Stratigraphic section of the Kimberley Mines. Note the abutment of the Goedgenoeg/Makwassie Formation against the Archaean Basement high.





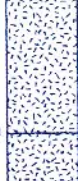



Formation	Depth	Log	Lithological Description	Chemical Facies
RIETGAT Fm.	550 m		Mafic, amygdaloidal lava flows (not observed)	Not Sampled
MAKWASSIE FORMATION	650 m		Quartz-feldspar porphyry (not observed)	Not Sampled
	Flow 1		Quartz-feldspar porphyry - light coloured and flow banded	Not Sampled
	760 m		Quartz-feldspar porphyry - light-coloured and flow banded	Mr facies
	Flow 3 820 m		Complex unit with lapilli and blocks	Mr facies
	Flow 4		Quartz-feldspar porphyry - massive, green to red in colour	Md facies
GOEDGE-NOEG Fm.	920 m		Quartz-feldspar porphyry - massive, green-coloured	Gs facies
ARCHAEOAN GRANITE	995 m		Metagranites (not observed)	

FIGURE 6.8: Litho- and chemostratigraphy of the Goedgenoeg and Makwassie Formations, as exposed in Wesselson Mine. (Depths in metres below surface. Not to scale).

During the first visit to the mine, the section from 660 m to 785 m was investigated. The existence of the uppermost unit (from 550 m to 650 m) was verified by T. McGhee of De Beers in Kimberley. During a second visit to collect samples, the only accessible exposure was between 785 m and 904 m. The individual flow-units between 760 m and 995 m were sampled for geochemical analyses, with results as listed in Table 6.2.

6.3.2 Detail of Examined Ash-Flow Units

Units 1 and 2 (\pm 650 m - 760 m and 760 m - 820 m): These two units both have a reddish colour and are lithologically similar. The upper parts are amygdaloidal

with the amygdales changing downwards from elongated to spherical in shape. The middle parts of both units are cryptocrystalline with very small (1 to 2 mm) fragmented phenocrysts of quartz and feldspar. Lamination is visible (Fig. 6.9) and small, ash-sized (less than 4 mm) inclusions occur, increasing to lapilli-size (4 mm to 16 mm) in the lower parts (Fig. 6.10). The lamination is better developed or preserved in the lowermost part of the units and is often locally contorted with tight flow-folds (Fig. 6.10 and 6.11). It drapes over lapilli and rotation of some lapilli is evident. A very fine-grained, light-coloured layer of less than 200 mm thick occurs at the base of the upper unit at 760 m. This layer is contorted and in places has a complex relationship to the underlying unit. It is interpreted as a basal vitrophyre, a common feature in pyroclastic-flow deposits (Cas and Wright, 1988). The lower flow has a thin, slightly discoloured zone (Figs. 6.10 and 6.12) at its base (at 820 m). In thin section the lamination is poorly defined by variation in the chlorite content in the matrix and preferential concentration of secondary minerals along parallel zones. Opaque oxides, secondary sericite and calcite are ubiquitous. The feldspar phenocrysts are totally altered to secondary amorphous minerals, while quartz phenocrysts are clouded and have reaction rims. The matrix displays granophyric textures, ascribed to rapid crystallization during devitrification of the matrix.



FIGURE 6.9: Upper Makwassie ash-flow unit (760 - 820 m) in Wesselton Mine. Note the flow lamination. When compared with the Makwassie Formation in the Bothaville area, the quartz and feldspar phenocrysts are smaller and less abundant. A minor fault is visible in the left part of the photograph. The dark areas in the middle of the photograph are chloritic shear partings. (The pen is 12 cm in length).



FIGURE 6.10: Contorted lamination and tight flow-folds in the porphyry at the base of the 760 - 820 m flow-unit. Note the quartz-feldspar porphyry lapilli in the centre of the picture. The contact with the dark-coloured underlying flow-unit is visible. A thin, discolouration zone at the base of the light-coloured flow-unit can be discerned and is interpreted as a vitrophyre. (The pen is 13 cm in length).



FIGURE 6.11: Contorted lamination in the basal part of the 760 - 820 m flow-unit. (The chisel is 30 cm in length).

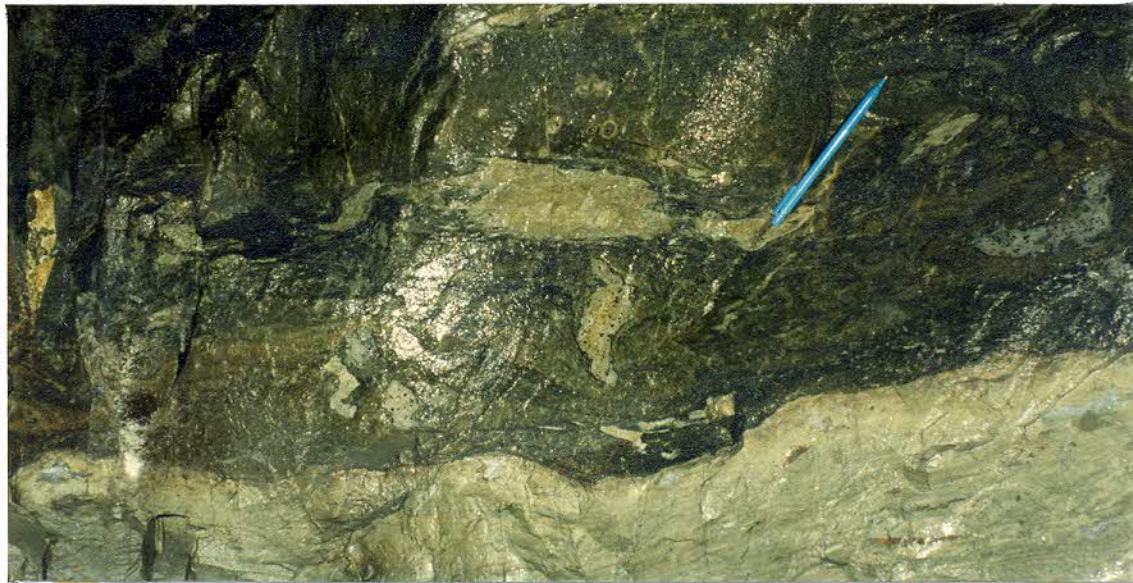


FIGURE 6.12: The dark-coloured 820 m flow-unit with abundant inclusions. Note the distortion of some of the inclusions. The discolouration zone at the base of the upper light-coloured flow-unit is interpreted as a vitrophyre. (The pen is 14 cm in length).

Unit 3 (820 m): A unit of ± 5 m in thickness occurs at the 820 m level and is markedly different from the other flow-units. The unit is dark-coloured and contains abundant lapilli- and block-size inclusions of quartz-feldspar porphyry, as well as sedimentary rock (Fig. 6.12). Some of these inclusions are deformed and flattened. The unit is composed of multiple layers with complex relationships, as is illustrated by the overlying flow-unit dragging part of the dark-coloured unit into its base (Fig. 6.13). In thin section cryptocrystalline material defines fine lamination. Larger lithic fragments indent the underlying laminae while overlying laminae drape over it. The lapilli display perlitic-crack textures and abundant amygdales.

Unit 4 (820 m - \pm 920 m): The top of this unit is highly amygdaloidal and brecciated. It is green-coloured and contains abundant quartz and feldspar phenocrysts, all with conspicuous reaction rims. Silicified spherulites, which appear as white specs in hand specimen, are hosted in the matrix.

Unit 5 (below 920 m): Drill drives from the 920 m level have established the existence of another unit (75 m thick) below this level. Borehole-core samples of the upper part of this unit have a dark-green colour and are highly amygdaloidal. Thin sections show occasional large quartz phenocrysts and abundant, altered feldspar phenocrysts in a granophyric matrix.



FIGURE 6.13: Part of the 820 m flow-unit (dark-coloured rock) which was dragged into the base of the overlying, light-coloured flow-unit during emplacement. This indicates the unconsolidated state of the 820 m unit at the time of deposition of the upper unit. (The pen is 14 cm in length).

6.3.3 Geochemical Composition

Each flow-unit has a distinctive geochemical composition (Table 6.2). Unit 5 correlates with the Gs facies of the Goedgenoeg Formation, unit 4 with the Md facies and units 2 and 3 with the Mr facies of the Makwassie Formation (Fig. 6.14). Unit 2 has a high incompatible/compatible element ratio and unit 3 a low incompatible/compatible element ratio. The geochemical stratigraphy of the Goedgenoeg and Makwassie Formations at Wesselton exhibits a trend from basic (unit 5) at the base to acidic at the top (unit 2), similar to that in the Bothaville area.

6.3.4 Discussion

The ash-flow units display a well-defined or well-preserved flow lamination and are interpreted as high-temperature ash-flows rather than rhyolite lava flows on the basis of fragmented phenocrysts and lack of autobreccia. The 820 m flow-unit is interpreted as a partially welded to welded pyroclastic flow, emplaced at a lower temperature than the underlying and overlying flows. The Goedgenoeg and Makwassie Formations at Wesselton correlate lithologically and geochemically with the occurrence in the Bothaville area and similar geochemical facies are present at both localities. The Makwassie rocks in Wesselton Mine have slightly lower concentrations of incompatible elements such as zirconium and phosphorous, possibly due to magmatic fractionation involving zircon and apatite.

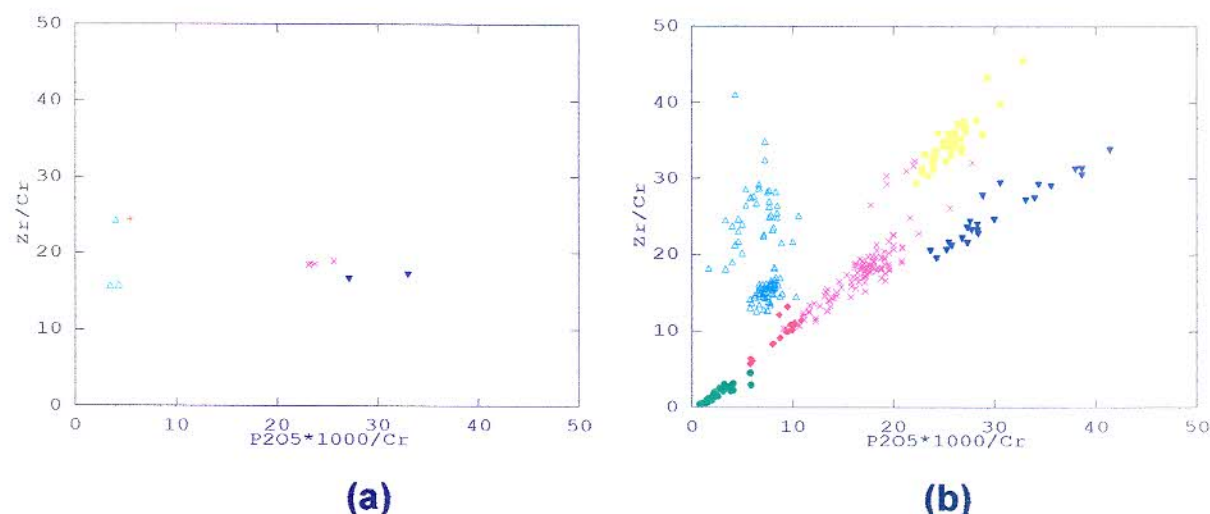


FIGURE 6.14: (a) P_2O_5/Cr vs Zr/Cr plot of porphyry samples from Wesselton Mine. The symbol colours are as follows: unit 2 - red; unit 3 - turquoise; unit 4 - magenta; unit 5 - dark blue. (b) A similar diagram for the Goedgenoeg and Makwassie Formations in the Bothaville area. The geochemical facies are indicated by the coloured symbols: green - Gm; red - Gi; blue - Gs; yellow - Gz; magenta - Md; turquoise - Mr.

TABLE 6.2: Average geochemical compositions of the individual flow-units in Wesselton Mine, Kimberley. The Ritchie Formation analyses are from Potgieter and Lock (1978). N = number of samples. Normalized data. Major elements in weight % volatile free and trace elements in parts per million.

FLOW-UNIT	2	3	4	5	RITCHIE
Depth (m)	760-820	820	820-920	920-995	
FACIES	Mr-High	Mr-Low	Md	Gs	Mr-High
N	1	3	4	2	4
SiO ₂	76.40	72.97	65.82	56.87	77.37
TiO ₂	.42	0.38	1.13	1.27	0.13
Al ₂ O ₃	11.45	13.53	13.58	13.53	11.85
Fe ₂ O ₃	2.89	3.70	7.68	10.74	1.14
MnO	0.04	0.04	0.11	0.23	0.02
MgO	0.90	2.42	1.80	2.12	1.45
CaO	0.96	1.60	4.56	10.94	0.02
Na ₂ O ₃	1.74	0.74	2.09	1.82	0.07
K ₂ O	5.13	4.55	2.84	2.02	8.94
P ₂ O ₅	0.07	0.06	0.38	0.45	0.01
Zr	316	288	297	253	152
Y	26	24	37	41	34
Sr	62	45	125	313	47
Rb	128	119	78	64	324
Ba	1078	519	661	852	642
Nb	11	11	12	12	15
V	27	35	135	203	-
Cr	13	16	16	15	-
Co	5	6	15	17	-

The geochemical consistency of the Goedgenoeg and Makwassie volcanics at widespread localities in the Ventersdorp depository is remarkable. The presence of the Goedgenoeg Formation at Wesselton indicates that this formation is widespread in the Ventersdorp Supergroup depository. The absence of an interbedded mafic unit in the Makwassie Formation substantiates that such units, e.g. the Garfield Member, are localized and of limited lateral extent.

6.3.5 Note on the Ritchie Formation (Locality 3, Fig. 6.1)

The Ritchie Formation occurs near the confluence of the Modder and Riet Rivers, approximately 40 km south of Kimberley. It is composed of quartz-feldspar porphyry, separated into eutaxitic ignimbrites and rheoignimbrites by Potgieter and Lock (1978). The eutaxitic ignimbrites are the most widespread and appear similar to the porphyries of the T'Kuip Quartz Porphyry Formation (Potgieter and Lock, 1978). They mention that the rheoignimbrites resemble rhyolite lava flows, as almost all original pyroclastic textures are destroyed through flow deformation. The rheoignimbrites display prominent, complex flow folding, which are *"...contorted, sharply folded and often knotted"* (Du Toit, 1907). Potgieter (1974) also described "melanocratic" quartz-feldspar porphyry in the basal part of the Ritchie outcrop, and mingled dark and light-coloured rheoignimbrite in other parts of the outcrop.

Potgieter (1974) and Potgieter and Lock (1978) correlated the Ritchie Formation with the Makwassie Formation and are supported by S.A.C.S. (1980). The present study correlates the Ritchie Formation with the Makwassie porphyry intersected in Wesselton Mine. The basal parts of the Makwassie flow-units above the 820 m level in Wesselton Mine are laminated, and resemble the rheomorphic ignimbrites of Ritchie. The "melanocratic" Ritchie ignimbrite of Potgieter (1974) may correlate with the Wesselton flow-units below the 820 m level, while the intermingled dark and light-coloured Ritchie ignimbrite (Potgieter, 1974) may be equivalent to the subordinate, dark-coloured unit at the 820 m level in Wesselton Mine.

The geochemical composition of the Ritchie Formation (Potgieter and Lock, 1978) is listed in Table 6.2. The composition compares with the Mr facies of the Makwassie Formation and has a high incompatible/compatible element ratio. Considering the stratigraphic position of the 760-820 m flow-unit (with high ratio) at Wesselton Mine, an equivalent of the 820-995 m flow-unit may therefore be present, but not exposed, at the Ritchie locality.

6.4 OUTCROP ON VAALKOPPIES 8, BETWEEN WELKOM AND BULT-FONTEIN (Locality 8, Fig. 6.1)

This outcrop consists of two small hills situated on the flood plain of the Vet River, to the northwest of the farmhouse on Vaalkoppies 8. This occurrence is indicated on the Geological Map of South Africa (Geological Survey of South Africa, 1984). The outcrop is highly sheared and altered; thin sections show mostly cryptocrystalline material with quartz and feldspar phenocrysts almost obliterated. Behounek (1980) distinguished two flow-units on the basis of colour difference and reported rare quartz phenocrysts of between 0.5 mm and 3 mm, and highly altered feldspar phenocrysts.

On Goudkoppies 461 to the east of Vaalkoppies 8, the Makwassie porphyries are overlain by immature conglomerate and quartzite. The conglomerate was quarried for road-building material and large blocks are exposed. Behounek (1980) assigned this outcrop to the Rietgat Formation and not the Bothaville Formation, the reason being the immature lithology and the statement by Winter (1965) that the Bothaville Formation pinches out against the Wesselsbron Arch. In this area the Makwassie Formation probably abuts against the Wesselsbron Arch. Granite of the Wesselsbron Arch is exposed in a gravel pit on Geduld 37 to the north of Vaalkoppies 8, north of the Sand River. The granite is extensively weathered and is overlain by Rietgat Formation lava, tuff and arkose. Behounek (1980) described this outcrop in detail.

6.5 OUTCROPS ON SWEET HOME 280 AND WILDEBEESTFONTEIN 471, BETWEEN BULTFONTEIN AND DEALESVILLE (Locality 7, Fig. 6.1)

To the west of Bultfontein the Makwassie Formation is poorly exposed on a small rise next to a large pan and is overlain by Rietgat Formation lava and Bothaville Formation arkose. This occurrence is shown on the Geological Map of South Africa (Geological Survey of South Africa, 1984). The outcrop consists of massive quartz-feldspar porphyry with abundant, large phenocrysts of up to 4 mm. Flow-units could not be distinguished and the contact with overlying rock types is covered by soil.

6.6 OUTCROPS ON HONIGLAAGTE 1234, HONIGKOP 1002 AND GOUDKOP 1496, NORTH OF BOSHOFF (Locality 6, Fig. 6.1)

A low-lying northwest striking ridge, composed of quartz-feldspar porphyry, occurs to the east of the Boshoff - Christiana gravel road. The occurrence is indicated on the Geological Map of South Africa (Geological Survey of South Africa, 1984). The outcrop appears massive, with abundant quartz veins and

jasper. It contains numerous large (up to 20 mm) feldspar phenocrysts, the largest observed during this study. Although plentiful, quartz phenocrysts are small (± 2 mm). The quartz-feldspar porphyry is extensively altered and brownish in colour. In thin section the feldspar phenocrysts reveal alteration to cryptocrystalline, opaque oxides. Using colour differences Behounek (1980) recognized 3 flow-units in the outcrop. Behounek also reported another, even more altered, outcrop to the west of the road. This outcrop has conspicuous green, chloritic spots which can possibly be attributed to devitrification spherulites. These outcrops are surrounded by alluvium, calcrete and dolerite and their relationship to other Ventersdorp Supergroup formations could not be established. Behounek (1980) inferred the presence of Rietgat lava under the alluvium and calcrete.

6.7 THE VRYBURG AREA (Localities 9, 10, 11 and 12, Fig. 6.1)

6.7.1 Outcrop on Vaarwel 683 and Schatkist 716 (Locality 11, Fig. 6.1)

This single outcrop is situated to the east of Vryburg, south of the Vryburg - Delareyville road and is indicated as Kraaipan Group on the Geological Map of South Africa (Geological Survey of South Africa, 1984). This small outcrop consists of phenocryst-rich quartz-feldspar porphyry with numerous quartz veins, jasper and chert. The large phenocrysts are up to 8 mm in length and thin sections show the feldspar to be highly altered and hosted in an epidotized matrix. The porphyry is overlain by tuffaceous sediments, possibly of the Rietgat Formation; the contact relationships are obscured by soil cover. The quartz-feldspar porphyry is lithologically similar to the massive middle zones of flow-units in the Bothaville area and is considered to be a Makwassie Formation correlative.

6.7.2 Kareefontein Formation, NW of Vryburg (Localities 9 and 10, Fig. 6.1)

This is the type area of the Zoetlief Group as described by Du Toit (1906), which is subdivided into the Oasis Formation (conglomerates and arkoses), the Kareefontein Formation (quartz-feldspar porphyry) and the Vogelvlei Formation (tuff, arenaceous tuffaceous sediments and lava) (S.A.C.S., 1980). S.A.C.S. (Ventersdorp Task Group Meeting, 1995) accepted that the Oasis, Kareefontein and Vogelvlei Formations are correlated with the Kameeldoorns, Makwassie and Rietgat Formations respectively.

The Kareefontein quartz-feldspar porphyry on Manchester 593, along the Vryburg - Tosca road, is intersected by quartz veins, but otherwise appears massive and phenocryst-rich. At Karee Fontein 454 the porphyry is dark blue-grey in colour, with conspicuous glassy, purplish-coloured bands (Figs. 6.15 and

6.16). These parallel bands weather positively and some bands terminate abruptly, while others display folds. The glassy bands appear similarly porphyritic as the host porphyry, with some phenocrysts continuing across the contact between the band and host porphyry. In thin sections it is evident that these bands and globules are silicification fronts, similar to siliceous nodular devitrification structures at Benambra, southeastern Australia (Personal communication, R. Allen; Allen, 1988). Comparable textures were also observed in borehole DF1 in the Bothaville area.

On Vogel Vlei 450 massive feldspar porphyry underlies the Kareefontein quartz-feldspar porphyries. The top of the feldspar porphyry is amygdaloidal, has a grey-green colour and contains scattered, broken feldspar phenocrysts. Microscopically, granophyric textures are visible in the matrix. This porphyry is considered to be equivalent to the Goedgenoeg Formation in the Bothaville area.

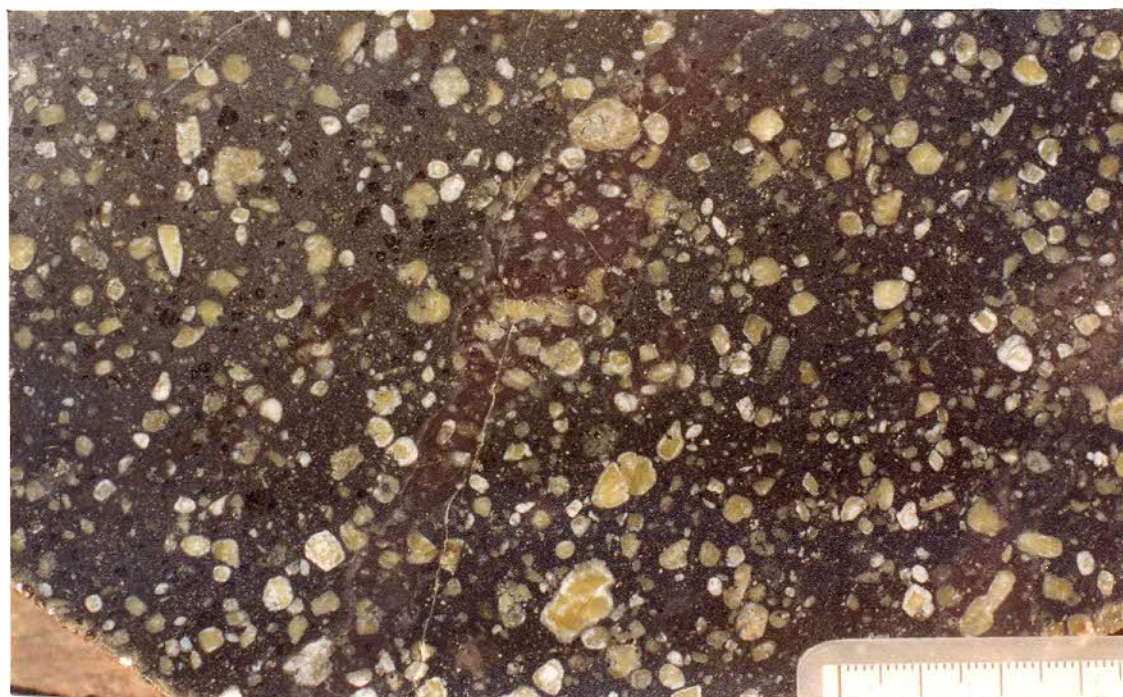


FIGURE 6.15: Silicification front, visible as a purplish-coloured band in quartz-feldspar porphyry outcrop near Vryburg. Note unconnected globules of similar material in the host porphyry. Sample LNV014; Kareefontein Formation, Zoetlief Group. (Scale in mm).

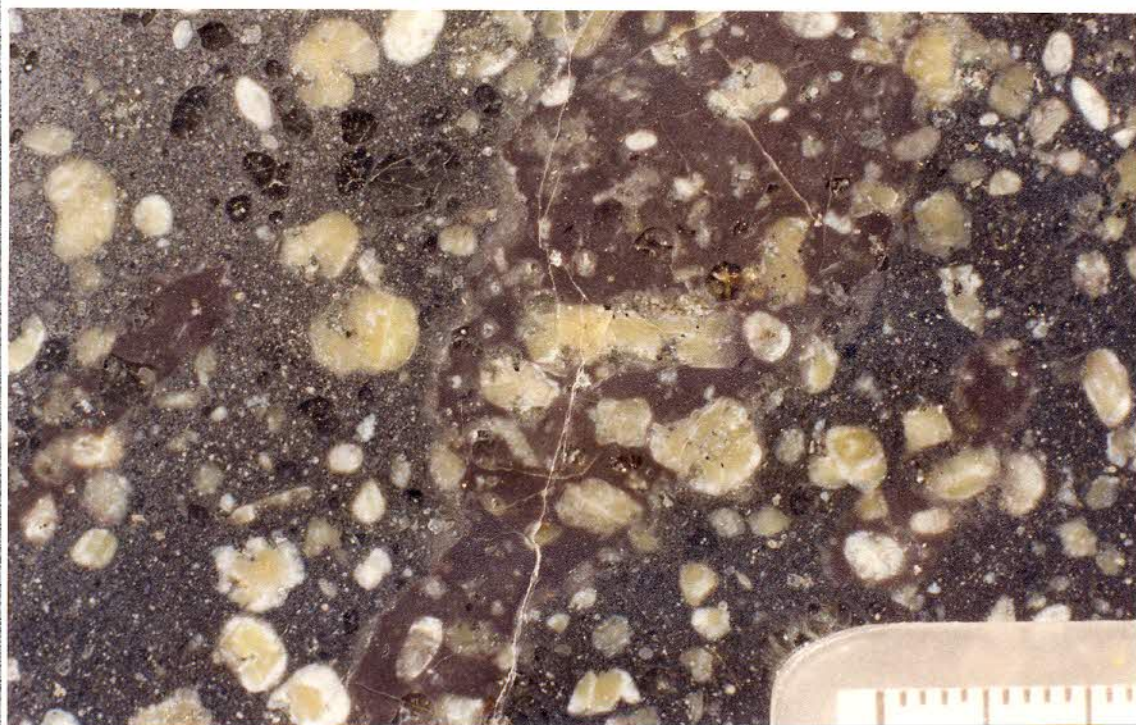


FIGURE 6.16: Detail of the silicification front in Fig. 6.15. Note that feldspar phenocrysts straddle the contact between silicified band and host porphyry. (Scale in mm).

6.7.3 Geochemical Composition

The geochemical compositions of samples from the above outcrops are listed in Table 6.3. The samples from Schatkist, Vaarwel and Manchester correlate with the Mr facies of the Makwassie Formation and have a high incompatible/compatible element ratio (Table 6.3). The banded porphyry at Karee Fontein possibly correlates with the Md facies of the Makwassie Formation (Fig. 6.17); the rocks suffered excessive alteration as indicated by silicification. The glassy bands contain more silica than the host porphyry (Table 6.3), confirming that they are silicification fronts. The host porphyry in the immediate area next to the glassy bands are depleted in the major elements SiO_2 and K_2O , but are enriched in most of the other major elements (Table 6.3). The feldspar porphyry on Vogel Vlei 450 correlates with the Gm facies of the Goedgenoeg Formation (Fig. 6.17). This outcrop further demonstrates the extensive occurrence of the Goedgenoeg Formation over the area of Ventersdorp Supergroup depository.

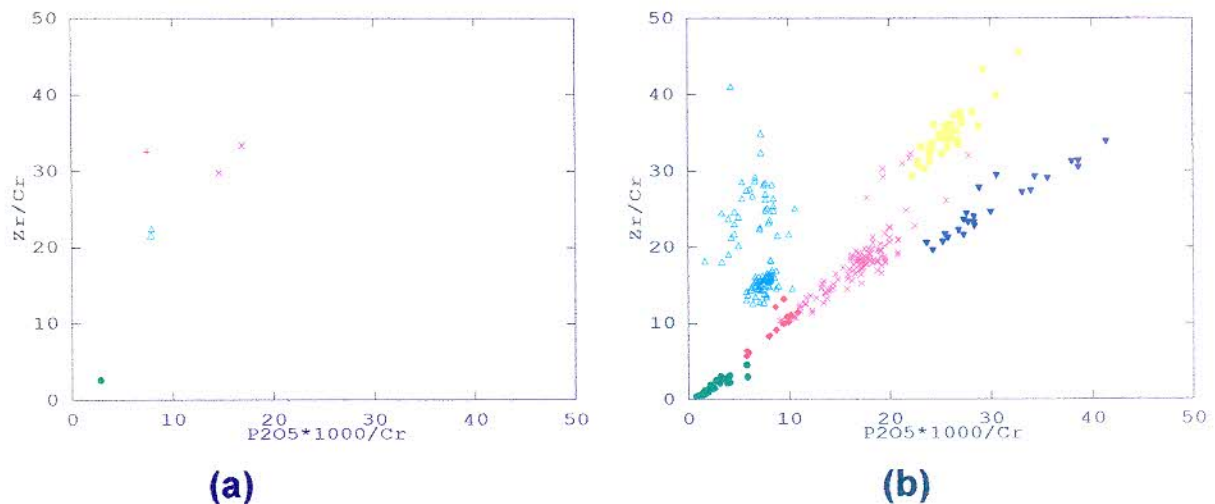


FIGURE 6.17: (a) P_2O_5/Cr - Zr/Cr plot of porphyry samples from the Vryburg area. The symbols represent samples from the following localities: turquoise - Schatkist and Vaarwel; red - Manchester; magenta - Karee Fontein; green - feldspar-porphyry at Vogel Vlei. (b) A similar diagram for the Goedgenoeg and Makwassie Formations in the Bothaville area. The geochemical facies are indicated by: green - Gm; red - Gi; blue - Gs; yellow - Gz; magenta - Md; turquoise - Mr.

TABLE 6.3: Average geochemical compositions of samples from the Vryburg area. The sample from Vogel Vlei is a feldspar porphyry; the others are quartz-feldspar porphyries. The first Karee Fontein sample is of the host porphyry, while the second sample is of a glassy band (silicification fronts). N = number of samples.

Farm	SCHATKIST	MANCHESTER	KAREE F.	KAREE F.	VOGEL VLEI
Facies	Mr-High	Mr-High	Md?		Gm
N	2	1	1	1	1
SiO ₂	77.01	75.44	67.99	73.37	61.46
TiO ₂	0.44	0.47	0.74	0.63	1.11
Al ₂ O ₃	11.73	11.69	13.50	12.37	13.93
Fe ₂ O ₃	1.61	2.89	5.96	2.18	7.38
MnO	0.02	0.03	0.10	0.04	0.11
MgO	0.43	0.76	1.50	0.22	2.87
CaO	0.74	1.29	1.07	0.76	4.61
Na ₂ O ₃	0.26	1.87	4.12	3.88	5.45
K ₂ O	7.66	5.48	4.79	6.35	2.62
P ₂ O ₅	0.11	0.09	0.22	0.19	0.45
Zr	308	390	433	387	392
Y	32	38	51	40	45
Sr	68	53	151	291	408
Rb	147	112	102	144	61
Ba	1187	985	1803	2380	1422
Nb	16	16	19	17	17
V	32	32	66	43	136
Cr	14	12	13	13	152
Co	6	5	9	4	25

SECTION B - MAKWASSIE FORMATION CORRELATIVES NOT EXAMINED DURING THIS STUDY

6.8 THE T'KUIP QUARTZ PORPHYRY FORMATION, SODIUM GROUP

(Locality 1, Fig. 6.1)

The T'Kuip Quartz Porphyry Formation originated as high-temperature ash-flows (Grobler *et al.*, 1989). It consists of massive, phenocryst-rich quartz-feldspar porphyry, with minor laterally impersistent tuff and arkose interbeds (S.A.C.S., 1980). Colour differences, phenocryst size, ratio of quartz to feldspar phenocrysts, and variation in weathering style are indicative of various flows (S.A.C.S., 1980). The quartz-feldspar porphyry is overlain by mafic lava of the Omdraaivlei Formation, which is correlated with the Rietgat Formation.

Du Toit (1908) gave a thorough description of the felsic volcanics, stating that the feldspar phenocrysts consist of orthoclase and predominant plagioclase, altered to a mixture of quartz, mica and chlorite. The common occurrence of plagioclase indicates a dacitic composition, while quartz-free varieties towards the top of the succession can be termed felsites or trachytes (Du Toit, 1908). The ferromagnesian constituents of the volcanics are represented by alteration products such as chlorite while pseudomorphs after enstatite were also recognized (Du Toit, 1908). The groundmass is altered by silicification, but colourless to brownish glass and perlitic textures were also noted (Du Toit, 1908). In some samples, quartz phenocrysts have been shattered and the broken portions separated from one another (Du Toit, 1908), which was attributed to primary brecciation.

Grobler and Emslie (1975-76) reinterpreted Emslie's (1972) map of the T'Kuip Hills and correlated the T'Kuip Quartz Feldspar Porphyry Formation with the Makwassie Formation of the Ventersdorp Supergroup. Grobler *et al.* (1989) quotes 328 m as the thickness of the T'Kuip Quartz Porphyry Formation, but mentioned that duplication through faulting may be possible. The felsic volcanics range from quartz porphyry at the base to dacitic rocks without primary free quartz near the top (Grobler and Emslie, 1975-76). A total of 11 flow-units were recognized by Van der Westhuizen and Grobler (1987). They mentioned that the quartz-feldspar porphyry displays flow textures and banding, which is sometimes contorted, in the lower part of the succession. Upwards the porphyry becomes massive (Grobler and Emslie, 1975-76; Grobler *et al.*, 1989). On Vilets Kuil 198 to the east of Omdraai Vlei, "agglomerate" occurs at the base of the porphyry.

consisting of inclusions of unknown composition in the T'Kuip porphyry (Lemmer, 1977). The T'Kuip Quartz Porphyry Formation is underlain by the arkose of the Ongers River Arkose Formation, which has an increasingly tuffaceous component towards the top of the succession. The upper part of the Ongers River Arkose Formation succession contains units with well preserved accretionary lapilli, mudrock desiccation cracks and raindrop imprints (Van der Westhuizen *et al.*, 1989).

Geochemically the T'Kuip quartz-feldspar porphyry correlates with the Mr facies of the Makwassie Formation and has a high incompatible/compatible element ratio (Fig. 6.18). (See Appendix C for the geochemical data). An equivalent of the Goedgenoeg Formation is absent in outcrops of the Sodium Group.

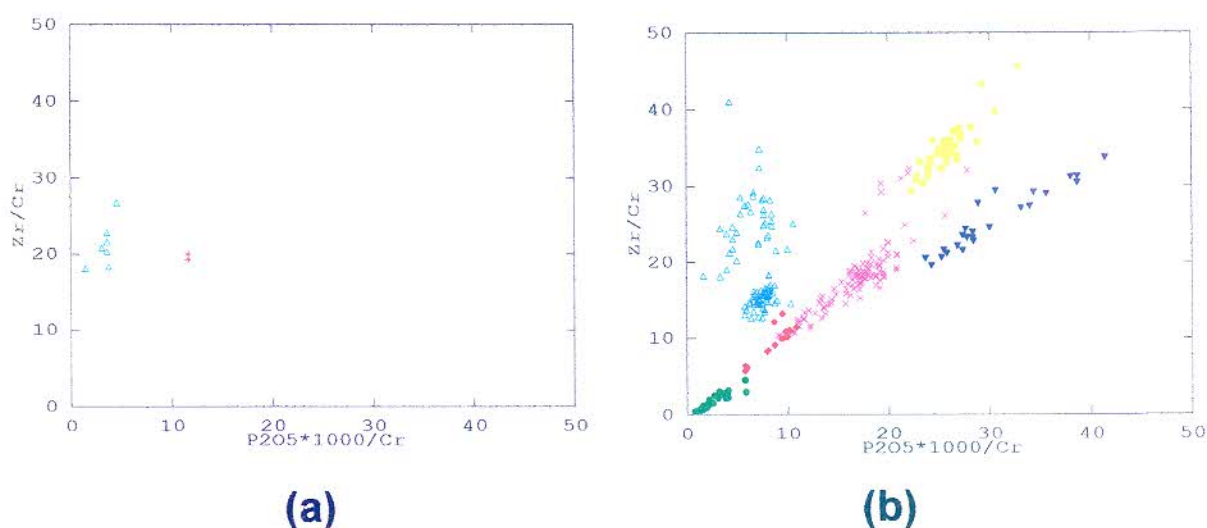


FIGURE 6.18: (a) P_2O_5/Cr - Zr/Cr plot of T'Kuip Formation samples (blue). Two samples from the top of the succession (red) have a slightly different composition from the rest. (b) The same diagram for the Makwassie Formation in the Botahville area. The geochemical facies are indicated by: green - Gm; red - Gi; blue - Gs; yellow - Gz; magenta - Md; turquoise - Mr.

6.9 THE RITCHIE FORMATION (Locality 3, Fig. 6.1; See paragraph 6.3.5)

6.10 THE HEREFORD FORMATION (Locality 2, Fig. 6.1)

On Hereford 202 in the Herbert district, rhyolitic vitric and lithic tuffs, accretionary lapilli-tuff, volcanic sandstone, tuffaceous siltstone and shale attain a thickness of about 40 m (Potgieter, 1973; Potgieter and Visser, 1976). The Hereford Formation lies on Basement Igneous Complex and is in turn overlain by the Bothaville Formation (S.A.C.S., 1980). Ash-flow deposits form the largest part of the succession, while ash-falls and water-reworked volcanic material are

subordinate. The Hereford Formation is correlated with the Makwassie Formation of the Ventersdorp Supergroup (S.A.C.S., 1980).

6.11 OUTCROP TO THE SOUTHWEST OF WARRENTON (Locality 5, Fig. 6.1)

Kleynhans (1979) described an outcrop of quartz-feldspar porphyry with minor intercalated mafic lava flows and volcaniclastics on the Vaalharts Nedersetting which he correlated with the Makwassie Formation. Kleynhans (1979) also reported a small, isolated quartz-feldspar porphyry outcrop on Just In Time 39, 15 km to the northeast of Warrenton, with a minimum thickness of 260 m. Various flow-units were recognized on the basis of quartz and feldspar phenocryst proportions, colour differences and weathering characteristics. The porphyry flows are intercalated with andesitic lava, breccia, tuff and tuffaceous chert (Kleynhans, 1979). The breccias and tuffs display fluvial textures such as wave-ripples, indicating that they were reworked or deposited in a shallow aqueous environment. The tuffs also display well-preserved glass-shard textures while some of the associated mafic lava contains pillow structures, again indicating aqueous depositional conditions.

6.12 THE PHOKWANE FORMATION OF THE HARTSWATER GROUP NEAR TAUNG (Locality 24, Fig. 6.1)

Quartz-feldspar porphyry with occasional well-developed flow banding occurs in the Taung area, where it is overlain by tuff, tuffaceous shale and lenses of andesitic lava and chert (S.A.C.S., 1980). This succession is assigned to the Phokwane Formation of the Hartswater Group by S.A.C.S. (1980), who supports the suggestion by Visser *et al.* (1975-76) and Liebenberg (1977) that this succession correlates with the Makwassie Formation. Liebenberg (1977) reported a maximum thickness of 200 m for the Makwassie Formation in the area and he regarded the flow-banded felsic volcanics as rheoignimbrites. Although other Ventersdorp formations crop out between Warrenton and Taung, quartz-feldspar porphyry is absent in the area around Hartswater.

6.13 THE PAARDEFONTEIN FORMATION OF THE AMALIA GROUP (Locality 25, Fig. 6.1)

The Paardefontein Formation occurs to the north of Amalia, southeast of Vryburg. It consists of quartz-feldspar porphyry, feldspar porphyry and banded rhyolite. Du Toit (1906) and later Van Eeden *et al.* (1963) correlated this succession with the Kareefontein Formation of the Zoetlief Series, while S.A.C.S. (1980) states that it is possibly a Makwassie Formation correlative.

The Paardefontein Formation is overlain by well-bedded tuff, known as the Marokane Tuff Formation, which is correlated with the Vogelvllei Formation (Zoetlief Group) and consequently, with the Rietgat Formation (S.A.C.S., 1980).

6.14 OUTCROPS AT KLERKSDORP TOWNLANDS, THE BUFFELSDOORN GRABEN AND PLATBERG (Localities 14, 15 and 16, Fig. 6.1)

Myers (1990) described the Makwassie Formation in the Klerksdorp area. In the Buffelsdoorn Graben it consists of minor mafic lava (Goedgenoeg Formation), chemical sedimentary rocks with stromatolitic textures, and quartz-feldspar porphyry (J.M. Myers *et al.*, 1990). The porphyritic volcanics are interpreted as pyroclastic-flow deposits represented by both block and ash-flows, highly-welded tuffs and lava flows of rhyolite to basaltic-andesite composition from the base to the top respectively (Myers, 1990). The Klerksdorp Townlands occurrence consists of a basal pyroclastic block and ash breccia, followed by massive quartz-feldspar porphyry, possibly with multiple flow-units (Myers, 1990). At Platberg the Makwassie Formation comprises minor mafic lava (Goedgenoeg Formation) and particularly phenocryst-rich quartz-feldspar porphyry. The porphyry consists of a well-banded crystal tuff with an increasing mafic lithic component with stratigraphic height (Myers, 1990).

6.15 OUTCROPS AT THE VREDEFORT DOME (Locality 17, Fig. 6.1)

Although not reported in the literature, quartz-feldspar porphyry of the Makwassie Formation possibly outcrops at the north-western collar of the Vredefort Dome (M. Brink, personal communication 1990). No detail of this alluded Makwassie correlative is, however, available.

6.16 OUTCROPS AT THE JOHANNESBURG DOME (Locality 23, Fig. 6.1)

Stanistreet and McCarthy (1990) reported an outcrop of quartz-feldspar porphyry on the western side of the Johannesburg Dome, which they correlate with the Ventersdorp Supergroup. The reported porphyry unit has a maximum thickness of 160 m and is highly deformed, appearing as cream-coloured quartz-sericite schist in outcrop, but flow-banding is still apparent on fresh surfaces (Stanistreet and McCarthy, 1990). This outcrop could be a correlative of the Makwassie Formation.

6.17 OUTCROPS IN SOUTHEASTERN BOTSWANA AND NORTH OF MAFIKENG, NORTH CAPE (Localities 18 and 19, Fig. 6.1)

A series of felsic lavas along the eastern border of Botswana, from west of Zeerust to south of Gaborone, were correlated with the Ventersdorp System by

Kynaston (1911). These outcrops continue south across the border into the Republic of South Africa, north of Mafikeng. On the Geological Map of South Africa (Geological Survey of South Africa, 1997) some of this outcrop within the borders of the RSA is correlated with the Platberg Group. An outcrop in the Derdepoort area has been interpreted as Makwassie Formation by Tyler (1979a), but this correlation is still uncertain even though it is correlated with the Platberg Group on the Geological Map of South Africa (Geological Survey of South Africa, 1997).

Across the border in eastern Botswana, Crockett (1971) correlated the Plantation Porphyry with the Makwassie Formation. The Makwassie Formation possibly outcrops to a limited extent north of Mafikeng, northwestwards across the border into Botswana, and then eastwards to the north of the Bushveld Igneous Complex, where it could be represented in the Seokangwana and Derdepoort Belts. The possibility that some of these outcrops are Dominion correlatives cannot, however, be excluded (S.A.C.S., 1980). Most likely both the Ventersdorp Supergroup and Dominion Group are present in the area.

6.18 THE WITFONTEINRANT FORMATION OF THE BUFFELSFONTEIN GROUP, THABAZIMBI AREA (Locality 22, Fig. 6.1)

The Witfonteinrant Formation comprises felsic volcanics, viz predominantly dark-coloured felsites, pink rhyolites, quartz and feldspar porphyries, variolitic lavas, basalts, various breccias and intercalated sedimentary rocks (Tyler, 1979b). Although the Buffelsfontein succession has previously been correlated with the Dominion Group (Truter, 1949; Schutte *et al.*, 1960) and the Ventersdorp System (Kynaston, 1911; Thabazimbi Sheet of the Geological Survey of South Africa, 1974), Tyler (1978; 1979b) considered it a lithological, and possible age, correlative of the Wolkberg Group of the Transvaal Supergroup. This correlation is supported by S.A.C.S. (1980). The possibility that the Buffelsfontein rocks correlate with the Ventersdorp Supergroup cannot be excluded and a thorough geochemical study of these rocks is required.

6.19 SUMMARY

There is still uncertainty about the true extent and correlation of the Goedgenoeg and Makwassie Formations. Although correlatives in the North Cape and North West Provinces are fairly well established, the occurrence of these Formations in the far western North West Province and the north of the western lobe of the Bushveld Complex is still uncertain. The status of the Kanye

Formation as an older volcanic sequence and not a Ventersdorp correlative is also still in dispute and might well prove not to be the case.

The lithology of most of the established occurrences is analogous to that of the Goedgenoeg and Makwassie Formations in the Bothaville area and are interpreted as high-temperature ash-flow deposits (Table 6.4), but less highly-welded ash-flow tuffs also occur. The Goedgenoeg Formation is less porphyritic to non-porphyritic towards the western and northwestern parts of the Ventersdorp Supergroup depository and apparently only the Gm and Gs geochemical facies are present. The Makwassie Formation is widespread and the Mr facies predominates in the areas to the west and northwest of the Bothaville area. The Md facies, although sporadically developed, retains its stratigraphic position with respect to the Goedgenoeg Formation.

TABLE 6.4: Comparison between the interpreted mode of deposition of the individual Goedgenoeg and Makwassie Formation occurrences. Interpretation of those occurrences which were not investigated during this study, were made from lithological descriptions in the literature. The abbreviations are HTAF - high-temperature ash-flow tuff; WAF - welded, partially-welded or unwelded ash-flow tuff; RAF - rheomorphic ash-flow tuff; and RLF - rhyolite lava flow.

LOCALITY	HTAF	WAF	RAF	RLF
Bothaville area	X			
Wolmaransstad area	X			
Kimberley Mines	X	X	X	
Vaalkoppies	X			
Sweet Home/Wildebeestfontein	X			
Honiglaagte/Honigkop/Goudkop	X			
Vaarwel/Schatkist	X			
Vryburg (Kareefontein Formation)	X			
T'Kuip (T'Kuip Quartz Porphyry Formation)	X			
Ritchie (Ritchie Formation)			X	
Hereford (Hereford Formation)		X		
Southwest of Warrenton	X	X?		
Taung (Phokwane Formation)	X?	X?	X	
Amalia	X?	X?	X?	
Klerksdorp Townlands	X	X		
Buffelsdoorn Graben	X	X		
Platberg	X			
Vredefort Dome	X?			
Pretoria Dome	X?			
Southeastern Botswana	X?		X?	

7. PETROGENESIS OF THE GOEDGENOEG AND MAKWASSIE FORMATIONS

7.1 INTRODUCTION

A genetic model of the Goedgenoeg and Makwassie Formations has to address the lithological, petrographical and chemical characteristics of the formation as described in the previous chapters. Some of the more remarkable features of the Goedgenoeg and Makwassie Formations are the widespread occurrence and voluminosity of the felsic volcanics, extreme variation in thickness over short lateral distances, lateral and vertical lithological and chemical homogeneity of thick parts of the succession, lack of emplacement textures, virtual absence of sedimentary rocks in the volcanic pile, and the bimodal chemical composition.

7.2 EMPLACEMENT

7.2.1 Intrusive vs Extrusive Origin

Pyroclastic flows are recognized by textures such as pumice, fiamme, glass-shards, welding or non-welding of such fragments, vesicles, inclusions that originated from underlying rock types, flow banding, breccia, gas elutriation pipes, vitrophyres, and fragmented phenocrysts. Pyroclastic flows also have low aspect ratios (flow bodies with a large lateral extent relative to flow thickness). In contrast felsic lava flows display intact phenocrysts, flow lamination, extensively developed autobreccias, domal flow anatomies and have high aspect ratios (thick flow bodies with limited lateral extent).

Although the Goedgenoeg and Makwassie Formation porphyries largely lack emplacement textures, as described in Chapter 3, it does not necessarily point to an intrusive origin as these textures could also be destroyed by welding. Welding is the fusion of hot pumice fragments and glass shards under a compactional load and occurs in most pyroclastic flows, especially in the lower and middle parts of a flow unit (Ross and Smith, 1961). Rapidly deposited superimposed flow units may cool as a single unit (a single ignimbrite) and such an ignimbrite can have zones with different degrees of welding, ranging from unwelded, partially welded to densely welded. Compactional flattening of lithic fragments and glass shards are observed in welded zones (Cas and Wright, 1988). Flattened pumice (fiamme) may define lineation which developed during secondary flowage (rheomorphism) of pyroclastic-flow deposits during welding. The above features are all readily recognizable, so that pyroclastic flow origins can be determined with certainty.

Some ash-flows, however, have recently been recognized that lack extensively developed emplacement textures and display features of both ash-flows and of rhyolite lava flows (Bristow and Cleverley, 1979; Cleverley and Bristow, 1982; Saggerson and Bristow, 1983; Bristow, 1989b). These ash-flows have undergone extreme welding so that lithic fragments and glass shards were destroyed and the ash-flow appears massive, apart from textures such as flow-banding preserved in the upper part of the flow. These ash-flows were interpreted as high-temperature (1100°C for rhyolites), low-volatile ash-flows (Saggerson and Bristow, 1983) and subsequently various occurrences of such high-temperature ash-flows have been envisaged (Table 7.1). The Makwassie quartz-feldspar porphyries in the Bothaville area are interpreted to be such high-temperature ash-flows (Table 7.2). Evidence for the extrusive origin of the quartz-feldspar and feldspar porphyries is found in relict glass-shard textures, perlitic-crack textures, devitrification textures, amygdales, autobreccias and contact relationships. The Makwassie flow-units compare favourably with those of the southern Lebombo rhyolite flows described by Saggerson and Bristow (1983).

Most of the Makwassie ash-flow units are separated by co-pyroclastic flow (co-ignimbrite) ash-fall deposits, which originally were composed of ash-size particles, lithic fragments, accretionary lapilli and glass shards. These tuffs are generally disturbed by the next ash-flow deposit, which demonstrates the violent emplacement mechanism of the ash-flow deposits. Pyroclastic clasts of lapilli and block sizes are frequently embedded in the tuff, indenting the tuff layering. Fluvial processes do not seem to have played a major role in deposition of the fine-grained rocks.

The high phenocryst content of the Makwassie quartz-feldspar porphyries as well as the massive thickness of units can be used to argue against an extrusive origin. The phenocryst content, however, rarely exceeds 35% and flow thickness (± 80 m) of the Makwassie porphyries are well within the constraints of ash-flow deposits. Thickness of individual ash-flow deposits vary greatly and may be very thick (>300 m) if ponded in depressions (Cas and Wright, 1988). Ash-flow tuffs with a phenocryst content of <35% by volume are common (Cas and Wright, 1988), while there are also numerous reports in literature of ash-flow tuffs with up to 60% phenocrysts (Table 7.3).

TABLE 7.1: Possible high-temperature rhyolitic ash-flow tuff localities (adapted from Bristow, 1989a).

LOCALITY	REFERENCE
PERALKALINE ASSOCIATIONS	
Pantelleria, Italy	Borsi <i>et al.</i> , 1963
Monte Amiata, Italy	Rittman, 1962
Nye County, Nevada, USA	Noble, 1968
Unnamed ash-flow, North-West Nevada	Noble, 1968; Noble <i>et al.</i> , 1964
Kane Springs Wash Caldera, S-E Nevada	Noble, 1968
Mogán Formation, Gran Canaria, Canary Islands	Schmincke and Swanson, 1967
Wagontire Mountain Tuff, Oregon, USA	Schmincke, 1990
Belted Range Tuff, Nevada	Walker and Swanson, 1968
Latir Volcanics, New Mexico	Noble, 1968; Hoover, 1964
Kap Washington, Greenland	Johnson and Lipman, 1988
Bumbeni Complex, South Africa	Brown <i>et al.</i> , 1987
Rammes Volcano, Oslo Graben	Wolmarans, 1988
	Rutten and Van Everdingen, 1961
OTHER THAN PERALKALINE ASSOCIATIONS	
Thirsty Canyon Tuff, Nevada, USA	Noble <i>et al.</i> , 1964
Timber Mountain Tuff, Nevada, USA	Noble <i>et al.</i> , 1964; Orkild, 1965
Paroc Sequence, Maine, USA	Noble <i>et al.</i> , 1964; Rawkin, 1960
Baja California, Mexico	Hausback, 1987
Gribbles Run, Colorado, USA	Chapin and Lowell, 1979
Bruneau-Jarbridge, Snake River Plain, USA	Ekren <i>et al.</i> , 1984
Trans Pecos, Texas, USA	Bonnichsen and Kauffman, 1987
Parana, South America	Henry <i>et al.</i> , 1988
Etendeka, Namibia	Mazzoni, personal communication to Bristow, 1989a;
Erongo Complex, Namibia	Milner, 1986
Lebombo, South Africa/Mozambique	Pirajno, 1988
Nuanetsi, Zimbabwe	Bristow and Cleverley, 1979
	Cleverley and Bristow, 1982
Nathins Cove Form., Newfoundland	Monkman, 1961; K.G. Cox, personal communication to Bristow, 1989a;
New South Wales, Australia	Lock, 1972
Sinclair Formation, Namibia	Cas, 1978
Soutpansberg, South Africa	Watters, 1974; Brown <i>et al.</i> , 1987
Rooiberg Felsites, South Africa	Barker, 1978; Bristow, 1986
	Clubley-Armstrong, 1977; Twist and French, 1983; Twist, 1985/86
Springs Well Tuff, Australia	Giles, 1982
Nsuze Group, Mpongoza Inlier, South Africa	Preston, 1987a; Preston, 1987b
Witfonteinrand Formation, Buffalo Springs Group, South Africa	Tyler, 1979b
MAKWASSIE FORMATION CORRELATIVES (?)	
T'Kuip, South Africa	Van der Westhuizen and Grobler, 1987
	Grobler <i>et al.</i> , 1989
Hereford Formation, North Cape Province, South Africa	Potgieter and Visser, 1976; Lock, 1977
Ritchie, South Africa	Potgieter and Lock, 1978
Plantation Porphyry, Botswana	Crockett, 1971
Acid volcanics, Derdepoort Belt, S. Africa	Tyler, 1979a
Acid volcanics, Seokangwana Belt, S. Africa	Tyler, 1979a

TABLE 7.2: Criteria for distinction between ash-flows, rhyolite lava flows and high-temperature ash-flows. (After Saggerson and Bristow, 1983; Bristow, 1989a; Bristow 1989b; Bonnicksen and Kauffman, 1987; Henry *et al.*, 1988). Characteristics of the Makwassie quartz-feldspar porphyries in the Bothaville area are indicated by #.

FLOW CHARACTERISTICS	ASH-FLOWS	FELSIC LAVA FLOWS	HIGH-T ASH-FLOWS
Low aspect ratios (extensive sheets)	x	rare	x(#)
High aspect ratios (domes)		x	
Columnar-jointed cliffs	x		x
Eutaxitic textures	x		
Extensive lithophysal horizons at flow base	x(#)		
Gas elutriation pipes	x		
Pumice	x		
Fiamme	x		rare
Lithic fragments	x		rare(#)
Glass shards	x		rare(#)
Absence of glass shards		x	#
Crystalline and/or devitrified		x	#
Welded and/or devitrified	x		#
Non-welded tops, bottoms and sides	x		
Broken phenocrysts predominate	x		#
Air-fall ash beneath flow	#		
Contorted flow-banding and folding		x	x(#)
Vertical and lateral zoning	x		#
Colour banding	x	x	#
Amygdales and elongated vesicles		#	rare
Vesicularity	x		rare
Subparallel flow marks			#
Autobreccias at flow top, bottom or throughout	x(#)		
Vitrophyres at or near top		#	
Complex basal vitrophyres		x(#)	

TABLE 7.3: Examples of ash-flow tuff deposits with high phenocryst content (by volume).

LOCALITY	PHENO-CRYSTS	REFERENCE
Lake Toba, Sumatra	60%	Ross and Smith, 1961
Ammonia Tanks Member, Timber Mountain Tuff, Timber Mountain-Oasis Valley Complex, Nevada	50%	Byers <i>et al.</i> , 1976
La Jara Canyon Member, Treasure Mountain Tuff, Platoro Caldera Complex, Colorado	50%	Lipman, 1975
Fish Canyon Tuff, Nevada	50%	Lipman, 1975
Snobs Creek sequence, Rubicon Rhyolite, Victoria Australia	55%	Birch, 1978; Clemens and Wall, 1984
Violet Town Volcanics, Victoria, Australia	65%	Birch, 1978; Clemens and Wall, 1984

7.2.2 Eruption Style

Large-volume ignimbrites are envisaged to form either through continuous gravitational collapse of a plinian eruptive column, or through a 'boiling-over' process (Cas and Wright, 1988). Since ignimbrites formed through plinian eruptions are frequently underlain by **plinian** pyroclastic-fall deposits (Cas and Wright, 1988), which are absent in the Makwassie porphyries, a 'boiling-over' process (during caldera collapse) is preferred. Bristow (1989a) considers that the high-temperature ash-flows of the Jozini rhyolites have been emplaced in a similar way, which enhances heat-retention to produce high-temperature ash-flows.

7.2.3 Eruption Source

Ignimbrites are often associated with calderas, but voluminous ignimbrites have previously been coupled with linear fissure eruptions, or continuous ring fissure eruptions (Cas and Wright, 1988). Only small-volume ignimbrites (and only few of them) were, however, witnessed in historic times, such as Mt St Helens in 1980 and El Chichón in Mexico in 1982. Cas and Wright (1988) pointed out that the vent type and eruption mechanism of large ignimbrites are still unresolved. Some of the model occurrences of fissure, large-volume ignimbrites were subsequently proved to have originated from calderas, *i.e.* the Valley of Ten Thousand Smokes ignimbrite at Katmai in Alaska (Curtis, 1968).

The Fish River Canyon Tuff may suggest a vent system for large-volume ignimbrites (Self and Wright, 1983), where crustal failure of an entire area takes place over a shallow magma chamber, possibly in a linear area on a complex tensional fracture system. A similar situation exists in the western USA in the Rio Grande rift (Baldrige *et al.*, 1989). The presence of shallow magma chambers have not yet been proven for the Goedgenoeg or Makwassie Formation, but crustal failure over a large area would explain the large effusion rates. Even though ash-flows can travel up to more than 200 km from its source, *i.e.* the Morrinsville ignimbrite (Cas and Wright, 1988), distances of more than a 100 km are exceptional. Multiple eruption centres are therefore envisaged for the widespread occurrence of the Goedgenoeg and Makwassie volcanics.

According to Henry *et al.* (1989) older calderas are difficult to detect once these features have been covered by younger deposits. In the case of the Ventersdorp Supergroup this problem is even greater. Goedgenoeg or Makwassie caldera structures have not yet been identified, even though numerous seismic traverses have been made over the Ventersdorp Supergroup depository in

evaluations of the underlying Witwatersrand Supergroup strata. Hence, in the case of the Goedgenoeg and Makwassie Formations, the problem of the apparent lack of intracaldera facies and caldera structures still remains.

Production of large volumes of felsic volcanics may indicate immense magma development that may lead to the formation of granite batholiths (Thurston *et al.*, 1985). The Ventersdorp Supergroup depository can therefore be expected to contain Makwassie-age granites, but such granites have not yet been reported. Since seismic recordings regularly look at depths of up to 10 km and more, shallow magma chambers should be detected. However, small magma chamber bodies of less than 2 km in diameter may be difficult to interpret as such on seismic profiles (personal communication, C. Spencer). Various granite domes occur in the Ventersdorp Supergroup depository, but are older than the Makwassie Formation (Robb, 1992) and therefore cannot represent shallow Makwassie magma chambers. High-temperature ash-flows, such as the Makwassie porphyries, have possibly erupted from depth without magma accumulation in a shallow reservoir, thereby enabling the high eruptive temperatures. Deep magma chambers, however, will prevent the development of calderas.

Huppert and Sparks (1988) attested that porphyritic silicic volcanism does not necessarily require large, high-level, long-lived magma chambers where phenocrysts form. The cyclic occurrence of mafic lavas associated with increasing volumes of felsic volcanics is common in many volcanic systems. This results from the progressive heating of the crust by the intrusion of mafic magma, until the source region is partially molten and basalt can no longer penetrate (Huppert and Sparks, 1988; Walker, 1989). Every new input of basalt into the source region will trigger rapid formation of silicic magma. During melting, crystallization can occur and eruption of porphyritic magmas therefore do not require a shallow magma chamber (Huppert and Sparks, 1988).

J.M. Myers *et al.* (1990) demonstrated individual Makwassie volcanic centres in the Klerksdorp area on the basis of lithological and eruptive style differences, but the eruptive vents could not be identified. These Makwassie occurrences are, however, restricted and apparently form outliers outside the main Makwassie Formation depository.

7.2.4 Eruption And Magma Volumes

Successive ash-flow deposits which form a coherent succession (ignimbrite), can reach volumes of up to 3 000 km³, i.e. the Fish Canyon Tuff in the San Juan volcanic field (Lipman, 1975). The total volume of the Goedgenoeg feldspar porphyries and the Makwassie quartz-feldspar porphyries are conservatively calculated to be more than 7 700 km³ for the 9 600 km² Bothaville area alone (Table 7.4). Quartz-feldspar porphyries comprise about half of this volume. Considering that the Makwassie Formation depository covers some 200 000 km² and that the formation reaches a thickness of more than 2 000 m in some of the grabens to the west of the Bothaville area, a conservative average thickness of 500 m over the depository calculates a total volume of 100 000 km³ of acidic volcanics. This makes the Goedgenoeg and Makwassie Formations probably one of the largest composite ash-flow deposits in the world. The Rooiberg Felsite or Rooiberg Group of the Transvaal Supergroup, however, comprises an estimated volume of 300 000 km³ of erupted acidic magma (Twist, 1985).

TABLE 7.4: Volume calculations for the Goedgenoeg and Makwassie Formation volcanics in the Bothaville area. The Bothaville area is defined as the area between 2 960 000 and 3 080 000 metres south of the equator, and between 10 000 and 90 000 metres west of 27° longitude. The volumes were calculated with the *SURFER* software programme from the isopach maps depicted in Chapter 4.

STRATIGRAPHIC UNIT	VOLUME
Goedgenoeg Formation	3 100 km ³
Makwassie Formation (including the Garfield Member)	4 700 km ³
TOTAL	7 800 km³
Garfield Member	800 km ³

7.2.5 Lack Of Interbedded Sedimentary Rocks

Epclastic sedimentary processes are a prominent feature of volcanic provinces (Cas and Wright, 1988). Individual volcanic eruptions are short-lived in the total time span of a volcanic episode and during periods of repose between eruptions degradational epclastic processes dominate. In active volcanic terrains the abundance of loose debris, steep slopes and the erodible nature of volcanic rocks lead to rapid erosion and redeposition. The aggradation rate during active volcanic periods is, however, much greater than the degradation rate during

repose periods, so that epiclastic sedimentary deposits represents a minor constituent of volcanic sequences (Cas and Wright, 1988).

Thin beds of epiclastic volcanoclastic conglomerate and fine-grained sedimentary rocks at the contact between the Goedgenoeg and Makwassie Formations, and between the Makwassie Formation and the Garfield Member, indicate a hiatus, albeit small, between deposition of these units. The virtual absence of interbedded epiclastic sedimentary rocks, apart from the above, and the lack of evidence for major erosion within the Goedgenoeg and Makwassie Formations, indicate that effusion rates were very rapid during deposition of these formations. However, the lack of exposures and inadequate representation through borehole cores must be considered; it is possible that significant syn-Goedgenoeg and Makwassie sedimentary rocks may exist elsewhere in the Ventersdorp Supergroup depository. By analogy with younger volcanic provinces, it is clear that in such old volcanic deposits as the Ventersdorp Supergroup, a very incomplete record of all the cycles of erosion and volcanism will be preserved.

7.3 TECTONIC SETTING

7.3.1 The Witwatersrand Supergroup

The tectonic setting of the Goedgenoeg and Makwassie Formations is better understood if regarded in the context of the larger scenario of the Witwatersrand and Ventersdorp Supergroups.

West Rand Basin and Lower Central Rand

The Witwatersrand Supergroup was deposited in a foreland basin (Burke *et al.*, 1986; Winter, 1986; Robb *et al.*, 1991; Stanistreet and McCarthy, 1991). The epicontinental style of deposition of the early West Rand Group either took place in response to thermal cooling and subsidence after outpouring of the voluminous bimodal Dominion volcanics (Clendenin *et al.*, 1988c), or with the initiation of a foreland basin (Burke *et al.*, 1986). The upper West Rand Group and Central Rand Group were deposited in a foreland basin, possibly through convergence initiated by the collision of the Zimbabwe Craton from the north (Burke *et al.*, 1986; Winter, 1986; Stanistreet and McCarthy, 1991). Granite emplacement could also have taken place during this stage, although poorly represented in the present geochronological data base due to lack of research (Robb *et al.*, 1991).

Upper Central Rand

Research by Robb *et al.* (1991) indicates that the foreland basin stage of the Witwatersrand Basin ended with the deposition of the lower Central Rand. During upper Central Rand times sediments were deposited in a shrinking basin under compressional stress, the shrinking brought on by the Witwatersrand Basin being “squeezed out” towards the southeast in response to the tectonic escape of crust from the continental interior during collision of the Kaapvaal and Zimbabwe Cratons (Stanistreet and McCarthy, 1991). Alluvial fan sedimentation was controlled by block faulting (R.E. Myers *et al.*, 1990). High-level granite plutons were emplaced adjacent to the edge of the Central Rand Group basin (Robb *et al.*, 1991), *i.e.* the Wesselsbron Dome which may have been responsible for overturning of the upper Central Rand in the Welkom region.

7.3.2 The Ventersdorp Supergroup

The Ventersdorp Supergroup represents a continental rift system (Bickle and Eriksson, 1982; Tankard *et al.*, 1982; Burke *et al.*, 1985; Clendenin, 1989). The rift features of the Ventersdorp are not comparable to a narrow continental rift system such as the African Rift Valley, but compare to the broad rift system features of the Basin and Range Province in the western United States and to the Rotliegendes Troughs in central Europe (Clendenin *et al.*, 1988c). The Platberg Group structures are over 200 km wide, while the characteristic width of continental rifts (Ramberg and Morgan, 1984) is only 30 to 50 km. Wernicke (1985) proposed a normal simple-shear tectonic model to explain the features of the Basin and Range Province and this model was adapted for the Ventersdorp Supergroup by Clendenin *et al.* (1988c).

Both the Basin and Range Province and the Rotliegendes basin have been interpreted as foreland rifts (Jowett and Jarvis, 1984). The process of foreland rifting can be closely linked to the Ventersdorp Supergroup (Clendenin *et al.*, 1988c), as follows:

1. An initial period of compressional tectonism caused by subduction of buoyant oceanic lithosphere; *i.e.* compressional tectonics during closure of the Central Rand Basin.
2. Thrusting and folding, with associated foreland basin or clastic wedge sedimentation; *i.e.* thrusting, folding and deposition of the Central Rand Group along the western margin of the Central Rand Basin in the Welkom area.

3. Lateral extensional forces due to viscous drag of mantle material by the descending oceanic slab; *i.e.* extensional tectonics which led to eruption of the Klipriviersberg Group flood basalts.
4. Stretching and thinning of the foreland lithosphere occur when the oceanic slab continues to sink after the compressional force, which countered the extensional force of the viscous drag, is removed by cessation of subduction; *i.e.* thinning of the crust towards the end of the Klipriviersberg Group volcanism.
5. Extensional tectonism due to the above extensional force; *i.e.* the onset of the Platberg Group rifting event.
6. Bimodal igneous activity; *i.e.* the basaltic, dacitic and rhyolitic volcanics of the Platberg Group.
7. Regional uplift and rapid sedimentation within subsiding rift basins; *i.e.* the graben-style sedimentary rocks of the Kameeldoorns Formation and the graben-fill volcanics of the Platberg Group.

Broad continental rift zones are characterized by the widespread (hundreds of kilometres) occurrence of bimodal volcanics and multiple, localized, structurally controlled sedimentary basins (Cas, 1983), which is analogous to the Ventersdorp Supergroup assemblage. Similar to the Ventersdorp Supergroup both basaltic and acidic volcanics, with additional occurrence of intermediate rocks, are the major rock types in the Basin and Range Province (Christiansen and Lipman, 1972).

Klipriviersberg Group

The Klipriviersberg Group lavas represent tholeiitic continental flood basalts (Tyler, 1979a; Tankard *et al.*, 1982) and the group was earlier thought to be exclusively confined to the Central Rand Basin. Klipriviersberg rocks are now known to occur to the northwest of the Central Rand Basin, as indicated on maps recently published by the Geological Survey. The paucity of sediments interbedded with the lavas indicate rapid effusion contemporaneous with faulting (Tyler, 1979a; Clendenin *et al.*, 1988c).

According to R.E. Myers *et al.* (1990) and McCarthy *et al.* (1990) the initial outpouring of Klipriviersberg lavas took place under compressional stress, which relaxed during the later stages of effusion. Stanistreet and McCarthy (1991) rationalized, however, that the paradox of the Klipriviersberg being at once compressional and extensional is resolved by tectonic escape related extension during the Kaapvaal-Zimbabwe Craton collision episode.

Komatiitic basalts of the Meredale Member at the base of the Klipriviersberg Group (McIver *et al.*, 1982) indicate that these lavas were derived directly from partial melting in the mantle (Burke *et al.*, 1985). The occurrence of komatiite implies that regional tensional stress was high (Nisbet, 1982).

The Platberg Group

The Platberg Group is developed to the west and north-west of the Central Rand Basin and indicates a shift to the west in both faulting and deposition (Clendenin *et al.*, 1988c). The Platberg Group was deposited during major graben development and represents a failed rift (Clendenin *et al.*, 1988b). An idealized section across the Bothaville area demonstrates the relationship between the Platberg Group, Klipriviersberg Group and Witwatersrand Supergroup (Fig. 7.1). From this figure it can be seen that the Klipriviersberg Group is largely confined to the Central Rand Group Basin as far as the area of this section is concerned. Platberg age faults uplifted the Witwatersrand Supergroup and Klipriviersberg Group rocks, leading to deposition of the Kameeldoorns Formation sedimentary rocks during the initial stage of graben formation. The Goedgenoeg and Makwassie volcanics were deposited contemporaneously with the formation of the grabens and progressively filled these structures, while the Rietgat Formation was deposited in reactivated subsiding areas and newly formed graben structures. Details of the western edge of the rift structure are not known. Although the eastern area was uplifted prior to Platberg times, major post-Platberg and post-Ventersdorp uplift led to complete removal of the Platberg Group and Pniel Sequence in this eastern area. Granite plutons apparently had a long-standing influence, although some granite plutons could represent the plutonic phase of Makwassie volcanism.

According to Stanistreet and McCarthy (1991) the Platberg Group represents the impactogenel rifting stage as end phase of the Kaapvaal and Zimbabwe Craton collision. The Platberg Group was deposited in a broad extensional rift system (Clendenin *et al.*, 1988c), which consisted of multiple smaller rifts. The individual rift zones are separated from each other by granitic terranes, as delineated in Fig. 7.2. Most of the faulting occurred early in the Platberg graben development (Burke *et al.*, 1985). J.M. Myers *et al.* (1990) indicated that sedimentation and volcanism during deposition of the Platberg Group were

controlled by faulting. Although sedimentation, now represented by the Kameeldoorns Formation, dominated during the early phase of Platberg rifting, sedimentary rocks are subordinate in volume to volcanic rocks in the Platberg Group.

Initial deposition of the Goedgenoeg intermediate volcanics took place in the most active parts of the rift grabens, *i.e.* presently at greatest depth. The first extrusives are interbedded and intermingled with sediments of the Kameeldoorns Formation, *e.g.* borehole DHK1. The intermingling indicates that some of the sediments were unconsolidated at the onset of Goedgenoeg volcanism and interbedded sedimentary rocks at the base of the Goedgenoeg Formation imply that sedimentation was still active. (This lower part of the Goedgenoeg Formation was described as the Vaal Bend Formation by Whiteside (1970), which was erroneously correlated with the Klipriviersberg Group).

The dacitic and rhyolitic volcanism (quartz-feldspar porphyries) that followed the intermediate volcanics (feldspar porphyries) further filled the active graben structures. Minor interbedded sedimentary rocks at, or close to the contact between the Goedgenoeg and Makwassie Formations suggest that there was at least a minor hiatus after the deposition of the Goedgenoeg Formation. The dacitic and rhyolitic volcanics are more widespread than the underlying intermediate volcanics, indicating that later volcanic deposits filled and even spread beyond the deepest graben structures. Rifting was probably already abating towards the end of Makwassie deposition.

The Rietgat Formation appears to be constricted to within reactivated grabens and newly formed grabens (Fig. 7.1). The Rietgat lavas have a chemical composition similar to the Goedgenoeg Formation, but are largely non-porphyritic, which implies that the graben reactivation resulted in the direct extrusion of magma without residence time in the crust which would allow growth of phenocrysts. The Rietgat Formation represents the reactivation stage after caldera formation, possibly involving andesitic to dacitic doming and rapid sedimentation in a moat setting.

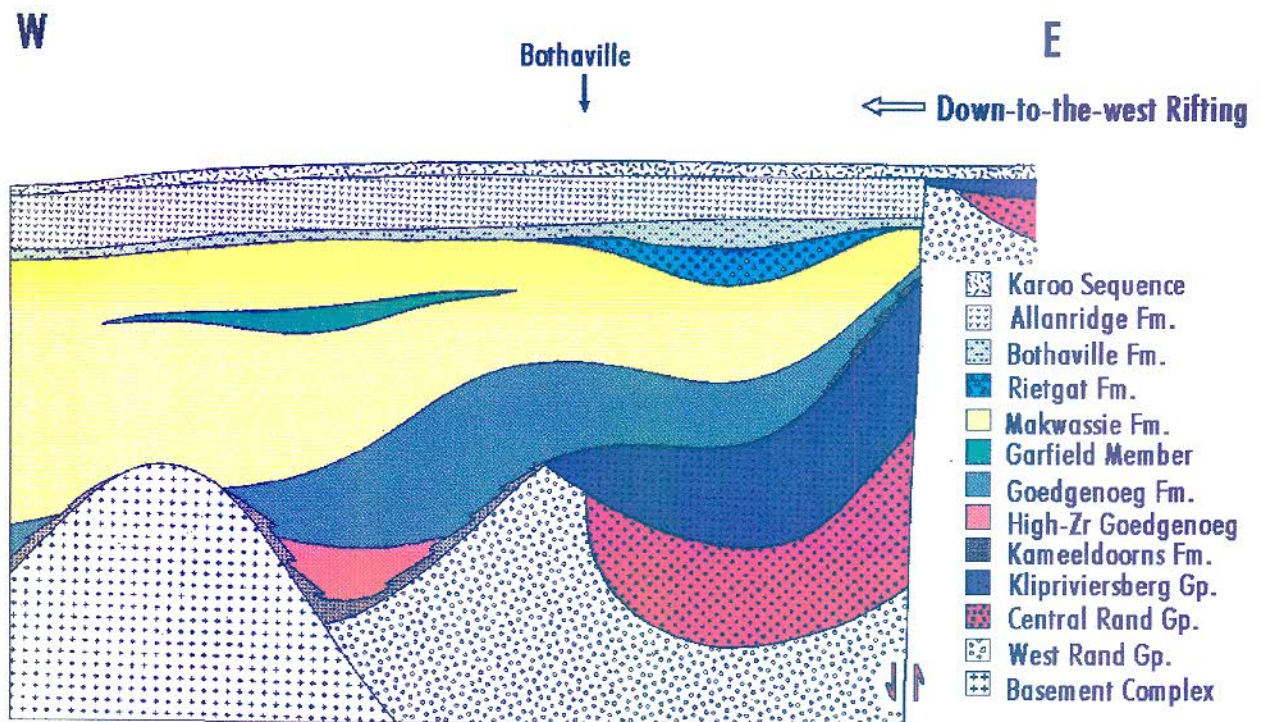


FIGURE 7.1: A simplified and idealized east-west cross section of the geology in the Bothaville area, without structural detail. This section is in agreement with that of Winter (1976). (Not to scale; the horizontal view is about 70 km, while the vertical is about 4 km.)

Pniel Sequence

The Platberg rifting ended before deposition of the Pniel Sequence and the sedimentary Bothaville Formation was deposited during a post-graben tectonic subsidence stage (Clendenin *et al.*, 1988a) or as a result of gravitational collapse (Stanistreet and McCarthy, 1991). A major unconformity separates the Rietgat Formation and the Pniel Sequence, so that erosion of pre-Pniel formations took place along the flanks of the Platberg grabens.

The Allanridge Formation comprises flood basalts during renewed rifting (Burke *et al.*, 1985) or early stages of thermal subsidence (Clendenin *et al.*, 1988c). The presence of localized komatiites at the base of the Allanridge Formation (Van der Westhuizen *et al.*, in prep.) may, however, hold important implications for the tectonic development of the Ventersdorp Supergroup (Van der Westhuizen *et al.*, 1991).

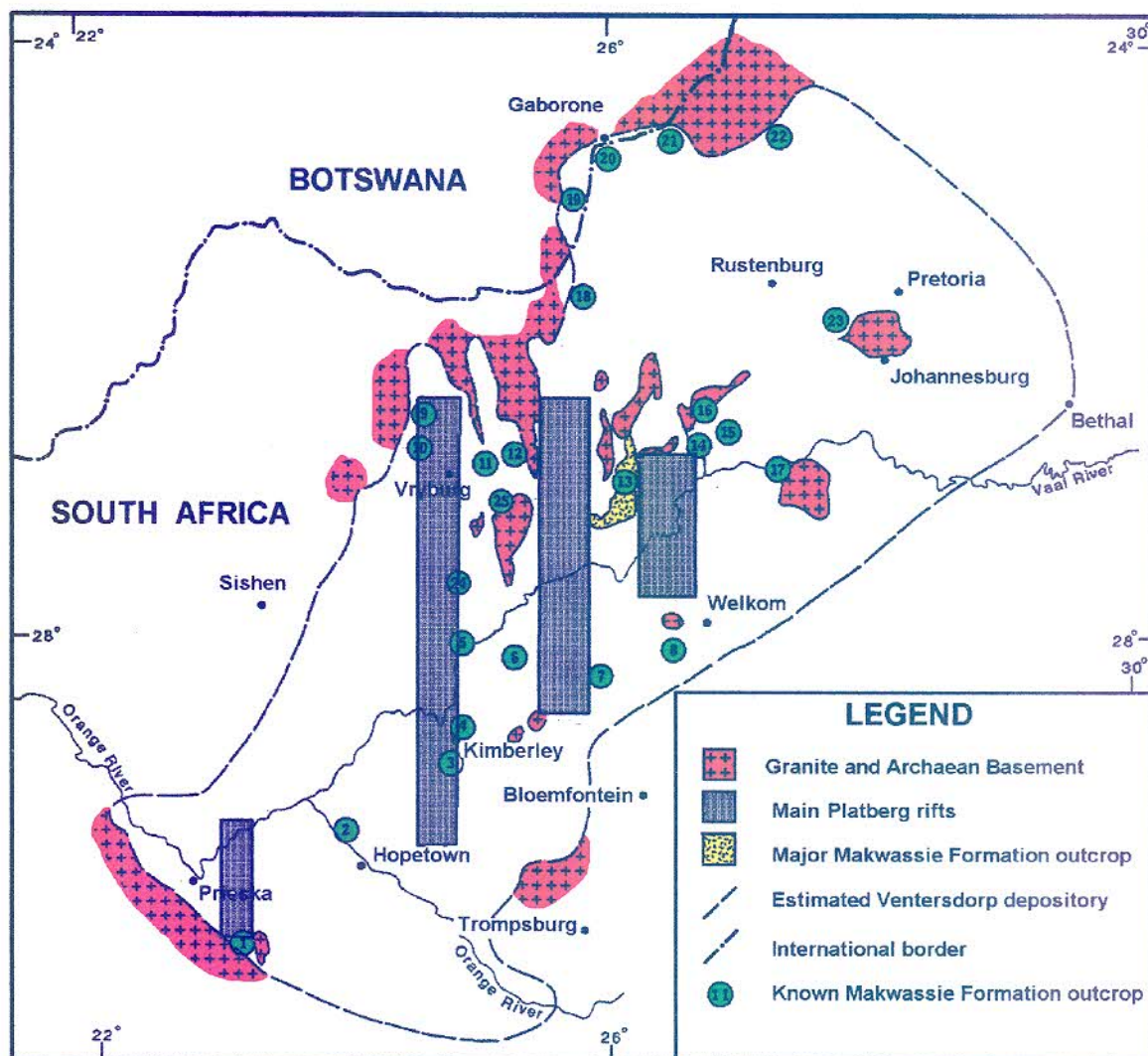


FIGURE 7.2: Individual rift zones in the Platberg multiple rift system. The rifts are separated from each other by granitic terranes, as indicated by the shaded areas lines. The numbered Makwassie Formation outcrops are listed in Figure 6.1.

Post Ventersdorp Supergroup Events

Recent evidence from exploration drilling indicates that the effects of post-Ventersdorp fault reactivation and subsequent erosion were often underestimated. Large displacements on faults through the Ventersdorp Supergroup are commonplace (Figs. 7.1) and the upper Ventersdorp succession is overturned in the northern Free State Gold Field. Since there is a gap of ± 2 Ga in the stratigraphic record between the Ventersdorp Supergroup and Karoo Supergroup over large parts of the Ventersdorp depository, post-Ventersdorp tectonic movements are difficult to discern and evaluate. The faulting and

erosion of the Ventersdorp Supergroup which are evident today, cannot be attributed to syndepositional tectonism alone.

7.3.3 Geochemical classification

Most geochemical tectonic discrimination techniques were designed for basaltic rocks, e.g. Pearce and Cann (1973), Pearce *et al.* (1977), Shervais (1982), Meschede (1986), etc. One of the few methods for granitic rocks that utilize immobile elements is that of Pearce *et al.* (1984), which makes use of Y and Nb or Yb and Ta. The Goedgenoeg and Makwassie data of this study plot as Within Plate Granites (WPG) on the Y-Nb diagram (Fig. 7.3a). Syn-collision granites (syn-COLG) could plot anywhere on this diagram but not in the Orogenic Granites (ORG) field. When the data are plotted on the Y+Nb vs Rb diagram of Pearce *et al.* (1984), the WPG classification still holds (Fig. 7.3b), even though Rb must have been remobilised during alteration of the Ventersdorp Supergroup as is evident in the scatter of Rb.

Following the classification scheme of Manior and Piccoli (1989), which makes use of mobile elements, the Goedgenoeg and Makwassie samples classify as rift-related and continental uplift (Fig. 7.4). This conforms with the tectonic setting of the Platberg Group as discussed earlier.

The R1-R2 diagram of Batchelor and Bowden (1985) indicates pre-plate collision to syn-collision magmatism (Fig. 7.5), which appears to be in conflict with the previous classifications. If, however, the Platberg volcanics represent back-arc rifting the magma may actually still reflect the collision signature of the foreland orogenic belt.

The metaluminous to peralkaline composition of the volcanics (Chapter 5) also conforms with a continental setting. The tholeiitic (Goedgenoeg Fm.) to calc-alkaline (Makwassie Fm.) character is typical of continental rift-related volcanism, which normally grades from an initial tholeiitic character to a later calc-alkaline composition.

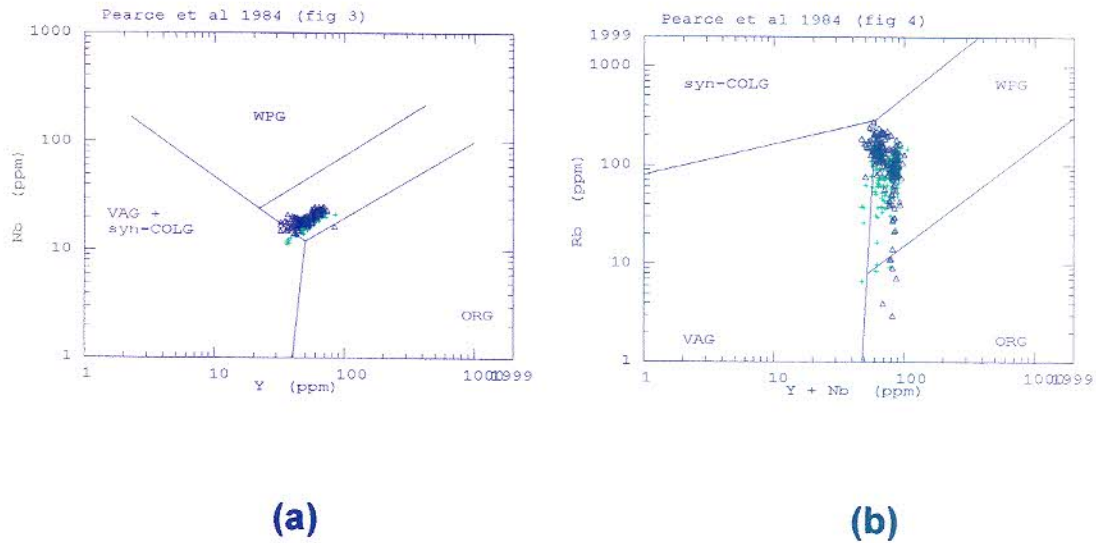


FIGURE 7.3: Within plate (WPG) classification of the Goedgenoeg (green) and Makwassie (black) Formations on the Y-Nb and (Y+Nb)-Rb diagrams of Pearce *et. al* (1984). Other fields are ocean ridge (ORG), volcanic arch (VAG) and syn-collision (syn-COLG) granites. Note that secondary mobility of Rb account for the scatter of some of the plots. (Data from the Bothaville area).

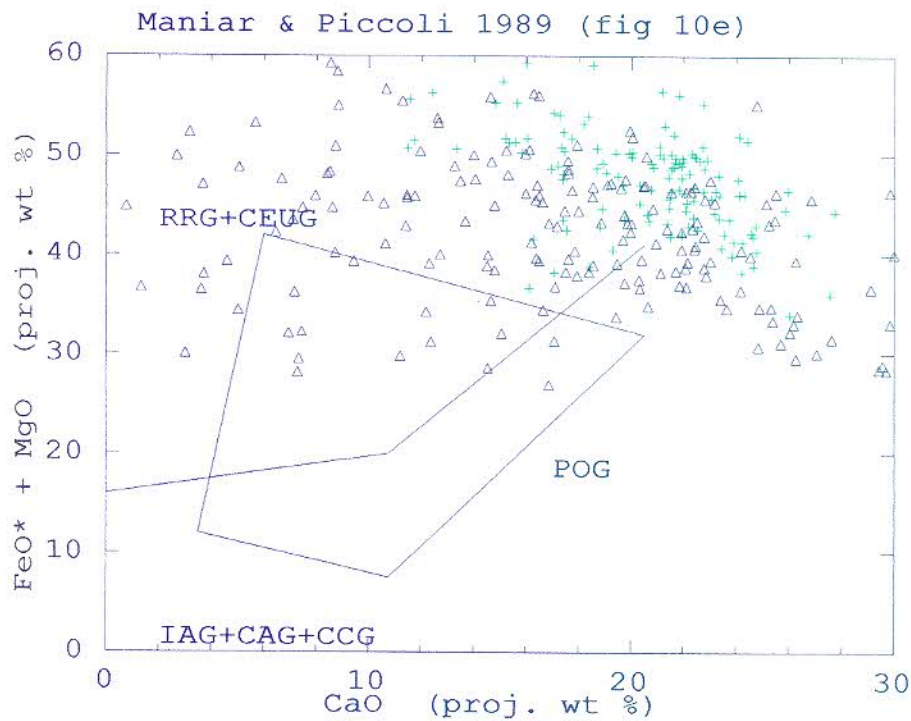


FIGURE 7.4: (RRG+CEUG) classification of the Goedgenoeg (green) and Makwassie (black) Formations on the Cao-(FeO+MgO) diagram of Maniar and Piccoli (1989). Symbols are rift-related (RRG), continental epeirogenic uplift (CEUG), island arc (IAG), continental arc (CAG), continental collision (CCG) and post-orogenic (POG) granitoids. (Data from the Bothaville area).

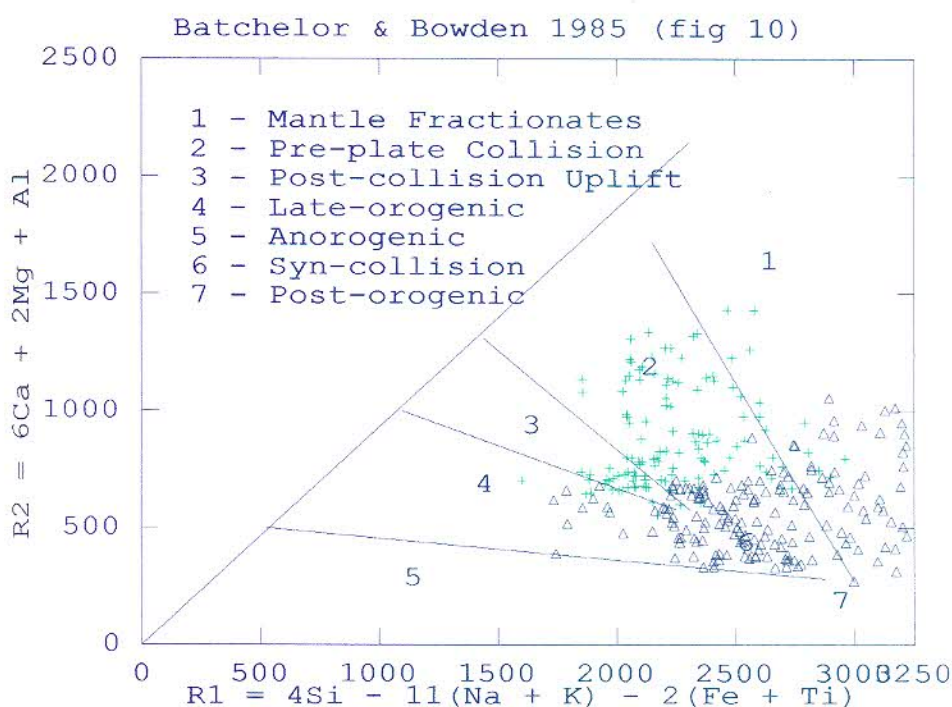


FIGURE 7.5: Classification of the geochemical facies of the Goedgenoeg and Makwassie Formation on the R1-R2 diagram of Batchelor and Bowden (1985). The Goedgenoeg Formation samples are indicated in green and the Makwassie Formation samples in black. (Data from the Bothaville area).

7.4 PETROGENESIS

7.4.1 Introduction

The observed compositional range from andesite to rhyolite of the Goedgenoeg and Makwassie eruptives indicates rudimentary changes in the original magma composition. Fundamental processes that can lead to this variation are partial melting, fractional crystallization, assimilation and magma mixing. Partial melting alone is unlikely to account for the complete variation. The true history of a felsic magma source is probably very complex, with partial melting, fractional crystallization, periodic replenishment of the magma chamber with incomplete or complete mixing of magmas and assimilation of country rock taking place. The dominant processes, however, should still be reflected in the geochemistry.

7.4.2 Note on Chemical Analysis of Porphyritic Rocks

Whole rock chemical analyses of porphyritic samples do not necessarily yield the original parent magma composition from which the rock crystallized as the

individual phenocrysts did not necessarily crystallize from the same magma. Some of these crystals could be remnants of crustal material that was assimilated, or they could be crystals that crystallized in an earlier magma that was subjected to mixing prior to extrusion. The glassy matrix of a porphyritic volcanic rock should represent the parent magma composition as it is the quenched phase. Magma modelling on fresh porphyritic volcanics constitutes separation of phenocrysts from the quenched glassy groundmass. However, in the case of the Archaean-age Makwassie porphyries it is not possible to separate the phenocryst and matrix components, especially since the phenocrysts are highly fragmented. Pervasive metamorphism of the rock further precludes isolation of possible original magma material. Microprobe analysis of the phenocryst crystals should reveal different genetic populations, but analyses are precluded by alteration related to the pervasive metamorphism. Bulk chemical analyses of the Makwassie porphyries nevertheless still give a broad indication of the chemical character of the original magma(s) involved in the genesis of the volcanics. The chemical stratigraphy of the succession also reflects the chemical evolution that took place during emplacement. This discussion of the Makwassie magma genesis consequently considers the broader aspects of the magmatic evolution that took place.

7.4.3 Previous Genetic Models

Few genetic models of the Makwassie volcanics have been presented in the literature. Most of these studies were conducted as overview studies of the Ventersdorp or Witwatersrand triad volcanics and then on limited databases too. Detailed lithostratigraphic research on the Platberg Group has up to recently received little attention.

M.P. Bowen (1984) concluded that the Platberg Group lavas are not genetically related to any other magma type in the Witwatersrand triad. He also proposed that the Goedgenoeg and Rietgat volcanics represent hybrid magmas which contain both mantle and crustal components, whereas the Makwassie quartz-feldspar porphyries represent the crustal-derived acid end member. A basic end member is not represented in the Ventersdorp volcanics.

The magma mixing or crustal contamination model was opposed by Myers (1990) who suggested that the lower mafic Goedgenoeg lava is the parent magma for the overlying acidic Makwassie rocks, as well as for the Rietgat lavas. The Makwassie Formation in the Klerksdorp area where Myers studied the formation, has an inverted chemical stratigraphy; the formation becomes

less differentiated and more basic with stratigraphic height. (The present study indicates the opposite for the Bothaville area). Myers accounted for the inverted stratigraphy by envisioning ponding of small volumes of Goedgenoeg magma within the crust, which differentiated rapidly to the acidic Makwassie composition and then erupted. Progressively, magma injected into these ponded chambers had less residential time and erupted as less differentiated lava. Lava eventually erupted directly from the deep source without differentiation to form the Rietgat lavas, which have a composition similar to the Goedgenoeg lavas. According to O'Hara and Mathews (1981), however, the chemical processes in frequently replenished high-level magma chambers can be very complicated.

Crow and Condie (1988) favoured batch melting and fractional crystallization of an enriched source to produce the Goedgenoeg and Rietgat lavas. Fractional crystallization of this Goedgenoeg/Rietgat magma can then produce the acidic lavas of the Makwassie.

Observed negative ε_{Nd} values and LREE (Light Rare Earth Elements) enrichment of the Ventersdorp lavas indicate crustal assimilation (Nelson *et al.*, 1990) and although inherited zircons in the Makwassie lavas (Armstrong *et al.*, 1992) support this observation, their relative low abundance in the Ventersdorp volcanics is irreconcilable with the extensive amounts of crustal assimilation which is required to explain the observed ε_{Nd} and LREE trends (Nelson *et al.*, 1990). The Sm-Nd isotopic investigation of Nelson *et al.* (1992) led them to conclude that the Ventersdorp volcanics were derived from enriched mantle sources. This is supported by the observation of Neumann and Ramberg (1978) that the source region of continental rift magmas is generally enriched mantle with marked heterogeneities.

7.4.4 Genetic Modelling

In order to determine the genesis of the different units (Gm, Gi, Gz, Gs, Md and Mr) that make up the Goedgenoeg and Makwassie Formations of the Platberg Group, use was made of a spidergram to ascertain enrichment and depletion of different elements. Data were Primitive Chondrite normalised (Taylor and McLennan, 1985) and the resulting spidergram is depicted in Figure 7.6. This figure clearly illustrates the relative enrichment of the different units as regards K, Rb, Nb, Sr, Zr Ti and Y, while the rocks are severely depleted in V, Zn, Cu, Ni, and Cr. Depletion of these elements is also evident in analyses of units of the Klipriviersberg Group (Linton *et al.*, 1990), with the exception that Ni-depletion is not as striking as Cu enrichment (Fig. 7.6).

When considering the formation of these units, the assumption that they are derived from Rayleigh fractionation was tested. Use was made of the NEWPET software programme, with additional mineral K_D values from the MODULUS software (Knoper, 1992). Using any of the formations of the Klipriviersberg Group as a starting liquid, it was indicated that the Goedgenoeg and Makwassie Formations could not have formed from simple fractional crystallisation of a more mafic source. Using the Westonia, Alberton and Orkney Formations as possible sources, it transpires that the Gm, Gi and Gz facies are distinctly enriched in Zr, while depletion in Ni is very evident in all units of the Goedgenoeg and the Makwassie Formations with the exception of the Gm facies (Fig. 7.7). The positions of the Gi and Gz facies on a plot of Zr against Ni (Fig. 7.7) lay between the lines of total equilibrium and surface equilibrium. The positions of the Gs and Md facies fall almost on the line representing 80% fractionation (Fig. 7.7).

The position of all these points on the diagram indicates that these rocks cannot be derived from a system of fractional crystallisation. Taking into account the distinctly Zr enriched nature of the Gm facies, the source of this unit was probably highly enriched in Zr. The involvement of an enriched source is well established by previous researchers (e.g. Schweitzer and Kröner, 1985; Crow and Condie, 1988). This also accounts for the enrichment in Ba and Y, and if the source is depleted in Cu, Ni and Cr it will also explain the depletion in these elements with respect to the Gm facies.

It is therefore likely that the magma responsible for the development of the Gm facies is from a separate source, or that it is derived from a mixture of fractionated Klipriviersberg magma and material from an unknown source. Data from the Gm facies on a plot of Zr against Ni indicate that for the greater part the different rocks of this unit are formed by fractional crystallisation (Fig. 7.8). Internal changes in the ratios are explained by injection of new material into the magma chamber, which will affect the composition of the extruded material. Magma chamber(s) that was periodically replenished, mixed, fractionated and tapped with accompanying assimilation was probably involved to produce lavas with different compositions as exhibited by the Gm facies.

The development of the Gi and Gz facies was also tested in terms of Rayleigh fractionation (Fig. 7.9) by using Gm as starting material. It is clear from the diagram that, although less depleted in terms of Zr, Ni depletion is greater with the data falling outside the region of the calculated fractionation curves. This is

explained by either progressive injection of new and even more Ni depleted and Zr enriched material and mixing with existing fractionated Gm material (Fig. 7.9). Or on the other hand, if Gz is the result of mixing between Gm and another depleted magma, then mixing between Gm and Gz could result in the formation of Gi. This model was tested using the MIXER software, written by the University of Cape Town. The data are presented in Table 7.5.

From the data presented in Table 7.5 it is evident that Gi could have originated from a combination of 18% Gm and 82% Gz, which results in a cumulative discrepancy of 1.65%. Major differences between the calculated and observed values are evident in Na_2O and K_2O , but all others correspond closely. It is therefore likely that either Gi is a combination of Gm and Gz, or it is a less evolved combination of Gm and the contaminant responsible for the development of Gz.

Considering the position of Mr on the diagram of Zr against Ni (Fig. 7.7), it is apparent that this rock type is not related to any fractional crystallisation of pre-existing mafic magmas, except if it was contaminated by a source depleted in Ni and Zr. It is thus regarded as derived from a separate source.

The position of Gs on the diagram of Zr against Ni (Fig. 7.7) attests that it is more depleted in Ni and Zr than either Gi or Gz. This is further indicative that this unit was not derived from fractional crystallisation, but rather a mixing of two individual magmas. This hypothesis was tested by means of the MIXER programme which indicated that it is a combination of Gi and Mr (Table 7.6). A similar situation is observed for the data from Md (Fig. 7.7) and therefore a similar origin is proposed for this unit. This data are also presented in Table 7.6.

It can consequently be concluded that the Gm facies is not the result of fractional crystallisation of a more mafic source only. Contamination by an additional source along with periodic injection of additional material, as evidenced by the distribution of Zr against Ni (Fig. 7.7) and the Primitive Chondrite normalised spidergram (Fig. 7.6) certify to this conclusion. Crow and Condie (1988) also found that the Platberg volcanics are not derived from fractional crystallisation of a Klipriviersberg source, but that an enriched mantle source must be involved. Development of the Gz facies is the result of mixing of fractionated Gm with another more Zr enriched and Ni depleted source. This, in different proportions, may also have been responsible for the generation of Gi magma, or mixing between Gm and Gz in fixed proportions could also have resulted in the formation of this unit.

It is envisaged that the Mr represents a separate melt and is not related to any of the precursors in the Ventersdorp Supergroup by means of fractional crystallisation alone. The Mr facies is regarded as a crystallisation product from an enriched mantle source. Mixing of Mr with different combinations of Gi resulted in the development of both the Gs and Md facies.

TABLE 7.5: Data depicting the mixing of 18.23% Gm and 81.77% Gz to produce the magma responsible for the development of Gi.

	Observed	Calculated	Difference
SiO ₂	65.18	64.46	-0.72
TiO ₂	1.24	1.34	0.10
Al ₂ O ₃	13.47	13.35	0.08
Fe ₂ O ₃	7.21	7.70	0.49
MnO	0.10	0.12	0.02
MgO	2.00	1.91	-0.09
CaO	4.60	4.24	-0.36
Na ₂ O	3.10	2.77	-0.33
K ₂ O	2.62	3.41	0.79
P ₂ O ₅	0.48	0.50	0.02
			Σ 1.65

TABLE 7.6: Data depicting the mixing of Gi and Mr to produce the magmas responsible for the development of Gs and Md respectively.

	Md Obs.	Md Calc.	Diff.	Gs Obs.	Gs Calc.	Diff.
SiO ₂	68.20	67.66	-0.54	65.58	66.10	.52
TiO ₂	1.09	1.04	-0.05	1.27	1.17	-0.10
Al ₂ O ₃	13.21	13.25	0.04	13.22	13.39	0.17
Fe ₂ O ₃	6.27	5.99	-0.28	7.38	6.76	-0.62
MnO	0.10	0.09	-0.01	0.09	0.09	0.00
MgO	1.54	1.64	0.10	1.32	1.87	0.55
CaO	3.37	3.67	0.30	3.57	4.26	0.69
Na ₂ O	2.71	2.91	0.20	3.77	3.03	-0.74
K ₂ O	3.07	3.36	0.29	3.29	2.90	-0.39
P ₂ O ₅	0.44	0.38	-0.06	0.53	0.44	-0.09
%Gi		71.17			89.32	
%Mr		28.83			10.68	
Σ Diff.			0.60			2.18

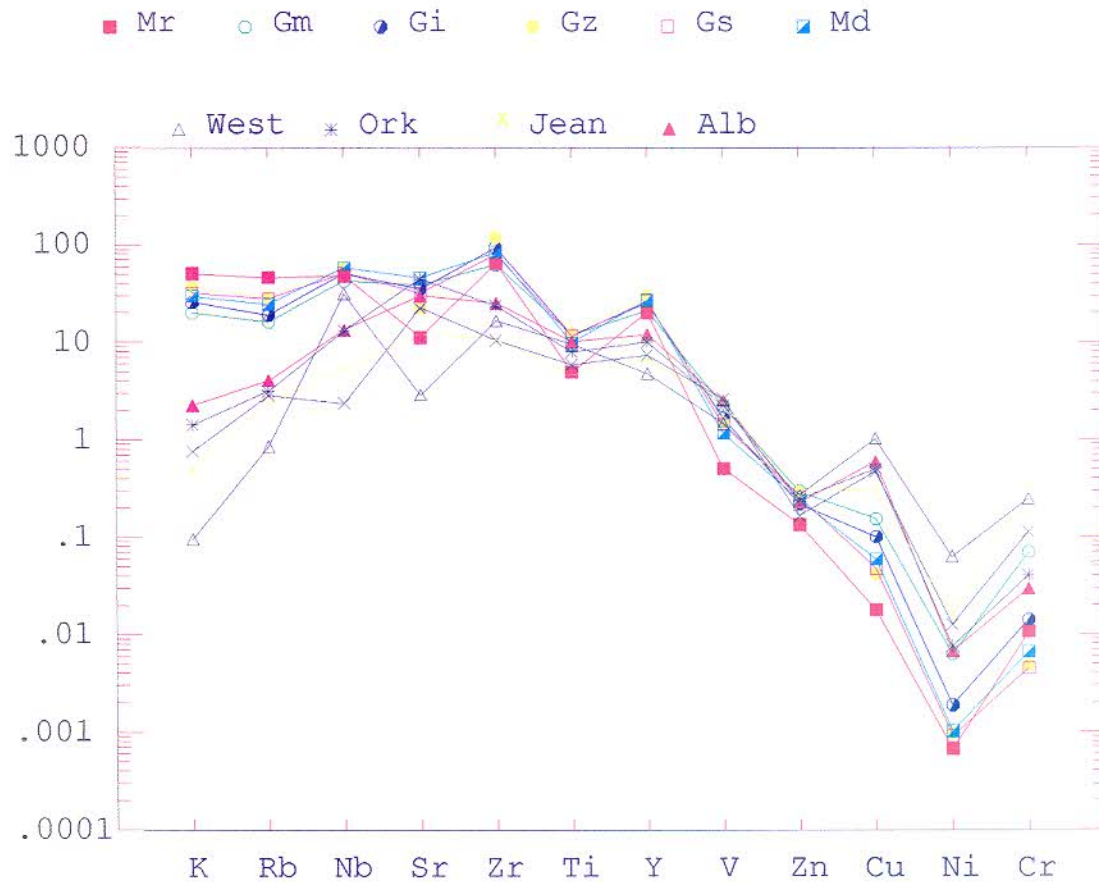


FIGURE 7.6: Spidergram of Primitive Chondrite normalised data of the Klipriviersberg Formations and the geochemical facies of the Goedgenoeg and Makwassie Formations.

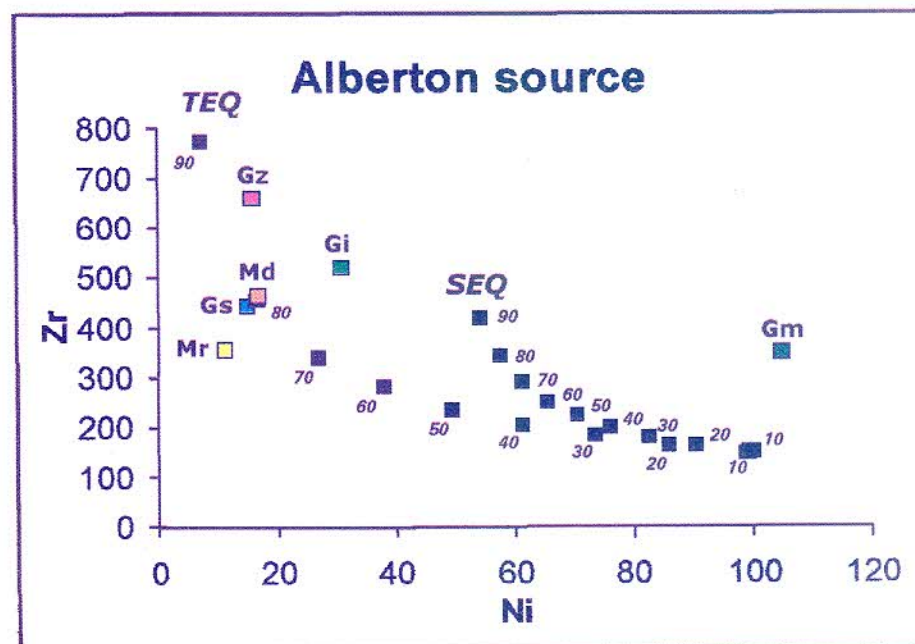


FIGURE 7.7: Fractionation of Alberton as source magma in terms of 10% intervals. Note the plot positions of the Goedgenoeg and Makwassie facies.

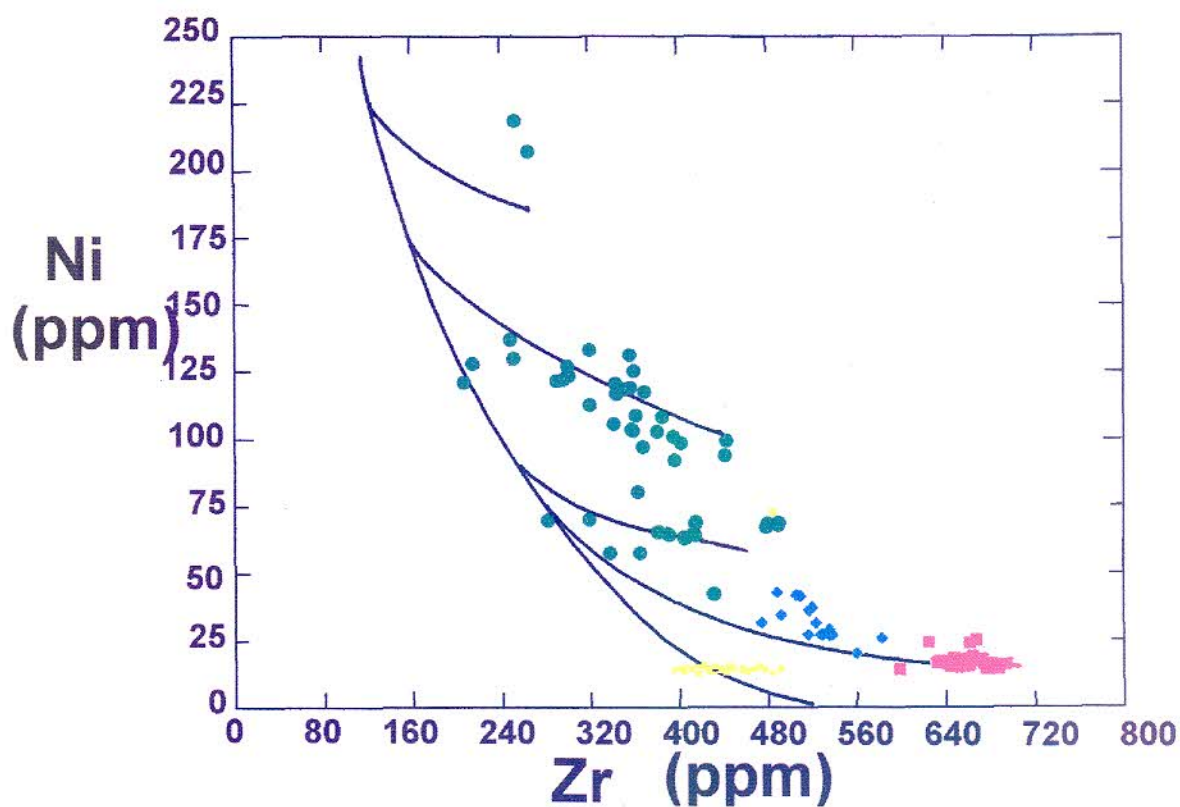


FIGURE 7.8: Possible fractionation trends for the Gm facies (green). The other Goedgenoeg facies are also plotted (Gi = blue, Gs = yellow, Gz = magenta).

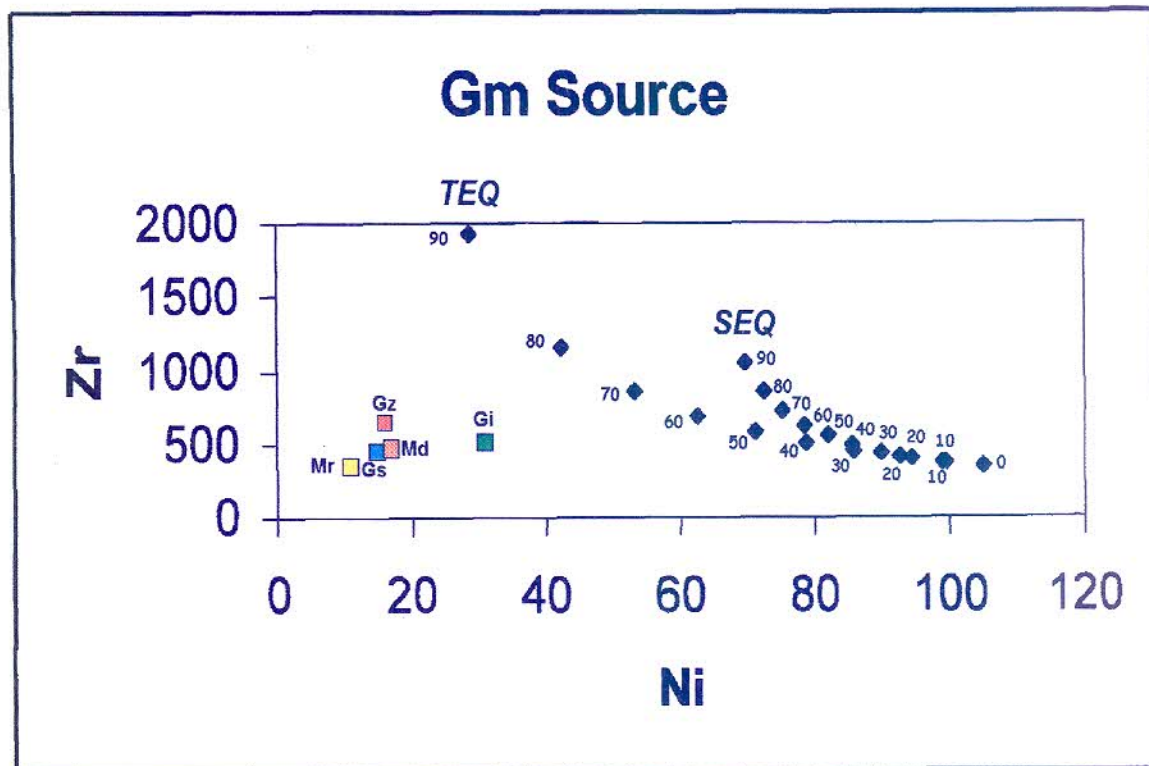


FIGURE 7.9: Fractionation of Gm as source magma in terms of 10% intervals. Note the plot positions of the other Goedgenoeg and Makwassie facies.

8. SUMMARY

8.1 LITHOSTRATIGRAPHY

The felsic volcanics of the Platberg Group are subdivided into a lower intermediate feldspar porphyry succession (the Goedgenoeg Formation) and an upper felsic quartz-porphyry succession (the Makwassie Formation). The lower feldspar porphyry succession was previously grouped with the Makwassie Formation (S.A.C.S., 1980). Sedimentary rocks occur only rarely at the top contact of the Goedgenoeg Formation or are interbedded with the top volcanics of the Goedgenoeg Formation, indicating a minor unconformity between the two formations.

The thickness of the Goedgenoeg Formation varies widely, as can be expected from volcanic succession. The formation is best developed and preserved in the deepest Platberg grabens, where it reaches a thickness in excess of 2 000 m. The Makwassie Formation is more widely spread with less dramatic thickness variation of mostly between 300 m and 800 m, although it too can reach more than 2 000 m in thickness.

Although the Goedgenoeg Formation is dominated by feldspar porphyries, interbedded non-porphyritic lavas are also prominent. Apart from the top contact, sedimentary rocks are locally also interbedded with the volcanics at the base of the formation, suggesting a gradual transition to volcanism from the sedimentation of the Kameeldoorns Formation.

The phenocryst concentrations of the feldspar porphyries vary from low to very high and consist of plagioclase (predominant), alkali-feldspar, chloritised amphibole(?) and biotite(?), apatite, zircon, sphene, spinel and titanomagnetite. Chloritization is prevalent. Most of the feldspar porphyries were emplaced as sub aerial pyroclastic ash-flows and the flow units can still be recognised. The non-porphyritic lavas and the feldspar porphyries with low phenocryst concentrations originated as normal liquid lava flows.

The quartz-feldspar porphyries of the Makwassie Formation are interbedded with minor feldspar porphyries and non-porphyritic lavas, especially toward the base of the Makwassie succession. Towards the top of the succession thick feldspar-porphyry units occur locally and one such unit in the Bothaville area was previously (Winter, 1976) described as the Garfield Member.

The phenocrysts are fragmented, but still of relative large size and concentrations in the quartz-feldspar porphyries are mostly very high (about 35%), with a similar population (but for the addition of quartz) as in the feldspar porphyries. The matrix invariably displays a felsitic texture with pervasive silicification being evident, rather than chloritization being dominant as in the feldspar porphyries. In the Bothaville area the lower part of the succession contains numerous macroscopic and microscopic inclusions of non-porphyritic intermediate lava.

Ash-flow units are discernible in the quartz-feldspar porphyries, often separated by minor co-ignimbrite air-fall tuffs. The general lack of flow textures, pumice and other pyroclastic or lava flow features in the bulk of the ash-flow units indicates that they represent high-temperature ash-flows, as defined by Saggerson and Bristow (1983), rather than normal welded ash-flows. Normal welded pyroclastic ash-flows, however, do also occur at various localities, e.g. at the Kimberley Mines, and in boreholes west of the Welkom Gold Field and near Vryburg. Rheomorphic flows have also been observed at Ritchie near Kimberley and in a borehole near Hoopstad.

The Ventersdorp Supergroup rocks underwent burial metamorphism which have reached the greenschist facies. The Goedgenoeg and Makwassie volcanics are highly altered and the typical products of greenschist facies metamorphism predominate the mineralogical composition, such as quartz, chlorite, epidote, actinolite, calcite and sericite. Differential alteration caused false pyroclastic textures in places. The feldspar phenocrysts are altered to such a state that the original compositions could not be determined reliably, not even by the use of the electron microprobe.

The typical lithological characteristics of the Goedgenoeg and Makwassie volcanics are listed in Table 8.1.

TABLE 8.1: Macroscopic lithological characteristics of the 3 main rock types of the Makwassie Formation in the Bothaville area. Predominant lithology is indicated by (P), subordinate lithology by (S) and minor lithology by (m). QFP = quartz-feldspar porphyry; FP = feldspar porphyry; and NON-P = non-porphyritic lava.

LITHOLOGY	QFP	FP	NON-P
Green-coloured		P	P
Grey-green to grey-white coloured	P	S	
Non-porphyritic interbeds	S	P	
Sedimentary interbeds	P	S	
Silicified	P	S	
Chloritized	S	P	P
FLOW-UNITS			
Thickness	<300 m	<200 m	<25 m
Phenocryst-rich units	P	P	
Quartz phenocrysts	P	m	
Feldspar phenocrysts	P	P	m
Fragmented phenocrysts	P	P	
Euhedral phenocrysts			S
Amygdales	P	P	P
Ash-flow units	P	P?	

8.2 GEOCHEMICAL COMPOSITION

The volcanic rocks of the Goedgenoeg and Makwassie Formations are subalkaline, bimodal and mostly metaluminous in composition. They are clearly oversaturated in silica, but alteration has, however, effected the original concentrations of those elements which are mobile under low to medium grade metamorphism, such as silica, Ca, K, Na, Ba, Rb and Sr. The less mobile elements, *i.e.* Ti, P, Cr, V, Co, Ni, Nb, Zr and Y were little affected but care must therefore be taken when interpreting the geochemical data.

Silica concentrations in the Goedgenoeg Formation vary between 56% and 69%, although secondary alteration could have affected these concentrations. The Goedgenoeg volcanics are metaluminous and tholeiitic in composition, with medium to high potassium. These rocks classify as high-andesites to dacites on discrimination diagrams that utilise immobile elements. Four geochemical facies are recognised. The high-andesite to low-dacite Gm facies represents the non-porphyritic to slightly porphyritic rocks, which occur throughout the Goedgenoeg

succession and typically have silica concentrations of 56% to 64%. The Gi facies has a silica range of 63% to 68% and mostly occurs as feldspar porphyries in the middle to upper parts of the Goedgenoeg succession. Compared to the Gi facies, the Gz facies has very high Zr (and Y) concentrations and is only encountered in the deepest areas of the Platberg grabens, near the base of the Goedgenoeg succession. Although the Gs facies occurs higher up in the succession, and only rarely at that, its composition is similar to that of the Gz facies, except for much lower Zr (and Y) concentrations. The Gi, Gz and Gs facies are all dacitic feldspar porphyries, but the Gz and Gs do contain sparse quartz phenocrysts. See Table 8.2 for the average composition of these facies for the Bothaville area.

The geochemical composition of the Makwassie Formation ranges from metaluminous to peraluminous, as can be expected from continental felsic volcanics. It is further calc-alkaline rather than tholeiitic, mostly high in potassium and the volcanics classify as dacites to rhyodacites. The lower, dacitic Md facies (65% - 74% SiO₂) and the upper rhyodacitic Mr facies (70% - 80% SiO₂) are distinguished. The Mr facies could be further subdivided through the use of incompatible/compatible element ratios (*i.e.* Cr/Zr). The Md facies represents the lower part of the Makwassie succession that typically contains numerous mafic inclusions. See Table 8.2 for the average composition of these facies for the Bothaville area.

The feldspar porphyries and non-porphyritic lavas of the Garfield Member have similar composition as the Gm facies, as do other mafic lavas interbedded with the Makwassie quartz-feldspar porphyries. Magma of Gm facies composition has therefore co-erupted with other magmas throughout the Goedgenoeg and Makwassie volcanic event.

8.3 DISTRIBUTION

The felsic volcanics of the Platberg Group are widespread throughout the Ventersdorp Supergroup depository, but are poorly exposed. The volcanics are preserved in deep and extensive graben structures developed in a broad continental rift zone. To the west of the Central Rand Basin the graben structures have a more or less north-south orientation and most are bounded on their eastern margin by massive faults with down-to-the-west throw of more than 3 000 m.

TABLE 8.2: The average compositions of the geochemical facies of the Goedgenoeg and Makwassie Formations and of the Garfield Member **for the Bothaville area only**. (Normalised data in weight % or ppm volatile free).

	Goedgenoeg Formation				Makwassie Formation		Garfield Member
	Gm	Gi	Gz	Gs	Md	Mr	(Gm)
SiO ₂	59.12	65.18	65.65	65.58	68.20	73.80	59.75
TiO ₂	1.31	1.24	1.35	1.27	1.09	0.54	1.34
Al ₂ O ₃	14.29	13.47	13.38	13.22	13.21	12.71	14.29
Fe ₂ O ₃	9.54	7.21	7.29	7.38	6.27	2.97	9.44
MnO	0.14	0.10	0.11	0.09	0.10	0.05	0.14
MgO	4.35	2.00	1.36	1.32	1.54	0.75	4.45
CaO	5.98	4.60	3.85	3.57	3.37	1.39	5.24
Na ₂ O ₃	2.65	3.10	2.80	3.77	2.71	2.44	2.53
K ₂ O	2.06	2.62	3.71	3.29	3.07	5.20	2.25
P ₂ O ₅	0.56	0.48	0.49	0.53	0.44	0.14	0.57
Zr	350	522	659	440	466	356	365
Y	48	57	66	60	61	45	47
Sr	466	422	263	380	551	133	379
Rb	56	66	99	96	85	158	63
Cu	26	17	7	8	10	3	21
Zn	137	101	130	117	111	62	151
Ni	105	31	16	15	17	11	106
Ba	1069	1153	1444	1448	1287	1343	912
Nb	16	19	22	19	22	18	16
V	192	143	129	122	101	43	197
Cr	279	57	19	18	27	20	273
Co	32	19	12	16	12	6	31

To the north of the Central Rand Group the orientation is east-west. Late Platberg stage reactivation and renewed graben formation are evident west of the Central Rand Group, with northeast-southwest orientation. Post Ventersdorp tectonic events have reactivated some of the older structures and in places the

Ventersdorp strata has even been folded, e.g. in the Target Project area of the Free State Gold Field.

The Goedgenoeg Formation is preserved in the deep grabens, where it can reach a thickness in excess of 2 000 m. This formation rarely crops out on surface. The Makwassie Formation is more widespread and appears to 'overflow' the graben structures. This is very much in line with the distribution of rhyolites and dacites in volcanic terrains, where they tend to drape over previous topography and flatten out the terrain. Late Platberg and post Platberg erosion has eliminated or attenuated the Goedgenoeg and Makwassie successions over large areas of its previous domain. The Goedgenoeg Formation nevertheless occurs not only in the Bothaville graben, but also in the Kimberley, Vryburg, Hartebeestfontein and Wolmaransstad areas. Due to limited drilling data and poor correlation outside the Central Rand Group Basin, the full distribution of the Goedgenoeg Formation is far from fully established.

The Gm facies of the Goedgenoeg Formation appears to be the most widespread outside the Bothaville graben, where it typically displays a non-porphyritic, medium-crystalline texture. This has led to correlation with the Klipriviersberg Group or classification as a new volcanic succession.

The Mr facies of the Makwassie Formation is prevalent outside the Bothaville graben, but the Md facies is largely confined to the Bothaville area (please note that this area stretches up to Klerksdorp, where the Md facies also occurs). The Md facies does occur locally at the Kimberley Mines and Vryburg areas, where it appears to be a minor member of the succession. The Mr facies volcanics commonly display rheomorphic flow textures and autobrecciation, which is not observed in the Bothaville area. This has again led to confusion and erroneous correlation during exploration drilling outside the Central Rand Basin.

The small variation and widespread consistency in the geochemical composition of the Goedgenoeg and Makwassie Formations are really remarkable and can only indicate continental volcanism of massive scale over a very short period. The previously described Garfield Member is a locally developed unit, similar to other localised mafic units in the Makwassie Formation.

Volume calculations of the preserved volcanics in the closely drilled Bothaville area give an indication of the massive eruption volumes involved, with $\sim 3\,100\text{ km}^3$ for the Goedgenoeg Formation and $\sim 3\,900\text{ km}^3$ for the Makwassie Formation being calculated. Considering the small area of the Bothaville graben compared to the rest of the Ventersdorp depository and the size of some of the other known Platberg grabens, the total erupted volume for Goedgenoeg and Makwassie magma could be well in excess of $100\,000\text{ km}^3$.

8.4 GENESIS

The Goedgenoeg and Makwassie igneous rocks are of extrusive origin and were emplaced as pyroclastic ash-flows and liquid lava flows under aerial conditions. The quartz-feldspar porphyries and most of the feldspar porphyries were emplaced as high-temperature ash-flows, which indicate high eruption volumes from deep seated magma chambers. These volcanics must have originated from calderas, but such structures have not yet been identified. Eruption of large volume felsic volcanics is invariably from calderas and not from extensive fissures as with large volumes of basaltic lava. The very thick accumulations of Platberg volcanics, such as at borehole LLE1 at the Makwassie Hills, most probably represents the thick intracaldera facies. The Goedgenoeg Formation is largely restricted to the intracaldera area or immediate surround, while Makwassie of "normal" thickness ($<1\,000\text{ m}$) form the outflow facies. Other very thick successions of Platberg volcanics, which possibly represents calderas, can be recognised from aeromagnetic surveys, where these areas tend to form magnetic low anomalies of $50 - 70\text{ km}$ in diameter, e.g. Makwassie Hills, Hertzogville and south of Vryburg. If the Rietgat Formation lavas and sediments indeed represent the resurgent volcanism and moats typically associated with calderas, the distribution of the Rietgat Formation should then indicate the near presence of a caldera.

The Gm facies magma has erupted throughout the Goedgenoeg and Makwassie episode and possibly even formed part of the Rietgat Formation volcanics. The Gm facies is probably the result of fractional crystallisation of a periodically replenished magma and does not have any direct correlation with any of the Klipriviersberg Group magmas. The Gz facies formed through mixing of fractionated Gm magma with another more compatible element (especially Zr)

enriched and incompatible element (such as Ni) depleted source. Mixing of Gm and Gz material could have resulted in the formation of the Gi unit.

The Mr facies of the Makwassie Formation represents a separate melt, which cannot be related to the other Ventersdorp Supergroup magmas through simple fractionation processes alone. It is regarded as a crystallisation product from an enriched mantle source and mixing of this Mr magma with different combinations of the Gi magma resulted in the development of both the Gs and Md facies.

8.5 STRATIGRAPHIC RECOGNITION

The Goedgenoeg and Makwassie Formations are distinguished from the other Ventersdorp Supergroup volcanic formations by their predominant porphyritic character and felsic composition. The extreme thickness of the Goedgenoeg and Makwassie successions at some localities, however, necessitate the identification of marker horizons to facilitate evaluation during drilling of exploration boreholes. Specific stratigraphic horizons within the Goedgenoeg or Makwassie Formation are not readily identified lithologically and geochemical techniques are applied to differentiate between units.

Quartz-feldspar porphyries characterise the Makwassie Formation and feldspar porphyries the underlying Goedgenoeg Formation. Interbedded feldspar porphyry lavas may pose a problem in the Makwassie Formation, especially where such a unit attains substantial thickness as is the case with the Garfield Member. There is no simple solution to this problem, but close observation of the top contact of such a unit may indicate the presence of a small unconformity, as is the case with the top contact of the Goedgenoeg Formation. Furthermore, in the Bothaville area the distribution of the Garfield Member is fairly well delineated (see Chapter 4) and in fact the member can be used as a marker horizon in these areas. The basal part of the Makwassie Formation in the Bothaville area contains numerous mafic inclusions and geochemically classifies as the Md facies and can again be used as a marker horizon.

The Goedgenoeg Formation is restricted to the deepest Platberg grabens, where it surpasses the Makwassie Formation in thickness. In the deepest depositories in the Bothaville area, the lower part of the Goedgenoeg is interbedded with clastic sedimentary rocks of the underlying Kameeldoorns Formation and is uniquely

enriched in Zr. Unfortunately there is no consistent lithological or geochemical stratigraphy evident in the Goedgenoeg Formation. Aeromagnetic surveys, however, readily show up these deep Platberg grabens and if correct interpretations are made, they can be avoided during exploration drilling.

In areas where the Goedgenoeg Formation consists largely of non-porphyrific lavas, it may be difficult to recognise as such by the uninitiated and has indeed been correlated with the Klipriviersberg lavas in the past. The medium-crystalline texture and light yellowish-green colour of the lavas, however, readily distinguish it as being Goedgenoeg. The stratigraphic position also prevents confusion with the Allanridge Formation lavas.

T.B. Bowen (1984) devised a diagram to geochemically discriminate between the volcanic formations of the Witwatersrand triad. The data of this study, however, indicate that the Makwassie Formation field of this diagram has to be adjusted as rhyolitic samples of the Makwassie Formation plot in the Dominion Group porphyries field. There is little overlap, however, with the actual Dominion Group plots of T.B. Bowen (1984). Regrettably, this diagram is not effective for discriminating between the different geochemical facies described earlier, but a simple plot of the P_2O_5 , Cr and Zr ratios, as described in Chapter 5, will accomplish that.

8.6 POTENTIAL FOR ECONOMIC MINERAL DEPOSITS

Volcanic successions are ideal hosts for mineral deposits, especially where deep fault structures and the right volcanic features such as calderas are present. The root zones of volcanoes are the typical setting for large-scale mineral deposits, such as Cu-porphyries, while smaller but no less important deposits typically occur associated with calderas, particularly in the moat areas. Indeed, pyrite mineralisation is very common in the Rietgat Formation sediments, albeit without significant base metal concentrations.

Plausible reasons for the lack of known mineral deposits in the Platberg volcanics is the lack of deep erosion to uncover the root zones of the volcanism and the lack of interest to explore the Ventersdorp Supergroup systematically. The erosion level of the Ventersdorp Supergroup progresses deeper in a northern to north-western direction on the Kaapvaal Craton, consequently the best potential

for discoverable deposits is in these regions. The unresolved correlation of the Kanye volcanics and other such rocks in Botswana is also of concern. Furthermore, the on-craton setting of most of the better known Platberg rocks (through drilling for Central Rand Group) would be less favourable for mineralisation and exploration should indeed be focused to the edges of the Kaapvaal Craton, e.g. south-eastern Botswana.

8.7 RECOMMENDATIONS

This study highlights the lack of knowledge on various aspects of the Ventersdorp Supergroup, specifically the following:

- Analyses of the rare-earth element concentrations will be of tremendous aid to unravel the magmatic genesis of the Platberg volcanics. It will especially assist to further explain the origin of the individual geochemical facies and their possible link to the Klipriviersberg Group. Such a study will also give insight into the magmatic history of the Kaapvaal Craton.
- More detailed age determinations are needed for the Platberg volcanics. SHRIMP analyses of samples across the Platberg distribution area may indicate the progressive tectonic evolution of the Platberg rifting event.
- The Rietgat Formation is still poorly understood. The stratigraphy, geochemistry, distribution and genesis need to be studied to understand how it fits in with the rest of the Platberg volcanics and to determine the relation with the Goedgenoeg Formation. The structural setting needs to be clarified, especially the possibility of the Rietgat representing resurgent volcanics after the voluminous felsic Makwassie event and the formation of moats.
- The Allanridge volcanics are still very poorly studied and the genetic and tectonic relationship with the Platberg and Klipriviersberg Groups need to be delineated.
- There are numerous volcanic formations that occur in the western Kaapvaal Craton that may correlate with the Ventersdorp Supergroup, such as the Kanye and Buffelsfontein volcanics. In the light of this study's findings and the new geochemical database, these volcanic formations can now be studied in more detail.
- The existence and nature of high-temperature ash-flows are still controversial, even though there are reports of such pyroclastic deposits from around the world. The Makwassie Formation presents an ideal opportunity to throw light on the style of ancient volcanism.

- The Platberg volcanics had to have emanated from calderas. These structures are there and need to be identified.
- For Late Archaean rocks, the Ventersdorp Supergroup is relatively undeformed and it offers an unique opportunity to study the early evolution of the earth and the style of geological processes during this early history of the earth.

ACKNOWLEDGEMENTS

I am indebted to numerous colleagues and friends:

Dr Nic Grobler introduced me to the Ventersdorp Supergroup and initiated this research project. His enthusiastic interest in the Ventersdorp Supergroup was highly inspiring, as was his professional approach.

Prof. Willem van der Westhuizen and Dr Derick de Bruijn ably acted as study leaders and were always willing to assist.

Anglo American Prospecting Services funded this project and made borehole core available. Various staff members at AAPS were of assistance, in particular Messrs Kowie Weyers, Digby Dewar and Tony Jamison. Mr Meiring Strydom must be singled out for always being willing to share his vast knowledge on the Ventersdorp Supergroup.

Mr A. van Zyl of De Beers in Kimberley approved and arranged underground visits at the Kimberley Mines, while Mr Tom McGhee accompanied us on underground visits.

Financial assistance from the FRD are gratefully acknowledged.

At the Geology Department of the UOFS, the following persons were of special help:

Prof. Willem van der Westhuizen and Prof. L.D.C. Bok did the geochemical analyses while Dr Derick de Bruijn carried out the microprobe analyses. Fruitful discussions with the late Prof. Org Geringer contributed towards the genetic model of the Makwassie Formation.

Mr Jonas Choane prepared the samples for geochemical analyses and Mr Daniël Radikgomo made the thin sections.

The drafts were done by Mr James Stellenberg and Mr Andries Felix.

My father and late mother financed me during my pregraduate studies, which is sincerely appreciated. To my sister and brothers: Don't worry, I'll be doing some **real** work at last!

REFERENCES

- Allen R.L. (1988). False pyroclastic textures in altered silicic lavas, with implications for volcanic-associated mineralization. *Econ. Geol.*, **83**: 1424-1446.
- Anhaeusser C.R. (1973). The evolution of the early Precambrian crust of southern Africa. *Philos. Trans. Roy. Soc. London*, **A273**: 359-388.
- Armstrong R.A., Compston W., Retief E.A. & Welke H.J. (1986). Ages and isotopic evolution of the Ventersdorp volcanics. *Abstr. Geocongress '86, Geol. Soc. S. Afr.*, Johannesburg, 89-92.
- Armstrong R.A., Compston W., Retief E., Williams I.S. & Welke H.J. (1992). Zircon ion microprobe studies bearing on the age and evolution of the Witwatersrand Triad. *Precamb. Res.*, **53**: 243-266.
- Baldrige W.S., Perry F.V., Vaniman D.T., Nealy L.D., Leavy B.D., Laughlin A.W., Kyle P., Bartov Y., Steinitz G. & Gladney E.S. (1989). Magmatism associated with lithospheric extension: Middle to late Cenozoic magmatism of the southeastern Colorado Plateau and central Rio Grande rift, New Mexico and Arizona. Excursion 8A, IAVCEI, *New Mexico Bureau of Mines and Mineral Resources, Mem. 46*: 187-230.
- Barker D.S. (1970). Compositions of granophyre, myrmekite, and graphic granite. *Geol. Soc. Am. Bull.*, **81**: 3339-3350.
- Barker D.S. (1983). *IGNEOUS ROCKS*. Prentice-Hall, New Jersey, 417pp.
- Barker O.B. (1978). *A CONTRIBUTION TO THE GEOLOGY OF THE SOUTPANSBERG GROUP, WATERBERG SUPERGROUP, NORTHERN TRANSVAAL*. MSc Thesis (unpubl.), Univ. Witwatersrand, Johannesburg, 113pp.
- Batchelor R.A. & Bowden P. (1985). Petrogenetic interpretation of granitoid rock series using mylticationic parameters. *Chem. Geol.*, **48**: 43-55.
- Beetz P.F.W. (1936). Contributions to the geology of the Klerksdorp District from results of the drilling activities by the Western Reefs Exploration and Development Company, Limited. *Trans. Geol. Soc. S. Afr.*, **39**: 223-261.
- Behounek N.J. (1980). *THE GEOLOGY OF AN AREA WEST OF WELKOM, ORANGE FREE STATE*. MSc Thesis (unpubl.), Univ. Orange Free State, Bloemfontein, 162pp.
- Beswick A.E. & Soucie G. (1978). A correction procedure for metasomatism in an Archean greenstone belt. *Precamb. Res.*, **6**: 235-248.

- Bickle M.J. & Eriksson K.A. (1982). Evolution and subsidence of early Precambrian sedimentary basins. *Phil. Trans. R. Soc. London*, **A305**: 225-247.
- Birch W.D. (1978). Petrogenesis of some Palaeozoic rhyolites in Victoria. *J. Geol. Soc. Austr.*, **25**: 75-87.
- Bonnichsen B. & Kauffman D.F. (1987). Physical features of rhyolite lava flows in the Snake River Plain volcanic province, southwestern Idaho. In: Fink J.H. (Ed.). The emplacement of silic domes and lava flows. *Geol. Soc. Am. Spec. Paper*, **212**: 119-145.
- Booth J.M. (1987). Acid volcanism in the Platberg Group around Klerksdorp: Examples of ash-flow and air-fall type pyroclastic deposits. *Workshop on pyroclastic volcanism and associated deposits: Abstr.*, Pietermaritzburg, 22-23.
- Borsi S., Marinelli G., Mazzocini F., Mitterpergher M. & Tedesco C. (1963). Reconnaissance of some ignimbrites at Pantelleria and Eolian islands. *Bull. Volcanol.*, **25**: 359-363.
- Bowen M.P. (1984). *THE PETROGENESIS OF THE VOLCANIC ROCKS OF THE WITWATERSRAND TRIAD IN THE KLERKSDORP AREA, TRANSVAAL*. MSc Thesis (unpubl.), Rhodes Univ., Grahamstown, 204pp.
- Bowen M.P., Bowen T.B., Marsh J.S. & Eales H.V. (1986). Geochemical stratigraphy of the volcanic rocks of the Witwatersrand triad. *Abstr. Geocongress '86, Geol. Soc. S. Afr.*, Johannesburg, 99-102.
- Bowen T.B. (1984). *THE GEOCHEMICAL STRATIGRAPHY OF THE VOLCANIC ROCKS OF THE WITWATERSRAND TRIAD IN THE KLERKSDORP AREA, TRANSVAAL*. MSc Thesis (unpubl.), Rhodes Univ., Grahamstown, 223pp.
- Bowen T.B., Marsh J.S., Bowen M.P. & Eales H.V. (1986). Volcanic rocks of the Witwatersrand Triad, South Africa. I: Description, classification and geochemical stratigraphy. *Precamb. Res.*, **31**: 297-324.
- Bristow J.W. & Cleverley R.W. (1979). Volcanology of the Lebombo rhyolites. *Abstr. Geocongress '79, Geol. Soc. S. Afr.*, Port Elizabeth, 76-78.
- Bristow J.W. (1986). An overview of the Soutpansberg sedimentary and volcanic rocks. *Koedoe*, **29**: 59-68.
- Bristow J.W. (1989a). Retracing Vulcan's fiery footsteps. *Nuclear Active*, **41**: 30-37.
- Bristow J.W. (1989b). The Jozini rhyolites: a new type of pyroclastic rock. *Guide to the Geology of the southern Lebombo volcanics*, Joint Publ. of the Natal Branch of the Geol. Soc. of S.A. and the Univ. of Natal (Durban), Spec. Publ. **1**, 37pp.
- Brown P.E., Parsons I. & Becker S.M. (1987). Peralkaline volcanicity in the Arctic Basin - the Kap Washington Volcanics, petrology and palaeotectonics. *J. Geol. Soc. London*, **44**: 707-715.

- Buddington A.F. & Lindsley D.H. (1964). Iron-titanium oxide minerals and synthetic equivalents. *J. Petr.*, **5**: 310-357.
- Burger A.J. & Coertze F.J. (1973/4). Radiometric age measurements on rocks from Southern Africa to the end of 1971. *Bull. Geol. Surv. S. Afr.*, **58**, 46pp.
- Burke K., Kidd W.S.F. & Kusky T. (1985). Is the Ventersdorp rift system of Southern Africa related to a continental collision between the Kaapvaal and Zimbabwe Cratons at 2.64 Ga ago? *Tectonophysics*, **115**: 1-24.
- Burke K., Kidd W.S.F. & Kusky T. (1986). Archaean foreland basin tectonics in the Witwatersrand, South Africa. *Tectonics*, **5**: 439-456.
- Byers F.M.(Jr), Carr W.J., Orkild P.P., Quinlivan W.D. & Sargent K.A. (1976). Volcanic suites and related cauldrons of Timber Mountain - Oasis Valley Caldera Complex, Southern Nevada. *U.S. Geol. Surv. Prof. Paper* **919**, 70pp.
- Cann J.R. (1970). Rb, Sr, Y, Zr and Nb in some ocean floor basaltic rocks. *Earth Planet. Sci. Letters*, **10**: 7-11.
- Cas R.A.F. (1978). Silicic lavas in Palaeozoic flyschlike deposits in New South Wales, Australia: Behaviour of deep subaqueous silicic flows. *Geol. Soc. Am. Bull.*, **89**: 1708-1714.
- Cas R.A.F. (1983). A review of the palaeogeographic and tectonic development of the Palaeozoic Lachlan Fold Belt of southeastern Australia. *Geol. Soc. Aust. Spec. Publ.*, **10**. **Cited in:** Cas R.A.F. & Wright J.V. (1988). *VOLCANIC SUCCESSIONS: MODERN AND ANCIENT*. Unwin Hyman, London, 526pp.
- Cas R.A.F. & Wright J.V. (1988). *VOLCANIC SUCCESSIONS: MODERN AND ANCIENT*. Unwin Hyman, London, 526pp.
- Chapin C.E. & Lowell G.R. (1979). Primary and secondary flow structures in ash-flows of the Gribbles Run paleovalley, Central Colorado. *Geol. Soc. Am. Spec. Paper*, **180**: 137-153.
- Cheney E.S., Roering C. & Winter H. de la R. (1990). The Archean-Proterozoic boundary in the Kaapvaal Province of Southern Africa. *Precamb. Res.*, **46**: 329-340.
- Christiansen R.L. & Lipman P.W. (1972). Cenozoic volcanism and plate-tectonic evolution of the western United States. II: Late Cenozoic. *Phil. Trans. R. Soc. London*, **A271**: 249-284.
- Clarke D.B. (1992). *GRANITOID ROCKS*. Chapman & Hall, London, 280pp.
- Clemens J.D. & Wall V.J. (1984). Origin and evolution of a peraluminous silicic ignimbrite suite: the Violet Town Volcanics. *Contrib. Miner. Petr.*, **88**: 354-371.
- Clendenin C.W., Charlesworth E.G. & Maske S. (1988a). An early Proterozoic three-stage rift system, Kaapvaal Craton, South Africa. *Tectonophysics*, **145**: 73-96.

- Clendenin C.W., Charlesworth E.G. & Maske S. (1988b). Tectonic style and mechanism of early Proterozoic successor basin development, Southern Africa. *Tectonophysics*, **156**: 275-291.
- Clendenin C.W., Charlesworth E.G., Maske S. & de Gasparis A.A. (1988c). Normal simple shear model for the structural evolution of the early Proterozoic Ventersdorp Supergroup, Southern Africa. *Econ. Geol. Res. Unit*, Univ. Witwatersrand, Johannesburg, Inform. Circ. **201**, 20pp.
- Clendenin C.W. (1989). *TECTONIC INFLUENCE ON THE EVOLUTION OF THE EARLY PROTEROZOIC TRANSVAAL SEA, SOUTHERN AFRICA*. PhD Thesis (unpubl.), Univ. Witwatersrand, Johannesburg, 367pp.
- Cleverley R.W. & Bristow J.W. (1982). Flow-banded and contorted tuffs: Examples from southern Africa (Lebombo Province) and western North America. *Abstracts G.S.A.*, **14(7)**, 464pp.
- Clubley-Armstrong A.R. (1977). *THE GEOLOGY OF THE SELONSRIVER AREA, NORTH OF MIDDELBURG, TRANSVAAL*. MSc Thesis (unpubl.), Univ. Pretoria, Pretoria. **Cited in:** Bristow J.W. (1989). Retracing Vulcan's fiery footsteps. *Nuclear Active*, **41**: 30-37.
- Coetzee C.B. (1960). The geology of the Orange Free State Gold-Field. *Mem. Geol. Surv. S. Afr.*, **49**: 197pp.
- Cornell D.H. (1978). Petrologic studies at T'Kuip: Evidence for metamorphism and metasomatic alteration of volcanic formations beneath the Transvaal volcanosedimentary pile. *Trans. Geol. Soc. S. Afr.*, **81**: 261-270.
- Cox K.G., Bell J.D. & Pankhurst R.J. (1979). *THE INTERPRETATION OF IGNEOUS ROCKS*. George Allen & Unwin, London, 450pp.
- Crampton D.G.V. (1973). *THE GEOCHRONOLOGY OF THE ACID IGNEOUS ROCKS OF THE DERDEPOORT AREA, N.W. TRANSVAAL*. MSc Thesis (unpubl.), Univ. Witwatersrand, Johannesburg, 34pp.
- Crockett R.N. (1971). The rocks of the Ventersdorp System of the Lobatse and Ramotswa areas, Republic of Botswana; their possible origins and regional correlations. *Trans. Geol. Soc. S. Afr.*, **74**: 1-24.
- Crow C. & Condie K.C. (1988). Geochemistry and origin of Late Archean volcanics from the Ventersdorp Supergroup, South Africa. *Precamb. Res.*, **42**: 19-37.
- Curtis G.H. (1968). The stratigraphy of the ejecta from the 1912 eruption of Mount Katmai and Novarupta, Alaska. **Cited in:** Cas R.A.F. & Wright J.V. (1988). *VOLCANIC SUCCESSIONS: MODERN AND ANCIENT*. Unwin Hyman, London, 526pp.

- Dahms P.H. (1891). Über einige Eruptivgesteine aus Transvaal in Süd-Afrika. *Neues Jahrb. f. Min., B. Bd.* **14**: 90-131. **Cited in:** Hatch F.H. & Corstorphine G.S. (1905). *THE GEOLOGY OF SOUTH AFRICA*. MacMillan & Co., London, 348pp.
- De Bruijn H., Van der Westhuizen W.A. & Grobler N.J. (1984). Lithogeochemistry and multivariate statistics as aids to the stratigraphic characterization of Proterozoic Ventersdorp lavas. *S. Afr. J. Science*, **80**: 280-282.
- De La Roche H., Leterrier J., Grandclaude P. & Marchal M. (1980). A classification of volcanic and plutonic rocks using R₁R₂-diagram and major-element analysis - its relationship with current nomenclature. *Chemical Geol.*, **29**: 183-210.
- Donaldson C.H. (1976). An experimental investigation of olivine morphology. *Contrib. Mineral. Petrol.*, **57**: 187-213.
- Du Toit A.L. (1906). Geological survey of portions of the Divisions of Vryburg and Mafeking. *10th Ann. Rep. Geol. Comm. Cape Good Hope* (for 1905), 205-258.
- Du Toit A.L. (1907). Geological survey of the eastern portion of Griqualand West. *11th Ann. Rep. Geol. Comm. Cape Good Hope* (for 1906), 87-106.
- Du Toit A.L. (1908). Geological survey of portions of Hopetown, Britstown, Prieska and Hay. *12th Ann. Rep. Geol. Comm. Cape Good Hope* (for 1907), 159-192.
- Ekren E.B., McIntyre D.H. & Bennett E.H. (1984). High-temperature, large-volume, lavalike ash-flow tuffs without calderas in southwestern Idaho. *U.S. Geol. Surv. Prof. Paper* **1272**, 75pp.
- Elsdon R. (1975). Iron-titanium oxide minerals in igneous and metamorphic rocks. *Minerals Sci. Engng.*, **7**: 48-70.
- Emslie D.P. (1972). *THE GEOLOGY OF AN AREA AROUND SODIUM, BRITSTOWN DISTRICT, NORTHERN CAPE*. MSc Thesis (unpubl.), Univ. Orange Free State, Bloemfontein, 99pp.
- Fenn P.M. (1977). The nucleation and growth of alkali feldspars from hydrous melts. *Can. Mineral.*, **15**: 135-161.
- Fisher R.V. & Schmincke H.-U. (1984). *PYROCLASTIC ROCKS*. Springer-Verlag, Berlin, 472pp.
- Floyd P.A. & Winchester J.A. (1975). Magma type and tectonic setting discrimination using immobile elements. *Earth Planet. Sci. Letters*, **27**: 211-218.
- Franklin R.R., Self S. & Wolff J.A. (1987). Lava-like tuffs of Trans-Pecos Texas: the Star Mountain Formation. *EOS*, **68**: 1544.
- Gibson H.L., Watkinson D.H. & Comba C.D.A. (1983). Silicification: Hydrothermal alteration in an Archean geothermal system within the Amulet Rhyolite Formation, Noranda, Quebec. *Econ. Geol.*, **78**: 954-971.

- Giles C.W. (1982) The geology and geochemistry of the Archaean Spring Wells felsic volcanic complex, Western Australia. *J. Geol. Soc. Austr.*, **29**: 205-220.
- Grobler N.J. & Emslie D.P. (1975-76). A re-examination of the Zoetlief-Ventersdorp relationship at the T'Kuip Hills, Britstown district. *Annals Geol. Surv. S. Afr.*, **11**: 99-117.
- Grobler N.J., Kleynhans E.P.J., Botha P.J. & de Bruijn H. (1982). Distinction between lavas of the Allanridge Andesite and Rietgat Formations in the northern Cape and western Transvaal. *Trans. Geol. Soc. S. Afr.*, **85**: 117-126.
- Grobler N.J., De Bruijn H., Van der Westhuizen W.A. & Schoch A.E. (1986). Komatiitic affinities at the bottom and top of the Late Archaean - Early Proterozoic intracratonic Ventersdorp volcanic pile. *Abstr. Geocongress '86, Geol. Soc. S. Afr.*, Johannesburg, 129-132.
- Grobler N.J., van der Westhuizen W.A. & Tordiffe E.A.W. (1989). The Sodium Group, South Africa: Reference section for Late Archaean cratonic cover sequences. *Austr. J. Earth Sci.*, **36**: 41-64.
- Harding R.R., Crockett R.N. & Snelling N.J. (1974). The Gaberone Granite, Kanye Volcanics and the Ventersdorp Plantation Porphyry, Botswana: geochronology and review. *Report Inst. Geol. Sci.*, **74/75**, 26pp.
- Hart S.R. (1969). K, Rb, Cs contents and K/Rb, K/Cs ratios of fresh and altered submarine basalts. *Earth Planet. Sci. Lett.*, **6**: 295-303.
- Hart S.R., Erlank A.J. & Kable E.J.D. (1974). Sea-floor basalt alteration: some chemical and Sr isotope effects. *Contrib. Mineral. Petrol.*, **44**: 219-230.
- Hartnady C.J.H. & Stowe C.W. (1991). The Archaean-Proterozoic transition in Southern Africa: A review of the Randian Erathem with reference to the accretionary tectonic evolution of the Kaapvaal and Zimbabwe Provinces. *Chamber of Mines Prec. Res. Unit, Univ. of Cape Town, Inf. Circ.* **2**, 18pp.
- Hatch F.H. (1898). A geological survey of the Witwatersrand and other Districts in the Southern Transvaal. *Quart. Journ. Geol. Soc. London*, **54**: 73-100. **Cited in:** Hatch F.H. & Corstorphine G.S. (1905). *THE GEOLOGY OF SOUTH AFRICA*. MacMillan & Co., London, 348pp.
- Hatch F.H. (1903). The Boulder Beds of Ventersdorp, Transvaal. *Trans. Geol. Soc. S. Afr.*, **6**: 95-97.
- Hatch F.H. & Corstorphine G.S. (1905). *THE GEOLOGY OF SOUTH AFRICA*. MacMillan & Co., London, 348pp.
- Haughton S.H. (1969). *GEOLOGICAL HISTORY OF SOUTHERN AFRICA*. Geol. Soc. S. Afr., Johannesburg, 535pp.

- Hausback B.P. (1987). An extensive, hot, vapor-charged rhyodacite flow, Baja California, Mexico. *In*: Fink J.H. (Ed.). The emplacement of silic domes and lava flows. *Geol. Soc. Am. Spec. Paper*, **212**: 119-145.
- Henry C.D., Price J.G., Rubin J.N., Parker D.F., Wolff J.A., Self S., Franklin R. & Barker D.S. (1988). Widespread, lavalike silicic volcanic rocks of Trans-Pecos Texas. *Geology*, **16**: 509-512.
- Henry C.D., Price J.G., Parker D.F. & Wolff J.A. (1989). Mid-Tertiary silicic alkalic magmatism of Trans-Pecos Texas: Rheomorphic tuffs and extensive silicic lavas. Excursion 9A, IAVCEI, *New Mexico Bureau of Mines and Mineral Resources, Mem.* **46**: 231-274.
- Holmes G.G. (1907). The geology of the south-western Transvaal. *Trans. Geol. S. Afr.*, **9**: 90-96.
- Hoover D.L. (1964). Flow structures in a welded tuff, Nye County, Nevada. *Geol. Soc. Am. Spec. Paper*, **76**, 83pp. **Cited in**: Bristow J.W. (1989). Retracing Vulcan's fiery footsteps. *Nuclear Active*, **41**: 30-37.
- Horwood C.B. (1911). Notes and analyses of typical Transvaal rocks. *Trans. Geol. Soc. S. Afr.*, **13**: 29-55.
- Hunter D.R. & Pretorius D.A. (1981). Chapter 8: Structural framework, p397-442. *In*: Hunter D.R. (Ed). *PRECAMBRIAN OF THE SOUTHERN HEMISPHERE*. Elsevier, Amsterdam, 882pp.
- Huppert H.E. & Sparks R.S.J. (1988). The generation of granitic magmas by intrusion of basalt into continental crust. *J. Petrol.*, **29**: 599-624.
- Irvine T.N. & Baragar W.R.A. (1971). A guide to the chemical classification of the common volcanic rocks. *Can. J. Earth. Sci.*, **8**: 523-548.
- Jacobsen W. (1940). Vulkanologische und tektonische Beobachtungen an der jungalgonkischen Ventersdorp-formation Südafrikas. *Geol. Rdsch.*, **31**: 255-284. **Cited in**: Winter H. de la R. (1965). *THE STRATIGRAPHY OF THE VENTERSDORP SYSTEM IN THE BOTHAVILLE DISTRICT AND ADJOINING AREAS*. PhD Thesis (unpubl.), Univ. Witwatersrand, Johannesburg, 131pp.
- Jacobsen W. (1943). Ausbildung und Petrographie der südafrikanischen Ventersdorp-Formation im südwestlichen Transvaal und nördlichen Oranje-Freistaat. *Neues Jb. Miner. Geol. Paläont. Abt. A., Abh.*: Bd. **78**: 217-282.
- Jensen L.S. (1976). A new cation plot for classifying volcanic rocks. *Ontario Div. of Mines, Ministry Nat. Res. Misc. Paper* **66**, 22pp.
- Johnson C.M. & Lipman P.W. (1988). Origin of metaluminous and alkaline volcanic rocks of the Latir volcanic field, northern Rio Grande rift, New Mexico. *Contrib. Mineral. Petrol.*, **100**: 107-128.

- Joubert C.W. (1973). *DIE GEOLOGIE VAN 'N GEBIED TUSSEN BOSHOF EN BARKLY-WES*. MSc Thesis (unpubl.), Univ. Orange Free State, Bloemfontein, 123pp.
- Jowett E.C. & Jarvis G.T. (1984). Formation of foreland rifts. *Sed. Geol.*, **40**: 51-72.
- Karpeta W.P. (1990). Eruptive style in an early Proterozoic tholeiite sequence - the Platberg Group in the Hartbeesfontein Basin, Republic of South Africa. *Abstr. Geocongress '90, Geol. Soc. S. Afr.*, Durban, 281-284.
- Kirkpatrick R.J. (1974). The kinetics of crystal growth in the system $\text{CaMgSi}_2\text{O}_6$ - $\text{CaAl}_2\text{SiO}_6$. *Am. J. Sci.*, **273**: 215-242.
- Kirkpatrick R.J. (1975). Crystal growth from the melt: A review. *Am. Mineral.*, **60**: 798-814.
- Kleynhans E.P.J. (1979). *THE GEOLOGY OF AN AREA AROUND WARRENTON, NORTHERN CAPE, WITH SPECIAL REFERENCE TO THE VOLCANOLOGY AND GEOCHEMISTRY OF THE VENTERSDORP SUPERGROUP*. MSc Thesis (unpubl.), Univ. Orange Free State, Bloemfontein, 214 pp.
- Knoper M.W. (1992). Modulus: A spreadsheet for modeling the petrogenesis of igneous rocks. (In prep.).
- Kranidiotis P. & MacLean W.H. (1987). Systematics of chlorite alteration at the Phelps Dodge massive sulfide deposit, Matagami, Quebec. *Econ. Geol.*, **82**: 1898-1911.
- Kuniyoshi S. & Liou J.G. (1976). Burial metamorphism of the Karmutsen volcanic rocks, northeastern Vancouver Island, British Columbia. *Am. J. Sci.*, **276**: 1096-1119.
- Kynaston H. (1911). The geology of a portion of the Rustenburg district lying north of the Pilanesberg. *Ann. Rep. Geol. Surv. S. Afr. (for 1912)*, 63-73.
- Le Bas M.J., Le Maitre R.W., Streckeisen A. & Zanettin B. (1986). A chemical classification of volcanic rocks based on the total alkali-silica diagram. *J. Petrol.*, **27**: 745-750.
- Le Maitre R.W. (Ed.) (1989). *A CLASSIFICATION OF IGNEOUS ROCKS AND GLOSSARY OF TERMS*. Blackwell, London, 193pp.
- Lemmer W.M. (1977). *DIE GEOLOGIE IN DIE OMGEWING VAN BRITSTOWN*. MSc Thesis (unpubl.), Univ. Orange Free State, Bloemfontein, 157pp.
- Liebenberg J. (1977). *DIE GEOLOGIE VAN DIE GEBIED 2724D (ANDALUSIA)*. MSc Thesis (unpubl.), Univ. Orange Free State, Bloemfontein, 232pp.
- Linton P.L., McCarthy T.S. & Myers R.E. (1990). A geochemical reappraisal of the stratigraphy of the Klipriviersberg Group in the type borehole LL1 in the Bothaville area. *S. Afr. J. Geol.*, **93**: 239-244.

- Lipman P.W. (1975). *EVOLUTION OF THE PLATORO CALDERA COMPLEX AND RELATED VOLCANIC ROCKS, SOUTHEASTERN SAN JUAN MOUNTAINS, COLORADO*. U.S. Geol. Surv. Prof. Paper **852**, 128pp.
- Lock B.E. (1977). Discussion: 'Precambrian ignimbrites and associated volcanoclastics from the Herbert District, northern Cape Province'. *Trans. Geol. Soc. S. Afr.*, **80**: 47-48.
- Lofgren G. (1971a). Experimentally produced devitrification textures in natural rhyolitic glass. *Geol. Soc. Am. Bull.*, **82**: 111-124.
- Lofgren G. (1971b). Spherulitic textures in glassy and crystalline rocks. *J. Geophys. Res.*, **76**: 5635-5648.
- Lofgren G. (1974). An experimental study of plagioclase morphology. *Am. J. Sci.*, **273**: 243-273.
- Lofgren G. (1980). Experimental studies on the dynamic crystallization of silicate melts. *Physics of magmatic processes*, Princeton University Press.
- MacKenzie W.S., Donaldson C.H. & Guilford C. (1982). *ATLAS OF IGNEOUS ROCKS AND THEIR TEXTURES*. Longman Group Ltd., Essex, 148pp.
- Maniar P.D. & Piccoli P.M. (1989). Tectonic discrimination of granitoids. *Geol. Soc. Am. Bull.*, **101**: 635-643.
- Marshall T.R. (1986). Morphotectonic analysis of the Wesselsbron panveld. *Econ. Geol. Res. Unit*, Univ. Witwatersrand, Johannesburg, Inform. Circ. **190**, 13pp.
- Matthysen J.L. (1953). 'N NUWE STRATIGRAFIESE INDELING VAN DIE VENTERSDORP-SISTEEM. MSc Thesis (unpubl.), Univ. Pretoria, Pretoria.
Cited in: Bowen T.B. (1984). *THE GEOCHEMICAL STRATIGRAPHY OF THE VOLCANIC ROCKS OF THE WITWATERSRAND TRIAD IN THE KLERKSDORP AREA, TRANSVAAL*. MSc Thesis (unpubl.), Rhodes Univ., Grahamstown, 223pp.
- McCarthy T.S., McCallum K., Myers R.E. & Linton P. (1990). Stress states along the northern margin of the Witwatersrand Basin during Klipriviersberg Group volcanism. *S. Afr. J. Geol.*, **93**: 245-269.
- McIver J.R., Cawthorn R.G. & Wyatt B.A. (1982). The Ventersdorp Supergroup - the youngest komatiitic sequence in South Africa. **In:** Arndt N.T. & Nisbet E.G. (Eds). *KOMATIITES*. George Allen & Unwin, London, 526pp.
- Meintjes P.G. (1988). *THE EVOLUTION OF VOLCANIC-SEDIMENTARY BASINS OF THE VENTERSDORP SUPERGROUP NEAR WELKOM*. MSc Thesis (unpubl.), Univ. Orange Free State, Bloemfontein, 211pp.

- Meschede M. (1986). A method of discriminating between different types of mid-ocean ridge basalts and continental toleites with the Nb-Zr-Y diagram. *Chem. Geol.*, **56**: 207-218.
- Milner S.C. (1986). The geological and volcanological features of the quartz latites of the Etendeka Formation. *Communs. Geol. Surv. SWA/Namibia*, **2**: 109-116.
Cited in: Bristow J.W. (1989). Retracing Vulcan's fiery footsteps. *Nuclear Active*, **41**: 30-37.
- Miyashiro A. (1974). Volcanic rock series in island arcs and active continental margins. *Am. J. Sci.*, **274**: 321-355.
- Monkman L.J. (1961). *THE GEOLOGY OF THE MOASE-MALIBANGWE RIVER BASINS WITH SPECIAL REFERENCE TO THE STORMBERG VULCANICITY OF SOUTHERN RHODESIA*. PhD Thesis (unpubl.), University of Leeds. **Cited in:** Bristow J.W. (1989). Retracing Vulcan's fiery footsteps. *Nuclear Active*, **41**: 30-37.
- Myers J.M., Myers R.E. & McCarthy T.S. (1988). Geology and geochemistry of the Makwassie Formation, Ventersdorp Supergroup, in the Klerksdorp area. *Abstr. Geocongress '88, Geol. Soc. S. Afr.*, Durban, 449-452.
- Myers J.M. (1990). *THE STRATIGRAPHY AND GEOCHEMISTRY OF THE KLIPRIVERSBERG AND PLATBERG GROUPS OF THE VENTERSDORP SUPERGROUP IN THE KLERKSDORP AREA, WESTERN TRANSVAAL*. MSc Thesis (unpubl.), Univ. Witwatersrand, Johannesburg, 294pp.
- Myers J.M., McCarthy T.S. & Stanistreet I.G. (1990). Platberg-age structures, sedimentation and volcanism in the Buffelsdoorn Graben, northeast of Klerksdorp. *S. Afr. J. Geol.*, **93**: 261-271.
- Myers R.E., McCarthy T.S., Bunyard M., Cawthorn R.G., Falatsa T.M., Hewitt T., Linton P., Myers J.M., Palmer K.J. & Spencer R. (1990). Geochemical stratigraphy of the Klipriviersberg Group volcanic rocks. *S. Afr. J. Geol.*, **93**: 224-238.
- Nel L.T. (1935). *THE GEOLOGY OF THE KLERKSDORP-VENTERSDORP AREA: AN EXPLANATION OF THE GEOLOGICAL MAP*. Geol. Surv. S. Afr., 159pp.
- Nel L.T. & Jansen H. (1957). *THE GEOLOGY OF THE COUNTRY AROUND VEREENIGING: AN EXPLANATION OF SHEET 62 (VEREENIGING)*. Geol. Surv. S. Afr., 90pp.
- Nel L.T. & Verster W.C. (1962). *DIE GEOLOGIE VAN DIE GEBIED TUSSEN BOTHAVILLE EN VREDEFORT: TOELIGTING VAN BLAAIE 2726B (BOTHAVILLE) EN 2727A (VREDEFORT)*. Geol. Surv. S. Afr., 50pp.
- Nelson D.R., Trendall A.F. & de Laeter J.R. (1990). *CORRELATION OF THE FORTESCUE GROUP*. Report 61, Minerals and Energy Research Institute of Western Australia (MERIWA), Perth, Australia, 71-103.

- Nelson D.R., Trendall A.F., de Laeter J.R., Grobler N.J. & Fletcher I.R. (1992). Isotope systematics and metamorphism of late Archaean supracrustal sequences from the Pilbara and Kaapvaal Cratons. *Precamb. Res.*, **54**: 231-256.
- Neumann E.-R. & Ramberg I.B. (1978). Paleorifts - Concluding remarks. **In:** Ramberg I.B. & Neumann E.-R. (Eds). (1978). *TECTONICS AND GEOPHYSICS OF CONTINENTAL RIFTS*. Reidel Publ. Co., Dordrecht, Holland, 409-424.
- Nisbet E.G. (1982). The tectonic setting and petrogenesis of komatiites. **In:** Arndt N.T. & Nisbet E.G. (Eds). *KOMATIITES*. George Allen & Unwin, London, 526pp.
- Noble D.C., Anderson R.E., Ekren E.B. & Connor J.T. (1964). Thirsty Canyon Tuff of Nye and Esmeralda Counties, Nevada. *U.S. Geol. Surv. Prof. Paper* **475-D**: 24-27.
- Noble D.C. (1968). Laminar viscous flowage structures in ash-flow tuffs from Gran Canaria, Canary Islands: A discussion. *J. Geol.*, **76**: 721-723.
- Norrish K. & Hutton J.T. (1969). An accurate X-ray spectrographic method for the analysis of a wide range of geological samples. *Geochim. et Cosmochim. Acta*, **33**: 431-453.
- O'Hara M.J. & Mathews R.E. (1981). Geochemical evolution in an advancing, periodically replenished, periodically tapped, continuously fractionated magma chamber. *J. Geol. Soc. London*, **138**: 237-277.
- Palmer K.J., Spencer R.M., Hewitt T. & McCarthy T.S. (1986). Geochemistry of the Klipriviersberg lavas as a stratigraphic guide in the Witwatersrand Basin. *Abstr. Geocongress '86, Geol. Soc. S. Afr.*, Johannesburg, 171-174.
- Pearce J.A. & Cann J.R. (1973). Tectonic setting of basic volcanic rocks determined using trace element analyses. *Earth Planet. Sci. Letters*, **19**: 290-300.
- Pearce J.A., Harris N.B.W. & Tindle A.G. (1984). Trace element discrimination diagrams for the tectonic interpretation of granitic rocks. *J. Petr.*, **25**: 956-983.
- Pearce T.H., Gorman B.E. & Birkett T.C. (1977). The relationship between major element chemistry and tectonic environment of basic and intermediate volcanic rocks. *Earth Planet. Sci. Letters*, **36**: 121-132.
- Pienaar P.J. (1956). *STRATIGRAPHY AND PETROGRAPHY OF THE VENTERSDORP SYSTEM IN THE ORANGE FREE STATE GOLDFIELD, SOUTH AFRICA*. MSc Thesis (unpubl.), Queen's Univ., Kingston, Ontario, 190pp. **Cited in:** Bowen T.B. (1984). *THE GEOCHEMICAL STRATIGRAPHY OF THE VOLCANIC ROCKS OF THE WITWATERSRAND TRIAD IN THE KLERKSDORP AREA, TRANSVAAL*. MSc Thesis (unpubl.), Rhodes Univ., Grahamstown, 223pp.

- Pirajno F. (1988). A preliminary assessment of the geology and mineralisation of the Erongo volcanic complex, Namibia. *Abstr. Geocongress '88, Geol. Soc. S. Afr.*, Durban, 461-464.
- Poldervaart A. & Gilkey A.K. (1954). On clouded plagioclase. *Am. Mineral.*, **39**: 75-91.
- Potgieter C. de W. (1973). *DIE GEOLOGIE VAN 'N GEBIED SUID VAN DOUGLAS, NOORD-KAAPLAND*. MSc Thesis (unpubl.), Univ. Orange Free State, Bloemfontein, 235pp.
- Potgieter G.J.A. (1974). *THE GEOLOGY OF AN AREA SOUTH OF KIMBERLEY*. MSc Thesis (unpubl.), Univ. Orange Free State, Bloemfontein, 91pp.
- Potgieter G.J.A. & Visser J.N.J. (1976). Precambrian ignimbrites and associated volcanoclastics from the Herbert District, northern Cape Province. *Trans. Geol. Soc. S. Afr.*, **79**: 27-30.
- Potgieter G.J.A. & Lock B.E. (1978). Correlation and lithology of the Ritchie Quartz Porphyry Formation along the Riet River, near Kimberley. *Trans. Geol. Soc. S. Afr.*, **81**: 41-46.
- Preston V.A. (1987a). Pyroclastics of the Nsuzze Group, Mpongoza Inlier, northern Natal. *Workshop on pyroclastic volcanism and associated deposits: Abstr.*, Pietermaritzburg, 16-19.
- Preston V.A. (1987b). *THE GEOLOGY AND GEOCHEMISTRY OF THE MPONGOZA INLIER, NORTHERN NATAL*. MSc Thesis (unpubl.), Univ. Natal, Pietermaritzburg, 282pp. **Cited in:** Bristow J.W. (1989). Retracing Vulcan's fiery footsteps. *Nuclear Active*, **41**: 30-37.
- Ramberg I.B. & Morgan P.A. (1984). Physical characteristics and evolutionary trends of continental rifts. **In:** *Tectonics, Proceedings of the 27th International Geological Congress 7*. Vnuscience, Utrecht, 165-216.
- Rickwood P.C. (1989). Boundary lines within petrologic diagrams which use oxides of major and minor elements. *Lithos*, **22**: 247-263.
- Rittman A. (1962). *VOLCANOES AND THEIR ACTIVITY*. Interscience, New York, 305pp. **Cited in:** Bristow J.W. (1989). Retracing Vulcan's fiery footsteps. *Nuclear Active*, **41**: 30-37.
- Robb L.J., Davis D.W. & Kamo S.L. (1991). Chronological framework for the Witwatersrand Basin and environs: towards a time-constrained depositional model. *S. Afr. J. Geol.*, **94**: 86-95.
- Robb L.J. (1992). A review of recent age determinations pertinent to the Witwatersrand triad. Abstracts: A short course reviewing recent developments in the understanding of the Witwatersrand Basin. *Econ. Geol. Res. Unit*, Univ. Witwatersrand, Johannesburg, 40-47.

- Roering C., Barton J.M. (Jr) & Winter H. de la R. (1990). The Vredefort structure: A perspective with regard to the new tectonic data from adjoining terranes. *Tectonophysics*, **171**: 7-22.
- Rogers A.W. & Du Toit A.L. (1909). *AN INTRODUCTION TO THE GEOLOGY OF THE CAPE COLONY: With a chapter on the fossil reptiles of the Karoo Formation by R. Broom*. 2nd Ed. Longmans, Green & Co., London, 491pp.
- Ross C.S. & Smith R.L. (1961). Ash-flow tuffs: Their origin, geologic relations and identification. *U.S. Geol. Surv. Prof. Paper* **366**, 159pp.
- Rutten M.G. & Van Everdingen R.O. (1961). Rheo-ignimbrites of the Rammes volcano. *Geol. Mijnbou*, **40**: 49-57.
- SACS (South African Committee for Stratigraphy), 1980. *STRATIGRAPHY OF SOUTH AFRICA. PART 1*. (Comp. L.E. Kent). Lithostratigraphy of the Republic of South Africa, South West Africa/Namibia, and the Republics of Boputhatswana, Transkei and Venda. *Handb. Geol. Surv. S. Afr.*, **8**.
- Saggerson E.P. & Bristow J.W. (1983). The geology and structural relationships of the southern Lebombo volcanic and intrusive rocks, South Africa. *Bull. Volcanol.*, **46**: 161-181.
- Schmincke H.-U. & Swanson D.A. (1967). Laminar viscous flowage structures in ash-flow tuffs from Gran Canaria, Canary Island. *J. Geol.*, **7**: 641-664.
- Schmincke H.-U. (1990). Geological field guide, Gran Canaria, 4th Ed. *Field Trip 7B1, IAVCEI Intern. Volcanol. Congress, Mainz, FRG.*, 212pp.
- Schutte I.C., Seeger K.G. & Wilke D.P. (1960). Die geologie van 'n gedeelte van die gebied 2426 (skaal 1:250 000) langs die Krokodilrivier, ten weste van Thabazimbi. *Unpubl. Rep. Geol. Surv. S. Afr.*, 7-25. **Cited in:** Tyler N. (1979b). The stratigraphy of the Early-Proterozoic Buffalo Springs Group in the Thabazimbi area, West-Central Transvaal. *Trans. Geol. Soc. S. Afr.*, **82**: 215-226.
- Schweitzer J. & Kröner A. (1985). Geochemistry and petrogenesis of early Proterozoic intracratonic volcanic rocks of the Ventersdorp Supergroup, South Africa. *Chem. Geol.*, **51**: 265-288.
- Self S. & Wright J.V. (1983). Large wave-forms from the Fish Canyon Tuff, Colorado. *Geology*, **11**: 443-446.
- Shand S.J. (1951). *THE STUDY OF ROCKS*. Thomas Murby and Co., London, 236pp.
- Shervais J.W. (1982). Ti-V plots and the petrogenesis of modern and ophiolitic lavas. *Earth Planet. Sci. Letters*, **59**: 101-118.

- Simpson A.B. (1964). A bibliography of the geology of the Ventersdorp System and other Pre-Bushveld extrusives and associated sediments. *Econ. Geol. Res. Unit*, Univ. Witwatersrand, Johannesburg, Inform. Circ. **18**, 66pp.
- Smith J.V. (1974). *FELDSPAR MINERALS: 2 - CHEMICAL AND TEXTURAL PROPERTIES*. Springer-Verlag, Berlin, 690pp.
- Sparks R.S.J., Self S. & Walker G.P.L. (1973). Products of ignimbrite eruptions. *Geology*, **1**: 115-118.
- Sparks R.S.J. (1976). Grain size variations in ignimbrites and implications for the transport of pyroclastic flows. *Sedimentology*, **23**: 147-188.
- Stanistreet I.G. & McCarthy T.S. (1990). Middle Ventersdorp graben development north of the Carletonville Goldfield and its relevance to the evolution of the Witwatersrand Basin. *S. Afr. J. Geol.*, **93**: 272-288.
- Stanistreet I.G. & McCarthy T.S. (1991). Changing tectono-sedimentary scenarios relevant to the development of the Late Archaean Witwatersrand Basin. *J. Afr. Earth Sciences*, **13**: 65-81.
- Tankard A.J., Jackson M.P.A., Eriksson K.A., Hobday D.K., Hunter D.R. & Minter W.E.L. (1982). *CRUSTAL EVOLUTION OF SOUTHERN AFRICA*. Springer-Verlag, New York, 523pp.
- Taylor S.R. & McLennan S.M. (1985). *THE CONTINENTAL CRUST: ITS COMPOSITION AND EVOLUTION*. Blackwell, Oxford, 312pp.
- Thurston P.C., Ayres L.D., Edwards G.R., G  linas L., Ludden J.N. & Verpa  lst P. (1985). Archean bimodal volcanism. In: Ayres L.D., Thurston P.C., Card K.D. & Weber W. (Eds). (1985). Evolution of Archean supracrustal sequences. *Geol. Assoc. Canada Spec. Paper*, **28**: 9-21.
- Truter F.C. & Strauss C.A. (1942). The Pre-Transvaal rocks at Taungs, Cape Province. *Trans. Geol. Soc. S. Afr.*, **44**: 161-166.
- Truter F.C. (1949). A review of volcanism in the geological history of South Africa. *Proc. Geol. Soc. S. Afr.*, **52**. Cited in: Tyler N. (1979b). The stratigraphy of the Early-Proterozoic Buffalo Springs Group in the Thabazimbi area, West-Central Transvaal. *Trans. Geol. Soc. S. Afr.*, **82**: 215-226.
- Twist D. & French B.M. (1983). Voluminous acid volcanism in the Bushveld Complex: A review of the Rooiberg Felsite. *Bull. Volcanol.*, **46**: 225-242.
- Twist D. (1985/86). Viscosity characteristics and mode of emplacement of the Rooiberg Felsite. *Annual Report 1985/86, Institute for Geological Research on the Bushveld Complex*, Univ. Pretoria, Pretoria.

- Twist D., Bristow J.W. & van der Westhuizen W.A. (1989). High-temperature ash-flows tuffs: A review of occurrences in southern Africa. *Abstr. IAVCEI, Bull. 131*. New Mexico Bureau of Mines & Mineral Resources, p273.
- Tyler N. (1978). *A STRATIGRAPHIC ANALYSIS OF THE PRE-CHUNIESPOORT-GROUP STRATA AROUND THE MAKOPPA DOME, WEST-CENTRAL TRANSVAAL*. PhD Thesis (unpubl.), Univ. Witwatersrand, Johannesburg, 206pp.
- Tyler N. (1979a). Stratigraphy, geochemistry and correlation of the Ventersdorp Supergroup in the Derdepoort area, West-Central Transvaal. *Trans. Geol. Soc. S. Afr.*, **82**: 133-147.
- Tyler N. (1979b). The stratigraphy of the Early-Proterozoic Buffalo Springs Group in the Thabazimbi area, West-Central Transvaal. *Trans. Geol. Soc. S. Afr.*, **82**: 215-226.
- Van der Westhuizen W.A. & Grobler N.J. (1987). Ignimbrites from the Sodium Group in the Britstown area. *Workshop on pyroclastic volcanism and associated deposits: Abstr.*, Pietermaritzburg, p24.
- Van der Westhuizen W.A., Grobler N.J., Bristow J.W. & Tordiffe E.A.W. (1988). High temperature ash-flows in the Ventersdorp Supergroup. *Abstr. Geocongress '88, Geol. Soc. S. Afr.*, Durban, 661-662.
- Van der Westhuizen W.A., Grobler N.J., Looock J.C. & Tordiffe E.A.W. (1989). Raindrop imprints in the Late Archaean - Early Proterozoic Ventersdorp Supergroup, South Africa. *Sed. Geol.*, **61**: 303-309.
- Van der Westhuizen W. A., De Bruijn H. & Meintjes P.G. (1991). The Ventersdorp Supergroup: an overview. *J. Afr. Earth Sci.*, **13**: 83-105.
- Van der Westhuizen W.A., De Bruijn H., Grobler N.J., Bristow J.W. & Bleeker N.J. (in prep.). Komatiitic basalt in the Allanridge Formation of the Ventersdorp Supergroup, southwest of Warrenton, South Africa.
- Van Eeden O.R. (1946). Die korrelasie van sekere Voor-Transvaal-Gesteentes in die distrik Schweizer Reneke. *Trans. Geol. Soc. S. Afr.* (for 1946), **49**: 277-290
- Van Eeden O.R., De Wet N. P. & Strauss C.A. (1963). The geology of an area around Schweizer-Reneke. *An explanation of sheets 2724B (Pudimoe) and 2725A (Schweizer-Reneke)*. Geol. Surv. S. Afr.
- Van Niekerk C.B. & Burger A.J. (1964). The age of the Ventersdorp System. *Ann. Geol. Surv. S. Afr.*, **3**: 75-86.
- Van Niekerk C.B. & Burger A.J. (1978). A new age for the Ventersdorp acidic lavas. *Trans. Geol. Soc. S. Afr.*, **81**: 155-163.

- Viereck L.G., Griffin B.J., Schmincke H.-U. & Pritchard R.G. (1982). Volcaniclastic rocks of the Reydarfjörður Drill Hole, eastern Iceland: 2 - Alteration. *J. Geophys. Res.*, **87**: 6459-6476.
- Visser J.N.J., Grobler N.J., Joubert C.W., Potgieter C.D., Potgieter G.J.A., McLaren C.H. & Liebenberg J. (1975-76). The Ventersdorp group between Taung and Britstown, Northern Cape Province. *Ann. Geol. Surv. S. Afr.*, **11**: 15-28.
- Von Backström J.W. (1962). Die geologie van die gebied om Ottosdal, Transvaal. Bladbeskrywing 2526D (Barberspan); 2626C (Ottosdal). *S. Afr. Geol. Surv.*
- Walker G.A. & Swanson D.A. (1968). Laminar flowage in a Pliocene soda rhyolite ash-flow tuff, Lake and Harney Counties, Oregon. *U.S. Geol. Surv. Prof. Paper 600-B*: B37-B47. **Cited in**: Bristow J.W. (1989). Retracing Vulcan's fiery footsteps. *Nuclear Active*, **41**: 30-37.
- Walker G.P.L. (1989). Gravitational (density) controls on volcanism, magma chambers and intrusions. *Austr. J. Earth Sci.*, **36**: 149-165.
- Walraven F., Armstrong R.A. & Kruger F.J. (1990). A chronostratigraphic framework for the north-central Kaapvaal Craton, the Bushveld Complex and Vredefort structure. *Tectonophysics*, **171**: 23-48.
- Watters B.R. (1974). Stratigraphy, igneous petrology and evolution of the Sinclair Group in southern South West Africa. *Chambers of Mines Prec. Res. Unit*, Univ. Cape Town, Bulletin **16**, 220pp. **Cited in**: Bristow J.W. (1989). Retracing Vulcan's fiery footsteps. *Nuclear Active*, **41**: 30-37.
- Wernicke B. (1985). Uniform-sense normal simple shear of the continental lithosphere. *Can. J. Earth Sci.*, **22**: 108-125.
- Whiteside H.C.M. (1970). Volcanic rocks of the Witwatersrand Triad, 73-87. **In**: Clifford T.N. & Gass I.G., Eds., *AFRICAN MAGMATISM AND TECTONICS*. Oliver & Boyd, Edinburgh, 461pp.
- Wilkinson J.F.G. (1986). Classification and average compositions of common basalts and andesites. *J. Petrol.*, **27**: 31-62.
- Williams A.F. (1932). *THE GENESIS OF THE DIAMOND, Vol. I*. Ernest Benn Limited, London, 352pp.
- Wilson C.J.N. (1980). The role of fluidisation in the emplacement of pyroclastic flows: An experimental approach. *J. Volcanol. Geotherm. Res.*, **8**: 231-249.
- Wilson M. (1989). *IGNEOUS PETROGENESIS*. Unwin Hyman, London, 466pp.
- Winchester J.A. & Floyd P.A. (1977). Geochemical discrimination of different magma series and their differentiation products using immobile elements. *Chem. Geol.*, **20**: 325-343.

- Winter F. (1995). *THE STRATIGRAPHY AND GEOCHEMISTRY OF THE ALBERTON FORMATION, VENTERSDORP SUPERGROUP, SOUTH-WEST OF KLERKSDORP*. Vol. 1. Msc Thesis (unpubl.), Univ. of the Orange Free State, Bloemfontein, 267pp.
- Winter H. de la R. (1965). *THE STRATIGRAPHY OF THE VENTERSDORP SYSTEM IN THE BOTHAVILLE DISTRICT AND ADJOINING AREAS*. PhD Thesis (unpubl.), Univ. Witwatersrand, Johannesburg, 131pp.
- Winter H. de la R. (1976). A lithostratigraphic classification of the Ventersdorp Succession. *Trans. Geol. Soc. S. Afr.*, **79**: 31-48.
- Winter H. de la R. (1986). Cratonic foreland model for the Witwatersrand Basin development in a continental back-arc plate tectonic setting. *Abstr. Gecongress '86, Geol. Soc. S. Afr.*, Johannesburg, 75-80.
- Wolmarans L.G. (1988). The Bumbeni Complex: A post-Karoo ash-flow tuff cauldron in the southern Lebombo Mountains. *Abstr. Gecongress '88, Geol. Soc. S. Afr.*, Durban, 745-748.
- Wyatt B.A. (1976). *THE GEOLOGY AND GEOCHEMISTRY OF THE KLIPRIVERSBERG VOLCANICS, VENTERSDORP SUPERGROUP, SOUTH OF JOHANNESBURG*. MSc Thesis (unpubl.), Univ. Witwatersrand, Johannesburg, 178pp.
- Wyley A. (1859). Notes on a journey in two directions across the Colony, made in the years 1857-8, with a view to determine the character and order of the various geological formations. *Appendix to C.G.H. Parl. Rep. G. '57-'59*.

APPENDIX A

BOREHOLES LOGGED DURING THIS STUDY

Anglo American Prospecting Services (Pty) Ltd made borehole core available for logging and sampling for the purposes of this study. Not all these boreholes penetrated the base of the Goedgenoeg/Makwassie Formation and the core of others was incomplete or in disorder. Borehole ST2 was made available by African Selection Trust. However, only short sections, at about 10 metre intervals, of this borehole's core were preserved so that only an estimated log could be construed.

The boreholes were logged on a scale of 1:200. Simplified logs were drafted from these on a scale of 1:2 500, as reproduced in this appendix.

The following legend is valid for the borehole logs:

-  - Quartz-feldspar porphyry
-  - Feldspar porphyry
-  - Igneous inclusions (mostly mafic lava inclusions)
-  - Quartz-feldspar porphyry inclusions
-  - Flow banding
-  - Non-porphyritic lava (mafic lava)
-  - Dolerite
-  - Regoliths (now silicified)
-  - Clastic sedimentary rock
-  - Fine-grained, dolomitic rock
-  - Shale and mudstone
-  - Fine-grained sedimentary rock (also tuff)
-  - Archaean Basement (mostly metagranite)

The abbreviations for the rock types are:

- Q** - Quartz-feldspar porphyry
- FQ** - Feldspar porphyry with rare quartz phenocrysts
- F** - Feldspar porphyry
- MF** - Mafic lava with only scattered feldspar phenocrysts
- M** - Mafic, non-porphyritic lava
- S** - Sedimentary rock (also tuffaceous sedimentary rocks)
- T** - Tuff
- I** - Intrusive rock
- G** - Basement Igneous Complex (mostly granitic)

DEPTHS are in metres, measured from the borehole collar downwards. Estimated depths are indicated by a \pm sign and uncertain depths by a question mark.

BOREHOLE CO-ORDINATES are given in the LO-27 grid system (metre-incremented grid with 27° longitude as Y-axis baseline and the equator as X-axis baseline). Therefore, positive signs indicate metres south from the equator for the X direction and metres west from the 27° longitude for the Y direction. Z co-ordinates are the collar elevation in metres above average mean sea level.

The **LITHOLOGICAL** descriptions begin with a non-genetic rock name given during logging of the core, followed by a short lithological description. The descriptions are concluded with the interpreted genetic rock name in brackets, given after petrographic and geochemical interpretation of the specific intersection.



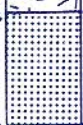

The term "flow units" is used as a non-genetic term to enable description of recognized sub-units in the volcanic facies. Compared to the typical porphyritic Makwassie rocks, flow units with only rare and scattered feldspar phenocrysts are regarded as non-porphyritic and were named as such during logging to enable distinction from the highly feldspar-phyric rocks typical of the Goedgenoeg Formation.

Feldspar-phyric rocks with only rare quartz phenocrysts are named feldspar porphyries to enable distinction from the proper quartz-feldspar porphyries typical of the Makwassie Formation.

Fine-grained and clastic units that separate flow units are indubitably recognized as pyroclastic rocks, but distinction between different types of pyroclastic rocks (pyroclastic-fall or pyroclastic-surge deposits) and their products, *i.e.* pyroclastic breccia, lapilli tuff, lithic tuff, crystal tuff, coarse-grained and fine-grained tuff, is not always possible due to various reasons, such as the limited diameter of borehole core. Some of these rocks may also represent water-reworked volcanics and therefore *sensu stricto* are sedimentary rocks.

The borehole code names (*i.e.* BES1) are given, as well as the farm name on which it was drilled.

BES1 - Estsamfra 78

Formation	Depth	Scale 1:2500	Rock Type
Rietgat	625		M
Makwassie	884		Q
GF	920		M
Makwassie	953		Q

BOREHOLE CO-ORDINATES

X - +3023250
Y - +40750
Z - 1300

ABBREVIATED BOREHOLE LOG

0 - 96 Karoo Sequence
96 - 404 Allanridge Formation
404 - 508 Bothaville Formation
508 - 625 Rietgat Formation
625 - 920 Makwassie Formation
920 - 953 Garfield Member
953 - 1182 Makwassie Formation
1182 - 2014 Goedgenoeg Formation
2014 - 2102 Kameeldoorns Formation
2102 - 2428 Klipriviersberg Group
2428 - Witwatersrand Supergroup

LITHOLOGY

NOTE: As this borehole intersects the complete Ventersdorp Supergroup, it was briefly investigated during the course of a previous research project done for Anglo American Corporation, in order to get acquainted with the stratigraphy of the Supergroup. Therefore, only limited information on the Platberg Group is available.

2014 - 1961 Feldspar porphyry with mylonite and breccia at the basal contact

1961 - 1945 Lapilli tuff, siltstone and lava breccia

1945 - 1899 Amygdaloidal, non-porphyritic lava

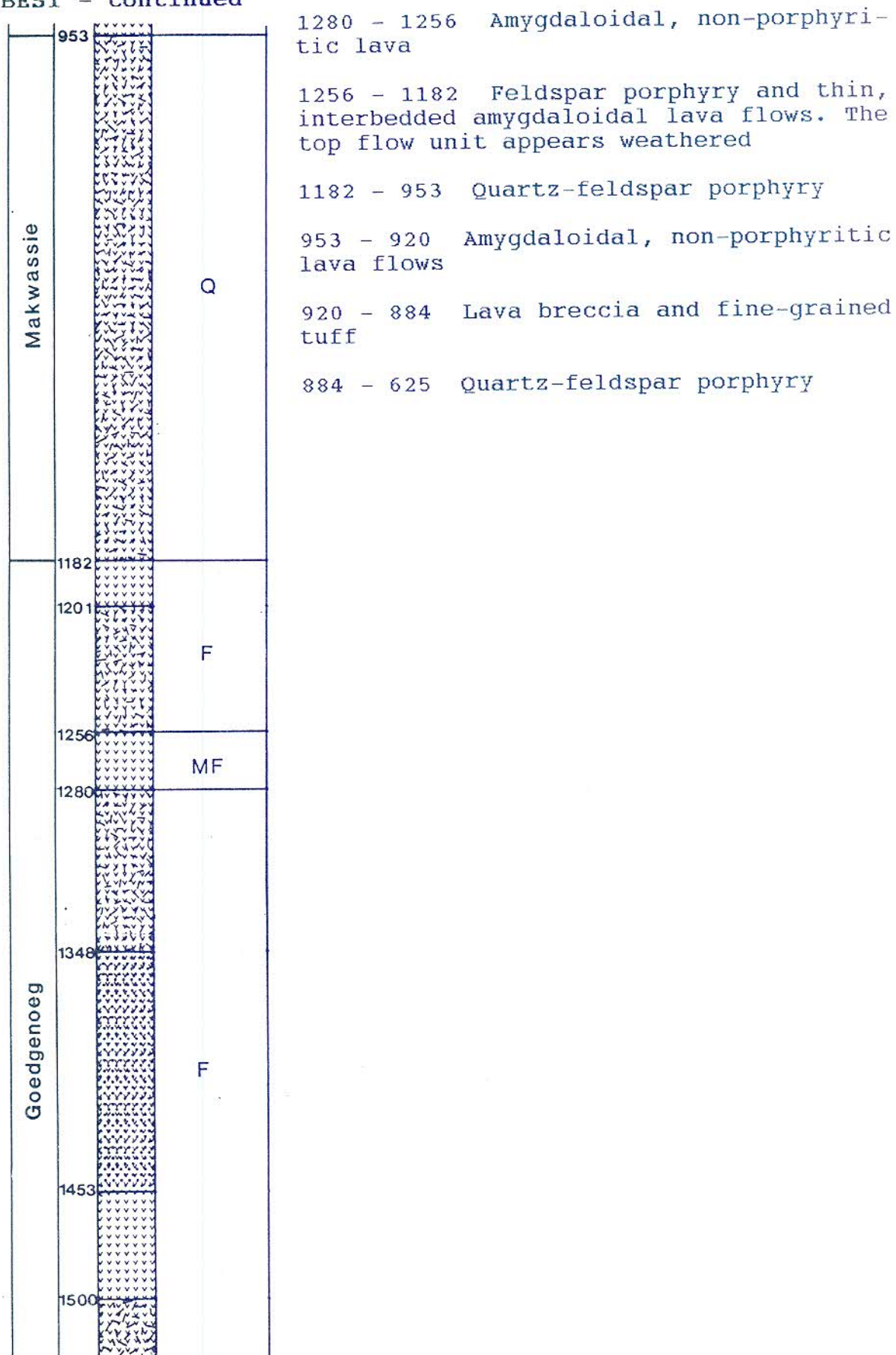
1899 - 1500 Feldspar porphyry

1500 - 1453 Numerous amygdaloidal, non-porphyritic lava flows

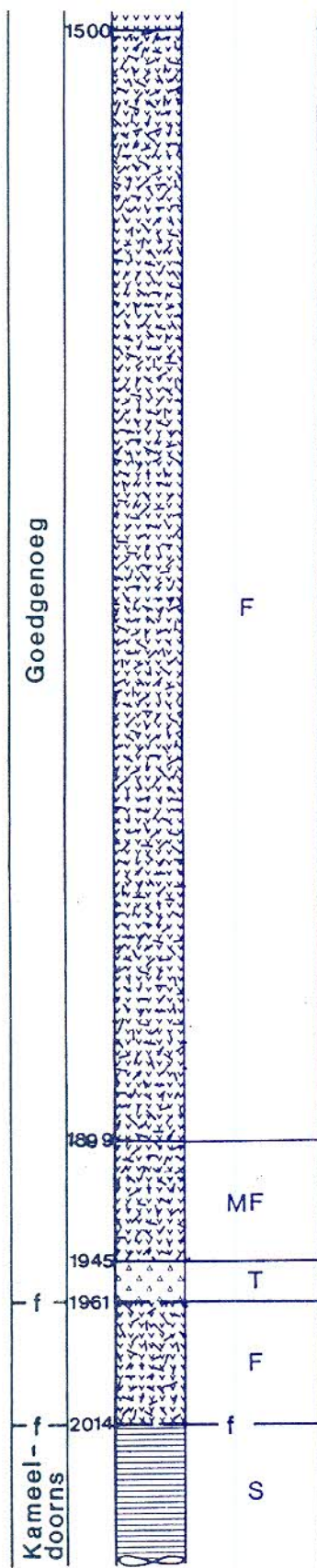
1453 - 1348 Amygdaloidal lava flows with scattered feldspar phenocrysts

1348 - 1280 Feldspar porphyry













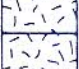
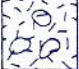
BES1 - continued



BES1 - continued



DF1 - Deelfontein 482

Formation	Depth	Scale 1:2500	Rock Type
Rietgat			M
Makwassie	279		Q
	300		
	320		
			
			
			
	464		
	482		
	519		
	554		
Klipriviersberg	567		M
	630		
	641		

BOREHOLE CO-ORDINATES

X - +3000582
Y - +40569
Z - 1289

ABBREVIATED BOREHOLE LOG







0 - 202 Allanridge Formation
202 - 279 Rietgat Formation
279 - 641 Makwassie Formation
641 - 1317 Klipriviersberg Group
1317 - Witwatersrand Supergroup

LITHOLOGY

641 - 630 Quartz-feldspar porphyry: Unwelded, poorly-sorted pyroclastic deposit overlying weathered mafic lava of the Klipriviersberg Group, with mylonitic fabric in places. [Base surge deposit]

630 - 279 Quartz-feldspar porphyry: Ignimbrite, composed of several units with unit contacts at 632, 630, 567, 554, 519, 464 and 279. [Ash-flow deposits, some separated by ash-fall deposits]

DHK1 - Driehoek 944

Formation	Depth	Scale 1:2500	Rock Type
Bothaville			S
Rietgat	562		M
	573		
	599		
Makwassie			Q
GF	855		M
	866		
Makwassie			Q
	1060		

BOREHOLE CO-ORDINATES

X - +3025005
Y - +43150
Z - 1304

ABBREVIATED BOREHOLE LOG

0 - 87 Karoo Sequence
87 - 354 Allanridge Formation
354 - 562 Bothaville Formation
562 - 573 Rietgat Formation
573 - 855 Makwassie Formation
855 - 866 Garfield Member
866 - 1128 Makwassie Formation
1128 - 1996 Goedgenoeg Formation
1996 - 2064 Kameeldoorns Formation
2064 - 2417 Klipriviersberg Group
2417 - Witwatersrand Supergroup

LITHOLOGY

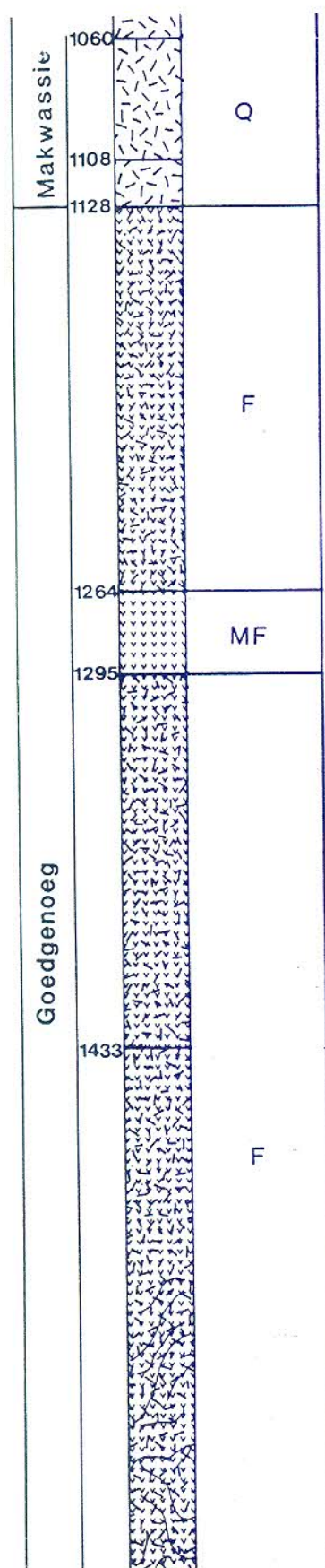
1996 - 1962 Feldspar porphyry: Feldspar phenocrysts in a very fine-crystalline matrix. [Ash-flow deposit]

1962 - 1938 Lapilli tuff: Layered units (4x) of lapilli tuff with variable lapilli size for each unit. [Ash-fall deposit in the form of lapilli-tuff]

1938 - 1933 Volcanic breccia: Partially welded, mafic volcanic breccia. [Lava flow-breccia]

1933 - 1912 Non-porphyritic lava: Very fine-crystalline lava with rare scattered feldspar phenocrysts. [Lava flow]

DHK1 - continued



1912 - 1295 Feldspar porphyry: The matrix is very fine-crystalline in the lower part of this intersection and is silicified higher up with silica spherulites. Flow lamination is also visible in the lower part. The matrix is reddish in colour higher up and contains abundant inclusions of fine-crystalline igneous material, some of up to a metre in diameter. The top of the section is magnetite-rich and amygdaloidal with elongated and flattened amygdales. The phenocryst contents is variable and, although no definite contacts were observed, the intersection is probably composed of several feldspar-phyric and less-porphyrific units. [Ash-flow deposits]

1295 - 1264 Non-porphyrific lava: Amygdaloidal lava with rare, small feldspar phenocrysts. [Lava flow]

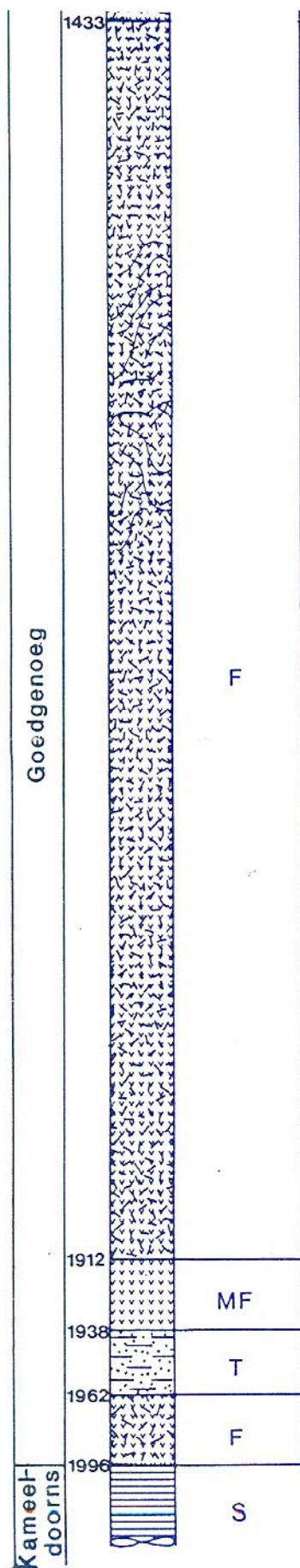
1264 - 1128 Feldspar porphyry: Scattered feldspar phenocrysts in a very fine-crystalline, altered matrix with feldspar spherulites in places. Possible unit contacts at 1210, 1160 and 1128. From 1160 the matrix is fine-crystalline. [Lava flow or ash-flow deposit]

1128 - 866 Quartz-feldspar porphyry: Units with relative large quartz and feldspar phenocrysts with crystalline, non-porphyrific inclusions in the lower unit. Unit contacts at 1108, 1060 and 866. Altered glass with visible perlitic cracks occur at the top of the 1108 to 1060 unit. [Ash-flow deposit]

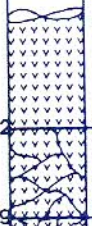

866 - 855 Non-porphyrific lava breccia: Crystalline lava breccia with fine-grained matrix and capped by layered, lithic tuff. [Block tuff and lithic tuff]

855 - 573 Quartz-feldspar porphyry: The top 30 metres of the unit are weathered and appear gravelly with brecciation. Thin intrusive diabase dykes occur at 599 and 587. [Ash-flow deposit]

DHK1 - continued



FS4 - Lombardy 1

Formation	Depth	Scale 1:2500	Rock Type
KLIPRIVERSBERG	2602		M
	2629		MF
GOEDGENOEG	2688		F

BOREHOLE CO-ORDINATES

X - +3021170
Y - +36830
Z - 1297

ABBREVIATED BOREHOLE LOG

0 - 80 Karoo Sequence
80 - 376 Allanridge Formation
376 - 494 Bothaville Formation
494 - 786 Rietgat Formation
786 - ±1040 Makwassie Formation
±1040 - ±1120 Garfield Member
±1120 - 1560 Makwassie Formation
1560 - ±2500 Goedgenoeg Formation
±2500 - 2629(f) Klipriviersberg Group
2629(f) - 2688 Goedgenoeg Formation
2688 End of hole
Duplicated Goedgenoeg Formation is estimated to continue to ±2850 m.

LITHOLOGY

2688 - 2629 Feldspar porphyry: Feldspar and rare quartz phenocrysts in a silicified matrix. [Ash-flow deposit]











2629 Fault

2629 - 2602 Non-porphyritic lava: Crystalline lava with scattered feldspar phenocrysts. [Lava flow]

2602 - ±2550 Non-porphyritic lava: Crystalline lava flows. [Lava flows]

±2550 - 786 Not logged (no core).

JWS6 - Wolvehuis 114

Formation	Depth	Scale 1:2500	Rock Type
Rietgat			M
Makwassie	279		Q
	327		
	352		
	398		
	417		
	446		
	462		
	485		
Goedgenoeg	504		S

BOREHOLE CO-ORDINATES

X - +2994625
Y - +41617
Z - 1280

ABBREVIATED BOREHOLE LOG

0 - 23 Karoo Sequence
23 - 279 Rietgat Formation
279 - 504 Makwassie Formation
504 - 558 Volcaniclastic conglomerate
(Goedgenoeg Formation)
558 - 674 Goedgenoeg Formation
674 - 773 Kameeldoorns Formation
773 - 1174 Klipriviersberg Group
1174 - Witwatersrand Supergroup




LITHOLOGY

674 - 558 Feldspar porphyry: (Not logged)

558 - 504 Volcaniclastic conglomerate: Moderately-sorted, sub-rounded, mafic lava pebbles, overlain by quartz-feldspar porphyry. [Epiclastic conglomerate]

504 - 279 Quartz-feldspar porphyry: Welded ignimbrite, multiple units with unit contacts at 485, 462, 446, 417, 398, 352, 327 and 279. Mafic Rietgat lava overlies the top unit. [Ash-flow deposits]

JWS7 - Wolvehuis 114

Formation	Depth	Scale 1:2500	Rock Type
Rietgat			M
Makwassie	365 400 464		Q
Goedgenoeg	530 545 555		S I F

BOREHOLE CO-ORDINATES

X - +2993004
Y - +41761
Z - 1276

ABBREVIATED BOREHOLE LOG

0(?) - 157 Allanridge Formation
157 - 220 Bothaville Formation
220 - 365 Rietgat Formation
365 - 530 Makwassie Formation
530 - 545 Volcaniclastic conglomerate
(Goedgenoeg Formation)
545 - 636 Goedgenoeg Formation
636 - 1533 Klipriviersberg Group
1533 - Witwatersrand Supergroup

LITHOLOGY






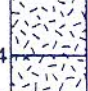


636 - 555 Feldspar porphyry: Multiple flow units with scattered feldspar phenocrysts, overlying non-porphyritic mafic Klipriviersberg lava. Flow contacts at 624, 591, 584, 578 and 560. [Lava flows]

555 - 545 Intrusive: Dense, light green-coloured, crystalline intrusive with scattered euhedral feldspar phenocrysts. [Feldspar-phyric intrusive - feeder dyke?]

545 - 530 Volcaniclastic conglomerate: Poorly sorted, angular to sub-rounded mafic lava clasts. [Epiclastic breccia]

530 - 365 Quartz-feldspar porphyry: Welded ignimbrite, consisting of several units separated by fine-grained tuff. Contacts between units at 464 and 400. The top unit is overlain by bedded tuff, followed by mafic Rietgat lava. [Ash-flow and ash-fall deposits]

JWS8 - Wolvehuis 114

Formation	Depth	Scale 1:2500	Rock Type
Rietgat			M
Makwassie	390		Q
	426		
	449		
	476		
	524		
Goedgenoeg	540		F
	589		

BOREHOLE CO-ORDINATES

X - +2992272

Y - +42224

X - 1297

ABBREVIATED BOREHOLE LOG

? - 159 Allanridge Formation
 159 - 161 Bothaville Formation
 161 - 390 Rietgat Formation
 390 - 589 Makwassie Formation
 589 - 599 Volcaniclastic conglomerate
 (Goedgenoeg Formation)
 599 - 852 Goedgenoeg Formation
 852 - 854 Kameeldoorns Formation
 854 - 2030 Klipriviersberg Group
 2030 - Witwatersrand Supergroup









LITHOLOGY

852 - 599 Feldspar porphyry: (Not logged)

599 - 589 Volcaniclastic conglomerate: Poorly sorted, sub-rounded mafic lava clasts, overlying feldspar porphyry. [Epiclastic conglomerate]

589 - 390 Quartz-feldspar porphyry: Welded ignimbrite, consisting of multiple units with contacts at 540, 524, 476, 449, 426 and 390. The top unit appears weathered and is followed by mafic Rietgat lava flows. [Ash-flow deposits]

KRF1 - Kransfontein 52

Formation	Depth	Scale 1:2500	Rock Type
Bothaville	696		S
Makwassie	889		Q
	904		F
	923		Q
	946		F
	1091		Q
Garfield	1111		F
	1168		MF

BOREHOLE CO-ORDINATES

X - +3018735
Y - +60160
Z - 1298

ABBREVIATED BOREHOLE LOG

0 - 26 Karoo Sequence
26 - 498 Allanridge Formation
498 - 696 Bothaville Formation
696 - 1091 Makwassie Formation
1091 - 1512 Garfield Member
1512 - 1993 Makwassie Formation
1993 - 3411 Goedgenoeg Formation
3411 End of hole
Goedgenoeg Formation estimated to continue to ±3800 m.

LITHOLOGY

3411 - 3107 Feldspar porphyry: No core available.

3107 - 3091 Feldspar porphyry: Feldspar phenocrysts in a green-coloured matrix, also with scattered quartz phenocrysts.

3091 - 3060 Tuff: Dark-coloured, pyritic tuff without visible layering. [Water-laid tuff]

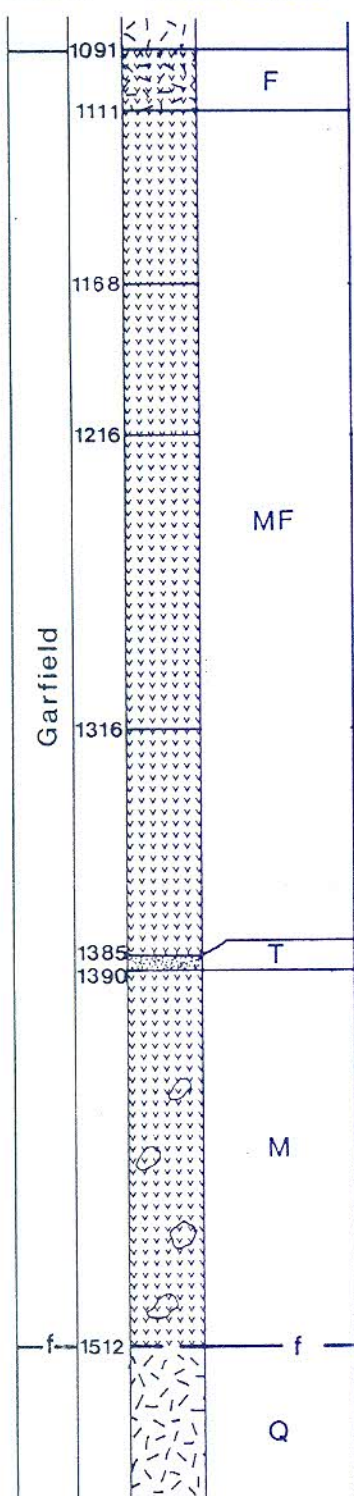
3060 - 2831 Mudrock and lava breccia: Lava and mudrock clasts in a mudrock matrix. [Lahar or debris flow deposit]

2831 - 2765 Feldspar porphyry: Relatively few feldspar phenocrysts and pyritic in the lower section. High-angle contact (70°) with the overlying unit. [Ash-flow deposit]

2765 - 2745 Mudrock and lava breccia: Lava and mudrock clasts in a feldspar-porphyry matrix. High-angle contact (60°) with the overlying unit. [Lahar or debris flow deposit]

2745 - 2720 Feldspar porphyry: Amygdaloidal unit. [Lava flow]

KRF1 - continued



2720 - 2694 Non-porphyritic lava: Amygdaloidal lava with inclusions of mudrock and feldspar-porphyry in the top 3 metres. [Lava flow with slumped or rafted debris on top]

2694 - 2658 Mudrock and lava breccia: Angular to sub-rounded lava and mudrock clasts. [Epiclastic breccia]

2658 - 2577 Non-porphyritic lava: Amygdaloidal lava flows (5x). [Lava flows]

2577 - 2534 Mudrock and lava breccia: Angular to sub-rounded lava and mudrock clasts, also with scattered quartz pebbles. [Epiclastic breccia]

NOTE: The core was only logged from 2545 downwards, but the following information was obtained:

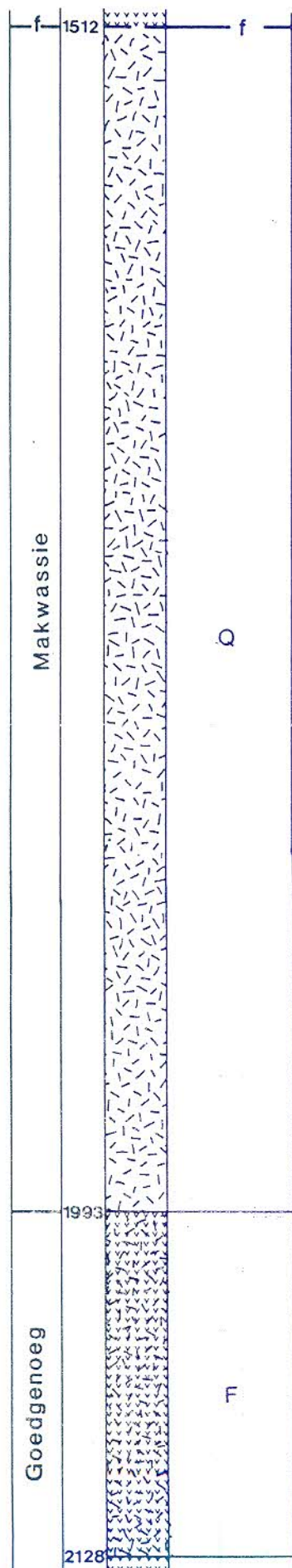
2534 - 2023 Feldspar-porphyry and non-porphyritic units. Some of the feldspar-porphyry units contain only scattered feldspar phenocrysts.

2023 - 1512 Quartz-feldspar porphyry units.

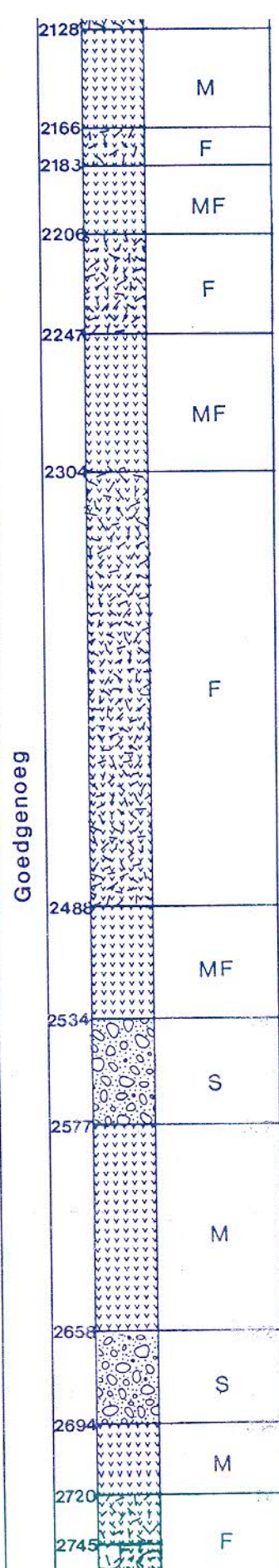
1512 - 1091 Non-porphyritic and feldspar-porphyry units.

1091 - 696 Quartz-feldspar porphyry with feldspar-porphyry units at 946 to 923 and 904 to 885.

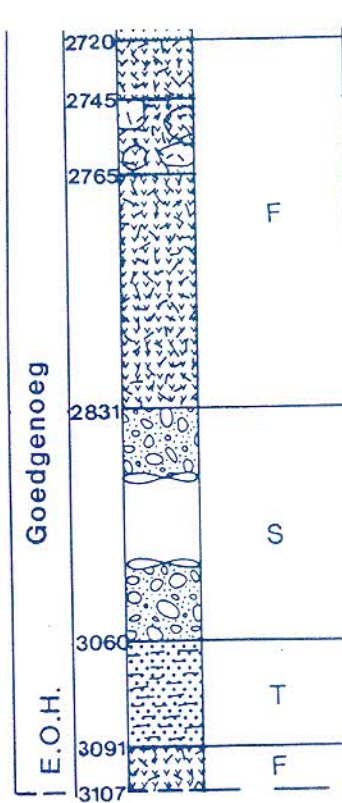
KRF1 - continued



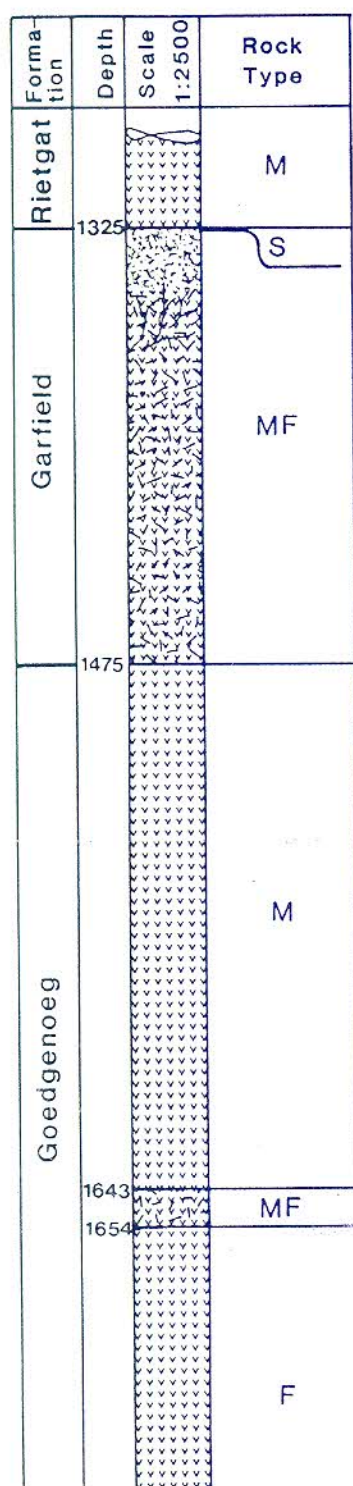
KRF1 - continued



KRF1 - continued



LL1 - Langgeleiven 597



BOREHOLE CO-ORDINATES

X - +3036460
Y - +29650
Z - 1301

ABBREVIATED BOREHOLE LOG

0 - 186 Karoo Sequence
186 - 835 Allanridge Formation
835 - 1042 Bothaville Formation
1042 - 1325 Rietgat Formation
1325 - ±1475 Garfield Member
±1475 - 1814 Goedgenoeg Formation
1814 - 1827 Kameeldoorns Formation
1827 - 3360 Klipriviersberg Group
3360 - Witwatersrand Supergroup

NOTE: Alternatively, the Garfield/Goedgenoeg contact can be at 1654 m.

LITHOLOGY

1814 - 1788 Feldspar-porphyry breccia: Unwelded, poorly sorted pyroclastic breccia composed of feldspar-phyric volcanic material and abundant non-porphyritic mafic clasts. [Base-surge deposit]

1788 - 1775 Non-porphyritic lava: Crystalline lava with scattered feldspar phenocrysts. [Lava flow]

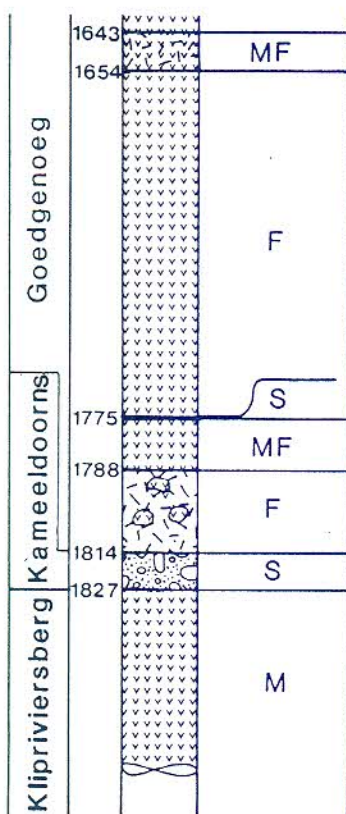
1775 - 1774 Shale: Laminated shale. [Lacustrine deposit]

1774 - 1654 Feldspar porphyry: Scattered feldspar phenocrysts and rare, small quartz phenocrysts. [Ash-flow deposit]

1654 - 1643 Non-porphyritic lava: Crystalline lava with scattered feldspar phenocrysts. [Lava flow]

1643 - 1475 Non-porphyritic lava: Crystalline lava. [Lava flows]

LL1 - continued



1475 - 1325 Non-porphyritic lava: Crystalline lava with scattered small feldspar-phenocrysts. The top of the unit is weathered and capped by a thin layer of shale. [Lava flow]

LLE1 - Leeuwfontein 185

Formation	Depth	Scale 1:2500	Rock Type
Makwassie	500		Q

BOREHOLE CO-ORDINATES

X - +3003050
Y - +87324
Z - 1420

ABBREVIATED BOREHOLE LOG

0 - 636 Makwassie Formation
636 - 848 Garfield Member
848 - 2604 Makwassie Formation
2604 - 3659 Goedgenoeg Formation
3659 End of hole
Goedgenoeg Formation estimated to continue to ± 4000 m.

LITHOLOGY

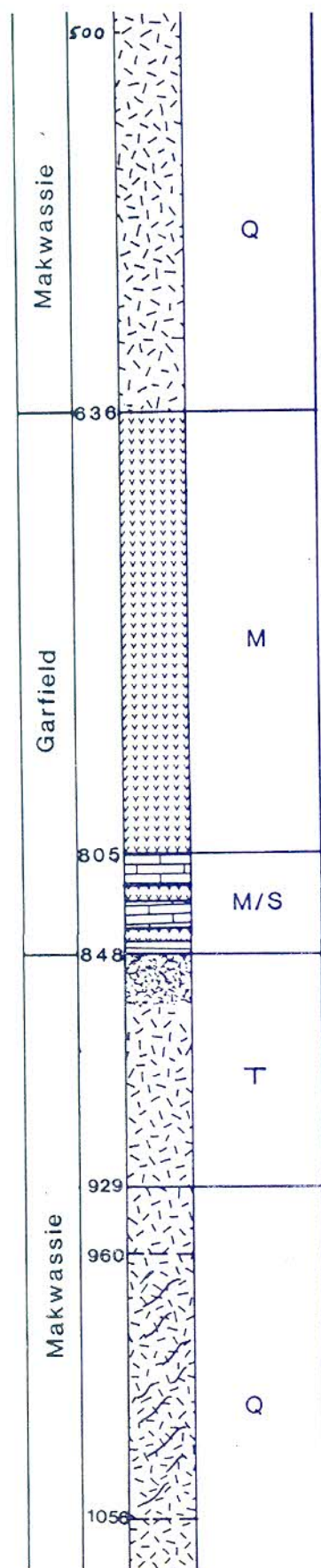
NOTE: The positive identification of flow units was hampered by previous sampling of the borehole core by AARL, during which complete sections of core was removed, apparently especially at flow-unit contacts.

3659 - 3648 Feldspar-porphyry breccia: Angular clasts of feldspar porphyry in fine-crystalline matrix. [Lava flow-top breccia]

3648 - 3560 Feldspar porphyry: Feldspar phenocrysts and rare, partially resorbed, small quartz phenocrysts in silicified and epidotized matrix. Quartz-filled amygdales occur at the top of the unit. [Ash-flow deposit]

3560 - 3218 Feldspar porphyry: Units, consisting of feldspar phenocrysts and rare, partially resorbed, small quartz phenocrysts in silicified and epidotized matrix. Granophyric intergrowths occur in the matrix. Mylonitic epidotized zones occur, which may be epidotized tuff-beds. Quartz-filled amygdales occur at the tops of units, with contacts at 3543, 3514, 3475, 3338, 3266 and 3218. [Ash-flow deposits]

LLE1 - continued



3218 - 3127 Quartz-feldspar porphyry: Abundant quartz phenocrysts, also feldspar phenocrysts in very fine-crystalline matrix. [Ash-flow deposit]

3127 - 2953 Quartz-feldspar porphyry: Units, mostly the same as the underlying unit (3210-3127), but with less quartz phenocrysts. Contacts between units at 3080, 2992 and 2953. [Ash-flow deposits]

2953 - 2876 Feldspar porphyry: Reddish-coloured unit with green-coloured epidotized bands. The unit appears tuffaceous or mylonitic and is capped by a 2 m layer of fine-grained, laminated tuff. [Ash-flow or ash-fall deposit]

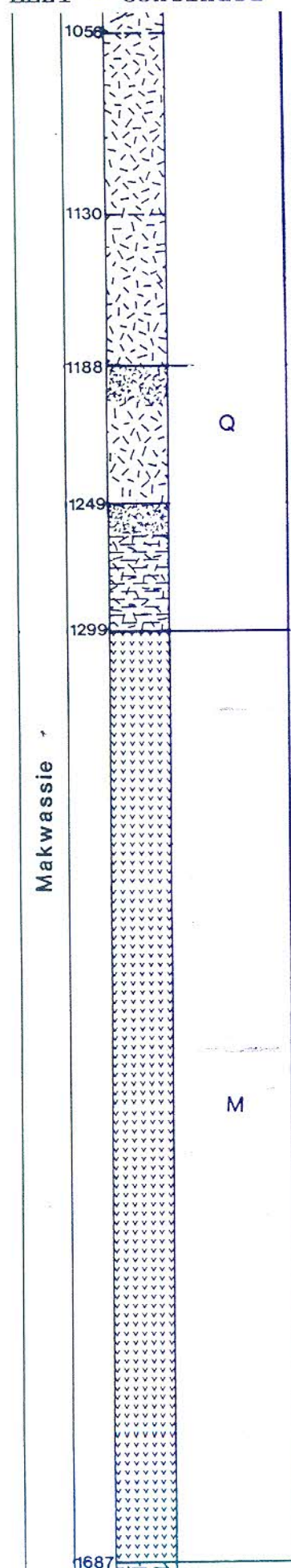
2876 - 2604 Feldspar porphyry: Units with feldspar and rare, partially resorbed, small quartz phenocrysts in a silicified matrix. Unit contacts at 2838 and 2604. The upper 30 m of the top unit is tuffaceous. [Ash-flow deposits]

2604 - 2404 Quartz-feldspar porphyry: Units with quartz and feldspar phenocrysts in silicified matrix. Unit contacts at 2588, 2566, 2420, and 2404. From 2566 the porphyry is amygdale-rich and less porphyritic, while the top (2420 - 2404) is composed of flow-top breccia and tuff. Fluorite veins cut through this zone. [Ash-flow and pyroclastic-fall deposits]

2404 - 2020 Quartz-feldspar porphyry: Possibly two units of porphyry with abundant quartz phenocrysts, also feldspar phenocrysts in highly silicified matrix (q = fsp <<< matrix). The top is tuffaceous and with fluorite veins. [Ash-flow deposits]

2020 - 2001 Tuff: Layered, fine to coarse-grained lithic tuff with layers of accretionary lapilli. [Ash-fall deposit]

LLE1 - continued



2001 - 1809 Quartz-feldspar porphyry: Units with abundant quartz and feldspar phenocrysts in silicified matrix. The matrix displays a streaky texture in places. Unit contacts at 1970, 1911 and 1809. [Ash-flow deposits]

1809 - 1687 Pyroclastic breccia: Multiple units of tuffaceous rock with angular quartz-feldspar porphyry clasts of variable size in places and amygdaloidal tops. Phenocrysts in the matrix are intensely fragmented. Unit contacts occur at 1785, 1753, 1747, 1736, 1718, 1693 and 1687. [Ash-flow (?) and pyroclastic-fall deposits]

1687 - 1413 Non-porphyrific lava: Numerous fine-crystalline lava flows with amygdaloidal bases and tops. [Lava flows]

1413 - 1410 Tuff: Very fine-grained heat-altered tuff. [Ash-fall deposit]

1410 - 1300 Non-porphyrific lava: Numerous fine-crystalline lava flows with amygdaloidal bases and tops. [Lava flows]

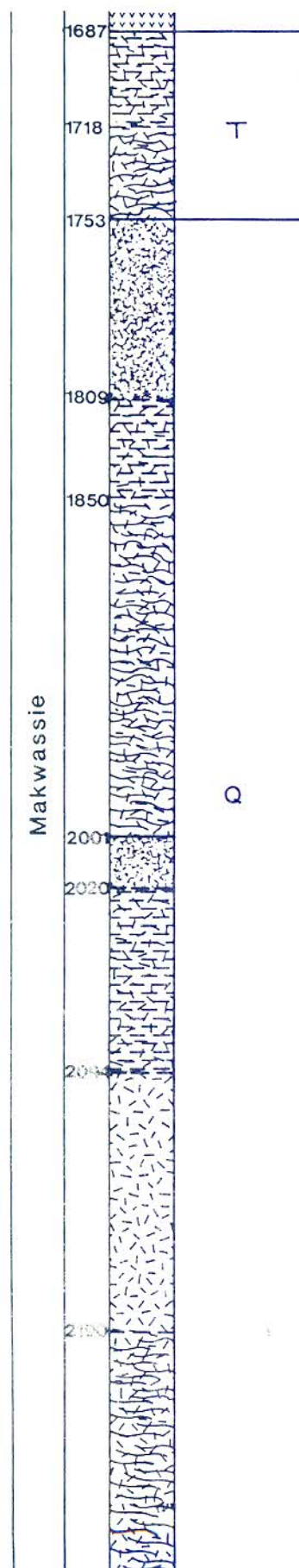
1300 - 1299 Lapilli tuff: Angular lava clasts in layered, lithic tuff. [Air-fall deposit]

1299 - 1130 Quartz-feldspar porphyry: Units with abundant quartz phenocrysts, also feldspar phenocrysts in silicified matrix. Unit contacts at 1249, 1226, 1188 and 1130. Lapilli tuff occurs between 1263 and 1249. [Ash-flow deposits]

1130 - 1072 Tuff: Fragmented phenocrysts in an altered glassy matrix. [Ash-fall deposits]

1072 - 929 Quartz-feldspar porphyry: Altered porphyry units with contacts at 1036 and 929. [Ash-flow deposits]

LLE1 - continued



929 - 848 Lapilli tuff: Angular porphyry clasts and fragmented phenocrysts in an altered glass matrix, with perlitic cracks still visible under the microscope. [Pyroclastic-fall deposit]

848 - 845 Shale: Dolomitic shale with pyrite and pyrrhotite laminae. [Water deposit]

845 - 838 Non-porphyritic lava: Thin amygdaloidal lava flows with contacts at 843, 841 and 838. The lava flows have finely brecciated lava at their bases and a thin shale layer occurs at 841. [Lava flows, which flowed into shallow water?]

838 - 824 Shale: Dolomitic shale with pyrite and pyrrhotite laminae, also with fenestral fabric in places. [Water deposit]

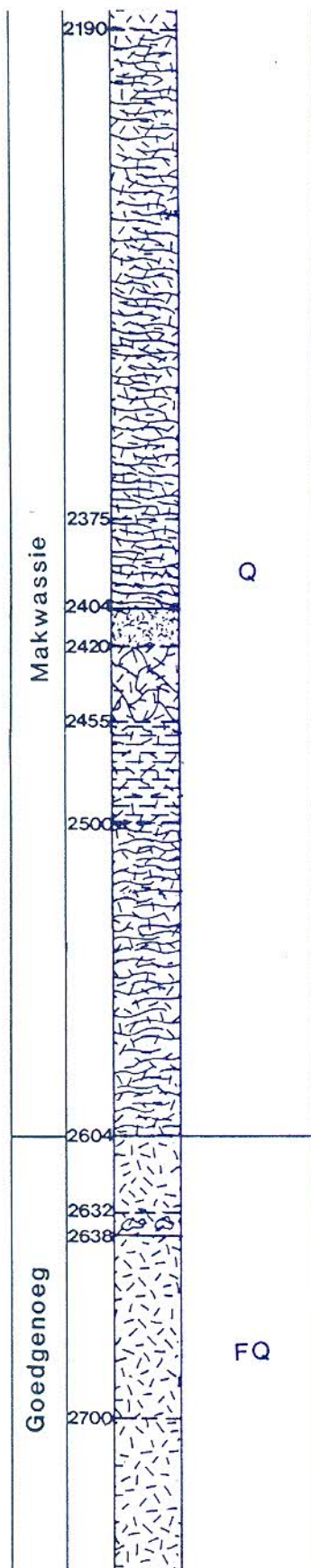
824 - 818 Non-porphyritic lava: Highly amygdaloidal lava. [Lava flow]

818 - 805 Shale: Dolomitic shale with pyrite and pyrrhotite laminae. [Water deposit]

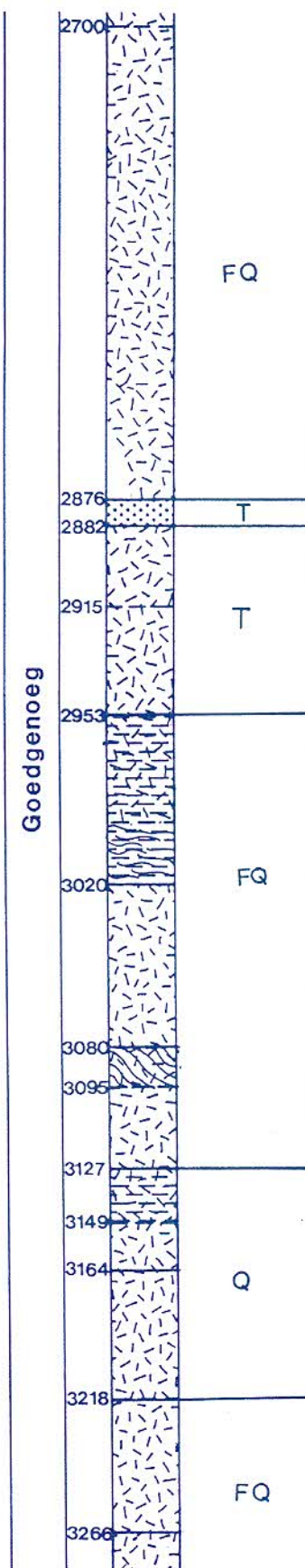
805 - ± 700 Non-porphyritic lava: Amygdaloidal lava flows. [Lava flows]

NOTE: The borehole was percussion-drilled from surface to ± 700 m.

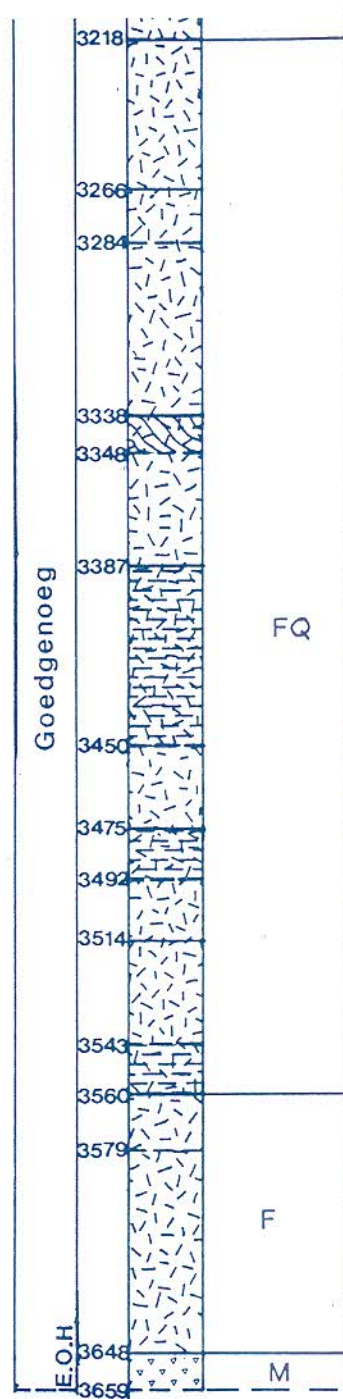
LLE1 - continued



LLE1 - continued



LLE1 - continued



OT1 - Ontario 832

Formation	Depth	Scale 1:2500	Rock Type
Rietgat			M
	1082		S
Garfield	1119		F
	1194		
	1224		M
	1251		S
Goedgenoeg			F
Kameeldoorns	1392		S

BOREHOLE CO-ORDINATES

X - +3019378
Y - +25840
Z - 1311

ABBREVIATED BOREHOLE LOG

0 - 258 Karoo Sequence
258 - 613 Allanridge Formation
613 - 1082 Rietgat Formation
1082 - ±1194 Garfield Member
±1194 - 1392 Goedgenoeg Formation
1392 - 1518 Kameeldoorns Formation
1518 - 2390 Klipriviersberg Group
2390 - Witwatersrand Supergroup

NOTE: Alternatively, the contact between the Garfield and Goedgenoeg Formation can be at 1251 m.

LITHOLOGY

1392 - 1251 Feldspar porphyry: Feldspar and rare quartz phenocrysts in a brownish-coloured matrix with amygdaloides at the top of the unit. [Ash-flow deposit]

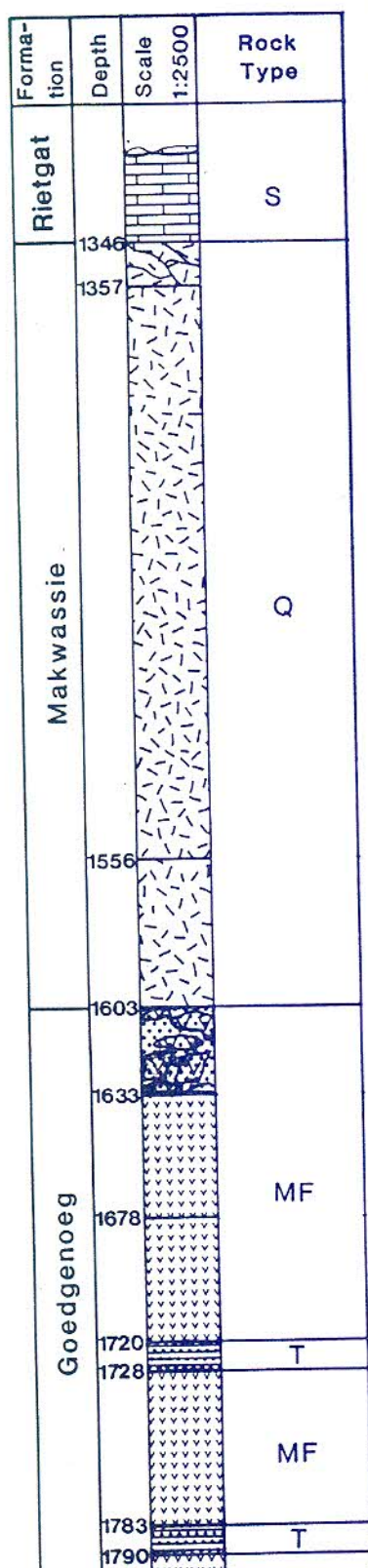
1251 - 1250 Laminated tuff: Partially welded lithic and crystal fragments in a matrix of partially welded, altered glass. [Partially welded lithic tuff]

1250 - 1194 Non-porphyrific lava: Crystalline lava flows with amygdaloidal tops and contacts at 1224 and 1194. [Lava flows]

1194 - 1082 Feldspar porphyry: Feldspar phenocrysts in a brownish-coloured matrix and amygdaloides at the top of the units, with contacts at 1119 and 1082. [Ash-flow deposits]

1082 - 1081 Laminated shale and chloritic, argillaceous sandstone [Lacustrine sediments - Rietgat Formation]

SHS1 - Smalfontein 495



BOREHOLE CO-ORDINATES

X - +3045750
Y - +54000
Z - 1300

ABBREVIATED BOREHOLE LOG

0 - ±120 Karoo Sequence
±120 - ±660 Allanridge Formation
±660 - 877 Bothaville Formation
877 - 1346 Rietgat Formation
1346 - ±1603 Makwassie Formation
±1603 - 2181 Goedgenoeg Formation
2181 End of hole
Goedgenoeg Formation estimated to continue to ±2240 m.

LITHOLOGY

2181 - 2106 Feldspar porphyry: Abundant, very fine-crystalline non-porphyrific inclusions in the lower part of the unit and with an amygdaloidal top. [Ash-flow deposit]

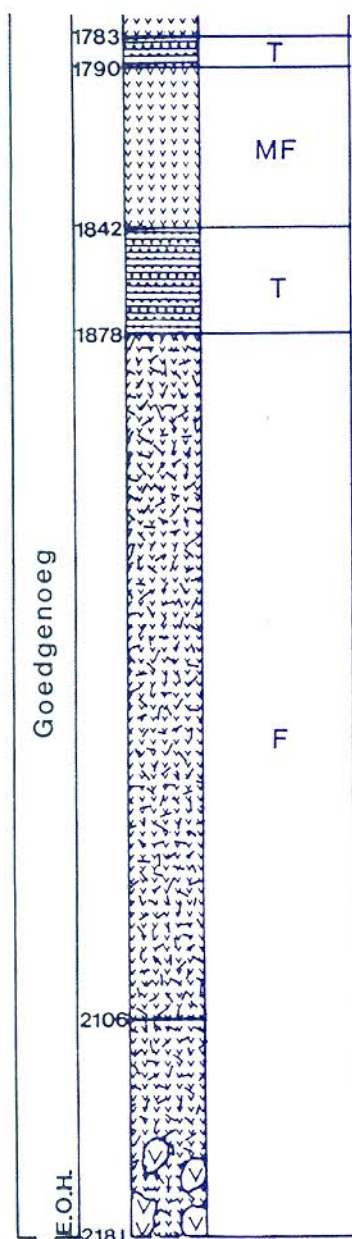
2106 - 1878 Feldspar porphyry: Unit with amygdales in the upper 60 metres. No subunits apparent. [Ash-flow deposit]

1878 - 1842 Laminated tuff: Lithic fragments of quartz and lava arranged in laminae are imbedded in an amorphous, chloritic matrix. The quartz fragments are angular to subrounded and some are polycrystalline under the microscope. Orientated glass shards are embedded with the lithic fragments. Upwards-fining units can be distinguished (<2 cm thick). [Water-reworked, lithic tuff]

1842 - 1790 Non-porphyrific lava: Amygdaloidal lava with scattered small feldspar phenocrysts and contacts between flows at 1814, 1797 and 1790. [Lava flows]

1790 - 1783 Laminated tuff: Laminae of lithic fragments and glass shards in a amorphous, chloritic matrix (matrix >> glass >> lithics). Less quartz fragments than the previous tuff. Abundant

SHS1 - continued



flattened and fractured accretionary lapilli arranged with the lithics in the laminae. Thin chert layers towards the top of the tuff unit. [Water-deposited lithic tuff]

1783 - 1728 Non-porphyritic lava: Amygdaloidal lava with scattered feldspar phenocrysts and contact between flows at 1760. The upper flow grades into a flow-top breccia or block-tuff at 1733. [Lava flows]

1728 - 1720 Laminated tuff: Cherty tuff similar to the 1790 to 1783 tuff unit. [Lithic tuff deposited in or reworked by water]

1720 - 1684 Non-porphyritic lava: Amygdaloidal lava flows with scattered feldspar phenocrysts with contacts between flows at 1699, 1692 and 1684. [Lava flows]

1684 - 1678 Lapilli tuff: Laminated lithic tuff with angular vesicular lava clasts, capped by a 1 metre thick, laminated tuff unit. [Lapilli tuff]

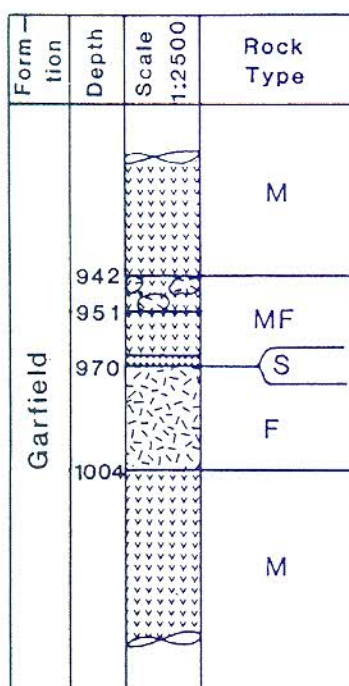
1678 - 1603 Non-porphyritic lava: Amygdaloidal lava flows with scattered feldspar phenocrysts and contacts between flows at 1662, 1650, 1633, 1620 and 1603. The flows are capped by lapilli-tuff or flow-top breccias. [Lava flows]

1603 - 1357 Quartz-feldspar porphyry: Units of quartz-feldspar porphyry with relative few quartz phenocrysts and an albitized (?) matrix. Contacts between units at 1571, 1556 and 1357; the upper 50 metres are brecciated and altered. [Ash-flow deposits]

1357 - 1346 Quartz-feldspar porphyry: Weathered and brecciated quartz porphyry. [Ash-flow deposits]

1346 - 1288 Mudrock: Fenestral dolomitic mudrock of the Rietgat Formation, followed by amygdaloidal lava flows.

SPP1 - Paardeplaats 265



BOREHOLE CO-ORDINATES

X - +2945347
Y - +65781
Z - 1533

ABBREVIATED BOREHOLE LOG

0	-	100	Bothaville Formation
100	-	550	Rietgat Formation
550	-	1328	Garfield Member
1328	-	1424	Kameeldoorns Formation
1424	-	1452	Diabase intrusive
1452	-	1462	Kameeldoorns Formation
1462	-	1742	Unknown felsic intrusive, probably a Dominion Group correlative
1742	-	1836	Basement
1836			End of hole

LITHOLOGY

1742 - 1462 Felsic, porphyritic igneous unit: Abundant unbroken euhedral feldspar phenocrysts, also quartz and amphibole in a very fine-crystalline matrix with extensive secondary silicification. Finer crystallinity apparent towards the upper and lower contact. Secondary granophyric overgrowths of feldspar phenocrysts. [Felsic intrusive]

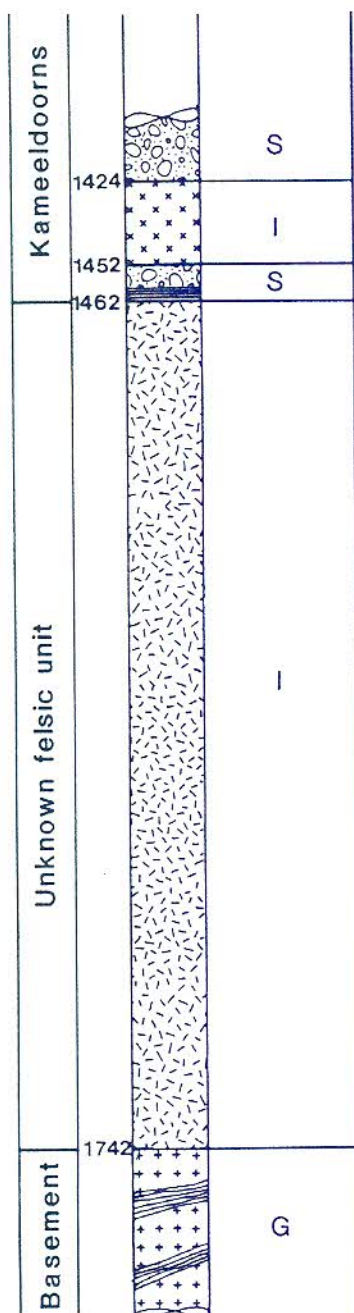
1462 - 1452 Feldspatic sandstone and conglomerate: Fine to coarse-grained sandstone and pebbly sandstone. [Immature proximal sedimentary rocks - Kameeldoorns Formation]

1452 - 1449 Mafic igneous rock: Very fine-crystalline, glassy rock. [Mafic intrusive]

1449 - 1424 Mafic igneous rock: Coarse-crystalline with scattered, large (10 mm) feldspar phenocrysts. [Diabase intrusive]

1424 - 1328 Sedimentary rock [Kameeldoorns Formation]

SPP1 - continued



1328 - 1004 Non-porphyrific and feldspar-phyric lava: Amygdaloidal, non-porphyrific lava flows and porphyritic units with only small, scattered feldspar phenocrysts. [Lava flows]

1004 - 970 Feldspar porphyry: Porphyry with larger and more abundant feldspar phenocrysts, a lighter green colour and flow lamination. [Ash-flow deposit]

970 - 968 Tuff: Fine-grained, laminated tuff. [Ash-fall deposit]

968 - 951 Non-porphyrific lava: Fine-crystalline lava. [Lava flow]

951 - 942 Non-porphyrific lava: Lava with numerous inclusions of feldspar porphyry. [Lava flow with porphyry breccia]

942 - 550 Non-porphyrific lava: Amygdaloidal lava flows, some with scattered, small feldspar phenocrysts. [Lava flows]

NOTE: The 550 - 942 intersection may alternatively be part of the Rietgat Formation.

SYF1 - Syferfontein 13

Formation	Depth	Scale 1:2500	Rock Type
Rietgat			M
Makwassie	387		Q
	409		
	459		
	494		
	530		
	552		
	580		
Goedgenoeg	592		F
	639		

BOREHOLE CO-ORDINATES

X - +2990725
Y - +67881
Z - 1366

ABBREVIATED BOREHOLE LOG

0 - 232 Allanridge Formation
232 - 250 Bothaville Formation
250 - 387 Rietgat Formation
387 - 639 Makwassie Formation
639 - 995 Goedgenoeg Formation
995 - 1212 Kameeldoorns Formation
1212 - 1440 Witwatersrand Supergroup
1440 - 2727 Dominion Group
2727 End of hole

LITHOLOGY

995 - 639 Feldspar porphyry: Not logged

639 - 387 Quartz-feldspar porphyry:
Magnetite-rich units with contacts at
592, 580, 552, 530, 494, 459, 409 and
387. The unit tops are amygdaloidal.
[Ash-flow deposits]

ULT1 - Ulster 128

Formation	Depth	Scale 1:2500	Rock Type
Garfield			M
	739		
	757		
			MF
	793		
Goedgenoeg	1367		
	1382		
			I
	1410		
			M
	1461		
			FQ
	1499		
	1504		M
E.O.H.	1563		
			FQ
	1607		
	1641		
	1683		
	1742		

BOREHOLE CO-ORDINATES

X - +3014630
Y - +45250
Z - 1285

ABBREVIATED BOREHOLE LOG

0 - 35 Karoo Sequence
35 - 494 Allanridge Formation
494 - 682 Bothaville Formation
682 - 833 Garfield Member
833 - 1250 Makwassie Formation
1250 - 1742 Goedgenoeg Formation
1742 End of hole

LITHOLOGY

1742 - 1683 Dolerite: Dark grey dolerite, not significantly affected by greenschist alteration and therefore considered as Karoo-age dolerite. [Dolerite intrusive]

1683 - 1607 Quartz-feldspar porphyry: Feldspar and scattered, resorbed quartz phenocrysts in units with contacts at 1641 and 1607. The tops are amygdaloidal. [Ash-flow deposits]

1607 - 1563 Quartz-feldspar porphyry: Unit with more quartz phenocrysts than in the previous units and with abundant inclusions of non-porphyritic lava. The unit is capped by lapilli, lithic and layered tuff and the whole unit may be pyroclastic. [Ash-flow deposit]

1563 - 1504 Quartz-feldspar porphyry: Feldspar and scattered, resorbed quartz phenocrysts in unit with amygdaloidal top. [Ash-flow deposit]

1504 - 1499 Non-porphyritic lava: Amygdaloidal. [Lava flow]

1499 - 1468 Quartz-feldspar porphyry: Feldspar and scattered resorbed quartz phenocrysts in unit capped by laminated tuff. The top metre is composed of cross-bedded tuff. [Ash-flow and base surge deposit]

ULT1 - continued

1468 - 1461 Quartz-feldspar porphyry: Feldspar and scattered, resorbed quartz phenocrysts in unit with amygdaloidal top. [Ash-flow deposit]

1461 - 1410 Non-porphyritic lava: Amygdaloidal lava flows with flow-top breccias and contacts between flows at 1456, 1440, 1426 and 1410. The uppermost flow is heat-altered. [Lava flows]


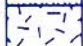




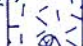

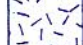
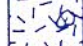

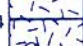
1410 - 1382 Dolerite: Dark, grey-coloured dolerite, not significantly affected by greenschist alteration and therefore considered as Karoo-age dolerite. [Dolerite intrusive]

1382 - 1260 Non-porphyritic lava: Amygdaloidal lava flows. [Lava flows]

1260 - 833 Quartz-feldspar porphyry: Porphyry with scattered quartz and feldspar phenocrysts. [Ash-flow deposits]

833 - 682 Non-porphyritic lava and feldspar porphyry: Amygdaloidal non-porphyritic lava flows and interbedded feldspar-phyric flow units. [Lava flows]

UTK1 - Uitkyk 91

Formation	Depth	Scale 1:2500	Rock Type
Garfield			M
Makwassie	980		Q
			
	1052		
			
	1134		
Kameeldoorns Klipriviersberg	1173		I/S
			
	1214		
	1239		
	255		S
			M

BOREHOLE CO-ORDINATES

X - +3002230
Y - +36800
Z - 1311

ABBREVIATED BOREHOLE LOG

0 - 33 Karoo Sequence
33 - 457 Allanridge Formation
457 - 471 Bothaville Formation
471 - ±720 Rietgat Formation
±720 - 980 Garfield Member
980 - 1214 Makwassie Formation
1214 - 1255 Kameeldoorns Formation
1255 - 1697 Klipriviersberg Group
1697 - Witwatersrand Supergroup








LITHOLOGY

NOTE: Two green-coloured intrusives were intersected in the Kameeldoorns Formation, which may be feeder dykes for the Platberg or Pniel lavas.

1214 - 980 Quartz-feldspar porphyry: Units with amygdaloidal tops, containing abundant non-porphyritic inclusions. Unit contacts at 1173, 1134, 1052 and 980. The upper unit is weathered. [Ash-flow deposit]

980 - ±720 Non-porphyritic and feldspar-phyrlic lava flows: Not logged

VE1 - Velshoek 341

Formation	Depth	Scale 1:2500	Rock Type
Rietgat	728		M
Makwassie	820		Q
GF	874		MF
Makwassie	896		Q
Goedgenoeg	1076		MF
	1107		
	1180		

BOREHOLE CO-ORDINATES

X - +3029030
Y - +22330
Z - 1335

ABBREVIATED BOREHOLE LOG

0 - 158 Karoo Sequence
158 - 604 Allanridge Formation
604 - 653 Bothaville Formation
653 - 728 Rietgat Formation
728 - 874 Makwassie Formation
874 - 896 Garfield Member
896 - 1076 Makwassie Formation
1076 - 1366 Goedgenoeg Formation
1366 - 1488 Kameeldoorns Formation
1488 - 2406 Klipriviersberg Group
2406 End of hole

LITHOLOGY

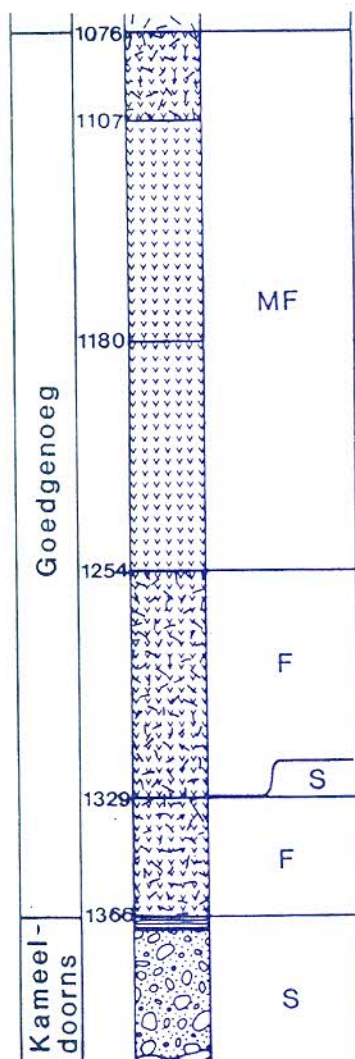
1366 - 1329 Feldspar porphyry: Fine-crystalline feldspar-phyric lava with amygdalites at the top. [Lava flow]

1329 - 1325 Volcaniclastic conglomerate: Upwards-fining cycles (3x), composed of coarse-grained, poorly sorted volcanic gravel and pebbles. Some clasts are porphyritic. [Intraformational epiclastic conglomerate]

1325 - 1254 Feldspar porphyry: Feldspar-porphyry with abundant inclusions of crystalline lava. The top is amygdaloidal and capped by very fine-grained sedimentary rock. [Lava or ash-flow deposit, capped by an ash-fall deposit]

1254 - 1107 Non-porphyritic lava: Fine-crystalline units with scattered feldspar phenocrysts and amygdalites at tops, with unit contacts at 1210, 1180, 1163, 1145, 1136 and 1107. [Lava flows]

VE1 - continued



1107 - 1076 Pyroclastic rock: Fine-crystalline lava blocks and smaller clasts, embedded in fine-grained, layered sedimentary rock. The top of the unit is overlain by a fine-grained, layered bed a metre thick. [Lava flow, block and lapilli tuff, capped by an ash-fall deposit]

1076 - 896 Quartz-feldspar porphyry: Welded ignimbrite with abundant large quartz phenocrysts. [Ash-flow deposit]

896 - 874 Non-porphyrific lava: Fine-crystalline units with scattered small feldspar phenocrysts in a chloritic matrix. Amygdales at the top of units with contacts at 886 and 874. [Lava flows]

874 - 820 Quartz-feldspar porphyry: Yellowish-green, glassy quartz-feldspar porphyry with a streaky and laminated fabric. In thin section the phenocrysts show strong resorption and the matrix is cryptocrystalline. [Strongly welded ash-flow deposit]

820 - 728 Not logged: No core available, but probably a continuation of the above.

WS3 - Wolvehuis 114

BOREHOLE CO-ORDINATES

X - +2994889
Y - +45823
Z - 1300

ABBREVIATED BOREHOLE LOG

±0 - 338 Allanridge Formation
338 - 451 Bothaville Formation
451 - 923 Makwassie Formation
923 - 977 Goedgenoeg Formation
977 - 998 Kameeldoorns Formation
998 - ±2300 Klipriviersberg Group
±2300 - Witwatersrand Supergroup

LITHOLOGY (not logged below 926)

926 - 925 Lapilli tuff: Laminated, fine-grained tuff with angular porphyry clasts of variable size. [Pyroclastic fall deposit]

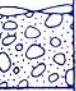
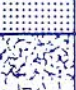
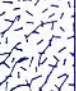







925 - 923 Non-porphyritic lava: Very fine-crystalline amygdaloidal lava with scattered feldspar phenocrysts. [Lava flow]

923 - 920 Quartz-feldspar porphyry: Scattered feldspar and quartz phenocrysts in crystalline matrix with abundant small igneous inclusions. [Ash-flow deposit, intermingled with mafic lava flow]

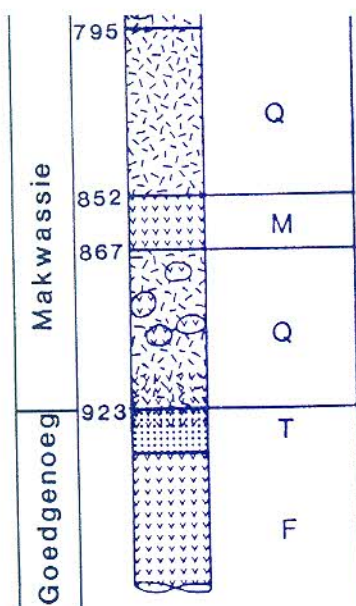
920 - 873 Quartz-feldspar porphyry: Porphyry with abundant inclusions of igneous rock. [Ash-flow deposit]

873 - 867 Lapilli tuff: Fine-grained tuff with lithic fragments and lapilli-size clasts. [Pyroclastic fall deposit]

867 - 852 Non-porphyritic lava: Amygdaloidal crystalline lava. [Lava flow]

Formation	Depth	Scale 1:2500	Rock Type
Bothaville	451		S
Makwassie	508		Q
	553		
	563		
	602		
	677		
	795		
	852		
	867		
			M

WS3 - continued



852 - 451 Quartz-feldspar porphyry:
Flow units with abundant quartz and
feldspar phenocrysts. Some units display
flow banding and others igneous
inclusions. Contacts between units at
795, 768, 677, 602, 563, 553, 508 and
451. [Ash-flow deposits]

WS4 - Wolvehuis 114

For- mation	Depth	Scale 1:2500	Rock Type
Rietgat			M
Makwassie	375		Q
	409		
	448		
	490		
	504		
	560		
	595		
	659		
	743		
Goed- genoeg			F

BOREHOLE CO-ORDINATES

X - +2991646

Y - +44341

Z - 1300

ABBREVIATED BOREHOLE LOG

±0 - 232 Allanridge Formation
 232 - 280 Bothaville Formation
 280 - 375 Rietgat Formation
 375 - 743 Makwassie Formation
 743 - 1078 Goedgenoeg Formation
 1078 - 1133 Kameeldoorns Formation
 1133 - ±2340 Klipriviersberg Formation
 ±2340 - Witwatersrand Supergroup

LITHOLOGY

1078 - 743 Not logged




743 - 375 Quartz-feldspar porphyry:
 Multiple flow units composed of abundant
 quartz and feldspar phenocrysts in
 cherty matrix, some with abundant
 igneous inclusions. Unit contacts at
 659, 595, 560, 504, 490, 478, 448, 409
 and 375. The topmost unit appears
 weathered. [Ash-flow deposits]

WS5 - Wolvehuis 114

BOREHOLE CO-ORDINATES

X - 2990318
Y - 42149
Z - 1300

ABBREVIATED BOREHOLE LOG

Formation	Depth	Scale 1:2500	Rock Type
Rietgat			M
MAK- WAS- SIE	564		Q
Goedgenoeg	585		T
			F









±0 - 147 Allanridge Formation
147 - 176 Bothaville Formation
176 - 564 Rietgat Formation
564 - 585 Makwassie Formation
585 - 927 Goedgenoeg Formation
927 - 963 Kameeldoorns Formation
963 - ±2400 Klipriviersberg Group
±2400 - Witwatersrand Supergroup

LITHOLOGY

927 - 585 Not logged. The topmost 10 metres are composed of feldspar porphyry, overlain by a thin layer of fine-grained tuff. [Ash-fall deposit]

585 - 564 Quartz-feldspar porphyry: Highly altered porphyry, composed of angular porphyry clasts in laminated, silicified, fine-grained matrix. [Pyroclastic flow deposit]

YYS1 - Yzerspruit 15

Formation	Depth	Scale 1:2500	Rock Type
Rietgat	708		M
Makwassie	750		Q
	868		
	885		
	917		
	941		M
Goedgenoeg	971		Q
	988		F

BOREHOLE CO-ORDINATES

X - +2991476
Y - +47885
Z - 1350

ABBREVIATED BOREHOLE LOG

±0 - 380 Allanridge Formation
380 - 430 Bothaville Formation
430 - 708 Rietgat Formation
708 - 988 Makwassie Formation
988 - 1526 Goedgenoeg Formation
1526 - 1821 Kameeldoorns Formation
1821 - 2620 Klipriviersberg Group
2620 - Witwatersrand Supergroup

LITHOLOGY

1526 - 988 Not logged.

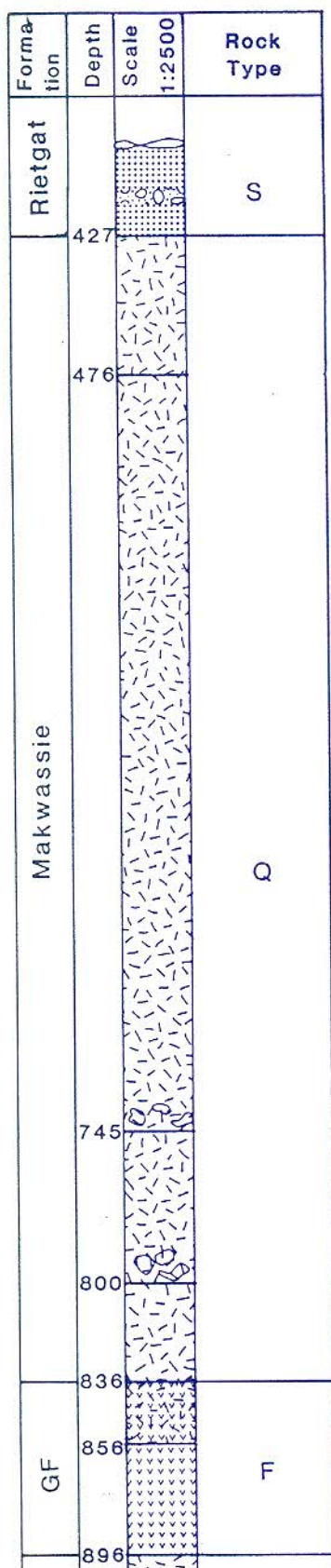
988 - 971 Non-porphyritic lava: Amygdaloidal fine-crystalline lava flows with contacts at 981, 979 and 971. [Lava flows]

971 - 941 Quartz-feldspar porphyry: Porphyry with abundant igneous and porphyry inclusions. [Mixed ash-flow deposit?]

941 - 917 Non-porphyritic lava: Amygdaloidal, fine-crystalline flow units with scattered phenocrysts of Makwassie-type quartz and feldspar phenocrysts. Unit contacts at 936, 935, 927, 919 and 917. [Lava flows]

917 - 708 Quartz-feldspar porphyry: Porphyry units composed of quartz and feldspar phenocrysts in cherty matrix, some with igneous and porphyry inclusions. Unit contacts at 985, 868, 750 and 709. The topmost unit appears weathered. [Ash-flow deposits]

ZH1 - Zonderhout 71



BOREHOLE CO-ORDINATES

X - +3021500
Y - +73250
Z - 1300

ABBREVIATED BOREHOLE LOG

0 - 305 Allanridge Formation
305 - 427 Bothaville Formation
427 - 836 Makwassie Formation
836 - 896 Garfield Member
896 - 1583 Makwassie Formation
1583 - ±1800 Kameeldoorns Formation

LITHOLOGY

1583 - 1580 Quartz-feldspar porphyry breccia: Angular quartz-feldspar porphyry lapilli embedded in calcitized matrix, overlying Kameeldoorns conglomerate. [Pyroclastic-fall deposit]

1580 - 1479 Quartz-feldspar porphyry: Welded ignimbrite, consisting of 2 units, separated by layered, fine-grained tuff at 1567. [Ash-flow and ash-fall deposits]

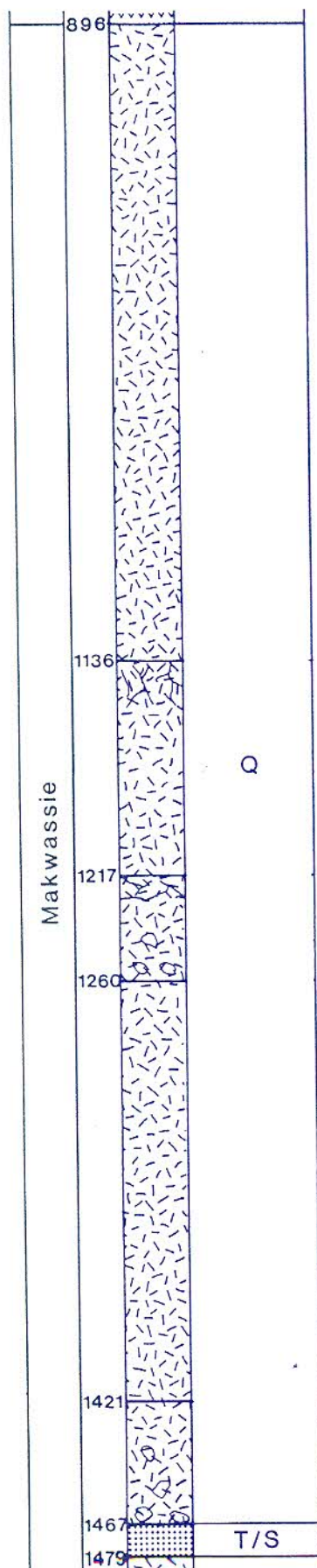
1479 - 1475 Tuff: Layered, fine-grained tuff. [Ash-fall deposit]

1475 - 1467 Volcaniclastic breccia: Two breccia units of poorly sorted, angular to sub-rounded quartz-feldspar porphyry, tuff and strongly-welded tuff clasts in cherty matrix, underlain by reverse-graded tuffaceous sandstone. [Lahar or fluvial deposit]

1467 - 896 Quartz-feldspar porphyry: Multiple welded ignimbrite units, separated by fine-grained tuff. Contacts between units at 1421, 1260, 1217 and 1136. [Ash-flow units, separated by ash-fall deposits]

896 - 856 Feldspar porphyry: Mafic lava with scattered feldspar and rare quartz phenocrysts. [Lava flow]

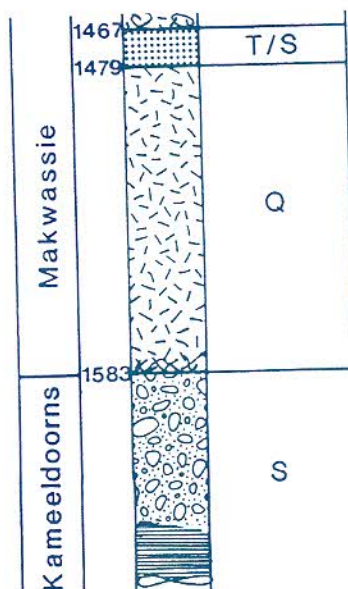
ZH1 - continued



856 - 836 Felspar porphyry: Banded mafic lava with scattered feldspar and quartz phenocrysts, less porphyritic than "normal" Makwassie Quartz Porphyry. [Strongly welded ash-flow]

836 - 427 Quartz-feldspar porphyry: Multiple welded ignimbrite units, separated by fine-grained tuff with unit contacts at 800, 745 and 476. The top unit (476-427) appears weathered and is overlain by Bothaville conglomerate and quartzite. [Ash flow units, separated by ash-fall deposits]

ZH1 - continued



ST2 - Drooggekraal 27

BOREHOLE CO-ORDINATES

X - +2998000
 Y - +82200
 Z - 1400

ABBREVIATED BOREHOLE LOG

0 - 215 Allanridge Formation
 215 - 305 Bothaville Formation
 305 - 590 Rietgat Formation
 590 - 775 Makwassie Formation
 775 - 986 Goedgenoeg Formation
 986 - 1255 Kameeldoorns Formation
 1255 - ±1700 Klipriviersberg Formation

LITHOLOGY

? - 1255 Non-amygdaloidal lava flows
 1255 - 1085 Dolomitic mudrock
 1085 - 1076 Amygdaloidal, non-porphyritic lava flow
 1076 - 1044 Dolomitic mudrock
 1044 - 996 Amygdaloidal, non-porphyritic lava flow
 996 - 985 Dolomitic mudrock
 985 - 775 Feldspar-porphyry and non-porphyritic lavas
 775 - 590 Quartz-feldspar porphyry with abundant large phenocrysts
 590 - 305 Rietgat lava with mudrock units

NOTE: The core was obtained from African Selection Trust Exploration in Klerksdorp. Only short sections of borehole core at regular intervals of the borehole were kept. A thin layer of mudrock occurs at 775 m between the Goedgenoeg and Makwassie Formation, with a normal relation between the mudrock and the overlying quartz-feldspar porphyry. The contact between the mudrock and underlying feldspar porphyry is very irregular, with heat-alteration in the mudrock. The feldspar-porphyry is very fine-crystalline close to the contact zone and do not show weathering. The rest of the Goedgenoeg Formation between 775 and 985 m consists of feldspar porphyry and non-porphyritic amygdaloidal lavas. The relationship between the two rock types is not represented in the kept core. In thin section the feldspar porphyry exhibits unusual coarse-crystallinity and no extrusive features normally associated with the Goedgenoeg Formation are visible. The feldspar porphyry between 775 and 985 is therefore intrusive and intruded into mudrock and non-porphyritic lava flows.

This implies that the intersection from 775 to 985 metres may correlate with the non-porphyritic lava and dolomitic mudrock occurring from 636 to 848 metres in borehole LLE1; therefore, it may be Garfield Member and not Goedgenoeg.

APPENDIX B

ADDITIONAL BOREHOLE DATA

For the purposes of the study, additional borehole data were obtained from various sources. However, core of these boreholes was not available for logging and the data had to be interpreted with the logged boreholes in Appendix A as basis, particularly to delineate the possible occurrence and position of the Goedgenoeg and Makwassie Formations. The borehole positions are indicated in Chapter 3 of the dissertation.

The borehole code, farm on which it was drilled, co-ordinates of the borehole collar and an abbreviated borehole log are given for each borehole. The X and Y co-ordinates are based on the LO-27 grid system, that is the X co-ordinates are in metres south of the equator and the Y co-ordinates in metres west of the 27° parallel. The Z co-ordinate give the collar elevation in metres above average mean sea level. Most of the borehole co-ordinates are only estimates as the surveyed co-ordinates are not available. They are however, still fairly accurate as the farm positions are known. The indicated intersections of the Goedgenoeg and Makwassie Formations and of the Garfield Member are interpretations done during this study and the possible occurrence of these units at depths deeper than the boreholes are also listed (flagged by an asterisk). *E.O.H.* is an abbreviation for 'End of Borehole'.

Borehole	Farm	Stratigraphy	From	To	Thickness
BOREHOLE DATA FROM ANGLO AMERICAN CORPORATION					
DPR1	Delports Rust 30	Karoo	0	272	272
	X +3 094 080	Bothaville	272	307	35
	Y +38 340	Rietgat	307	861	554
	Z +1 308	Makwassie	861	1207	346
		Kameeldoorns	1207	1486	279
		Klipriviersberg	1486	1596	110
		Basement	1596	1662	66
		E.O.H.	1662		
BH1	Hendrik Theron (?)	Karoo	0	102	102
	X +3 044 360	Allanridge	102	556	454
	Y +68 650	Bothaville	556	676	120
	Z +1 301	Makwassie	676	1660	984
		Garfield	840	1000	160
		Goedgenoeg	1660	2056	396
		Basement	2056	2148	92
		E.O.H.	2148		
KA1	Karokom 480	Karoo	0	222	222
	X +3 008 320	Allanridge	222	737	515
	Y +29 110	Bothaville	737	764	27
	Z +1 323	Rietgat	764	1310	546
		Makwassie	1310	2340	1030
		Garfield	1420	1724	304
		Goedgenoeg	2340	2499	159
		Kameeldoorns	2499	2664	165
		Klipriviersberg	2664	3912	1248
		E.O.H.	3912		
LRQ1	Ladies Request 46	Karoo	0	100	100
	X +3 056 600	Allanridge	100	444	344
	Y +69 160	Bothaville	444	602	158
	Z +1 277	Rietgat	602	796	194
		Makwassie	796	1023	227
		Kameeldoorns	1023	1066	43
		Basement	1066	1112	46
		E.O.H.	1112		
MNT1	Nooitgedach 378	Makwassie	794	832	38
	X +3 072 000	(No further data available)			
	Y +44 000				
	Z +1 300				
RH1	Red Hill 484	Karoo	0	113	113
	X +3 016 020	Transvaal	113	972	859
	Y +18 360	Allanridge	972	1304	332
	Z +1 347	Bothaville	1304	1312	8
		Makwassie	1312	1550	238
		Garfield	1312	1400	88
		Goedgenoeg	1550	1928	378
		Kameeldoorns	1928	1980	52
		Klipriviersberg	1980	2725	745
		E.O.H.	2725		

Borehole	Farm	Stratigraphy	From	To	Thickness
BH1	Salisbury 79	Karoo	0	116	116
	X +3 009 480	Transvaal	116	1184	1068
	Y +21 210	Allanridge	1184	1663	479
	Z +1 344	Makwassie	1663	1900	237
		Garfield	1663	1740	77
		Goedgenoeg	1900	2109	209
		Klipriviersberg	2109	2457	348
		E.O.H.	2109		
SCT1	Scott 559	Karoo	0	296	296
	X +3 026 130	Allanridge	296	881	585
	Y +30 050	Bothaville	881	933	52
	Z +1 318	Rietgat	933	1310	377
		Makwassie	1310	1530	220
		Garfield	1470	1500	30
		Goedgenoeg	1530	1749	219
		Klipriviersberg	1749	2747	998
		Witwatersrand	2747	3962	1215
		E.O.H.	3962		
BH1	Vergenoeg 325	Karoo	0	219	219
	X +3 014 130	Transvaal	219	271	52
	Y +27 000	Allanridge	271	743	472
	Z +1 341	Bothaville	743	791	48
		Rietgat	791	1320	529
		Makwassie	1320	1760	440
		Garfield	1450	1593	143
		Goedgenoeg	1760	2002	242
		Kameeldoorns	2002	2183	181
		Klipriviersberg	2183	3554	1371
		E.O.H.	3554		
Y1	Yzerspruit 15	Allanridge	0	410	410
	X +2 991 828	Bothaville	410	497	87
	Y +49 983	Rietgat	497	722	225
	Z +1 326	Makwassie	722	1228	506
		Goedgenoeg	1228	1771	543
		Kameeldoorns	1771	2110	339
		Klipriviersberg	2110	2869	759
		Witwatersrand	2869	3137	268
		E.O.H.	3137		
BOREHOLE DATA FROM WINTER'S Ph.D. THESIS (Winter, 1965)					
(NOTE: The XY-coordinates of the borehole collars were calculated from Winter's map)					
EH1	Edgar's Hope (?)	Karoo	0	58	58
	X +3 004 750	Allanridge	58	479	421
	Y +38 500	Rietgat	479	672	193
	Z +1 329	Makwassie	672	998	326
		Kameeldoorns	998	1015	17
		Klipriviersberg	1015	1648	633
		E.O.H.	1648		
EL1	Escol 519	Karoo	0	90	90
	X +3 038 500	Allanridge	90	412	322
	Y +60 200	Bothaville	412	493	81
	Z +1 250	Witwatersrand	493	1334	841

Borehole	Farm	Stratigraphy	From	To	Thickness
		E.O.H.	1334		
FS3	Jacoba 878	Karoo	0	43	43
	X +3 005 250	Allanridge	43	367	324
	Y +43 000	Bothaville	367	389	22
	Z +1 317	Makwassie	389	863	474
		Goedgenoeg	863	1050	187
		Klipriviersberg	1050	2165	1115
		Witwatersrand	2165	2273	108
		E.O.H.	2273		
FV1	Fairview (?)	Karoo	0	141	141
	X +3 050 200	Allanridge	141	836	695
	Y +47 680	Bothaville	836	1179	343
	Z +1 298	Rietgat	1179	1690	511
		Makwassie	1690	1914	224
		E.O.H.	1914		
		*Makwassie	1690	2120	430
GD1	Grootdeel 29	Karoo	0	13	13
	X +3 001 750	Allanridge	13	328	315
	Y +45 000	Makwassie	328	720	392
	Z +1 311	Goedgenoeg	720	930	210
		Kameeldoorns	930	964	34
		Klipriviersberg	964	1982	1018
		E.O.H.	1982		
GF1	Garfield 579	Karoo	0	23	23
	X +3 000 000	Allanridge	23	190	167
	Y +38 750	Rietgat	190	389	199
	Z +1 298	Makwassie	389	874	485
		Garfield	389	541	152
		Kameeldoorns	874	964	90
		Klipriviersberg	964	1129	165
		Witwatersrand	1129	1982	853
		E.O.H.	1982		
GLV1	Gelykvlakte 142	Karoo	0	140	140
	X +3 005 000	Allanridge	140	732	592
	Y +35 500	Bothaville	732	747	15
	Z +1 329	Rietgat	747	986	239
		Makwassie	986	1369	383
		Garfield	986	1065	79
		Klipriviersberg	1369	1960	591
		E.O.H.	1960		
GR2	Groenfontein 513	Karoo	0	44	44
	X +2 992 250	Transvaal	44	504	460
	Y +25 000	Allanridge (?)	504	1265	761
	Z +1 326	Makwassie	1265	1763	498
		Garfield	1265	1763	498
		E.O.H.	1763		
		*Garfield	1265	1800	535
		*Makwassie	1800	2500	700
JY4	Jersey 145	Karoo	0	57	57
	X +2 992 500	Transvaal	57	190	133

Borehole	Farm	Stratigraphy	From	To	Thickness
	Y +28 500	Allanridge (?)	190	836	646
	Z +1 305	Makwassie	836	1712	876
		Garfield	836	1473	637
		E.O.H.	1712		
		*Makwassie	1473	2220	747
KF1	Klipfontein 459	Karoo	0	31	31
	X +3 018 480	Allanridge	31	374	343
	Y +38 800	Bothaville	374	486	112
	Z +1 280	Rietgat	486	614	128
		Makwassie	614	1240	626
		Garfield	840	950	110
		Goedgenoeg	1240	1594	354
		E.O.H.	1594		
		*Goedgenoeg	1240	2300	1060
KPD1	Klipplaatdrift 87	Karoo	0	54	54
	X +3 028 000	Allanridge	54	380	326
	Y +56 250	Bothaville	380	441	61
	Z +1 265	Makwassie	441	1096	655
		Garfield	441	632	191
		Goedgenoeg	1096	2231	1135
		E.O.H.	1096		
		*Goedgenoeg	1096	2800	1704
LRP1	Le Roux Pan 220	Karoo	0	125	125
	X +3 062 250	Allanridge	125	201	76
	Y +33 250	Bothaville	201	414	213
	Z +1 292	Rietgat	414	682	268
		Goedgenoeg	682	896	214
		Kameeldoorns	896	1457	561
		Klipriviersberg	1457	1892	435
		E.O.H.	1892		
LRP2	Le Roux Pan 220	Karoo	0	161	161
	X +3 067 250	Bothaville	161	311	150
	Y +35 000	Rietgat	311	548	237
	Z +1 302	Makwassie	548	629	81
		Kameeldoorns	629	1183	554
		Klipriviersberg	1183	1699	516
		E.O.H.	1699		
BH1	Middelburg 246	Karoo	0	67	67
	X +3 068 750	Allanridge	67	221	154
	Y +45 000	Bothaville	221	571	350
	Z +1 295	Rietgat	571	1030	459
		Makwassie	1030	1547	517
		Kameeldoorns	1547	1806	259
		Klipriviersberg	1806	2046	240
		E.O.H.	2046		
MN1	Modderfontein 343	Karoo	0	104	104
	X +3 074 750	Allanridge	104	709	605
	Y +48 250	Rietgat	709	1003	294
	Z +1 292	Makwassie	1003	1277	274
		Basement	1277	1298	21
		E.O.H.	1298		

Borehole	Farm	Stratigraphy	From	To	Thickness
MO1	Moddefontein Oost 883	Karoo	0	45	45
	X +3 037 000	Allanridge	45	355	310
	Y +66 250	Makwassie	355	1524	1169
	Z +1 250	Garfield	780	880	100
		E.O.H.	1524		
		*Makwassie	355	1620	1265
		*Goedgenoeg	1620	2200	580
Moir	Moir 119	Karoo	0	192	192
	X +3 001 250	Allanridge	192	771	579
	Y +30 500	Rietgat	771	933	162
	Z +1 344	Makwassie	933	1280	347
		Garfield	933	1188	255
		E.O.H.	1280		
		*Makwassie	933	1780	847
NKR1	Niekerks Rust 298	Karoo	0	167	167
	X +3 024 600	Transvaal	167	640	473
	Y +12 950	Makwassie	640	990	350
	Z +1 356	Garfield	700	850	150
		Goedgenoeg	850	1308	458
		Klipriviersberg	1308	1828	520
		E.O.H.	1828		
OTF1	One Tree Farm 84	Karoo	0	87	87
	X +3 061 800	Allanridge	87	376	289
	Y +56 650	Bothaville	376	593	217
	Z +1 280	Rietgat	593	634	41
		Makwassie	634	803	169
		Kameeldoorns	803	1018	215
		Basement	1018	1059	41
		E.O.H.	1059		
PM1	Palmietfontein 250	Karoo	0	74	74
	X +3 036 250	Allanridge	74	481	407
	Y +55 000	Bothaville	481	511	30
	Z +1 295	Makwassie	511	1320	809
		Garfield	680	880	200
		Goedgenoeg	1320	2001	681
		E.O.H.	2001		
		*Goedgenoeg	1320	2720	1400
RG1	Rietgat 251	Karoo	0	136	136
	X +3 053 450	Allanridge	136	844	708
	Y +44 140	Bothaville	844	1232	388
	Z	Rietgat	1232	1798	566
		Makwassie	1798	2159	361
		Goedgenoeg	2159	2691	532
		Kameeldoorns	2691	2852	161
		E.O.H.	2852		
SB1	Klein Brittanje 76	Karoo	0	98	98
	X +3 060 400	Allanridge	98	552	454
	Y +44 170	Bothaville	552	978	426
	Z +1 285	Rietgat	978	1641	663
		Makwassie	1641	1880	239

Borehole	Farm	Stratigraphy	From	To	Thickness
		Goedgenoeg	1880	1997	117
		E.O.H.	1997		
		*Goedgenoeg	1880	2450	570
SB2	Goud Kwarts 64	Allanridge	0	351	351
	X +3 065 230	Bothaville	351	674	323
	Y +51 430	Makwassie	674	1295	621
	Z +1 304	E.O.H.	1295		
		*Makwassie	674	1400	726
SW2	Samara 856	Karoo	0	31	31
	X +2 996 500	Allanridge	31	587	556
	Y +34 000	Bothaville	587	610	23
	Z +1 317	E.O.H.	610		
TEA1	Teneriffe 33	Karoo	0	104	104
	X +2 994 500	Allanridge	104	656	552
	Y +28 750	Bothaville	656	688	32
	Z +1 326	Makwassie	688	1486	798
		Garfield	688	1036	348
		Kameeldoorns	1486	1593	107
		Klipriviersberg	1593	1981	388
		E.O.H.	1981		
TF1	The Flats 635	Karoo	0	162	162
	X +3 055 250	Allanridge	162	536	374
	Y +30 250	Bothaville	536	737	201
	Z +1 308	Rietgat	737	927	190
		Goedgenoeg	927	1206	279
		E.O.H.	1206		
		*Goedgenoeg	927	1230	303
UC16	Palmietfontein 250	Karoo	0	38	38
	X +3 032 250	Allanridge	38	471	433
	Y +53 250	Bothaville	471	674	203
	Z +1 265	Makwassie	674	1330	656
		Garfield	674	827	153
		Goedgenoeg	1330	1530	200
		E.O.H.	1530		
		*Goedgenoeg	1330	2900	1570
UC18	Susannaskraal 467	Karoo	0	174	174
	X +3 038 500	Allanridge	174	760	586
	Y +35 500	Bothaville	760	875	115
	Z +1 256	Rietgat	875	906	31
		Makwassie	906	1529	623
		Garfield	906	1150	244
		E.O.H.	1529		
		*Makwassie	906	2060	1154
UC73	Klipfontein 598	Karoo	0	253	253
	X +3 038 500	Transvaal	253	256	3
	Y +35 500	Allanridge	256	1018	762
	Z +1 256	Bothaville	1018	1258	240
		Rietgat	1258	1855	597
		Makwassie	1855	2134	279
		E.O.H.	2134		

Borehole	Farm	Stratigraphy	From	To	Thickness
		*Makwassie	1855	2220	365
		*Goedgenoeg	2220	2800	580
UH1	Uitenhaag 65	Karoo	0	119	119
	X +3 065 250	Bothaville	119	277	158
	Y +41 750	Rietgat	277	578	301
	Z +1 298	Goedgenoeg	578	999	421
		Kameeldoorns	999	1554	555
		Klipriviersberg	1554	2923	1369
		E.O.H.	2923		
ZN1	Zandfontein 271	Karoo	0	49	49
	X +3 036 500	Allanridge	49	416	367
	Y +57 750	Bothaville	416	533	117
	Z +1 295	Makwassie	533	1066	533
		Garfield	720	820	100
		E.O.H.	1066		
		*Makwassie	533	1600	1067
NOTE: Winter (1965) has indicated the possible occurrence of West Rand Group from 897 m to the end of the hole at 1 066 m.					
WS1	Wolvehuis 114	Allanridge	0	365	365
	X +2 997 000	Makwassie	365	424	59
	Y +43 500	Klipriviersberg	424	1393	969
	Z +1 289	Witwatersrand	1393	2417	1024
		E.O.H.	2417		
The following boreholes did not intersect the Goedgenoeg or Makwassie Formations, but did intersect overlying or underlying formations and is therefore delineating the distribution limits of these formations.					
AW1	Albon 841	Karoo	0	30	30
		Klipriviersberg	30	177	147
		Witwatersrand	177	619	442
		E.O.H.	619		
BH1	Tredenham 133	Allanridge	0	92	92
		Bothaville	92	269	177
		Klipriviersberg	269	995	726
		Witwatersrand	995	1779	784
		E.O.H.	1779		
BH2	Tredenham 133	Karoo	0	150	150
		Klipriviersberg	150	1981	1831
		Witwatersrand	1981	2295	314
		E.O.H.	2295		
BP1	Bovenlandsplaats 114	Karoo	0	180	180
		Allanridge	180	559	379
		Bothaville	559	727	168
		Rietgat	727	1291	564
		Kameeldoorns	1291	1380	89
		Basement	1380	1442	62
		E.O.H.	1442		
CC1	Concord 392	Karoo	0	282	282

Borehole	Farm	Stratigraphy	From	To	Thickness
		Klipriviersberg	282	365	83
		Witwatersrand	365	693	328
		E.O.H.	693		
Diamant	Diamant 37	Karoo	0	155	155
		Klipriviersberg	155	1661	1506
		Witwatersrand	1661	2476	815
		E.O.H.	2476		
DP1	Damplaats 220	Karoo	0	146	146
		Allanridge	146	372	226
		Bothaville	372	456	84
		Klipriviersberg	456	1187	731
		E.O.H.	1187		
DPL1	Damplaats 361	Karoo	0	186	186
		Kameeldoorns	186	484	298
		Klipriviersberg	484	1300	816
		Witwatersrand	1300	2233	933
		E.O.H.	2233		
EG3	Eerste Geluk 61	Karoo	0	105	105
		Bothaville	105	222	117
		Kameeldoorns	222	397	175
		Klipriviersberg	397	461	64
		Witwatersrand	461	641	180
		E.O.H.	641		
EO1	Edom 277	Transvaal	0	168	168
		Rietgat	168	226	58
		Klipriviersberg	226	926	700
		Witwatersrand	926	954	28
		Fault	954		
		Klipriviersberg	954	964	10
		Witwatersrand	964	1630	666
		E.O.H.	954		
GB1	Gibea 825	Karoo	0	57	57
		Witwatersrand	57	418	361
		E.O.H.	418		
GG1	Graspan 40	Karoo	0	180	180
		Klipriviersberg	180	1631	1451
		Witwatersrand	1631	2499	868
		E.O.H.	2499		
GV1	Gras Vlei 46	Karoo	0	152	152
		Allanridge	152	270	118
		Bothaville	270	437	167
		Rietgat	437	466	29
		Kameeldoorns	466	1739	1273
		E.O.H.	1739		
JY1	Jersey 145	Karoo	0	43	43
		Klipriviersberg	43	503	460
		Witwatersrand	503	760	257
		E.O.H.	760		

Borehole	Farm	Stratigraphy	From	To	Thickness
KZ1	Kromdraai Zuid 187	Karoo	0	118	118
		Allanridge	118	374	256
		Bothaville	374	479	105
		Rietgat	479	801	322
		Kameeldoorns	801	1376	575
		Klipriviersberg	1376	1987	611
		E.O.H.	1987		
Lekkerl.	Lekkerleven 308	Karoo	0	196	196
		Allanridge	196	467	271
		Bothaville	467	472	5
		Klipriviersberg	472	1207	735
		Witwatersrand	1207	1799	592
		E.O.H.	1799		
RB1	Roodebloem 344	Karoo	0	134	134
		Allanridge	134	193	59
		Bothaville	193	267	74
		Klipriviersberg	267	1501	1234
		Witwatersrand	1501	1981	480
		E.O.H.	1981		
SK1	Stukpan 435	Karoo	0	199	199
		Witwatersrand	199	1601	1402
		E.O.H.	1601		
SW1	Samara 856	Karoo	0	29	29
		Klipriviersberg	29	320	291
		Witwatersrand	320	1003	683
		E.O.H.	1003		
TE1	Teneriffe 33	Karoo	0	102	102
		Witwatersrand	102	1373	1271
		E.O.H.	1373		
UC11	Johannes Rust 529	Klipriviersberg	0	797	797
		Witwatersrand	797	990	193
		E.O.H.	990		
UC13	Jonkers Kraal 475	Klipriviersberg	0	717	717
		Witwatersrand	717	855	138
		E.O.H.	855		
UC15	Boschoek 466.	Klipriviersberg	0	573	573
		Witwatersrand	573	1830	1257
		E.O.H.	1830		
UC22	Taljaards Dam 86	Karoo	0	231	231
		Klipriviersberg	231	461	230
		Witwatersrand?	461	1077	616
		E.O.H.	1077		
UC55	Taljaards Dam 86	Karoo	0	187	187
		Allanridge	187	207	20
		Bothaville	207	292	85
		Rietgat?	292	418	126

Borehole	Farm	Stratigraphy	From	To	Thickness
		Kameeldoorns?	418	2217	1799
		E.O.H.	2217		
UC6	Avonds Rust 543	Klipriviersberg	0	551	551
		Witwatersrand	551	863	312
		E.O.H.	863		
UC9	Jonkers Kraal 475	Klipriviersberg	0	743	743
		Witwatersrand	743	839	96
		E.O.H.	839		
Vergenoeg	Vergenoeg 89	Karoo	0	174	174
		Transvaal	174	921	747
		Klipriviersberg	921	1355	434
		Witwatersrand	1355	2465	1110
		E.O.H.	2465		
WE8	Katbosch 583	Karoo	0	160	160
		Kameeldoorns	160	187	27
		Klipriviersberg	187	1027	840
		Witwatersrand	1027	1772	745
		E.O.H.	1772		
WV1	Weestevreden 269	Karoo	0	123	123
		Witwatersrand	123	907	784
		E.O.H.	907		
BOREHOLE DATA FROM VON BACKSTROM (1962)					
NOTE: The stratigraphy is interpreted.					
KCG1	Klippan 324	Allanridge	0	120	120
	X +2 982 000	Rietgat	120	251	131
	Y +63 500	Makwassie	251	415	164
	Z +1 425	Goedgenoeg	415	1082	667
		Dominion	1082	1336	254
		E.O.H.	1336		
KCG4	Klipfontein 311	Makwassie	0	974	974
	X +2 983 250	E.O.H.	974		
	Y +90 001	*Makwassie	0	1160	1160
	Z +1 475	*Garfield	586	1160	574
RF1	Rietfontein 284	Makwassie	0	964	964
	X +2 964 500	E.O.H.	964		
	Y +89 750	*Makwassie	0	1160	1160
	Z +1 525	*Garfield	255	1160	905
RF2	Rietfontein 284	Rietgat	0	207	207
	X +2 965 250	Makwassie	207	458	251
	Y +87 000	E.O.H.	458		
	Z +1 525	Makwassie	207	1260	1053
		Garfield	660	1260	600
VF10	Vlakfontein 315	Rietgat	0	278	278
	X +2 978 250	Makwassie	278	485	207
	Y +83 250	Basement	485	497	12

Borehole	Farm	Stratigraphy	From	To	Thickness
	Z +1 525	E.O.H.	497		
		*Garfield	354	485	131
VF13	Vlakfontein 315	Makwassie	0	35	35
	X +2 976 250	Basement	35	47	12
	Y +84 000	E.O.H.	47		
	Z +1 525				
BOREHOLE DATA FROM WHITESIDE (1970)					
HB1	Hart van Boomtuin (?)	Karoo	0	10	10
	X +3 003 000	Allanridge	10	380	370
	Y +49 000	Bothaville	380	580	200
	Z +1 300	Makwassie	580	1190	610
		Garfield	1050	1115	65
		Goedgenoeg	1190	2200	1010
		Kameeldoorns	2200	3065	865
		Witwatersrand	3065		
Note that the Kameeldoorns Fm. is interbedded with Goedgenoeg lavas and tuff and thus is actually part of the Goedgenoeg Fm. - this is the "Vaal Bend" unit of Whiteside (1970)					

APPENDIX C

WHOLE-ROCK GEOCHEMICAL DATA

SAMPLING METHODS

Samples were taken from the massive middle zones of recognized flow-units. In general, all visibly altered areas and zones were avoided, although samples were taken close to the facies contact zones to enable determination of geochemical change in these areas. More or less 20 cm of core (diameter 45 mm) were sampled and the core was split by diamond saw in order to leave a half-core sample in the core tray. In the light of extensive alteration of the Ventersdorp Supergroup, a hand specimen was kept of each geochemical sample in order to have a reference sample in case chemical analysis showed up an anomalous chemical composition. For the same reason, a thin section was prepared of each sample so that the influence of secondary alteration can be verified. Some flow units, e.g. borehole WS3, were sampled thoroughly, *i.e.* samples were taken from the welded basal zone, welded middle zone and amygdaloidal top zone, in order to determine the geochemical variations in a single flow unit. A total of 483 samples were taken from 21 boreholes and all were analyzed for major and trace elements.

SAMPLE PREPARATION

Due to the phenocryst-rich nature of the porphyries it was not possible to separate the phenocrysts from the groundmass for separate analyses, especially since numerous fragments of broken phenocrysts are hosted in the groundmass. In the case of non-porphyritic rocks, amygdaloidal-rich flow tops were avoided during sampling, but amygdales that were still present in samples were not removed for the same reason as above.

Samples were ground to -300 mesh in 2 rock crushers and a centrifugal crusher. Two of these crushers are constructed of cobalt-tungsten steel, while the third is made of carbon steel. Cobalt contamination of the samples may therefore influence the analyses.

ANALYTICAL TECHNIQUES

Whole rock geochemical analyses were processed on a PHILLIPS PW 1404 X-ray spectrometer by Dr W.A. van der Westhuizen of the Geochemistry Division at the Geology Department, University of the O.F.S. Major element analyses were executed on fused glass discs, using the technique of Norrish and Hutton (1969). Trace elements and Na were analyzed for on pressed power briquettes. Corrections were made for different matrices and for the spectral overlap. Loss at 110°C was determined and is reported as H₂O⁻. Loss on ignition at 1000°C was determined and is reported as L.O.I.

DATA PRESENTATION

The geochemical data is reported in this appendix without any corrections for volatile content, except for the Vryburg data set. In general, the analyses are very accurate due to low volatile content of the samples, as reflected in H₂O⁻ and L.O.I. (Loss On Ignition). All applications of the geochemical data in the dissertation, however, uses data recalculated to a 100% volatile-free basis.

The legend for each sample is:

BOREHOLE - The borehole from which the sample was taken.

FACIES - The formation and geochemical facies:

- Gm - Goedgenoeg Fm., basic facies
- Gi - Goedgenoeg Fm., intermediate facies
- Gs - Goedgenoeg Fm., low-Zr facies
- Gz - Goedgenoeg Fm., high-Zr facies
- Md - Makwassie Fm., dacitic facies
- Mr - Makwassie Fm., rhyolitic facies
- GF - Makwassie Fm., Garfield Member
- Mm - Makwassie Fm., interbedded mafic lava
- Ga - Goedgenoeg Fm., anomalously altered
- Ma - Makwassie Fm., anomalously altered
- Mx - Makwassie Fm., inclusion-rich zone (mixed lava)

DEPTH - The depth in metres, measured from the borehole collar or below surface, at which the sample was taken.

TOTAL - The major element total, including H₂O⁻ and LOI.

NOTE: Iron was analyzed as total Fe and is listed as Fe₂O₃.

B'hole	Facies	Depth	Sample	SiO2	TiO2	Al2O3	Fe2O3	MnO	MgO	CaO	Na2O	K2O	P2O5	H2O-	LOI	TOTAL	Zr	Y	Sr	Rb	Cu	Zn	Ni	Ba	Nb	V	Cr	Co
WS3	Gm	953	FVM001	56.55	1.20	14.16	8.22	0.15	4.03	5.75	3.27	2.49	0.53	0.02	3.11	99.48	398	53	550	60	25	157	62	945	18	172	144	29
WS3	Gm	952	FVM002	58.20	1.22	14.12	8.25	0.13	2.74	6.43	2.89	1.31	0.52	0.01	3.05	98.87	397	48	775	32	13	129	66	794	17	162	126	28
WS3	Gm	951	FVM003	57.93	1.19	13.82	8.09	0.15	3.49	6.22	3.50	1.71	0.53	0.02	3.00	99.65	392	50	650	42	42	136	61	751	18	166	136	30
WS3	Ga	950	FVM004	49.11	1.71	15.94	14.85	0.20	4.59	4.36	2.94	0.51	0.87	0.04	3.04	98.16	388	50	640	36	18	139	63	714	17	164	140	30
WS3	Ga	925	FVM005	59.97	0.72	13.56	9.15	0.10	4.50	1.63	0.14	5.90	0.12	0.11	2.88	98.78	201	34	114	139	38	113	176	3406	13	171	419	36
WS3	Ma	923	FVM006	49.28	1.61	14.42	13.33	0.22	7.27	4.39	2.42	0.08	0.85	0.11	3.66	97.64	236	43	268	6	25	158	160	68	13	245	377	48
WS3	Ma	921	FVM007	54.11	1.23	10.77	10.74	0.20	5.83	6.56	1.21	0.38	0.63	0.08	6.94	98.68	178	35	155	13	22	133	119	192	10	171	252	39
WS3	Ma	920	FVM008	51.13	1.66	14.79	11.38	0.17	5.98	3.86	1.94	1.15	0.84	0.13	4.16	97.19	306	50	192	30	21	156	129	528	17	221	319	41
WS3	Ma	919	FVM009	53.52	1.41	13.51	10.76	0.20	4.98	5.44	1.88	2.03	0.72	0.13	2.85	97.43	287	50	404	49	27	140	114	1056	16	192	255	36
WS3	Ma	918	FVM010	57.04	1.28	12.89	9.08	0.13	3.51	5.19	2.94	3.12	0.62	0.15	2.62	98.57	338	57	491	73	21	126	78	1586	20	151	163	28
WS3	Ma	917	FVM011	60.32	1.26	13.20	8.55	0.17	3.90	4.87	1.58	3.42	0.59	0.16	2.06	100.08	357	57	540	78	23	118	71	1517	19	141	144	24
WS3	Ma	915	FVM012	52.67	1.34	13.04	9.59	0.22	4.92	6.96	2.21	2.07	0.65	0.21	5.14	99.02	298	51	375	49	23	135	104	832	17	169	217	31
WS3	Mx	914	FVM013	60.03	1.15	13.43	7.94	0.13	2.59	6.71	2.42	2.45	0.53	0.18	2.39	99.95	417	59	1067	59	21	102	51	1105	21	126	94	20
WS3	Mx	912	FVM014	57.63	1.19	14.04	8.25	0.11	2.84	6.27	2.56	1.50	0.51	0.22	3.88	99.00	314	56	280	36	29	186	119	597	16	190	279	34
WS3	Mx	909	FVM015	55.19	1.49	14.46	10.91	0.19	4.61	4.80	2.65	1.49	0.74	0.13	1.79	98.45	400	58	473	74	34	122	33	1316	21	96	58	17
WS3	Mx	897	FVM016	64.95	1.08	12.87	6.70	0.11	3.07	3.46	2.13	2.77	0.44	0.16	1.98	99.72	418	58	402	61	7	111	32	1158	21	95	58	12
WS3	Mx	895	FVM017	65.50	1.09	13.24	6.92	0.11	2.58	3.34	2.65	3.00	0.45	0.02	1.83	100.73	403	60	419	66	15	104	32	1291	21	105	57	19
WS3	Mx	888	FVM018	63.63	1.09	12.84	6.80	0.13	1.76	3.44	3.37	3.36	0.46	0.03	2.22	99.13	424	63	403	73	14	106	29	1403	22	97	49	15
WS3	Mx	878	FVM019	66.92	1.10	13.18	5.67	0.10	1.79	2.00	2.29	4.03	0.46	0.05	1.41	99.00	423	61	62	169	11	95	31	1874	22	95	51	11
WS3	Mx	875	FVM020	62.51	1.08	12.64	6.23	0.10	1.82	4.50	3.20	3.80	0.47	0.17	3.33	99.85	474	70	195	117	8	97	37	1884	22	98	47	18
WS3	Mx	874	FVM021	61.48	1.23	14.77	7.95	0.04	3.92	2.63	2.93	1.18	0.54	0.08	2.71	99.46	447	62	1316	31	29	160	48	719	21	115	104	20
WS3	Mx	873	FVM022	62.33	1.03	12.74	6.92	0.14	1.63	7.34	2.61	0.23	0.44	0.10	2.18	97.69	449	55	180	18	9	75	37	107	20	113	65	16
WS3	Mm	867	FVM023	54.50	1.21	10.80	7.94	0.29	3.57	8.77	2.50	0.13	0.62	0.20	7.47	98.00	505	76	87	208	83	120	114	51	10	147	219	35
WS3	Mm	864	FVM024	62.90	1.04	12.37	6.65	0.11	2.10	3.66	3.10	3.09	0.44	0.12	4.62	100.20	474	65	291	61	23	215	150	170	14	232	343	51
WS3	Md	852	FVM025	64.32	1.07	13.41	7.61	0.10	3.30	2.30	0.69	3.82	0.43	0.35	3.21	100.61	407	54	283	81	3	116	20	916	23	103	35	13
WS3	Md	848	FVM026	64.11	1.14	14.63	5.77	0.11	2.76	1.94	2.55	2.55	0.47	0.24	2.21	98.48	440	57	307	79	6	103	19	649	24	103	35	14
WS3	Md	843	FVM027	66.51	1.06	13.29	5.96	0.08	1.57	6.22	2.38	0.68	0.43	0.23	1.46	99.87	395	60	277	29	8	113	18	214	23	101	35	11
WS3	Md	823	FVM028	66.04	1.09	13.44	5.76	0.11	3.26	1.82	6.32	0.45	0.44	0.15	1.65	100.53	422	57	1769	11	11	124	18	247	20	71	32	14
WS3	Mx	812	FVM029	60.74	1.29	15.15	6.75	0.10	2.86	2.13	0.64	5.38	0.53	0.12	2.79	98.48	192	52	173	9	10	115	18	1705	27	120	34	12
WS3	Mx	789	FVM030	63.40	1.11	14.38	6.12	0.10	2.25	2.31	3.61	1.36	0.45	0.19	2.00	97.28	267	48	128	25	6	115	18	432	23	98	33	11
WS3	Mx	783	FVM031	65.90	0.87	11.02	4.29	0.15	1.83	5.07	1.23	2.94	0.36	0.10	4.18	97.94	360	56	142	119	37	85	15	1138	17	71	30	9
WS3	Md	763	FVM032	66.27	1.14	12.78	5.98	0.07	1.13	2.43	2.15	4.84	0.45	0.05	2.00	99.29	454	64	213	159	6	98	17	2253	21	98	20	11
WS3	Md	760	FVM033	65.84	1.10	12.59	6.49	0.13	2.21	2.85	2.59	4.55	0.46	0.10	2.07	100.98	487	64	266	112	5	120	16	1727	23	99	23	10
WS3	Md	753	FVM034	65.94	1.08	12.72	5.98	0.14	1.44	3.03	2.12	3.71	0.46	0.09	2.25	98.96	461	63	321	102	14	106	16	1273	22	102	22	14
WS3	Md	711	FVM035	66.46	1.07	12.69	6.17	0.11	1.32	2.81	1.54	3.49	0.43	0.04	2.64	98.77	437	61	197	106	23	111	18	1265	22	105	30	12
WS3	Md	686	FVM036	68.42	1.00	12.14	5.28	0.07	0.82	2.53	3.02	3.18	0.43	0.09	2.19	99.17	431	58	171	98	3	107	16	1159	21	100	25	10
WS3	Mx	669	FVM037	62.93	0.85	9.32	9.98	0.01	0.47	3.18	1.15	2.88	0.35	0.07	6.64	97.83	350	52	144	88	20	48	16	1075	21	70	23	19
WS3	Md	641	FVM038	67.85	1.09	13.10	5.64	0.04	1.10	1.43	2.27	3.06	0.45	0.04	1.74	97.81	455	59	195	104	10	111	17	1777	21	109	25	10
WS3	Md	634	FVM039	68.72	1.19	13.14	4.58	0.04	1.19	1.61	0.28	5.31	0.49	0.06	2.11	98.72	473	66	114	162	5	109	15	3225	24	119	26	12

B'hole	Facies	Depth	Sample	SiO2	TiO2	Al2O3	Fe2O3	MnO	MgO	CaO	Na2O	K2O	P2O5	H2O-	LOI	TOTAL	Zr	Y	Sr	Rb	Cu	Zn	Ni	Ba	Nb	V	Cr	Co
WS3	Md	625	FVM040	65.70	1.22	13.15	8.12	0.11	2.62	1.63	0.70	3.65	0.50	0.03	2.43	99.86	454	57	137	114	0	169	20	2718	24	100	24	20
WS3	Md	597	FVM041	66.52	1.09	12.88	5.66	0.06	0.80	3.23	2.87	3.03	0.46	0.04	3.00	99.44	459	61	292	104	7	112	16	1538	22	101	22	9
WS3	Md	592	FVM042	71.10	1.03	11.65	4.28	0.07	0.79	2.48	1.43	2.91	0.42	0.06	2.28	98.50	450	54	196	100	3	83	14	1785	19	99	24	12
WS3	Md	578	FVM043	61.67	1.17	14.31	7.47	0.14	3.12	2.49	1.98	1.82	0.49	0.00	3.08	97.74	509	66	251	71	5	132	18	1285	24	116	26	15
WS3	Mx	528	FVM044	54.06	1.28	16.08	9.49	0.20	4.03	3.98	2.25	2.04	0.52	0.15	4.81	98.89	551	68	256	81	15	204	21	1143	27	124	28	18
WS3	Md	526	FVM045	63.95	0.95	12.31	7.75	0.17	3.78	3.25	0.81	1.85	0.39	0.11	4.15	99.47	374	57	139	80	10	139	18	1071	19	109	24	10
WS3	Md	509	FVM046	64.44	1.13	13.29	6.29	0.13	3.13	2.95	0.91	3.05	0.47	0.07	3.72	99.58	442	61	105	130	4	102	16	1483	22	118	24	9
WS3	Mx	500	FVM047	56.44	1.18	14.61	12.38	0.21	5.48	2.18	1.50	0.64	0.48	0.09	4.22	99.41	464	46	159	26	15	249	23	443	23	93	30	25
WS3	Md	477	FVM048	64.83	1.14	13.49	8.35	0.13	4.14	1.23	1.10	1.53	0.46	0.10	3.21	99.71	457	56	101	50	9	176	19	464	21	118	27	15
WS3	Md	466	FVM049	66.04	0.98	11.45	8.07	0.13	3.68	2.39	1.48	1.16	0.41	0.06	4.04	99.89	376	54	92	38	8	138	18	290	19	98	26	13
WS3	Mx	458	FVM050	72.23	0.90	10.14	5.68	0.10	2.58	2.24	0.00	2.28	0.38	0.08	3.61	100.22	414	48	47	69	59	166	17	487	17	92	24	11
WS4	Ga	749	FVM051	50.53	1.59	13.91	13.20	0.14	6.30	6.44	1.86	0.22	0.83	0.04	3.70	98.76	269	51	454	10	31	201	152	228	16	221	299	45
WS4	Ga	747	FVM052	54.75	1.60	12.72	10.52	0.18	5.13	5.61	3.12	0.21	0.83	0.01	3.07	97.75	285	50	487	9	27	130	139	162	15	202	295	37
WS4	Ma	746	FVM053	51.15	1.55	13.52	10.42	0.14	4.82	6.63	2.31	0.15	0.79	0.02	5.95	97.45	280	48	385	8	23	141	147	88	14	195	300	42
WS4	Ma	743	FVM054	54.13	1.48	17.31	8.99	0.00	3.98	2.59	0.84	7.16	0.63	0.01	3.02	100.14	558	87	225	219	17	184	20	3266	30	116	26	17
WS4	Ma	742	FVM055	69.82	0.98	11.01	5.12	0.07	2.32	1.72	0.25	5.66	0.40	0.03	1.85	99.23	379	51	102	178	7	87	16	1486	19	80	27	11
WS4	Ma	741	FVM056	57.18	1.55	17.44	6.76	0.10	2.62	2.44	1.21	5.53	0.63	0.10	2.31	97.87	661	95	310	269	8	117	20	3217	32	130	30	14
WS4	Md	728	FVM057	64.24	1.06	12.70	6.40	0.11	1.08	2.78	4.59	3.35	0.43	0.03	1.86	98.63	442	62	372	83	9	110	17	1218	21	96	31	13
WS4	Md	712	FVM058	65.07	1.10	13.13	7.05	0.10	2.14	2.00	2.04	3.09	0.46	0.06	1.91	98.15	458	62	346	75	8	145	20	1078	22	110	43	14
WS4	Md	693	FVM059	67.20	1.05	12.84	5.52	0.07	0.68	2.10	2.95	4.65	0.43	0.27	1.58	99.34	445	59	181	101	10	122	16	1594	22	94	24	11
WS4	Md	678	FVM060	63.89	1.12	14.28	6.80	0.11	2.13	1.72	6.23	0.19	0.46	0.05	1.76	98.74	482	62	146	7	14	123	16	78	23	101	32	17
WS4	Md	672	FVM061	63.65	1.17	13.75	6.63	0.11	3.05	1.88	2.26	2.09	0.48	0.09	2.08	97.24	477	70	251	101	7	110	17	832	22	112	29	17
WS4	Md	661	FVM062	68.41	0.94	11.28	5.65	0.11	1.68	2.78	1.66	3.46	0.39	0.05	2.57	98.98	374	55	207	144	10	91	16	1208	19	87	20	12
WS4	Md	650	FVM063	65.43	1.06	12.76	6.04	0.11	1.37	3.02	2.45	3.64	0.46	0.03	2.05	98.42	457	64	368	91	12	102	16	1117	22	98	25	11
WS4	Md	635	FVM064	65.38	1.11	12.64	6.19	0.11	1.80	2.49	2.47	3.47	0.48	0.08	2.02	98.24	457	64	311	78	16	115	17	1346	23	100	28	13
WS4	Md	619	FVM065	65.52	1.13	12.87	6.18	0.11	0.80	1.99	3.87	4.53	0.47	0.04	1.55	99.06	495	64	235	96	12	116	18	2127	23	106	26	14
WS4	Mx	614	FVM066	60.24	1.26	14.83	8.99	0.06	1.80	3.93	2.65	1.87	0.52	0.03	2.90	99.08	492	76	511	40	8	153	17	904	25	113	25	18
WS4	Mx	603	FVM067	69.66	0.88	10.39	7.16	0.14	2.63	1.79	1.69	1.77	0.35	0.05	2.33	98.84	366	48	167	83	11	104	15	539	17	84	34	17
WS4	Md	580	FVM068	66.35	1.14	12.92	6.60	0.13	2.21	3.14	3.38	1.01	0.46	0.04	2.15	99.53	474	68	422	39	10	221	18	590	23	103	29	12
WS4	Mx	583	FVM069	74.96	0.74	9.02	3.68	0.03	1.06	3.61	1.07	2.37	0.32	0.05	3.12	100.03	296	50	154	94	10	57	14	987	13	68	20	8
WS4	Mx	553	FVM070	68.11	0.89	11.47	5.25	0.11	2.28	2.49	0.60	4.88	0.37	0.05	2.90	99.40	337	50	93	166	40	80	14	1806	16	96	20	13
WS4	Md	538	FVM071	66.42	1.09	14.15	6.26	0.00	2.83	3.69	2.33	1.12	0.44	0.20	1.89	100.42	430	64	850	54	9	139	17	365	21	121	24	13
WS4	Md	506	FVM072	63.58	1.07	13.03	7.14	0.14	2.41	2.69	1.53	3.13	0.45	0.15	2.93	98.25	471	65	311	130	5	140	17	1660	22	88	26	14
WS4	Md	490	FVM073	64.02	1.16	13.69	6.66	0.14	2.20	4.57	3.81	0.88	0.48	0.20	1.87	99.68	479	67	1439	42	36	130	18	284	23	102	27	14
WS4	Md	467	FVM074	64.83	1.12	13.01	6.62	0.06	1.36	3.73	1.99	3.01	0.47	0.16	3.22	99.58	468	63	513	80	5	108	20	1144	22	100	27	13
WS4	Md	426	FVM075	65.43	1.05	12.74	5.95	0.10	1.10	3.30	2.75	3.32	0.46	0.12	2.84	99.16	421	61	474	88	10	112	17	1544	21	90	24	11
WS4	Md	380	FVM076	68.14	0.83	10.62	8.77	0.14	3.59	1.64	0.75	1.43	0.34	0.11	2.97	99.33	344	51	146	56	22	141	17	695	17	98	24	17
WS4	Mx	378	FVM077	53.55	1.47	18.12	7.80	0.10	3.04	2.95	1.48	4.05	0.61	0.10	4.00	97.27	570	81	297	155	7	131	17	1863	31	167	29	13
YYS1	Gm	1026	FVM082	58.74	1.21	14.20	8.08	0.10	2.91	6.36	2.79	1.66	0.57	0.21	2.83	99.66	377	49	621	37	23	105	63	698	16	167	144	25

B'hole	Facies	Depth	Sample	SiO2	TiO2	Al2O3	Fe2O3	MnO	MgO	CaO	Na2O	K2O	P2O5	H2O-	LOI	TOTAL	Zr	Y	Si	Rb	Cu	Zn	Ni	Ba	Nb	V	Cr	Co
YYS1	Gm	1020	FVM083	58.09	1.20	14.30	8.41	0.10	2.93	6.32	2.69	2.25	0.55	0.19	2.89	99.72	371	49	587	51	27	105	63	801	17	170	146	23
YYS1	Ga	994	FVM084	51.01	1.93	14.29	12.65	0.12	6.65	5.00	2.25	0.20	1.09	0.20	3.92	99.31	354	58	411	7	58	151	182	177	20	236	345	51
YYS1	Ma	987	FVM085	56.04	1.54	14.12	9.87	0.09	5.09	4.67	3.28	1.48	0.80	0.18	2.37	99.53	276	47	291	34	27	113	122	790	15	210	279	38
YYS1	Ma	983	FVM086	55.25	1.47	13.64	10.78	0.14	4.82	6.73	2.00	2.24	0.76	0.16	2.47	100.46	273	47	518	52	35	118	127	1187	15	210	279	38
YYS1	Mm	976	FVM087	48.65	1.60	14.48	13.37	0.17	5.38	5.50	2.36	0.53	0.81	0.26	5.57	98.68	244	46	188	19	33	132	147	444	15	233	314	51
YYS1	Ma	971	FVM088	51.11	1.57	13.84	12.50	0.15	4.86	5.10	2.67	0.45	0.81	0.26	4.79	98.11	258	47	181	18	41	130	138	509	15	223	305	44
YYS1	Mx	954	FVM089	63.48	1.06	13.79	7.28	0.10	0.89	8.58	2.53	0.69	0.49	0.20	1.31	100.40	459	62	2351	21	7	63	36	580	21	118	71	13
YYS1	Mm	931	FVM090	47.04	1.71	14.63	14.50	0.18	6.61	7.07	1.84	1.34	0.90	0.16	3.60	99.58	274	54	568	37	41	147	164	1426	15	240	326	47
YYS1	Mm	923	FVM091	56.39	1.37	13.02	10.03	0.12	4.05	6.29	2.76	0.80	0.71	0.23	3.30	99.07	308	50	462	22	27	120	112	588	16	174	256	35
YYS1	Md	913	FVM092	67.41	1.07	12.59	6.31	0.10	0.98	6.62	3.02	0.40	0.47	0.26	1.38	100.61	451	64	1743	22	2	113	15	148	21	93	25	14
YYS1	Md	901	FVM093	65.91	1.13	13.12	6.61	0.09	0.61	2.73	4.07	3.52	0.49	0.29	1.47	100.04	447	64	346	91	11	103	16	1151	23	102	25	12
YYS1	Md	854	FVM094	65.89	1.17	13.33	6.88	0.09	1.13	3.36	3.37	3.32	0.51	0.25	1.33	100.63	470	63	480	86	12	109	17	1496	23	106	26	14
YYS1	Md	840	FVM095	63.95	1.10	12.62	6.17	0.08	1.24	3.10	3.12	3.31	0.48	0.24	5.04	100.45	441	65	393	92	8	104	17	1632	22	97	23	13
YYS1	Md	801	FVM096	65.30	1.09	13.03	6.30	0.08	1.29	2.83	3.50	3.24	0.47	0.51	2.56	100.20	422	61	365	80	8	104	16	1246	22	99	25	13
YYS1	Md	770	FVM097	67.49	1.09	12.98	6.15	0.06	0.35	1.89	2.33	6.32	0.48	0.45	1.05	100.64	415	63	165	141	10	98	16	2664	23	90	25	13
YYS1	Md	741	FVM098	70.20	0.96	11.63	5.76	0.08	1.37	2.05	1.96	3.14	0.43	0.41	1.81	99.80	380	55	225	116	13	87	15	1165	18	95	25	14
SPP1	GF	1026	FVM101	54.20	1.25	14.37	10.10	0.12	3.71	7.86	2.63	0.92	0.58	0.41	3.64	99.79	254	45	1037	25	37	125	94	528	12	194	247	35
SPP1	GF	1008	FVM102	52.13	1.29	14.45	9.96	0.11	3.79	6.79	2.75	1.28	0.58	0.40	5.34	98.87	254	44	554	34	30	127	87	590	13	198	256	35
SPP1	GF	1002	FVM103	64.23	1.30	12.81	7.17	0.08	1.36	4.32	2.15	3.22	0.55	0.25	2.23	99.67	418	63	700	105	8	110	12	2596	21	122	15	12
SPP1	GF	993	FVM104	63.42	1.36	12.97	7.93	0.09	1.26	3.75	2.82	3.46	0.59	0.29	1.83	99.77	423	63	507	87	8	118	13	1370	20	127	14	13
SPP1	GF	987	FVM105	63.59	1.30	12.71	7.53	0.10	1.33	3.69	2.89	3.44	0.56	0.07	2.40	99.61	414	63	454	87	8	121	12	1561	19	125	15	15
SPP1	GF	982	FVM106	64.21	1.27	12.32	6.90	0.10	0.92	4.08	1.48	5.03	0.55	0.11	2.41	99.38	417	63	471	136	8	111	13	2345	20	114	16	14
SPP1	GF	978	FVM107	62.00	1.37	13.57	7.76	0.09	1.28	3.53	5.13	1.11	0.59	0.12	2.45	99.00	434	64	389	28	8	124	13	2541	19	120	15	14
SPP1	GF	975	FVM108	63.71	1.26	12.27	6.80	0.09	0.95	4.22	1.00	5.44	0.53	0.15	3.02	99.44	390	61	350	147	6	108	11	878	13	167	141	28
SPP1	GF	965	FVM109	57.71	1.06	14.77	8.69	0.12	3.05	5.40	3.08	2.18	0.44	0.14	2.93	99.57	293	38	626	56	21	104	49	698	13	153	135	27
SPP1	GF	958	FVM110	57.10	1.07	14.76	8.21	0.01	3.25	5.59	3.13	2.17	0.44	0.22	3.64	99.59	290	38	551	56	26	107	48	698	13	153	135	27
LLE1	Gm	3657	FVM114	56.13	1.03	13.90	10.29	0.12	5.81	5.49	2.97	1.51	0.45	0.07	1.85	99.62	203	35	429	37	61	119	118	1148	11	183	287	35
LLE1	Gm	3652	FVM115	55.59	1.05	13.80	10.08	0.13	5.86	4.95	3.04	1.38	0.48	0.11	1.97	98.44	208	36	372	36	40	121	123	1016	11	196	344	38
LLE1	Gs	3640	FVM116	66.88	1.15	12.73	6.31	0.08	0.77	3.53	3.00	3.79	0.49	0.06	0.69	99.48	401	59	482	112	7	105	12	1425	19	104	19	13
LLE1	Gs	3637	FVM117	65.88	1.18	13.01	6.69	0.07	0.94	3.14	4.47	3.21	0.50	0.10	0.56	99.75	417	60	348	9	6	109	12	1208	18	108	18	15
LLE1	Gs	3628	FVM118	65.58	1.17	12.89	6.63	0.12	1.27	3.28	3.63	3.43	0.47	0.04	0.56	99.07	413	60	363	96	8	112	13	1470	18	111	17	15
LLE1	Gs	3586	FVM119	65.61	1.21	13.02	6.89	0.10	1.13	3.25	3.68	3.82	0.51	0.14	0.61	99.97	410	61	333	125	9	113	12	1377	19	107	15	14
LLE1	Gs	3544	FVM120	65.55	1.24	12.74	7.24	0.09	1.77	2.34	2.83	3.94	0.51	0.24	1.35	99.84	417	57	228	106	9	134	12	2236	20	97	17	17
LLE1	Gs	3499	FVM121	65.52	1.24	12.88	7.02	0.09	1.10	3.19	4.00	3.68	0.51	0.08	0.72	100.03	419	61	307	113	9	114	12	1399	19	109	19	14
LLE1	Gs	3456	FVM122	67.02	1.16	12.60	6.81	0.11	1.72	2.53	4.81	1.82	0.45	0.12	0.80	99.95	388	53	263	89	5	123	13	867	16	108	19	15
LLE1	Gs	3412	FVM123	62.87	1.30	13.70	8.00	0.11	1.66	3.20	5.07	2.43	0.54	0.15	1.05	100.08	431	62	308	97	9	135	14	1147	19	124	19	16
LLE1	Gs	3358	FVM124	66.43	1.17	12.75	7.00	0.08	1.32	3.17	5.19	1.64	0.48	0.16	0.93	100.32	391	52	321	61	6	106	13	914	16	105	19	14
LLE1	Gs	3323	FVM125	65.08	1.23	13.20	7.30	0.01	1.20	3.83	3.86	3.69	0.51	0.13	1.01	101.05	409	59	351	119	9	111	13	1514	19	119	21	15
LLE1	Gs	3265	FVM126	64.16	1.20	13.45	7.37	0.11	1.26	3.93	3.86	3.15	0.52	0.16	0.90	100.07	408	59	378	101	7	113	12	1276	18	121	19	13

B'hole	Facies	Depth	Sample	SiO2	TiO2	Al2O3	Fe2O3	MnO	MgO	CaO	La2O	K2O	P2O5	H2O-	LOI	TOTAL	Zr	Y	Sr	Rb	Cu	Zn	Ni	Ba	Nb	V	Cr	Co
LLE1	Gs	3240	FVM127	64.74	1.25	13.18	7.27	0.09	1.21	3.72	3.68	3.43	0.51	0.13	0.79	100.00	416	60	355	111	8	113	13	1435	18	121	18	16
LLE1	Ga	3174	FVM128	60.26	1.36	14.64	8.52	0.13	1.76	3.84	5.95	1.33	0.57	0.29	1.52	100.17	457	57	364	107	4	148	15	492	19	135	18	18
LLE1	Gs	3116	FVM129	65.36	1.25	13.05	7.40	0.08	1.10	3.84	3.09	3.52	0.52	0.15	1.05	100.41	498	63	391	61	7	109	13	1368	18	118	18	14
LLE1	Gs	3060	FVM130	64.65	1.25	13.08	7.45	0.08	1.27	3.85	3.81	3.02	0.52	0.17	1.03	100.18	445	56	421	115	8	116	13	1271	18	127	19	18
LLE1	Gs	3048	FVM131	65.31	1.23	13.17	7.41	0.09	1.21	3.74	3.71	3.18	0.51	0.11	0.93	100.60	431	57	425	88	8	113	12	1515	20	123	20	15
LLE1	Gs	3022	FVM132	64.81	1.20	13.15	7.09	0.08	1.13	3.60	3.98	3.25	0.51	0.16	1.07	100.03	429	56	425	86	8	104	13	1395	20	116	18	15
LLE1	Gs	2984	FVM133	64.07	1.26	13.06	7.55	0.08	1.42	2.99	3.39	3.68	0.53	0.12	1.47	99.62	433	57	451	108	6	122	12	1449	20	121	16	16
LLE1	Ga	2928	FVM134	56.84	1.45	15.73	8.66	0.14	2.28	4.07	4.38	1.87	0.60	0.24	2.78	99.04	502	68	447	57	4	167	14	1181	24	122	20	19
LLE1	Ga	2890	FVM135	72.69	0.81	11.27	4.23	0.04	0.27	1.96	3.09	4.55	0.32	0.15	1.09	100.47	409	42	199	107	8	53	9	1683	14	56	15	8
LLE1	Gs	2872	FVM136	64.22	1.29	13.13	7.40	0.10	1.23	3.74	3.76	3.08	0.55	0.02	1.00	99.52	466	61	382	94	8	118	13	1340	20	127	16	15
LLE1	Gs	2845	FVM137	63.99	1.34	13.11	7.79	0.10	1.34	4.04	3.46	2.89	0.57	0.03	1.09	99.75	467	62	440	81	8	116	12	1377	20	133	15	18
LLE1	Gs	2814	FVM138	63.80	1.35	13.12	7.70	0.11	1.33	4.33	3.46	2.80	0.58	0.04	1.26	99.88	456	61	467	77	9	115	12	1319	20	134	15	16
LLE1	Gs	2771	FVM139	63.92	1.36	13.07	7.79	0.10	0.95	3.99	4.35	2.79	0.58	0.06	1.18	100.14	468	62	437	83	9	118	13	1372	20	136	15	17
LLE1	Gs	2722	FVM140	63.72	1.37	12.90	7.88	0.11	1.24	4.28	3.40	3.11	0.57	0.05	1.70	100.33	463	62	422	78	6	121	12	1409	20	129	16	16
LLE1	Gs	2689	FVM141	63.33	1.37	13.07	7.56	0.10	1.25	3.78	2.44	4.68	0.58	0.04	1.49	99.69	471	65	405	160	8	111	12	2624	21	129	14	16
LLE1	Ms	2599	FVM142	68.71	0.89	13.20	5.06	0.08	0.69	2.68	3.71	3.93	0.32	0.04	1.12	100.43	476	51	390	116	5	90	9	1400	17	74	18	8
LLE1	Ms	2566	FVM143	68.47	0.89	13.08	5.00	0.07	0.65	2.67	3.74	3.82	0.31	0.05	1.17	99.92	467	50	344	107	6	92	10	1427	17	71	16	9
LLE1	Ms	2571	FVM144	68.89	0.90	13.04	4.97	0.07	0.57	2.82	3.94	3.69	0.33	0.05	1.16	100.43	475	51	371	99	6	92	9	1320	18	72	15	9
LLE1	Ms	2514	FVM145	68.14	0.87	12.75	4.74	0.08	1.03	3.17	3.02	4.34	0.29	0.04	2.25	100.72	454	50	243	106	2	84	9	1381	18	70	15	10
LLE1	Ms	2478	FVM146	69.79	0.83	12.84	4.48	0.06	0.34	2.47	2.68	4.71	0.31	0.03	1.77	100.31	451	48	265	134	7	74	9	1420	17	67	14	8
LLE1	Ms	2429	FVM147	69.72	0.89	12.72	4.59	0.05	0.44	2.54	3.46	4.52	0.32	0.03	1.57	100.85	464	50	214	115	1	62	8	1426	17	74	15	9
LLE1	Ms	2387	FVM148	76.27	0.44	12.60	1.91	0.02	0.01	0.80	3.32	4.98	0.11	0.02	0.52	101.00	330	40	283	151	2	49	6	1362	17	20	13	8
LLE1	Ms	2316	FVM149	76.22	0.42	12.16	1.84	0.02	0.00	1.36	3.56	4.95	0.10	0.00	0.90	101.53	338	43	161	129	2	42	6	1129	16	19	12	7
LLE1	Ms	2251	FVM150	74.85	0.42	12.50	2.17	0.03	0.00	1.03	3.99	4.71	0.10	0.03	0.60	100.43	341	42	164	119	2	51	6	1271	17	21	13	6
LLE1	Ms	2207	FVM151	74.24	0.44	12.92	2.16	0.03	0.00	1.11	4.50	4.44	0.10	0.03	0.62	100.59	369	44	186	124	1	55	7	1346	18	22	13	6
LLE1	Ms	2154	FVM152	74.86	0.43	12.65	2.17	0.04	0.00	1.29	4.02	4.59	0.10	0.04	0.68	100.87	350	44	213	137	2	54	6	1369	17	21	13	7
LLE1	Ms	2112	FVM153	75.01	0.42	12.31	2.23	0.06	0.12	1.30	4.01	4.46	0.07	0.02	0.75	100.76	343	44	196	124	3	54	6	1403	18	20	13	6
LLE1	Ms	2070	FVM154	74.65	0.44	12.73	2.10	0.04	0.00	1.32	3.96	4.58	0.11	0.05	0.96	100.94	322	46	159	137	2	48	7	1318	18	22	13	8
LLE1	Ms	1999	FVM155	75.29	0.41	12.16	2.18	0.04	0.00	1.18	4.03	4.65	0.10	0.07	0.71	100.82	323	43	151	128	2	48	7	1347	17	23	13	7
LLE1	Ms	1974	FVM156	73.86	0.47	12.52	2.46	0.03	0.14	1.65	3.24	4.75	0.12	0.02	1.14	100.40	348	45	204	141	2	55	7	1425	18	28	15	6
LLE1	Ms	1928	FVM157	74.94	0.40	12.29	2.24	0.04	0.01	1.19	3.74	4.51	0.10	0.05	0.74	100.25	313	45	175	132	2	48	6	1287	18	22	14	6
LLE1	Ms	1875	FVM158	74.69	0.45	12.54	2.33	0.04	0.09	1.22	4.44	4.28	0.11	0.06	0.86	101.11	352	46	169	116	1	58	7	1213	18	23	14	5
LLE1	Ms	1832	FVM159	75.56	0.43	12.65	2.01	0.04	0.00	0.82	3.83	5.09	0.11	0.05	0.68	101.27	343	43	187	157	5	42	7	1426	19	22	13	7
LLE1	Ms	1798	FVM160	77.51	0.41	11.38	2.18	0.03	0.16	1.23	2.33	3.90	0.10	0.05	1.28	100.56	316	39	145	179	1	47	7	1255	16	28	14	6
LLE1	Ms	1755	FVM161	71.92	0.41	13.98	2.02	0.05	0.13	0.99	6.61	2.80	0.09	0.07	0.75	99.82	338	32	155	76	2	64	6	1232	18	20	12	6
LLE1	Ms	1747	FVM162	71.43	0.55	12.97	3.43	0.04	0.33	1.79	3.67	3.69	0.18	0.06	1.61	99.75	336	44	164	124	0	81	11	1369	18	50	21	10
LLE1	Ms	1741	FVM163	73.32	0.58	12.02	3.07	0.04	0.15	1.61	3.05	4.52	0.21	0.02	1.30	99.89	350	40	160	150	3	55	11	1368	17	46	24	11
LLE1	Ms	1735	FVM164	74.32	0.46	12.28	2.57	0.02	0.00	1.24	3.42	4.70	0.14	0.03	1.10	100.28	322	41	156	144	2	39	10	1342	17	38	20	8
LLE1	Ms	1720	FVM165	68.98	0.79	12.61	4.70	0.08	1.08	2.83	2.74	4.08	0.26	0.01	2.53	100.69	433	50	220	142	9	76	15	1408	19	85	29	10

Bhole	Facies	Depth	Sample	SiO2	TiO2	Al2O3	Fe2O3	MnO	MgO	CaO	Na2O	K2O	P2O5	H2O-	LOI TOTAL	Zr	Y	Sr	Rb	Cu	Zn	Ni	Ba	Nb	V	Cr	Co	
LLE1	Mr	1699	FVM166	71.96	0.79	12.25	4.02	0.03	0.34	1.89	4.25	3.85	0.31	0.00	1.25	100.94	436	48	116	86	12	57	14	1074	17	77	30	6
LLE1	Mm	1681	FVM167	54.68	1.34	13.84	10.16	0.14	6.36	5.39	2.71	1.13	0.61	0.03	3.74	100.13	251	42	615	19	24	119	141	1336	13	191	259	38
LLE1	Mm	1674	FVM168	53.30	1.12	11.37	10.63	0.15	8.84	7.05	1.13	1.66	0.49	0.03	3.95	99.72	203	38	419	35	37	119	303	789	11	194	950	48
LLE1	Mm	1655	FVM169	52.89	1.07	10.90	10.91	0.16	9.43	6.06	1.58	1.26	0.46	0.03	4.10	98.85	190	34	582	24	31	123	308	700	11	193	954	51
LLE1	Mm	1648	FVM170	54.03	0.96	9.69	11.93	0.06	12.99	5.34	1.06	1.33	0.42	0.03	3.80	101.64	160	26	245	48	25	126	422	340	7	187	1410	59
LLE1	Mm	1305	FVM171	55.96	1.27	13.69	9.59	0.01	3.96	6.43	2.80	0.94	0.59	0.03	4.19	99.46	252	40	750	25	30	108	85	454	12	195	199	28
LLE1	Ma	1296	FVM172	65.65	0.70	16.25	4.10	0.05	1.46	1.29	5.23	3.29	0.23	0.03	1.38	99.66	428	45	405	86	3	85	15	2171	22	57	27	7
LLE1	Mr	1287	FVM173	71.98	0.64	12.68	3.75	0.04	0.27	1.71	3.67	4.42	0.21	0.06	1.36	100.79	362	48	217	122	4	56	13	1398	19	55	27	8
LLE1	Mr	1221	FVM174	72.28	0.60	13.04	3.46	0.03	0.30	2.14	3.33	4.40	0.19	0.05	1.30	101.12	361	46	291	123	5	59	13	1389	18	48	24	7
LLE1	Mr	1169	FVM175	71.68	0.61	12.82	3.67	0.05	0.36	1.73	3.94	4.11	0.19	0.03	1.26	100.45	374	49	236	113	6	68	12	1335	19	50	23	7
LLE1	Mr	1133	FVM176	72.12	0.56	12.87	3.22	0.04	0.42	1.56	3.93	4.26	0.18	0.05	1.42	100.63	349	45	149	115	2	52	12	1343	18	46	24	6
LLE1	Mr	1101	FVM177	72.02	0.57	12.77	3.19	0.05	0.39	1.78	2.74	4.89	0.18	0.28	1.49	100.35	401	45	211	159	5	60	10	1538	19	45	22	7
LLE1	Mr	1061	FVM178	72.46	0.53	12.74	3.25	0.04	0.52	1.82	3.52	4.29	0.14	0.02	1.17	100.50	339	44	297	123	6	57	11	1257	18	44	21	5
LLE1	Mr	1008	FVM179	72.70	0.56	12.78	3.33	0.07	0.30	1.72	3.21	4.47	0.15	0.00	1.63	100.92	346	45	232	127	6	59	12	1342	18	47	22	6
LLE1	Mr	967	FVM180	72.81	0.57	12.49	3.24	0.05	0.31	1.39	3.21	4.67	0.16	0.08	1.15	100.13	372	46	217	142	7	55	12	1405	18	48	24	8
LLE1	Mr	929	FVM181	74.38	0.56	12.38	2.85	0.04	0.20	0.75	3.93	4.74	0.15	0.11	0.64	100.73	345	44	159	111	8	41	11	1208	17	47	24	8
LLE1	Mr	907	FVM182	71.73	0.55	12.43	3.34	0.06	1.67	1.22	3.88	4.50	0.15	0.13	1.06	100.72	352	45	170	108	12	73	11	1239	18	50	24	8
LLE1	Mr	900	FVM183	71.02	0.60	13.41	3.50	0.05	0.80	1.21	4.31	3.68	0.16	0.13	1.33	100.20	370	41	166	80	3	81	14	1498	20	58	27	9
LLE1	Mr	873	FVM184	73.22	0.58	12.34	3.07	0.06	0.78	1.16	2.48	5.65	0.15	0.18	1.13	100.80	368	43	133	130	3	26	10	2433	20	44	26	6
LLE1	GF	803	FVM185	54.84	1.62	13.05	10.85	0.13	5.54	6.05	1.37	1.35	0.76	0.08	3.78	99.42	365	53	540	28	38	136	126	757	18	200	275	43
LLE1	GF	782	FVM186	53.53	1.67	13.68	10.16	0.17	4.23	7.10	2.29	2.65	0.79	0.10	2.76	99.13	385	55	865	57	41	135	114	1427	19	196	282	35
LLE1	GF	774	FVM187	53.24	1.63	13.13	11.26	0.18	6.08	6.35	2.62	1.01	0.75	0.15	2.46	98.86	385	55	599	22	21	109	124	826	19	203	264	39
LLE1	GF	741	FVM188	53.64	1.50	13.19	10.45	0.15	5.05	7.29	1.67	2.65	0.68	0.13	2.92	99.32	356	53	705	58	34	127	119	1227	18	188	330	39
JWS7	Gm	550	FVM189	56.68	1.38	14.47	6.99	0.11	2.14	5.83	3.20	2.27	0.62	0.15	4.30	98.14	340	40	383	51	36	113	75	955	16	179	152	29
JWS7	Gm	549	FVM190	55.32	1.45	15.50	9.74	0.10	5.87	4.24	3.02	0.33	0.64	0.17	4.38	100.76	354	43	353	8	31	133	93	76	16	208	166	33
JWS7	Md	549	FVM191	63.96	1.16	13.01	6.79	0.10	1.26	2.18	3.18	3.68	0.48	0.16	1.80	97.76	539	61	323	76	8	120	17	1988	24	106	24	16
JWS7	Md	522	FVM191	63.96	1.16	13.01	6.79	0.10	1.26	2.18	3.18	3.68	0.48	0.16	1.80	97.76	539	61	323	76	8	120	17	1988	24	106	24	16
JWS7	Md	514	FVM192	64.66	1.13	13.10	6.85	0.09	2.90	2.56	4.03	3.28	0.46	0.24	2.01	101.31	474	60	268	63	10	114	17	2108	23	106	28	13
JWS7	Md	488	FVM193	66.32	1.05	13.29	5.56	0.10	0.95	5.90	3.62	0.50	0.43	0.15	1.78	99.65	444	61	1233	21	2	75	16	129	21	117	25	12
JWS7	Md	457	FVM194	66.59	1.13	12.84	6.74	0.09	1.68	3.09	3.23	3.35	0.46	0.23	2.03	101.46	493	61	439	67	8	110	17	1233	23	98	28	14
JWS7	Md	429	FVM195	64.99	1.08	12.78	6.29	0.09	1.48	2.97	2.95	3.47	0.46	0.21	2.16	98.93	475	61	456	74	8	107	16	1357	22	102	23	13
JWS7	Md	398	FVM196	68.62	1.06	13.37	6.69	0.08	2.14	1.71	5.66	0.28	0.42	0.17	1.71	101.81	461	49	228	4	5	98	18	117	20	88	25	14
JWS6	Md	501	FVM199	68.45	0.97	12.42	5.72	0.08	1.10	6.33	2.16	1.32	0.40	0.15	1.55	100.65	426	57	2416	39	3	86	15	722	21	88	25	15
JWS6	Md	486	FVM200	67.85	1.09	13.12	5.83	0.06	1.07	1.63	1.44	7.23	0.44	0.17	1.21	101.14	498	58	262	140	9	98	15	3951	24	86	26	9
JWS6	Md	477	FVM201	68.58	1.03	12.14	5.66	0.09	1.80	5.70	2.15	1.24	0.43	0.19	2.63	101.64	478	56	1439	43	12	97	15	392	20	74	22	12
JWS6	Md	459	FVM202	68.65	1.07	12.37	6.10	0.10	1.05	5.61	2.92	0.75	0.44	0.17	1.83	101.06	430	60	1903	28	4	99	16	259	21	93	23	14
JWS6	Md	424	FVM203	67.33	1.06	13.70	5.55	0.08	1.22	5.20	3.42	0.94	0.44	0.15	1.62	100.71	464	62	1280	37	3	78	17	249	21	111	25	12
JWS6	Md	411	FVM204	67.99	1.06	12.70	5.88	0.09	1.68	5.30	3.35	0.39	0.44	0.21	1.37	100.46	442	60	1987	14	3	86	14	119	21	104	25	10
JWS6	Md	392	FVM205	69.13	1.05	12.47	5.75	0.11	1.45	5.47	2.61	0.98	0.44	0.14	1.84	101.44	448	60	1790	40	4	83	15	244	21	101	23	10
JWS6	Md	344	FVM206	65.15	1.11	14.19	6.11	0.08	1.90	2.60	6.66	0.14	0.45	0.21	2.25	100.85	476	51	167	0	2	98	16	72	20	86	25	13

B'hole	Facies	Depth	Sample	SiO2	TiO2	Al2O3	Fe2O3	MnO	MgO	CaO	Na2O	K2O	P2O5	H2O-	LOI	TOTAL	Zr	Y	Sr	Rb	Cu	Zn	Ni	Ba	Nb	V	Cr	Co
JWS6	Md	311	FVM207	65.81	1.13	13.82	6.79	0.11	2.72	1.98	4.96	0.51	0.46	0.19	2.08	100.56	472	58	318	11	2	123	18	340	21	94	26	17
JWS8	Md	581	FVM209	66.71	1.04	12.76	5.76	0.09	1.25	5.76	1.70	2.31	0.43	0.14	1.51	99.46	444	59	1366	56	3	99	15	956	22	89	22	12
JWS8	Mx	560	FVM210	61.32	1.20	15.12	7.01	0.11	2.13	1.87	6.10	0.56	0.49	0.28	1.78	97.97	574	61	153	5	20	152	19	174	24	92	25	15
JWS8	Md	533	FVM211	68.29	1.00	12.20	6.00	0.09	0.78	6.02	1.95	1.75	0.42	0.03	1.39	99.92	448	59	1867	46	6	91	15	958	21	91	22	12
JWS8	Md	502	FVM212	66.22	1.06	12.93	6.22	0.10	2.12	2.27	3.00	3.54	0.42	0.05	1.97	99.90	452	59	322	72	11	105	16	1259	21	103	23	12
JWS8	Md	470	FVM213	64.22	1.13	13.41	6.58	0.10	0.66	2.37	3.34	4.26	0.46	0.03	1.76	98.32	459	62	253	87	5	118	16	1538	23	109	29	13
JWS8	Md	446	FVM214	67.23	1.04	12.66	5.67	0.09	0.72	5.93	3.24	0.82	0.43	0.05	1.33	99.21	426	62	2422	29	7	78	15	353	21	97	25	12
JWS8	Md	426	FVM215	66.24	1.05	13.10	6.02	0.09	0.75	4.18	3.46	1.26	0.43	0.04	2.49	101.11	473	60	870	50	7	105	15	262	20	93	24	12
ZH1	Md	1554	FVM216	64.44	1.04	12.59	5.87	0.10	0.87	3.70	2.08	4.56	0.39	0.03	3.59	99.26	448	54	302	138	3	96	10	1545	17	100	14	11
ZH1	Md	1532	FVM217	64.82	1.06	12.53	5.96	0.10	1.33	3.44	3.16	3.63	0.39	0.02	2.96	99.40	446	54	322	98	6	134	11	1283	17	106	18	14
ZH1	Md	1540	FVM218	66.91	1.05	12.49	5.06	0.09	1.36	2.74	1.40	5.86	0.41	0.03	2.83	100.23	417	47	174	137	2	134	11	1480	17	96	16	4
ZH1	Mr	1439	FVM219	73.67	0.42	12.53	1.94	0.05	0.12	1.15	2.57	6.12	0.08	0.06	1.36	100.07	344	42	111	150	1	48	5	1228	17	22	12	6
ZH1	Mr	1406	FVM220	73.95	0.45	12.03	2.35	0.05	0.91	0.81	1.47	7.05	0.09	0.04	1.05	100.25	373	45	132	182	3	57	6	1638	18	23	14	6
ZH1	Mr	1374	FVM221	74.72	0.42	12.17	2.25	0.05	0.64	1.00	3.12	5.06	0.08	0.03	1.25	100.79	350	43	155	146	1	55	6	1228	17	22	12	6
ZH1	Mr	1323	FVM222	75.05	0.39	11.54	1.86	0.05	0.21	0.97	2.25	6.04	0.07	0.04	1.05	99.52	329	40	164	165	1	51	5	1367	16	17	12	5
ZH1	Mr	1289	FVM223	74.43	0.43	12.10	2.05	0.04	0.29	0.99	1.86	6.60	0.08	0.09	1.35	100.31	356	43	129	177	2	62	7	1490	17	22	11	5
ZH1	Mr	1242	FVM224	72.66	0.47	12.61	2.60	0.04	0.28	1.23	3.27	2.99	0.08	0.10	1.95	98.28	383	42	107	132	1	45	6	686	16	30	11	5
ZH1	Mr	1200	FVM225	71.37	0.51	11.98	2.72	0.05	0.38	1.55	1.31	6.95	0.13	0.13	1.78	98.86	376	43	104	176	2	50	8	1350	17	37	16	5
ZH1	Mr	1181	FVM226	75.79	0.38	11.97	2.04	0.03	1.13	0.69	2.54	5.69	0.06	0.14	1.04	101.50	320	52	89	154	2	47	6	1185	18	23	13	6
ZH1	Mr	1095	FVM227	72.90	0.36	11.98	1.82	0.06	0.66	1.75	1.19	6.98	0.06	0.12	1.87	99.75	297	49	81	211	2	80	5	1243	18	19	14	8
ZH1	Mr	1067	FVM228	75.81	0.36	11.81	1.60	0.04	1.54	1.21	1.39	6.55	0.06	0.16	1.45	101.98	282	43	85	206	4	43	6	1338	17	18	13	7
ZH1	Mr	1039	FVM229	74.87	0.36	11.93	1.90	0.04	0.60	1.09	3.44	4.39	0.06	0.17	1.38	100.23	299	42	77	139	2	78	7	872	17	23	13	4
ZH1	Mr	982	FVM230	72.83	0.34	11.37	1.75	0.04	0.72	1.07	0.91	7.10	0.06	0.17	1.42	97.78	287	46	69	213	1	42	5	1250	18	17	12	6
ZH1	Mr	951	FVM231	77.11	0.37	11.56	1.39	0.03	0.33	0.26	0.23	8.61	0.07	0.22	0.86	101.04	283	36	52	243	1	50	5	1451	18	19	14	4
ZH1	Mr	923	FVM232	79.32	0.34	10.95	2.48	0.04	1.36	0.42	1.53	3.12	0.05	0.16	1.72	101.49	271	32	55	186	0	62	6	619	15	27	15	7
ZH1	Mr	893	FVM233	59.00	1.23	13.35	8.04	0.12	2.82	4.03	1.84	3.49	0.52	0.14	4.73	99.31	437	51	152	112	6	142	87	1154	18	170	218	28
ZH1	GF	819	FVM234	56.11	1.29	14.07	8.31	0.15	3.17	4.70	1.60	3.11	0.54	0.20	5.51	98.76	466	42	131	133	6	156	93	983	18	179	218	17
ZH1	GF	868	FVM235	57.65	1.24	13.53	7.53	0.13	3.26	4.86	1.31	2.98	0.51	0.18	5.74	98.92	475	47	132	146	14	139	82	927	19	170	206	19
ZH1	GF	848	FVM236	58.31	1.16	13.09	5.44	0.11	2.17	5.95	1.84	3.31	0.43	0.15	6.55	98.51	498	54	151	161	4	105	34	884	20	126	89	12
ZH1	Mr	775	FVM237	69.85	0.61	12.24	3.52	0.05	1.66	2.21	0.44	6.19	0.18	0.21	3.23	100.39	366	48	79	201	1	101	12	1407	18	58	23	7
ZH1	Mr	746	FVM238	68.54	0.56	12.11	3.48	0.04	1.08	2.56	0.09	6.82	0.17	0.17	3.10	98.72	355	43	63	228	3	77	12	1591	18	44	22	9
ZH1	Mr	733	FVM239	70.75	0.62	12.19	3.89	0.08	1.80	1.90	0.25	5.69	0.18	0.30	3.12	100.77	342	45	57	202	1	107	12	1285	18	56	22	6
ZH1	Mr	716	FVM240	69.29	0.68	12.97	3.81	0.06	1.29	1.67	0.80	6.10	0.20	0.29	2.66	99.82	411	56	66	198	4	93	13	1420	20	59	25	6
ZH1	Mr	689	FVM241	70.19	0.62	12.06	3.15	0.08	1.65	2.38	0.09	6.60	0.19	0.29	3.30	100.60	346	39	64	203	3	110	11	1368	18	54	25	7
ZH1	Mr	663	FVM242	73.09	0.59	11.83	3.09	0.05	2.34	0.54	0.07	6.94	0.16	0.25	1.73	100.68	355	39	37	190	2	128	11	1264	19	56	24	4
ZH1	Mr	627	FVM243	74.33	0.62	12.30	2.60	0.04	1.12	0.56	0.07	6.59	0.17	0.24	1.88	100.52	373	47	29	208	3	73	12	1146	19	51	23	6
ZH1	Mr	595	FVM244	70.28	0.64	12.71	2.91	0.07	1.41	1.91	0.09	6.85	0.19	0.20	2.96	100.22	362	53	54	215	2	75	11	1265	19	58	23	4
ZH1	Mr	576	FVM245	72.46	0.62	12.57	3.55	0.05	2.02	0.65	0.08	6.83	0.18	0.24	2.11	101.36	363	55	40	194	2	71	12	1228	19	59	27	2
ZH1	Mr	520	FVM246	67.92	0.68	13.12	4.85	0.09	3.29	1.54	0.34	4.00	0.18	0.09	3.93	100.03	402	41	42	195	0	166	17	805	19	61	22	8

B'hole	Facies	Depth	Sample	SiO2	TiO2	Al2O3	Fe2O3	MnO	MgO	CaO	Na2O	K2O	P2O5	H2O-	LOI TOTAL	Zr	Y	Sr	Rb	Cu	Zn	Ni	Ba	Nb	V	Cr	Co	
ZH1	Mr	494	FVM247	69.32	0.65	13.36	3.24	0.08	2.19	2.13	0.58	4.47	0.18	0.14	3.98	100.32	381	51	53	205	1	64	12	825	16	59	23	7
ZH1	Mr	463	FVM248	71.11	0.61	12.92	5.46	0.06	2.44	0.36	0.04	4.51	0.18	0.23	2.81	100.73	371	34	25	173	2	129	15	855	18	68	25	9
ZH1	Mr	1455	FVM249	74.57	0.44	12.11	2.28	0.04	0.17	0.80	2.27	5.86	0.07	0.20	1.38	100.19	371	42	118	150	3	46	6	1699	17	23	13	6
ZH1	Mr	1144	FVM250	74.80	0.47	13.19	2.68	0.04	0.74	0.53	3.11	3.16	0.08	0.17	1.79	100.76	359	41	108	172	4	53	16	888	20	38	13	6
ZH1	Mr	1133	FVM251	77.16	0.35	11.43	1.49	0.03	0.34	0.68	0.34	7.74	0.06	0.17	1.25	101.04	285	40	74	232	0	55	5	1927	17	17	15	5
SYF1	Md	614	FVM266	65.72	1.11	13.00	6.55	0.09	0.84	2.32	3.22	3.83	0.44	0.15	2.08	99.35	510	63	199	98	13	117	17	1226	23	102	24	9
SYF1	Mx	588	FVM267	62.63	1.26	14.03	7.47	0.12	1.67	4.18	3.01	1.54	0.51	0.09	2.15	98.66	559	72	1417	63	12	138	20	541	25	116	33	12
SYF1	Mx	575	FVM268	58.92	1.34	15.93	8.65	0.09	1.71	2.03	3.96	2.25	0.54	0.09	2.00	97.51	618	78	337	109	2	161	19	756	26	119	39	18
SYF1	Mx	562	FVM269	48.79	1.37	16.99	16.11	0.22	3.95	2.14	2.34	1.23	0.54	0.11	3.65	97.44	528	72	411	53	12	297	21	627	27	125	38	25
SYF1	Md	554	FVM270	66.80	1.02	12.36	5.60	0.09	1.50	2.95	1.00	5.19	0.41	0.08	2.62	99.62	452	64	291	176	9	105	18	1580	21	91	24	10
SYF1	Md	508	FVM271	67.34	0.76	9.45	5.06	0.12	1.40	6.12	0.37	4.03	0.32	0.08	5.07	100.12	362	39	443	131	40	87	16	1458	17	69	24	7
SYF1	Md	491	FVM272	64.72	1.04	12.74	5.95	0.08	0.84	3.33	1.82	5.47	0.42	0.08	2.77	99.26	476	62	298	118	9	137	16	1880	22	98	26	11
SYF1	Md	481	FVM273	67.44	1.05	12.74	4.81	0.06	0.40	2.87	2.43	4.79	0.42	0.07	2.32	99.40	473	58	298	146	9	57	13	2272	22	93	24	11
SYF1	Md	440	FVM274	65.54	1.08	12.89	6.17	0.09	0.77	3.00	3.10	3.47	0.44	0.16	2.54	99.25	493	60	277	80	2	112	16	1649	22	98	24	8
SYF1	Md	424	FVM275	66.82	1.02	12.57	5.78	0.09	0.88	2.86	2.50	3.23	0.40	0.19	2.74	99.08	466	54	170	83	14	115	16	1658	21	101	24	12
SYF1	Md	420	FVM276	64.47	1.02	12.62	5.97	0.10	0.99	3.90	1.97	3.82	0.41	0.16	3.72	99.15	438	58	170	83	6	122	16	2131	22	96	24	9
SYF1	Md	415	FVM277	66.68	1.00	12.24	5.44	0.09	0.95	3.26	1.56	3.93	0.40	0.17	3.13	98.85	432	58	133	92	5	125	15	2162	21	91	24	11
SYF1	Mx	399	FVM278	55.70	1.31	15.69	10.76	0.12	2.88	3.05	2.09	2.16	0.53	0.09	3.79	98.17	547	65	219	76	4	212	21	1117	28	123	29	24
DF1	Md	640	FVM283	66.14	1.04	12.77	6.33	0.08	2.92	2.40	1.52	2.60	0.42	0.25	2.54	99.01	437	62	316	111	9	116	19	1374	21	104	33	13
DF1	Md	633	FVM284	67.68	1.01	12.62	6.02	0.09	1.00	5.61	3.48	1.08	0.41	0.14	1.23	100.37	445	61	1755	27	7	65	19	583	20	97	37	15
DF1	Md	625	FVM285	65.82	1.05	12.63	6.05	0.09	1.02	3.03	2.97	3.87	0.42	0.02	2.10	99.07	468	58	323	93	6	95	21	1410	21	96	38	12
DF1	Md	602	FVM286	64.87	1.03	12.60	6.19	0.09	1.44	3.18	3.12	3.24	0.41	0.06	2.19	98.42	454	58	377	74	8	108	20	1275	20	97	44	10
DF1	Md	586	FVM287	65.42	1.05	12.90	5.92	0.09	1.23	3.10	3.28	3.51	0.41	0.04	2.29	99.24	453	58	356	79	22	106	18	1423	20	94	31	11
DF1	Md	571	FVM288	67.92	0.97	12.71	5.28	0.09	0.54	7.22	4.14	0.09	0.39	0.04	1.35	100.74	403	61	2900	3	14	49	17	82	20	85	35	11
DF1	Md	567	FVM289	64.44	1.03	13.01	5.08	0.09	1.46	4.56	2.82	2.25	0.41	0.08	2.73	97.96	460	61	1173	76	27	97	19	2639	22	94	28	12
DF1	Mx	560	FVM290	56.65	1.31	15.73	7.75	0.09	1.82	4.64	1.42	3.91	0.54	0.05	4.11	98.02	569	69	351	190	24	95	20	1389	27	120	29	12
DF1	Md	558	FVM291	69.07	1.02	12.34	4.93	0.09	0.61	6.75	3.63	0.26	0.42	0.07	1.06	100.25	434	60	2323	9	56	52	15	111	21	94	31	6
DF1	Md	554	FVM292	68.50	1.02	12.89	5.03	0.07	0.43	2.28	1.53	5.70	0.42	0.06	1.71	99.64	454	56	188	142	7	90	17	2236	21	94	25	14
DF1	Md	531	FVM293	63.29	1.18	13.95	7.29	0.09	2.27	2.57	2.17	2.77	0.48	0.08	2.43	98.57	487	64	370	113	5	129	19	1144	23	113	25	14
DF1	Md	524	FVM294	62.95	1.11	13.24	6.42	0.10	1.76	3.31	2.03	3.12	0.44	0.06	3.17	97.71	507	61	222	130	12	106	18	987	22	107	27	10
DF1	Md	515	FVM295	65.74	1.06	12.64	6.19	0.09	0.55	3.23	2.88	3.78	0.42	0.06	2.32	98.96	474	58	368	92	6	105	17	1400	20	101	21	14
DF1	Md	461	FVM296	66.66	1.07	12.56	6.12	0.08	0.66	2.44	1.82	5.26	0.43	0.10	1.80	99.00	484	60	304	114	11	100	18	2152	22	98	28	14
DF1	Md	441	FVM297	65.44	1.01	12.92	6.48	0.09	1.63	2.48	2.52	3.39	0.41	0.05	2.14	98.56	463	52	403	79	13	115	20	1516	20	95	45	15
DF1	Md	419	FVM298	65.59	1.07	12.70	6.93	0.09	1.38	2.92	2.57	3.40	0.42	0.03	2.55	99.65	485	57	342	79	11	123	18	1332	21	95	26	11
DF1	Md	397	FVM299	64.86	1.04	12.61	6.37	0.09	1.23	3.42	2.67	3.16	0.42	0.07	2.90	98.84	429	57	288	77	8	119	18	1182	21	103	40	14
DF1	Md	361	FVM300	64.68	1.09	12.81	6.26	0.09	1.13	3.56	2.11	3.32	0.45	0.06	3.34	98.90	461	61	208	90	18	107	17	1484	22	108	33	9
DF1	Md	346	FVM301	65.44	1.05	12.98	5.92	0.08	1.07	3.12	2.05	3.40	0.41	0.06	3.20	98.78	465	53	145	94	4	100	17	1870	21	110	35	8
DF1	Md	330	FVM302	64.44	1.06	12.56	6.35	0.10	1.02	4.04	1.94	3.15	0.43	0.05	3.92	99.06	456	58	208	84	21	111	19	1238	21	99	29	13
DF1	Md	313	FVM303	66.01	1.07	12.83	5.34	0.09	1.11	3.61	1.59	3.28	0.43	0.06	3.89	99.31	463	59	119	95	12	100	17	1639	21	103	37	10

B'hole	Facies	Depth	Sample	SiO2	TiO2	Al2O3	Fe2O3	MnO	MgO	CaO	Na2O	K2O	P2O5	H2O-	LOI	TOTAL	Zr	Y	Sr	Rb	Cu	Zn	Ni	Ba	Nb	V	Cr	Co
DF1	Md	297	FVM304	65.10	1.01	12.19	5.07	0.10	1.19	4.74	1.15	3.19	0.40	0.07	5.30	99.51	448	52	99	88	7	83	15	1064	20	94	33	10
DF1	Mx	283	FVM305	61.91	1.36	16.50	5.12	0.07	1.64	2.84	0.98	4.71	0.57	0.08	4.10	99.88	595	79	116	162	21	66	17	1155	27	135	50	13
DHK1	Gm	1987	FVM307	56.02	1.13	14.04	8.03	0.15	3.49	5.77	2.81	2.48	0.46	0.06	3.78	98.22	267	36	343	59	7	118	66	765	12	160	181	26
DHK1	Gm	1973	FVM308	57.03	1.15	14.18	9.22	0.16	3.88	4.09	1.94	3.77	0.45	0.03	2.79	98.69	349	45	287	100	6	96	55	1910	15	160	142	28
DHK1	Gm	1971	FVM309	56.83	1.14	14.24	8.61	0.16	4.08	4.17	2.17	3.51	0.46	0.03	3.12	98.52	322	41	234	95	6	118	55	1965	13	160	148	31
DHK1	Gm	1927	FVM310	54.71	1.17	13.75	9.95	0.19	5.61	4.58	1.71	4.15	0.52	0.07	2.23	98.64	240	41	333	106	24	150	132	2963	13	189	401	35
DHK1	Gm	1920	FVM311	54.20	1.14	13.58	10.31	0.22	4.99	5.05	1.79	2.39	0.49	0.00	3.26	97.42	236	40	373	73	22	207	122	4684	13	194	431	38
DHK1	Gz	1894	FVM312	63.22	1.37	12.95	8.21	0.09	1.27	3.18	2.81	4.04	0.51	0.03	1.55	99.23	645	66	279	92	5	91	17	1886	22	129	19	13
DHK1	Gz	1906	FVM313	64.62	1.36	13.11	7.68	0.10	0.95	3.55	3.79	2.43	0.49	0.06	1.42	99.56	644	65	379	58	6	69	17	1270	22	131	22	10
DHK1	Gz	1864	FVM314	64.77	1.36	13.42	7.88	0.14	1.11	3.62	3.87	3.51	0.51	0.06	1.00	100.25	633	66	454	90	7	248	16	1591	22	119	19	13
DHK1	Gz	1854	FVM315	63.30	1.32	13.14	8.00	0.14	1.48	3.25	2.74	4.66	0.48	0.26	1.26	100.03	643	68	383	116	5	173	14	2235	23	117	20	14
DHK1	Gz	1840	FVM316	62.68	1.40	13.09	7.65	0.11	1.54	3.26	2.90	4.28	0.52	0.24	1.61	99.28	643	67	260	94	5	155	17	1540	23	120	18	12
DHK1	Gz	1813	FVM317	61.14	1.36	12.94	7.70	0.11	1.68	4.77	2.64	3.74	0.51	0.24	2.50	99.33	636	67	374	80	5	153	16	1337	22	116	19	13
DHK1	Gz	1794	FVM318	63.91	1.35	13.16	7.48	0.10	1.44	3.12	3.06	3.90	0.48	0.24	1.34	99.58	651	64	288	82	9	153	18	1541	22	115	20	13
DHK1	Gz	1771	FVM319	63.33	1.31	13.02	7.56	0.10	1.54	3.97	3.34	3.23	0.48	0.24	1.89	100.01	639	62	340	70	5	154	15	1021	21	115	17	11
DHK1	Gz	1749	FVM320	63.02	1.31	13.25	8.10	0.11	1.50	3.34	2.75	3.90	0.49	0.18	1.65	99.60	658	64	266	86	5	170	17	1462	22	120	18	13
DHK1	Gz	1736	FVM321	64.49	1.32	12.87	6.79	0.13	1.41	4.77	2.40	3.35	0.48	0.15	1.67	99.83	632	65	438	73	7	163	15	1299	21	123	18	16
DHK1	Gz	1705	FVM322	65.09	1.33	13.29	6.71	0.11	1.20	3.48	4.10	2.28	0.48	0.16	1.53	99.76	654	66	319	48	30	160	24	1066	21	121	21	14
DHK1	Gz	1684	FVM323	62.98	1.26	12.81	7.50	0.11	1.30	4.17	3.24	3.38	0.45	0.15	2.19	99.54	631	64	306	77	4	155	14	1321	21	116	17	11
DHK1	Gz	1668	FVM324	62.92	1.27	12.86	7.01	0.10	1.22	4.31	3.53	3.21	0.46	0.18	2.34	99.41	624	62	302	77	5	141	14	1462	20	112	19	12
DHK1	Gz	1647	FVM325	63.62	1.30	12.86	6.68	0.11	1.17	4.28	4.05	2.19	0.46	0.18	2.18	99.08	626	60	263	52	6	157	17	1128	21	115	18	9
DHK1	Gz	1620	FVM326	63.24	1.28	12.91	7.35	0.11	1.11	3.59	3.30	3.83	0.46	0.08	2.04	99.30	637	65	227	88	14	147	16	1634	22	117	19	9
DHK1	Gz	1600	FVM327	63.69	1.24	12.79	7.08	0.10	1.20	3.46	3.03	4.06	0.46	0.06	1.98	99.15	637	65	246	95	8	185	14	1664	21	113	14	12
DHK1	Gz	1585	FVM328	64.31	1.24	12.73	6.90	0.10	0.85	3.38	3.53	3.59	0.45	0.08	1.87	99.03	620	62	245	80	10	158	16	1514	20	115	18	9
DHK1	Gz	1572	FVM329	63.52	1.29	12.69	7.25	0.13	1.16	3.69	3.03	3.94	0.47	0.06	2.21	99.44	634	64	250	92	5	190	14	1785	21	114	18	13
DHK1	Gz	1538	FVM330	64.75	1.31	12.90	7.16	0.12	1.15	3.26	3.39	3.49	0.47	0.05	1.33	99.38	647	64	249	76	6	160	16	1479	21	121	18	12
DHK1	Gz	1525	FVM331	66.19	1.32	12.66	6.47	0.10	1.07	2.25	3.39	3.80	0.48	0.05	1.33	99.11	646	63	186	82	5	129	17	1491	21	120	21	13
DHK1	Gz	1510	FVM332	63.96	1.27	13.05	7.05	0.12	1.23	3.17	2.36	4.84	0.46	0.04	2.32	99.87	632	64	157	115	4	123	16	1861	21	121	17	11
DHK1	Gz	1498	FVM333	62.82	1.29	12.89	7.59	0.14	1.53	3.35	2.10	4.10	0.47	0.04	3.05	99.37	631	64	170	103	5	140	16	1651	21	130	18	11
DHK1	Gz	1497	FVM334	64.93	1.30	12.48	7.08	0.17	1.26	2.63	2.46	4.11	0.47	0.05	3.03	99.97	605	61	150	108	14	103	23	1668	20	123	20	13
DHK1	Gs	1419	FVM335	61.71	1.21	13.23	7.29	0.10	2.31	3.27	2.40	3.85	0.49	0.03	2.96	98.85	469	54	304	101	7	118	69	1584	18	155	16	19
DHK1	Gm	1403	FVM336	61.02	1.19	12.93	7.29	0.11	2.44	4.59	2.74	2.82	0.48	0.04	3.98	99.63	459	52	384	72	28	122	65	1216	18	148	150	22
DHK1	Gm	1383	FVM337	59.41	1.25	13.31	8.23	0.12	2.87	4.21	3.06	1.76	0.51	0.07	3.92	98.72	464	53	274	40	11	121	65	928	18	171	187	20
DHK1	Gl	1368	FVM338	60.87	1.18	12.87	6.94	0.09	1.78	4.11	2.82	3.37	0.46	0.09	3.73	98.31	508	55	287	84	6	91	25	1183	19	150	47	16
DHK1	Gl	1351	FVM339	62.10	1.19	12.97	6.44	0.11	2.05	4.16	2.51	3.48	0.47	0.04	3.50	99.02	486	55	433	90	45	108	39	1335	19	142	58	20
DHK1	Gm	1335	FVM340	56.39	1.33	13.28	8.85	0.14	3.30	4.99	2.42	2.45	0.55	0.08	4.31	98.09	377	51	456	66	14	149	92	967	15	184	242	26
DHK1	Gl	1310	FVM341	64.93	1.09	12.01	5.57	0.08	1.34	4.22	2.90	3.61	0.45	0.09	3.26	99.55	456	46	232	89	5	64	30	1316	16	110	45	15
DHK1	Gl	1297	FVM342	65.99	1.13	12.59	5.36	0.06	1.59	3.35	2.81	4.28	0.45	0.13	2.42	100.16	480	52	278	100	5	64	33	1629	17	122	44	15
DHK1	Gm	1281	FVM343	54.60	1.24	12.86	8.65	0.13	4.13	6.55	2.38	0.81	0.52	0.07	6.35	98.29	295	44	254	15	17	132	103	458	13	176	264	28

B'hole	Facies	Depth	Sample	SiO2	TiO2	Al2O3	Fe2O3	MnO	MgO	CaO	Na2O	K2O	P2O5	H2O-	LOI	TOTAL	Zr	Y	Sr	Rb	Cu	Zn	Ni	Ba	Nb	V	Cr	Co
DHK1	Gm	1270	FVM344	55.80	1.40	13.41	9.80	0.13	4.77	4.35	2.51	0.50	0.60	0.16	5.06	98.49	299	45	235	9	21	149	124	284	13	215	373	40
DHK1	Gm	1262	FVM345	50.98	1.40	13.71	9.48	0.12	4.60	6.65	1.87	1.42	0.58	0.08	6.56	97.45	324	46	269	34	12	145	119	715	15	201	316	25
DHK1	Gm	1241	FVM346	54.94	1.36	13.03	8.50	0.12	3.72	6.44	2.42	1.11	0.56	0.10	6.01	98.31	317	44	408	27	20	137	111	594	14	187	324	28
DHK1	Gm	1207	FVM347	57.57	1.38	13.40	8.46	0.12	3.42	4.41	2.76	2.55	0.57	0.12	4.05	98.81	361	48	388	70	20	142	97	1060	16	185	257	27
DHK1	Gm	1194	FVM348	59.01	1.36	13.47	8.96	0.15	3.85	3.16	2.67	2.60	0.56	0.11	3.23	99.13	380	51	326	71	14	170	96	1222	17	197	245	28
DHK1	Gm	1169	FVM349	54.31	1.39	13.41	9.80	0.16	4.38	5.30	2.28	1.23	0.59	0.12	5.28	98.25	359	50	236	34	23	196	100	641	16	188	254	27
DHK1	Gm	1156	FVM350	57.38	1.18	13.07	9.71	0.15	4.73	3.70	2.03	0.95	0.49	0.14	4.55	98.08	338	43	410	29	19	221	101	1008	14	190	239	31
DHK1	Mx	1127	FVM351	62.44	1.12	12.74	7.34	0.10	2.72	3.27	2.32	2.86	0.40	0.13	3.43	98.87	492	53	244	78	3	125	39	1462	19	138	93	19
DHK1	Mx	1120	FVM352	65.85	1.07	12.61	6.30	0.09	2.13	2.08	2.62	3.22	0.38	0.12	2.49	98.96	478	48	159	77	5	104	39	1556	18	129	97	16
DHK1	Mx	1109	FVM353	64.43	1.09	12.02	6.20	0.11	1.94	3.51	2.55	2.87	0.41	0.12	3.32	98.57	472	54	170	76	4	91	36	1462	18	123	91	15
DHK1	Mx	1107	FVM354	62.84	1.08	12.98	6.53	0.08	1.88	3.20	2.05	4.68	0.40	0.10	2.99	98.81	496	56	198	148	5	86	36	1931	21	125	84	14
DHK1	Mx	1100	FVM355	64.21	1.10	12.95	6.42	0.08	2.18	3.34	2.47	4.24	0.41	0.11	2.93	100.44	504	58	262	118	51	139	34	1650	21	124	76	12
DHK1	Mx	1097	FVM356	63.25	1.10	12.97	6.59	0.08	1.75	3.43	2.14	4.98	0.40	0.09	2.92	99.70	477	57	220	147	11	71	33	1561	20	117	71	12
DHK1	Mx	1091	FVM357	62.73	1.13	12.86	6.79	0.07	1.97	3.34	2.58	3.93	0.40	0.11	2.88	98.79	494	57	262	116	23	76	37	1463	20	130	87	12
DHK1	Mr	1064	FVM358	69.09	0.73	14.18	4.42	0.06	1.33	1.49	2.39	4.04	0.23	0.11	2.27	100.34	450	50	133	183	4	51	17	1511	20	87	28	8
DHK1	Mr	1058	FVM359	70.93	0.69	12.58	3.67	0.05	0.87	1.47	2.15	5.20	0.21	0.09	1.61	99.52	406	46	101	144	1	46	16	1506	18	59	24	8
DHK1	Mr	1051	FVM360	69.70	0.74	12.48	4.08	0.07	0.85	2.65	2.66	4.99	0.21	0.13	2.28	100.84	439	51	172	131	6	42	16	1338	19	66	28	6
DHK1	Mr	1046	FVM361	69.68	0.70	12.71	4.31	0.05	0.88	1.90	2.41	5.33	0.21	0.16	1.89	100.23	433	49	172	164	7	44	17	1589	18	70	30	8
DHK1	Mr	1032	FVM362	71.04	0.66	12.73	3.72	0.05	0.92	1.40	2.38	5.51	0.19	0.17	1.51	100.28	417	46	168	150	4	57	16	1755	18	63	27	9
DHK1	Mr	1016	FVM363	69.49	0.67	12.50	3.91	0.06	0.89	1.79	3.21	4.86	0.19	0.20	1.73	99.50	400	47	177	127	4	61	16	1450	18	62	27	6
DHK1	Mr	997	FVM364	69.10	0.68	12.78	4.18	0.06	0.83	1.95	3.07	5.11	0.20	0.22	1.94	100.12	390	49	159	135	6	65	18	1620	19	64	25	5
DHK1	Mr	975	FVM365	70.08	0.68	12.32	4.01	0.06	0.79	1.80	2.47	5.20	0.19	0.09	1.90	99.59	392	48	146	157	4	61	15	1693	19	63	27	6
DHK1	Mr	957	FVM366	69.64	0.69	12.80	3.82	0.06	0.72	2.31	2.44	5.30	0.21	0.08	1.90	99.59	384	48	143	169	4	56	16	1561	18	67	26	6
DHK1	Mr	941	FVM367	70.62	0.68	12.94	2.85	0.07	0.63	2.16	2.44	5.45	0.20	0.08	2.34	100.41	384	48	143	175	8	53	15	1560	18	53	25	5
DHK1	Mr	927	FVM368	72.56	0.69	12.84	2.66	0.05	0.55	1.51	2.46	5.88	0.20	0.07	1.77	101.04	407	48	137	165	8	49	16	1934	18	59	24	7
DHK1	Mr	899	FVM369	69.90	0.71	12.92	4.08	0.07	0.86	2.13	2.80	4.76	0.20	0.00	2.38	100.81	407	39	117	131	3	70	16	1400	20	67	26	7
DHK1	Mr	874	FVM370	67.95	0.79	14.73	3.44	0.06	0.90	2.30	3.17	3.72	0.23	0.06	2.85	100.20	467	40	129	166	7	81	16	1122	19	94	28	7
DHK1	GF	865	FVM371	50.29	1.35	12.84	11.84	0.15	5.37	6.77	1.35	0.72	0.55	0.04	8.03	99.30	270	39	144	38	7	304	166	189	12	217	376	32
DHK1	GF	861	FVM372	54.11	1.43	13.53	11.92	0.14	5.42	3.99	1.46	0.77	0.57	0.04	5.91	99.29	284	39	108	34	8	305	164	204	13	243	447	33
DHK1	Ma	843	FVM373	67.75	0.88	12.87	5.10	0.08	1.18	2.05	2.63	4.58	0.31	0.10	2.34	99.87	418	39	140	133	3	101	26	1473	17	97	51	10
DHK1	Mr	822	FVM374	69.42	0.60	12.28	2.93	0.05	0.48	2.25	3.15	4.85	0.16	0.06	2.08	98.31	361	47	114	138	2	57	15	1353	17	54	24	4
DHK1	Mr	790	FVM375	69.48	0.73	12.73	4.15	0.06	0.74	1.89	3.27	4.41	0.22	0.05	1.82	99.55	396	46	113	129	2	68	17	1324	18	71	31	7
DHK1	Mr	762	FVM376	70.00	0.65	12.66	3.32	0.08	0.56	2.15	2.71	5.25	0.18	0.04	2.27	99.87	377	82	116	126	4	64	16	1674	16	56	25	7
DHK1	Mr	724	FVM378	72.96	0.56	11.48	3.84	0.08	0.96	1.69	2.10	4.57	0.16	0.03	2.08	100.51	315	43	116	103	17	67	15	1686	15	58	25	7
DHK1	Mr	669	FVM379	73.22	0.59	13.42	3.16	0.04	1.36	0.36	0.53	5.76	0.16	0.07	1.91	100.58	387	46	165	5	5	65	13	1555	18	49	18	6
DHK1	Mr	646	FVM380	72.44	0.64	13.59	3.06	0.05	1.29	1.09	0.40	5.66	0.18	0.03	2.54	100.97	426	48	172	2	2	46	11	1426	18	48	17	5
DHK1	Mr	621	FVM381	71.78	0.58	13.03	3.29	0.05	1.65	1.30	0.07	4.70	0.18	0.04	3.06	99.73	390	45	32	150	2	46	11	1053	17	46	18	4
FS4	Gi	2685	FVM382	66.12	1.24	12.90	6.19	0.08	1.78	4.14	3.25	1.95	0.48	0.06	1.62	99.81	518	55	444	41	8	73	26	574	19	126	47	18
FS4	Gi	2671	FVM383	62.88	1.27	13.44	7.59	0.11	2.13	4.54	2.89	2.44	0.50	0.07	1.61	99.47	523	60	368	66	24	98	26	1093	20	154	53	24

B'hole	Facies	Depth	Sample	SiO ₂	TiO ₂	Al ₂ O ₃	Fe ₂ O ₃	MnO	MgO	CaO	Na ₂ O	K ₂ O	P ₂ O ₅	H ₂ O	LOI	TOTAL	Zr	Y	Sr	Rb	Cu	Zn	Ni	Ba	Nb	V	Cr	Co
FS4	GI	2667	FVM384	63.00	1.26	13.64	7.32	0.10	2.04	4.46	2.95	2.58	0.50	0.06	1.66	99.57	518	57	360	72	20	111	26	1182	19	144	52	20
FS4	GI	2660	FVM385	63.30	1.23	13.14	7.67	0.12	1.92	4.97	3.13	2.27	0.50	0.05	1.39	99.69	507	58	375	89	15	103	26	1065	20	150	50	20
FS4	GI	2655	FVM386	63.32	1.25	13.14	7.16	0.11	1.96	4.89	3.15	2.45	0.50	0.05	1.39	99.37	524	58	413	72	15	100	28	909	20	140	46	20
FS4	GI	2649	FVM387	63.01	1.28	13.48	7.61	0.11	2.50	4.36	3.16	2.38	0.50	0.17	1.45	100.01	508	57	363	71	26	105	35	802	19	143	83	21
FS4	Gm	2642	FVM388	58.06	1.28	13.45	9.16	0.14	4.08	5.18	2.60	2.32	0.54	0.06	1.56	98.43	384	50	351	74	15	137	89	1170	17	185	335	29
FS4	Gm	2641	FVM389	57.72	1.26	13.42	9.15	0.13	4.37	5.74	2.64	2.04	0.54	0.08	1.45	98.54	348	46	371	64	25	137	100	991	15	184	358	31
FS4	Gm	2639	FVM390	56.66	1.25	13.40	9.29	0.14	4.44	6.57	2.20	2.26	0.55	0.04	1.60	98.40	331	48	377	71	33	119	102	1107	15	181	342	33
FS4	Gm	2636	FVM391	55.65	1.32	13.60	10.26	0.14	4.99	6.74	2.07	2.17	0.58	0.04	1.82	99.38	294	46	346	69	44	118	122	996	16	189	358	38
FS4	Gm	2635	FVM392	55.47	1.34	13.23	10.14	0.15	5.17	7.12	2.24	1.53	0.59	0.04	1.77	98.79	285	44	375	49	56	127	118	546	15	199	357	37
FS4	Gm	2634	FVM393	54.43	1.36	13.59	10.30	0.16	5.22	7.18	2.31	1.88	0.61	0.04	1.77	98.85	291	46	331	60	35	114	120	859	15	198	326	36
FS4	Gm	2632	FVM394	54.33	1.37	13.70	10.40	0.15	5.20	6.93	2.50	1.86	0.62	0.08	1.84	98.98	292	47	298	59	32	119	123	915	15	197	325	38
OT1	Gz	1390	FVM398	63.28	1.30	12.61	6.54	0.10	1.67	3.92	1.39	3.11	0.48	0.05	3.97	98.42	624	80	110	137	4	74	22	695	20	142	20	13
OT1	Gz	1384	FVM399	63.30	1.31	12.65	5.54	0.09	1.22	4.93	1.70	4.34	0.49	0.05	4.09	99.71	628	62	114	115	3	53	16	1315	20	132	19	12
OT1	Gz	1373	FVM400	65.59	1.30	12.37	5.47	0.09	0.97	3.92	2.06	4.01	0.48	0.06	3.14	99.46	611	58	116	101	13	55	16	1227	20	121	19	10
OT1	Gz	1362	FVM401	63.24	1.28	12.38	6.39	0.09	1.13	3.82	2.40	3.60	0.46	0.07	3.40	98.26	625	58	111	81	3	66	14	1119	20	120	17	9
OT1	Gz	1336	FVM402	62.56	1.32	13.25	7.12	0.09	1.75	3.54	1.18	4.12	0.48	0.04	3.67	99.12	649	69	86	143	2	75	14	1100	21	173	19	8
OT1	Gz	1324	FVM403	62.19	1.27	12.58	6.78	0.12	1.61	4.06	1.86	3.97	0.45	0.05	3.97	98.91	617	65	148	122	9	88	15	1238	21	129	18	4
OT1	Gz	1314	FVM404	63.67	1.33	12.93	6.29	0.11	1.42	3.52	1.90	4.52	0.47	0.05	3.39	99.60	636	66	148	126	3	88	15	1414	20	134	18	6
OT1	Gz	1296	FVM405	66.49	1.22	11.99	6.07	0.09	1.35	3.18	2.11	3.65	0.44	0.04	3.23	99.86	578	53	134	100	9	80	13	1335	18	115	17	7
OT1	Gz	1286	FVM406	64.13	1.30	12.40	7.04	0.09	1.69	3.63	1.13	3.97	0.47	0.04	3.91	99.80	615	61	74	135	2	93	15	1187	21	135	18	8
OT1	Gz	1271	FVM407	61.20	1.38	13.72	7.10	0.09	1.92	3.71	1.70	4.30	0.49	0.03	3.88	99.52	650	64	109	129	7	98	15	1233	22	141	18	10
OT1	GF	1247	FVM409	52.74	1.28	13.77	9.10	0.14	6.44	5.36	1.77	1.52	0.55	0.05	6.35	99.07	255	41	146	31	12	194	138	573	12	217	392	40
OT1	GF	1241	FVM410	53.44	1.28	13.63	8.90	0.16	5.70	5.03	2.03	1.76	0.54	0.06	5.64	98.17	258	41	274	37	30	186	156	906	12	214	472	39
OT1	GF	1230	FVM411	55.26	1.12	13.31	9.16	0.19	5.20	4.69	2.42	2.42	0.47	0.06	3.24	97.54	277	38	459	53	32	141	150	1260	13	177	476	35
OT1	GF	1218	FVM412	52.96	1.18	12.92	9.57	0.15	6.08	4.56	1.79	1.95	0.50	0.04	5.34	97.04	238	37	206	37	41	165	139	586	11	202	391	39
OT1	GF	1212	FVM413	55.67	1.06	12.90	9.39	0.15	5.63	5.23	2.36	2.03	0.44	0.07	3.26	98.19	258	40	485	45	19	141	144	938	13	173	419	32
OT1	GF	1200	FVM414	54.54	1.07	13.06	9.18	0.15	4.91	5.80	2.66	2.07	0.45	0.04	3.74	97.67	264	40	278	42	39	129	138	710	12	184	383	36
OT1	GF	1190	FVM415	57.64	1.20	13.52	8.51	0.13	4.58	3.81	2.74	3.26	0.49	0.08	2.25	98.21	367	48	260	74	14	121	86	1746	16	192	178	33
OT1	GF	1184	FVM416	58.39	1.26	13.90	7.53	0.11	3.09	3.39	3.14	3.46	0.50	0.17	3.07	98.01	426	50	264	80	9	99	50	1343	17	170	108	22
OT1	GF	1172	FVM417	58.52	1.24	13.55	7.63	0.12	3.67	4.62	2.98	3.29	0.53	0.03	2.18	98.36	368	47	408	79	31	103	93	1704	16	176	224	27
OT1	GF	1162	FVM418	57.42	1.22	13.19	9.07	0.13	4.54	4.37	2.63	2.76	0.53	0.08	2.35	98.29	349	45	396	70	15	131	107	1158	16	183	298	34
OT1	GF	1153	FVM419	56.76	1.25	13.46	8.60	0.14	3.57	5.73	2.55	2.66	0.53	0.07	3.11	98.43	370	48	692	65	16	114	91	1243	16	178	219	26
OT1	GF	1137	FVM420	59.45	1.24	12.08	7.67	0.12	4.13	5.38	3.17	2.67	0.53	0.11	2.27	98.82	365	41	322	60	6	115	101	1213	16	155	218	25
OT1	GF	1118	FVM421	60.77	1.23	13.28	7.86	0.12	3.99	3.33	3.19	2.01	0.51	0.08	2.64	99.01	431	50	283	47	19	120	94	1019	17	174	241	23
OT1	GF	1114	FVM422	61.19	1.20	12.90	8.54	0.13	4.49	2.73	2.83	1.51	0.50	0.03	3.05	99.10	422	49	218	32	6	138	95	893	16	175	236	25
OT1	GF	1098	FVM423	59.81	1.11	12.54	7.59	0.12	3.34	4.65	2.37	2.73	0.46	0.08	4.54	99.34	388	39	189	58	51	102	89	744	15	142	209	17
OT1	GF	1088	FVM424	58.28	1.37	12.90	10.83	0.15	4.44	3.70	1.97	1.49	0.59	0.04	3.91	99.67	379	54	408	32	5	135	95	698	16	210	251	21
OT1	GF	1083	FVM425	51.41	1.54	13.75	14.64	0.19	5.86	4.58	0.04	2.92	0.65	0.05	4.08	99.71	418	57	1041	72	7	167	111	1778	20	227	277	31
OT1	GF	1074	FVM426	50.59	1.34	13.87	7.72	0.14	3.68	8.15	2.76	1.15	0.61	0.06	7.17	97.24	282	43	281	26	4	116	124	459	13	197	298	29

Bhole	Facies	Depth	Sample	SiO2	TiO2	Al2O3	Fe2O3	MnO	MgO	CaO	Na2O	K2O	P2O5	H2O-	LOI	TOTAL	Zr	Y	Sr	Rb	Cu	Zn	Ni	Ba	Nb	V	Cr	Co
OT1	GF	1068	FVM427	54.41	1.33	13.50	9.72	0.15	4.23	5.53	2.51	2.36	0.58	0.06	3.64	98.02	281	43	504	62	36	125	133	1321	14	206	303	34
OT1	GF	1047	FVM428	52.58	1.34	13.81	9.24	0.12	5.07	5.55	2.63	1.05	0.59	0.04	5.64	97.66	288	42	204	22	5	129	139	487	13	225	318	32
VE1	Gm	1354	FVM429	56.05	1.19	13.58	9.88	0.15	4.53	6.51	2.46	2.48	0.50	0.01	2.24	99.58	336	46	675	63	26	108	113	1017	16	181	280	32
VE1	Gm	1337	FVM430	55.28	1.27	14.07	9.43	0.14	5.00	5.98	2.81	1.83	0.55	0.04	2.81	99.21	355	49	673	44	20	118	113	905	16	196	290	30
VE1	Gm	1316	FVM431	60.35	1.18	13.11	8.32	0.11	3.42	5.64	2.39	2.06	0.49	0.01	2.11	99.19	429	51	683	51	17	106	91	998	19	152	223	25
VE1	Gm	1301	FVM432	59.49	1.25	13.14	8.56	0.12	3.44	5.97	2.39	1.95	0.52	0.03	2.56	99.42	429	51	611	48	20	106	96	859	18	163	237	26
VE1	Gm	1240	FVM433	55.56	1.21	13.60	9.78	0.15	4.51	6.48	2.18	2.48	0.50	0.02	2.99	99.46	288	41	470	58	31	116	118	818	14	172	274	34
VE1	Gm	1219	FVM434	55.80	1.17	12.96	9.24	0.15	4.06	5.46	2.80	1.66	0.49	0.02	2.46	97.27	326	44	460	35	34	131	111	893	15	181	288	33
VE1	Mr	1070	FVM435	73.93	0.44	12.38	2.70	0.04	0.48	0.59	2.43	5.58	0.11	0.02	0.95	99.65	248	36	141	154	5	47	11	1559	15	30	19	6
VE1	Mr	1066	FVM436	74.38	0.46	12.72	2.51	0.04	0.48	0.80	3.18	4.52	0.13	0.01	1.10	100.33	259	42	115	139	1	52	12	953	14	26	18	5
VE1	Mr	1048	FVM437	74.29	0.52	12.74	2.88	0.05	0.54	0.80	2.61	4.84	0.15	0.02	1.25	100.69	253	38	148	167	1	53	13	1023	16	36	20	7
VE1	Mr	992	FVM438	71.46	0.48	12.66	2.86	0.07	0.62	1.91	3.02	4.41	0.14	0.05	2.01	99.69	247	40	121	126	2	61	12	841	14	35	18	8
VE1	Mr	956	FVM439	73.22	0.50	12.80	2.87	0.05	0.56	1.47	2.55	5.01	0.13	0.03	1.77	100.95	269	44	117	141	1	56	13	1154	15	35	17	6
VE1	GF	891	FVM440	63.47	1.29	14.59	6.94	0.07	2.59	1.89	3.68	1.28	0.57	0.04	2.53	98.94	333	33	96	54	2	119	56	180	12	201	110	26
VE1	GF	880	FVM441	60.98	1.31	14.80	8.97	0.08	3.18	1.78	3.27	1.07	0.56	0.02	2.82	98.84	335	36	83	47	30	187	47	172	13	209	110	33
VE1	GF	878	FVM442	59.33	1.32	14.76	7.17	0.11	2.61	4.75	2.86	1.68	0.57	0.03	4.84	100.03	333	34	152	74	2	143	49	215	12	212	105	23
VE1	Mr	869	FVM443	71.37	0.35	15.90	2.37	0.03	1.97	0.48	0.51	5.68	0.03	0.02	2.73	101.44	287	36	42	274	0	59	8	680	21	10	7	4
VE1	Mr	858	FVM444	78.14	0.25	11.58	1.62	0.03	0.69	0.56	0.88	5.60	0.03	0.19	1.36	100.93	220	32	91	167	0	29	9	1259	17	8	9	5
VE1	Mr	848	FVM445	77.37	0.24	11.13	1.54	0.03	0.30	0.59	1.50	5.51	0.02	0.16	1.08	99.47	218	36	139	148	1	34	9	1091	16	7	12	4
VE1	Mr	825	FVM446	77.84	0.26	11.63	1.48	0.04	0.55	0.52	1.56	4.90	0.04	0.18	1.36	100.36	237	35	114	162	0	24	10	969	15	10	10	4
UTK1	Mx	1211	FVM447	61.50	1.21	12.99	7.49	0.11	2.03	5.03	2.33	2.96	0.52	0.19	2.78	99.14	426	56	1028	62	18	108	57	1039	20	123	99	19
UTK1	Mx	1193	FVM448	62.09	1.10	12.74	6.90	0.07	1.63	4.42	2.90	2.60	0.49	0.15	3.63	98.72	399	51	300	87	174	82	56	936	18	127	109	21
UTK1	Mx	1169	FVM449	60.51	1.21	12.91	7.69	0.14	2.53	3.87	2.70	3.04	0.55	0.13	3.17	98.45	430	55	418	74	31	16	66	1432	19	140	133	20
UTK1	Mx	1154	FVM450	60.38	1.26	12.83	7.78	0.09	4.13	3.18	2.56	2.08	0.56	0.13	3.70	98.68	381	52	143	62	2	117	65	830	17	129	157	21
UTK1	Mx	1132	FVM451	63.20	1.17	12.79	7.15	0.08	2.39	3.61	2.19	3.03	0.52	0.12	3.54	99.79	437	53	182	111	13	92	53	935	19	136	101	18
UTK1	Mx	1101	FVM452	62.27	1.13	12.72	7.62	0.11	2.14	3.11	2.29	3.02	0.47	0.12	3.03	98.03	431	55	249	89	3	122	43	1096	21	125	81	17
UTK1	Mx	1090	FVM453	62.76	1.15	12.81	6.83	0.10	2.05	4.03	3.12	2.50	0.49	0.08	2.95	98.87	430	56	591	55	5	109	44	1062	19	115	82	19
UTK1	Mx	1053	FVM454	69.24	1.04	11.75	4.78	0.08	1.63	3.08	3.79	0.93	0.45	0.13	2.24	99.14	370	46	380	43	1	78	50	470	15	108	104	16
UTK1	Md	1027	FVM455	65.87	1.08	12.57	6.07	0.09	0.97	3.60	2.62	3.27	0.43	0.05	2.93	99.55	460	57	534	94	9	101	17	1165	21	102	37	15
UTK1	Md	1010	FVM456	66.25	1.09	12.69	5.72	0.10	1.04	3.31	2.68	3.77	0.43	0.04	2.52	99.64	495	60	490	92	7	103	17	1356	22	99	32	11
KRF1	Gi	3106	FVM457	64.21	1.12	13.13	6.75	0.10	1.75	3.67	2.82	2.43	0.39	0.03	2.43	98.83	540	58	509	45	15	109	19	1548	19	127	41	15
KRF1	Gi	3100	FVM458	63.78	1.14	13.04	6.70	0.10	1.93	4.05	3.03	1.27	0.40	0.04	3.50	98.98	556	56	410	29	10	120	24	1091	19	131	46	15
KRF1	Gz	2824	FVM459	64.06	1.33	13.51	7.25	0.09	0.98	3.47	2.22	1.83	0.44	0.05	7.09	97.68	629	65	341	60	3	100	14	889	18	130	19	10
KRF1	Gz	2800	FVM460	59.23	1.25	12.59	6.46	0.13	0.92	5.04	2.66	1.83	0.44	0.05	7.09	97.68	629	65	341	60	3	100	14	889	18	130	19	10
KRF1	Gz	2775	FVM461	63.82	1.36	13.58	6.86	0.10	1.00	3.42	2.35	2.86	0.49	0.04	3.73	99.61	656	64	302	94	11	92	15	1404	23	145	19	16
ULT1	Gi	1665	FVM462	61.06	1.23	13.30	7.56	0.11	2.07	5.85	3.27	2.22	0.49	0.04	1.92	99.12	508	57	699	56	27	100	30	1078	20	151	56	19
ULT1	Gi	1632	FVM463	61.44	1.23	13.19	7.64	0.10	1.89	3.70	4.05	1.53	0.48	0.03	3.66	98.94	495	52	305	35	12	99	35	956	18	146	60	19
ULT1	Gi	1545	FVM464	62.18	1.19	13.07	7.48	0.10	2.14	5.44	2.64	2.26	0.45	0.03	2.72	99.70	490	55	534	47	14	110	40	1049	19	141	77	21
ULT1	Gi	1541	FVM465	62.36	1.21	12.93	7.79	0.11	2.11	5.50	2.61	2.03	0.48	0.03	2.51	99.67	474	55	543	43	19	114	41	1045	19	146	83	17

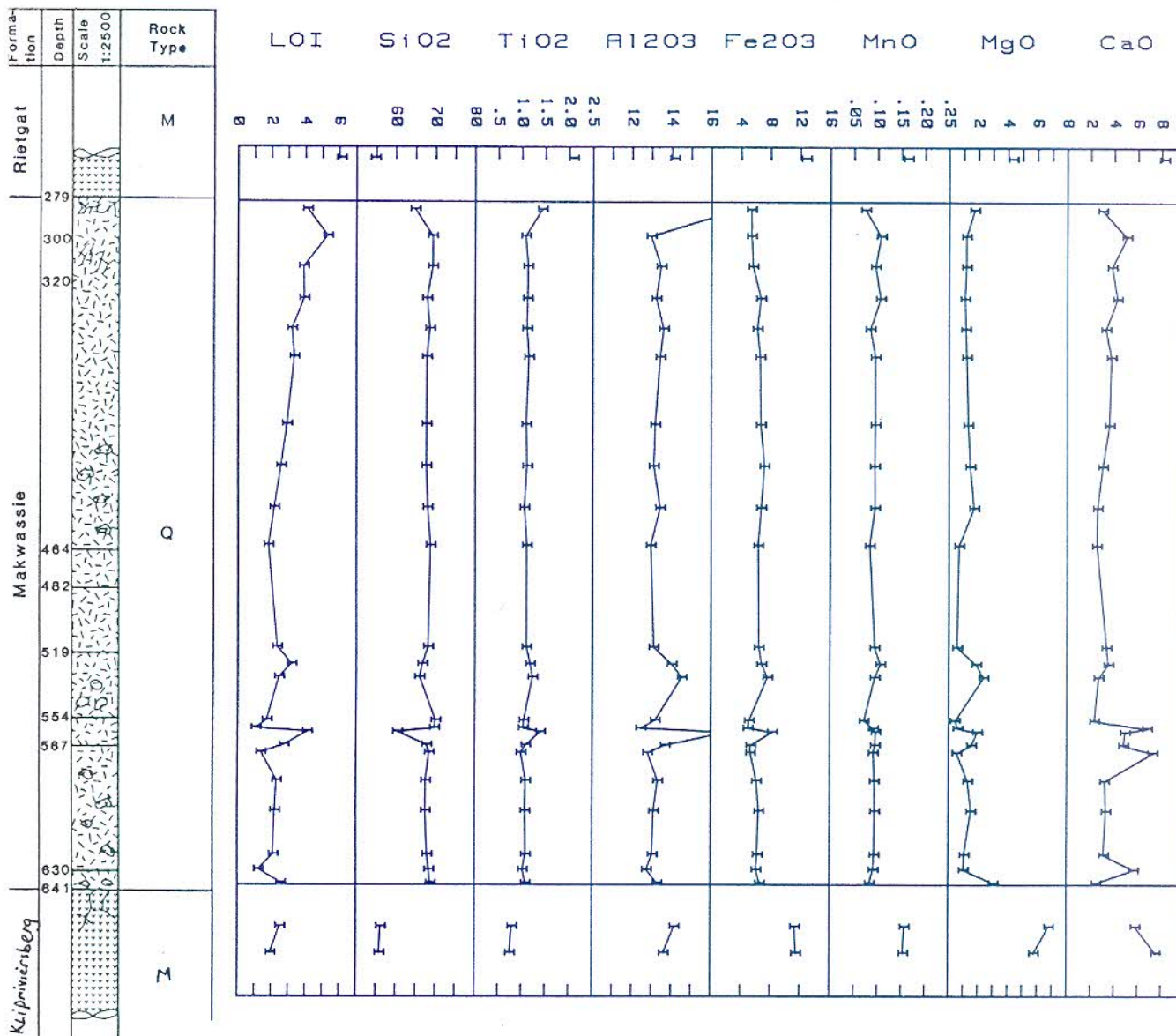
Bhole	Facies	Depth	Sample	SiO2	TiO2	Al2O3	Fe2O3	MnO	MgO	CaO	Na2O	K2O	P2O5	H2O-	LOI TOTAL	Zr	Y	Sr	Rb	Cu	Zn	Ni	Ba	Nb	V	Cr	Co	
SHS1	Gz	2141	FVM502	59.20	1.36	12.64	7.08	0.13	1.64	4.83	3.15	2.29	0.49	0.07	4.79	97.67	636	65	327	70	2	125	14	1395	20	108	16	13
SHS1	Gz	2092	FVM503	63.38	1.20	12.93	6.76	0.08	1.33	2.90	2.67	4.05	0.44	0.06	3.08	98.88	646	63	285	137	9	127	15	1552	20	125	18	12
SHS1	Gz	2048	FVM504	61.15	1.26	12.68	7.00	0.09	1.12	4.38	2.68	3.35	0.46	0.06	4.36	98.59	637	64	336	122	9	117	13	1441	19	129	17	14
SHS1	Gz	2008	FVM505	61.75	1.24	12.87	6.85	0.09	1.26	4.02	2.28	3.69	0.45	0.10	4.26	98.86	624	64	308	143	8	114	14	1442	20	126	18	13
SHS1	Gz	1961	FVM506	61.54	1.22	12.98	7.03	0.10	1.37	3.39	2.97	3.57	0.46	0.04	3.40	98.07	643	65	336	111	14	124	13	1577	20	129	18	15
SHS1	Gz	1941	FVM507	60.86	1.22	12.93	6.84	0.13	1.39	4.01	3.43	2.95	0.44	0.07	3.75	98.02	648	62	474	84	8	117	13	1474	19	100	15	15
SHS1	Gz	1941	FVM507	60.86	1.22	12.93	6.84	0.13	1.39	4.01	3.43	2.95	0.44	0.07	3.75	98.02	648	62	474	84	8	117	13	1474	19	100	15	15
SHS1	Gm	1807	FVM508	54.31	1.13	12.83	8.38	0.11	3.40	5.96	2.38	2.40	0.49	0.11	5.67	97.17	326	43	617	85	28	116	109	1062	13	193	258	31
SHS1	Gm	1776	FVM509	52.92	1.22	13.47	9.08	0.12	3.01	6.99	1.94	2.38	0.58	0.04	5.99	97.74	293	42	592	82	19	115	64	804	14	203	99	30
SHS1	Gm	1746	FVM510	56.51	1.18	13.87	8.03	0.10	2.02	5.05	3.02	2.43	0.51	0.09	4.60	97.41	400	47	578	105	16	111	39	758	15	183	88	27
SHS1	Gm	1707	FVM511	52.46	1.09	12.92	9.12	0.13	5.51	7.38	2.13	0.89	0.48	0.10	5.66	97.87	235	34	608	24	25	108	201	445	11	186	547	39
SHS1	Gm	1694	FVM512	53.27	1.05	12.31	8.93	0.12	6.42	7.08	2.39	0.29	0.45	0.11	4.72	97.14	246	33	562	6	19	106	191	183	11	178	560	35
SHS1	Gm	1648	FVM513	54.16	1.35	13.34	9.26	0.12	3.30	6.35	2.59	1.98	0.56	0.09	4.49	97.59	335	48	594	57	32	123	116	865	14	193	310	31
SHS1	Mx	1595	FVM514	60.28	1.11	13.48	6.98	0.09	2.55	4.70	2.61	2.04	0.41	0.14	2.93	97.32	505	54	1068	66	10	110	46	1185	19	131	111	20
SHS1	Mx	1549	FVM515	60.53	1.13	12.71	6.67	0.10	1.99	4.74	2.78	2.79	0.41	0.09	3.72	97.66	478	52	387	79	18	102	53	970	18	131	150	20
SHS1	Mx	1504	FVM516	61.91	1.07	12.82	6.53	0.09	1.86	4.40	3.26	2.11	0.39	0.11	3.71	98.26	478	51	401	59	18	97	46	890	18	123	120	14
SHS1	Mx	1467	FVM517	62.18	1.10	12.89	6.35	0.09	1.90	3.97	3.46	2.33	0.40	0.13	3.36	98.16	499	51	388	61	16	131	46	944	18	126	111	19
SHS1	Mx	1419	FVM518	63.58	1.10	12.84	6.48	0.08	1.65	3.40	3.13	2.39	0.39	0.09	3.24	98.37	493	52	351	67	14	104	42	1104	19	134	109	17
SHS1	Mx	1392	FVM519	63.07	1.14	13.50	7.00	0.08	1.26	2.43	3.39	3.11	0.41	0.12	2.51	98.02	525	51	283	64	15	87	46	1601	19	146	116	15
TKUIP QUARTZ PORPHYRY FORMATION																												
TKuip	Mr	0	LVA049	69.86	0.70	11.46	5.08	0.07	0.99	2.56	2.25	4.10	0.26	0.04	2.40	99.77	346	29	120	73	93	73	15	1852	12	52	18	8
TKuip	Mr	0	LVA063	69.26	0.71	12.36	4.82	0.08	1.03	1.68	1.77	4.26	0.21	0.12	2.11	98.41	359	31	89	100	4	47	12	1527	12	79	18	9
TKuip	Mr	0	LVA078	78.78	0.28	10.03	1.99	0.05	0.45	0.38	2.15	3.82	0.02	0.12	0.92	98.99	253	18	68	105	1	35	9	1131	10	16	14	7
TKuip	Mr	0	LVA079	74.96	0.38	11.47	2.60	0.07	0.58	0.79	2.58	4.07	0.06	0.10	1.20	98.86	293	24	81	101	3	46	10	1134	11	25	16	6
TKuip	Mr	0	LVA080	76.85	0.38	11.20	2.08	0.05	0.54	0.50	2.91	3.56	0.05	0.09	0.98	99.19	302	24	95	87	0	39	9	1045	11	23	14	8
TKuip	Mr	0	LVA081	76.55	0.38	11.42	1.46	0.04	0.45	0.60	3.48	3.42	0.05	0.05	1.02	98.92	294	25	97	87	1	32	9	1007	10	22	11	9
TKuip	Mr	0	LVA082	74.79	0.39	11.79	3.18	0.06	0.60	0.57	2.28	4.24	0.05	0.14	1.28	99.37	319	23	62	105	0	51	10	1138	12	27	14	8
TKuip	Mr	0	LVA083	76.97	0.35	11.07	2.36	0.04	0.47	0.48	2.55	3.49	0.05	0.14	1.15	99.12	284	20	64	86	2	34	9	87	10	24	14	4
TKuip	Mr	0	LVA084	77.68	0.32	10.75	1.83	0.04	0.46	0.72	2.02	4.27	0.04	0.16	1.29	99.58	270	21	91	103	1	31	9	1467	11	18	13	7

B'hole	Facies	Depth	Sample	SiO2	TiO2	Al2O3	Fe2O3	MnO	MgO	CaO	Na2O	K2O	P2O5	H2O-	LOI	TOTAL	Zr	Y	Sr	Rb	Cu	Zn	Ni	Ba	Nb	V	Cr	Co
WESSELTON MINE																												
Wessel	Mr	785	LWS001	74.88	0.41	11.22	2.83	0.04	0.88	0.94	1.71	5.03	0.07	0.04	1.72	99.77	316	26	62	128	-	-	-	1078	11	27	13	5
Wessel	Md	835	LWS005	62.37	1.07	12.96	8.04	0.10	2.30	3.69	2.61	1.69	0.39	0.03	4.58	99.83	302	35	115	50	-	-	-	459	12	143	16	17
Wessel	Md	850	LWS007	61.53	1.07	12.80	7.01	0.11	2.12	4.41	0.89	3.58	0.35	0.02	5.82	99.71	297	39	107	106	-	-	-	763	12	132	16	17
Wessel	Md	886	LWS009	62.47	1.08	12.88	6.96	0.10	1.34	4.56	2.19	2.86	0.36	0.02	5.01	99.83	296	38	134	81	-	-	-	780	12	132	16	10
Wessel	Md	920	LWS011	62.85	1.07	12.78	7.06	0.11	1.06	4.61	2.23	2.60	0.35	0.04	5.04	99.80	294	36	143	75	-	-	-	641	12	131	16	17
Wessel	Gs	995	LWS017	54.21	1.10	11.98	9.11	0.23	2.08	8.32	1.68	1.84	0.37	0.03	8.99	99.94	248	41	125	63	-	-	-	1139	11	211	15	16
Wessel	Gs	995	LWS018	48.13	1.19	12.35	10.20	0.19	1.74	11.32	1.60	1.79	0.44	0.03	10.58	99.56	257	40	501	64	-	-	-	564	13	195	15	18
Wessel	Mr	820	LWS019	74.01	0.36	11.97	1.73	0.04	1.16	1.87	0.75	4.65	0.06	0.03	3.27	99.90	282	23	59	119	-	-	-	504	11	28	18	5
Wessel	Mr	820	LWS020	65.12	0.38	14.49	7.10	0.03	4.39	0.35	0.33	4.02	0.05	0.06	3.55	99.87	315	26	20	116	-	-	-	670	11	53	13	12
Wessel	Mr	820	LWS021	71.70	0.37	12.62	1.86	0.04	1.43	2.41	1.05	4.49	0.07	0.03	3.79	99.86	267	22	57	124	-	-	-	383	10	24	17	2
RITCHIE FORMATION																												
Ritchie	Mr	0	RIT001	76.00	0.13	11.55	1.14	0.03	0.48	0.03	0.08	9.26	0.01	0.11	0.65	99.47	147	34	59	281	-	-	-	1049	15	-	-	-
Ritchie	Mr	0	RIT002	77.18	0.13	11.65	0.91	0.02	0.45	0.02	0.08	8.47	0.01	0.00	0.76	99.68	153	34	44	340	-	-	-	430	14	-	-	-
Ritchie	Mr	0	RIT003	76.63	0.13	12.07	0.83	0.01	0.34	0.00	0.05	8.50	0.01	0.03	0.78	99.38	156	40	39	356	-	-	-	435	15	-	-	-
Ritchie	Mr	0	RIT004	75.83	0.13	11.54	1.64	0.03	0.51	0.02	0.07	9.07	0.01	0.03	0.67	99.55	153	28	48	318	-	-	-	656	16	-	-	-
VRYBURG AREA (Data normalised volatile free)																												
Schatkist	Mr	0	LNV001	75.52	0.46	12.20	1.99	0.02	0.48	1.21	0.25	7.76	0.11	-	-	100.00	314	32	64	149	-	-	-	1145	16	33	14	5
Schatkist	Mr	0	LNV002	78.51	0.41	11.26	1.23	0.01	0.37	0.27	0.26	7.55	0.11	-	-	100.00	302	32	71	144	-	-	-	1229	16	30	14	6
Manchester	Mr	0	LNV011	75.44	0.47	11.69	2.89	0.03	0.76	1.29	1.87	5.48	0.09	-	-	100.00	390	38	53	112	-	-	-	985	16	32	12	5
Karee F.	Md	0	LNV014A	67.99	0.74	13.50	5.96	0.10	1.50	1.07	4.12	4.79	0.22	-	-	100.00	433	51	151	102	-	-	-	1803	19	66	13	9
Karee F.	Md	0	LNV014B	73.37	0.63	12.37	2.18	0.04	0.22	0.76	3.88	6.35	0.19	-	-	100.00	387	40	291	144	-	-	-	2380	17	43	13	4
Vogel Vlei	Gm	0	LNV015	61.46	1.11	13.93	7.38	0.11	2.87	4.61	5.45	2.62	0.45	-	-	100.00	392	45	408	61	-	-	-	1422	17	136	152	25

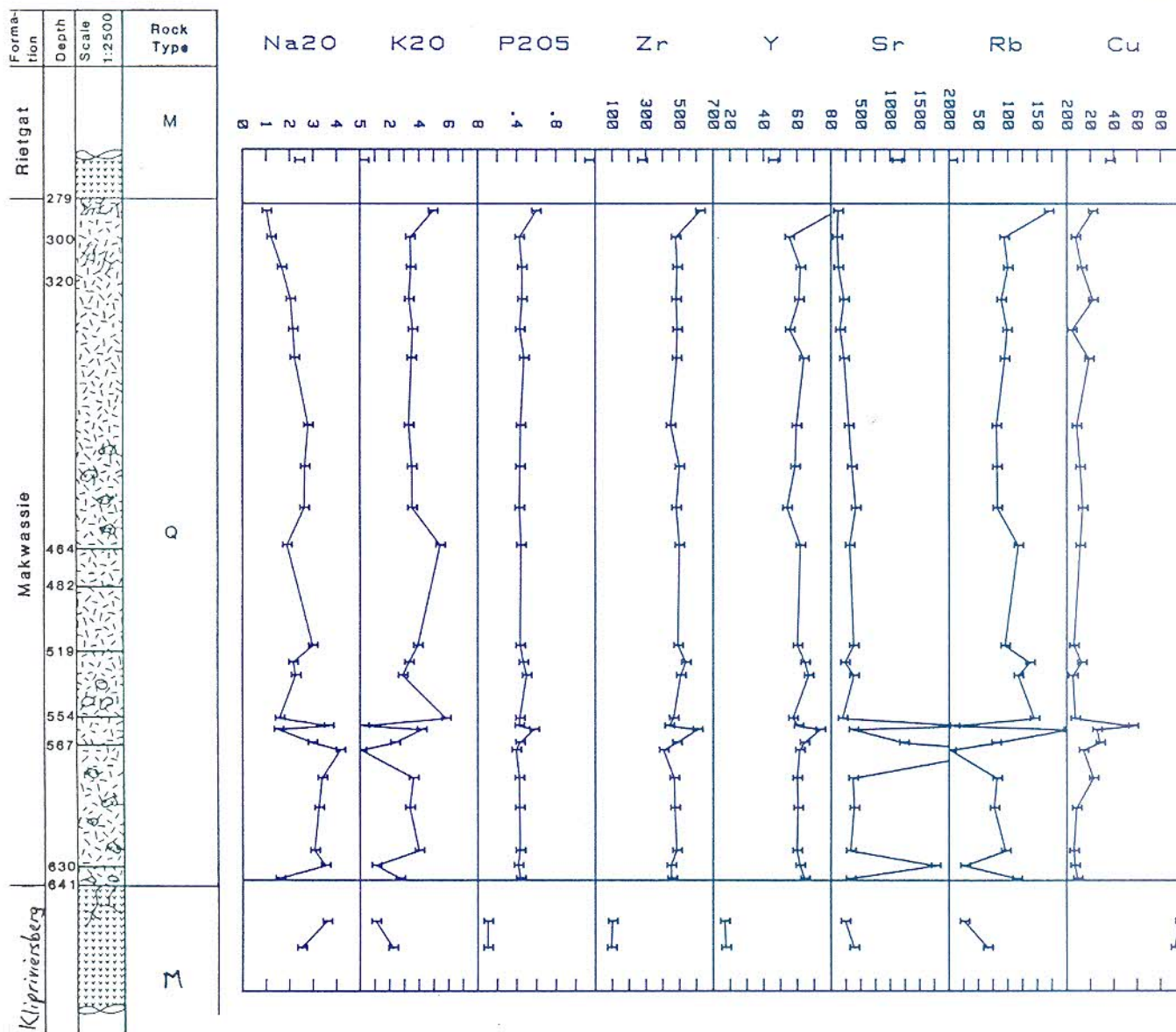
APPENDIX D

DOWNHOLE GEOCHEMICAL LOGS

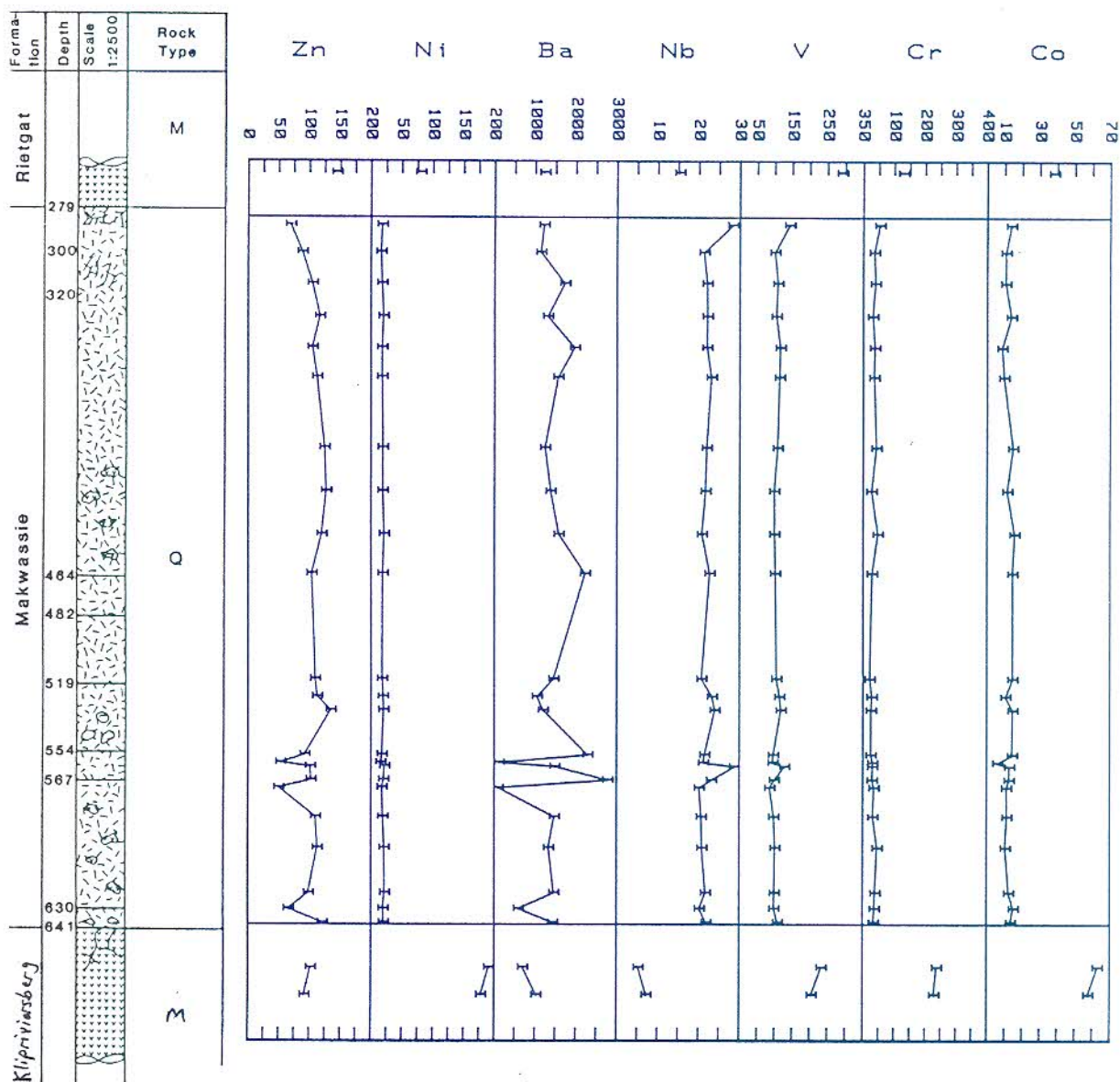
Downhole geochemical logs were made for each sampled borehole in the Bothaville area. The logs are to the same scale as the accompanying borehole logs, which are described in Appendix A. The original plots were on a scale of 1:2 500 on A3-size paper, which was reduced to A4 size (or by 70.7%). Therefore, the present scale is $\pm 1:3\ 500$. Data that were utilized in these plots were normalized by recalculation to 100% volatile free and each borehole is accompanied by a table of the relevant normalized geochemical data. Trace elements were normalized by the same factor as for major elements.



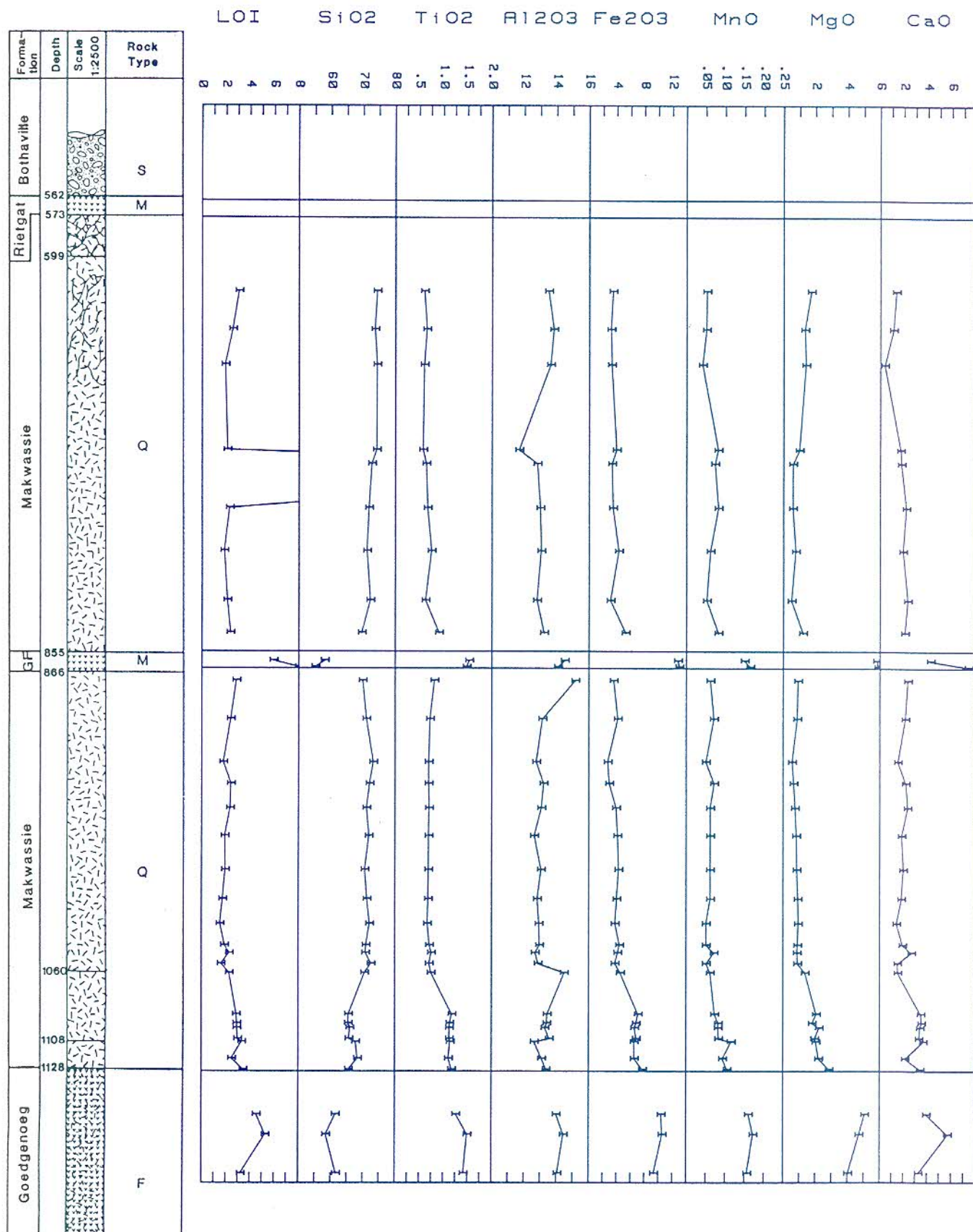
BOREHOLE FORMATION	DF1	DF1	DF1	DF1	DF1	DF1	DF1	DF1	DF1	DF1
			MAKW.	MAKW.	MAKW.	MAKW.	MAKW.	MAKW.	MAKW.	MAKW.
DEPTH	677	663	640	633	625	602	586	571	567	560
SAMPLE No	281	282	283	284	285	286	287	288	289	290
SiO ₂	55.85	56.20	68.74	68.36	67.89	67.45	67.51	68.36	67.72	60.36
TiO ₂	0.75	0.80	1.08	1.02	1.08	1.07	1.08	0.98	1.08	1.40
Al ₂ O ₃	13.61	14.16	13.27	12.75	13.03	13.10	13.31	12.79	13.67	16.76
Fe ₂ O ₃	11.47	11.31	6.58	6.08	6.24	6.44	6.11	5.31	5.34	8.26
MnO	0.15	0.16	0.08	0.09	0.09	0.09	0.09	0.09	0.09	0.10
MgO	5.78	6.79	3.03	1.01	1.05	1.50	1.27	0.54	1.53	1.94
CaO	7.55	5.83	2.49	5.67	3.13	3.31	3.20	7.27	4.79	4.94
SiO ₂	2.51	3.58	1.58	3.52	3.06	3.24	3.38	4.17	2.96	1.51
TiO ₂	2.22	1.07	2.70	1.09	3.99	3.37	3.62	0.09	2.36	4.17
Al ₂ O ₃	0.10	0.10	0.44	0.41	0.43	0.43	0.42	0.39	0.43	0.58
TOTAL	100.00	100.00	100.00	100.00	100.00	100.00	100.00	100.00	100.00	100.00
Loss	96	102	454	449	483	472	467	406	483	606
Loss	17	17	64	62	60	60	60	61	64	74
Loss	393	241	328	1773	333	392	367	2919	1233	374
Loss	66	26	115	27	96	77	82	3	80	202
Loss	93	96	9	7	6	8	23	14	28	26
Loss	92	102	121	66	98	112	109	49	102	101
Loss	178	191	20	19	22	21	19	17	20	21
Loss	1024	693	1428	589	1454	1326	1468	83	2774	1480
Loss	7	5	22	20	22	21	21	20	23	29
Loss	205	233	108	98	99	101	97	86	99	128
Loss	229	238	34	37	39	46	32	35	29	31
Loss	58	63	14	15	12	10	11	11	13	13

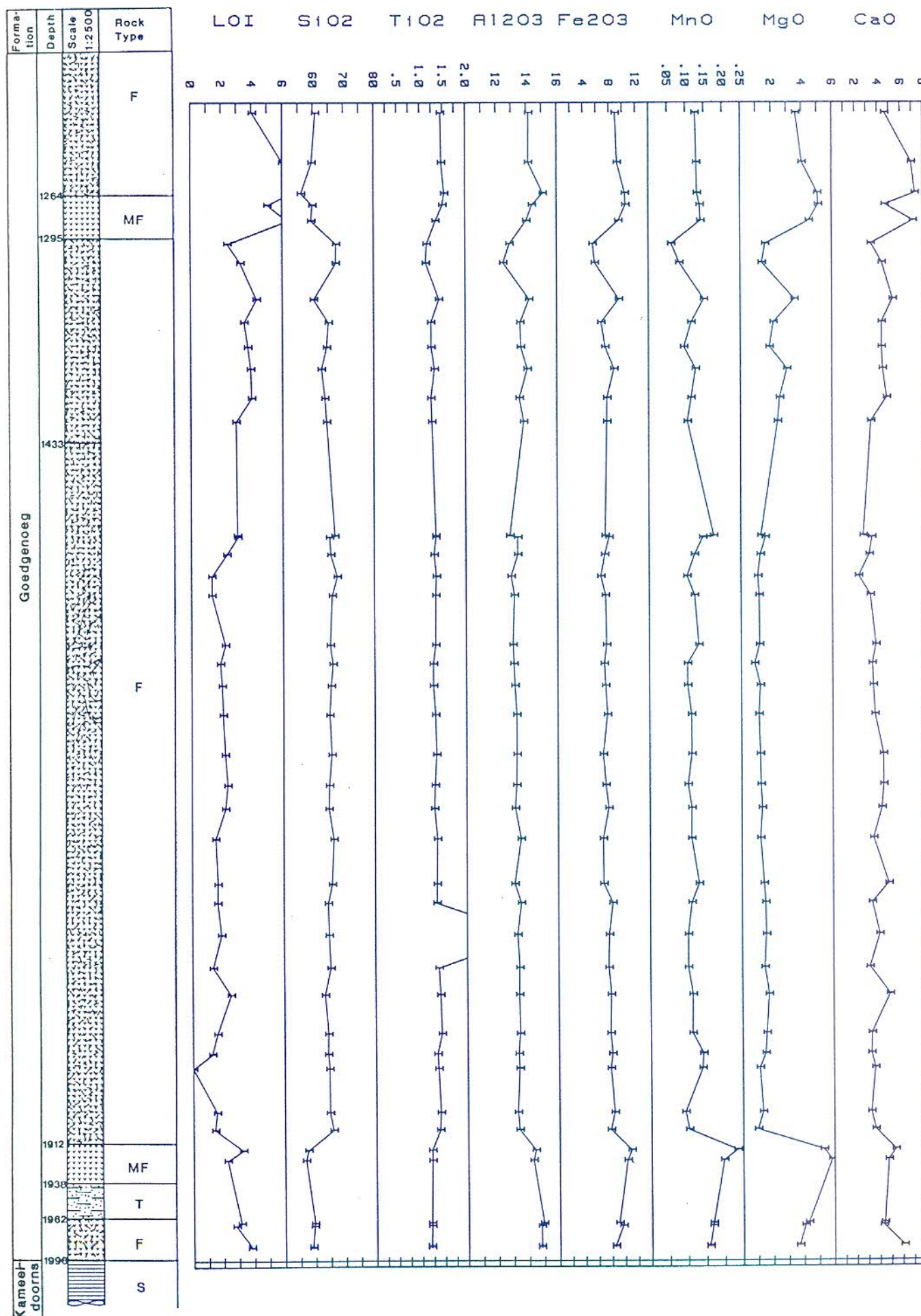


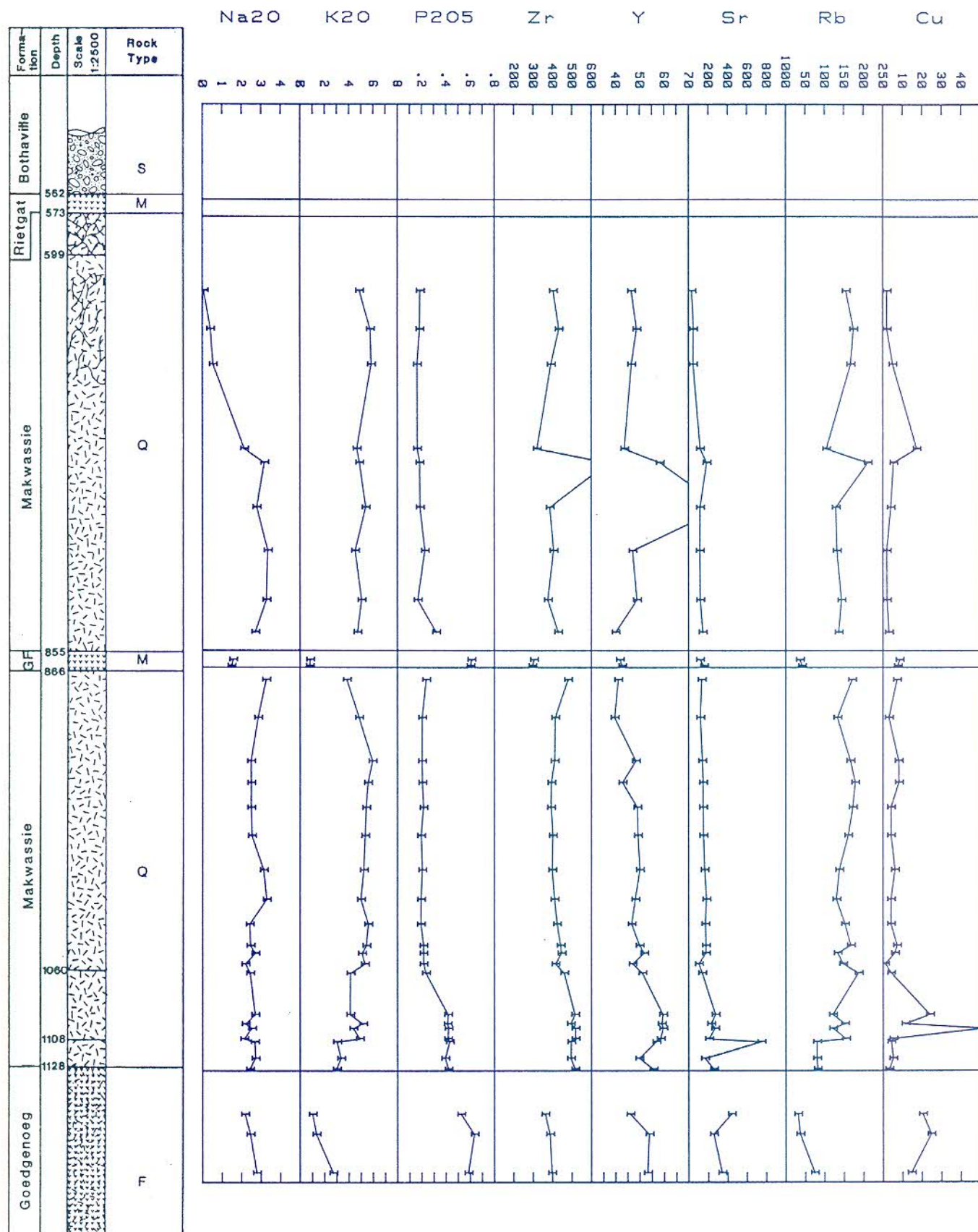
BOREHOLE FORMATION	DF1 MAKW.	DF1 MAKW.	DF1 MAKW.	DF1 MAKW.	DF1 MAKW.	DF1 MAKW.	DF1 MAKW.	DF1 MAKW.	DF1 MAKW.	DF1 MAKW.
DEPTH	558	554	531	524	515	461	441	419	397	361
SAMPLE No	291	292	293	294	295	296	297	298	299	300
SiO2	69.68	69.99	65.89	66.63	68.07	68.65	67.90	67.57	67.65	67.73
TiO2	1.03	1.04	1.23	1.17	1.10	1.10	1.05	1.10	1.08	1.14
Al2O3	12.45	13.17	14.52	14.01	13.09	12.94	13.41	13.08	13.15	13.41
Fe2O3	4.97	5.14	7.59	6.80	6.41	6.30	6.72	7.14	6.64	6.55
MnO	0.09	0.07	0.09	0.11	0.09	0.08	0.09	0.09	0.09	0.09
MgO	0.62	0.44	2.36	1.86	0.57	0.68	1.69	1.42	1.28	1.18
CaO	6.81	2.33	2.68	3.50	3.34	2.51	2.57	3.01	3.57	3.73
Na2O	3.66	1.56	2.26	2.15	2.98	1.87	2.61	2.65	2.79	2.21
K2O	0.26	5.82	2.88	3.30	3.91	5.42	3.52	3.50	3.30	3.48
P2O5	0.42	0.43	0.50	0.47	0.43	0.44	0.43	0.43	0.44	0.47
TOTAL	100.00	100.00	100.00	100.00	100.00	100.00	100.00	100.00	100.00	100.00
Zr	438	464	507	537	491	498	480	500	447	483
Y	61	57	67	65	60	62	54	59	59	64
Sr	2344	192	385	235	381	313	418	352	300	218
Rb	9	145	118	138	95	117	82	81	80	94
Cu	56	7	5	13	6	11	13	11	8	19
Zn	52	92	134	112	109	103	119	127	124	112
Ni	15	17	20	19	18	19	21	19	19	18
Ba	112	2285	1191	1045	1450	2216	1573	1372	1233	1554
Nb	21	21	24	23	21	23	21	22	22	23
V	95	96	118	113	105	101	99	98	107	113
Cr	31	26	26	29	22	29	47	27	42	35
Co	6	14	15	11	14	14	16	11	15	9

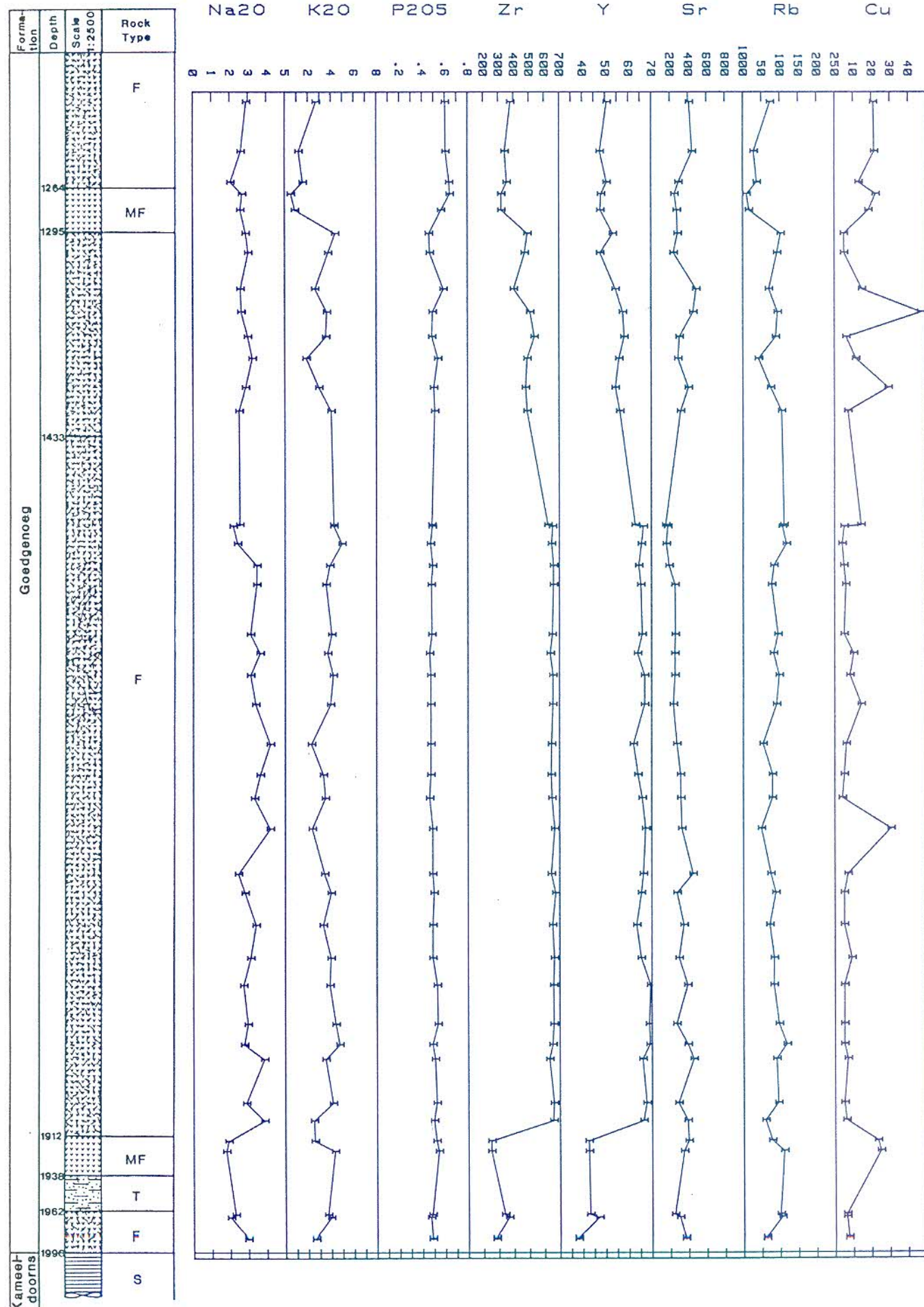


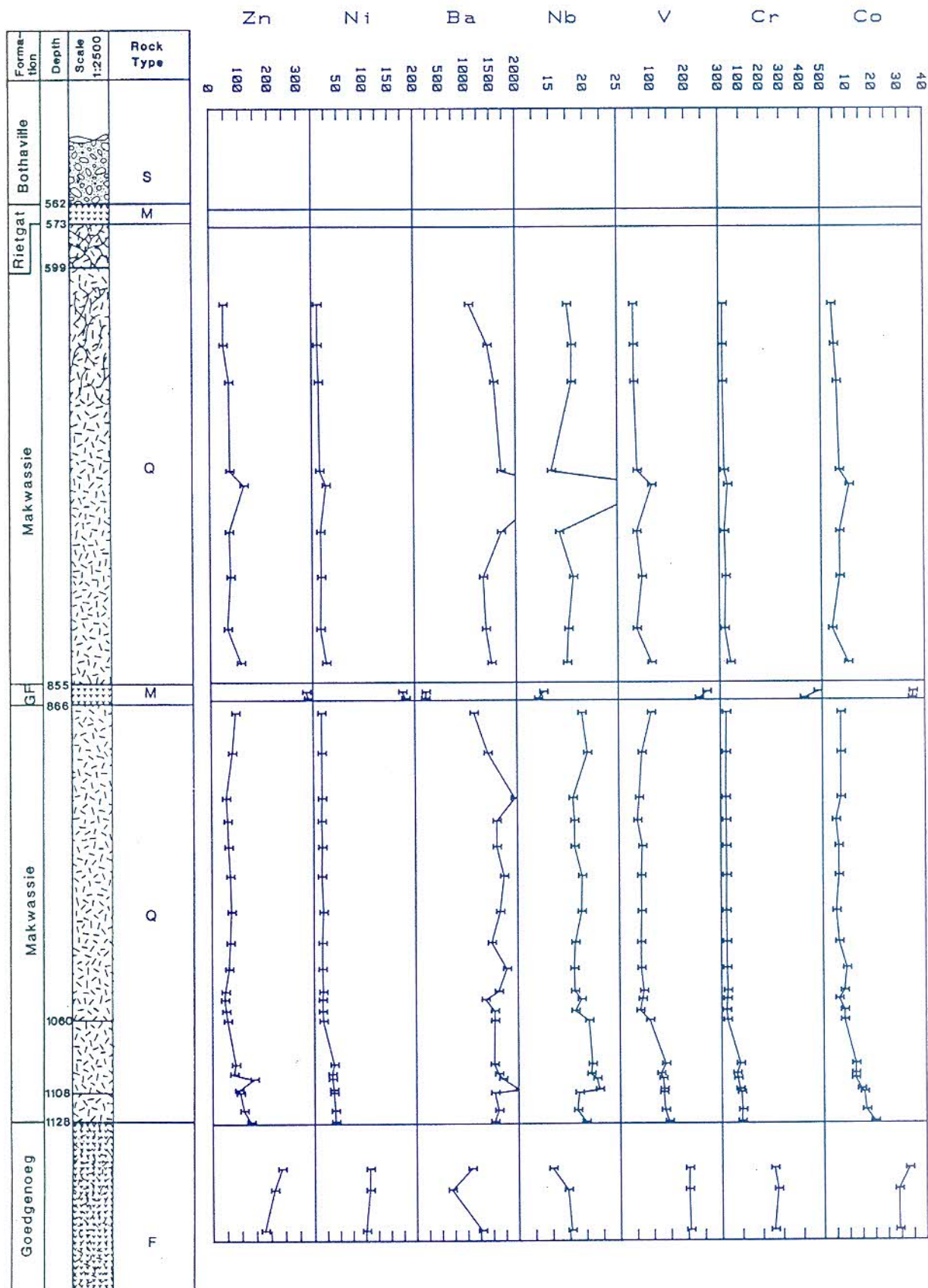
BOREHOLE FORMATION	DF1 MAKW.	DF1 MAKW.	DF1 MAKW.	DF1 MAKW.	DF1 MAKW.	DF1 RIETG.
DEPTH	346	330	313	297	283	256
SAMPLE No	301	302	303	304	305	306
SiO2	68.51	67.77	69.22	69.15	64.69	54.64
Al2O3	1.10	1.11	1.12	1.07	1.42	2.08
Fe2O3	13.59	13.21	13.45	12.95	17.24	14.12
MnO	6.20	6.68	5.60	5.39	5.35	12.71
CaO	0.08	0.11	0.09	0.11	0.07	0.16
MgO	1.12	1.07	1.16	1.26	1.71	4.29
Na2O	3.27	4.25	3.79	5.04	2.97	8.19
K2O	2.15	2.04	1.67	1.22	1.02	2.42
P2O5	3.56	3.31	3.44	3.39	4.92	0.26
TOTAL	0.43	0.45	0.45	0.42	0.60	1.14
	100.00	100.00	100.00	100.00	100.00	100.00
Zn	487	480	486	476	622	278
Ni	55	61	62	55	83	46
Ba	152	219	125	105	121	1115
Nb	98	88	100	93	169	5
V	4	22	13	7	22	37
Cr	105	117	105	88	69	144
Co	18	20	18	16	18	79
	1958	1302	1719	1130	1207	1220
	22	22	22	21	28	15
	115	104	108	100	141	289
	37	30	39	35	52	128
	8	14	10	11	14	38

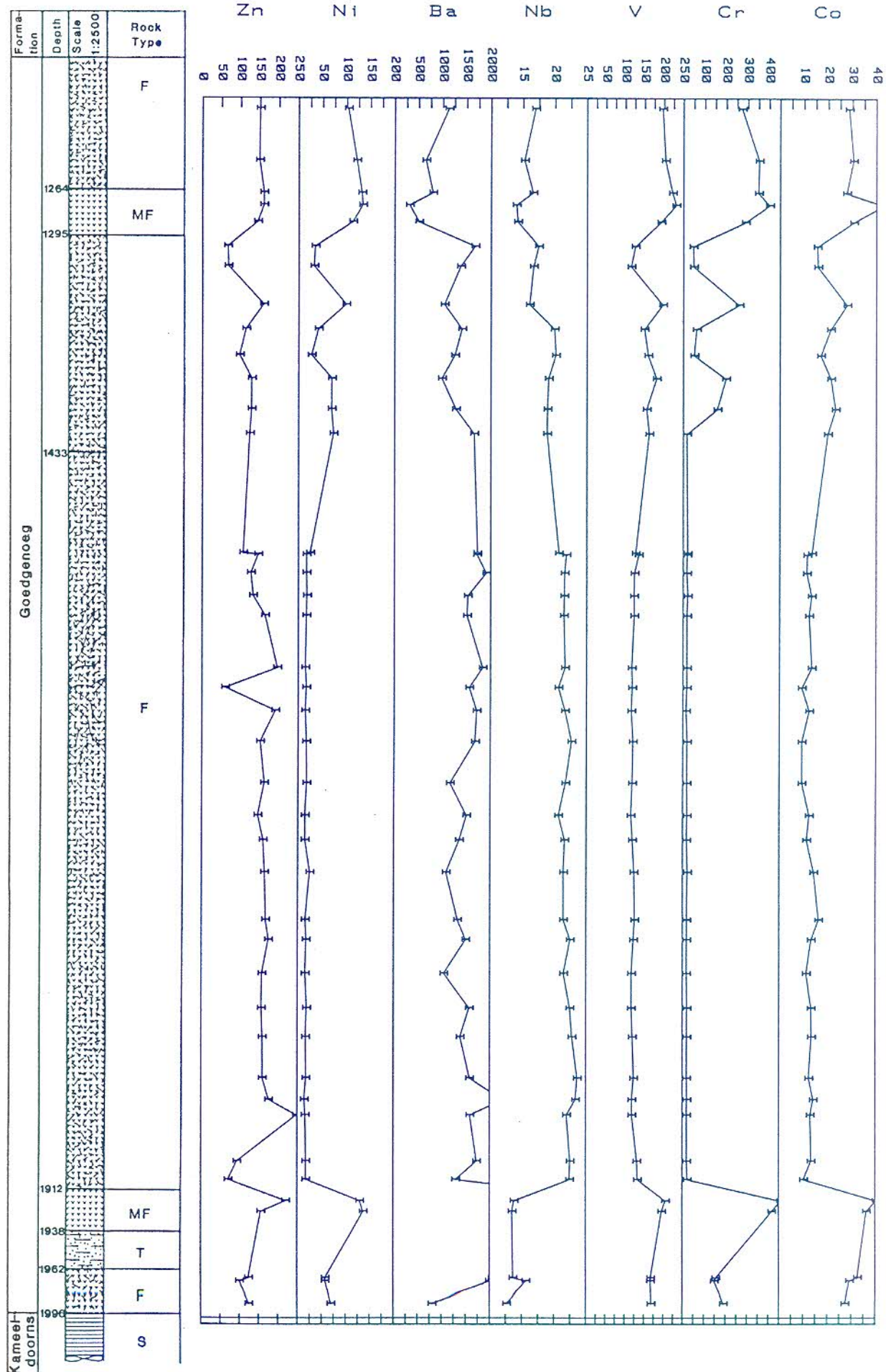












BOREHOLE FORMATION	DHK1 GOEDG.	DHK1 GOEDG.	DHK1 GOEDG.	DHK1 GOEDG.	DHK1 GOEDG.	DHK1 GOEDG.	DHK1 GOEDG.	DHK1 GOEDG.	DHK1 GOEDG.
DEPTH	1987	1973	1971	1927	1920	1894	1906	1864	1854
SAMPLE No	307	308	309	310	311	312	313	314	315
SiO2	59.36	59.49	59.59	56.79	57.56	64.74	65.88	64.65	64.26
TiO2	1.20	1.20	1.20	1.21	1.21	1.40	1.39	1.36	1.34
Al2O3	14.88	14.79	14.93	14.27	14.42	13.26	13.37	13.39	13.34
Fe2O3	8.51	9.62	9.03	10.33	10.95	8.41	7.83	7.87	8.12
MnO	0.16	0.17	0.17	0.20	0.23	0.09	0.10	0.14	0.14
MgO	3.70	4.05	4.28	5.82	5.30	1.30	0.97	1.11	1.50
CaO	6.11	4.27	4.37	4.75	5.36	3.26	3.62	3.61	3.30
Na2O	2.98	2.02	2.28	1.77	1.90	2.88	3.86	3.86	2.78
K2O	2.63	3.93	3.68	4.31	2.54	4.14	2.48	3.50	4.73
P2O5	0.49	0.47	0.48	0.54	0.52	0.52	0.50	0.51	0.49
TOTAL	100.00	100.00	100.00	100.00	100.00	100.00	100.00	100.00	100.00
Zr	283	364	338	249	251	661	657	632	653
Y	38	47	43	43	42	68	66	66	69
Sr	363	299	245	346	396	286	386	453	389
Rb	63	104	100	110	78	94	59	90	118
Cu	7	6	6	25	23	5	6	7	5
Zn	125	100	124	156	220	93	70	248	176
Ni	70	57	58	137	130	17	17	16	14
Ba	811	1992	2060	3076	4975	1727	1295	1588	2269
Nb	13	16	14	13	14	23	22	22	23
V	170	167	168	196	206	132	134	119	119
Cr	192	148	155	416	458	19	22	19	20
Co	28	29	33	36	40	13	10	13	14

BOREHOLE FORMATION	DHK1 GOEDG.	DHK1 GOEDG.	DHK1 GOEDG.	DHK1 GOEDG.	DHK1 GOEDG.	DHK1 GOEDG.	DHK1 GOEDG.	DHK1 GOEDG.	DHK1 GOEDG.
DEPTH	1840	1813	1794	1771	1749	1736	1705	1684	1668
SAMPLE No	316	317	318	319	320	321	322	323	324
SiO2	64.33	63.30	65.21	64.70	64.46	65.80	66.37	64.79	64.94
TiO2	1.44	1.41	1.38	1.34	1.34	1.35	1.36	1.30	1.31
Al2O3	13.44	13.40	13.43	13.30	13.55	13.13	13.55	13.18	13.27
Fe2O3	7.85	7.97	7.63	7.72	8.28	6.93	6.84	7.72	7.24
MnO	0.11	0.11	0.10	0.10	0.11	0.13	0.11	0.11	0.10
MgO	1.58	1.74	1.47	1.57	1.53	1.44	1.22	1.34	1.26
CaO	3.35	4.94	3.18	4.06	3.42	4.87	3.55	4.29	4.45
Na2O	2.98	2.73	3.12	3.41	2.81	2.45	4.18	3.33	3.64
K2O	4.39	3.87	3.98	3.30	3.99	3.42	2.32	3.48	3.31
P2O5	0.53	0.53	0.49	0.49	0.50	0.49	0.49	0.46	0.47
TOTAL	100.00	100.00	100.00	100.00	100.00	100.00	100.00	100.00	100.00
Zr	660	658	664	653	673	645	667	649	644
Y	69	69	65	63	65	66	67	66	64
Sr	267	387	294	347	272	447	325	315	312
Rb	96	83	84	72	88	74	49	79	79
Cu	5	5	9	5	5	7	31	4	5
Zn	159	158	156	157	174	166	163	159	146
Ni	17	17	18	15	17	15	24	14	14
Ba	1581	1384	1572	1043	1495	1325	1087	1359	1509
Nb	24	23	22	21	23	21	21	22	21
V	123	120	117	117	123	125	123	119	116
Cr	18	20	20	17	18	18	21	17	20
Co	12	13	13	11	13	16	14	11	12

BOREHOLE FORMATION	DHK1 GOEDG.	DHK1 GOEDG.	DHK1 GOEDG.	DHK1 GOEDG.	DHK1 GOEDG.	DHK1 GOEDG.	DHK1 GOEDG.	DHK1 GOEDG.	DHK1 GOEDG.
DEPTH	1647	1620	1600	1585	1572	1538	1525	1510	1498
SAMPLE No	325	326	327	328	329	330	331	332	333
SiO2	65.78	65.08	65.59	66.24	65.37	66.07	67.73	65.59	65.25
TiO2	1.34	1.32	1.28	1.28	1.33	1.34	1.35	1.30	1.34
Al2O3	13.30	13.28	13.17	13.11	13.06	13.16	12.95	13.38	13.39
Fe2O3	6.91	7.56	7.29	7.11	7.46	7.31	6.62	7.23	7.88
MnO	0.11	0.11	0.10	0.10	0.13	0.12	0.10	0.12	0.15
MgO	1.21	1.14	1.24	0.88	1.19	1.17	1.09	1.26	1.59
CaO	4.43	3.69	3.56	3.48	3.80	3.33	2.30	3.25	3.48
Na2O	4.19	3.40	3.12	3.64	3.12	3.46	3.47	2.42	2.18
K2O	2.26	3.94	4.18	3.70	4.05	3.56	3.89	4.96	4.26
P2O5	0.48	0.47	0.47	0.46	0.48	0.48	0.49	0.47	0.49
TOTAL	100.00	100.00	100.00	100.00	100.00	100.00	100.00	100.00	100.00
Zr	647	655	656	639	652	660	661	648	655
Y	62	67	67	64	66	65	64	66	66
Sr	272	234	253	252	257	254	190	161	177
Rb	54	91	98	82	95	78	84	118	107
Cu	6	14	8	10	5	6	5	4	5
Zn	162	151	191	163	196	163	132	126	145
Ni	18	16	14	16	14	16	17	16	17
Ba	1166	1681	1714	1560	1837	1509	1526	1909	1715
Nb	22	23	22	21	22	21	21	22	22
V	119	120	116	118	117	123	123	124	135
Cr	19	20	14	19	19	18	21	17	19
Co	9	9	12	9	13	12	13	11	11

BOREHOLE FORMATION	DHK1 GOEDG.	DHK1 GOEDG.	DHK1 GOEDG.	DHK1 GOEDG.	DHK1 GOEDG.	DHK1 GOEDG.	DHK1 GOEDG.	DHK1 GOEDG.	DHK1 GOEDG.
DEPTH	1497	1419	1403	1383	1368	1351	1335	1310	1297
SAMPLE No	334	335	336	337	338	339	340	341	342
SiO2	67.01	64.38	63.82	62.72	64.42	65.04	60.18	67.49	67.61
TiO2	1.34	1.26	1.24	1.32	1.25	1.25	1.42	1.13	1.16
Al2O3	12.88	13.80	13.52	14.05	13.62	13.58	14.17	12.48	12.90
Fe2O3	7.31	7.60	7.62	8.69	7.34	6.74	9.45	5.79	5.49
MnO	0.18	0.10	0.12	0.13	0.10	0.12	0.15	0.08	0.06
MgO	1.30	2.41	2.55	3.03	1.88	2.15	3.52	1.39	1.63
CaO	2.71	3.41	4.80	4.44	4.35	4.36	5.33	4.39	3.43
Na2O	2.54	2.50	2.87	3.23	2.98	2.63	2.58	3.01	2.88
K2O	4.24	4.02	2.95	1.86	3.57	3.64	2.61	3.75	4.38
P2O5	0.49	0.51	0.50	0.54	0.49	0.49	0.59	0.47	0.46
TOTAL	100.00	100.00	100.00	100.00	100.00	100.00	100.00	100.00	100.00
Zr	624	489	480	490	538	509	402	474	492
Y	63	56	54	56	58	58	54	48	53
Sr	155	317	402	289	304	453	487	241	285
Rb	111	105	75	42	89	94	70	93	102
Cu	14	7	29	12	6	47	15	5	5
Zn	106	123	128	128	96	113	159	67	66
Ni	24	72	68	69	26	41	98	31	34
Ba	1722	1652	1272	980	1252	1398	1032	1368	1669
Nb	21	19	19	19	20	20	16	17	17
V	127	162	155	181	159	149	196	114	125
Cr	21	17	157	197	50	61	258	47	45
Co	13	20	23	21	17	21	28	16	15

BOREHOLE FORMATION	DHK1 GOEDG.	DHK1 GOEDG.	DHK1 GOEDG.	DHK1 GOEDG.	DHK1 GOEDG.	DHK1 GOEDG.	DHK1 GOEDG.	DHK1 GOEDG.	DHK1 MAKW.
DEPTH	1281	1270	1262	1241	1207	1194	1169	1156	1127
SAMPLE No	343	344	345	346	347	348	349	350	351
SiO2	59.43	59.83	56.14	59.59	60.83	61.60	58.49	61.44	65.51
TiO2	1.35	1.50	1.54	1.48	1.46	1.42	1.50	1.26	1.18
Al2O3	14.00	14.38	15.10	14.13	14.16	14.06	14.44	14.00	13.37
Fe2O3	9.42	10.51	10.44	9.22	8.94	9.35	10.55	10.40	7.70
MnO	0.14	0.14	0.13	0.13	0.13	0.16	0.17	0.16	0.10
MgO	4.50	5.11	5.07	4.03	3.61	4.02	4.72	5.06	2.85
CaO	7.13	4.66	7.32	6.98	4.66	3.30	5.71	3.96	3.43
Na2O	2.59	2.69	2.06	2.62	2.92	2.79	2.46	2.17	2.43
K2O	0.88	0.54	1.56	1.20	2.69	2.71	1.32	1.02	3.00
P2O5	0.57	0.64	0.64	0.61	0.60	0.58	0.64	0.52	0.42
TOTAL	100.00	100.00	100.00	100.00	100.00	100.00	100.00	100.00	100.00
Zr	321	321	357	344	381	397	387	362	516
Y	48	48	51	48	51	53	54	46	56
Sr	276	252	296	443	410	340	254	439	256
Rb	16	10	37	29	74	74	37	31	82
Cu	19	23	13	22	21	15	25	20	3
Zn	144	160	160	149	150	177	211	237	131
Ni	112	133	131	120	102	100	108	108	41
Ba	499	304	787	644	1120	1276	690	1079	1534
Nb	14	14	17	15	17	18	17	15	20
V	192	231	221	203	195	206	202	203	145
Cr	287	400	348	351	272	256	274	256	98
Co	30	43	28	30	29	29	29	33	20

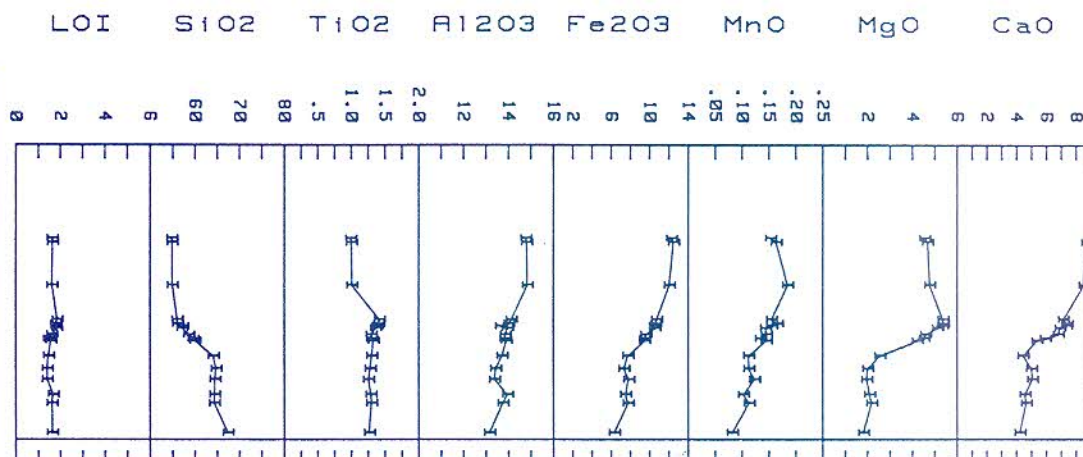
BOREHOLE FORMATION	DHK1 MAKW.	DHK1 MAKW.	DHK1 MAKW.	DHK1 MAKW.	DHK1 MAKW.	DHK1 MAKW.	DHK1 MAKW.	DHK1 MAKW.	DHK1 MAKW.
DEPTH	1120	1109	1107	1100	1097	1091	1064	1058	1051
SAMPLE No	352	353	354	355	356	357	358	359	360
SiO2	68.34	67.73	65.65	65.92	65.42	65.48	70.53	72.51	70.81
TiO2	1.11	1.15	1.13	1.13	1.14	1.18	0.75	0.71	0.75
Al2O3	13.09	12.64	13.56	13.30	13.41	13.42	14.48	12.86	12.68
Fe2O3	6.54	6.52	6.82	6.59	6.82	7.09	4.51	3.75	4.15
MnO	0.09	0.12	0.08	0.08	0.08	0.07	0.06	0.05	0.07
MgO	2.21	2.04	1.96	2.24	1.81	2.06	1.36	0.89	0.86
CaO	2.16	3.69	3.34	3.43	3.55	3.49	1.52	1.50	2.69
Na2O	2.72	2.68	2.14	2.54	2.21	2.69	2.44	2.20	2.70
K2O	3.34	3.02	4.89	4.35	5.15	4.10	4.12	5.32	5.07
P2O5	0.39	0.43	0.42	0.42	0.41	0.42	0.23	0.21	0.21
TOTAL	100.00	100.00	100.00	100.00	100.00	100.00	100.00	100.00	100.00
Zr	494	496	518	517	493	516	459	415	446
Y	50	57	59	60	59	59	51	47	52
Sr	165	179	207	269	228	273	136	103	175
Rb	80	80	155	121	152	121	187	147	133
Cu	5	4	5	52	11	24	4	1	6
Zn	108	96	90	143	73	79	52	47	43
Ni	40	38	38	35	34	39	17	16	16
Ba	1615	1537	2017	1694	1614	1527	1542	1540	1359
Nb	19	19	22	22	21	21	20	18	19
V	134	129	131	127	121	136	89	60	67
Cr	101	96	88	78	73	91	29	25	28
Co	17	16	15	12	12	13	8	8	6

BOREHOLE FORMATION	DHK1 MAKW.	DHK1 MAKW.	DHK1 MAKW.	DHK1 MAKW.	DHK1 MAKW.	DHK1 MAKW.	DHK1 MAKW.	DHK1 MAKW.	DHK1 MAKW.
DEPTH	1046	1032	1016	997	975	957	941	927	899
SAMPLE No	361	362	363	364	365	366	367	368	369
SiO2	70.97	72.05	71.22	70.54	71.80	71.07	72.03	73.15	71.01
TiO2	0.71	0.67	0.69	0.69	0.70	0.70	0.69	0.70	0.72
Al2O3	12.95	12.91	12.81	13.05	12.62	13.06	13.20	12.74	13.13
Fe2O3	4.39	3.77	4.01	4.27	4.11	3.90	2.91	2.68	4.15
MnO	0.05	0.05	0.06	0.06	0.06	0.06	0.07	0.05	0.07
MgO	0.90	0.93	0.91	0.85	0.81	0.73	0.64	0.55	0.87
CaO	1.94	1.42	1.83	1.99	1.84	2.36	2.20	1.52	2.16
Na2O	2.45	2.41	3.29	3.13	2.93	2.49	2.49	2.48	2.84
K2O	5.43	5.59	4.98	5.22	5.33	5.41	5.56	5.93	4.84
P2O5	0.21	0.19	0.19	0.20	0.19	0.21	0.20	0.20	0.20
TOTAL	100.00	100.00	100.00	100.00	100.00	100.00	100.00	100.00	100.00
Zr	441	423	410	398	402	392	394	410	413
Y	50	47	48	50	49	49	43	48	40
Sr	175	170	181	162	150	146	146	138	119
Rb	167	152	130	138	161	172	178	166	133
Cu	7	4	4	6	4	4	8	8	3
Zn	45	58	63	66	63	57	54	49	71
Ni	17	16	16	18	15	16	15	16	16
Ba	1618	1780	1486	1654	1735	1593	1591	1950	1422
Nb	18	18	18	19	19	18	18	18	20
V	71	64	64	65	65	68	54	59	68
Cr	31	27	28	26	28	27	25	24	26
Co	8	9	6	5	6	6	5	7	7

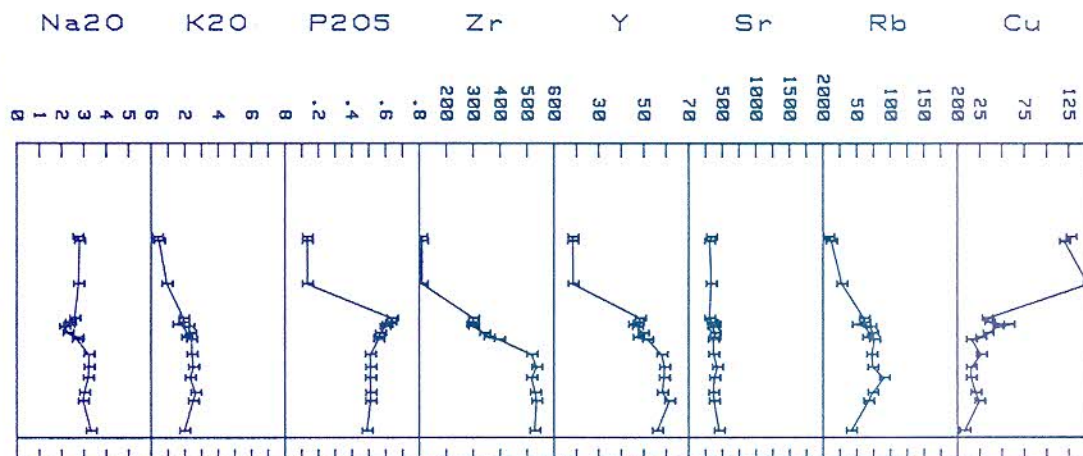
BOREHOLE FORMATION	DHK1 MAKW.	DHK1 GARF.	DHK1 GARF.	DHK1 MAKW.	DHK1 MAKW.	DHK1 MAKW.	DHK1 MAKW.	DHK1 MAKW.	DHK1 MAKW.
DEPTH	874	865	861	843	822	790	762	733	724
SAMPLE No	370	371	372	373	374	375	376	377	378
SiO2	69.84	55.12	57.97	69.54	72.18	71.13	71.75	72.64	74.15
TiO2	0.81	1.48	1.53	0.90	0.62	0.75	0.67	0.64	0.57
Al2O3	15.14	14.07	14.50	13.21	12.77	13.03	12.98	12.79	11.67
Fe2O3	3.54	12.98	12.77	5.23	3.05	4.25	3.40	3.26	3.90
MnO	0.06	0.16	0.15	0.08	0.05	0.06	0.08	0.07	0.08
MgO	0.93	5.89	5.81	1.21	0.50	0.76	0.57	0.58	0.98
CaO	2.36	7.42	4.27	2.10	2.34	1.93	2.20	1.79	1.72
Na2O	3.26	1.48	1.56	2.70	3.28	3.35	2.78	3.17	2.13
K2O	3.82	0.79	0.82	4.70	5.04	4.51	5.38	4.87	4.64
P2O5	0.24	0.60	0.61	0.32	0.17	0.23	0.18	0.18	0.16
TOTAL	100.00	100.00	100.00	100.00	100.00	100.00	100.00	100.00	100.00
Zr	480	296	304	429	375	405	386	687	320
Y	41	43	42	40	49	47	84	58	44
Sr	133	158	116	144	119	116	119	186	118
Rb	171	42	36	137	143	132	129	211	105
Cu	7	8	9	3	2	2	4	5	17
Zn	83	333	327	104	59	70	66	117	68
Ni	16	182	176	27	16	17	16	27	15
Ba	1153	207	219	1512	1407	1355	1716	2765	1713
Nb	20	13	14	17	18	18	16	31	15
V	97	238	260	100	56	73	57	102	59
Cr	29	412	479	52	25	32	26	42	25
Co	7	35	35	10	4	7	7	11	7

BOREHOLE FORMATION	DHK1 MAKW.	DHK1 MAKW.	DHK1 MAKW.
DEPTH	669	646	621
SAMPLE No	379	380	381
SiO2	74.26	73.62	74.28
TiO2	0.60	0.65	0.60
Al2O3	13.61	13.81	13.48
Fe2O3	3.20	3.11	3.40
MnO	0.04	0.05	0.05
MgO	1.38	1.31	1.71
CaO	0.37	1.11	1.35
Na2O	0.54	0.41	0.07
K2O	5.84	5.75	4.86
P2O5	0.16	0.18	0.19
TOTAL	100.00	100.00	100.00
Zr	392	433	404
Y	47	49	47
Sr	47	50	33
Rb	167	175	155
Cu	5	2	2
Zn	66	47	48
Ni	13	11	11
Ba	1577	1449	1090
Nb	18	18	18
V	50	49	48
Cr	18	17	19
Co	6	5	4

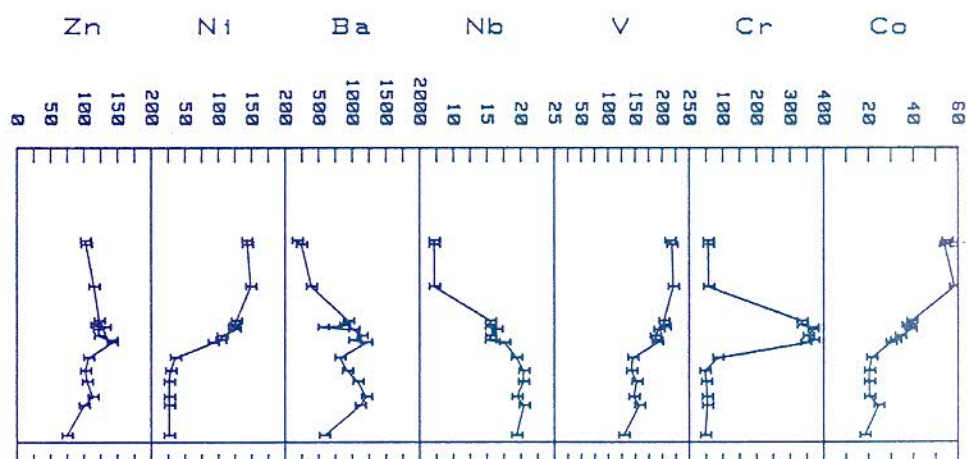
Formation	Depth	Scale	Rock Type
Klipriviersberg	2602	1:2500	M
Goedgenoeg	2625		MF
	2688		F



Formation	Depth	Scale	Rock Type
Klipriviersberg	2602	1:2500	M
Goedgenoeg	2625		MF
	2688		F



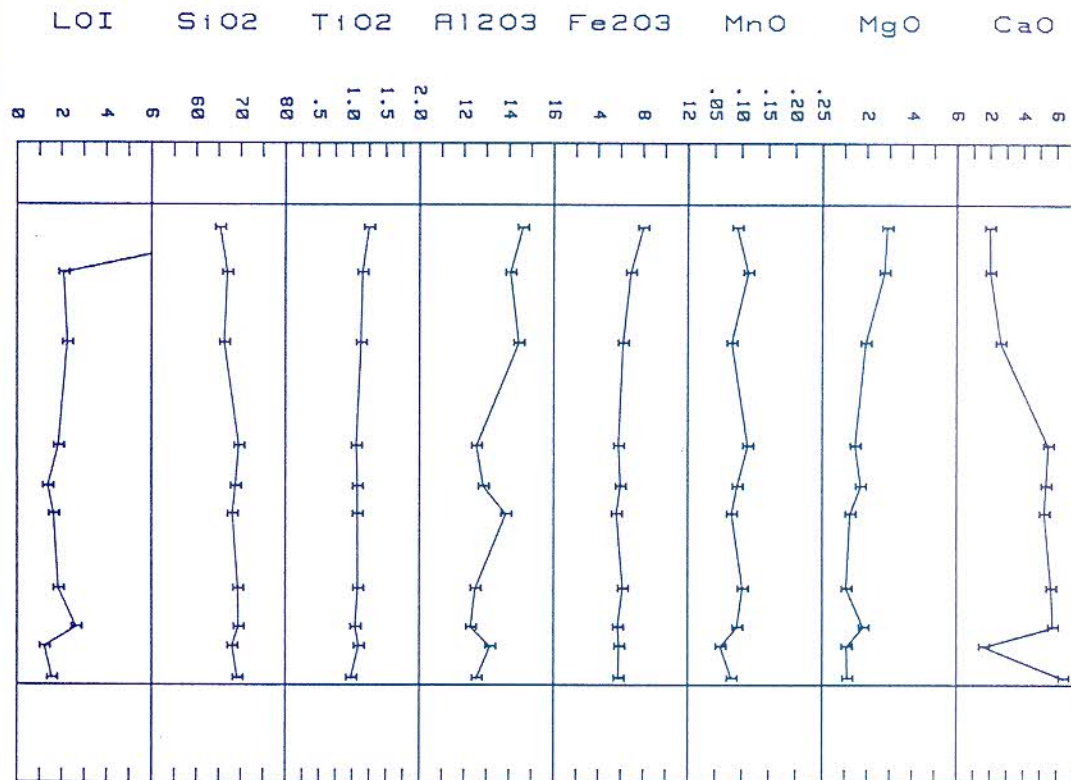
Formation	Depth	Scale	Rock Type
Klipriviersberg	2602	1:2500	M
Goedgenoeg	2625		MF
	2688		F



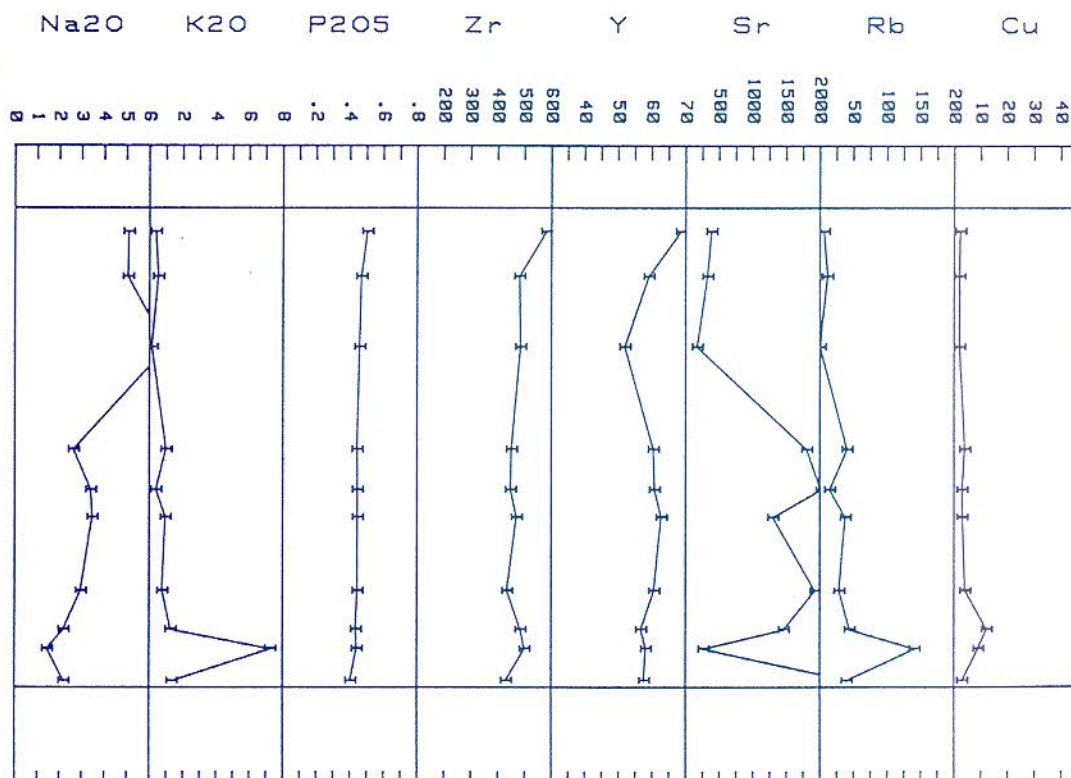
BOREHOLE FORMATION	FS4 GOEDG.	FS4 GOEDG.	FS4 GOEDG.	FS4 GOEDG.	FS4 GOEDG.	FS4 GOEDG.	FS4 GOEDG.	FS4 GOEDG.	FS4 GOEDG.
DEPTH	2685	2671	2667	2660	2655	2649	2642	2641	2639
SAMPLE No	382	383	384	385	386	387	388	389	390
SiO2	67.38	64.30	64.38	64.43	64.66	64.04	59.97	59.50	58.56
TiO2	1.26	1.30	1.29	1.25	1.28	1.30	1.32	1.30	1.29
Al2O3	13.15	13.74	13.94	13.37	13.42	13.70	13.89	13.83	13.85
Fe2O3	6.31	7.76	7.48	7.81	7.31	7.73	9.46	9.43	9.60
MnO	0.08	0.11	0.10	0.12	0.11	0.11	0.14	0.13	0.14
MgO	1.81	2.18	2.08	1.95	2.00	2.54	4.21	4.50	4.59
CaO	4.22	4.64	4.56	5.06	4.99	4.43	5.35	5.92	6.79
Na2O	3.31	2.96	3.01	3.19	3.22	3.21	2.69	2.72	2.27
K2O	1.99	2.50	2.64	2.31	2.50	2.42	2.40	2.10	2.34
P2O5	0.49	0.51	0.51	0.51	0.51	0.51	0.56	0.56	0.57
TOTAL	100.00	100.00	100.00	100.00	100.00	100.00	100.00	100.00	100.00
Zr	528	535	529	516	535	516	397	359	342
Y	56	61	58	59	59	58	52	47	50
Sr	452	376	368	382	422	369	363	382	390
Rb	42	67	74	91	74	72	76	66	73
Cu	8	25	20	15	15	26	15	26	34
Zn	74	100	113	105	102	107	142	141	123
Ni	26	27	27	26	29	36	92	103	105
Ba	585	1118	1208	1084	928	815	1209	1022	1144
Nb	19	20	19	20	20	19	18	15	16
V	128	157	147	153	143	145	191	190	187
Cr	48	54	53	51	47	84	346	369	353
Co	18	25	20	20	20	21	30	32	34

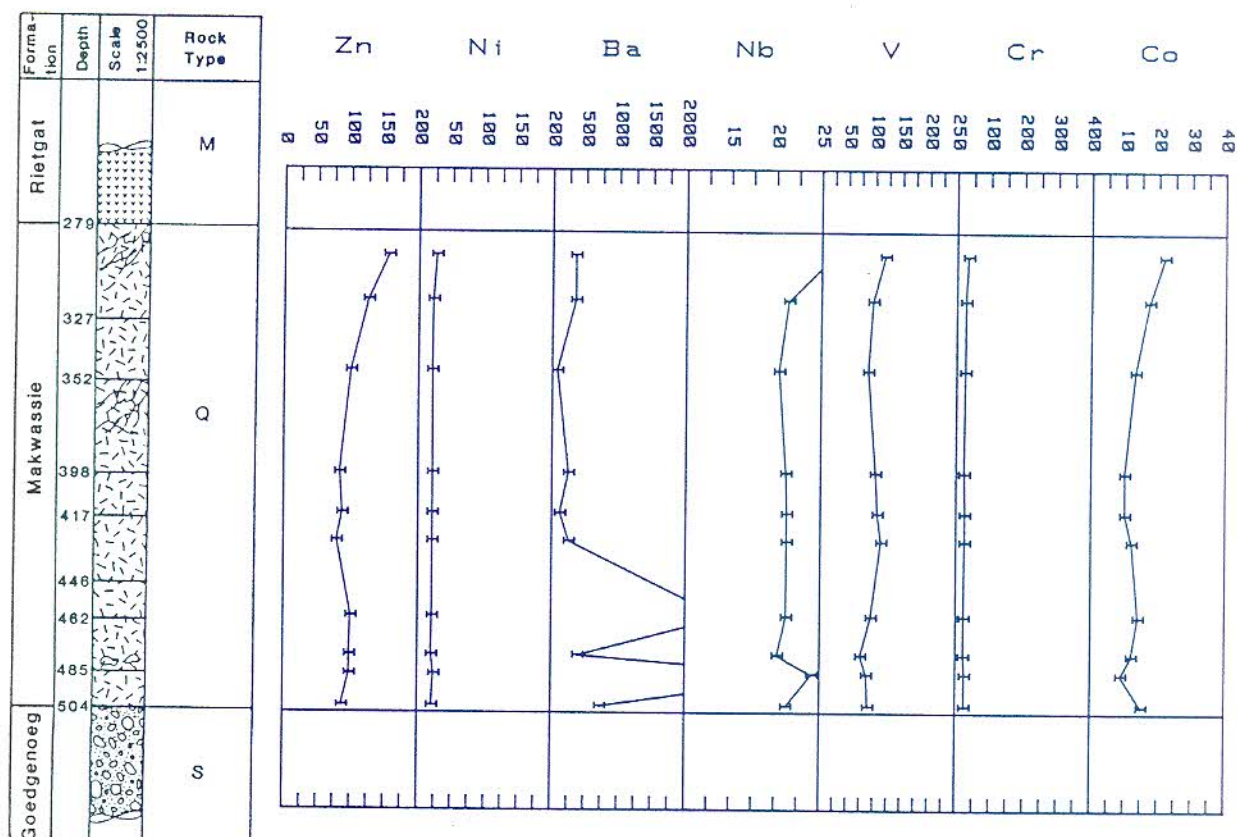
BOREHOLE FORMATION	FS4 GOEDG.	FS4 GOEDG.	FS4 GOEDG.	FS4 GOEDG.	FS4 KLIPR.	FS4 KLIPR.	FS4 KLIPR.
DEPTH	2636	2635	2634	2632	2616	2596	2594
SAMPLE No	391	392	393	394	395	396	397
SiO2	57.07	57.20	56.09	55.98	54.88	54.85	54.81
TiO2	1.35	1.38	1.40	1.41	1.00	1.00	0.99
Al2O3	13.95	13.64	14.00	14.11	14.83	14.80	14.76
Fe2O3	10.52	10.46	10.61	10.72	12.02	12.44	12.26
MnO	0.14	0.15	0.16	0.15	0.18	0.16	0.15
MgO	5.12	5.33	5.38	5.36	4.76	4.67	4.54
CaO	6.91	7.34	7.40	7.14	8.51	8.70	9.29
Na2O	2.12	2.31	2.38	2.58	2.75	2.79	2.71
K2O	2.23	1.58	1.94	1.92	0.92	0.47	0.36
P2O5	0.59	0.61	0.63	0.64	0.13	0.13	0.13
TOTAL	100.00	100.00	100.00	100.00	100.00	100.00	100.00
Zr	301	294	300	301	111	111	109
Y	47	45	47	48	18	18	18
Sr	355	387	341	307	330	305	334
Rb	71	51	62	61	28	12	8
Cu	45	58	36	33	146	120	127
Zn	121	131	117	123	115	103	102
Ni	125	122	124	127	148	143	143
Ba	1021	563	885	943	390	241	179
Nb	16	15	15	15	7	7	7
V	194	205	204	203	220	218	214
Cr	367	368	336	335	57	56	56
Co	39	38	37	39	58	54	55

Formation	Rietgat	Makwassie	Goedgenoeg	Rock Type
Depth	279	327	352	M
Scale 1:2500	398	417	446	Q
	462	485	504	S



Formation	Rietgat	Makwassie	Goedgenoeg	Rock Type
Depth	279	327	352	M
Scale 1:2500	398	417	446	Q
	462	485	504	S

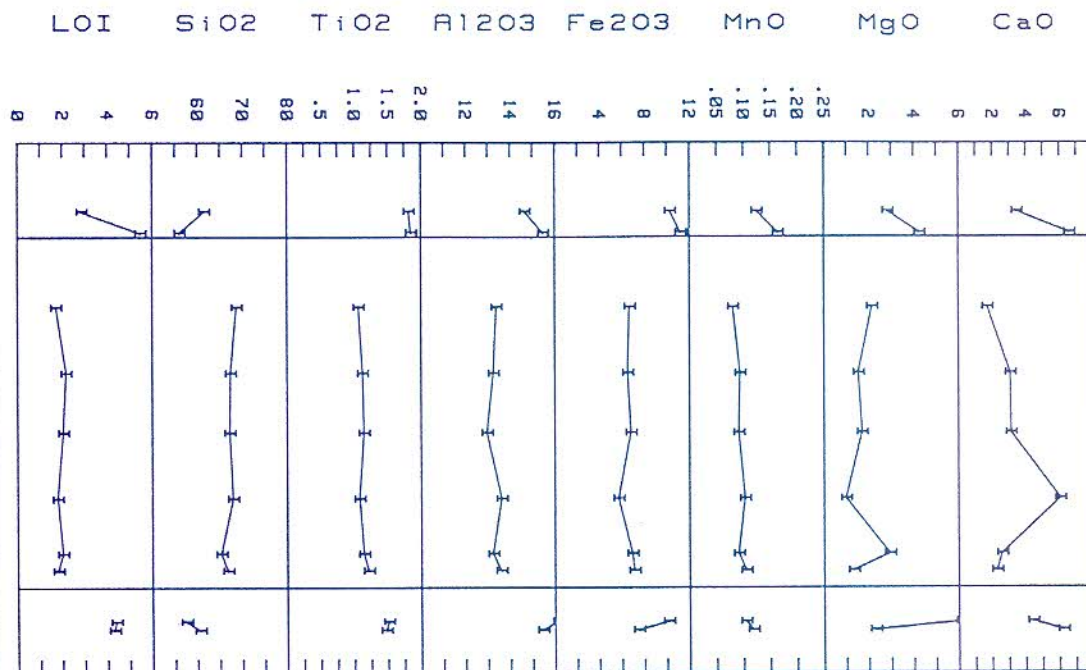




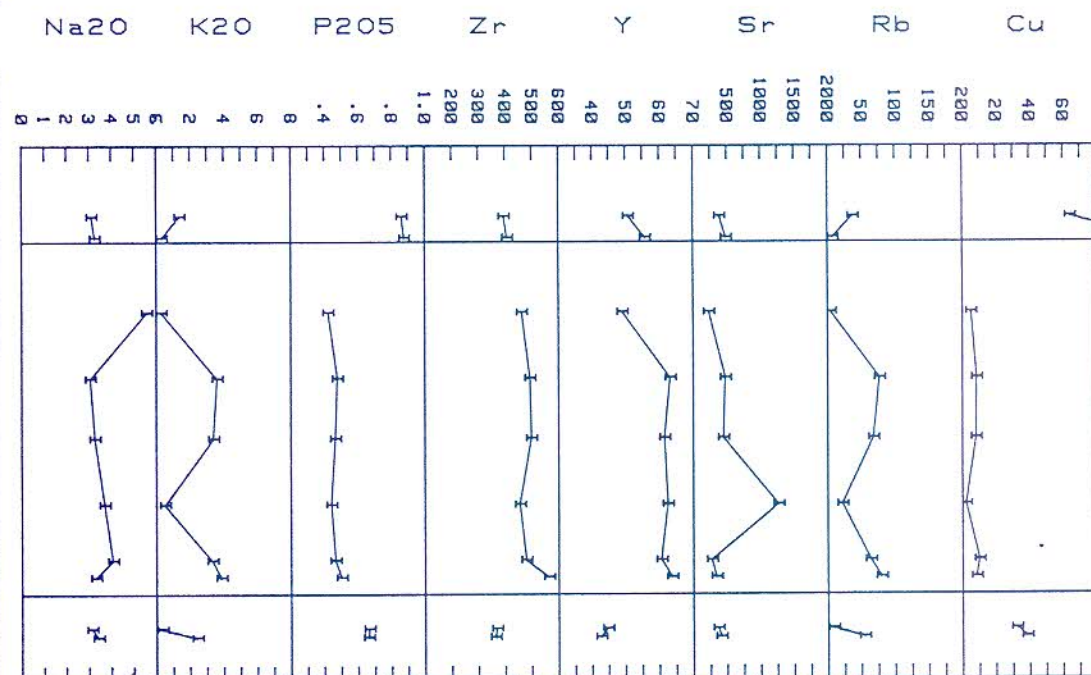
BOREHOLE FORMATION	JWS6 MAKW.	JWS6 MAKW.	JWS6 MAKW.	JWS6 MAKW.	JWS6 MAKW.	JWS6 MAKW.	JWS6 MAKW.	JWS6 MAKW.	JWS6 MAKW.	JWS6 MAKW.
DEPTH	501	486	477	459	424	411	392	344	311	290
SAMPLE No	199	200	201	202	203	204	205	206	207	208
SiO2	69.18	68.01	69.40	69.30	68.05	68.76	69.51	66.22	66.95	65.26
TiO2	0.98	1.09	1.04	1.08	1.07	1.07	1.06	1.13	1.15	1.25
Al2O3	12.55	13.15	12.28	12.49	13.85	12.84	12.54	14.42	14.06	14.61
Fe2O3	5.78	5.84	5.73	6.16	5.61	5.95	5.78	6.21	6.91	8.00
MnO	0.08	0.06	0.09	0.10	0.08	0.09	0.11	0.08	0.11	0.09
MgO	1.11	1.07	1.82	1.06	1.23	1.70	1.46	1.93	2.77	2.88
CaO	6.40	1.63	5.77	5.66	5.26	5.36	5.50	2.64	2.01	1.98
Na2O	2.18	1.44	2.18	2.95	3.46	3.39	2.62	6.77	5.05	5.07
K2O	1.33	7.25	1.25	0.76	0.95	0.39	0.99	0.14	0.52	0.37
P2O5	0.40	0.44	0.44	0.44	0.44	0.44	0.44	0.46	0.47	0.50
TOTAL	100.00	100.00	100.00	100.00	100.00	100.00	100.00	100.00	100.00	100.00
Zr	431	499	484	434	469	447	450	484	480	580
Y	58	58	57	61	63	61	60	52	59	69
Sr	2442	263	1456	1921	1294	2010	1800	170	324	383
Rb	39	140	44	28	37	14	40	0	11	6
Cu	3	9	12	4	3	3	4	2	2	2
Zn	87	98	98	100	79	87	83	100	125	155
Ni	15	15	15	16	17	14	15	16	18	23
Ba	730	3961	397	261	252	120	245	73	346	343
Nb	21	24	20	21	21	21	21	20	21	26
V	89	86	75	94	112	105	102	87	96	118
Cr	25	26	22	23	25	25	23	25	26	33
Co	15	9	12	14	12	10	10	13	17	22

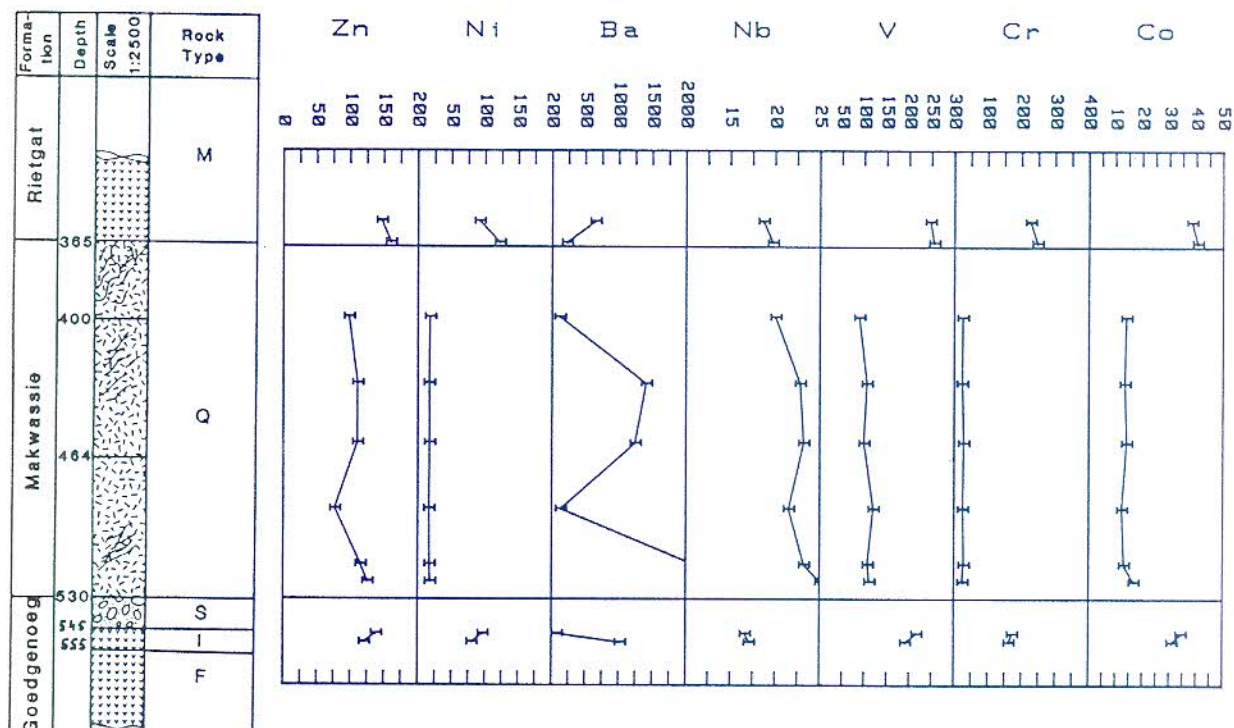
BOREHOLE JWS7

Formation	Depth	Scale	Rock Type
Rietgat	365		M
Makwassie	400		Q
Goedgenoeg	530		S
	545		I
	555		F



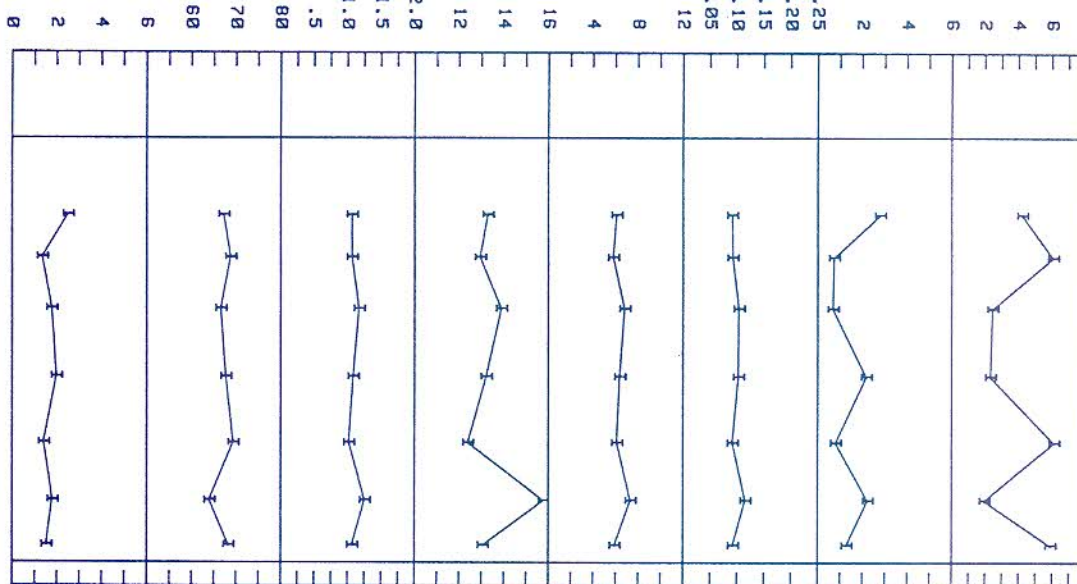
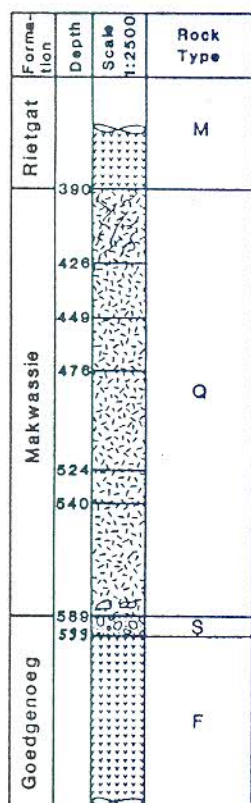
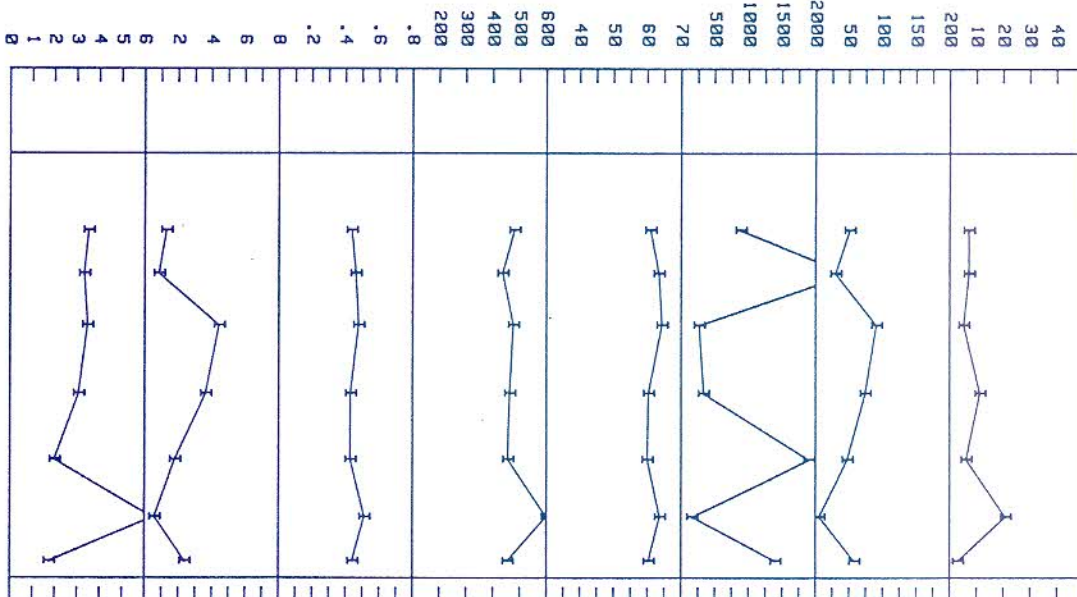
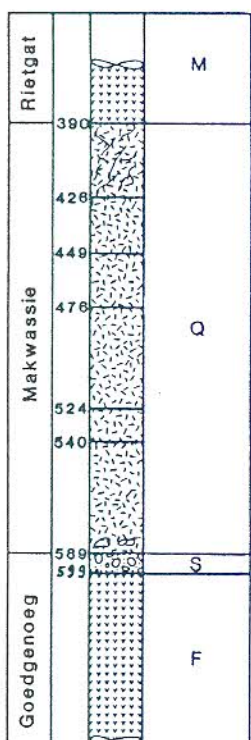
Formation	Depth	Scale	Rock Type
Rietgat	365		M
Makwassie	400		Q
Goedgenoeg	530		S
	545		I
	555		F

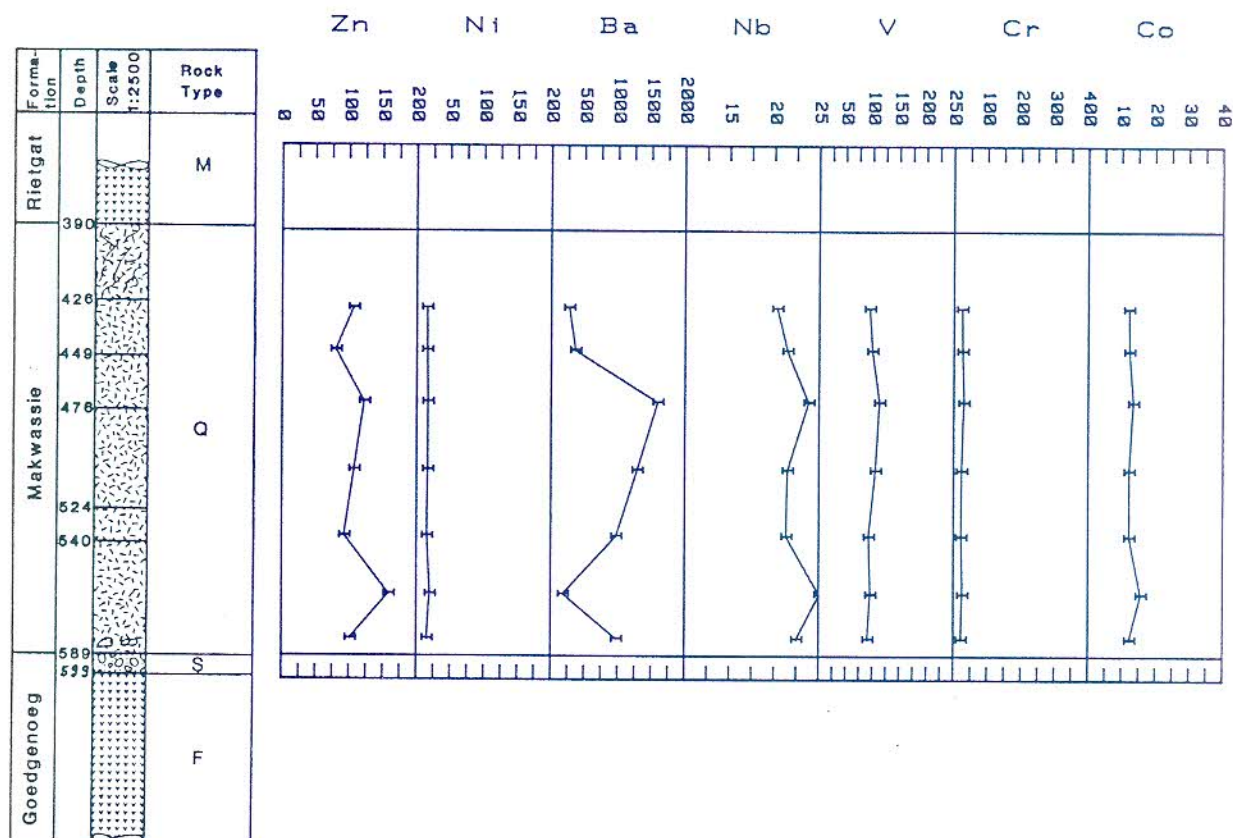




BOREHOLE FORMATION	JWS7 GOEDG.	JWS7 GOEDG.	JWS7 MAKW.	JWS7 MAKW.	JWS7 MAKW.	JWS7 MAKW.	JWS7 MAKW.	JWS7 MAKW.	JWS7 RIETG.	JWS7 RIETG.
DEPTH	550	549	522	514	488	457	429	398	363	353
SAMPLE No	189	190	191	192	193	194	195	196	197	198
SiO2	60.50	57.50	66.76	65.27	67.87	67.13	67.31	68.67	56.02	61.50
TiO2	1.47	1.51	1.21	1.14	1.07	1.14	1.12	1.06	1.85	1.81
Al2O3	15.44	16.11	13.58	13.22	13.60	12.94	13.24	13.38	15.47	14.65
Fe2O3	7.46	10.12	7.09	6.92	5.69	6.79	6.51	6.69	11.20	10.27
MnO	0.12	0.10	0.10	0.09	0.10	0.09	0.09	0.08	0.16	0.12
MgO	2.28	6.10	1.32	2.93	0.97	1.69	1.53	2.14	4.25	2.84
CaO	6.22	4.41	2.28	2.58	6.04	3.11	3.08	1.71	6.60	3.45
Na2O	3.42	3.14	3.32	4.07	3.70	3.26	3.06	5.56	3.26	3.12
K2O	2.42	0.34	3.84	3.31	0.51	3.38	3.59	0.28	0.32	1.37
P2O5	0.66	0.67	0.50	0.46	0.44	0.46	0.48	0.42	0.87	0.86
TOTAL	100.00	100.00	100.00	100.00	100.00	100.00	100.00	100.00	100.00	100.00
Zr	363	368	563	478	454	497	492	461	408	395
Y	43	45	64	61	62	61	63	49	56	51
Sr	409	367	337	271	1262	443	472	228	487	389
Rb	54	8	79	64	21	68	77	4	8	37
Cu	38	32	8	10	2	8	8	5	109	64
Zn	121	138	125	115	77	111	111	98	160	146
Ni	80	97	18	17	16	17	17	18	121	91
Ba	1019	79	2075	2128	132	1243	1405	117	221	644
Nb	17	17	25	23	21	23	23	20	20	19
V	191	216	111	107	120	99	106	88	255	247
Cr	162	173	25	28	26	28	24	25	246	226
Co	31	34	17	13	12	14	13	14	40	38

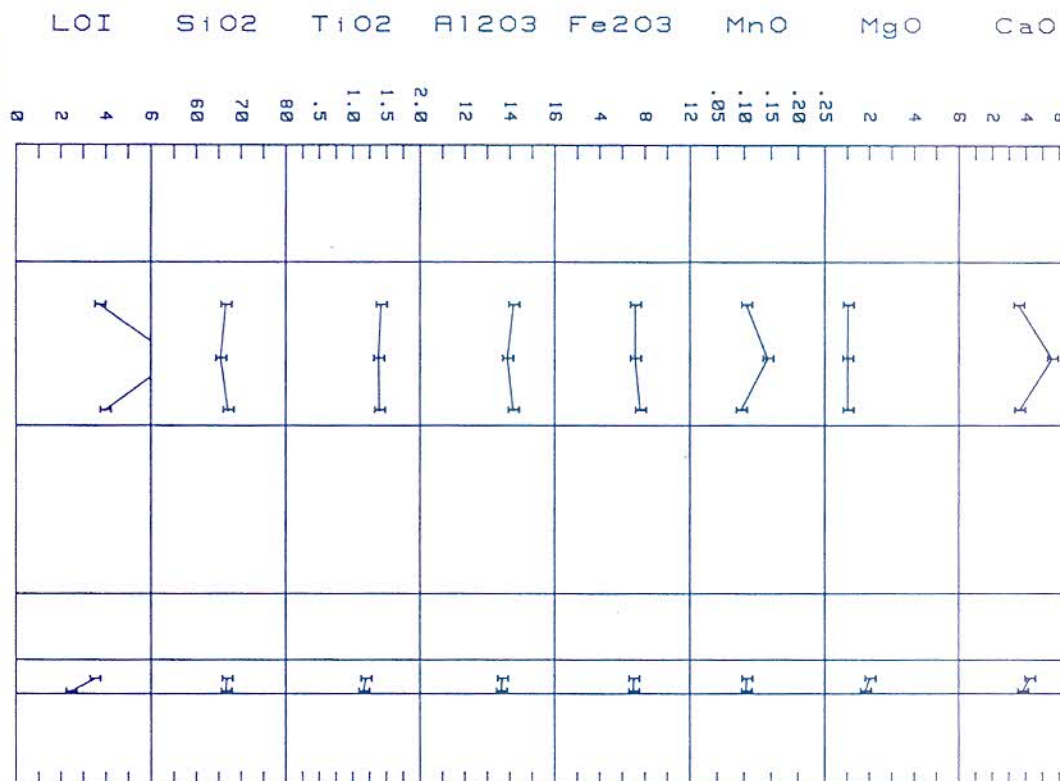
BOREHOLE JWS8

LOI SiO₂ TiO₂ Al₂O₃ Fe₂O₃ MnO MgO CaONa₂O K₂O P₂O₅ Zr Y Sr Rb Cu

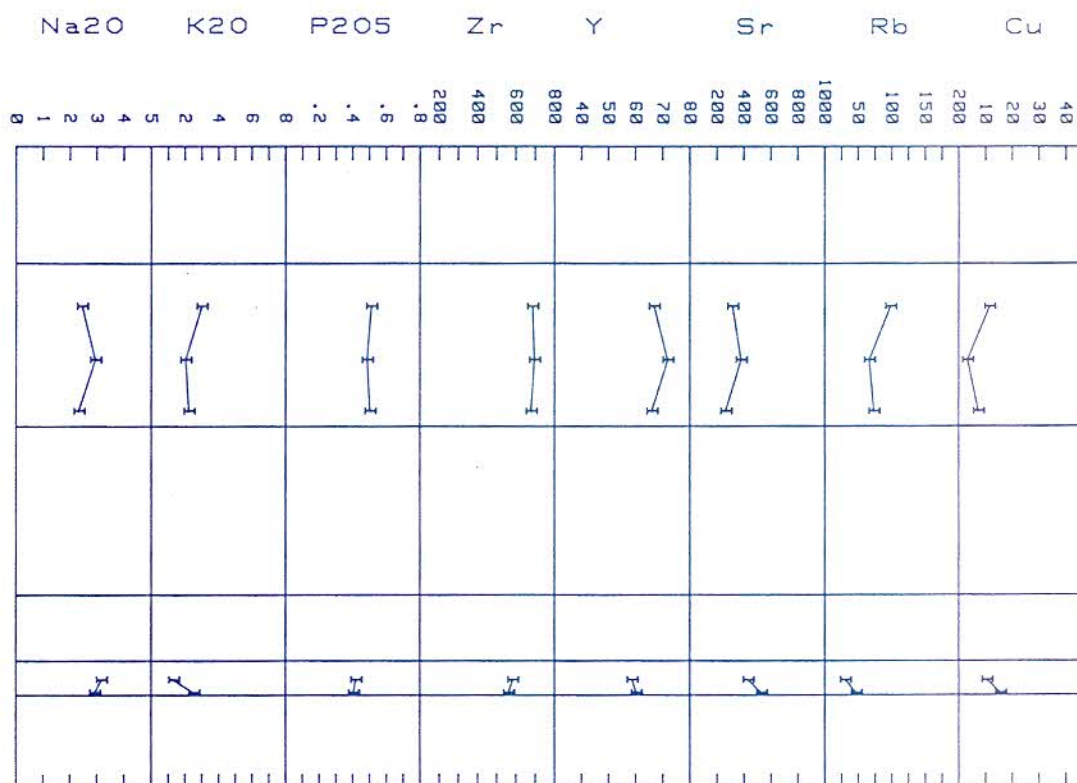


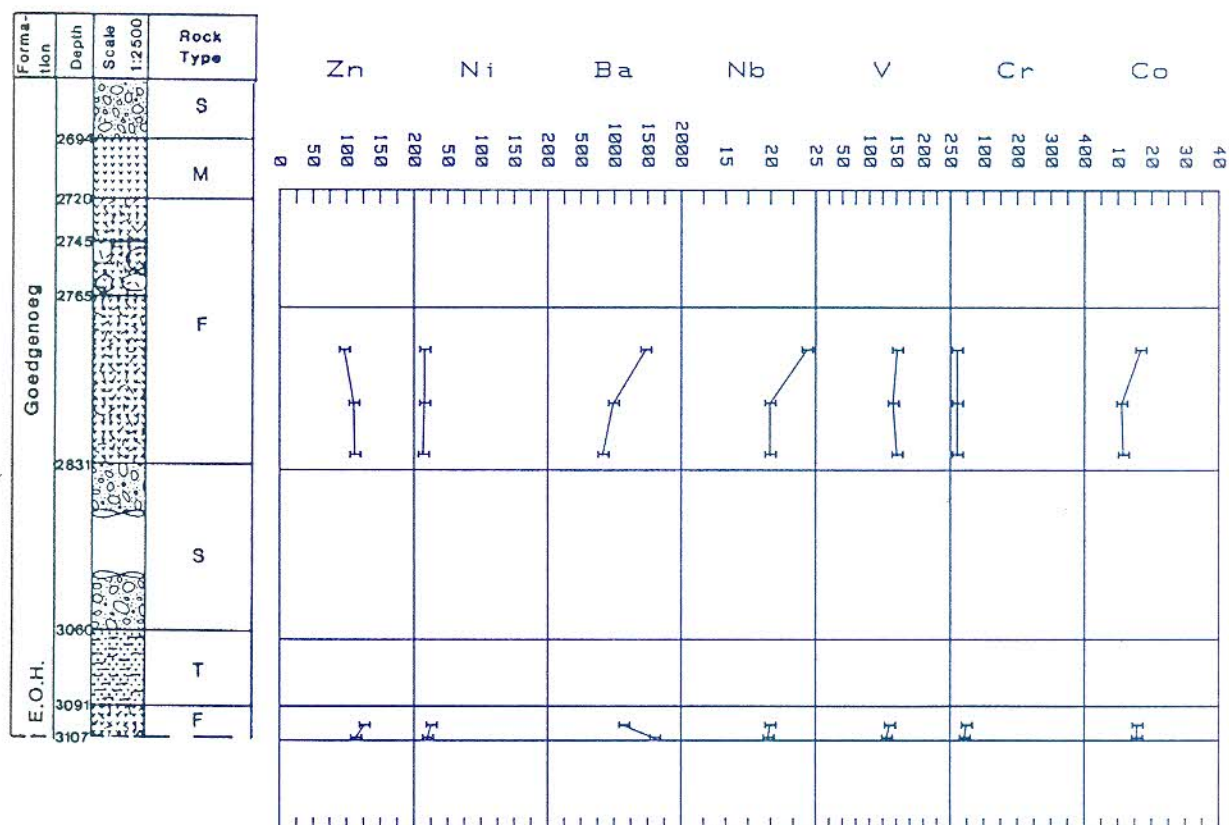
BOREHOLE FORMATION	JWS8 MAKW.	JWS8 MAKW.	JWS8 MAKW.	JWS8 MAKW.	JWS8 MAKW.	JWS8 MAKW.	JWS8 MAKW.
DEPTH	581	560	533	502	470	446	426
SAMPLE No	209	210	211	212	213	214	215
SiO2	68.20	63.93	69.33	67.65	66.53	68.72	67.19
TiO2	1.06	1.25	1.02	1.08	1.17	1.06	1.07
Al2O3	13.05	15.76	12.39	13.21	13.89	12.94	13.29
Fe2O3	5.89	7.31	6.09	6.35	6.82	5.80	6.11
MnO	0.09	0.11	0.09	0.10	0.10	0.09	0.09
MgO	1.28	2.22	0.79	2.17	0.68	0.74	2.79
CaO	5.89	1.95	6.11	2.32	2.46	6.06	4.24
Na2O	1.74	6.36	1.98	3.06	3.46	3.31	3.51
K2O	2.36	0.58	1.78	3.62	4.41	0.84	1.28
P2O5	0.44	0.51	0.43	0.43	0.48	0.44	0.44
TOTAL	100.00	100.00	100.00	100.00	100.00	100.00	100.00
Zr	454	598	455	462	475	435	480
Y	60	64	60	60	64	63	61
Sr	1397	160	1895	329	262	2476	883
Rb	57	5	47	74	90	30	51
Cu	3	21	6	11	5	7	7
Zn	101	158	92	107	122	80	107
Ni	15	20	15	16	17	15	15
Ba	977	181	973	1286	1593	361	266
Nb	22	25	21	21	24	21	20
V	91	96	92	105	113	99	94
Cr	22	26	22	23	30	26	24
Co	12	16	12	12	13	12	12

Formation	Depth	Scale	Rock Type
E.O.H.	2694	1:2500	S
	2720		M
	2745		F
	2765		
	2831		
	3060		S
E.O.H.	3091		T
	3107		F

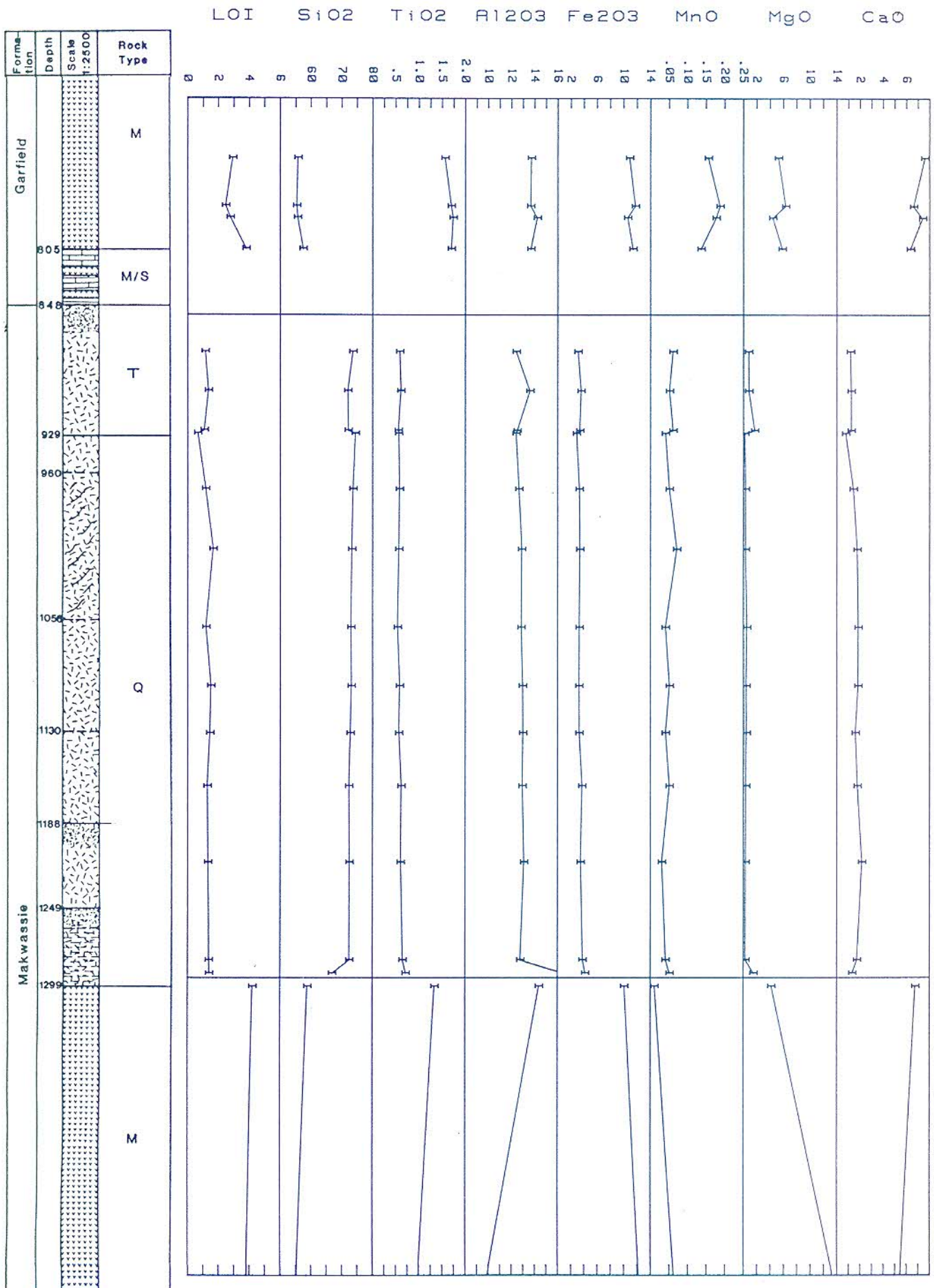


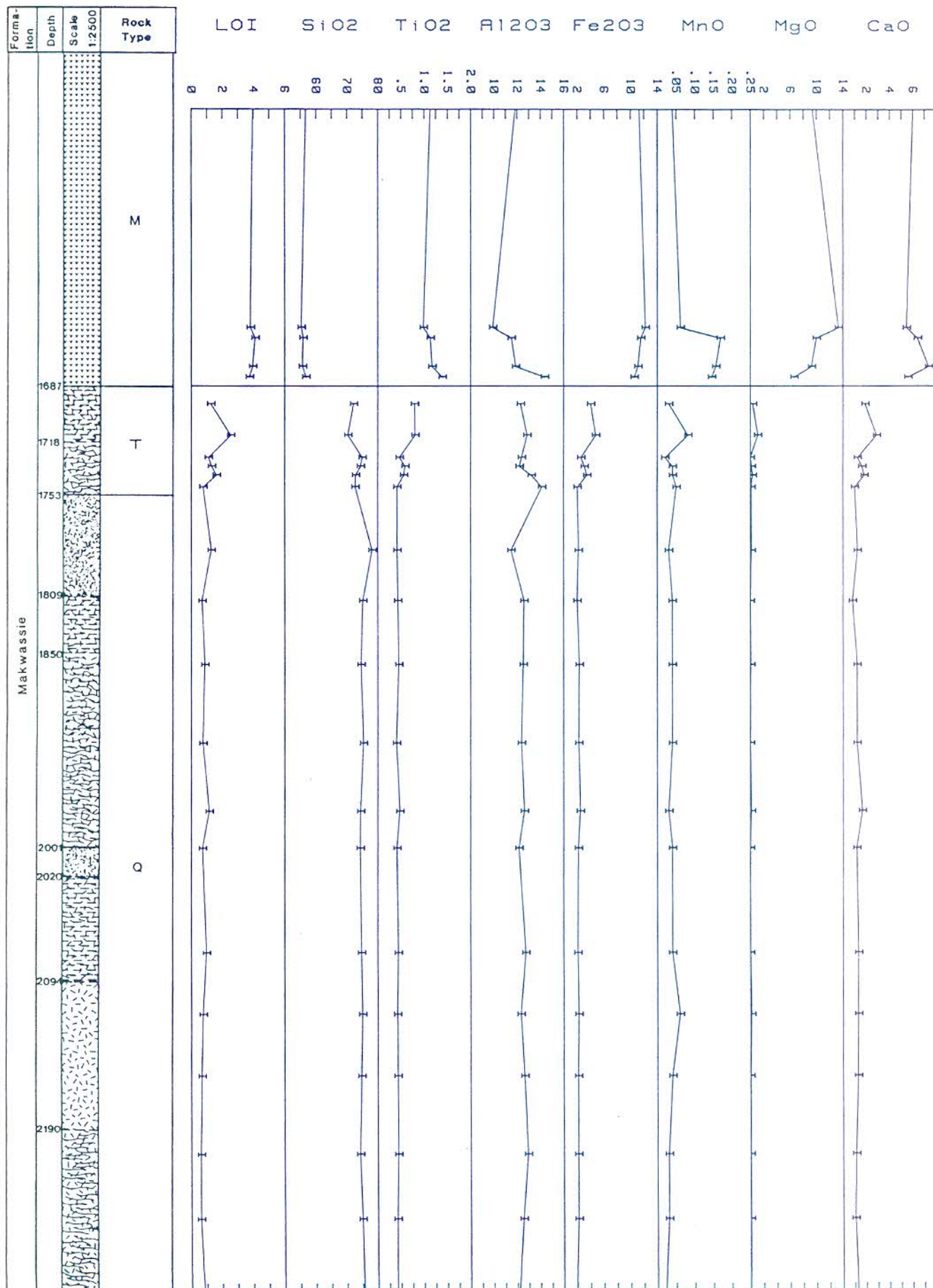
Formation	Depth	Scale	Rock Type
E.O.H.	2694	1:2500	S
	2720		M
	2745		F
	2765		
	2831		
	3060		S
E.O.H.	3091		T
	3107		F

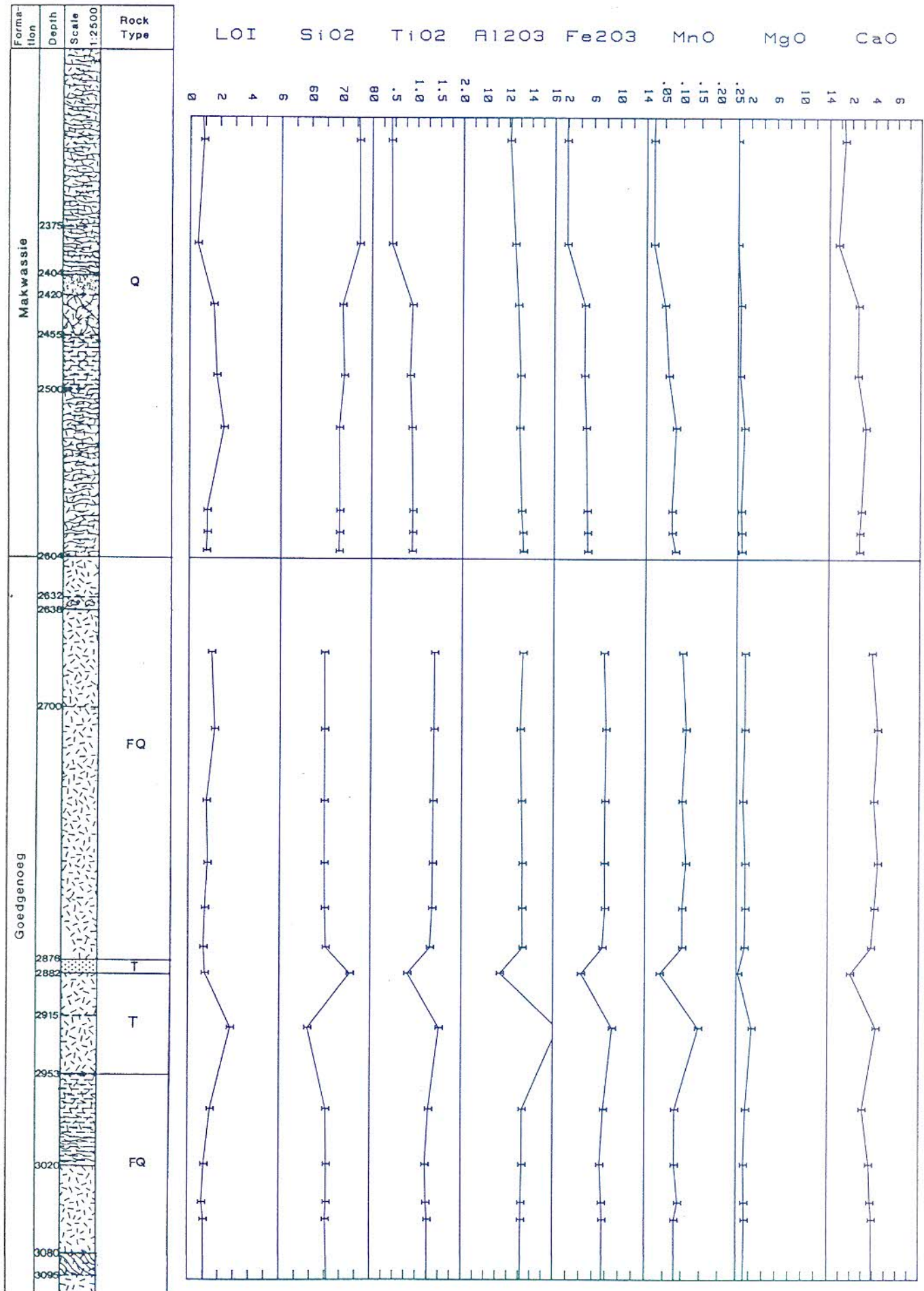


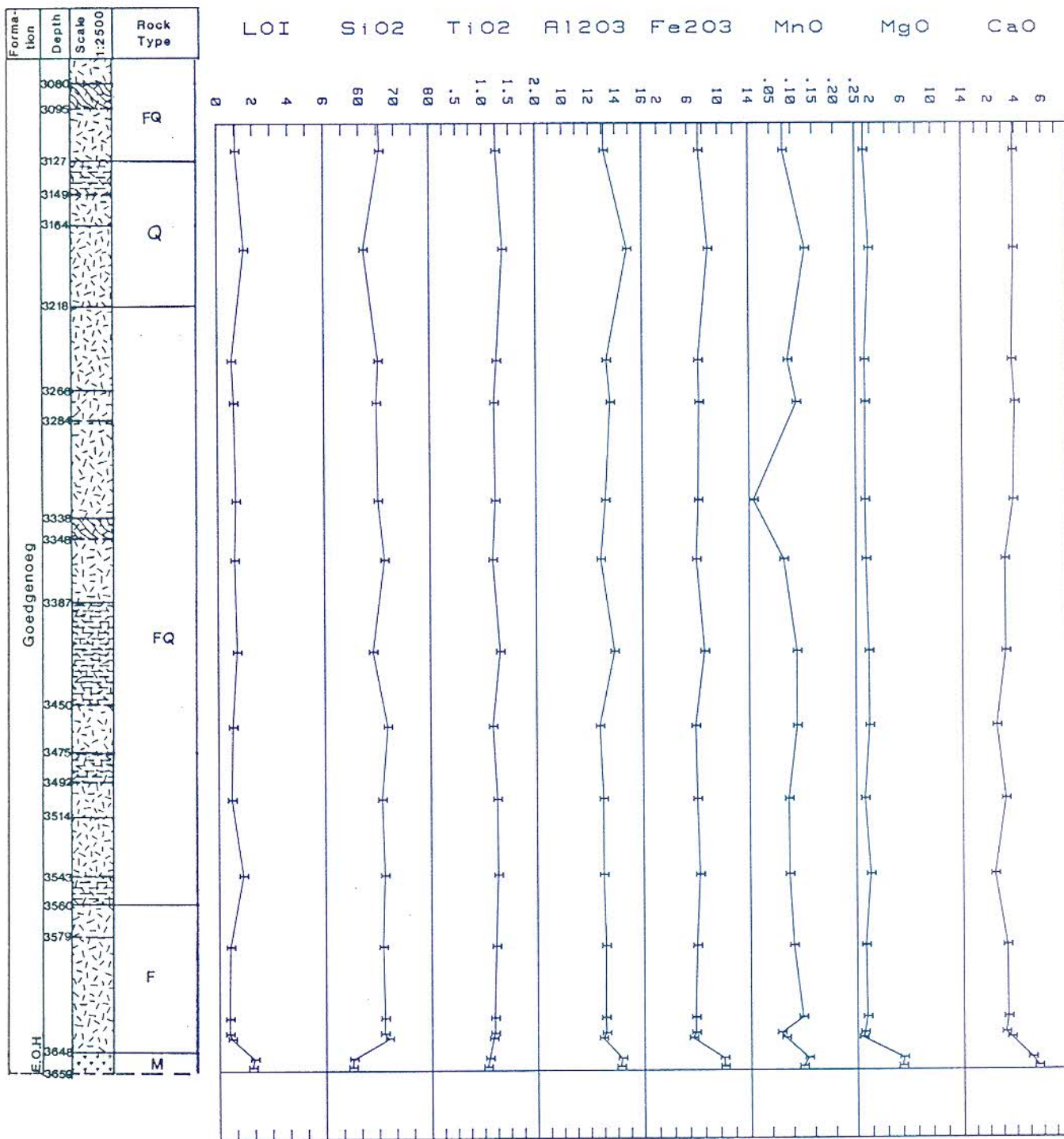


BOREHOLE FORMATION	KRF1 GOEDG.	KRF1 GOEDG.	KRF1 GOEDG.	KRF1 GOEDG.	KRF1 GOEDG.
SAMPLE No	3106	3100	2824	2800	2775
MNST. NO	457	458	459	460	461
SiO2	66.63	66.83	67.07	65.42	66.59
TiO2	1.16	1.19	1.39	1.38	1.42
Al2O3	13.62	13.66	14.15	13.89	14.17
Fe2O3	7.00	7.02	7.59	7.13	7.16
MnO	0.10	0.10	0.09	0.14	0.10
MgO	1.82	2.02	1.03	1.02	1.04
CaO	3.81	4.24	3.63	5.57	3.57
Na2O	2.93	3.17	2.32	2.94	2.45
K2O	2.52	1.33	2.22	2.02	2.98
P2O5	0.40	0.42	0.50	0.49	0.51
TOTAL	100.00	100.00	100.00	100.00	100.00
Zr	560	583	678	695	684
Y	60	59	66	72	67
Sr	528	430	265	377	315
Rb	47	30	73	66	98
Cu	16	10	7	3	11
Zn	113	126	112	110	96
Ni	20	25	14	15	16
Ba	1606	1143	826	982	1465
Nb	20	20	20	20	24
V	132	137	151	144	151
Cr	43	48	21	21	20
Co	16	16	12	11	17

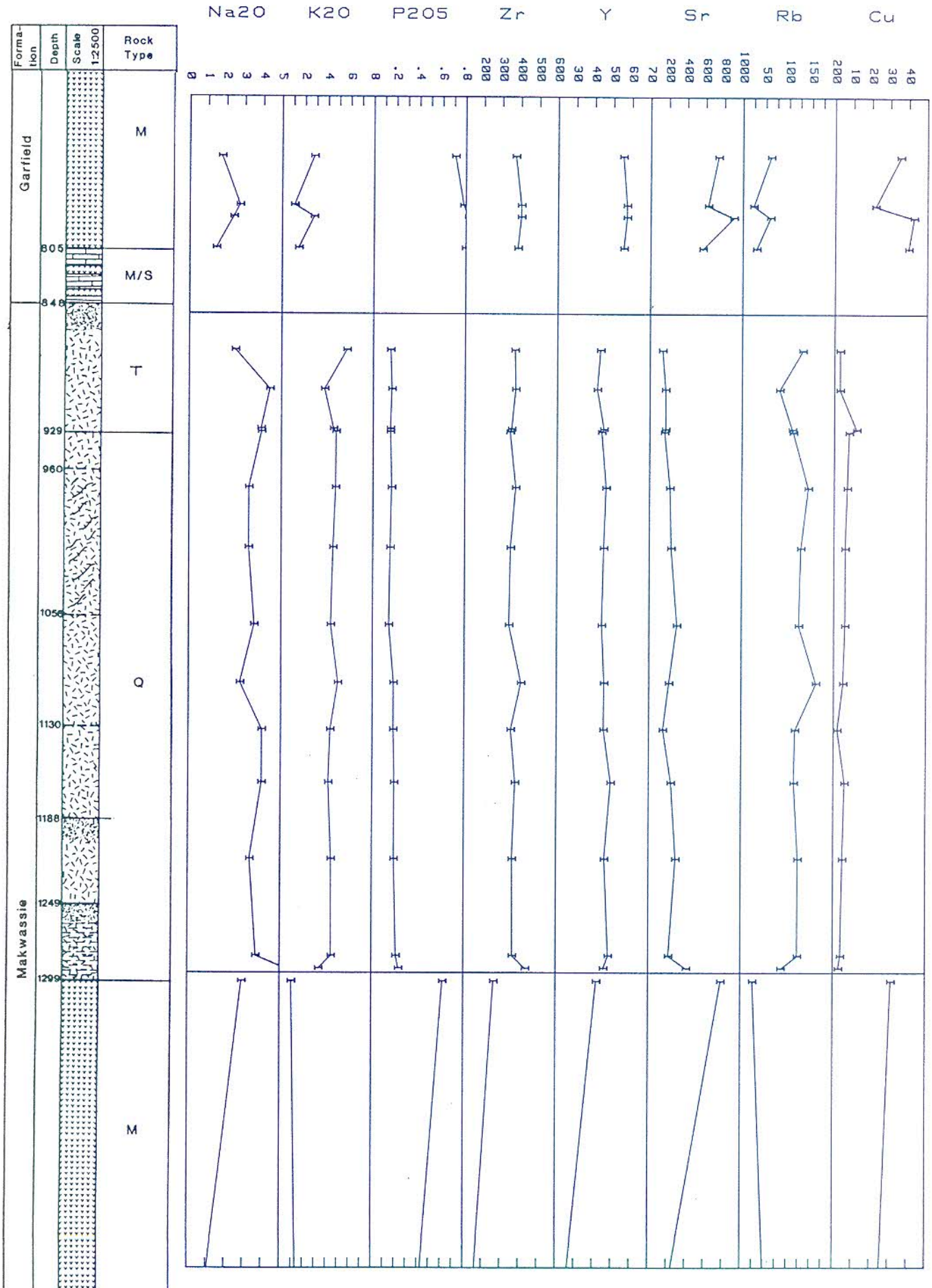


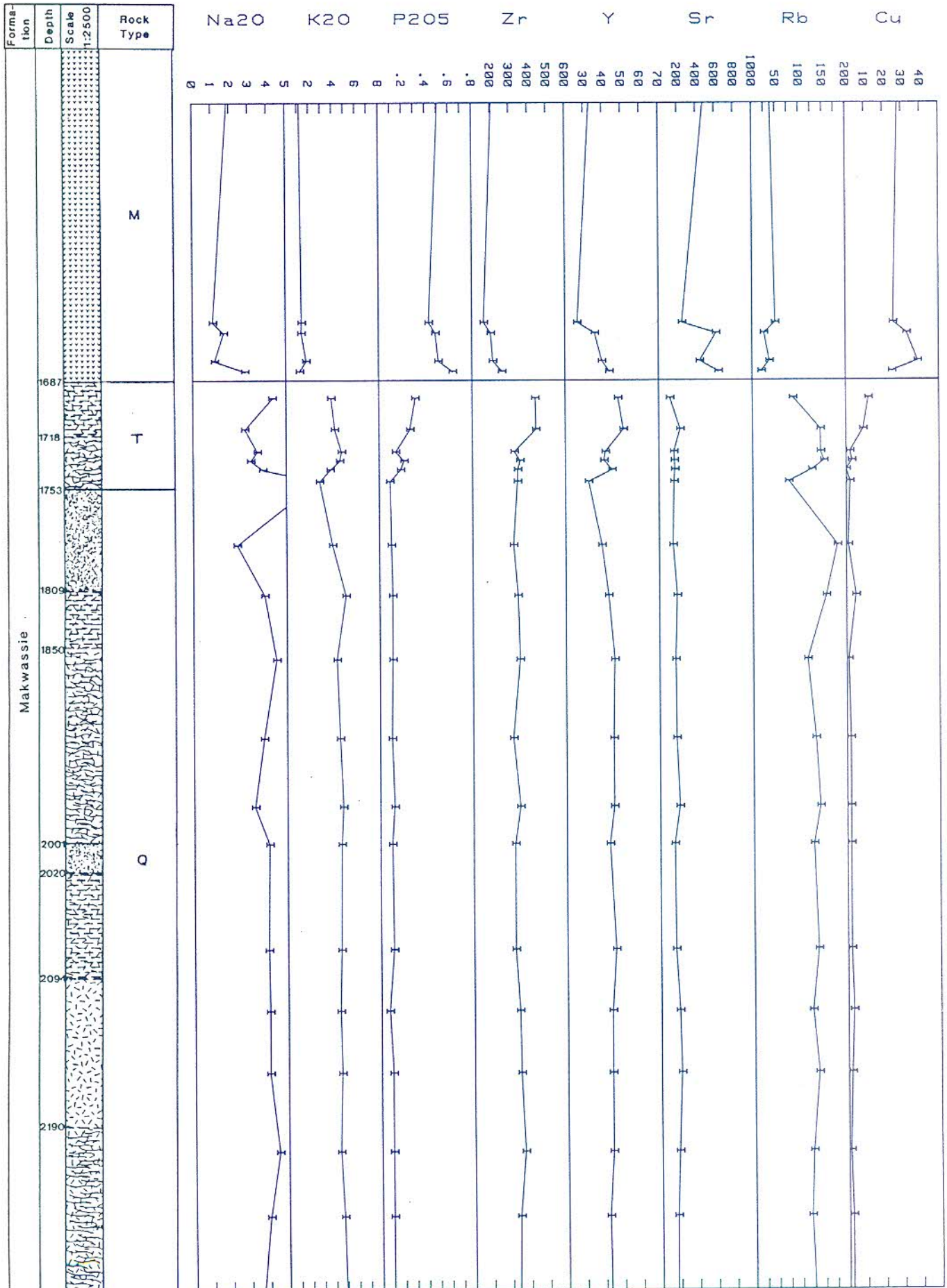


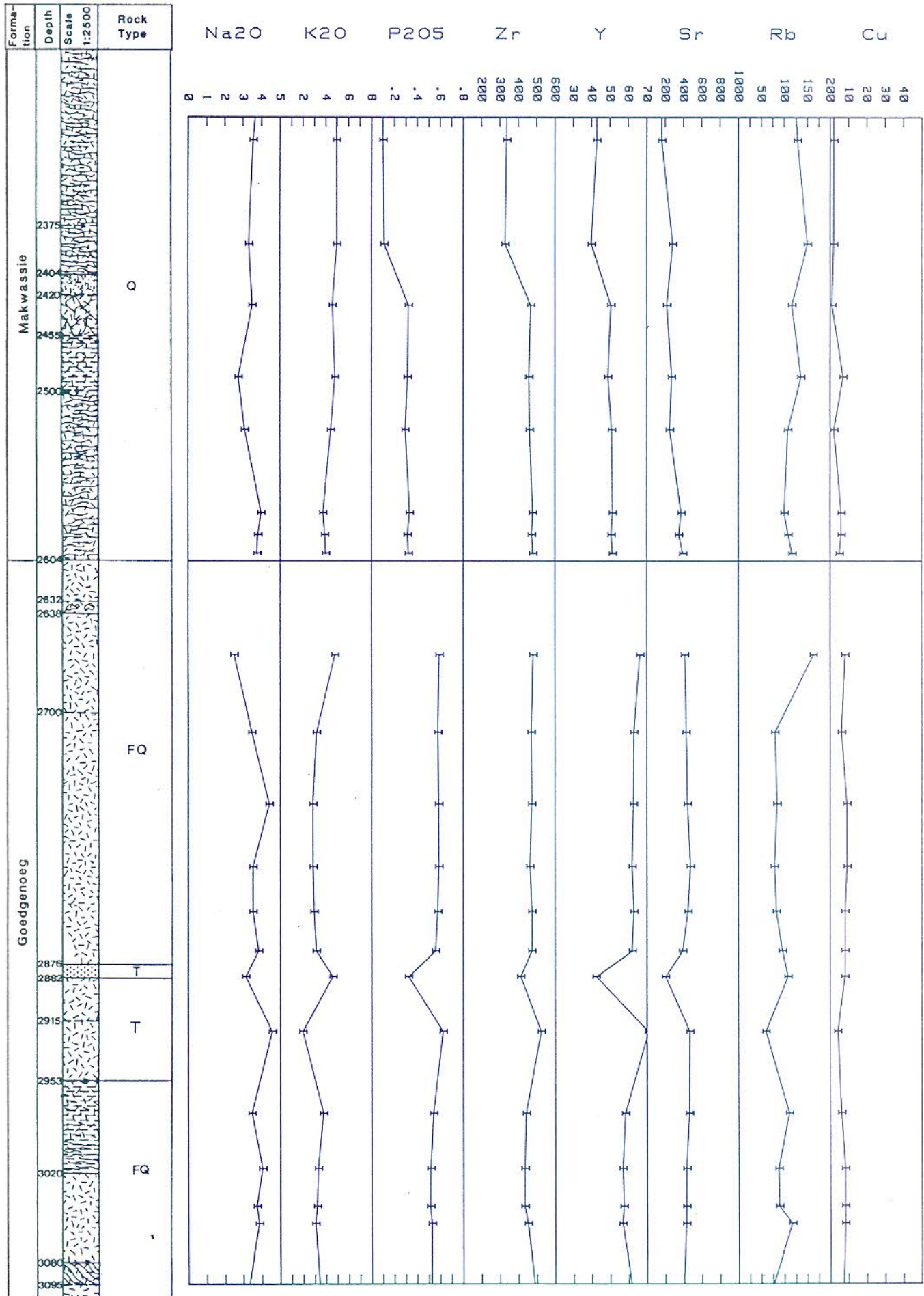


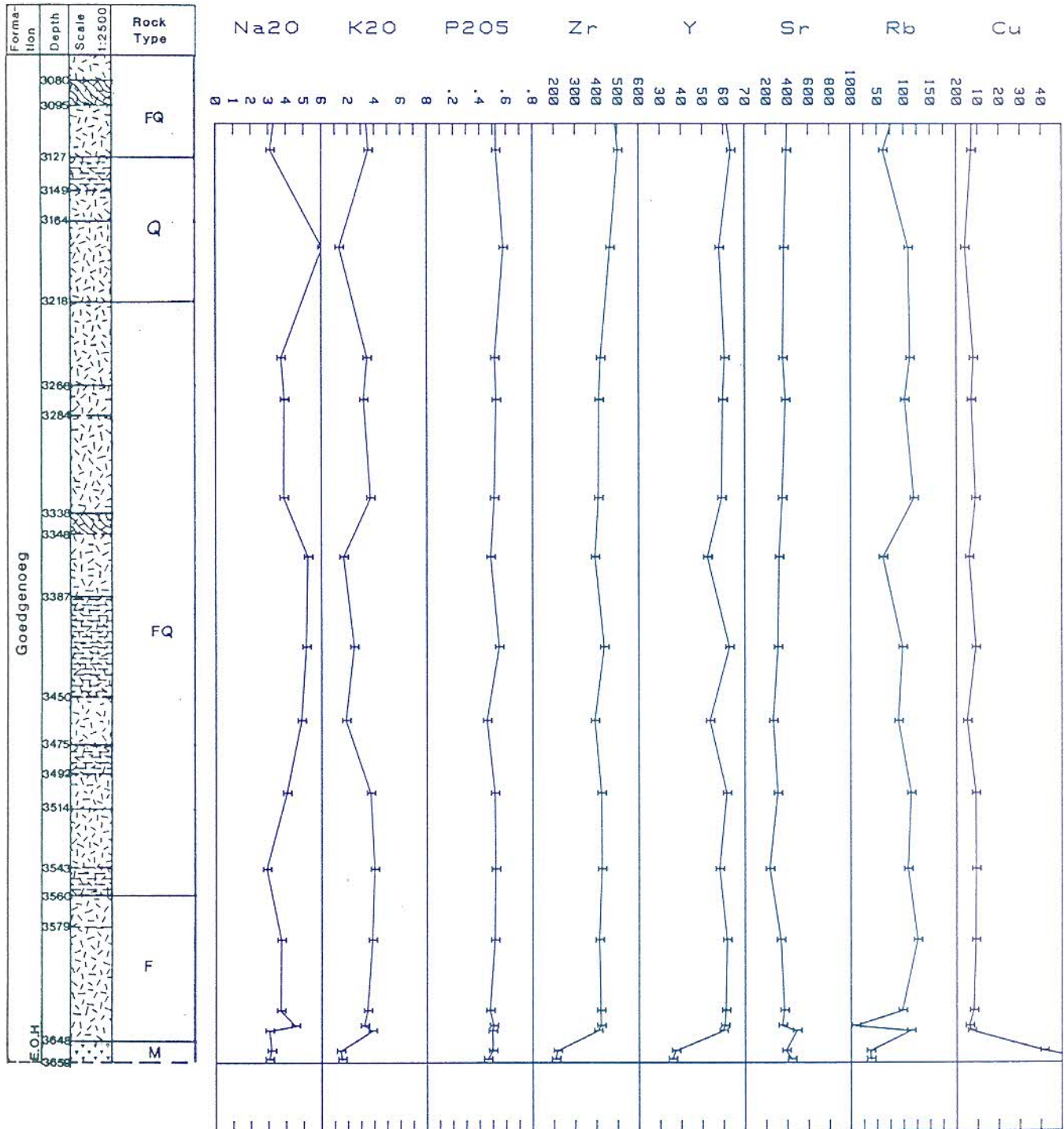


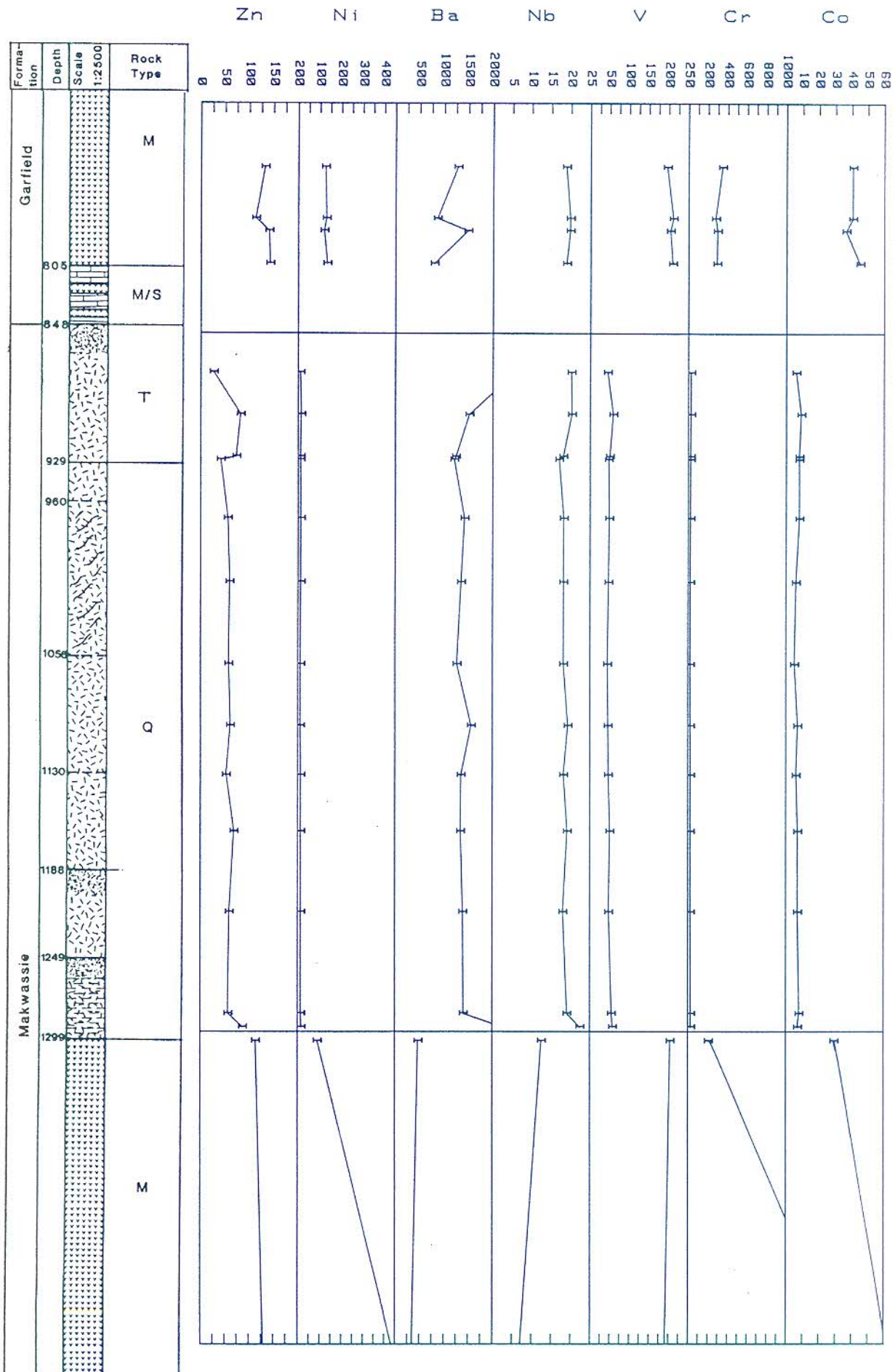
LLE1 /Continued 4

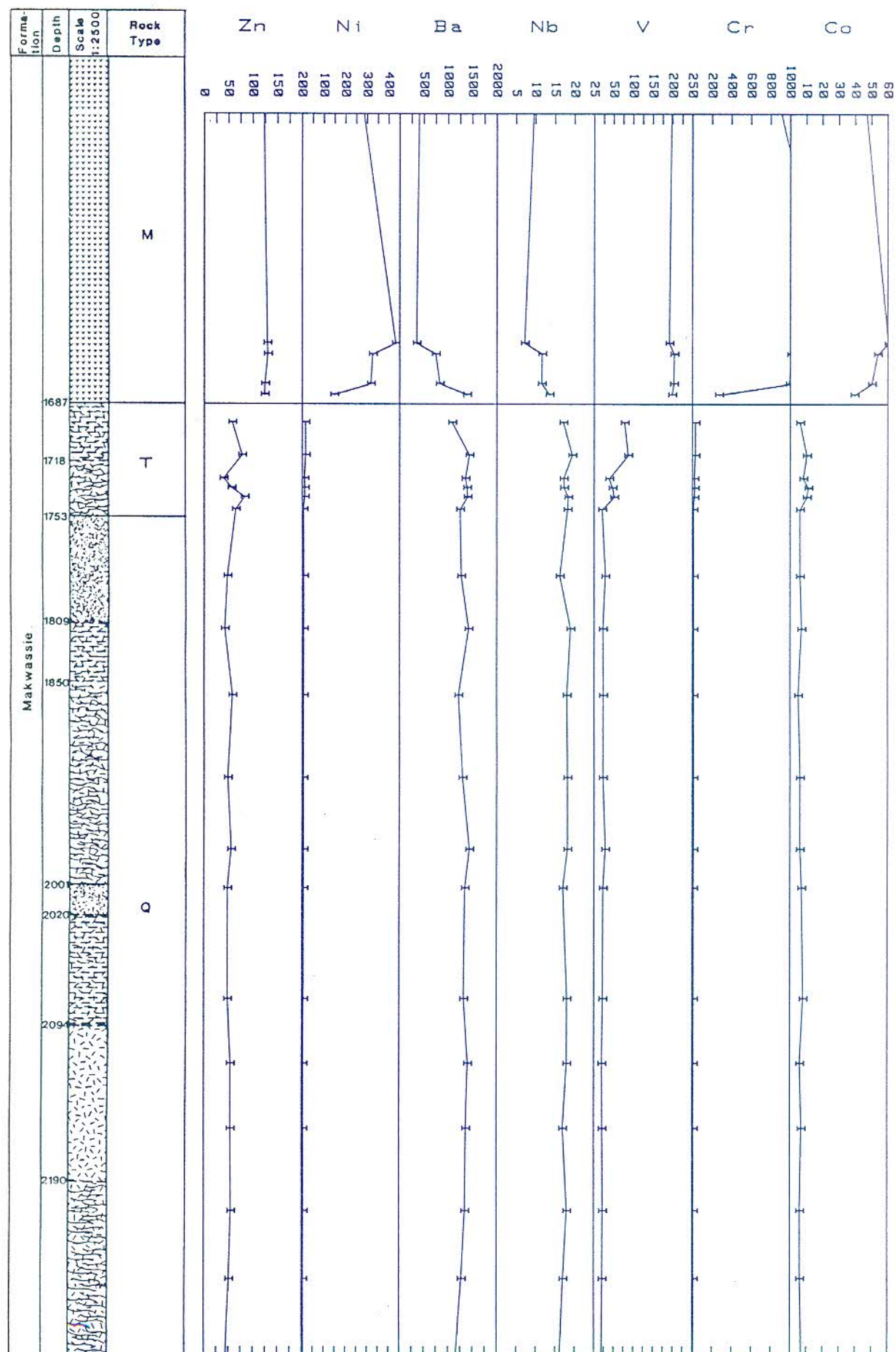


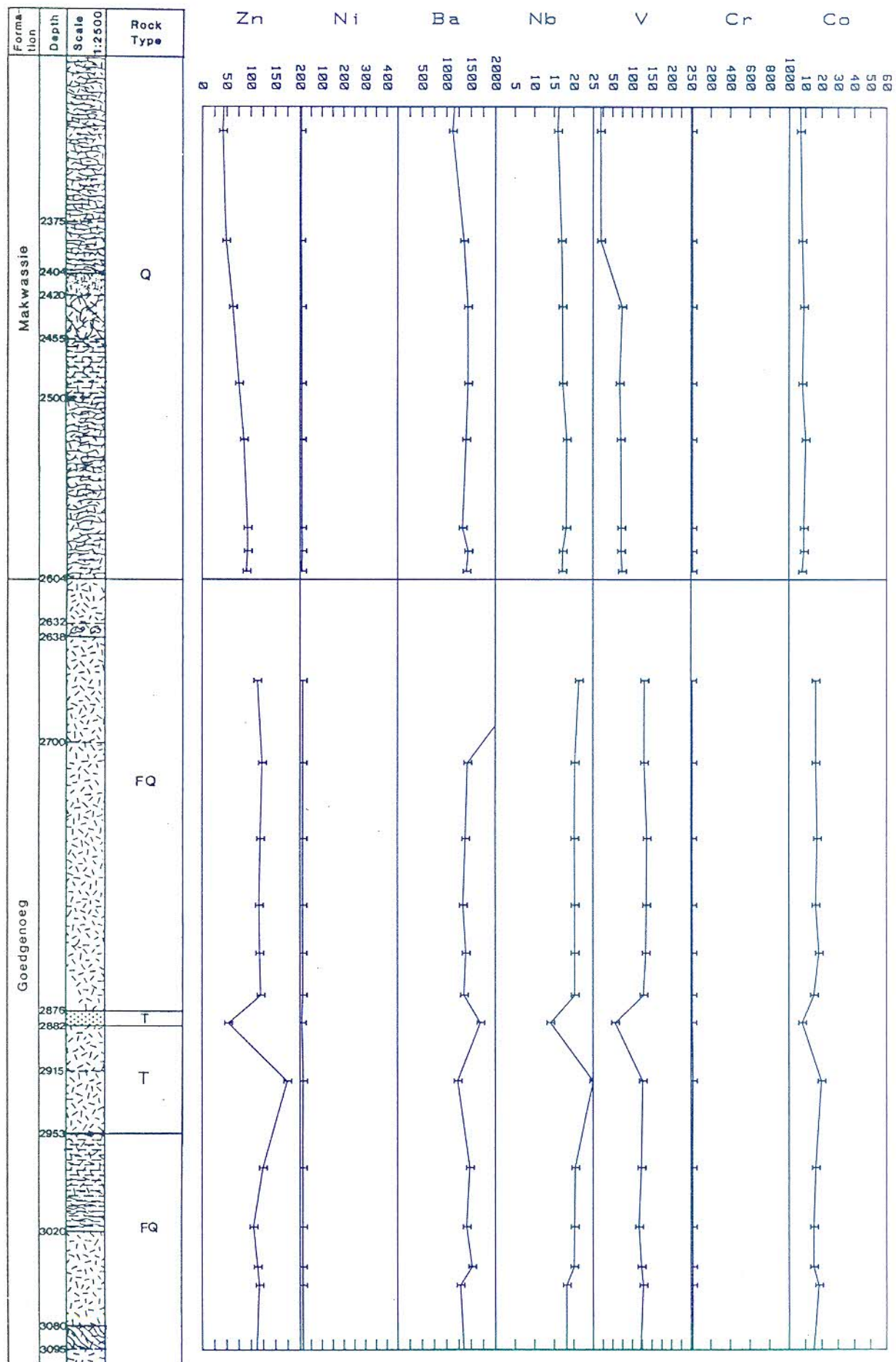


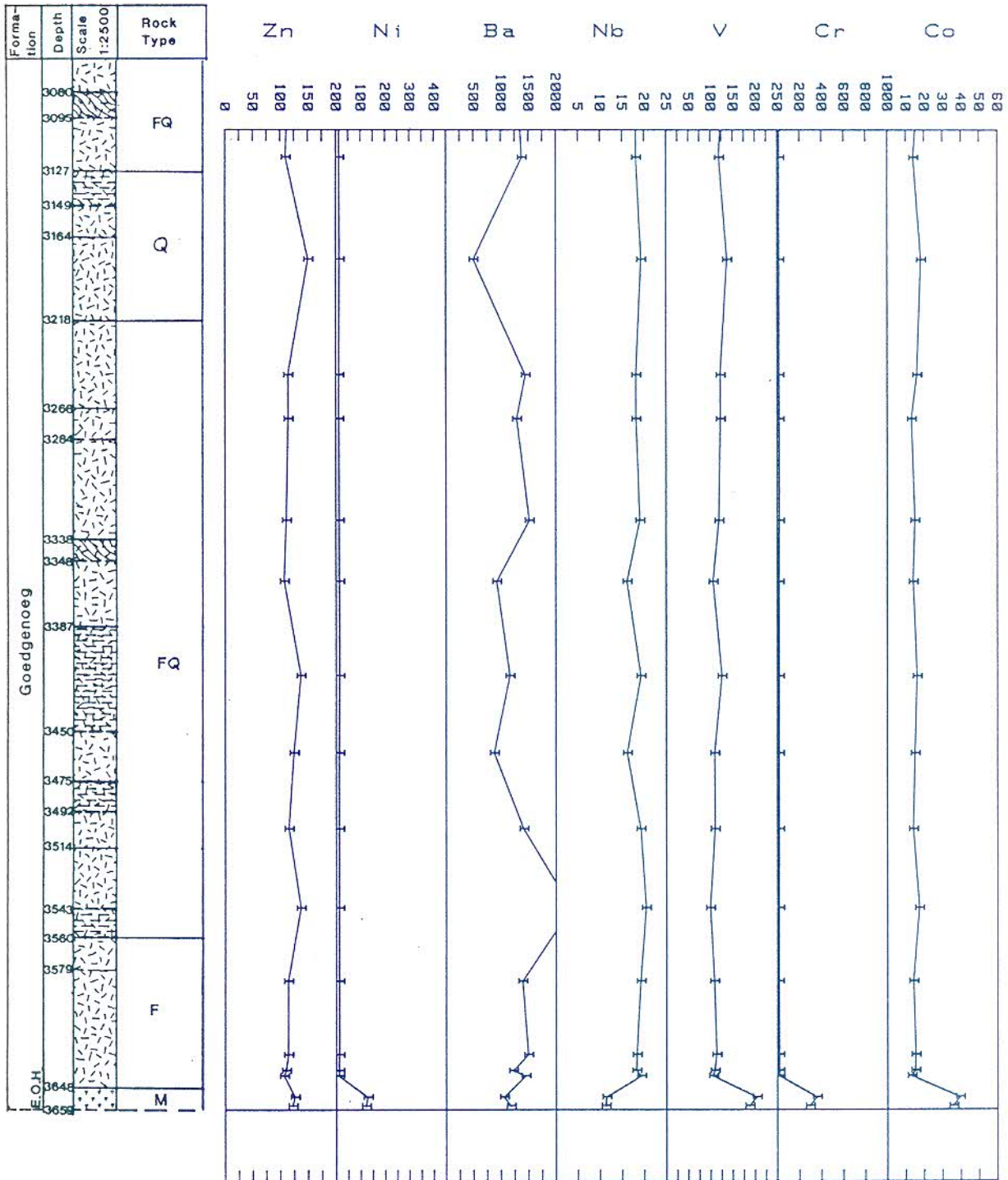












BOREHOLE FORMATION	LLE1 GOEDG.	LLE1 GOEDG.	LLE1 GOEDG.	LLE1 GOEDG.	LLE1 GOEDG.	LLE1 GOEDG.	LLE1 GOEDG.	LLE1 GOEDG.	LLE1 GOEDG.
DEPTH	3657	3652	3640	3637	3628	3586	3544	3499	3456
SAMPLE No	114	115	116	117	118	119	120	121	122
SiO2	57.45	57.69	67.74	66.49	66.60	66.13	66.72	66.03	67.68
TiO2	1.05	1.09	1.16	1.19	1.19	1.22	1.26	1.25	1.17
Al2O3	14.23	14.32	12.89	13.13	13.09	13.12	12.97	12.98	12.72
Fe2O3	10.53	10.46	6.39	6.75	6.73	6.94	7.37	7.07	6.88
MnO	0.12	0.13	0.08	0.07	0.12	0.10	0.09	0.09	0.11
MgO	5.95	6.08	0.78	0.95	1.29	1.14	1.80	1.11	1.74
CaO	5.62	5.14	3.58	3.17	3.33	3.28	2.38	3.21	2.55
Na2O	3.04	3.15	3.04	4.51	3.69	3.71	2.88	4.03	4.86
K2O	1.55	1.43	3.84	3.24	3.48	3.85	4.01	3.71	1.84
P2O5	0.46	0.50	0.50	0.50	0.48	0.51	0.52	0.51	0.45
TOTAL	100.00	100.00	100.00	100.00	100.00	100.00	100.00	100.00	100.00
Zr	208	216	406	421	419	413	424	422	392
Y	36	37	60	61	61	61	58	61	54
Sr	439	386	488	351	369	336	232	309	266
Rb	38	37	113	9	97	126	108	114	90
Cu	62	42	7	6	8	9	9	9	5
Zn	122	126	106	110	114	114	136	115	124
Ni	121	128	12	12	13	12	12	12	13
Ba	1175	1054	1443	1219	1493	1388	2276	1410	875
Nb	11	11	19	18	18	19	20	19	16
V	187	203	105	109	113	108	99	110	109
Cr	294	357	19	18	17	15	17	19	19
Co	36	39	13	15	15	14	17	14	15

BOREHOLE FORMATION	LLE1 GOEDG.	LLE1 GOEDG.	LLE1 GOEDG.	LLE1 GOEDG.	LLE1 GOEDG.	LLE1 GOEDG.	LLE1 GOEDG.	LLE1 GOEDG.	LLE1 GOEDG.
DEPTH	3412	3358	3323	3265	3240	3174	3116	3060	3048
SAMPLE No	123	124	125	126	127	128	129	130	131
SiO2	63.58	66.95	65.14	64.80	65.34	61.26	65.88	65.32	65.60
TiO2	1.31	1.18	1.23	1.21	1.26	1.38	1.26	1.26	1.24
Al2O3	13.86	12.85	13.21	13.58	13.30	14.88	13.15	13.21	13.23
Fe2O3	8.09	7.05	7.31	7.44	7.34	8.66	7.46	7.53	7.44
MnO	0.11	0.08	0.01	0.11	0.09	0.13	0.08	0.08	0.09
MgO	1.68	1.33	1.20	1.27	1.22	1.79	1.11	1.28	1.22
CaO	3.24	3.19	3.83	3.97	3.75	3.90	3.87	3.89	3.76
Na2O	5.13	5.23	3.86	3.90	3.71	6.05	3.11	3.85	3.73
K2O	2.46	1.65	3.69	3.18	3.46	1.35	3.55	3.05	3.19
P2O5	0.55	0.48	0.51	0.53	0.51	0.58	0.52	0.53	0.51
TOTAL	100.00	100.00	100.00	100.00	100.00	100.00	100.00	100.00	100.00
Zr	436	394	409	412	420	465	502	451	433
Y	63	52	59	60	61	58	64	57	57
Sr	311	323	351	382	358	370	394	425	427
Rb	98	61	119	102	112	109	61	116	88
Cu	9	6	9	7	8	4	7	8	8
Zn	137	107	111	114	114	150	110	117	113
Ni	14	13	13	12	13	15	13	13	12
Ba	1160	921	1515	1289	1448	500	1379	1284	1522
Nb	19	16	19	18	18	19	18	18	20
V	125	106	119	122	122	137	119	128	124
Cr	19	19	21	19	18	18	18	19	20
Co	16	14	15	13	16	18	14	18	15

BOREHOLE FORMATION	LLE1 GOEDG.	LLE1 GOEDG.	LLE1 GOEDG.	LLE1 GOEDG.	LLE1 GOEDG.	LLE1 GOEDG.	LLE1 GOEDG.	LLE1 GOEDG.	LLE1 GOEDG.
DEPTH	3022	2984	2928	2890	2872	2845	2814	2771	2722
SAMPLE No	132	133	134	135	136	137	138	139	140
SiO2	65.60	65.36	59.20	73.25	65.20	64.88	64.72	64.63	64.64
TiO2	1.21	1.29	1.51	0.82	1.31	1.36	1.37	1.38	1.39
Al2O3	13.31	13.32	16.38	11.36	13.33	13.29	13.31	13.22	13.09
Fe2O3	7.18	7.70	9.02	4.26	7.51	7.90	7.81	7.88	7.99
MnO	0.08	0.08	0.15	0.04	0.10	0.10	0.11	0.10	0.11
MgO	1.14	1.45	2.37	0.27	1.25	1.36	1.35	0.96	1.26
CaO	3.64	3.05	4.24	1.98	3.80	4.10	4.39	4.03	4.34
Na2O	4.03	3.46	4.56	3.11	3.82	3.51	3.51	4.40	3.45
K2O	3.29	3.75	1.95	4.59	3.13	2.93	2.84	2.82	3.15
P2O5	0.52	0.54	0.62	0.32	0.56	0.58	0.59	0.59	0.58
TOTAL	100.00	100.00	100.00	100.00	100.00	100.00	100.00	100.00	100.00
Zr	434	442	523	412	473	473	463	473	470
Y	57	58	71	42	62	63	62	63	63
Sr	430	460	466	201	388	446	474	442	428
Rb	87	110	59	108	95	82	78	84	79
Cu	8	6	4	8	8	8	9	9	6
Zn	105	124	174	53	120	118	117	119	123
Ni	13	12	15	9	13	12	12	13	12
Ba	1412	1478	1230	1696	1360	1396	1338	1387	1429
Nb	20	20	25	14	20	20	20	20	20
V	117	123	127	56	129	135	136	138	131
Cr	18	16	21	15	16	15	15	15	16
Co	15	16	20	8	15	18	16	17	16